EMERGING
INFECTIOUS DISEASES®

Fungal Infections

September 2021

EMERGING INFECTIOUS DISEASES®

EDITOR-IN-CHIEF
D. Peter Drotman

EMERGING INFECTIOUS DISEASES®

Fungal Infections

September 2021

Research

Medscape
EDUCATION
ACTIVITY

On the Cover

Mattia di Nanni di Stefano (1403–1433), *Scipio Africanus* **ca. 1425–1430.** Poplar, bog oak and other wood inlay, rosewood, tin, bone, traces of green coloring, 24.19 in x 17.13 in/61.5 cm x 43.3 cm. Public domain image courtesy of The Metropolitan Museum of Art, New York, NY, USA.

Synopses

2353

Dispatches

2390

2452

EMERGING INFECTIOUS DISEASES®

2463

⦿DPDx

Diagnostic Assistance and Training in Laboratory Identification of Parasites

A free service of CDC available to laboratorians, pathologists, and other health professionals in the United States and abroad

Diagnosis from photographs of worms, histological sections, fecal, blood, and other specimen types

Expert diagnostic review

Formal diagnostic laboratory report

Submission of samples via secure file share

Visit the DPDx website for information on laboratory diagnosis, geographic distribution, clinical features, parasite life cycles, and training via Monthly Case Studies of parasitic diseases.

Epidemiology of Coronavirus Disease Outbreak among Crewmembers on Cruise Ship, Nagasaki City, Japan, April 2020

Haruka Maeda,[1] Eiichiro Sando,[1] Michiko Toizumi,[1] Yuzo Arima,[1] Tomoe Shimada, Takeshi Tanaka,
Masato Tashiro, Ayumi Fujita, Katsunori Yanagihara, Hayato Takayama, Ikkoh Yasuda, Nobuyuki Kawachi,
Yoshitaka Kohayagawa, Maiko Hasegawa, Katsuaki Motomura, Rie Fujita, Katsumi Nakata, Jiro Yasuda,
Koichi Morita, Shigeru Kohno, Koichi Izumikawa, Motoi Suzuki,[2] Konosuke Morimoto[2]

In April 2020, a coronavirus disease (COVID-19) outbreak occurred on the cruise ship Costa Atlantica in Nagasaki, Japan. Our outbreak investigation included 623 multinational crewmembers onboard on April 20. Median age was 31 years; 84% were men. Each crewmember was isolated or quarantined in a single room inside the ship, and monitoring of health status was supported by a remote health monitoring system. Crewmembers with more severe illness were hospitalized. The investigation found that the outbreak started in late March and peaked in late April, resulting in 149 laboratory-confirmed and 107 probable cases of infection with severe acute respiratory syndrome coronavirus 2. Six case-patients were hospitalized for COVID-19 pneumonia, including 1 in severe condition and 2 who required oxygen administration, but no deaths occurred. Although the virus can spread rapidly on a cruise ship, we describe how prompt isolation and quarantine combined with a sensitive syndromic surveillance system can control a COVID-19 outbreak.

Severe acute respiratory syndrome coronavirus 2 (SARS-CoV-2) was first reported from Wuhan, China (1), and led to outbreaks of coronavirus disease (COVID-19), which was declared a pandemic

by the World Health Organization on March 11, 2020. COVID-19 also has been affecting global economies, leading to several recessions (2). Japan experienced an outbreak of COVID-19 on the cruise ship Diamond Princess during the early stages of the epidemic in February 2020 (3–5). The government of Japan prohibited entry into the country at the end of March, declaring a state of emergency in 7 prefectures on April 7, which became a nationwide policy on April 16. Against this backdrop, the Italian cruise ship Costa Atlantica had remained docked at Nagasaki City since January 2020 for full maintenance. In April 2020, we identified an outbreak of COVID-19 on this cruise ship.

COVID-19 spreads easily on cruise ships because of the "3 Cs": crowded places, close-contact settings, and confined and enclosed spaces (6–9). Given the specialized setting of a cruise ship and its closed population, a cruise ship can offer important insights about infectious disease epidemiology and transmission dynamics (10). How to manage an outbreak of COVID-19 on a cruise ship is a matter of debate, especially in a resource-limited situation. To improve our understanding of COVID-19 and prepare for outbreaks to come, studies of outbreaks on cruise ships are valuable. In this article we describe the epidemiology of the COVID-19 outbreak on Costa Atlantica and approaches taken for managing and responding to this outbreak.

Methods

Setting
On April 19, 2020, officials of Costa Atlantica, which had been docked in Nagasaki City since January

Author affiliations: Nagasaki University, Nagasaki, Japan
(H. Maeda, E. Sando, M. Toizumi, T. Tanaka, M. Tashiro, A. Fujita,
K. Yanagihara, H. Takayama, I. Yasuda, N. Kawachi, J. Yasuda,
K. Morita, S. Kohno, K. Izumikawa, K. Morimoto); Fukushima
Medical University, Fukushima, Japan (E. Sando, I. Yasuda);
National Institute of Infectious Diseases, Tokyo, Japan (Y. Arima,
T. Shimada, M. Suzuki); Disaster Medical Center of Japan, Tokyo
(Y. Kohayagawa); Nagasaki Prefecture Government, Nagasaki
(M. Hasegawa, K. Nakata); Nagasaki City Public Health Center,
Nagasaki (K. Motomura); Northern Nagasaki Public Health Center,
Nagasaki (R. Fujita)

[1]These authors contributed equally to this article.

[2]These authors were co–principal investigators.

2020, reported to Nagasaki City Public Health Center that they had febrile crewmembers (*11,12*). No passengers were on board the ship. All 623 crewmembers had already completed their quarantine upon entry in Japan, but they had been asked to refrain from leaving the ship unless necessary as part of the public health policy to prevent the spread of COVID-19. Because of cruise ship employment contracts, 56 crewmembers embarked during March 14–April 3. Given the COVID-19 pandemic, the body temperature of all crewmembers had been checked daily since the end of February. Beginning March 22, at the discretion of the cruise ship company, any crewmember with a body temperature $\geq$37.1°C was to be isolated in a single-passenger cabin room of the ship; beginning April 19, every nonessential worker was isolated or quarantined in a single-passenger cabin room. Essential workers were defined as crewmembers who were involved in the operation of the ship or in maintaining its operation and functionality, such as the captain, engineers, and food preparation staff.

On April 20, we performed PCR assays for SARS-CoV-2 for 4 crewmembers who had a body temperature $\geq$37.1°C, resulting in 1 positive result. During April 21–25, all crewmembers underwent universal screening for infection by using loop-mediated isothermal amplification (LAMP) for SARS-CoV-2. After the universal screening, each nonessential worker remained isolated or quarantined in a single passenger cabin room. Even for those whose test results were positive, crewmembers with mild illness or without signs or symptoms remained on the ship, and the health status of all crewmembers was monitored daily. If clinically indicated, regardless of test results, ill persons were transported and admitted to hospitals in Nagasaki City at the discretion of the ship's medical doctor.

Data Collection and Definitions
The study population included 623 crewmembers who were on board on April 20, 2020. The cruise ship company provided demographic and body temperature data (ship's medical record) during March 14–May 27 for all crewmembers on board. Demographic data included sex, date of birth, nationality, and occupation category. Before disembarkation from the ship, crewmembers also provided information regarding their smoking history, presence of any underlying disease, height and weight, daily body temperature, and clinical signs or symptoms during April 28–May 29 by using a smartphone-based remote health monitoring system (*13*). Obesity, as

a risk factor for severe COVID-19, was defined as a body mass index (BMI) $\geq$30 (*14,15*). Clinical signs and symptoms of COVID-19 were fever (body temperature $\geq$37.5°C), cough, shortness of breath, nasal congestion, sore throat, nausea or vomiting, conjunctival congestion, headache, fatigue, myalgia or arthralgia, diarrhea, olfactory dysfunction, and taste disorder (loss of taste), which are globally recognized COVID-19 signs and symptoms (*1,13,16–18*). In managing this outbreak, the threshold value of a body temperature $\geq$37.1°C was applied on the basis of the cruise ship's definition for illness and criteria for isolation precaution.

We defined laboratory-confirmed cases as illness in anyone with a positive test result for SARS-CoV-2 by PCR or LAMP. We defined a probable case was defined as illness in anyone with signs or symptoms indicative of COVID-19 but with a negative test result (*19*). We divided the severity of COVID-19 into 4 groups (*20*): severe pneumonia that required intubation or intensive care unit admission, moderate pneumonia that required oxygen administration, mild illness with COVID-19 signs or symptoms that did not require oxygen administration, and an asymptomatic condition without any clinical signs or symptoms. We performed chest radiographs or chest computed tomography scans only for those suspected of having pneumonia, such as prolonged fever or shortness of breath, and those who were hospitalized.

Testing Strategy
We confirmed SARS-CoV-2 infection by using PCR or LAMP. We conducted PCR according to the protocol recommended by Japan's National Institute of Infectious Diseases (*21*). LAMP is used for the detection of SARS-CoV-2 because of its fast turnaround time and acceptable levels of sensitivity and specificity (*22–24*). LAMP was conducted at the Institute of Tropical Medicine at Nagasaki University and Nagasaki University Hospital. Persons who tested positive were allowed to disembark and travel back to their countries after negative test results were confirmed in subsequent tests and their signs or symptoms had resolved.

Data Analysis
We constructed an epidemic curve on the basis of illness onset date, which was based on a body temperature $\geq$37.1°C according to the ship's medical record or the smartphone-based health monitoring system; the onset date of body temperature $\geq$37.1°C was defined as the date when body temperature was $\geq$37.1°C with a body temperature <37.1°C until the

previous day. For the epidemic curve, we used body temperature ≥37.1°C for 2 reasons: first, it was the cruise ship's definition for illness and criteria for isolation precaution; second, describing the epidemic curve based on the test results of SARS-CoV-2 from the universal screening would not give an accurate picture of this outbreak because screening was introduced ≈1 month after the beginning of the outbreak and would only detect infections prevalent at the time of screening.

In addition to monitoring such incident events, we monitored the daily prevalent numbers of crewmembers with a body temperature ≥37.1°C or signs or symptoms. To evaluate the spatial distribution of infection, we plotted on the ship's map the cabin rooms of crewmembers with a body temperature ≥37.1°C before isolation. We noted the demographic characteristics of all crewmembers according to their test results and presence of signs or symptoms. We calculated attack rates for both laboratory-confirmed case-patients (laboratory-confirmed case-patients divided by all crewmembers) and with the addition of probable case-patients (laboratory-confirmed case-patients and probable case-patients divided by all crewmembers). We also plotted the clinical course of symptomatic crewmembers individually by calendar date.

We expressed continuous variables as medians and interquartile ranges (IQRs). We summarized categoric variables as numbers and proportions. We conducted statistical analyses by using Stata 16 (StataCorp, https://www.stata.com).

Ethics
The governments of Nagasaki City and Nagasaki Prefecture conducted the surveillance of the COVID-19 outbreak on this cruise ship during April 20–May 29, 2020, under authorization by the Infectious Diseases Control Law. This study was approved by the Institutional Review Board at the Institute of Tropical Medicine at Nagasaki University (approval no. 200619242).

Results

Demographic Characteristics of the Crewmembers
Among the 623 crewmembers, the median age was 31 years (IQR 26–40 years), and 84% (523/623) were men (Table 1). Thirty-six nations were represented by the crewmembers, including (in descending order) the Philippines, India, Indonesia, and China; most (80%) crewmembers were from countries in Asia. Characteristic data were available for 593

crewmembers. Of those, 25% (148/592) had a history of smoking, and 3.7% (22/593) had underlying diseases, including hypertension (2.0% [12/592]), diabetes (1.7% [10/592]), cardiovascular disease (0.2% [1/592]), and asthma (0.2% [1/592]). Median BMI was 24.1 (IQR 21.7–26.7), and 9.4% (49/523) crewmembers had obesity (BMI ≥30).

Overview of the COVID-19 Outbreak on the Cruise Ship
A body temperature ≥37.1°C was first detected in a crewmember on March 22, and afterwards, 5 other crewmembers had a body temperature ≥37.1°C during March 24–27 (Figure 1, panel A). Their crew cabin rooms were not concentrated in a single area on the ship (Figure 2, panel A). However, all of these crewmembers belonged to the entertainment occupation group that boarded the cruise ship from several countries in Europe on March 18 and 19 (Appendix Figure 1, https://wwwnc.cdc.gov/EID/article/27/9/20-4596-App1.pdf). On April 2, another crewmember had a body temperature ≥37.1°C, and the number of persons with incident fever increased and peaked on April 28, decreasing thereafter (Figure 1, panel A). During March 22–May 29, a total of 211 (34%) had a body temperature ≥37.1°C. One crewmember who had a body temperature ≥37.1°C associated with cellulitis was excluded. Apart from the first wave of persons with a body temperature ≥37.1°C in late March, SARS-CoV-2 infection was distributed similarly across sex, and age group, nationality, and occupation type (Appendix Figure 1). The crew cabin rooms of crewmembers who had a body temperature ≥37.1°C also were widely distributed throughout the ship (Figure 2, panel B). No information on the ventilation system on the cruise ship was available. We compiled the daily number of crewmembers with a body temperature ≥37.1°C or with signs or symptoms; a peak occurred on April 28, after which the number gradually decreased until the end of May (Figure 1, panel B).

Among all 623 crewmembers, 149 cases were laboratory-confirmed and 107 probable case-patients who tested negative had clinical signs or symptoms indicative of COVID-19. Restricted to laboratory-confirmed cases, the attack rate for infection was 24%. When probable cases were included, the attack rate was 41%.

Outbreak Control Measures and Management of Disembarkation
An emergency operations center was established in the prefecture office, and an onsite field response center was set up in the harbor near the cruise ship (12).

Company staff stayed on board to communicate with both the ship and public health authorities, and company staff introduced interventions to the ship. Online meetings among company staff on board, the on-site field response center, the emergency operations center, and Nagasaki University Hospital took place almost every morning. In the evening, online meetings between Japan's Ministry of Health, Labour and Welfare and the emergency operations center took place. Through these communication and coordination mechanisms, we were able to share information, make informed decisions jointly, and implement interventions on the cruise ship.

Every nonessential worker had been separately isolated or quarantined in a single passenger cabin room and not allowed to leave his or her room since

Table 1. Selected characteristics of crewmembers on cruise ship where a coronavirus disease outbreak occurred, by SARS-CoV-2 test result and symptomatic status, Nagasaki, Japan, 2020*

Characteristic	All crewmembers	Test-positive, n = 149		Test-negative, n = 474	
		Symptomatic	Asymptomatic	Symptomatic	Asymptomatic
Total	623 (100)	96 (100)	53 (100)	107 (100)	367 (100)
Age, y					
Median (IQR)	31 (26–40)	32 (27–39)	32 (23–42)	29 (25–35)	31 (26–41)
Distribution					
10–19	3 (0.5)	1 (1.0)	1 (1.9)	0	1 (0)
20–29	271 (43)	37 (39)	20 (38)	55 (51)	159 (43)
30–39	184 (30)	36 (38)	14 (26)	33 (31)	101 (28)
40–49	123 (20)	17 (18)	15 (28)	13 (12)	78 (21)
50–59	34 (5.5)	4 (4.2)	2 (3.8)	6 (5.6)	22 (6.0)
≥60	8 (1.3)	1 (1.0)	1 (1.9)	0	6 (1.6)
Sex					
M	523 (84)	82 (85)	46 (87)	88 (82)	307 (84)
F	100 (16)	14 (15)	7 (13)	19 (18)	60 (16)
Nationality					
Philippines	206 (33)	35 (36)	6 (11)	40 (37)	125 (34)
India	104 (17)	16 (17)	14 (26)	16 (15)	58 (16)
Indonesia	84 (13)	10 (10)	13 (25)	13 (12)	48 (13)
China	82 (13)	14 (15)	7 (13)	13 (12)	48 (13)
Italy	40 (6.4)	5 (5.2)	3 (5.7)	6 (5.6)	26 (7.1)
Other	107 (17)	16 (17)	10 (19)	19 (18)	62 (17)
Occupation category					
Essential worker					
Engine	75 (12)	6 (6.3)	11 (21)	10 (8.1)	48 (13)
Hotel	73 (12)	13 (14)	3 (5.7)	6 (5.0)	51 (14)
Deck	70 (11)	11 (11)	10 (19)	11 (9.4)	38 (10)
Nonessential worker					
Restaurant	96 (15)	13 (14)	6 (11)	21 (20)	56 (15)
Galley	77 (12)	18 (19)	5 (9.4)	22 (21)	32 (8.7)
Housekeeping	72 (12)	8 (8.3)	7 (13)	7 (6.5)	50 (14)
Entertainment	49 (7.9)	8 (8.3)	6 (11)	13 (12)	22 (6.0)
Technician	21 (3.4)	4 (4.2)	2 (3.8)	3 (2.8)	12 (3.3)
Others	90 (14)	15 (16)	3 (5.7)	14 (13)	58 (16)
Smoking history, n = 592†					
Yes	148 (25)	20 (22)	13 (28)	36 (35)	79 (23)
Underlying disease, n = 593†‡					
Any	22 (3.7)	5 (5.5)	2 (4.4)	2 (1.9)	13 (3.7)
Hypertension	12 (3.0)	2 (2.2)	1 (2.2)	0	9 (2.6)
Diabetes	10 (1.7)	1 (1.1)	1 (2.2)	0	8 (2.3)
Cardiovascular disease	1 (0.2)	1 (1.1)	0	0	0
Asthma	1 (0.2)	0	0	1 (1.0)	0
BMI, n = 523†					
Median (IQR)	24.1 (21.7–26.7)	23.6 (21.3–26.0)	24.7 (21.6–28.0)	23.9 (21.3–26.7)	24.1 (22.0–26.5)
Distribution					
Underweight, BMI < 18.5	29 (5.5)	5 (6.2)	3 (7.5)	2 (2.0)	19 (6.3)
Normal, 18.5 ≤ BMI < 25	278 (53)	45 (56)	18 (45)	58 (59)	157 (52)
Overweight, 25 ≤ BMI < 30	167 (32)	22 (27)	15 (36)	27 (28)	103 (34)
Obese, BMI ≥30	49 (9.4)	9 (11)	4 (10)	11 (11)	25 (8.2)

*Values are no. (%) except as indicated. Symptomatic was defined as having any clinical sign or symptom of coronavirus disease (i.e., fever (≥37.5°C), cough, shortness of breath, nasal congestion, sore throat, nausea or vomiting, conjunctival congestion, headache, fatigue, myalgia or arthralgia, diarrhea, olfactory dysfunction, or taste disorder [loss of taste]). BMI, body mass index; IQR, interquartile range, SARS-CoV-2, severe acute respiratory coronavirus 2.
†Among crewmembers who entered data into the health monitoring system since its introduction on April 28, 2020.
‡Two crewmembers had both hypertension and diabetes.
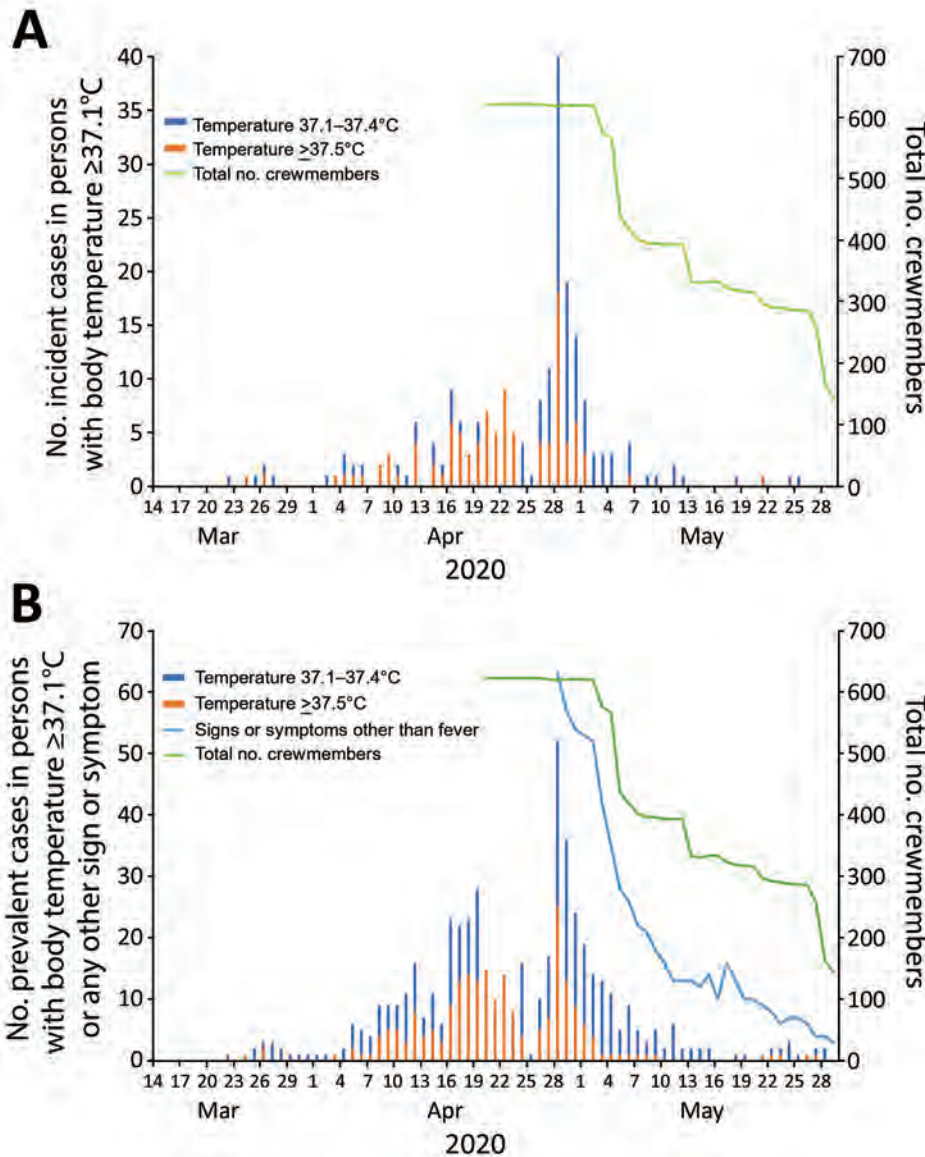
Figure 1. Number of incident cases of persons with body temperature ≥37.1°C and number of prevalent cases of persons with body temperature ≥37.1°C or any sign or symptom of coronavirus disease on a cruise ship, Nagasaki, Japan, March 14–May 29, 2020. A) Number of persons with illness onset, by date. Crewmembers started disembarking on May 3. B) Daily number of crewmembers who reported having a body temperature ≥37.1°C or coronavirus disease signs or symptoms. Signs or symptoms other than fever: cough, nasal congestion, sore throat, headache, olfactory dysfunction, taste disorder, conjunctival congestion, diarrhea, myalgia or arthralgia, fatigue, shortness of breath, and nausea or vomiting.

April 19. Essential workers who tested negative and had no signs or symptoms served meals or collected laundry for nonessential workers. When medically indicated, a nonessential worker was transported out of the room for medical care. To prevent secondary infection, several interventions were taken. Essential workers were provided with guidance and training for infection prevention on April 26. To ensure that the essential workers did not interact directly with isolated or quarantined crewmembers in their rooms, some interventions were put in place, such as distributing an individual thermometer to each crewmember on April 28 and streaming educational videos on COVID-19 infection prevention in the cabin rooms on April 29. To avoid missing the signs of disease

progression and to be able to respond to critical patients in a timely manner, a field clinic was established, along with provision of a vehicle equipped with a computed tomography scanner and a medical transportation system. A remote health monitoring system was developed and introduced to support the cruise ship from outside of the ship (*17*). After the initial universal screening in April, only essential workers and medical personnel were reexamined when a sign or symptom indicative of COVID-19 was noted; reexaminations were limited in this way to prevent potential spread of the infection.

Starting May 3, those crewmembers who tested negative at universal screening were given priority to disembark; the ship's medical doctor made

Figure 2. Initial cabin room locations of the crewmembers on cruise ship where a coronavirus disease outbreak occurred, Nagasaki, Japan, 2020. A) Red indicates distribution of crewmembers with onset of body temperature ≥37.1°C during March 22–27. Green indicates cabin rooms of crewmembers who did not have a body temperature ≥37.1°C. B) Red indicates distribution of crewmembers with onset of body temperature ≥37.1°C during March 22–April 19. Green indicates cabin rooms of crewmembers who did not have a body temperature ≥37.1°C.

the decision on the basis of the crewmember's body temperature and signs or symptoms. Starting May 14, crewmembers who tested positive were able to disembark and travel back to their countries of origin, provided that they had a subsequent negative test result. Through this predisembarkation testing policy, a total of 495 crewmembers were able to disembark and leave Japan. On May 31, the cruise ship set sail for Manila, the Philippines, with the remaining 126 essential workers, none of whom had a positive test result.

Clinical Outcomes

We compiled the clinical outcomes of all crewmembers and their signs or symptoms during their respective observation periods (Table 2). Among all crewmembers,

0.2% (1/623) had severe pneumonia, 0.3% (2/623) had moderate pneumonia, 32% (200/623) had mild illness, and 67% (420/623) had no signs or symptoms. Among crewmembers with laboratory-confirmed cases, 0.7% (1/149) had severe pneumonia, 1.3% (2/149) had moderate pneumonia, 62% (93/149) had mild illness, and 36% (53/149) had no signs or symptoms. Of the 11 crewmembers admitted to a hospital, 6 had COVID-19 pneumonia.

Clinical Course of Crewmembers Who Had Signs or Symptoms

During the observation period, 96 persons with laboratory-confirmed cases and 107 with probable cases experienced signs or symptoms. The median number of symptomatic days among laboratory-confirmed

case-patients was 4 days (IQR 1–8 days) (Appendix Table). Among laboratory-confirmed case-patients who were asymptomatic at the time of universal screening, 58 (52%) subsequently experienced signs or symptoms. Among 38% of the symptomatic crewmembers, symptoms were intermittent, or additional COVID-19 signs or symptoms appeared sporadically over time (Appendix Figure 2).

Discussion

We have described the key findings from the COVID-19 outbreak that occurred on a cruise ship with multinational crewmembers in Nagasaki City during April 20–May 29, 2020. Six crewmembers were hospitalized for COVID-19 pneumonia, 1 of whom had a severe case, but no deaths occurred. Our retrospective investigation revealed that the outbreak likely started in late March, with the infection introduced into this population from the entertainment occupation group that boarded the ship, which then spread widely inside the ship, irrespective of occupational group, nationality, or crew cabin room location, resulting in 149 laboratory-confirmed cases and 107 probable cases. Because transmission of SARS-CoV-2 from presymptomatic or asymptomatic patients is known to occur (25), certain social activities on the ship could have facilitated transmission which ultimately spread throughout the ship. The epidemic curve (Figure 1, panel A) shows that the number of incident case-patients with a body temperature ≥37.1°C peaked on April 28. The period between the universal implementation of the quarantine policy (April 19) and the peak of onset (April 28) was longer than the expected incubation period (17,26). This fact might be attributable to several reasons. For instance, before receiving training for infection prevention, essential workers might not have been able to sufficiently prevent infection transmission. Because an essential worker who was measuring body temperatures of isolated or quarantined crewmembers tested positive for SARS-CoV-2 on May 3, we speculate that infection could have spread through any interactions during those measurements or through sharing of the thermometers among the isolated or quarantined crewmembers. These factors might have contributed to further transmissions even after quarantine measures were enforced.

Management of the outbreak on Costa Atlantica was different from that observed on the Diamond Princess or other cruise ship outbreaks. The main difference was that the Costa Atlantica had only crewmembers whereas the Diamond Princess had both passengers and crewmembers. On Costa Atlantica, because passenger cabin rooms inside the ship were empty, crewmembers could be isolated or quarantined inside the ship, which was not possible on the Diamond Princess or other cruise ship outbreaks with passengers. For the outbreak on the Diamond Princess, priority testing was given to

Table 2. Clinical outcomes of crewmembers on cruise ship where a coronavirus disease outbreak occurred, by SARS-CoV-2 test result, Nagasaki, Japan, 2020*

Clinical outcome†	All crewmembers	Test-positive	Test-negative
Total	623 (100)	149 (100)	474 (100)
Severe pneumonia	1 (0.2)	1 (0.7)	0
Moderate pneumonia	2 (0.3)	2 (1.3)	0
Mild illness	200 (32)	93 (62)	107 (23)
Asymptomatic	420 (67)	53 (36)	367 (77)
Fever (≥37.5°C)	121 (19)	51 (34)	70 (15)
Symptom, n = 593‡			
Cough	45 (7.6)	32 (23)	13 (2.9)
Nasal congestion	34 (5.7)	23 (17)	11 (2.4)
Sore throat	32 (5.4)	22 (16)	10 (2.2)
Headache	32 (5.4)	18 (13)	14 (3.1)
Olfactory dysfunction	31 (5.2)	25 (18)	6 (1.3)
Taste disorder	28 (4.7)	23 (17)	5 (1.1)
Conjunctival congestion	24 (4.1)	13 (9.5)	11 (2.4)
Diarrhea	16 (2.7)	12 (8.8)	4 (0.9)
Myalgia or arthralgia	13 (2.2)	11 (8.0)	2 (0.4)
Fatigue	11 (1.9)	7 (5.1)	4 (0.9)
Shortness of breath	8 (1.4)	7 (5.1)	1 (0.2)
Nausea or vomiting	5 (0.8)	4 (2.9)	1 (0.2)

*Values are no. (%) except as indicated. SARS-CoV-2, severe acute respiratory coronavirus 2.
†Severe pneumonia defined as illness requiring with intubation or intensive care unit admission; moderate pneumonia defined as illness requiring oxygen administration; mild illness defined as illness in patients who had coronavirus disease signs or symptoms without oxygen administration; asymptomatic, no clinical signs or symptoms. Body temperature data were obtained from the ship's medical records and from the health monitoring system introduced by investigators on April 28, 2020.
‡Among 593 crewmembers who entered data into the health monitoring system introduced by investigators; 137 crewmembers tested positive and 456 tested negative for SARS-CoV-2.

the high-risk population. Passengers with positive test results for SARS-CoV-2 were transported to medical facilities, and their clinical courses followed. For those passengers without positive test results, a 14-day health observation period was set before disembarking (27,28). One study suggested the possibility that evacuating all on board early would have prevented many on the Diamond Princess from becoming infected (29). Early evacuation of all crewmembers was thus initially considered in the Costa Atlantica outbreak. However, there were not enough medical facilities or accommodations to isolate or quarantine all crewmembers in the city, and preparing other isolation facilities would have required installing sewage systems and using communal toilets, which could promote transmission, making such options both impractical and of questionable value. Because we regarded the area inside the ship as contaminated, we developed and introduced a health monitoring system (13), aiming to rapidly detect crewmembers requiring medical attention and to minimize the risk for secondary infection, which was an issue on the Diamond Princess (13,30). Debate is ongoing as to how to manage an outbreak of COVID-19 on a cruise ship, but we should take measures that are best suited for the particular context, especially in resource-limited situations.

As for clinical outcomes, we detected 3 crewmembers with moderate to severe pneumonia (2.0% of laboratory-confirmed cases and 1.2% of laboratory-confirmed and probable cases); this proportion was lower than that noted in a previous report in China, in which 14% of case-patients had severe illness and 5% had critical illness (30). However, the population on the Costa Atlantica included only crewmembers, who were considerably younger and healthier by selection (i.e., healthy worker effect).

Among the laboratory-confirmed cases, we determined 36% (42/149) to be in persons who were asymptomatic (25,31). In the Diamond Princess outbreak, the asymptomatic proportion was reported to be 55% (4), but after transfer to medical facilities, ≈20% of asymptomatic subjects had onset of signs or symptoms (32,33). We were able to follow the clinical courses of all laboratory-confirmed case-patients for >20 days, which prevented misclassification of presymptomatic cases as asymptomatic cases. We also obtained detailed clinical information after introducing the health monitoring system, which had a high usage rate, enabling individual crewmembers to report their signs or symptoms easily on a daily basis. These differences resulted in a lower proportion of asymptomatic cases in our study, which we think to be a more valid picture of the COVID-19 severity spectrum.

Of note, we did not repeat LAMP and PCR tests for SARS-CoV-2 for nonessential workers in our testing strategy. The main goal for our outbreak management was to prevent the spread of infection and to rapidly detect those persons who required medical attention (to provide them with appropriate and timely treatment); thus, repeat testing was not considered necessary as long as nonessential workers who were asymptomatic or had mild illness were isolated or quarantined. On the other hand, essential workers were repeatedly tested because of the potential to spread the infection. Before the ship's departure, 107 probable cases were reported, which accounted for 23% of crewmembers with negative test results. With limited frequency of testing, some interval-censored infections might have been missed, but with a sensitive health monitoring system and an isolation and quarantine policy in place, we believe our operations were justifiable and effective.

Our study's first limitation is that we might have underestimated the number of laboratory-confirmed cases because most crewmembers were only tested once. Second, the clinical signs or symptoms of the crewmembers before the introduction of the health monitoring system or after disembarkation could not be tracked, meaning additional symptomatic cases might have occurred.

In conclusion, we have described the epidemiology, along with our management approach, of a COVID-19 outbreak on a cruise ship with crewmembers isolated or quarantined inside the ship. Although SARS-CoV-2 can spread rapidly in closed settings, prompt isolation and quarantine and a sensitive surveillance system using a remote health monitoring approach could successfully control a COVID-19 outbreak on a cruise ship and result in timely medical care for affected persons.

About the Author

Dr. Maeda is a researcher at the Institute of Tropical Medicine at Nagasaki University and the Nagasaki University Graduate School of Biomedical Science. Her primary research interests include infectious disease epidemiology and public health.

References

1. Huang C, Wang Y, Li X, Ren L, Zhao J, Hu Y, et al. Clinical features of patients infected with 2019 novel coronavirus in Wuhan, China. Lancet. 2020;395:497–506. https://doi.org/10.1016/S0140-6736(20)30183-5

2. World Bank. Global economic prospects. pandemic, recession: the global economy in crisis [cited 2021 Apr 28]. https://www.worldbank.org/en/publication/global-economic-prospects

3. Expert Taskforce for the COVID-19 Cruise Ship Outbreak. Epidemiology of COVID-19 outbreak on cruise ship quarantined at Yokohama, Japan, February 2020. Emerg Infect Dis. 2020;26:2591–7. https://doi.org/10.3201/eid2611.201165

4. Ministry of Health, Labour and Welfare. Official report on the cruise ship Diamond Princess, May 1, 2020 [cited 2021 Apr 28]. https://www.mhlw.go.jp/stf/newpage_11146.html

5. Yamagishi T, Kamiya H, Kakimoto K, Suzuki M, Wakita T. Descriptive study of COVID-19 outbreak among passengers and crew on Diamond Princess cruise ship, Yokohama Port, Japan, 20 January to 9 February 2020. Euro Surveill. 2020; 25:2000272. https://doi.org/10.2807/1560-7917.ES.2020.25.23.2000272

6. Furuse Y, Sando E, Tsuchiya N, Miyahara R, Yasuda I, Ko YK, et al. Clusters of coronavirus disease in communities, Japan, January–April 2020. Emerg Infect Dis. 2020;26:2176–9. https://doi.org/10.3201/eid2609.202272

7. Moriarty LF, Plucinski MM, Marston BJ, Kurbatova EV, Knust B, Murray EL, et al.; CDC Cruise Ship Response Team; California Department of Public Health COVID-19 Team; Solano County COVID-19 Team. Public health responses to COVID-19 outbreaks on cruise ships—worldwide, February–March 2020. MMWR Morb Mortal Wkly Rep. 2020;69:347–52. https://doi.org/10.15585/mmwr.mm6912e3

8. World Health Organization. COVID-19. Avoid the three Cs. 2020 [cited 2021 Apr 28]. https://www.who.int/brunei/news/infographics---english

9. Oshitani H; Expert Members of The National COVID-19 Cluster Taskforce at The Ministry of Health, Labour and Welfare, Japan. Cluster-based approach to coronavirus disease 2019 (COVID-19) response in Japan, from February to April 2020. Jpn J Infect Dis. 2020;73:491–3. https://doi.org/10.7883/yoken.JJID.2020.363

10. Mallapaty S. What the cruise-ship outbreaks reveal about COVID-19. Nature. 2020;580:18. https://doi.org/10.1038/d41586-020-00885-w

11. National Institute of Infectious Diseases. Outbreak of novel coronavirus disease (COVID-19) on a cruise ship docked in Nagasaki City: preliminary interim report. 2020 [cited 2021 Apr 28]. https://www.niid.go.jp/niid/en/2019-ncov-e/2484-idsc/9650-covid19-14-200323-e-2.html

12. Nagasaki Prefecture. Investigation report on the outbreak of novel coronavirus cluster aboard the cruise ship "Costa Atlantica" 2020 [cited 2021 Apr 20]. https://www.pref.nagasaki.jp/shared/uploads/2021/02/1613627203.pdf

13. Sando E, Morimoto K, Narukawa S, Nakata K. COVID-19 outbreak on the Costa Atlantica cruise ship: use of a remote health monitoring system. J Travel Med. 2021;28:taaa163. https://doi.org/10.1093/jtm/taaa163

14. Petrakis D, Marginǎ D, Tsarouhas K, Tekos F, Stan M, Nikitovic D, et al. Obesity—a risk factor for increased COVID19 prevalence, severity and lethality [review]. Mol Med Rep. 2020;22:9–19. https://doi.org/10.3892/mmr.2020.11127

15. Centers for Disease Control and Prevention. Defining adult overweight and obesity [cited 2021 Apr 28]. https://www.cdc.gov/obesity/adult/defining.html

16. Giacomelli A, Pezzati L, Conti F, Bernacchia D, Siano M, Oreni L, et al. Self-reported olfactory and taste disorders in SARS-CoV-2 patients: a cross-sectional study. Clin Infect Dis. 2020;71:889–90. https://doi.org/10.1093/cid/ciaa330

17. Guan WJ, Ni ZY, Hu Y, Liang WH, Ou CQ, He JX, et al.; China Medical Treatment Expert Group for Covid-19. Clinical characteristics of coronavirus disease 2019 in China. N Engl J Med. 2020;382:1708–20. https://doi.org/10.1056/NEJMoa2002032

18. Wang D, Hu B, Hu C, Zhu F, Liu X, Zhang J, et al. Clinical Characteristics of 138 hospitalized patients with 2019 novel coronavirus-infected pneumonia in Wuhan, China. JAMA. 2020;323:1061–9. https://doi.org/10.1001/jama.2020.1585

19. European Centre for Disease Prevention and Control. Case definition for coronavirus disease 2019 (COVID-19) [cited 2021 Apr 28]. https://www.ecdc.europa.eu/en/covid-19/surveillance/case-definition

20. Ministry of Health, Labour and Welfare. Clinical management of patients with COVID-19. A guide for front-line healthcare workers. Version 2.1 [cited 2021 Apr 28]. http://www.mhlw.go.jp/content/000646531.pdf

21. National Institute of Infectious Diseases. Manual for the detection of pathogen 2019-nCoVver.2.6. [cited 2021 Apr 28]. http://www.niid.go.jp/niid/images/lab-manual/2019-nCoV20200319.pdf

22. Park G-S, Ku K, Baek S-H, Kim S-J, Kim SI, Kim B-T, et al. Development of reverse transcription loop-mediated isothermal amplification assays targeting severe acute respiratory syndrome coronavirus 2 (SARS-CoV-2). J Mol Diagn. 2020;22:729–35. https://doi.org/10.1016/j.jmoldx.2020.03.006

23. Yan C, Cui J, Huang L, Du B, Chen L, Xue G, et al. Rapid and visual detection of 2019 novel coronavirus (SARS-CoV-2) by a reverse transcription loop-mediated isothermal amplification assay. Clin Microbiol Infect. 2020;26:773–9. https://doi.org/10.1016/j.cmi.2020.04.001

24. Yoshikawa R, Abe H, Igasaki Y, Negishi S, Goto H, Yasuda J. Development and evaluation of a rapid and simple diagnostic assay for COVID-19 based on loop-mediated isothermal amplification. PLoS Negl Trop Dis. 2020; 14:e0008855. https://doi.org/10.1371/journal.pntd.0008855

25. Furukawa NW, Brooks JT, Sobel J. Evidence supporting transmission of severe acute respiratory syndrome coronavirus 2 while presymptomatic or asymptomatic. Emerg Infect Dis. 2020;26(7):e1–6. https://doi.org/10.3201/eid2607.201595

26. Lauer SA, Grantz KH, Bi Q, Jones FK, Zheng Q, Meredith HR, et al. The incubation period of coronavirus disease 2019 (COVID-19) from publicly reported confirmed cases: estimation and application. Ann Intern Med. 2020;172:577–82. https://doi.org/10.7326/M20-0504

27. Nakazawa E, Ino H, Akabayashi A. Chronology of COVID-19 cases on the Diamond Princess cruise ship and

ethical considerations: a report from Japan. Disaster Med Public Health Prep. 2020;14:506–13. https://doi.org/10.1017/dmp.2020.50

28. Takeuchi I. COVID-19 first stage in Japan—how we treat 'Diamond Princess Cruise Ship' with 3700 passengers? Acute Med Surg. 2020;7:e506. https://doi.org/10.1002/ams2.506

29. Rocklöv J, Sjödin H, Wilder-Smith A. COVID-19 outbreak on the Diamond Princess cruise ship: estimating the epidemic potential and effectiveness of public health countermeasures. J Travel Med. 2020;27:taaa030.

30. Ministry of Health, Labour and Welfare. To all medical aid workers on board the cruise ship [cited 2021 Apr 28]. https://www.mhlw.go.jp/content/10900000/000596279.pdf

31. Bai Y, Yao L, Wei T, Tian F, Jin DY, Chen L, et al. Presumed asymptomatic carrier transmission of COVID-19. JAMA. 2020;323:1406–7. https://doi.org/10.1001/jama.2020.2565

32. Sakurai A, Sasaki T, Kato S, Hayashi M, Tsuzuki SI, Ishihara T, et al. Natural history of asymptomatic SARS-CoV-2 infection. N Engl J Med. 2020;383:885–6. https://doi.org/10.1056/NEJMc2013020

33. Tabata S, Imai K, Kawano S, Ikeda M, Kodama T, Miyoshi K, et al. Clinical characteristics of COVID-19 in 104 people with SARS-CoV-2 infection on the Diamond Princess cruise ship: a retrospective analysis. Lancet Infect Dis. 2020;20:1043–50. https://doi.org/10.1016/S1473-3099(20)30482-5

Address for correspondence: Konosuke Morimoto, Department of Respiratory Infections, Institute of Tropical Medicine, Nagasaki University, 1-12-4 Sakamoto, Nagasaki, 852-8523, Japan; email: komorimo@nagasaki-u.ac.jp
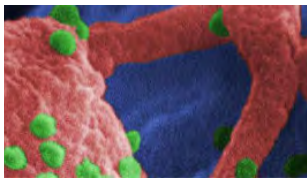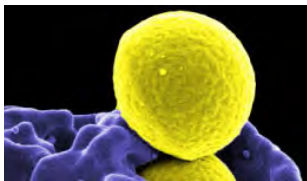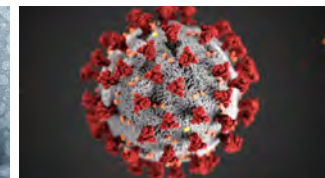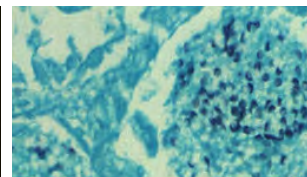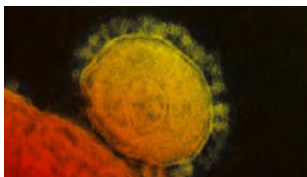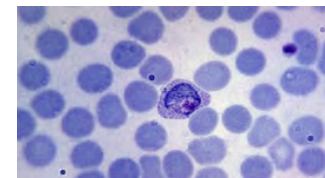
Seroprevalence and Virologic Surveillance of Enterovirus 71 and Coxsackievirus A6, United Kingdom, 2006–2017

Everlyn Kamau, Dung Nguyen, Cristina Celma, Soile Blomqvist, Peter Horby, Peter Simmonds, Heli Harvala

Enterovirus A71 (EV-A71) and coxsackievirus A6 (CVA6) cause hand, foot and mouth disease (HFMD) and are occasionally linked to severe neurologic complications and large outbreaks worldwide. We estimated EV-A71 and CVA6 seroprevalence using cross-sectional age-stratified samples collected in 2006, 2011, and 2017. Seroprevalences of EV-A71 and CVA6 increased from 32% and 54% at 6–11 months to >75% by 10 years of age. Antibody titers declined after 20 years, which could indicate infrequent re-exposure in older populations. Age profiles for acquiring infections and mean titers were comparable in the 3 testing years, despite the marked increase in incidence of CVA6-related HFMD from 2010. The uncoupling of changes in disease severity from the infection kinetics of CVA6 as we inferred from the seroprevalence data, rather than incidence of infection over the 11-year study period, provides further evidence for a change in its pathogenicity.

Enteroviruses within species A are the primary cause of hand, foot and mouth disease (HFMD), mostly affecting infants and young children. HFMD is highly contagious and manifests as a self-limiting illness; it typically includes fever, skin eruptions on hands and feet, and vesicles in the mouth (*1,2*). In severe disease, patients develop neurologic and systemic complications that can be fatal, including meningoencephalitis, pulmonary edema, and acute flaccid paralysis (*3,4*).

Enterovirus A71 (EV-A71) is the predominant cause of HFMD outbreaks. In the Asia-Pacific region,

Author affiliations: University of Oxford, Oxford, UK (E. Kamau, D. Nguyen, P. Horby, P. Simmonds); Public Health England, London, UK (C. Celma); National Institute for Health and Welfare, Helsinki, Finland (S. Blomqvist); National Health Service Blood and Transplant, London, UK (H. Harvala); University College London, London, UK (H. Harvala)

the effects of the virus on public health have been substantial; in Europe these infections are considered mild and often remain undiagnosed (*5*), although severe neurologic manifestations and small outbreaks have been reported more recently (*6–10*). EV-A71 is classified into 7 genogroups (A–G) and several sub-genogroups (B0–B5, C1–C5) based on the viral protein 1 gene; the appearance of novel EV-A71 genogroups has been associated with large HFMD outbreaks (*5*).

Coxsackievirus A6 (CVA6) has become another major cause of HFMD since 2008 (*11,12*). CVA6 infections have often been linked to a febrile atypical form of HFMD, affecting both pediatric and adult populations (*13–15*). The severity of the clinical manifestations associated with CVA6 infections and the recent increase of HFMD cases associated with EV-A71 and CVA6 in Europe (*10*) may have originated through the evolution of recombinant forms or changes in pathogenicity of emerging strains (*16,17*). Alternatively, their clinical prominence may have resulted from an increase in infections in a larger previously unexposed and susceptible populations. To investigate that theory, we determined the age-stratified seroprevalence of EV-A71 and CVA6 in representative cross-sections of the UK population in 2006, 2011, and 2017; we used serotype-specific microneutralization assays and compared our findings with the numbers of infections reported through public health surveillance.

The 2011 timepoint corresponded to the approximate timing of large EV-A71 outbreaks, especially in Vietnam and China (*12,18*) in addition to emergence of CVA6 infections associated with atypical clinical phenotypes (*11,19*). Whereas the 2006 timepoint was selected to precede these recorded events and the 2017 to measure population immunity post-CVA6 emergence period, the last timepoint also corresponded to recorded EV-A71 outbreaks in Spain and elsewhere in Europe in 2016 (*4,7,8*). Collectively, these selected

timepoints reflected changed activity of both viruses and hence enabled us to measure their effects on population immunity.

Materials and Methods

Serum Samples

We obtained a convenience sample of 1,573 residual serum samples collected in 2006 (n = 514), 2011 (n = 498), and 2017 (n = 561) from the seroepidemiology unit archive collection of Public Health England (PHE; Manchester, UK). This archive is an opportunistic collection of residual clinical samples from laboratories throughout England. Case-patients were divided into 7 age groups: <6 months, 6–11 months, 1–5 years, 6–10 years, 11–20 years, 21–40 years, and >40 years. We aimed to obtain 100 samples from each group (Appendix, https://wwwnc.cdc.gov/EID/article/27/9/20-4915-App1.pdf). We anonymized all samples and unlinked any patient identifying information; we retained age, sex, date of collection, sample type, and contributing laboratory information.

Virus Strains

We obtained 2 CVA6 strains isolated in Finland in 2008 and 2016 from the National Institute for Health and Welfare (Helsinki, Finland). The CVA6/2008 isolate was obtained during a HFMD outbreak in Finland (20), and the CVA6/2016 isolate was a contemporary clinical strain. We used the EV-A71 genogroup B4 strain isolated in Singapore (5865/SIN/000009). We propagated EV-A71 viruses in a rhabdomyosarcoma cell line obtained from the American Type Culture Collection. We propagated CVA6 viruses in TE32 or 130T cells obtained from the UK National Institute for Biologic Standards and Control. We determined the 50% tissue culture infective dose ($TCID_{50}$) of virus stocks by means of endpoint dilution using the Reed and Muench method: in a 96-well format, 8 replicates of a 10-fold serial dilution were incubated with cells in Dulbecco minimum essential medium (DMEM; Sigma-Aldrich, https://www.sigmaaldrich.com) containing 2% vol/vol fetal bovine serum (FBS; Sigma-Aldrich) and penicillin/streptomycin (10,000 U/mL; Sigma-Aldrich) at 37°C in 5% CO_2 for 4–5 days.

Neutralization Assays

The microneutralization assay was performed as previously described (21) (Appendix). In brief, we inactivated serum samples for 3 min at 56°C, and then diluted 2-fold serially in 2% DMEM-FBS from 1:8 to 1:1,024. We mixed 50μL of diluted samples and 100

$TCID_{50}$ of virus stock diluted in 50 μL in 96-well microplates and incubated at 37°C for 1 hour. We added 100 μL of cell suspension containing average of 20,000 rhabdomyosarcoma cells in 10% DMEM-FBS for EV-A71 assays and average of 20,000 TE32 cells in 5% DMEM-FBS for CVA6 assays. We observed cytopathic effect in an inverted microscope after incubating at 37°C in 5% CO_2 for 4–5 days. We used pooled adult serum with known neutralizing antibody titer (nAb; 13/328, obtained from the UK National Institute for Biologic Standards and Control) as a positive control and inactivated horse serum (obtained from American Type Culture Collection) as negative control. We included a virus control and an uninfected cell control for each batch of tests. We tested each sample in duplicate and calculated results as their geometric mean titers (GMT).

To determine the optimal strain for the CVA6 neutralizing assay, we compared titers of 36 serum samples collected in 2006 against the 2 CVA6 clinical isolates. We selected 18 samples each for the 1–5-year (representing serologic responses acquired during 2001–2006) and >40-year (representing serologic responses acquired substantially before 2006) age groups. For the 1–5-year age group, 16/18 samples tested were seropositive for the CVA6/2008 and 17/18 samples tested were seropositive for CVA6/2016 isolates. All 18 samples tested from the >40-year age group were seropositive for both CVA6 isolates. GMT to both CVA6 isolates were comparable between the 1–5-year and >40-year age groups (Appendix, Figure 1). Samples collected from the >40-year age group in 2006 had proportionately higher nAb against the CVA6/2008 isolate (p = 0.008 by paired Wilcoxon signed rank test). Because the differences in GMT between the CVA6 isolates were minor, we selected the more contemporary CVA6/2016 strain for the assay used in this study.

We reported the neutralizing titer as the reciprocal titer of serum dilutions that inhibited 50% virus growth. For both EV-A71 and CVA6, samples with nAb titers of $\geq$1:8 were considered seropositive as previously reported (22,23). For GMT calculations, we excluded titers <1:8; we assigned a value of 2,048 to titers $\geq$1:1,024. We classified GMT values as low (<1:64), moderate (1:64–1:256), and high ($\geq$1:512).

Virological Surveillance Data

We collected information on enterovirus-positive samples submitted for typing to the PHE Enteric Virus Unit (London, UK), during 2006–2017. Local diagnostic laboratories in England and Wales were asked to forward samples in which EV RNA has been detected

for typing, for the purposes of national enhanced enterovirus surveillance. Data collected included a total number of enterovirus-positive samples submitted for typing and the number identified as EV-A71 or CVA6 per month, patient age group, and sample type.

We used these data to compare the prevalence of infections estimated from serologic data with EV-A71– and CVA6-associated infections reported through this voluntary enhanced enterovirus surveillance.

Statistical Analysis

We compared rates of seropositivity in different groups using χ^2 or Fisher exact test, with Bonferroni adjustment for multiple comparison. We compared age-stratified GMTs between the serum collection time points using the Mann-Whitney U or Kruskal-Wallis test with Dunn's post hoc analysis. We calculated 95% CIs of the seroprevalence rates according to the Wilson method (http://vassarstats.net/prop1.html) and considered p<0.05 statistically significant. We computed all the statistical analyses in R (https://www.r-project.org).

Results

Enterovirus Reporting in the United Kingdom, 2006–2017

We identified 402 EV-A71–positive and 1,519 CVA6-positive samples from 20,221 enterovirus-positive samples referred to PHE for typing (Figure 1, panel A). Over the study period, the numbers of enterovirus-positive samples referred for typing increased substantially from 189 in 2006 to 1,479 in 2017. At the same time, the proportion of samples typed as CVA6 increased sharply, from ≈1% in 2007–2008 to 10% in 2016–2017, and the proportion of samples typed as EV-A71 decreased.

Most EV-A71 infections were reported in even years; ≈10% of all enterovirus-positive samples were identified as EV-A71 in 2006, 2008, and 2010, whereas this proportion has remained at ≈3% since 2012. The peak months for EV-A71 detections were July–August and for CVA6 detections were October–December. The highest monthly detections were 20 of EV-A71 in July 2013 and 74 of CVA6 in October 2017 (Figure 1, panel B).

EV-A71 infections were mostly identified in feces (122/381, 32%; data not available for 21 samples), followed by cerebrospinal fluid (CSF) (100/381, 26.2%), respiratory specimens (46/381, 12.1%), vesicle or skin swabs (21/381, 5.5%), and blood (24/381, 6.3%) (Table). Consistent with its association with HFMD in the UK, CVA6 was mostly detected in vesicle or skin swabs (759/1,033, 73.5%; data not available for 486 samples), followed by respiratory specimens (136/1,033, 13.2%), feces (84/1,033, 8.1%), CSF (44/1,033, 4.3%), and blood (42/1,033, 4.1%).

Patient age data were available for 9,636/20,211 total samples. Age data were available for 381/402 EV-A71 samples, and for 1,029/1,519 CVA6 samples. Most enterovirus-positive samples were obtained from young children <3 months of age (3,730/9,636, 39%), or young adults (2,309/9,636, 24%) (Figure 2, panel A). EV-A71 detections were highest in infants <3 months (222/381, 58%), whereas 58/381 (15%) were identified in children 4–12 months of age and 63/381 (17%) in children 1–5 years of age. CVA6 infections were diagnosed most often in older children 1–5 years of age (52%, 537/1,029), followed by
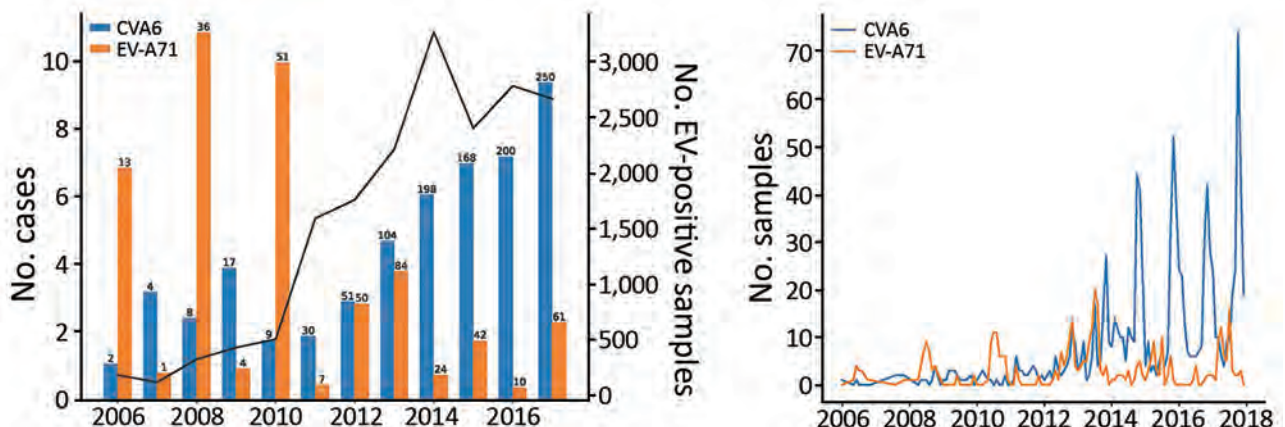
Figure 1. EV-A71 and CVA6 identified in enterovirus-positive samples referred to Public Health England from laboratories throughout England, UK, by year, 2006–2017. A) Percentage of samples typed as EV-A71 and CVA6 in each referral year (total no. cases above each bar). Solid black line indicates number of samples referred for virus typing. B) Distribution of EV-A71 (n = 381) and CVA6 (n = 1,033) clinical detections in England, using monthly totals for the period 2006–2017. CVA6, coxsackievirus A6; EV, enterovirus; EV-A71, enterovirus A71.

Table. EV-A71– and CVA6-positive samples submitted to the Public Health England Enteric Virus Reference Department, United Kingdom, 2006–2017*

Virus	Blood	CSF	Gastrointestinal	Respiratory	Skin	Tissue	Total
EV-A71	24 (6.3)	100 (26.2)	122 (32)	46 (12.1)	21 (5.5)	25 (6.6)	381
CVA6	42 (4.1)	44 (4.3)	84 (8.1)	136 (13.2)	759 (73.4)	19 (1.8)	1,084
*Totals of positive samples are given as no. (%). CSF, cerebrospinal fluid; CVA6, coxsackievirus A6; EV-A71, enterovirus A71.							

children 4–12 months of age (23%, 239/1,029). In contrast, a small number of CVA6 infections were reported in infants <3 months of age (56/1,029, 5%). We observed no change in EV-A71 or CVA6 detection by age group for 2006–2017 (Figure 2, panels B and C).

Seroprevalence of EV-A71
The overall seropositivity rate of EV-A71 was 74% (95% CI 71.8%–76.2%). The seropositivity rates for the 3 timepoints were comparable at 71% (95% CI 66.8%–75.0%) in 2006, 73% (95% CI 69.1%–77.0%) in 2011, and 77% (95% CI 73.8%–80.9%) in 2017. Age-specific seroprevalence of EV-A71 nAb in each timepoint were lowest in children 6–11 months of age and gradually increased with age category (p<0.001 by χ^2 test for trend) (Figure 3; Appendix Table 1). The seropositivity rate for the >40-year age group increased from 77% in 2011 to 91% in 2017 (p = 0.003 Fisher exact test).

The proportion of samples with moderate (64–256) and high (≥512) nAb titers increased with age from 1–20 years but decreased thereafter; most (>85%) samples from adults >20 years had titers ≤256 (Figure 3). For example, in 2006, the proportion of patients with high titers decreased from 30% in the 11–20-year age group to 6.7% in the 21–40-year age group and to 3.8% in the >40-year age group. We observed a similar trend of declining titers through 2011, in which the proportion of patients with high titers dropped by age group, from 12% (11–20 years) to 9% (21–40 years) to 2% (>40 years), and through 2017, when titers drop from 19% (11–20 years) to 11% (21–40 years) to 5% (>40 years).

The seropositive samples from infants (<6 months of age) in 2006 had a GMT 5-fold higher than the same age group in 2017, whereas those from children 6–11 months of age in 2006 had a geometric mean titer 3.6-fold higher than the same age group in 2017. Similarly, the samples from children 1–5 years of age in 2011 had a GMT 5.5-fold higher than in 2017 (Appendix, Appendix Table 1). Significant increases in titers of seropositive samples were found among children <6 months (p = 0.014 by Kruskal-Wallis test) and 1–5 years of age (p = 0.0026) and also among patients aged 11–20 years of age (p = 0.0067) (Appendix, Appendix Figure).

Seroprevalence of CVA6
The seropositivity for CVA6 was 80% (95% CI 78.2–82.3) overall and 82% (95% CI 78.7–85.3) for 2006, 78% (95% CI 74–81.8) for 2011, and 80% (76.7–83.3) for 2017; seropositivity similarly increased with increasing age group (p<0.001 by χ^2 test for trend) (Figure 3; Appendix, Appendix Table 2). The seropositivity rates were comparable across age groups (p>0.05 by Fisher exact test). We observed significant differences in CVA6 antibody titers among seropositive samples from children <6 months of age (p<0.001 by Kruskal-Wallis test), 1–5 years of age (p = 0.005), and 6–10 years of age (p<0.001). Neutralizing antibody titers were significantly lower in 2011 for seropositive samples (titer ≥8) in the 21–40-year and >40-year age groups (Appendix, Appendix Figure 2).

The proportion of infants <6 months of age with titers ≥64 was significantly higher in 2006 (75%) than
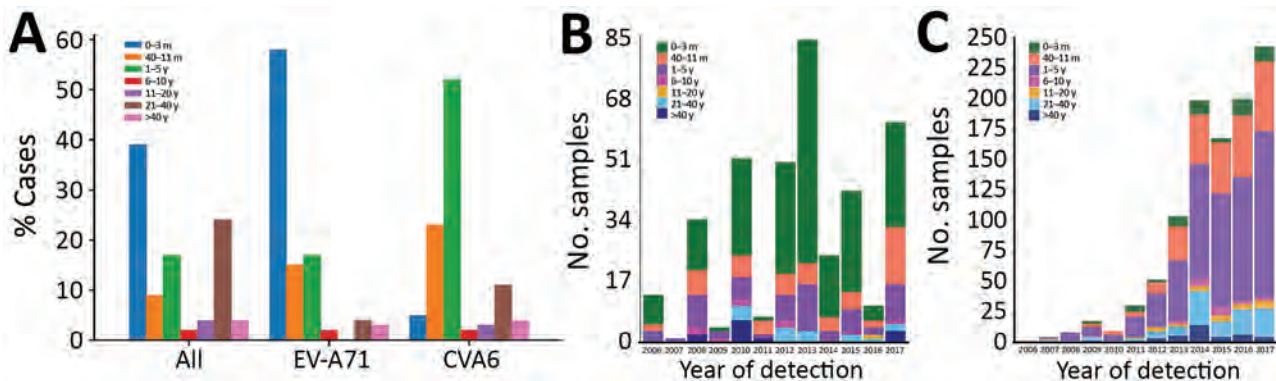
Figure 2. EV-A71 and CVA6 identified in enterovirus-positive samples referred to Public Health England from laboratories throughout England, UK, by age, 2006–2017. A) Percentage of all enterovirus-positive samples, by age group. B, C) EV-A71 (B) and CVA6 (C) detection by age group and by year of sampling. CVA6, coxsackievirus A6; EV-A71, enterovirus A71.
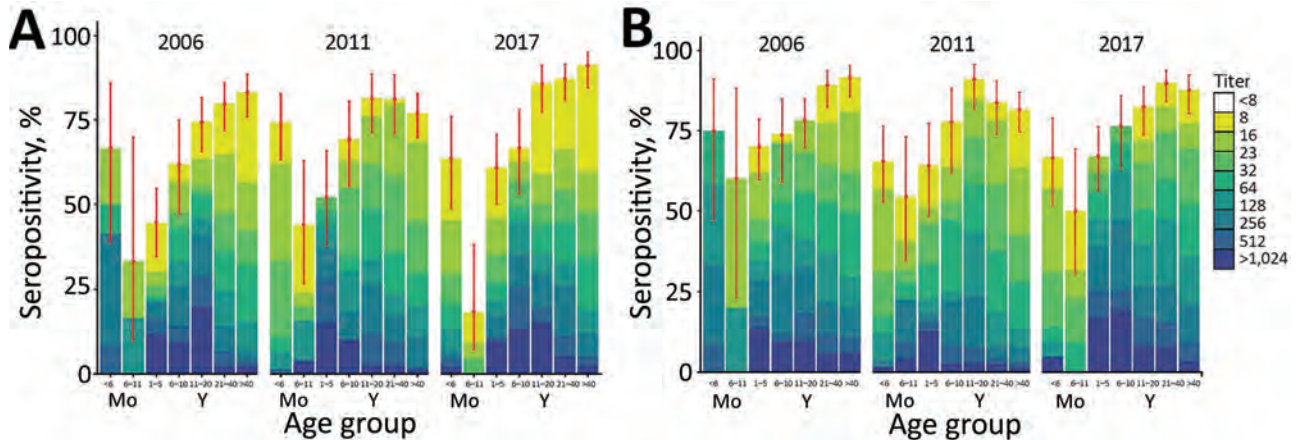
Figure 3. EV-A71(A) and CVA6 (B)seroprevalence in England, UK, in 2006, 2011, and 2017, by age group. Results are expressed as percentage of samples displaying neutralizing antibody titers <8 to ≥1,024 (colored bars). Red dots represent point estimates of the seropositive proportion; error bars indicate 95% CI. Samples were scored seropositive if neutralization was achieved at serum dilution of ≥1:8. CVA6, coxsackievirus A6; EV-A71, enterovirus A71.

in 2011 (17%) and 2017 (14%), whereas the proportion of adults >40 years of age with moderate titers was significantly lower in 2011 (27.8%) than in 2006 (49.2%) and 2017 (51.7%) (p<0.001 by Fisher exact test) (Figure 3). Geometric mean titers were highest in children 1–10 years of age in 2017 and >5-fold higher in 2006 for the <6-month-olds (Appendix Table 2).

Discussion

Seroepidemiology findings in this study showed that EV-A71 and CVA6 infections were highly prevalent among children and adults in the United Kingdom. From the minimum values in the 6–11-month age group after the decline of maternally conferred immunity (24,25), we determined that EV-A71 and CVA6 neutralizing antibody detection frequencies and titers increased steadily with age, which indicates ongoing exposure and infection throughout childhood. EV-A71 seropositivity rates observed in the United Kingdom were comparable to those observed among preschool children <6 years of age (63.4%) in Germany (26) and in children ≤5 years of age in the Netherlands (27). EV-A71 seroprevalence in adults (>75%) was comparable for the United Kingdom, the Netherlands, and Germany.

The number of persons with high titers of EV-A71 neutralizing antibodies declined with age; this finding is consistent with previous seroepidemiological studies, including the report of high EV-A71 antibody titers in the 10–14-year age group in Germany (28), and comparable to the peak titers recorded in the 11–20-year age group in our study. These findings indicate that EV-A71 primarily circulates in and infects children, and the subsequent decline in titers but not fre-

quencies of seropositivity indicates that re-exposure in the older population is uncommon (28–30). The decline in titers may also reflect the differences between acute serologic responses post-infection in the younger population and homeostatic antibody levels in the older population that become established years after infection (30). Related to this decline, the >4-fold attrition in mean EV-A71 neutralizing antibody titers in the 21–40-year age group (Appendix Table 1) may also create the low mean titers of maternally derived antibodies observed in children <6 months of age. This finding may underpin the high incidence of EV-A71 diagnosis reported in the 0–3-month age group when infants are most susceptible to severe infection outcomes (Figure 3). Of note, the largest share (39%) of enterovirus-positive samples were obtained from this age group, which might attest to infants' vulnerability and higher likelihood of sampling.

The global emergence of CVA6 since 2008 has been linked to an increase in pathogenicity of CVA6 around 2010 (31), becoming another major causative agent for HFMD in several countries worldwide (23). This change was reflected in the number of atypical HFMD caused by CVA6 in Scotland in 2014 (19) and also in the increasing numbers of reported CVA6 infections in our study (Figure 1). Our seroprevalence data show that CVA6 circulated widely before the emergence of atypical HFMD in 2008 (25); seroprevalence approached 90% in adults >40 years of age as recorded in 2006 (Figure 3). This observation discounts the idea that the increased incidence of CVA6-associated HFMD simply reflects a change in its infection incidence and the existence of a widely susceptible population.

Comparing the 2 serotypes, CVA6 seroprevalence was higher than EV-A71 seroprevalence in younger children (1–10 years) in each study year (Figure 3; Appendix Tables 1, 2). However, this difference was not reflected in the peak age group for CVA6 infections (1–5 years) (Figure 2), which contrasts with the predominance of EV-A71 infections recorded in neonates and infants. CVA6 infections were predominantly detected in skin vesicle fluids (Table; Appendix), which would primarily be associated with HFMD manifestations (*32–34*).

Over the study period, the number of samples referred to PHE substantially increased (Figure 1), but rather than indicating more enterovirus-associated disease, this finding is more likely a reflection of improvements in detection through exclusive introduction of PCR in the clinical laboratories (*35*). Diagnostic practices in general, and for enteroviruses in particular, have changed over time in England and Wales as previously described (*35*). The use of PCR has increased rapidly, from 36% in 2000 to 45% in 2011, and probably approached 100% in 2015, replacing the slow and laborious virus culture entirely.

Changes in clinical practice or diagnostic procedures, such as the threshold for investigating and hospitalizing patients with suspected viral infections, or performing lumbar puncture (*35*), may have further influenced the number of samples submitted to PHE. Controlled cohort-based surveillance studies are required to better infer EV incidence.

A limitation of this study is that we based our inferences of incidences of EV-A71 and CVA6 infections on referral of clinical samples for typing at PHE. The much lower numbers of EV-A71–positive samples identified from older children and adults (Figure 2) at a time when seroprevalence was increasing (Figure 3) is indicative of subclinical infections or benign disease in these age groups. Differences in clinical practices could have also influenced the number of samples obtained and referred from older children and adults to PHE. For instance, CSF samples are more likely to be obtained for enterovirus testing from these patients who had any neurologic symptoms, compared with throat, fecal, or rectal swab specimens from which the viral loads would be higher and virus excretion prolonged (*36,37*). In addition, delayed lumbar puncture also reduces the likelihood of a positive pathogen detection. Atypical and varying clinical manifestations, especially in older adults, and the absence of CSF pleocytosis may also impede the timely diagnosis of enteroviral infections and consequently reduce the number of samples found to be positive and referred to PHE.

We used a convenience sample of residual serum samples from diagnostic laboratories throughout England. Although we attempted to include equal sample sizes for all ages, the serosurvey was not powered to provide precise seroprevalence estimates for certain age groups. The volume of available specimens, particularly for the younger age groups, was insufficient, thus limiting the number of samples tested and generalization of our results to the larger pediatric population. Convenience samples are also prone to chance variations in sampling between geographic regions. Lack of additional information on participants' risk factors for exposure was another limitation.

In summary, we provide an analysis of age-stratified seroprevalence of EV-A71 and CVA6 in the UK population. Prevalence of infection by both viruses inferred from age-related changes in seroprevalence varied little over the 11-year study period despite the emergence of CVA6-associated HFMD in 2010, implying changes in CVA6 pathogenicity rather than changes in population susceptibility to severe infection outcomes. This study will enable a more detailed understanding of population susceptibility, the emergence of enterovirus serotypes, and potential changes in serotype pathogenicity and transmissibility.

About the Author

Ms. Kamau is a doctoral candidate at the University of Oxford, UK. Her primary research interest is epidemiology of infectious diseases.

References

1. Aswathyraj S, Arunkumar G, Alidjinou EK, Hober D. Hand, foot and mouth disease (HFMD): emerging epidemiology and the need for a vaccine strategy. Med Microbiol Immunol (Berl). 2016;205:397–407. https://doi.org/10.1007/s00430-016-0465-y
2. Klein M, Chong P. Is a multivalent hand, foot, and mouth disease vaccine feasible? Hum Vaccin Immunother. 2015;11:2688–704. https://doi.org/10.1080/21645515.2015.1049780
3. Chang LY, Lin HY, Gau SS, Lu CY, Hsia SH, Huang YC, et al. Enterovirus A71 neurologic complications and long-term sequelae. J Biomed Sci. 2019;26:57. https://doi.org/10.1186/s12929-019-0552-7
4. Karrasch M, Fischer E, Scholten M, Sauerbrei A, Henke A, Renz DM, et al. A severe pediatric infection with a novel

enterovirus A71 strain, Thuringia, Germany. J Clin Virol. 2016;84:90–5. https://doi.org/10.1016/j.jcv.2016.09.007

5. Hassel C, Mirand A, Lukashev A, TerletskaiaLadwig E, Farkas A, Schuffenecker I, et al. Transmission patterns of human enterovirus 71 to, from, and among European countries, 2003 to 2013. Euro Surveill. 2015;20:30005. https://doi.org/10.2807/1560-7917.ES.2015.20.34.30005

6. Ngangas ST, Lukashev A, Jugie G, Ivanova O, Mansuy JM, Mengelle C, et al. Multirecombinant enterovirus A71 subgenogroup C1 isolates associated with neurologic disease, France, 2016–2017. Emerg Infect Dis. 2019;25:1204–8. https://doi.org/10.3201/eid2506.181460

7. Casas-Alba D, de Sevilla MF, Valero-Rello A, Fortuny C, García-García JJ, Ortez C, et al. Outbreak of brainstem encephalitis associated with enterovirus-A71 in Catalonia, Spain (2016): a clinical observational study in a children's reference centre in Catalonia. Clin Microbiol Infect. 2017;23:874–81. https://doi.org/10.1016/j.cmi.2017.03.016

8. Antona D, Kossorotoff M, Schuffenecker I, Mirand A, Leruez-Ville M, Bassi C, et al. Severe paediatric conditions linked with EV-A71 and EV-D68, France, May to October 2016. Euro Surveill. 2016;21. https://doi.org/10.2807/1560-7917.ES.2016.21.46.30402

9. Solomon T, Lewthwaite P, Perera D, Cardosa MJ, McMinn P, Ooi MH. Virology, epidemiology, pathogenesis, and control of enterovirus 71. Lancet Infect Dis. 2010;10:778–90. https://doi.org/10.1016/S1473-3099(10)70194-8

10. Bubba L, Broberg EK, Jasir A, Simmonds P, Harvala H, et al.; Enterovirus study collaborators. Circulation of non-polio enteroviruses in 24 EU and EEA countries between 2015 and 2017: a retrospective surveillance study. Lancet Infect Dis. 2020;20:350–61. https://doi.org/10.1016/S1473-3099(19)30566-3

11. Bian L, Wang Y, Yao X, Mao Q, Xu M, Liang Z. Coxsackievirus A6: a new emerging pathogen causing hand, foot and mouth disease outbreaks worldwide. Expert Rev Anti Infect Ther. 2015;13:1061–71. https://doi.org/10.1586/14787210.2015.1058156

12. Anh NT, Nhu LNT, Van HMT, Hong NTT, Thanh TT, Hang VTT, et al. Emerging coxsackievirus A6 causing hand, foot and mouth disease, Vietnam. Emerg Infect Dis. 2018;24:654–62. https://doi.org/10.3201/eid2404.171298

13. Mathes EF, Oza V, Frieden IJ, Cordoro KM, Yagi S, Howard R, et al. "Eczema coxsackium" and unusual cutaneous findings in an enterovirus outbreak. Pediatrics. 2013;132:e149–57. https://doi.org/10.1542/peds.2012-3175

14. Feder HM Jr, Bennett N, Modlin JF. Atypical hand, foot and mouth disease: a vesiculobullous eruption caused by coxsackie virus A6. Lancet Infect Dis. 2014;14:83–6. https://doi.org/10.1016/S1473-3099(13)70264-0

15. Harris PNA, Wang AD, Yin M, Lee CK, Archuleta S. Atypical hand, foot, and mouth disease: eczema coxsackium can also occur in adults. Lancet Infect Dis. 2014;14:1043. https://doi.org/10.1016/S1473-3099(14)70976-4

16. Chen YJ, Chang SC, Tsao KC, Shih SR, Yang SL, Lin TY, et al. Comparative genomic analysis of coxsackievirus A6 strains of different clinical disease entities. PLoS One. 2012;7:e52432. https://doi.org/10.1371/journal.pone.0052432

17. Gaunt E, Harvala H, Österback R, Sreenu VB, Thomson E, Waris M, et al. Genetic characterization of human coxsackievirus A6 variants associated with atypical hand, foot and mouth disease: a potential role of recombination in emergence and pathogenicity. J Gen Virol. 2015;96:1067–79. https://doi.org/10.1099/vir.0.000062

18. Xing W, Liao Q, Viboud C, Zhang J, Sun J, Wu JT, et al. Hand, foot, and mouth disease in China, 2008–12: an epidemiological study. Lancet Infect Dis. 2014;14:308–18. https://doi.org/10.1016/S1473-3099(13)70342-6

19. Sinclair C, Gaunt E, Simmonds P, Broomfield D, Nwafor N, Wellington L, et al. Atypical hand, foot and mouth disease associated with coxsackievirus A6 infection, Edinburgh, United Kingdom, January to February 2014. Euro Surveill. 2014;19:20745. https://doi.org/10.2807/1560-7917.ES2014.19.12.20745

20. Österback R, Vuorinen T, Linna M, Susi P, Hyypiä T, Waris M. Coxsackievirus A6 and hand, foot and mouth disease, Finland. Emerg Infect Dis. 2009;15:1485–8. https://doi.org/10.3201/eid1509.090438

21. Kamau E, Harvala H, Blomqvist S, Nguyen D, Horby P, Pebody R, et al. Increase in enterovirus D68 infections in young children, United Kingdom, 2006–2016. Emerg Infect Dis. 2019;25:1200–3. https://doi.org/10.3201/eid2506.181759

22. Nguyet LA, Thanh TT, Nhan LNT, Hong NTT, Nhu LNT, Van HMT, et al. Neutralizing antibodies against enteroviruses in patients with hand, foot and mouth disease. Emerg Infect Dis. 2020;26:298–306. https://doi.org/10.3201/eid2602.190721

23. Ang LW, Tay J, Phoon MC, Hsu JP, Cutter J, James L, et al. Seroepidemiology of coxsackievirus A6, coxsackievirus A16, and enterovirus 71 infections among children and adolescents in Singapore, 2008–2010. PLoS One. 2015; 10:e0127999. https://doi.org/10.1371/journal.pone.0127999

24. Yang B, Wu P, Wu JT, Lau EH, Leung GM, Yu H, et al. Seroprevalence of enterovirus 71 antibody among children in China. Pediatr Infect Dis J. 2015;34:1399–406. https://doi.org/10.1097/INF.0000000000000900

25. Luo ST, Chiang PS, Chao AS, Liou GY, Lin R, Lin TY, et al. Enterovirus 71 maternal antibodies in infants, Taiwan. Emerg Infect Dis. 2009;15:581–4. https://doi.org/10.3201/1504.081550

26. Diedrich S, Weinbrecht A, Schreier E. Seroprevalence and molecular epidemiology of enterovirus 71 in Germany. Arch Virol. 2009;154:1139–42. https://doi.org/10.1007/s00705-009-0413-x

27. van der Sanden SM, Koen G, van Eijk H, Koekkoek SM, de Jong MD, Wolthers KC. Prediction of protection against Asian enterovirus 71 outbreak strains by cross-neutralizing capacity of serum from Dutch donors, the Netherlands. Emerg Infect Dis. 2016;22:1562–9. https://doi.org/10.3201/eid2209.151579

28. Rabenau HF, Richter M, Doerr HW. Hand, foot and mouth disease: seroprevalence of coxsackie A16 and enterovirus 71 in Germany. Med Microbiol Immunol (Berl). 2010;199:45–51. https://doi.org/10.1007/s00430-009-0133-6

29. Ooi EE, Phoon MC, Ishak B, Chan SH. Seroepidemiology of human enterovirus 71, Singapore. Emerg Infect Dis. 2002;8:995–7. https://doi.org/10.3201/eid0809.010397

30. Tran CB, Nguyen HT, Phan HT, Tran NV, Wills B, Farrar J, et al. The seroprevalence and seroincidence of enterovirus71 infection in infants and children in Ho Chi Minh City, Viet Nam. PLoS One. 2011;6:e21116. https://doi.org/10.1371/journal.pone.0021116

31. Pons-Salort M, Grassly NC. Serotype-specific immunity explains the incidence of diseases caused by human enteroviruses. Science. 2018;361:800–3. https://doi.org/10.1126/science.aat6777

32. Xing W, Liao Q, Viboud C, Zhang J, Sun J, Wu JT, et al. Hand, foot, and mouth disease in China, 2008–12: an epidemiological study. Lancet Infect Dis. 2014;14:308–18. https://doi.org/10.1016/S1473-3099(13)70342-6

33. Ju Y, Tan Z, Huang H, Chen M, Tan Y, Zhang C, et al. Clinical and epidemiological characteristics of coxsackievirus A6– and enterovirus 71–associated clinical stage 2 and 3

severe hand, foot and mouth disease in Guangxi, Southern China, 2017. J Infect. 2020;80:121–42. https://doi.org/10.1016/j.jinf.2019.09.021

34. Chen S-C, Chang H-L, Yan T-R, Cheng Y-T, Chen K-T. An eight-year study of epidemiologic features of enterovirus 71 infection in Taiwan. Am J Trop Med Hyg. 2007;77:188–91.

35. Kadambari S, Bukasa A, Okike IO, Pebody R, Brown D, Gallimore C, et al. Enterovirus infections in England and Wales, 2000–2011: the impact of increased molecular diagnostics. Clin Microbiol Infect. 2014;20:1289–96. https://doi.org/10.1111/1469-0691.12753

36. Kupila L, Vuorinen T, Vainionpää R, Marttila RJ, Kotilainen P. Diagnosis of enteroviral meningitis by use of

polymerase chain reaction of cerebrospinal fluid, stool, and serum specimens. Clin Infect Dis. 2005;40:982–7. https://doi.org/10.1086/428581

37. Harvala H, Broberg E, Benschop K, Berginc N, Ladhani S, Susi P, et al. Recommendations for enterovirus diagnostics and characterization within and beyond Europe. J Clin Virol. 2018;101:11–7. https://doi.org/10.1016/j.jcv.2018.01.008

Address for correspondence: Everlyn Kamau, Peter Medawar Building for Pathogen Research, South Parks Road, Oxford OX13SY, UK; email: everlyn.kamau@ndm.ox.ac.uk

EMERGING INFECTIOUS DISEASES

To revisit the April 2021 issue, go to:

Epidemiology, Clinical Features, and Outcomes of Coccidioidomycosis, Utah, 2006–2015

Adrienne Carey, Morgan E. Gorris, Tom Chiller, Brendan Jackson, Wei Beadles, Brandon J. Webb

On the basis of a 1957 geographic *Coccidioides* sero-positivity survey, 3 counties in southwestern Utah, USA, were considered coccidioidomycosis-endemic, but there has been a paucity of information on the disease burden in Utah since. We report findings from a recent clinical and epidemiologic study of coccidioidomycosis in Utah. To describe clinical characteristics, we identified all coc-cidioidomycosis cases in an integrated health system in the state during 2006–2015. For epidemiologic analysis, we used cases reported to the Utah Department of Health during 2009–2015. Mean state incidence was 1.83 cases/100,000 population/year. Washington County, in southwestern Utah, had the highest incidence, 17.2 cases/100,000 population/year. In a generalized linear model with time as a fixed effect, mean annual temperature, population, and new construction were associated with regional variations in incidence. Using these variables in a spatiotemporal model, we estimated the adjusted regional variation by county to predict areas where *Coccidioides* infections might increase.

Coccidioidomycosis, also known as Valley fever, is caused by *Coccidioides immitis* and *C. posadasii*, endemic, dimorphic environmental fungi found in the soil of the southwestern United States, Mexico, and Central and South America (*1*). Clinical infection ranges from asymptomatic to diverse manifestations including pneumonia, soft tissue and osteoarticular infection, meningitis, and disseminated disease (*2*). On the basis of findings from the seminal 1957 seropositivity survey (*3*) that established the com-

monly accepted geographic distribution of *Coccidioides* in the United States, 6 states were classified as coccidioidomycosis-endemic (Arizona, California, Nevada, New Mexico, Texas, and Utah); California and Arizona had the highest seroprevalence (*4*). On the basis of that study, 3 counties in southwestern Utah were considered coccidioidomycosis-endemic: Iron, Kane, and Washington (*3*). With the exception of reports from a widely publicized 2001 outbreak of coccidioidomycosis at an archeological dig in Uintah County in the US Park Service's Dinosaur National Monument (*5–7*), there are few published data on this disease in Utah. However, recent data suggest that southwestern Utah might represent an area of increased disease burden (*8*). Here we report a description of the epidemiology of coccidioidomycosis in Utah and explore environmental and climatic factors contributing to regional variations in statewide incidence using data from cases reported to the Utah Department of Health (UDOH) during 2009–2015. We also describe clinical characteristics and outcomes using patient-level data from the Intermountain Healthcare System during 2006–2015.

Methods

Clinical Characteristics

To describe the clinical characteristics and outcomes of coccidioidomycosis, we used patient-level data from Intermountain Healthcare, an integrated health network with 21 hospitals and 180 clinics in urban and rural Utah. Each year, 1.5 million unique patients, over half of Utah's 2010 population of 2,763,885 (https://www.census.gov/quickfacts/UT), receive care in the Intermountain Healthcare network. We identified all cases of proven or probable coccidioidomycosis recorded during January 1, 2006–December 31, 2015, by applying a previously published query methodology to clinical data from the Intermountain electronic data warehouse. We used an iterative

Author affiliations: University of Utah School of Medicine, Salt Lake City, Utah, USA (A. Carey); Los Alamos National Laboratory, Los Alamos, New Mexico, USA (M. Gorris); Centers for Disease Control and Prevention, Atlanta, Georgia, USA (T. Chiller, B. Jackson); Utah Department of Health, Salt Lake City (W. Beadles); Intermountain Healthcare, Salt Lake City (B. Webb); Stanford University School of Medicine, Palo Alto, California, USA (B. Webb)

search process by querying each of 7 different types of clinical and diagnostic data associated with the diagnosis of coccidioidomycosis: codes from the International Classification of Diseases (ICD) 9th (code range 114.x) and 10th (code range B38.x) Revisions, laboratory tests for *Coccidioides*, microbiologic culture data, pathologic data, radiologic data, pharmacy data for antifungal medications, and composite data identifying immunocompromised patients at higher risk for fungal disease (*9*). Laboratory data included serologic assays for *Coccidioides*: IgM/IgG by ELISA, IgM/IgG by immunodiffusion, complement fixation (CF) titers for IgG (ARUP Laboratories, https://www.aruplab.com), and PCR for *Coccidioides* (Mayo Medical Laboratories, https://www.mayocliniclabs.com).

We extracted demographic and other clinical data for patients in the Intermountain electronic data warehouse cohort, then manually reviewed all potential cases identified by electronic query to verify the diagnosis by laboratory, microbiologic, and pathologic test results; we validated correlating clinical symptoms using imaging reports, clinical notes, and electronic medical record (EMR) data. We classified each case as proven or probable according to definitions established by the European Organization for Research and Treatment of Cancer/Invasive Fungal Infections Cooperative Group and Mycoses Study Group (EORTC/MSG) (*10*). We considered cases proven if they met ≥1 of the following requirements: histopathologic, cytopathologic, or direct microscopic evidence of *Coccidioides* spherules with tissue damage from sterile specimen or tissue biopsy; culture from any specimen or tissue biopsy positive for *C. immitis* or *C. posadasii*; positive blood culture for *C. immitis* or *C. posadasii*; positive *Coccidioides* serology in cerebrospinal fluid; or 2-dilution rise in *Coccidioides* CF titer measured in consecutive blood samples tested concurrently. We considered cases probable if case-patients had a *Coccidioides* CF titer >1:2 or positive IgM or IgG by enzyme immunoassay (EIA)/ELISA or immunodiffusion in the setting of a compatible clinical syndrome, which could include >1 of the following: 1) systemic infection with fever, chills, night sweats, weight loss; 2) cutaneous or musculoskeletal infection; 3) pulmonary involvement with nodules, cavitation, hilar lymphadenopathy; 4) meningitis; or 5) visceral infiltration. We included case data in the study if the cases met criteria for proven or probable infection (Figure 1).

For the Intermountain Healthcare cohort used for describing clinical characteristics, we included cases from small communities just outside the Utah border for which Intermountain Healthcare facilities serve as the primary access to healthcare. These cases were not included in the cohort used for epidemiologic analyses. We excluded cases in which it was clear from the EMR that the infection was acquired outside of Utah and surrounding communities. We also excluded cases that did not meet the EORTC/MSG definition for proven or probable infection. Because of the higher likelihood of a false positive test with ELISA IgM, we excluded cases if the ELISA IgM was positive but not the ELISA IgG and a diagnosis other than coccidioidomycosis was considered more likely. We also excluded cases with a positive ELISA IgG alone and no corresponding clinical signs or symptoms. We manually confirmed the location of diagnosis and management using the patient's residential ZIP code from EMRs. If the city of residence was identified but not the ZIP code, we randomly imputed 1 of the ZIP codes corresponding to that city. We reviewed clinical notes for information regarding disease presentation, reasons for testing for coccidioidomycosis, and interpretation of laboratory results by the physician. We also documented whether antifungal drugs were prescribed and the duration of treatment.

Epidemiologic Analyses

For epidemiologic analyses, we used data from UDOH to ensure we evaluated the entire state population. For this cohort, we included case counts by county by year during 2009–2015. We excluded cases from before 2009 because of acknowledged limitations in data accuracy before that time. As a sensitivity analysis, we compared agreement between results from the case-finding methodology applied to the Intermountain Healthcare data with records from UDOH of cases diagnosed within Intermountain Healthcare facilities.

Statistical Analysis

Descriptive statistics to compare clinical characteristics were performed using a χ^2 test for categorical data and the Mann-Whitney U-test for nonnormally distributed continuous data. To compare characteristics between patients with pulmonary and nonpulmonary disease, we developed a logistic regression model including factors significant at an α-significance of <0.1, then reduced it to a parsimonious model. We confirmed the goodness of fit using the Hosmer-Lemeshow method and fitted a simple least-squares linear regression to model the variation in statewide incidence over time.

To explore the association between environmental and anthropological features and geographic variation in observed coccidioidomycosis incidence, we developed a generalized linear model using year,

annual population for 2006–2015 (US Census Bureau, https://www.census.gov), PRISM AN81m mean annual air temperature and precipitation (https://prism.oregonstate.edu) (*11,12*), and total annual new construction permits per 100,000 population for 2006–2015 (Ivory-Boyer Construction Report and Database, https://gardner.utah.edu/economics/ivory-boyer-construction-database) as covariates. We included year to account for potential fixed-year effects and population to capture differences in signals and levels of cases between urban versus rural counties. We included temperature and precipitation data because both climate factors have been shown to correlate with cases in other endemic regions (*8,13–16*). Last, we included new construction permits because coccidioidomycosis outbreaks have occurred in areas with construction activity, caused by soil-disrupting activities that increase airborne dust containing *Coccidioides* spp. (*17–19*). We also explored the contributions of soil pH (SSURGO database, https://www.nrcs.usda.gov/wps/portal/nrcs/detail/soils/survey/?cid=nrcs142p2_053627) and soil frost-free days and freeze-free intervals (Utah Climate Center, https://climate.usu.edu) but ultimately did not include these in the final model. We assessed model fitness using F-test, R^2, and residuals. Then, to predict geographic variation in coccidioidomycosis incidence after accounting for environmental and construction factors and the secular trend, we used an analysis of covariance model using county as a fixed variable to estimate the adjusted mean incidence. We input these estimated adjusted incidences into a spatiotemporal geographic information systems model to map predicted incidence by county for the time period. Statistical analysis was conducted using SPSS Statistics 22 (IBM, https://www.ibm.com). This study was approved by the Intermountain Healthcare institutional review board.

Results

Demographic and Clinical Data
From the 788 cases we electronically identified initially, 364 patients had serologic, microbiological, or pathological evidence of proven or probable coccidioidomycosis (Figure 1); we excluded an additional 115 patients living in the endemic regions of Utah because they had positive IgG results from ELISA but no evidence of clinical disease. We classified 192 (52.7%) of the 364 cases as proven and 172 (47.3%) as probable (Table 1). Median age of case-patients was 61 years (range 1–97 years); 3.6% were <18 years of age. Over half (55.2%) of patients were male, and 87.9%
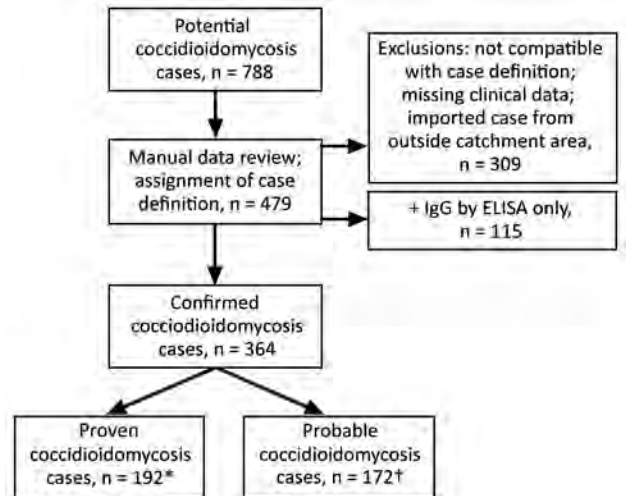
Figure 1. Flowchart showing process for inclusion of possible coccidioidomycosis studies in study of cases in Utah, 2006–2015. Confirmed cases had ≥1 of the following: 1) histopathological, cytopathological, or direct microscopic evidence of *Coccidioides* spherules with tissue damage from sterile specimen or tissue biopsy; 2) culture from any specimen or tissue biopsy positive for *C. immitis* or *C. posadasii*; 3) blood culture positive for *C. immitis* or *C. posadasii*; 4) positive *Coccidioides* serology in cerebrospinal fluid; or 5) two-dilution rise in *Coccidioides* CF titer measured in consecutive blood samples tested concurrently. Probable cases had a *Coccidioides* complement fixation titer >1:2 or positive IgM or IgG by EIA/ELISA or immunodiffusion in the setting of a compatible clinical syndrome and ≥1 of the following: 1) systemic infection with fever, chills, night sweats, weight loss; 2) cutaneous or musculoskeletal infection; 3) pulmonary involvement with nodules, cavitation, hilar lymphadenopathy; 4) meningitis; or 5) visceral infiltration. Definitions based on criteria set by the European Organization for Research and Treatment of Cancer/Invasive Fungal Infections Cooperative Group; National Institute of Allergy and Infectious Diseases Mycoses Study Group (*10*).

identified as white. Patients had a median Charlson comorbidity score of 2 (range 0–4); the most common coexisting conditions were chronic pulmonary disease (144, 39.6%), diabetes mellitus (81, 22.3%), and malignancy (76, 20.9%). Only a few patients were taking immunosuppressive medications (27, 7.4%) or undergoing chemotherapy (4, 1.1%) at the time of their diagnosis, and 154 (42.3%) patients were hospitalized for coccidioidomycosis with the length of stay 0–5 days (0 indicating only an emergency room visit); 25.3% of the cohort had ≥1 hospitalization within ≤6 weeks after diagnosis. All-cause mortality was 5.5% at 42 days and 9.1% at 1 year.

Sites of Infection
Primary pulmonary infection was the most common type of infection, in 323 (88.7%) of 364 patients; 4 (1.1%) pulmonary patients had meningitis. Of 41

Table 1. Demographic and clinical data from coccidioidomycosis cases identified in the Intermountain Healthcare system, Utah, USA, 2006–2015*

Variables	No. (%)
Total patients	364
Demographics	
Age, y, median (IQR)	61 (44–72)
Pediatric <18 y	13 (3.6)
Male sex	201 (55.2)
Race	
American Indian	5 (1.4)
Asian	2 (0.5)
Black	1 (0.3)
Hispanic	20 (5.5)
Pacific Islander	9 (2.5)
Unknown	7 (1.9)
White	320 (87.9)
Coexisting conditions/medical factors	
Charlson comorbidity score, median (IQR)	2 (0–4)
Diabetes mellitus	81 (22.3)
Hepatic disease	61 (16.8)
Chronic pulmonary disease	144 (39.6)
Connective tissue disease	27 (7.4)
Congestive heart failure	53 (14.6)
Neurologic disease	52 (14.3)
Renal disease	45 (12.4)
History of malignancy	76 (20.9)
Hematopoietic stem cell transplant	2 (0.5)
Solid organ transplant	2 (0.5)
Any immunosuppressive medication	27 (7.4)
Corticosteroids	25 (6.9)
Anti-TNF	3 (0.8)
Antimetabolite	2 (0.5)
Chemotherapy	4 (1.1)
Laboratory test results	
Lymphopenia, absolute lymphocyte count <500	12 (3.3)
Lymphopenia value at diagnosis, absolute lymphocyte count, median (IQR)	300 (300–400)
Outcomes	
Coccidioidomycosis-related hospital admission	154 (42.3)
Hospital length of stay, d, median (IQR)	0 (0–5)
42-d all-cause mortality	20 (5.5)
1-y all-cause mortality	33 (9.1)
Case classification	
Proven	192 (52.7)
Probable	172 (47.3)

*Values are no. (%) except as indicated. IQR, interquartile range; TNF, tumor necrosis factor.

patients with nonpulmonary disease, 11 (26.8%) had disseminated infection (Table 2; Appendix Table 1, https://wwwnc.cdc.gov/EID/article/27/9/21-0751-App1.pdf). We noted no significant differences in age or coexisting conditions, but did find a trend toward significance (p≤0.05) for chronic neurologic disease, diagnosed in 24.4% (10/41) of nonpulmonary disease patients compared with 13.0% (42/323; p = 0.08) of pulmonary disease patients (Appendix Table 1). Among all those with nonpulmonary disease, 22.2% (9/41) were nonwhite patients, but only 10.8% (35/323; p = 0.05) of patients with pulmonary disease were nonwhite. Nonpulmonary disease was also more common than pulmonary disease in patients receiving immunosuppressive medications, 14.6% (6/41) versus 6.5% (21/323; p = 0.06) and those with lymphopenia preceding diagnosis, 9.8% (4/41)

versus 2.5% (8/323; p = 0.04). In a multivariable logistic regression including use of any immunosuppressing medication, neurologic disease, and lymphopenia, only lymphopenia remained a predictor for nonpulmonary disease (OR 4.56, 95% CI 1.2–14.8).

Diagnosis and Management

We confirmed a coccidioidomycosis diagnosis with serologic testing in 51.9% of cases and with microbiologic or pathologic evidence of *Coccidioides* in 48.1% of cases (Table 2). Patients were diagnosed in a hospital in 110 (30.2%) cases; among outpatients, 23.1% were diagnosed by a pulmonologist, 11.8% by a primary care provider, 10.7% by a surgeon, and only 0.8% by an infectious disease physician. Of interest, 104 patients (28.6%) were diagnosed as part of a workup for malignancy, usually for an incidental pulmonary

nodule. Of the 364 patients in the study, 209 (57.4%) were treated with antifungal therapy alone; 12.6% of case-patients received no surgical or antifungal therapy (Appendix Table 2). Fluconazole (91.7%) was the most common antifungal agent prescribed, followed by amphotericin B (3.2%); 20.8% of patients received >1 different antifungal agent during their treatment.

Epidemiology and Geographic Variation

We found 366 cases reported during 2009–2015. Mean observed statewide incidence was 1.83 cases/100,000 population/year; yearly rates increased by a mean of 0.02 cases/100,000 population/year from 2009 through 2015 (R^2 = 0.018, Figure 2). Washington County, in the southwestern part of the state, accounted for the largest proportion (47.5%) of cases, a mean observed incidence of 17.2 cases/100,000 population/year (Figure 3, Table 3). Outside of Washington County, incidence was next highest in the adjacent southwestern counties of Beaver, Garfield, Iron, and Kane, then in Daggett and Rich Counties in the northeast corner of the state (Table 3; Figure 3). In the generalized linear model accounting for temporal trend, the factors that best explained regional variation in observed incidence included population (effect size [partial η^2] 0.068, p = 0.001), mean air temperature (effect size 0.246; p<0.001), and new construction permits/

100,000 population (effect size 0.072; p = 0.001), but precipitation was not significantly associated (effect 0.022; p = 0.059; R^2 = 0.42) (Appendix Table 3).

For the analysis of covariance model, in which we used county as a fixed effect and adjusted by secular trend, population, mean annual temperature, precipitation, and new construction permits, the estimated mean statewide incidence was 3.45 cases/100,000 population/year (R^2 = 0.92); (Table 3; Appendix Table 4). In this model, estimated adjusted mean incidence was highest in Washington County at 17.2 cases/100,000 population per year. The estimated incidence was higher than the observed incidence in Summit, Uintah, Duchesne, Morgan, and Rich Counties in northeastern Utah (Table 3).

Discussion

These data, representing the results of a modern epidemiologic study, confirm coccidioidomycosis as a clinically relevant endemic mycosis in Utah. Our analyses benefited from the granularity of patient-level data combined with UDOH statewide data. Although not on the scale of incidence reported for Arizona (154.6 cases/100,000 population/year) or California (9.37 cases/100,000 population/year) (20–22), the incidence (1.83 cases/100,000 population/year) in Utah during 2009–2015 was higher than

Table 2. Clinical features based on case classification from the Intermountain Healthcare system, Utah, USA, 2006–2015

Characteristic	No. (%) cases		
	Total	Proven	Probable
Total	364 (100)	192 (52.7)	172 (47.3)
Primary method of diagnosis			
Laboratory	189 (51.9)	17 (8.9)	172 (100)
Microbiology	43 (11.8)	43 (22.4)	0
Pathology	106 (29.1)	106 (55.2)	0
Microbiology, pathology	26 (7.1)	26 (13.5)	0
Infection site			
Abdomen, peritoneal fluid	1 (0.3)	1 (0.5)	0
Adrenal	2 (0.5)	2 (1.0)	0
Back	1 (0.3)	1 (0.5)	0
Disseminated	11 (3.0)	10 (5.2)	1 (0.6)
Extremity	6 (1.6)	6 (3.1)	0
Liver	1 (0.3)	0	1 (0.6)
Lung only	316 (86.8)	154 (80.2)	162 (94.2)
Lung and lymph node	7 (1.9)	7 (3.6)	0
Lymph node only	4 (1.1)	4 (2.1)	0
Meningitis	4 (1.1)	3 (1.6)	1 (0.6)
Skin	5 (1.4)	3 (1.6)	2 (1.2)
Unknown	6 (1.6)	1 (0.5)	5 (2.9)
Location of diagnosis			
Urgent care/emergency department	12 (3.3)	2 (1.0)	10 (5.8)
Inpatient hospital	110 (30.2)	59 (30.7)	51 (29.7)
Primary care provider	43 (11.8)	22 (11.5)	21 (12.2)
Pulmonary department	84 (23.1)	40 (20.8)	44 (25.6)
Infectious diseases	3 (0.8)	0	3 (1.7)
Surgery department	39 (10.7)	38 (19.8)	1 (0.6)
Other	24 (6.6)	19 (9.9)	5 (2.9)
Unknown	50 (13.7)	12 (6.3)	38 (22.1)
Diagnosed as work-up for malignancy	104 (28.6)	100 (52.1)	4 (2.33)
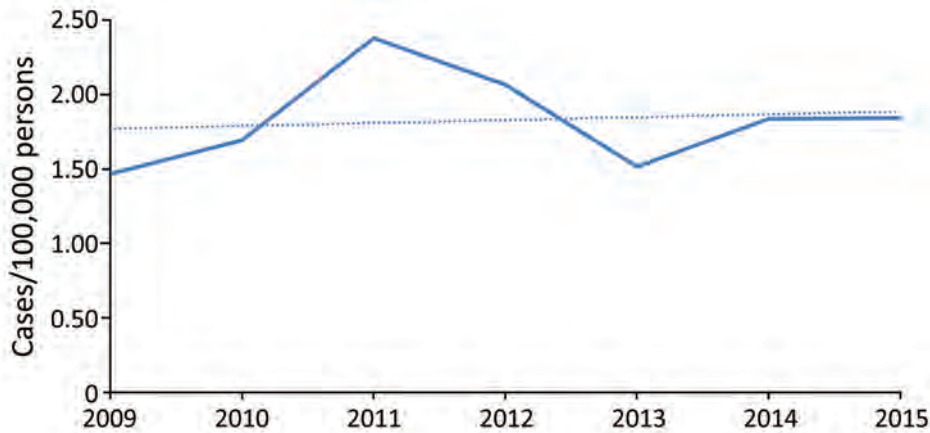
Figure 2. Annual statewide coccidioidomycosis incidence calculated from cases reported to the Utah Department of Health, Utah, 2009–2015. The dotted line represents the line of best fit for the data with an R^2 of 0.018.

previously reported, and Utah ranks as the third most endemic state (*4*).

Coccidioidomycosis clusters regionally within the state. Washington, Garfield, Beaver, Kane, and Iron Counties in the southwestern portion of the state account for the most cases. Although regional climate contributes to this distribution, rapid population growth and new construction in this area of the state might also play a role. As of 2018, St. George, located in Washington County, was one of the fastest growing metropolitan areas in the United States (US Census Bureau). Residential and commercial construction disrupts soil and exposes residents

to aerosolized arthroconidia, increasing the risk for contracting coccidioidomycosis (*19,23*). With increasing population growth in this area, we hypothesize that the rate of coccidioidomycosis incidence will also continue to rise. Future studies focusing on incidence among construction workers or residents living in areas with increased rates of construction will be key to further understand this association. Washington County also represents a large recreational area for travelers, both those commuting to other destinations in the Interstate 15 corridor and those traveling to Zion National Park, the fourth-most visited national park in the United States in
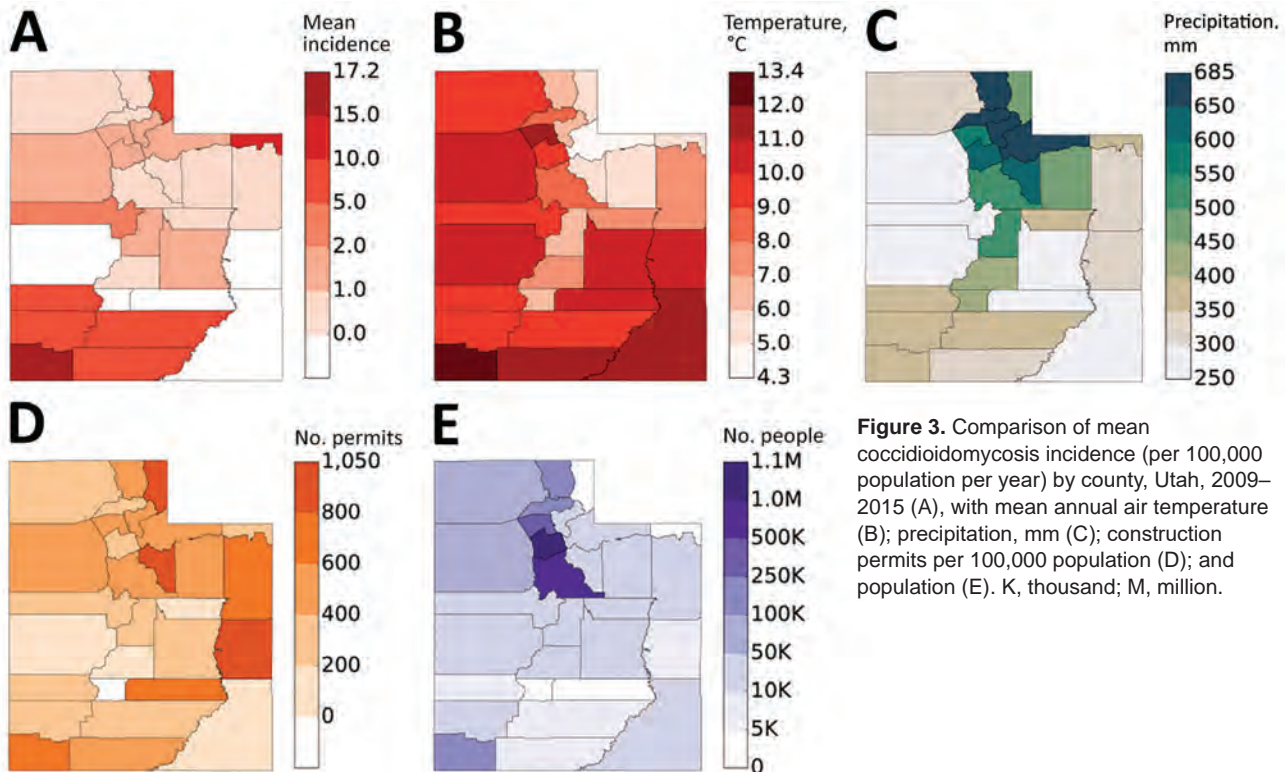
Figure 3. Comparison of mean coccidioidomycosis incidence (per 100,000 population per year) by county, Utah, 2009–2015 (A), with mean annual air temperature (B); precipitation, mm (C); construction permits per 100,000 population (D); and population (E). K, thousand; M, million.

Table 3. Distribution by county of coccidioidomycosis cases reported to the Utah Department of Health, Utah, USA, 2009–2015

County*	Total (%)†	Observed mean cases/year	Mean incidence/100,000 population/year	
			Observed	Estimated
Washington	174 (47.5)	24.9	17.2	17.2
Salt Lake	79 (21.6)	11.3	1.06	−0.01
Davis	23 (6.3)	3.29	1.02	−0.11
Utah	21 (5.7)	3.00	0.56	1.00
Iron	17 (4.6)	2.43	5.23	4.18
Weber	10 (2.7)	1.43	0.60	−0.79
Tooele	6 (1.6)	0.86	1.43	0.65
Summit	5 (1.4)	0.71	1.93	4.57
Beaver	4 (1.1)	0.57	8.83	6.93
Cache	4 (1.1)	0.57	0.50	1.14
Garfield	3 (0.8)	0.43	8.44	7.32
Box Elder	2 (0.5)	0.29	0.85	−0.03
Kane	2 (0.5)	0.29	5.95	4.73
Juab	2 (0.5)	0.29	2.78	0.64
Sanpete	2 (0.5)	0.29	1.01	0.20
Uintah	2 (0.5)	0.29	0.80	2.70
Carbon	1 (0.3)	0.14	0.68	−0.88
Daggett	1 (0.3)	0.14	12.9	13.7
Duchesne	1 (0.3)	0.14	0.71	2.62
Emery	1 (0.3)	0.14	1.34	−1.00
Morgan	1 (0.3)	0.14	1.40	2.43
Rich	1 (0.3)	0.14	6.33	11.0
Sevier	1 (0.3)	0.14	0.69	−0.98
Wasatch	1 (0.3)	0.14	0.58	5.66
Utah	366‡ (100)	52.3	1.83	3.45

*Counties with no cases included in the table: Grand, Millard, Piute, San Juan, and Wayne.
†Two cases in 2015 could not be classified by county.
‡Data from analysis of covariance model adjusting for year, mean annual temperature, mean annual precipitation, mean annual population, and mean number of new construction permits/100,000 population/year.

2018, which averages 4.3 million visitors/year (National Park Services Visitor Use Statistics, https://irma.nps.gov/STATS).

Of additional interest, when climate, population, and construction factors were taken into account, our model predicted a second hotspot for future high coccidioidomycosis incidence in the northeastern corner of the state. Although the current observed incidence in these counties is low, they are also sparsely populated but with substantial population growth expected, the incidence in these areas might also be expected to increase. This finding was especially intriguing in the context of the 2001 coccidioidomycosis outbreak (adjusted mean incidence: 2.70 cases/100,000 population/year) that occurred in Uintah County in northeast Utah, which includes part of Dinosaur National Monument.

In addition to the factors that we included in our analyses, other environmental factors such as soil pH and composition and the geographic distribution of small mammal species important in the lifecycle of *Coccidioides* (24) might also contribute to the geographic variation in disease incidence and merit additional research. Future studies including PCR testing of soil and air samples will be important to clarify the interactions between the environment and *Coccidioides* pathogens and enable more accurate epidemiologic forecasting.

The observed all-cause mortality in the study cohort was higher than reported in an earlier study (25). Because roughly one third of cases in our study were diagnosed in a hospital, delay in diagnosis because of lack of clinical awareness might have led to increased death. In addition, because of this finding of elevated death rates, potential differences in virulence among *Coccidioides* strains circulating in Utah should be considered to better understand this phenomenon (26). Congruent with findings from prior studies (27), persons of non-White race and those taking immunosuppressive medications were more likely to have the nonpulmonary form of the disease.

Given the high incidence in southwestern Utah, more widespread efforts to educate clinicians about coccidioidomycosis are urgently needed, especially as the population increases and ages. In these areas, where pulmonary and infectious diseases specialists are scarce, primary care providers and those working in urgent care settings serve as the front line for diagnosing and treating diseases such as coccidioidomycosis. Because nearly one third of patients in this cohort were diagnosed as part of a workup for malignancy, our findings suggest that additional awareness efforts should be targeted to the hematologists and oncologists serving a broad referral area in Utah, Nevada, and Arizona. Radiologists should also be included so that they might

consider coccidioidomycosis as a differential diagnosis in the presence of relevant radiological features.

An additional 115 patients living in southwestern Utah were excluded from the study although they had positive IgG ELISA results because of a lack of clinical disease evidence. It is unclear if these cases represent temporally remote or subclinical exposures with long-lasting seropositivity, questioning the current paradigm that *Coccidioides* IgG wanes over time. Additional analysis of that subgroup of the cohort will need to be conducted to further understand this phenomenon.

Our study's first limitation is that the reported demographic and clinical data are based on the subset of cases from Intermountain Healthcare identified within the state, but incidence data are based on cases reported to the state health department. When we manually compared Intermountain Healthcare patient-level data with statewide reportable disease data from UDOH for the same cases, there were differences, particularly for case confirmation and regional distribution (e.g., more reportable cases in northern counties). This might have been because of decreased specificity related to the granularity of laboratory-initiated health department data and decreased sensitivity in Intermountain Healthcare data, where not all possible cases might have been detected. For example, not all physicians used EMR, and in some cases clinical data were missing; therefore, we excluded those cases to maintain data integrity. This process likely led to an underestimation of the true number of cases within the state. Third, we used ZIP code information as a surrogate for the location of disease acquisition. Without a direct survey of patients to elucidate occupational and recreational exposures, this might skew the distribution of disease across the state. Last, we excluded cases from the demographic and clinical analyses when *Coccidioides* CF was positive at 1:2 titer, although UDOH includes cases with CF positive at that titer. However, manual review revealed only 2 cases excluded with an exact 1:2 titer without another positive serologic result. One case had missing clinical information that did not permit us to confirm symptomatology, and 1 case was imported from outside of the state.

In conclusion, we found that coccidioidomycosis incidence in Utah is higher than previously described and clusters primarily in the recognized endemic area in the southwestern part of the state. However, in geospatial modeling accounting for environmental factors, we identified a second potential area in the northeast that might have conditions conducive to future increases in *Coccidioides* incidence. Increasing the awareness of front-line providers and especially oncologists in southwestern Utah is necessary for early recognition and clinical management of the disease, but enhanced clinical surveillance in the northeast might increase case detection. Serologic and environmental testing might further elucidate distribution of *Coccidioides* organisms and determine the effects of air temperature, population growth, and construction on coccidioidomycosis disease burden in the state.

About the Author

Dr. Carey is an assistant professor in the Division of Infectious Diseases at the University of Utah School of Medicine in Salt Lake City. Her primary research interests include the epidemiology and clinical characteristics of coccidioidomycosis within the state.

References

1. Pappagianis D. Epidemiology of coccidioidomycosis. In: McGinnis M, editor. Current topics in medical mycology, vol. 2. New York City: Springer; 1988. p. 199–238.
2. Galgiani JN, Ampel NM, Blair JE, Catanzaro A, Geertsma F, Hoover SE, et al. 2016 Infectious Diseases Society of America (IDSA) clinical practice guideline for the treatment of coccidioidomycosis. Clin Infect Dis. 2016;63:e112–46. https://doi.org/10.1093/cid/ciw360
3. Edwards PQ, Palmer CE. Prevalence of sensitivity to coccidioidin, with special reference to specific and nonspecific reactions to coccidioidin and to histoplasmin. Dis Chest. 1957;31:35–60. https://doi.org/10.1378/chest.31.1.35
4. Centers for Disease Control and Prevention (CDC). Increase in reported coccidioidomycosis—United States, 1998-2011. MMWR Morb Mortal Wkly Rep. 2013;62:217–21.
5. Centers for Disease Control and Prevention. Coccidioidomycosis in workers at an archeologic site—Dinosaur National Monument, Utah, June–July 2001. JAMA. 2001;286:3072–3. https://doi.org/10.1001/jama.286.24.3072
6. Perera P, Stone S. Update on emerging infections: news from the Centers for Disease Control and Prevention Ann Emerg Med. 2002;39:566–9.

7. Petersen LR, Marshall SL, Barton-Dickson C, Hajjeh RA, Lindsley MD, Warnock DW, et al. Coccidioidomycosis among workers at an archeological site, northeastern Utah. Emerg Infect Dis. 2004;10:637–42. https://doi.org/10.3201/eid1004.030446

8. Gorris ME, Cat LA, Zender CS, Treseder KK, Randerson JT. Coccidioidomycosis dynamics in relation to climate in the southwestern United States. Geohealth. 2018;2:6–24. https://doi.org/10.1002/2017GH000095

9. Webb BJFJ, Ferraro JP, Rea S, Kaufusi S, Goodman BE, Spalding J. Epidemiology and clinical features of invasive fungal infection in a US health care network. Open Forum Infect Dis. 2018;5:ofy187. https://doi.org/10.1093/ofid/ofy187

10. De Pauw B, Walsh TJ, Donnelly JP, Stevens DA, Edwards JE, Calandra T, et al.; European Organization for Research and Treatment of Cancer/Invasive Fungal Infections Cooperative Group; National Institute of Allergy and Infectious Diseases Mycoses Study Group (EORTC/MSG) Consensus Group. Revised definitions of invasive fungal disease from the European Organization for Research and Treatment of Cancer/Invasive Fungal Infections Cooperative Group and the National Institute of Allergy and Infectious Diseases Mycoses Study Group (EORTC/MSG) Consensus Group. Clin Infect Dis. 2008;46:1813–21. https://doi.org/10.1086/588660

11. Daly C, Halbleib M, Smith JI, Gibson WP, Doggett MK, Taylor GH, et al. Physiographically sensitive mapping of climatological temperature and precipitation across the conterminous United States. Int J Climatol. 2008;28:2031–64. https://doi.org/10.1002/joc.1688

12. Daly C, Neilson RP, Phillips DL. A statistical–topographic model for mapping climatological precipitation over mountainous terrain. J Appl Meteorol. 1994;33:140–58. https://doi.org/10.1175/1520-0450(1994)033<0140:ASTMFM>2.0.CO;2

13. Kolivras KN, Comrie AC. Modeling valley fever (coccidioidomycosis) incidence on the basis of climate conditions. Int J Biometeorol. 2003;47:87–101. https://doi.org/10.1007/s00484-002-0155-x

14. Comrie AC. Climate factors influencing coccidioidomycosis seasonality and outbreaks. Environ Health Perspect. 2005;113:688–92. https://doi.org/10.1289/ehp.7786

15. Park BJ, Sigel K, Vaz V, Komatsu K, McRill C, Phelan M, et al. An epidemic of coccidioidomycosis in Arizona associated with climatic changes, 1998–2001. J Infect Dis. 2005;191:1981–7. https://doi.org/10.1086/430092

16. Weaver EA, Kolivras KN. Investigating the relationship between climate and valley fever (coccidioidomycosis). EcoHealth. 2018;15:840–52. https://doi.org/10.1007/s10393-018-1375-9

17. Cummings KC, McDowell A, Wheeler C, McNary J, Das R, Vugia DJ, et al. Point-source outbreak of coccidioidomycosis in construction workers. Epidemiol Infect. 2010;138:507–11. https://doi.org/10.1017/S0950268809990999

18. Laws RL, Cooksey GS, Jain S, Wilken J, McNary J, Moreno E, et al. Coccidioidomycosis outbreak among workers constructing a solar power farm—Monterey County, California, 2016–2017. MMWR Morb Mortal Wkly Rep. 2018;67:931–4. https://doi.org/10.15585/mmwr.mm6733a4

19. Wilken JA, Sondermeyer G, Shusterman D, McNary J, Vugia DJ, McDowell A, et al. Coccidioidomycosis among workers constructing solar power farms, California, USA, 2011–2014. Emerg Infect Dis. 2015;21:1997–2005. https://doi.org/10.3201/eid2111.150129

20. Arizona Department of Health Services, Office of Infectious Disease Services. Rates of reported cases of notifiable diseases by year for Arizona, 2005–2015, per 100,000 population [cited 2019 Jun 19]. https://www.azdhs.gov/documents/preparedness/epidemiology-disease-control/disease-data-statistics-reports/data-statistics-archive/t3a1-rates.pdf

21. California Department of Public Health, Division of Communicable Diseases Control, Infectious Diseases Branch, Surveillance and Statistics Section. Yearly summaries of selected general communicable diseases in California, 2001–2010 [cited 2019 Jun 19]. https://www.cdph.ca.gov/Programs/CID/DCDC/CDPH%20Document%20Library/YearlySummaryReportsofSelectedGenCommDiseasesinCA2001-2010.pdf

22. California Department of Public Health, Division of Communicable Diseases Control, Infectious Diseases Branch, Surveillance and Statistics Section. Epidemiologic summary of coccidioidomycosis in California, 2016 [cited 2019 Jun 19]. https://www.cdph.ca.gov/Programs/CID/DCDC/CDPH%20Document%20Library/CocciEpiSummary2016.pdf

23. Brown J, Benedict K, Park BJ, Thompson GR III. Coccidioidomycosis: epidemiology. Clin Epidemiol. 2013;5:185–97.

24. Taylor JW, Barker BM. The endozoan, small-mammal reservoir hypothesis and the life cycle of Coccidioides species. Med Mycol. 2019;57(Supplement_1):S16–20. https://doi.org/10.1093/mmy/myy039

25. Huang JY, Bristow B, Shafir S, Sorvillo F. Coccidioidomycosis-associated Deaths, United States, 1990-2008. Emerg Infect Dis. 2012;18:1723–8. https://doi.org/10.3201/eid1811.120752

26. Barker BM, Jewell KA, Kroken S, Orbach MJ. The population biology of *coccidioides*: epidemiologic implications for disease outbreaks. Ann N Y Acad Sci. 2007;1111:147–63. https://doi.org/10.1196/annals.1406.040

27. Odio CD, Marciano BE, Galgiani JN, Holland SM. Risk factors for disseminated coccidioidomycosis, United States. Emerg Infect Dis. 2017;23:308–11. https://doi.org/10.3201/eid2302.160505

Address for correspondence: Adrienne Carey, Division of Infectious Diseases, University of Utah School of Medicine, 30 N 1900 E, Rm 4B319, Salt Lake City, UT 84132, USA; email: adrienne.carey@hsc.utah.edu

etymologia

Talaromyces marneffei [tlæˈɹɒ maɪs ɪz mɑːneɪ]

Monika Mahajan

*T*alaromyces marneffei (formerly *Penicillium marneffei*) is a thermally dimorphic fungus that causes talaromycosis, which was previously called penicilliosis. The genus name *Talaromyces* is derived from the Greek words *tálaros* (basket) and *múkēs* (mushroom). Talaros aptly describes the ascocarp known as a gymnothecium (composed of fine woven hyphae) in which asci are formed. Asexual stages of *Talaromyces* species were previously known as the species *Penicillium* of the subgenus *Biverticillium*. Capponi and Sureau isolated the fungus at Institute Pasteur de Dalat in Vietnam in 1955 from Chinese bamboo rats (*Rhizomys sinensis*). In 1959, Gabriel Segretain, after an accidental finger prick with a needle containing the yeast cells, described the fungus as a new species, naming it *Penicillium marneffei* in honor of Hubert Marneffe (1901–1970), the Director of the Institute in Indochina.

Talaromycosis affects persons who live in or visit Southeast Asia, southern China, or northeastern India, and are immunocompromised because of HIV/AIDS, cancer, organ transplant, or adult-onset immunodeficiency syndrome. This disease occurs after inhalation of aerosolized fungal spores from the environment. Although the precise reservoir is unknown, *T. marneffei* is found in bamboo rats.

Figure 1. Hubert Marneffe (1901–1970) Source: Wikimanche, Institut Pasteur, public domain.

Figure 2. A) Ultrastructural morphology of *Talaromyces marneffei*, including chains of single-celled, teardrop-shaped conidia, each originating from its respective, flask-shaped phialide. Source: Libero Ajello, Centers for Disease Control and Prevention (https://phil.cdc.gov/Details.aspx?pid = 4240). B) Superior (front) view of a petri dish culture plate on which a wrinkled colony of *Penicillium marneffei* has been cultivated. Source: James Gathany, Centers for Disease Control and Prevention (https://phil.cdc.gov/Details.aspx?pid = 1879). C) Mouse testicle tissue specimen showing globe-shaped yeast cells of *T. marneffei* undergoing multiplication by binary fission not by mitosis (methenamine silver stain). Source: Libero Ajello, Centers for Disease Control and Prevention (https://phil.cdc.gov/Details.aspx?pid = 4235); D) Gradual conversion of mycelial phase of *T. marneffei* (growth at 25°C) to yeast phase on brain heart infusion agar after incubation at 37°C. Mycelial phase (first tube marked 25°C) shows diffusible red pigment. Source: Monika Mahajan, Postgraduate Institute of Medical Education and Research, Chandigarh, India; E) Loose network of hyphae of *T. marneffei* forming gymnothecium that contains asci. Source: https://istudy.pk/ascomycota-fruit-bodies/.
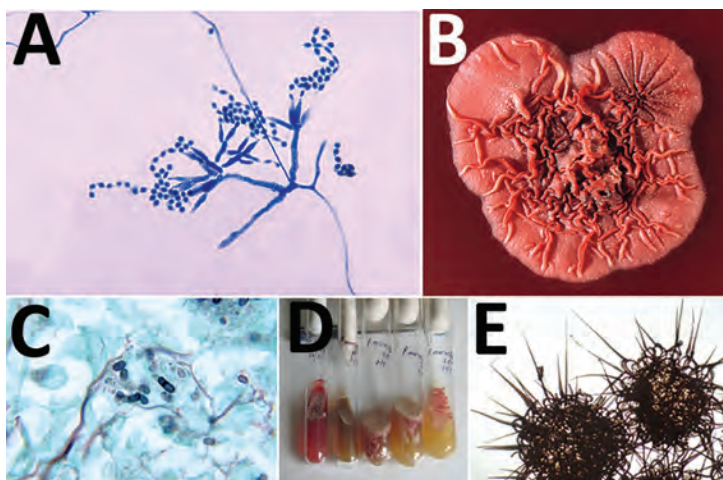
Sources

1. Pitt JI. *Penicillium* and *Talaromyces*. In: Batt C. Patel P, editors. Encyclopedia of food microbiology. New York: Elsevier; 2014. p. 6–13.
2. Talaromycosis (formerly penicilliosis) [cited 2021 Jun 10]. https://www.cdc.gov/fungal/diseases/other/talaromycosis.html
3. Tsang C-C, Lau SK, Woo PC. Sixty years from Segretain's description: what have we learned and should learn about the basic mycology of *Talaromyces marneffei?* Mycopathologia. 2019;184:721–9. https://doi.org/10.1007/s11046-019-00395-y
4. Vanittanakom N, Cooper CR Jr, Fisher MC, Sirisanthana T. *Penicillium marneffei* infection and recent advances in the epidemiology and molecular biology aspects. Clin Microbiol Rev. 2006;19:95–110. https://doi.org/10.1128/CMR.19.1.95-110.2006

Address for correspondence: Monika Mahajan, Postgraduate Institute of Medical Education and Research, Medical Microbiology, Research Block A, Sector 12, Chandigarh 160012, India; email: monideepmj@yahoo.com

Maternal Carriage in Late-Onset Group B *Streptococcus* Disease, Italy

Alberto Berardi, Caterina Spada, Roberta Creti, Cinzia Auriti, Lucia Gambini, Vittoria Rizzo, Mariagrazia Capretti, Nicola Laforgia, Irene Papa, Anna Tarocco, Angela Lanzoni, Giacomo Biasucci, Giancarlo Piccinini, Giovanna Nardella, Giuseppe Latorre, Daniele Merazzi, Laura Travan, Maria Letizia Bacchi Reggiani, Lorenza Baroni, Matilde Ciccia, Laura Lucaccioni, Lorenzo Iughetti, Licia Lugli

Author affiliations: Azienda Ospedaliero–Universitaria Policlinico, Modena, Italy (A. Berardi, C. Spada, L. Lucaccioni, L. Iughetti, L. Lugli); Istituto Superiore di Sanità, Rome, Italy (R. Creti); Ospedale Pediatrico Bambino Gesù, Rome (C. Auriti); Azienda Ospedaliero-Universitaria Policlinico, Parma, Italy (L. Gambini); Ospedale Civile M. Bufalini, Cesena, Italy (V. Rizzo); Azienda Ospedaliero–Universitaria S. Orsola–Malpighi, Bologna, Italy (M. Capretti, M.L. Bacchi Reggiani); Ospedale Policlinico, Bari, Italy (N. Laforgia); Ospedale Infermi, Rimini, Italy (I. Papa); Azienda Ospedaliero–Universitaria S. Anna, Ferrara, Italy (A. Tarocco); Ospedale Santa Maria della Scaletta, Imola, Italy (A. Lanzoni); Ospedale G. da Saliceto, Piacenza, Italy (G. Biasucci); Ospedale Santa Maria Delle Croci, Ravenna, Italy (G. Piccinini); Azienda Ospedaliero–Universitaria Ospedali Riuniti, Foggia, Italy (G. Nardella); Ospedale F. Miulli, Acquaviva delle Fonti, Italy (G. Latorre); Ospedale Valduce, Como, Italy (D. Merazzi); IRCCS Materno Infantile Burlo Garofolo, Trieste, Italy (L. Travan); Arcispedale Santa Maria Nuova, Reggio Emilia, Italy (L. Baroni); Ospedale Maggiore, Bologna (M. Ciccia)

We retrospectively investigated mother-to-infant transmission of group B *Streptococcus* (GBS) in 98 cases of late-onset disease reported during 2007–2018 by a network in Italy. Mothers with full assessment of vaginal/rectal carriage tested at prenatal screening (APS) and at time of late onset (ATLO) were included. Thirty-three mothers (33.7%) were never GBS colonized; 65 (66.3%) were vaginal/rectal colonized, of which 36 (36.7%) were persistently colonized. Mothers with vaginal/rectal colonization ATLO had high rates of GBS bacteriuria (33.9%) and positive breast milk culture (27.5%). GBS strains from mother–infant pairs were serotype III and possessed the surface protein antigen Rib. All but 1 strain belonged to clonal complex 17. GBS strains from 4 mother–infant pairs were indistinguishable through pulsed-field gel electrophoresis. At least two thirds of late-onset cases are transmitted from mothers, who often have vaginal/rectal carriage, positive breast milk culture, or GBS bacteriuria, which suggests heavy maternal colonization.

Group B *Streptococcus* (GBS; *Streptococcus agalactiae*) is a notable cause of sepsis and meningitis in infancy (*1*). Intrapartum antimicrobial prophylaxis (IAP) has substantially reduced the rates of early-onset disease (EOD; onset on day 0–6 postpartum) (*2,3*) but does not prevent late-onset disease (LOD; onset on day 7–89 postpartum) (*4*). Thus, in some settings, LOD has become the most common manifestation of neonatal GBS disease (*2,3*).

Prevention efforts are hampered by poor knowledge of both the pathogenesis of LOD and the relevance of any mode of GBS transmission. GBS can be transmitted from a mother to the neonate during passage through the birth canal or from sources other than delivery (*2*). A controversial issue concerns the transmission of GBS from a mother to the neonate in the postpartum period (*5,6*); because IAP does not eradicate maternal colonization (*5,7*), the mother remains a possible source of GBS transmission to the infant. The transmission of LOD GBS has been poorly investigated. Mothers of neonates with LOD show prenatal vaginal/rectal (VR) colonization ranging from 30% to 38% (*8,9*). However, also knowing the maternal VR status at the time of disease onset can help define the maternal carriage more precisely (*10*); this status may vary over time or, in some cases, be falsely negative at the time of screening (*11*). Breast milk has been suggested as a possible source of LOD, but its role remains controversial (*10,12–14*). It is not yet clear whether breast milk leads to LOD through repeated GBS transmission and persistent intestinal colonization (*13*) or is a marker for high levels of neonatal nasopharyngeal GBS colonization (*5*). Establishing the role of breast milk is necessary because ending breast-feeding can have long-term consequences. The literature concerning breast milk–associated cases of LOD is based almost exclusively on case reports, and we found no studies in large populations that provide stronger evidence. Finally, quantifying the burden of LOD transmitted from mothers can help in predicting the effects of future strategies, because a GBS vaccine might reduce maternal carriage (*15*).

To clarify the dynamics of GBS mother-to-infant transmission, we defined maternal carriage on the basis of VR status assessed both at the prenatal screening and at the time of disease onset with full assessment of maternal carriage. We used additional maternal cultures collected from urine and breast milk at disease onset to investigate further possible associations with neonatal LOD.

Methods

We retrospectively analyzed data from a network of hospitals in Italy. Episodes of LOD GBS are anonymously reported on a monthly basis to the coordinating center, Azienda Ospedaliero—Universitaria of Modena (Modena, Italy) (*10*). Hospitals participating in the network follow US Centers for Disease Control and Prevention (CDC) guidelines regarding antenatal GBS screening and IAP administration to women who are GBS-colonized (*11*). During January 1, 2007–December 31, 2018, we received notification of 175 cases of LOD, of which 98 had a full assessment of maternal carriage (see definitions in Appendix, https://wwwnc.cdc.gov/EID/article/27/9/21-0049-App1.pdf). We used a special form for surveillance, designed for both EOD and LOD reporting, that included patient demographics, mode of delivery, risk factors for EOD, and IAP administration. Surveillance officers extracted all clinical information from the labor and delivery records using this standardized form; they obtained any missing data by telephone from the coordinating center. To maintain patient confidentiality, spreadsheets submitted to the principal investigator were anonymous and did not include any identifiable data of patients or caregivers. The case reporting and isolate collection were determined to be non-research public health surveillance. The local ethical committee of Azienda Ospedaliero–Universitaria of Modena approved the study (no. 423/2019). We obtained a waiver of informed consent for each of the patients included.

Microbiological Methods

We processed vaginal and rectal samples according to CDC recommendations: growth in preenrichment broth and isolation in selected media. We collected and cultured breast milk samples as previously described (*10*). We processed blood, cerebrospinal fluid, and

urine cultures with automated systems, Bactec 9240 (Becton Dickinson, https://www.bd.com) and Bactalert (bioMérieux, https://www.biomerieux.com).

We sent the maternal and infant LOD GBS strains isolated at the time of onset to the National Reference Center for Streptococci at Istituto Superiore di Sanità (Rome, Italy). We performed species confirmation by determining group B Lancefield surface antigen using the Streptococcal Grouping kit (Oxoid, https://www.oxoid.com). We based serotyping on a commercial latex agglutination test, ImmuLex *Streptococcus* Group Kit (SSI Diagnostica, https://www.ssidiagnostica.com). We performed molecular typing of capsular types Ia-IX using a multiplex PCR assay (16); we identified surface protein antigens belonging to the α-like family by a multiplex PCR (17). We assessed bacterial genetic population structure by multilocus sequence typing (MLST) and, for selected strains, by pulsed-field gel electrophoresis (PFGE). We assessed antimicrobial susceptibility profile to erythromycin, clindamycin, and tetracycline as previously described (18,19). We identified pilus island gene content using PCR (20).

Maternal Cultures

We tested GBS carriage at the vaginal and rectal sites both at the prenatal screening and at the time of LOD onset in a full assessment of maternal carriage. We collected additional breast milk and urine cultures from mothers at LOD onset. We conducted molecular analyses on the available maternal GBS strains collected at the time of LOD onset.

Statistical Analyses

We used Stata/SE version 14.2 (StataCorp, https://www.stata.com) and MedCalc version 9.3 (MedCalc Software, https://www.medcalc.org). Continuous variables are expressed as mean $\pm$SD or median and interquartile range (IQR), and categorical data are expressed as numbers (percentages). We compared categorical and continuous variables across patient groups using a χ^2 test, Fisher exact test, Student t-test, or Mann-Whitney test, as appropriate. All p values refer to 2-tailed tests of significance; p<0.05 was considered significant.

Results

A full assessment of maternal carriage was available in 98 cases of LOD during 2007–2018. Most cases of LOD (89/98) came from a regional area-based surveillance in which incidence of EOD is 0.18/1,000 live births (21) and of LOD is 0.31/1,000 live births (10), and the prevalence of maternal VR colonization is 21% (22).

Eighty (81.6%) cases occurred in full-term neonates and 18 (18.4%) in preterm neonates (of which 10 were still in hospital at the time of LOD onset). Compared with full-term neonates, preterm neonates were less likely to be delivered vaginally and more likely to undergo mechanical ventilation (Table 1). Twenty mothers (3 preterm and 17 full-term) were exposed to adequate IAP; of those, 17 (85%) carried GBS at the time of LOD diagnosis.

Thirty-three (33.7%) of 98 mothers were persistently not GBS-colonized; the other 65 (66.3%) mothers were GBS-colonized, 36 (36.7%) persistently (Table 2).. Maternal VR colonization was more likely to be detected at the time of onset (58/65) than at the prenatal screening (43/65; p<0.01). At the time of LOD onset, 59.2% of mothers were colonized, 18.9% had asymptomatic GBS bacteriuria, and 20.5% had positive breast milk culture.

Table 1. Demographics and clinical data of neonates with late-onset group B *Streptococcus* disease, Italy*

Characteristic	LOD cases in preterm neonates, n = 18†	LOD cases in full-term neonates, n = 80	p value	Total, N = 98
Median birthweight, g (IQR)	1,285 (987–1,800)	3,185 (2,898–3,518)	NA	3,110 (2,570–3,425)
Gestational age at delivery, wks, median (IQR)	31.0 (27.0–33.0)	39.0 (38.0–40.0)	NA	39 (38–40)
Vaginal delivery	4 (22.2)	56 (70.0)	<0.01	60 (61.2)
Planned caesarean section	8 (44.4)	18 (22.5)	0.11	26 (26.5)
IAP exposure‡	9 (50.0)	29 (36.3)	0.42	38 (38.8)
Age at onset, median, d (IQR)	33 (26–45)	27 (15–43)	0.08	29 (16–43)
Mechanical ventilation	7 (38.9)	4 (5.0)	<0.01	11 (11.2)
Focal infection§	0	6 (7.5)	0.51	6 (6.1)
Meningitis with or without sepsis¶	8 (57.1)	32 (56.1)	0.82	40 (56.3·)
Brain lesions at discharge from hospital#	7 (38.9)	15 (18.8)	0.12	22 (22.4)
Death	1 (5.6)	1 (1.3)	0.81	2 (1.0)

*Values are no. (%) except as indicated. GBS, group B streptococcus; IAP, intrapartum antibiotic prophylaxis; IQR, interquartile range; LOD, late-onset disease; NA, not applicable.
†14 were early to moderate and 4 were late preterm neonates.
‡IAP was adequate (ampicillin, penicillin, or cefazolin given >4 h before delivery) in 3/9 (33.3%) cases in preterm neonates and in 17/29 (58.6%) cases in full-term neonates.
§GBS-positive blood culture result associated with focal signs outside the respiratory tract (cellulitis, arthritis, parotiditis, others) (10).
¶Percentage and significance were calculated based on findings from lumbar puncture (in preterm neonates, 14 cases; in full-term neonates, 57 cases). Meningitis was culture-proven in 36/40 cases.
#Brain lesions were confirmed through ultrasound, magnetic resonance study, or both.

Table 2. Maternal cultures of group B *Streptococcus*, Italy*

Culture	Preterm cases, n = 18	Missed cases	Full-term cases, n = 80	Missed cases	p value	Total cases, n = 98
Cultures before delivery						
VR tested	18 (100)	0	80 (100)	0	NA	98 (100)
Positive culture	8 (44.4)	0	35 (43.8)	0	0.83	43 (43.9)
Urine tested	18 (100)	0	74 (92.5)	6	0.51	92 (93.9)
GBS bacteriuria†	0 (0)	0	2 (2.7)	0	0.85	2 (2.2)
Cultures at onset of LOD						
VR tested	18 (100)	0	80 (100)	0	NA	98 (100)
Positive culture	7 (38.9)	0	51 (63.8)	0	0.09	58 (59.2)
Urine tested	18 (100)	0	72 (90.0)	8	0.36	90 (91.8)
GBS bacteriuria†	5 (27.8)	0	12 (16.7)	0	0.46	17 (18.9)
Breast milk tested‡	15 (83.3)	3	68 (85.0)	12	0·85	83 (84.7)
Positive culture†	2 (13.3)	0	15 (22.1)	0	0.69	17 (20.5)

*Values are no. (%) except as indicated. Samples were obtained during pregnancy (urine), at prenatal screening (VR), and at onset of LOD (urine, VR, and breast milk). GBS, group B *Streptococcus*; LOD, late-onset disease; NA, not assessible; VR, vaginal/rectal.
†Percentage and significance are calculated based on the patients who were tested.
‡Among 18 preterm neonates, 7 were exclusively fed breast milk (1 positive culture), 7 were fed pump-extracted milk (1 positive culture), 2 were fed formula milk, 1 was fed mixed breastmilk (missing culture), and 1 was fed donor human milk. Among 80 full-term neonates, 58 were exclusively fed breast milk (14 positive cultures and 1 missing culture), and 10 were fed mixed breast milk (1 positive culture and 1 missing culture).

All mothers with asymptomatic GBS bacteriuria also carried GBS at the VR site. Median urinary bacterial count was 40,000 CFU/mL (interquartile range [IQR] 10,000–100,000 CFU/mL; range 1,000–1 million CFU/mL). GBS bacteriuria was significantly more likely to be detected at the time of LOD onset (17/90 tested) rather than during pregnancy (2/92 tested; p<0.01).

Among 17 women with a positive breast milk culture, 1 mother had mastitis (1 million CFUs/mL) and 16 had no mastitis (median bacterial count 300,000 CFU/mL; IQR 100,000–725,000 CFU/mL; range 9,000–6,400,000 CFU/mL). Fourteen (82.4%) of the 17 mothers were GBS colonized at the VR site at the

prenatal screening or at the time of onset, or both, but the other 3 (17.6%) were persistently not colonized.

Urine and Breast Milk Cultures According to Maternal VR Carriage
Forty-three women tested GBS colonized at the VR site at the prenatal screening (Figure 1). At the time of LOD onset, most (36, 83.7%) were confirmed GBS-colonized at the VR site; of those, 11/34 tested (32.4%) also had GBS bacteriuria and 9/32 tested (28.1%) had positive breast milk culture.

Fifty-five women tested GBS-noncolonized at the prenatal VR screening (Figure 2). At the time of
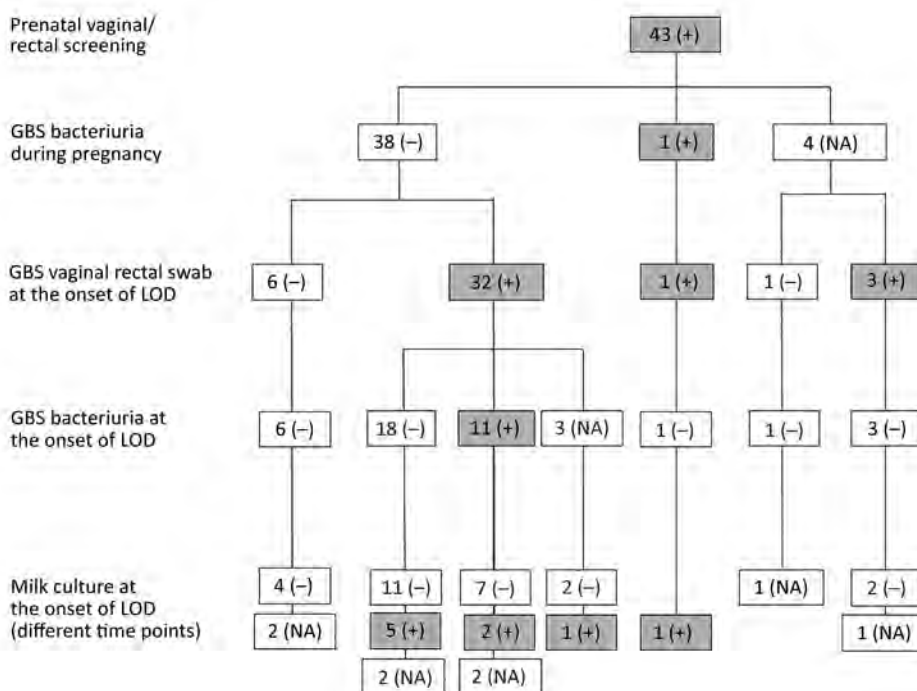
Figure 1. Longitudinal analysis of cultures obtained from women carrying GBS at the vaginal/rectal site at screening. Gray-shaded boxes represent GBS positivity. GBS, group B *Streptococcus*; LOD, late-onset disease; NA, not assessed; –, negative; +, positive.
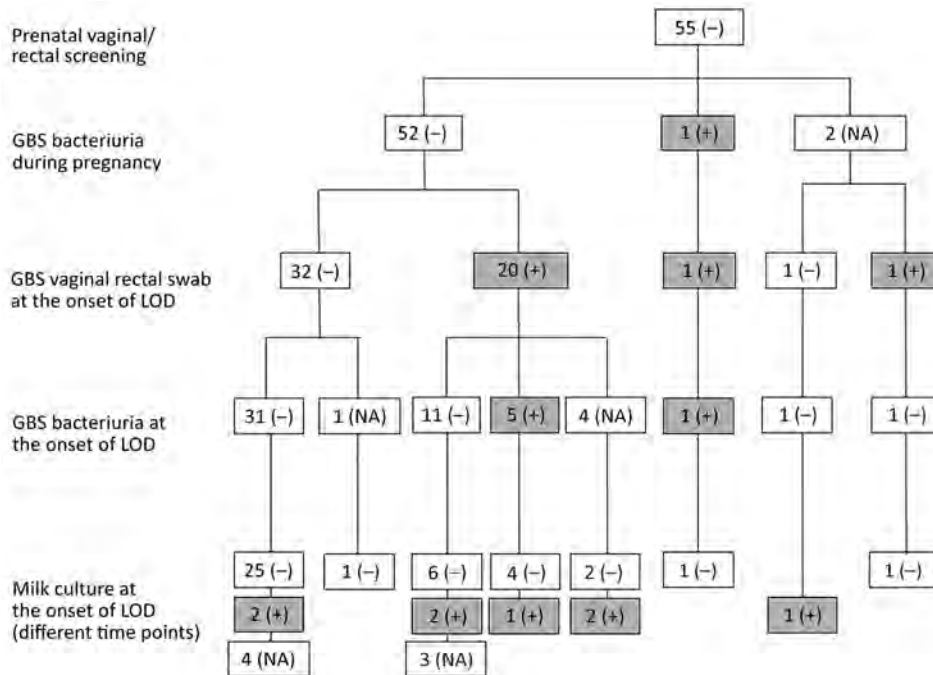
Figure 2. Longitudinal analysis of cultures obtained from women who did not carry GBS at the vaginal/rectal site at screening. GBS, group B *Streptococcus*; LOD, late-onset disease; NA, not assessed; –, negative; +, positive.

LOD onset, 40% (22/55) carried GBS at the VR site; of those, 31.6% (6/19 tested) also had GBS bacteriuria and 5/19 tested (26.3%) tested positive in the breast milk culture. Overall, we found very high frequencies of GBS bacteriuria (33.4%) and GBS-positive breast milk (27.5%) in women with VR colonization at the time of LOD onset, independent of the VR status at prenatal screening.

GBS Molecular Typing

Fifty-eight mothers were GBS colonized at the time of LOD onset, and the cultures obtained from 20 (34.5%) of them were available along with isolates from their infants for molecular typing. Overall, 57 bacterial isolates from different sources were available (Table 3). We collected 24 strains of neonatal isolates from blood, CSF, or both and collected maternal isolates from VR swab only (7 cases), milk only (3 cases), both VR swab and milk (7 cases), or both VR swab and urine (3 cases). All GBS strains were serotype III and possessed the surface protein *Rib* gene. At MLST analysis, all strains collected from mother–infant pairs were sequence type (ST) 17, which is part of the clonal complex (CC) 17 (*6,19*), except for 1 mother–infant pair whose strains were ST449. Each mother–infant pair displayed the same antimicrobial susceptibility profile; only strains from 3 pairs were resistant to both erythromycin and clindamycin, mediated by the *ermB* gene. Of note, these resistant strains were also resistant to tetracycline mediated by the *tetO*

gene and, unlike all other strains that possessed the pili island (PI) 1 and 2b, they lacked PI-1 and had only PI-2b (Table 3).

In addition, we analyzed 12 bacterial isolates from 4 mother–infant pairs by PFGE. We assigned strains within each pair the same PFGE type if they presented an identical genomic band pattern profile (*18*).

Discussion

It is crucial to understand the pathway of GBS transmission in LOD to determine the necessary interventions. We collected a large set of maternal cultures at the onset of LOD and focused on mothers with a full assessment of VR carriage. At the time of LOD onset, a substantial proportion of mothers were found to carry GBS at the VR site, although some of them were GBS-noncolonized at prenatal VR screening. Maternal GBS colonization is an important risk factor for GBS disease, and determining the extent and types of colonization is essential for the formulation of a vaccine against GBS (*8,23,24*).

Rates of maternal asymptomatic GBS bacteriuria were strikingly high (≈19%). GBS bacteriuria, which affects 2%–7% of pregnant women (*11*) (2.2% in a recent area-based study in Italy [*22*]), is a marker for heavy genital tract colonization. GBS bacteriuria is associated with an increased risk for EOD in neonates (*11*), but its role in LOD has not been previously investigated. GBS bacteriuria was present in approximately one third of the cases among

mothers with VR colonization at the time of LOD onset. This observation suggests that mothers, especially those heavily colonized, may be a main source of GBS exposure for their infants. Indeed, molecular typing indicated that GBS isolates collected from mother-infant pairs were closely related. All maternal and infant bacterial strains were serotype III and possessed the surface antigen Rib, and all but 1 pair displayed the same MLST type. The common origin of the bacterial maternal–infant pairs was confirmed by PFGE analysis when performed and the comparable antimicrobial susceptibility profile. This finding is consistent with a previous longitudinal study in 160 mother–infant pairs, which demonstrated that GBS strains isolated from healthy neonates and their mothers until 8 weeks postpartum were indistinguishable (i.e., had identical band patterns) by PFGE analyses (5). Globally, serotype III strains are clinically the most important, accounting for 25% of colonizing strains and 62% of strains causing invasive disease in infants, although geographic variation exists (1).

In this study, strains from all but 1 case belonged to clonal complex (CC) 17, a hypervirulent clonal lineage predominantly responsible for both EOD and LOD. In animal models, GBS CC17 shows higher abilities of intestinal colonization and translocation through physiologic barriers (25,26); >80% of cases of GBS serotype III LOD worldwide are caused by the hypervirulent CC17 (6,19,26,27). The emergence of a multidrug-resistant CC17 sublineage has been increasingly reported since its identification in China, Canada, and Europe (27–29); it is identifiable by the replacement of the pilus island 1 genetic locus by mobile elements carrying both *tetO* and *ermB* genes plus aminoglycoside resistance genes. The presence of the *tetO-ermB* genes along with that of PI-2b alone can be considered a marker of the emerging multidrug-resistant hypervirulent CC17 clonal lineage (27–29). Although we did not perform a detailed genomic analysis for all GBS strains, the antimicrobial resistance we detected was probably due to this multidrug-resistant CC17 subclone whose dissemination is still limited among neonatal infections in Italy. GBS resistance to clindamycin is well documented, but is relevant to only a small population of women and not to infants.

Mother-to-infant postdelivery GBS transmission can be assumed in some cases. Indeed, many neonates were born to mothers who had been exposed to IAP (which interrupts maternal-to-fetal transmission). Because maternal VR carriage at the time of late onset was confirmed in 85% of mothers who received adequate IAP, a postdelivery transmission is likely. This finding is consistent with recent studies showing risks of neonatal postpartum colonization from a maternal source (5,6,25). The importance of maternal colonization is probably greater in neonates born full-term because they have frequent and close contact with their mothers, whereas preterm neonates admitted to hospital have fewer chances for transmission of GBS during close contact with their mothers. Although in this study VR colonization

Table 3. Mother-infant pairs and isolates of group B *Streptococcus* in study of late-onset disease, Italy*

Pair	Maternal isolates			Infant isolates		Sequence type	Pili island gene content	Erythromycin resistance genes			Tetracycline resistance genes	
	Urine	VR	Breast milk	Blood	CSF			*erm*B	*erm*A	*mef*A/E	*tet*M	*tet*O
Pair 1			X	X	X	ST449	1+2b	–	–	–	+	–
Pair 2		X		X		ST17	1+2b	–	–	–	+	–
Pair 3		X	X	X		ST17	1+2b	–	–	–	+	–
Pair 4			X	X		ST17	1+2b	–	–	–	–	–
Pair 5		X	X	X	X	ST17	1+2b	–	–	–	+	–
Pair 6	X	X		X		ST17	1+2b	–	–	–	+	–
Pair 7			X	X		ST17	1+2b	–	–	–	+	–
Pair 8		X		X		ST17	1+2b	–	–	–	+	–
Pair 9	X	X		X		ST17	1+2b	–	–	–	+	–
Pair 10		X	X	X		ST17	1+2b	–	–	–	+	–
Pair 11	X	X		X		ST17	1+2b	–	–	–	–	–
Pair 12		X	X	X		ST17	1+2b	–	–	–	–	–
Pair 13		X	X	X		ST17	1+2b	–	–	–	+	–
Pair 14		X		X	X	ST17	1+2b	–	–	–	+	–
Pair 15		X		X		ST17	1+2b	–	–	–	+	–
Pair 16		X		X		ST17	1+2b	–	–	–	+	–
Pair 17		X		X		ST17	2b	+	–	–	–	+
Pair 18		X		X		ST17	1+2b	–	–	–	+	–
Pair 19		X*	X†	X		ST17	2b	+	–	–	–	+
Pair 20		X	X†	X	X	ST17	2b	+	–	–	–	+

*CSF, cerebrospinal fluid; ST, sequence type; VR, vaginal/rectal; –, negative; +, positive.
†Two samples were taken at different times.

rates at the time of LOD onset were higher in full-term mothers (64% vs. 39% in preterm mothers), the difference was not significant, perhaps because of the small sample size.

In this study, we found GBS in ≈20% of breast-feeding mothers. Mastitis in LOD was infrequent; mothers with positive breast milk culture were more often asymptomatic, although their milk bacterial counts were sometimes high. This finding suggests a silent maternal duct colonization, and it is consistent with case reports of GBS breast milk–associated LOD, in which most mothers have no sign of mastitis (*13*).

Furthermore, in our study most mothers with positive breast milk culture carried GBS at the VR site, which was often heavily colonized. Maternal VR carriage would appear to be associated with GBS transmission into breast milk, perhaps in some cases after translocation from the gastrointestinal tract through the lymphatic system to the mammary glands (*30*). In contrast, only 3 mothers who had positive breast milk culture were persistently GBS-noncolonized at the VR site. In such cases, a circular mechanism of GBS transmission to neonates could be implicated. The retrograde theory assumes that GBS, present in the infant's throat, colonizes the mammary ducts during breast-feeding; GBS load increases in the milk, and, in turn, the infant is infected during breast-feeding. Our data do not suggest that breast milk itself is a risk factor for LOD. Breast milk is known to contain immunomodulatory and antimicrobial components (*12*) (i.e., sIgA and cytokines) that may protect from LOD, and the lack of these components seems to increase the risk of persistent neonatal colonization (*31*) and LOD (*32*).

Taken all together, these results show that mothers are largely the predominant source of GBS in cases of LOD, both during childbirth (especially if IAP is not given) and in the postpartum period. GBS-positive breast milk is one of the ways by which heavily colonized mothers expose their infants to GBS.

The first limitation of our investigation is that it was an observational study without a control group. Therefore, the relevance of a positive breast milk in LOD could not be clearly assessed, because we do not know how many breastfeeding GBS-colonized mothers with healthy neonates have GBS-positive breast milk. However, Berardi et al. (*5*) found much lower rates (≈7%) of GBS-positive breast milk in a cohort of breastfeeding mothers (GBS-colonized at the VR site) who had healthy neonates. In addition, we cannot rule out an accidental contamination of some breast milk samples during collection,

although we had provided instructions for collection. Second, although we proposed doing so, we did not systematically perform full assessment of VR culture both at prenatal screening and at the time of disease onset; just over half of the mothers had the full assessment during surveillance. In fact, not all of them had prenatal screening; furthermore, the collection of cultures at the time of LOD diagnosis and then shipping the maternal strains were challenging to organize. Third, the PFGE analysis was available only in a few mother-infant pairs. However, previous studies demonstrate that the concordance of GBS strains collected from mothers and their own neonates at delivery or in the following weeks is very high, reaching ≈100% of cases (*5*,*6*,*18*). Finally, maternal colonization rates could be higher than we found as a result of inherent insufficient sensitivity of maternal VR cultures (*11*), which may lead to false-negative culture results. We did not investigate the possible role of the father in the transmission of GBS.

In conclusion, this study suggests that most cases of LOD are strictly associated with maternal VR colonization and that CC17 is the predominant clonal lineage. Rates of asymptomatic GBS bacteriuria at the time of LOD onset are strikingly high, and this finding suggests heavy maternal colonization. Positive breast milk culture is relatively common among asymptomatic breastfeeding mothers of neonates with LOD, especially if they carry GBS at the VR site. However, the causal role of breast-feeding remains uncertain, and our data do not lead to definitive conclusions. Mother-to-infant transmission may occur after delivery. Our findings call attention to maternal transmission after delivery as an underestimated source of neonatal LOD and may assist in predicting the impact of maternal GBS vaccination.

About the Author

Dr. Berardi is the head of the Unità Operativa di Terapia Intensiva Neonatale, Azienda Ospedaliero—Universitaria Policlinico di Modena, Italy. His primary research interests are group B *Streptococcus*, early- and late-onset sepsis, and neonatal infections.

References

1. Madrid L, Seale AC, Kohli-Lynch M, Edmond KM, Lawn JE, Heath PT, et al.; Infant GBS Disease Investigator Group. Infant group B streptococcal disease incidence and serotypes worldwide: systematic review and meta-analyses. Clin Infect Dis. 2017;65(suppl_2):S160–72. https://doi.org/10.1093/cid/cix656

2. Puopolo KM, Lynfield R, Cummings JJ; Committee on Fetus and Newborn; Committee on Infectious Diseases. Management of infants at risk for group B streptococcal disease. Pediatrics. 2019;144:e20191881. https://doi.org/10.1542/peds.2019-1881

3. Nanduri SA, Petit S, Smelser C, Apostol M, Alden NB, Harrison LH, et al. Epidemiology of invasive early-onset and late-onset group B streptococcal disease in the United States, 2006 to 2015: multistate laboratory and population-based surveillance. JAMA Pediatr. 2019;173:224–33. https://doi.org/10.1001/jamapediatrics.2018.4826

4. Seale AC, Bianchi-Jassir F, Russell NJ, Kohli-Lynch M, Tann CJ, Hall J, et al. Estimates of the burden of group B streptococcal disease worldwide for pregnant women, stillbirths, and children. Clin Infect Dis. 2017;65:suppl_2:S200–S219. https://doi.org/10.1093/cid/cix664

5. Berardi A, Rossi C, Creti R, China M, Gherardi G, Venturelli C, et al. Group B streptococcal colonization in 160 mother-baby pairs: a prospective cohort study. J Pediatr. 2013;163:1099–104.e1. https://doi.org/10.1016/j.jpeds.2013.05.064

6. Tazi A, Plainvert C, Anselem O, Ballon M, Marcou V, Seco A, et al. Risk factors for infant colonization by hypervirulent CC17 group B Streptococcus: toward the understanding of late-onset disease. Clin Infect Dis. 2019;69:1740–8. https://doi.org/10.1093/cid/ciz033

7. Manning SD, Lewis MA, Springman AC, Lehotzky E, Whittam TS, Davies HD. Genotypic diversity and serotype distribution of group B Streptococcus isolated from women before and after delivery. Clin Infect Dis. 2008;46:1829–37. https://doi.org/10.1086/588296

8. Lin FY, Weisman LE, Troendle J, Adams K. Prematurity is the major risk factor for late-onset group B Streptococcus disease. J Infect Dis. 2003;188:267–71. https://doi.org/10.1086/376457

9. Joubrel C, Tazi A, Six A, Dmytruk N, Touak G, Bidet P, et al. Group B Streptococcus neonatal invasive infections, France 2007–2012. Clin Microbiol Infect. 2015;21:910–6. https://doi.org/10.1016/j.cmi.2015.05.039

10. Berardi A, Rossi C, Lugli L, Creti R, Bacchi Reggiani ML, Lanari M, et al.; GBS Prevention Working Group, Emilia-Romagna. Group B Streptococcus late-onset disease: 2003–2010. Pediatrics. 2013;131:e361–8. https://doi.org/10.1542/peds.2012-1231

11. Verani JR, McGee L, Schrag SJ; Division of Bacterial Diseases, National Center for Immunization and Respiratory Diseases, Centers for Disease Control and Prevention (CDC). Prevention of perinatal group B streptococcal disease—revised guidelines from CDC, 2010. MMWR Recomm Rep. 2010;59(RR-10):1–36.

12. Le Doare K, Kampmann B. Breast milk and group B streptococcal infection: vector of transmission or vehicle for protection? Vaccine. 2014;32:3128–32. https://doi.org/10.1016/j.vaccine.2014.04.020

13. Filleron A, Lombard F, Jacquot A, Jumas-Bilak E, Rodière M, Cambonie G, et al. Group B streptococci in milk and late neonatal infections: an analysis of cases in the literature. Arch Dis Child Fetal Neonatal Ed. 2014;99:F41–7. https://doi.org/10.1136/archdischild-2013-304362

14. Zimmermann P, Gwee A, Curtis N. The controversial role of breast milk in GBS late-onset disease. J Infect. 2017;74(Suppl 1):S34–40. https://doi.org/10.1016/S0163-4453(17)30189-5

15. Le Doare K, Kampmann B, Vekemans J, Heath PT, Goldblatt D, Nahm MH, et al. Serocorrelates of protection against infant group B Streptococcus disease. Lancet Infect Dis. 2019;19:e162–71. https://doi.org/10.1016/S1473-3099(18)30659-5

16. Imperi M, Pataracchia M, Alfarone G, Baldassarri L, Orefici G, Creti R. A multiplex PCR assay for the direct identification of the capsular type (Ia to IX) of Streptococcus agalactiae. J Microbiol Methods. 2010;80:212–4. https://doi.org/10.1016/j.mimet.2009.11.010

17. Creti R, Fabretti F, Orefici G, von Hunolstein C. Multiplex PCR assay for direct identification of group B streptococcal alpha-protein-like protein genes. J Clin Microbiol. 2004;42:1326–9. https://doi.org/10.1128/JCM.42.3.1326-1329.2004

18. Imperi M, Gherardi G, Berardi A, Baldassarri L, Pataracchia M, Dicuonzo G, et al. Invasive neonatal GBS infections from an area-based surveillance study in Italy. Clin Microbiol Infect. 2011;17:1834–9. https://doi.org/10.1111/j.1469-0691.2011.03479.x

19. Creti R, Imperi M, Berardi A, Pataracchia M, Recchia S, Alfarone G, et al.; Italian Neonatal GBS Infections Working Group. Neonatal group B Streptococcus infections. Pediatr Infect Dis J. 2017;36:256–62. https://doi.org/10.1097/INF.0000000000001414

20. Springman AC, Lacher DW, Waymire EA, Wengert SL, Singh P, Zadoks RN, et al. Pilus distribution among lineages of group B Streptococcus: an evolutionary and clinical perspective. BMC Microbiol. 2014;14:159. https://doi.org/10.1186/1471-2180-14-159

21. Berardi A, Baroni L, Bacchi Reggiani ML, Ambretti S, Biasucci G, Bolognesi S, et al.; GBS Prevention Working Group Emilia-Romagna. The burden of early-onset sepsis in Emilia-Romagna (Italy): a 4-year, population-based study. J Matern Fetal Neonatal Med. 2016;29:3126–31. https://doi.org/10.3109/14767058.2015.1114093

22. Berardi A, Rossi C, Bacchi Reggiani ML, Bastelli A, Capretti MG, Chiossi C, et al. An area-based study on intrapartum antibiotic prophylaxis for preventing group B streptococcus early-onset disease: advances and limitations. J Matern Fetal Neonatal Med. 2017;30:1739–44. https://doi.org/10.1080/14767058.2016.1224832

23. Khatami A, Randis TM, Tavares L, Gegick M, Suzman E, Ratner AJ. Vaginal co-colonization with multiple group B Streptococcus serotypes. Vaccine. 2019;37:409–11. https://doi.org/10.1016/j.vaccine.2018.12.001

24. Carreras-Abad C, Cochet M, Hall T, Ramkhelawon L, Khalil A, Peregrine E, et al. Developing a serocorrelate of protection against invasive group B streptococcus disease in pregnant women: a feasibility study. Health Technol Assess. 2019;23:1–40. https://doi.org/10.3310/hta23670

25. Ratner AJ. Enhanced postnatal acquisition of hypervirulent group B Streptococcus. Clin Infect Dis. 2019;69:1749–51. https://doi.org/10.1093/cid/ciz035

26. Tazi A, Disson O, Bellais S, Bouaboud A, Dmytruk N, Dramsi S, et al. The surface protein HvgA mediates group B Streptococcus hypervirulence and meningeal tropism in neonates. J Exp Med. 2010;207:2313–22. https://doi.org/10.1084/jem.20092594

27. Campisi E, Rosini R, Ji W, Guidotti S, Rojas-López M, Geng G, et al. Genomic analysis reveals multi-drug resistance clusters in group B Streptococcus CC17 hypervirulent isolates

causing neonatal invasive disease in southern mainland China. Front Microbiol. 2016;7:1265. https://doi.org/10.3389/fmicb.2016.01265

28. Martins ER, Pedroso-Roussado C, Melo-Cristino J, Ramirez M; Portuguese Group for the Study of Streptococcal Infections. *Streptococcus agalactiae* causing neonatal infections in Portugal (2005–2015): diversification and emergence of a CC17/PI-2b multidrug resistant sublineage. Front Microbiol. 2017;8:499. https://doi.org/10.3389/fmicb.2017.00499

29. Teatero S, Ramoutar E, McGeer A, Li A, Melano RG, Wasserscheid J, et al. Clonal complex 17 group B *Streptococcus* strains causing invasive disease in neonates and adults originate from the same genetic pool. Sci Rep. 2016;6:20047. https://doi.org/10.1038/srep20047

30. Perez PF, Doré J, Leclerc M, Levenez F, Benyacoub J, Serrant P, et al. Bacterial imprinting of the neonatal immune system: lessons from maternal cells? Pediatrics. 2007;119:e724–32. https://doi.org/10.1542/peds.2006-1649

31. Le Doare K, Bellis K, Faal A, Birt J, Munblit D, Humphries H, et al. SIgA, TGF-β1, IL-10, and TNFα in colostrum are associated with infant group B *Streptococcus* colonization. Front Immunol. 2017;8:1269–79. https://doi.org/10.3389/fimmu.2017.01269

32. Dangor Z, Khan M, Kwatra G, Izu A, Nakwa F, Ramdin T, et al. The association between breast milk group B streptococcal capsular antibody levels and late-onset disease in young infants. Clin Infect Dis. 2020;70:1110–4.

Address for correspondence: Alberto Berardi, Unità Operativa di Terapia Intensiva Neonatale, Azienda Ospedaliero-Universitaria Policlinico di Modena, Via del Pozzo, 71-41124 Modena, Italy; email: alberto.berardi@unimore.it

etymologia revisited

Coronavirus

The first coronavirus, avian infectious bronchitis virus, was discovered in 1937 by Fred Beaudette and Charles Hudson. In 1967, June Almeida and David Tyrrell performed electron microscopy on specimens from cultures of viruses known to cause colds in humans and identified particles that resembled avian infectious bronchitis virus. Almeida coined the term "coronavirus," from the Latin corona ("crown"), because the glycoprotein spikes of these viruses created an image similar to a solar corona. Strains that infect humans generally cause mild symptoms. However, more recently, animal coronaviruses have caused outbreaks of severe respiratory disease in humans, including severe acute respiratory syndrome (SARS), Middle East respiratory syndrome (MERS), and 2019 novel coronavirus disease (COVID-19).

Originally published in May 2020

Sources:
1. Almeida JD, Tyrrell DA. The morphology of three previously uncharacterized human respiratory viruses that grow in organ culture. J Gen Virol. 1967;1:175–8. https://doi.org/10.1099/0022-1317-1-2-175
2. Beaudette FR, Hudson CB. Cultivation of the virus of infectious bronchitis. J Am Vet Med Assoc. 1937;90:51–8.
3. Estola T. Coronaviruses, a new group of animal RNA viruses. Avian Dis. 1970;14:330–6. https://doi.org/10.2307/1588476
4. Groupe V. Demonstration of an interference phenomenon associated with infectious bronchitis virus of chickens. J Bacteriol. 1949;58:23–32. https://doi.org/10.1128/JB.58.1.23-32.1949

Transmission of Severe Acute Respiratory Syndrome Coronavirus 2 to Close Contacts, China, January–February 2020

Yu Li,[1] Jianhua Liu,[1] Zhongcheng Yang,[1] Jianxing Yu, Chengzhong Xu, Aiqin Zhu,
Hao Zhang, Xiaokun Yang, Xin Zhao, Minrui Ren, Zhili Li, Jinzhao Cui, Hongting Zhao,
Xiang Ren, Chengxi Sun, Ying Cheng, Qiulan Chen, Zhaorui Chang, Junling Sun,
Lance E. Rodewald, Liping Wang, Luzhao Feng, George F. Gao,[2] Zijian Feng,[2] Zhongjie Li

We estimated the symptomatic, PCR-confirmed secondary attack rate (SAR) for 2,382 close contacts of 476 symptomatic persons with coronavirus disease in Yichang, Hubei Province, China, identified during January 23–February 25, 2020. The SAR among all close contacts was 6.5%; among close contacts who lived with an index case-patient, the SAR was 10.8%; among close-contact spouses of index case-patients, the SAR was 15.9%. The SAR varied by close contact age, from 3.0% for those <18 years of age to 12.5% for those $\geq$60 years of age. Multilevel logistic regression showed that factors significantly associated with increased SAR were living together, being a spouse, and being $\geq$60 years of age. Multilevel regression did not support SAR differing significantly by whether the most recent contact occurred before or after the index case-patient's onset of illness (p = 0.66). The relatively high SAR for coronavirus disease suggests relatively high virus transmissibility.

Transmissibility of an emerging infectious disease is a key factor for determining transmission dynamics in a population. The basic reproductive number, R_0, indicates the average number of new cases resulting from 1 infected person in a completely susceptible population (1). In December 2019, an outbreak of coronavirus disease (COVID-19), caused by severe acute respiratory syndrome coronavirus

2 (SARS-CoV-2), was identified in Wuhan, Hubei Province, China (2). The mean R_0 of COVID-19 was estimated to be in the range of 1.90–6.49 (3), indicating a high contagiousness that led to its rapid spread across the world (4). Another indicator of infectiousness is secondary attack rate (SAR), which is the probability that infection occurs among susceptible persons within a reasonable incubation period after known contact with an infectious person or an infectious source (5,6). Few estimates are available for the SAR for COVID-19 and its variation by type of contact, characteristics of index case-patients and contacts, and other factors. Information about factors associated with variation in SAR could help identify persons at high risk of transmitting the virus or acquiring COVID-19. Studies have reported transmission during the incubation period of COVID-19 (7–10) but with unclear quantification of risk. We estimated the SAR for COVID-19 and factors associated with risk for transmission.

Methods

We conducted this study from January 23 through February 25, 2020, in Yichang, Hubei Province, China; the city has a population of ≈4 million. In accordance with National Health Commission guidelines for prevention and control of COVID-19 (http://www.gov.cn/xinwen/2020-01/23/content_5471768.htm), close contacts of COVID-19 case-patients were placed under 14-day quarantine for medical observation, during which time they would be tested by PCR for SARS-CoV-2 one time if illness symptoms developed

Author affiliations: Chinese Center for Disease Control and Prevention, Beijing, China (Y. Li, J. Yu, A. Zhu, X. Yang, M. Ren, Zhili Li, J. Cui, H. Zhao, X. Ren, C. Sun, Y. Cheng, Q. Chen, Z. Chang, J. Sun, L.E. Rodewald, L. Wang, L. Feng, G.F. Gao, Z. Feng, Zhongjie Li); Yichang Center for Disease Control and Prevention, Yichang, China (J. Liu, Z. Yang, C. Xu, H. Zhang, X. Zhou)

[1]These authors contributed equally to this article.
[2]These authors are the senior authors.

but not tested if illness symptoms did not develop during the quarantine period.

Nasopharyngeal and pharyngeal swab samples from symptomatic quarantined persons were obtained and placed in airtight, freeze-tolerant tubes containing 3.5 mL of UTM (universal transport medium) viral transport medium. Sealed tubes were transported to the Yichang Center for Disease Control and Prevention laboratory (Yichang, China) within 24 hours of specimen collection. Viral RNA was extracted from samples and tested by using a commercial SARS-CoV-2 PCR diagnostic kit (Bioperfectus Technologies, https://www.bioperfectus.com) according to the manufacturer's instructions. The commercial kit targets the open reading frame 1ab and nucleocapsid protein genes of the SARS-CoV-2 genome.

An index case-patient was defined as a person in this study with a positive SARS-CoV-2 PCR result. A close contact was defined as someone who had contact with an index case-patient without effective protection and within 1 meter, regardless of contact duration. Persons who had close contact with the index case-patient during or 2 days before the index case-patient's illness onset were counted as close contacts. Secondary case-patients were close contacts with positive SARS-CoV-2 test results.

The types of contacts were considered mutually exclusive and were living together in the same household as an index case-patient, eating together (having meals together at a party, in a restaurant, or in another setting), caring for a patient (including doctors, nurses, and family members taking care of patients), sharing a vehicle (riding the same vehicle with an index case-patient but with no other close contact), or staying in a confined space (in the same confined space with an index case-patient, excluding in a vehicle, and with no other close contact). We included in our analyses close contacts who had completed their 14-day quarantine or who had positive SARS-CoV-2 results during quarantine in our study period. We excluded from our analyses close contacts of suspected case-patients for whom laboratory evidence of COVID-19 was lacking. We also excluded close contacts of >1 index case-patient or those whose information about contact type was missing.

We estimated the SAR by dividing the number of secondary cases by the number of close contacts. SAR in our study refers to secondary case-patients who had symptomatic, PCR-confirmed infection. We estimated the SAR for each type of close contact, tested statistical significance of differences by using χ^2 or Fisher exact tests as appropriate, and considered $p < 0.05$ to be significant. We further analyzed factors significantly associated with SAR in univariate analyses with multilevel logistic regression mixed-effect models. We estimated crude and adjusted odds ratios (ORs) and 95% CIs, accounting for random effects of index case-patients.

Surveillance and analysis of close contacts of COVID-19 case-patients is part of public health surveillance in China. These procedures are exempted from need for institutional review board approval.

Results

We included in our analyses 2,382 close contacts of 476 symptomatic index case-patients, all of whom completed their 14-day quarantine with assessed outcomes and who provided contact-related information (Figure). Close contacts were generally younger and more likely to be female than their corresponding
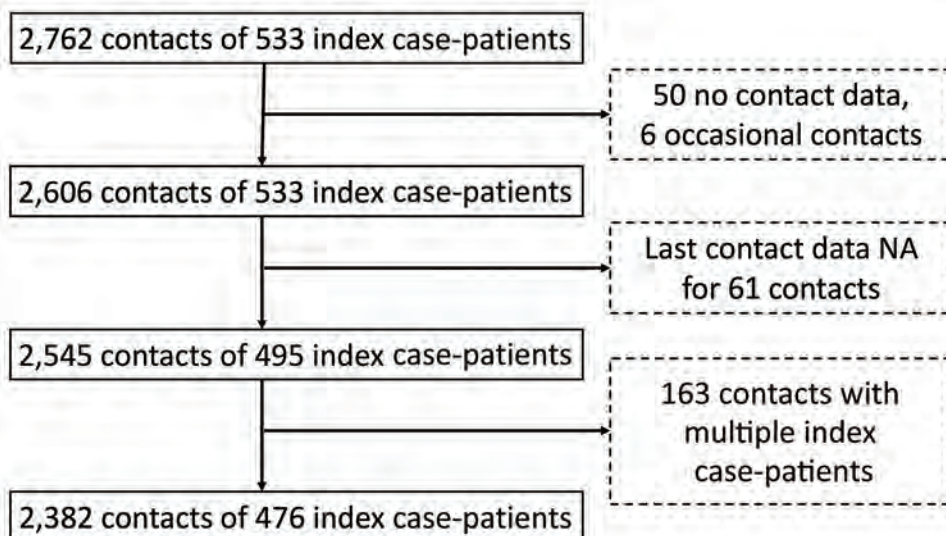
Figure. Enrollment of close contacts in study of transmission of severe acute respiratory syndrome coronavirus 2 to close contacts, China, January–February 2020.

Table 1. Characteristics of 476 index case-patients and 2,382 close contacts in study of transmission of severe acute respiratory syndrome coronavirus 2 to close contacts, China, January–February 2020*

Characteristic	Index case-patients	Close contacts
Age, y, mean (range)	49 (2–91)	43 (0–94)
Age group, y		
<18	5 (1)	267 (12)
18–59	339 (71)	1,559 (68)
≥60	132 (28)	465 (20)
Sex		
M	262 (55)	1,162 (49)
F	214 (45)	1,198 (51)
*Values are no. (%) unless otherwise indicated.		

index case-patients (Table 1). The overall SAR was 6.5%. SAR was 10.8% among close contacts who lived together with an index case-patient; this rate was significantly higher than that for other contact types, for which SAR ranged from 1.5% to 4.0% (Table 2). The SAR was 15.9% among spouses of index case-patients. SAR did not differ by sex of close contacts or of index case-patients. SAR increased with age, from 3.0% among close contacts <18 years of age to 12.5% among close contacts ≥60 years of age. A similar pattern by age was found for index case-patients (Table 2).

The SAR was 4.7% for close contacts whose most recent contact with an index case-patient was during the index case-patient's incubation period, compared

with a SAR of 7.3% for close contacts for whom the most recent contact occurred after index case-patient illness onset (p = 0.023). In multilevel univariate analysis that accounted for index case-patient variation, the pattern of ORs for factors associated with SAR was similar to the pattern described above (Table 3). In multilevel analysis that used a multivariate model with age of close contact, adjusted ORs for the following differed slightly from those for the univariate analysis: age of index case-patient, type of contact, whether the close contact and the index case-patient were spouses, and most recent contact time between close contact and index case-patient. Associations between SAR and the most recent contact time with the index case-patient (before/after illness onset) and age of the index case-patients (<60 years/≥60 years) were no longer statistically significant, although the directions of the associations were the same (Table 3). The associations of SAR with age of contact, living together with an index case-patient, and being the spouse of an index case-patient were still significant, although the point estimates of the adjusted ORs became smaller (Table 3).

Discussion

We found the SAR among all close contacts to be 6.5%. Because confirmed case-patients were centrally

Table 2. Secondary attack rate for coronavirus disease, overall and by characteristic, China, January–February 2020

Characteristic	Close contacts, no.	Secondary cases, no. (%)	p value
Overall	2,382	156 (6.5)	
Contact			
Type of contact			<0.001
Living together	1,020	110 (10.8)	
Eating together	835	33 (4.0)	
Care	80	2 (2.5)	
Sharing vehicle	68	1 (1.5)	
Stay in a confined space	379	10 (2.6)	
Most recent contact with index case-patient			0.023
Before illness onset	686	32 (4.7)	
After illness onset	1,696	124 (7.3)	
Whether contacts and index case-patients were spouses			<0.001
No	2,105	112 (5.3)	
Yes	277	44 (15.9)	
Close contacts			
Age			<0.001
<18 y	267	8 (3.0)	
18–59 y	1,559	89 (5.7)	
≥60 y	465	58 (12.5)	
Sex			0.644
M	1,162	71 (6.1)	
F	1,198	83 (6.9)	
Index case-patients			
Age			<0.001
<18 y	86	0	
18–59 y	1,747	90 (5.2)	
≥60 y	549	66 (12.0)	
Sex			0.704
M	1,303	82 (6.3)	
F	1,079	74 (6.9)	

Table 3. Univariate and multivariate analyses of factors associated with secondary attack rate for coronavirus disease, China, January–February 2020*

Characteristic of contact	Univariate		Multivariate†	
	Crude OR (95% CI)	p value	Adjusted OR (95% CI)	p value
Type of contact				
Not living together	Referent		Referent	
Living together	7.85 (3.89–15.83)	<0.01	5.12 (2.11–12.45)	<0.01
Spouse of index case-patient				
No	Referent		Referent	
Yes	6.46 (3.30–12.61)	<0.01	2.83 (1.31–6.11)	<0.01
Age of contact, y				
<60	Referent		Referent	
≥60	3.29 (1.86–5.82)	<0.01	2.61 (1.43–4.78)	0.01
Age of index case-patient, y				
<60	Referent		Referent	
≥60	5.13 (1.66–15.86)	<0.01	2.92 (0.80–10.59)	0.1
Most recent contact with index case-patient				
Before illness	Referent		Referent	
After illness	2.20 (1.06–4.59)	0.03	1.23 (0.49–3.07)	0.66

*Multilevel logistic regression model of mixed effects accounted for random effects of index cases. OR, odds ratio.
†Other covariates included in the model were contact type, whether the contact was a spouse of the index case-patient, age of contact, age of index case-patient, and most recent contact with index case-patient.

isolated and away from home, the SAR we measured may be lower than it would have been under conditions of home isolation. Factors independently associated with significantly higher risk of contracting COVID-19 were living in the same house as an index case-patient, being a spouse of an index case-patient, and being older. We found evidence of presymptomatic transmission, in which close contacts who only had contact with a COVID-19 case-patient during the incubation period subsequently had positive SARS-CoV-2 test results. The SAR among these close contacts was 4.7%, significantly lower than that for contacts whose most recent contact occurred after illness onset of the index case-patient.

We estimated the COVID-19 SAR in a household to be 10.8%, slightly higher than SAR estimates for seasonal influenza and pandemic influenza (H1N1) viruses in Hong Kong (*11*). Our results suggest that transmissibility of SARS-CoV-2 might be similar or slightly higher than that of influenza virus, which has a SAR of ≈10% in the household setting (*11*). This similarity is consistent with the finding that the R_0 for COVID-19 is also similar to or slightly higher than that for influenza (*12*). In contrast, the SAR in households is estimated to be 2%–7% for Middle East respiratory syndrome (*13*) and 6.2% for severe acute respiratory syndrome (*14*), suggesting slightly weaker transmissibility compared with COVID-19.

Our findings corroborated transmissibility of SARS-CoV-2 during the COVID-19 incubation period. Viral shedding has been observed during the CO-VID-19 incubation period (*15,16*). Our results were consistent with those of another study that estimated that 40% of the transmission events in COVID-19 clusters were attributed to presymptomatic virus

transmission in China (*17*). Our multivariate analysis did not find statistically significant differences in SAR before and after illness onset, which is consistent with a SAR study in southern China that found infectivity during the incubation period to not differ statistically from infectivity after illness onset. Although respiratory signs such as coughing and sneezing after illness onset increased the probability of virus transmission compared with during the incubation period (*18–20*), studies suggest that viral load peaks right before illness onset (*10,21*), highlighting the threat for presymptomatic SARS-CoV-2 transmission.

Risk of contracting COVID-19 was positively associated with intimacy between contacts and index case-patients. Living in the same household with index case-patients considerably increased risk for COVID-19. Being a spouse of an index case-patient independently increased the risk of contracting COVID-19, consistent with findings from another study (P. Cui et al., unpub. data, https://www.medrxiv.org/content/10.1101/2020.02.26.20028225v2). However, the SAR was relatively low among contacts who provided care to patients, implying that risk for infection can be reduced by using protective equipment and by protective behaviors.

Previous studies indicated that age was associated with risk for severe and fatal infection (*22*); however, few studies directly assessed the effect of age on risk of contracting COVID-19. Our study confirmed that senior persons are at high risk for contracting COVID-19, highlighting the need to pay special attention to facilities with numerous seniors, such as nursing homes. However, our findings also suggested that older age does not necessarily increase the risk of transmitting the virus; our multivariate analysis

found that the association between older age of index case-patients and SAR was not statistically significant, a finding consistent with a study showing that viral loads did not differ significantly by age (10).

The first limitation of our study is that for surveillance of close contacts, laboratory testing was initiated only when the contacts showed symptoms of illness. Asymptomatic infections with SARS-CoV-2 occur; for example, 1 study estimated that 17.9% of persons infected with SARS-CoV-2 did not have any symptoms (23). Therefore, our study will have missed asymptomatic case-patients and therefore underestimated the true SAR. Our estimates should therefore be interpreted as SAR limited to secondary case-patients with symptomatic COVID-19. The second limitation is that SAR is determined not only by infectiousness of the virus but also by protection levels, which might differ by geography, phase of the pandemic, education level of persons at risk, perceived threat from COVID-19, and other confounding factors. The third limitation is that the number of index case-patients <18 years of age and corresponding contacts was small; thus, our estimates of SAR for COVID-19 are more representative of transmissibility among adults than among children.

In conclusion, the SAR for COVID-19 is relatively high, suggesting relatively high transmissibility. This SAR is influenced by type of contact, level of intimacy between case-patients and contact, and age of contact. Our results provide additional evidence that SARS-CoV-2 can be transmitted by presymptomatic persons.

About the Author
Dr. Yu Li is an epidemiologist in the Division of Infectious Diseases of China CDC. His primary interests include the epidemiology and transmission dynamics of hand, foot, and mouth disease; zoonotic and vector-borne diseases such as rabies, dengue, anthrax; and fever with thrombocytopenia syndrome.

References
1. Delamater PL, Street EJ, Leslie TF, Yang YT, Jacobsen KH. Complexity of the basic reproduction number (R_0). Emerg Infect Dis. 2019;25:1–4. https://doi.org/10.3201/eid2501.171901
2. Zhu N, Zhang D, Wang W, Li X, Yang B, Song J, et al.; China Novel Coronavirus Investigating and Research Team. A novel coronavirus from patients with pneumonia in China, 2019. N Engl J Med. 2020;382:727–33. https://doi.org/10.1056/NEJMoa2001017
3. Alimohamadi Y, Taghdir M, Sepandi M. Estimate of the basic reproduction number for COVID-19: a systematic review and meta-analysis. J Prev Med Public Health. 2020;53:151–7. https://doi.org/10.3961/jpmph.20.076
4. Sanche S, Lin YT, Xu C, Romero-Severson E, Hengartner N, Ke R. High contagiousness and rapid spread of severe acute respiratory syndrome coronavirus 2. Emerg Infect Dis. 2020;26:1470–7. https://doi.org/10.3201/eid2607.200282
5. Yom-Tov E, Johansson-Cox I, Lampos V, Hayward AC. Estimating the secondary attack rate and serial interval of influenza-like illnesses using social media. Influenza Other Respir Viruses. 2015;9:191–9. https://doi.org/10.1111/irv.12321
6. Yang Y, Sugimoto JD, Halloran ME, Basta NE, Chao DL, Matrajt L, et al. The transmissibility and control of pandemic influenza A (H1N1) virus. Science. 2009;326:729–33. https://doi.org/10.1126/science.1177373
7. Buitrago-Garcia D, Egli-Gany D, Counotte MJ, Hossmann S, Imeri H, Ipekci AM, et al. Occurrence and transmission potential of asymptomatic and presymptomatic SARS-CoV-2 infections: a living systematic review and meta-analysis. PLoS Med. 2020;17:e1003346. https://doi.org/10.1371/journal.pmed.1003346
8. Furukawa NW, Brooks JT, Sobel J. Evidence supporting transmission of severe acute respiratory syndrome coronavirus 2 while presymptomatic or asymptomatic. Emerg Infect Dis. 2020;26. https://doi.org/10.3201/eid2607.201595
9. Sun K, Wang W, Gao L, Wang Y, Luo K, Ren L, et al. Transmission heterogeneities, kinetics, and controllability of SARS-CoV-2. Science. 2021;371:24. https://doi.org/10.1126/science.abe2424
10. He X, Lau EHY, Wu P, Deng X, Wang J, Hao X, et al. Temporal dynamics in viral shedding and transmissibility of COVID-19. Nat Med. 2020; 26:672–5. https://doi.org/10.1038/s41591-020-0869-5
11. Cowling BJ, Chan KH, Fang VJ, Lau LLH, So HC, Fung ROP, et al. Comparative epidemiology of pandemic and seasonal influenza A in households. N Engl J Med. 2010;362:2175–84. https://doi.org/10.1056/NEJMoa0911530
12. White LF, Wallinga J, Finelli L, Reed C, Riley S, Lipsitch M, et al. Estimation of the reproductive number and the serial interval in early phase of the 2009 influenza A/H1N1 pandemic in the USA. Influenza Other Respir Viruses. 2009; 3:267–76. https://doi.org/10.1111/j.1750-2659.2009.00106.x

13. Hui DS, Azhar EI, Kim YJ, Memish ZA, Oh MD, Zumla A. Middle East respiratory syndrome coronavirus: risk factors and determinants of primary, household, and nosocomial transmission. Lancet Infect Dis. 2018;18:e217–27. https://doi.org/10.1016/S1473-3099(18)30127-0

14. Goh DL, Lee BW, Chia KS, Heng BH, Chen M, Ma S, et al. Secondary household transmission of SARS, Singapore. Emerg Infect Dis. 2004;10:232–4. https://doi.org/10.3201/eid1002.030676

15. Hu Z, Song C, Xu C, Jin G, Chen Y, Xu X, et al. Clinical characteristics of 24 asymptomatic infections with COVID-19 screened among close contacts in Nanjing, China. Sci China Life Sci. 2020;63:706-11.

16. Pan Y, Zhang D, Yang P, Poon LLM, Wang Q. Viral load of SARS-CoV-2 in clinical samples. Lancet Infect Dis. 2020;20:411–2. https://doi.org/10.1016/S1473-3099(20)30113-4

17. Ren X, Li Y, Yang X, Li Z, Cui J, Zhu A, et al. Evidence for pre-symptomatic transmission of coronavirus disease 2019 (COVID-19) in China. Influenza Other Respir Viruses. 2020;15:19–26. https://doi.org/10.1111/irv.12787

18. Lindsley WG, Blachere FM, Thewlis RE, Vishnu A, Davis KA, Cao G, et al. Measurements of airborne influenza virus in aerosol particles from human coughs. PLoS One. 2010;5:e15100. https://doi.org/10.1371/journal.pone.0015100

19. To KK, Tsang OT, Yip CC, Chan KH, Wu TC, Chan JM, et al. Consistent detection of 2019 novel coronavirus in saliva. Clin Infect Dis. 2020;71:841–3. https://doi.org/10.1093/cid/ciaa149

20. Yan J, Grantham M, Pantelic J, Bueno de Mesquita PJ, Albert B, Liu F, et al.; EMIT Consortium. Infectious virus in exhaled breath of symptomatic seasonal influenza cases from a college community. Proc Natl Acad Sci U S A. 2018;115:1081–6. https://doi.org/10.1073/pnas.1716561115

21. Arons MM, Hatfield KM, Reddy SC, Kimball A, James A, Jacobs JR, et al.; Public Health–Seattle and King County and CDC COVID-19 Investigation Team. Presymptomatic SARS-CoV-2 infections and transmission in a skilled nursing facility. N Engl J Med. 2020;382:2081–90. https://doi.org/10.1056/NEJMoa2008457

22. Zhou F, Yu T, Du R, Fan G, Liu Y, Liu Z, et al. Clinical course and risk factors for mortality of adult inpatients with COVID-19 in Wuhan, China: a retrospective cohort study. Lancet. 2020;395:1054–62. https://doi.org/10.1016/S0140-6736(20)30566-3

23. Mizumoto K, Kagaya K, Zarebski A, Chowell G. Estimating the asymptomatic proportion of coronavirus disease 2019 (COVID-19) cases on board the Diamond Princess cruise ship, Yokohama, Japan, 2020. Euro Surveill. 2020;25. https://doi.org/10.2807/1560-7917.ES.2020.25.10.2000180

Address for correspondence: Zhongjie Li, Chinese Center for Disease Control and Prevention, 155 Changbai Rd, Changping District, Beijing 102206, China; email: lizj@chinacdc.cn

Human and Porcine Transmission of *Clostridioides difficile* Ribotype 078, Europe

Geraldine Moloney,[1] David W. Eyre,[1] Micheál Mac Aogáin, Máire C. McElroy,
Alison Vaughan, Tim E.A. Peto, Derrick W. Crook, Thomas R. Rogers

Genomic analysis of a diverse collection of *Clostridioides difficile* ribotype 078 isolates from Ireland and 9 countries in Europe provided evidence for complex regional and international patterns of dissemination that is not restricted to humans. These isolates are associated with *C. difficile* colonization and clinical illness in humans and pigs.

*C*lostridioides (formerly *Clostridium*) *difficile* was considered to be a predominantly nosocomial pathogen until findings of several whole-genome sequencing studies suggested a more complex epidemiology. For example, Eyre et al. reported that only 35% of nosocomial *C. difficile* infections (CDIs) were potentially attributable to other cases on the basis of genomic data, and only 19% were additionally linked through sharing possible hospital-based contact (*1*). This finding suggests that a major proportion of *C. difficile* from CDI cases occurring in healthcare institutions originates from other sources, including the community (*2*).

Community-associated CDI (CA-CDI) is now well recognized, accounting for ≈25% of cases in Australia, <25% of cases in Europe, and 33% of cases in the United States (*3*,*4*). There is increasing recognition that *C. difficile* is a near ubiquitous environmental organism and that humans have widespread environmental exposure to it. *C. difficile* has been detected in samples from parks (24.6%); water sources, including rivers, lakes, and sea water; homes (17.1%); commercial stores; and other premises (6.5%–8.1%), in addition to hospitals (16.5%) (*5*,*6*). Isolates of *C. difficile*

from these studies underwent ribotype analysis. Overall, ribotype 027 isolates were most commonly identified in hospital samples, and ribotype 014–020 isolates predominated in other environmental samples. Isolates of the most common ribotypes were not restricted to any particular location (*5*). These findings support the possibility that there are different sources for exposure to each *C. difficile* ribotype.

Occurrence of CDI caused by *C. difficile* ribotype 027 has been greatly reduced in the United Kingdom, most likely the result of the combination of antimicrobial stewardship and hospital infection prevention and control measures. However, these interventions have not reduced the incidence of infections caused by other ribotypes, including ribotype 078 (*7*).

Findings of genomic analysis of isolates from the European, Multi-Center, Prospective, Biannual, Point-Prevalence Study of *Clostridium difficile* Infection in Hospitalized Patients with Diarrhea (EUCLID) showed that specific *C. difficile* ribotypes were associated with healthcare clusters, and other ribotypes had an international distribution across Europe (*8*). For example, ribotype 078 isolates did not cluster by their country of origin, indicating a complex distribution unrelated to nosocomial transmission. The mechanisms of transmission have not been identified, but might be related to the movement of food, other animal-derived products, or persons across Europe (*8*).

C. difficile carriage and infection has been well described in livestock and other animals (*3*); certain ribotypes of *C. difficile* are considered to be major ribotypes from a One Health perspective. These ribotypes include ribotype 078, carriage of which has been reported in 9%–100% of piglets from North America, Europe, Asia, and Australia (*3*). Carriage rates in calves (56%) and cows (13%) have been lower.

[1]These authors contributed equally to this article.

Although many studies did not identify any major carriage in adult pigs, 1 study in the Netherlands reported a rate ranging from 6.6% to 100% (*3*).

We have reported *C. difficile* ribotype 078 in cases of typhlocolitis in neonatal piglets in Ireland (*9*), and Knetsch et al. found that ribotype 078 isolates carried by farmers in the Netherlands and their pigs were identical by whole-genome sequence analysis (*10*). These findings suggest that *C. difficile* isolates might be shared between humans and pigs when in close proximity. However, the mechanisms and directions of transmission are not known.

In this study, we investigated the genomic relationships between *C. difficile* ribotype 078 isolates of human and porcine origin collected from Ireland and compared these with international ribotype 078 isolates. We also investigated the extent to which geographic proximity could explain clusters of clonal isolates.

Methods

Samples and Settings

Clinical isolates of *C. difficile* ribotype 078 were collected prospectively as part of an investigation of consecutive episodes of CDI conducted at St. James's Hospital (Dublin, Ireland), a 900-bed tertiary referral center, during 2013–2016. Stool samples, sent from patients with diarrhea, had the *C. difficile* toxin B gene identified by using the EntericBio PCR Kit (Serosep, https://www.serosep.com). We reviewed medical notes of inpatients to obtain relevant clinical data, including antimicrobial drugs and proton pump inhibitors prescribed before the onset of diarrhea, features indicative of severe CDI with or without complications, and the antimicrobial drugs used for management of CDI. These data were pseudonymized and stored in a dedicated database.

We retrieved an additional 9 *C. difficile* 078 isolates from a study of recurrent CDI at St. James's Hospital during 2012–2013 (*11*). Five additional *C. difficile* ribotype 078 isolates were provided from those submitted to a national surveillance study of CA-CDI in Ireland conducted during 2015. Isolates of *C. difficile* were recovered from pigs that had been referred for autopsy at the Central Veterinary Research Laboratory (CVRL; Backweston, Ireland) during 2014–2015, irrespective of the suspected cause of death, by sampling colonic contents or feces that had positive results for *C. difficile* toxins A/B by using the Premier Elisa Kit (Meridian BioScience Inc., https://www.meridianbioscience.com). We treated human fecal and porcine colonic/fecal samples with ethanol shock before anaerobic incubation on cycloserine cefoxitin egg yolk medium. DNA was extracted from resulting colonies for PCR ribotype analysis and Illumina (https://www.illumina.com) genomic library preparation as described (*11*).

Whole-Genome Sequencing

Whole-genome sequencing was performed either on an Illumina MiSeq or MiniSeq platform at Trinity College (Dublin, Ireland) or on the Illumina HiSeq platform at the Wellcome Centre for Human Genetics, University of Oxford (Oxford, UK). Sequence data generated have been deposited in the National Center for Biotechnology Information Short Read Archive (https://www.ncbi.nlm.nih.gov/sra) under BioProject PRJNA692997.

We mapped sequence reads to the ribotype 078 reference genome M120 (GenBank accession no. FN665653.1), and identified high-quality variants by using an approach developed and calibrated for *C. difficile* (*1*) with later refinements (*12*) (Appendix, https://wwwnc.cdc.gov/EID/article/27/9/20-3468-App1.pdf). We obtained published comparison sequences from the EUCLID pan-European cross-sectional survey conducted during in 2012–2013 (*8*) and from farm animal and human isolates from the Netherlands (2002–2011) described by Knetsch et al. (*10*).

Sequence Comparisons

We compared sequences by using single-nucleotide polymorphisms (SNPs) and obtained differences between sequences from maximum-likelihood phylogenies corrected for recombination (Appendix). We reviewed phylogenetic analysis of closely related genomes in conjunction with available epidemiologic data. Within the clinical database, CDI recurrence was defined as identification of 2 isolates within 10 SNPs from 1 patient (*1*) for which that patient had clearly documented clinical resolution of symptoms after their first episode. On the basis of rates of *C. difficile* evolution and within-host diversity (*1*), we defined plausible, short-term, transmission/mutual exposure as isolates differing by 0–2 SNPs.

We made epidemiologic matches between patients who had in-patient admissions and demonstrable links with respect to time, location, or healthcare staff, where their *C. difficile* isolates were within 0–2 SNPs. Because epidemiologic details were not available for either the CA-CDI investigation in Ireland or the EUCLID isolates, we analyzed linkage between cases on the basis of genetic similarity alone. These genomic pairs were named by the isolate sources in chronologic order of identification.

Ethics

Investigation of hospital-associated CDI (HA-CDI) cases at St James's Hospital was conducted after obtaining approval from the St. James's Hospital/Tallaght Research Ethics Committee. Porcine isolates were exempt from requiring ethics approval.

Results

A total of 171 *C. difficile* ribotype 078 isolates were included in the analysis: 53 isolates from CDI episodes in 44 inpatients at St. James's Hospital, including 5 community-associated isolates; 20 porcine isolates from Ireland; 67 clinical, farmer, and porcine isolates from the Netherlands; and 31 clinical EUCLID isolates. We provide details of their country of origin, source, and date of isolation (Table 1). The EUCLID isolates were obtained from 9 countries in Europe. Six countries, including Ireland, submitted ≥2 isolates.

Of the 53 isolates causing CDI in Ireland, 9 were from recurrent CDI episodes in 7 patients (7 subsequent isolates were 0 SNPs different from, the baseline isolate, 1 was 1 SNP different, and 1 was 8 SNPs different). Only the first isolate from each patient was considered in subsequent analyses. We provide genomic relationships between the remaining 162 ribotype 078 isolates (Figure). Despite the diverse sampling frame, only limited diversity was seen; the greatest root-to-tip distance in the phylogenetic tree was 48 SNPs.

Isolates from Ireland were found throughout the tree, but specific clusters of these isolates were seen,

Table 1. Countries from which *Clostridioides difficile* 078 isolates originated, their identified sources, and timeframe of collection*

Origin and source of isolates	Timeframe of collection	No. isolates
Ireland (*11*)		
HA-CDI	2012–2016	48†
Porcine	2014–2015	20
CA-CDI	2015 Apr–Jun	5
Netherlands (*10*)		
CDI	2002–2011	31
Porcine	2009, 2011	20
Healthy farmers	2011	16
EUCLID (*8*), HA-CDI	2012 Dec–2013 Aug	
Germany		9
Italy		7
United Kingdom		4
France		3
Portugal		3
Ireland		2
Spain		1
Greece		1
Austria		1

*CDI, *C. difficile* infection; EUCLID, European, Multi-Center, Prospective, Biannual, Point-Prevalence Study of *Clostridium difficile* Infection in Hospitalized Patients with Diarrhea; HA-CDI, hospital-associated CDI.
†Includes 9 isolates from HA-CDI cases (*11*).

including, as shown at the ≈240° (≈8 o'clock) position (Figure), a cluster of cases that included isolates from HA-CDI and CA-CDI cases as well as cases from pigs. Within this cluster, several porcine isolates were directly ancestral to 1 HA-CDI case. Another 5 CDI cases, including 1 CA-CDI, had another porcine isolate directly ancestral. This finding suggests a porcine origin for these cases, either directly or by >1 or more intermediate (unsampled) transmission routes. This same cluster also contained an isolate from a pig and a farmer from the Netherlands. Several other clinical isolates from the Netherlands were closely related to porcine isolates (Figure).

We provide epidemiologic links between genetically related isolates within 0–2 SNPs (Table 2). Although nearly all genomic pairs occurred among isolates with the same country of origin, the epidemiologic information available can explain only a small proportion of transmissions/mutual exposures.

Discussion

Our findings support a complex regional and international distribution of *C. difficile* ribotype 078 isolates. In contrast to the EUCLID study, which obtained samples on single days in winter and summer, more dense sampling was undertaken in our study. In the EUCLID study, no evidence of clustering of ribotype 078 within countries was seen, which is consistent with a complex pattern of dissemination in Europe over timescales spanning years (Figure). However, our study showed evidence of sublineages of ribotype 078 that are predominantly found in isolates from the Netherlands and others predominantly found in isolates from Ireland (Figure). It is likely that this denser sampling has enabled recent, local, onward transmission to be better captured. We also identify a EUCLID isolate from Italy (2013) and a CA-CDI isolate from Dublin, Ireland (2014), that are within 2 SNPs, which is consistent with a temporally related transmission. However, we do not know of any epidemiologic link between these 2 cases.

For 10 pairs of isolates within 2 SNPs from inpatients who had HA-CDI, possible healthcare-based epidemiologic links could be made for 6 of these pairs but not the other 4. Plausible ward-based transmission only accounted for 3 pairs. For other genetically related isolates pertaining to inpatients in our study, there was a median of 559 days between their associated CDI episodes (range 147–651 days) without overlapping hospital admissions or appointments. Overall, nosocomial transmission accounted for 15% of closely genetically related (<2 SNPs) *C. difficile* ribotype 078 cases in this study, and

Figure. Recombination-adjusted maximum-likelihood phylogenetic tree of sequences from human and porcine *Clostridioides difficile* isolates from Ireland and 9 other countries in Europe. Isolates are shown as triangles for healthcare-associated *C. difficile* cases and circles for community-associated *C. difficile* cases. Isolates from pigs are shown as crosses and those from farmers as squares. The color at each tip indicates the country of origin of the isolate. The tree was based on 4,861 variable sites before correction for recombination, based on a median (interquartile ranges) of 93.4% (93.0%–93.8%) and (83.1%–96.2%) of the reference genome being called. Scale bar indicates single-nucleotide polymorphisms.

equal proportions were attributable to farms and unknown transmission routes. In a study in Leeds, UK, which had comparable phylogenetic analysis, hospital ward-based epidemiologic linkage was reported as 11% for ribotype 078 cases versus 64% for ribotype 027 cases (*13*).

A EUCLID isolate from Ireland (2013) forms a genomic cluster with 1 CA-CDI isolate (2015) and 2 HA-CDI isolates (July 2015 and December 2015). These 4 isolates were from patients in 3 Dublin healthcare facilities and from 1 case of CA-CDI that had been collected within a 3-year period. This finding suggests shared exposure across the greater Dublin area, and that nosocomial transmission is not the dominant route of acquisition of *C. difficile* ribotype 078.

This observation is consistent with the EUCLID study findings (*8*).

It is not clearly understood how persons who have CA-CDI acquired their infection because they do not have the risk factors for HA-CDI (*14*). Anderson et al. described proximity to livestock farms, agricultural industry, and nursing home facilities as risk factors for CA-CDI in North Carolina, USA, but they did not include analysis of *C. difficile* molecular data in their models (*15*). In contrast, Van Dorp et al. found no evidence of either localized point sources or livestock exposure as risk factors for *C. difficile* acquisition in the Netherlands (*16*). They included ribotype detail in their analysis, but found no evidence of geographic clustering of ribotype 078 CDI cases (*16*). This finding

Table 2. Pairs of *Clostridioides difficile* ribotype 078 isolates matched by country of origin and source case, with associated epidemiology*

Country	Source of isolate(s)	Country 2	Source of isolate(s)	No. pairs of isolates	Associated epidemiology
Ireland	CA-CDI	Ireland	CA-CDI	2	No known links
Ireland	CA-CDI	Ireland	HA-CDI	2	No known links
Ireland	HA-CDI	Ireland	HA-CDI	10	Possible transmission 6 pairs,† unknown for 4 pairs
Ireland	Porcine	Ireland	HA-CDI	3	No known links
Ireland	Porcine	Ireland	Porcine	12	8 pairs at 1 farm, 3 pairs at 1 farm, 1 pair at 1 farm, no pairs between farms
Ireland	CA-CDI	Italy	HA-CDI	1	Unknown
Ireland	HA-CDI	United Kingdom	HA-CDI	1	Unknown
Germany	HA-CDI	Germany	HA-CDI	1	Unknown
Netherlands	HA-CDI	Netherlands	HA-CDI	1	Unknown
Netherlands	CDI	Netherlands	Farmer	1	No known links
Netherlands	CDI	Netherlands	Porcine	1	No known links
Netherlands	Farmer	Netherlands	Farmer	3	Unknown
Netherlands	Farmer	Netherlands	Porcine	10	Farm exposures
Netherlands	Porcine	Netherlands	Porcine	1	No known links
Portugal	HA-CDI	Portugal	HA-CDI	1	Unknown

*CA-CDI, community-assocated *C. difficile* infection; HA-CDI, healthcare-associated *C. difficile* infection.
†The 6 possible healthcare-associated transmission pairs shared time and space on the same hospital ward (n = 3) or time on different hospital wards while under the care of the same medical team (n = 3).

is consistent with that of Knetsch et al., who reported clonal isolates of farm and clinical origin without a geographic basis for those clusters (*10*).

Knetsch et al. identified another genomic cluster of *C. difficile* ribotype 078 isolates, which included an isolate of animal origin from Canada (2004) and 8 isolates of clinical origin from the United Kingdom (2008–2012) (*17*). We also identified a cluster of clinical and porcine 078 isolates from Ireland, where there was no known occupational exposure of the affected patients who lived in urban locations far from relevant pig farms. Knight et al. reported clonal ribotype 014 isolates from Australia that were considerable geographic distances from each other, which is suggestive of long-range transmission and major community reservoirs (*18*). They concluded that this transmission was unlikely to have been caused by direct contact between the humans and animals involved, and suggested that by-products, such as manure or compost, could enable indirect transmission from animals and humans (*18*). In a study from the United States, biosolid-based compost had the highest rate of *C. difficile* recovery that included ribotype 078 isolates (*19*), which was also the most common ribotype in an investigation of manure from Japan (*20*).

Findings based on ribotype analysis alone are insufficient for clear identification of transmission events pertaining to community reservoirs (*21*). Moradigaravand et al. identified ≈90% of their collection of clinical and wastewater isolates as clade 1 (231/256), and only 10 (3.9%) as clade 5/ribotype 078 (*22*). When their ribotype 078 isolates were com-

pared with the same isolates from the Netherlands included in our analysis, they found divergence of ≈20 years between the isolates from the United Kingdom and the Netherlands. This finding suggests that water is not the primary reservoir or route for dissemination of *C. difficile* ribotype 078 isolates. It is still considered possible that dissemination of ribotype 078 isolates occurs by the food chain, the environment, or both (*23,24*). This view is supported by the presence and distribution of tetracycline-resistant determinants in *C. difficile* genomes, reflecting the antimicrobial drug selection pressure from tetracycline use in agriculture or veterinary practice, and thereby facilitating emergence and spread of ribotype 078 bacteria (*24*).

It is not completely understood how some livestock might have asymptomatic *C. difficile* colonization, whereas others show development of infection (*25*). The porcine isolates from Ireland in this analysis were from available samples processed at the CVRL. These isolates included samples from neonatal piglets that had typhlocolitis (*9*). We have identified genomic similarities among isolates causing human and veterinary infections. This finding augments the need for a One Health approach for *C. difficile* ribotype 078.

The strengths of this analysis include the large number of *C. difficile* ribotype 078 isolates included, from different sources including humans and animal species, and geographic origin. The limitations of this study include the lack of epidemiologic data available to the investigators for CA-CDI and the limited number of porcine strains from samples available at

the CVRL. In conclusion, our analysis of *C. difficile* ribotypes 078 isolates from Ireland and 9 other countries in Europe showed close overlap between isolates from humans and pigs, including the occurrence of plausible transmission, either directly or by an unknown intermediate source.

About the Author

Dr. Moloney is an infectious diseases physician at Cork University Hospital, Cork, Ireland. Her primary research interest is infections with *Clostridioides difficile*.

References

1. Eyre DW, Cule ML, Wilson DJ, Griffiths D, Vaughan A, O'Connor L, et al. Diverse sources of *C. difficile* infection identified on whole-genome sequencing. N Engl J Med. 2013;369:1195–205. https://doi.org/10.1056/NEJMoa1216064
2. Moloney G, Mac Aogáin M, Kelleghan M, O'Connell B, Hurley C, Montague E, et al. Possible interplay between hospital and community transmission of a novel *Clostridium difficile* sequence type 295 recognized by next-generation sequencing. Infect Control Hosp Epidemiol. 2016;37:680–4. https://doi.org/10.1017/ice.2016.52
3. Knight DR, Riley TV. Genomic delineation of zoonotic origins of *Clostridium difficile*. Front Public Health. 2019;7:164. https://doi.org/10.3389/fpubh.2019.00164
4. European Centre for Disease Prevention and Control. Healthcare-associated infections: *Clostridium difficile* infections. In: Annual epidemiological report for 2016. Stockholm: The Centre, 2018 [cited 2021 Jun 5]. https://www.ecdc.europa.eu/en/publications-data/healthcare-associated-infections-clostridium-difficile-infections-annual
5. Alam MJ, Walk ST, Endres BT, Basseres E, Khaleduzzaman M, Amadio J, et al. Community environmental contamination of toxigenic *Clostridium difficile*. Open Forum Infect Dis. 2017;4:ofx018. https://doi.org/10.1093/ofid/ofx018
6. al Saif N, Brazier JS. The distribution of *Clostridium difficile* in the environment of South Wales. J Med Microbiol. 1996;45:133–7. https://doi.org/10.1099/00222615-45-2-133
7. Dingle KE, Didelot X, Quan TP, Eyre DW, Stoesser N, Golubchik T, et al.; Modernising Medical Microbiology Informatics Group. Effects of control interventions on *Clostridium difficile* infection in England: an observational study. Lancet Infect Dis. 2017;17:411–21. https://doi.org/10.1016/S1473-3099(16)30514-X
8. Eyre DW, Davies KA, Davis G, Fawley WN, Dingle KE, De Maio N, et al.; EUCLID Study Group. Two distinct patterns of *Clostridium difficile* diversity across Europe indicating contrasting routes of spread. Clin Infect Dis. 2018;67:1035–44. https://doi.org/10.1093/cid/ciy252
9. McElroy MC, Hill M, Moloney G, Mac Aogáin M, McGettrick S, O'Doherty Á, et al. Typhlocolitis associated with *Clostridium* difficile ribotypes 078 and 110 in neonatal piglets from a commercial Irish pig herd. Ir Vet J. 2016;69:10. https://doi.org/10.1186/s13620-016-0070-9
10. Knetsch CW, Connor TR, Mutreja A, van Dorp SM, Sanders IM, Browne HP, et al. Whole genome sequencing reveals potential spread of *Clostridium difficile* between humans and farm animals in the Netherlands, 2002 to 2011. Euro Surveill. 2014;19:20954. https://doi.org/10.2807/1560-7917.ES2014.19.45.20954
11. Mac Aogáin M, Moloney G, Kilkenny S, Kelleher M, Kelleghan M, Boyle B, et al. Whole-genome sequencing improves discrimination of relapse from reinfection and identifies transmission events among patients with recurrent *Clostridium difficile* infections. J Hosp Infect. 2015;90:108–16. https://doi.org/10.1016/j.jhin.2015.01.021
12. De Silva D, Peters J, Cole K, Cole MJ, Cresswell F, Dean G, et al. Whole-genome sequencing to determine transmission of *Neisseria gonorrhoeae*: an observational study. Lancet Infect Dis. 2016;16:1295–303. https://doi.org/10.1016/S1473-3099(16)30157-8
13. Martin JS, Eyre DW, Fawley WN, Griffiths D, Davies K, Mawer DP, et al. Patient and strain characteristics associated with *Clostridium difficile* transmission and adverse outcomes. Clin Infect Dis. 2018;67:1379–87. https://doi.org/10.1093/cid/ciy302
14. Khanna S, Pardi DS, Aronson SL, Kammer PP, Baddour LM. Outcomes in community-acquired *Clostridium difficile* infection. Aliment Pharmacol Ther. 2012;35:613–8. https://doi.org/10.1111/j.1365-2036.2011.04984.x
15. Anderson DJ, Rojas LF, Watson S, Knelson LP, Pruitt S, Lewis SS, et al.; CDC Prevention Epicenters Program. Identification of novel risk factors for community-acquired *Clostridium difficile* infection using spatial statistics and geographic information system analyses. PLoS One. 2017;12:e0176285. https://doi.org/10.1371/journal.pone.0176285
16. van Dorp SM, Hensgens MP, Dekkers OM, Demeulemeester A, Buiting A, Bloembergen P, et al. Spatial clustering and livestock exposure as risk factor for community-acquired *Clostridium difficile* infection. Clin Microbiol Infect. 2019;25:607–12. https://doi.org/10.1016/j.cmi.2018.07.018
17. Knetsch CW, Kumar N, Forster SC, Connor TR, Browne HP, Harmanus C, et al. Zoonotic transfer of *Clostridium difficile* harboring antimicrobial resistance between farm animals and humans. J Clin Microbiol. 2018;56:e01384-17. https://doi.org/10.1128/JCM.01384-17
18. Knight DR, Squire MM, Collins DA, Riley TV. Genome analysis of *Clostridium difficile* PCR ribotype 014 lineage in Australian pigs and humans reveals a diverse genetic repertoire and signatures of long-range interspecies transmission. Front Microbiol. 2017;7:2138. https://doi.org/10.3389/fmicb.2016.02138
19. Dharmasena M, Jiang X. Isolation of toxigenic *Clostridium difficile* from animal manure and composts being used as biological soil amendments. Appl Environ Microbiol. 2018;84:e00738-18. https://doi.org/10.1128/AEM.00738-18
20. Usui M, Kawakura M, Yoshizawa N, San LL, Nakajima C, Suzuki Y, et al. Survival and prevalence of *Clostridium difficile* in manure compost derived from pigs. Anaerobe. 2017;43:15–20. https://doi.org/10.1016/j.anaerobe.2016.11.004

21. Knetsch CW, Lawley TD, Hensgens MP, Corver J, Wilcox MW, Kuijper EJ. Current application and future perspectives of molecular typing methods to study *Clostridium difficile* infections. Euro Surveill. 2013;18:20381. https://doi.org/10.2807/ese.18.04.20381-en

22. Moradigaravand D, Gouliouris T, Ludden C, Reuter S, Jamrozy D, Blane B, et al. Genomic survey of *Clostridium difficile* reservoirs in the East of England implicates environmental contamination of wastewater treatment plants by clinical lineages. Microb Genom. 2018;4. https://doi.org/10.1099/mgen.0.000162

23. Hensgens MP, Keessen EC, Squire MM, Riley TV, Koene MG, de Boer E, et al.; European Society of Clinical Microbiology and Infectious Diseases Study Group for Clostridium difficile (ESGCD). *Clostridium difficile*

24. Dingle KE, Didelot X, Quan TP, Eyre DW, Stoesser N, Marwick CA, et al. A Role for tetracycline selection in recent Evolution of agriculture-associated *Clostridium difficile* PCR ribotype 078. MBio. 2019;10:e02790-18. https://doi.org/10.1128/mBio.02790-18

infection in the community: a zoonotic disease? Clin Microbiol Infect. 2012;18:635–45. https://doi.org/10.1111/j.1469-0691.2012.03853.x

25. Weese JS. *Clostridium* (*Clostridioides*) *difficile* in animals. J Vet Diagn Invest. 2020;32:213–21. https://doi.org/10.1177/1040638719899081

Address for correspondence: Geraldine Moloney, Department of Infectious Diseases, Cork University Hospital, Wilton, Cork, Ireland; email: geraldinemoloney@physicians.ie

Risk Factors for Middle East Respiratory Syndrome Coronavirus Infection among Camel Populations, Southern Jordan, 2014–2018

Peter Holloway, Matthew Gibson, Neeltje van Doremalen, Stephen Nash,
Tanja Holloway, Michael Letko, Jacqueline M. Cardwell, Bilal Al Omari, Ahmad Al-Majali,
Ehab Abu-Basha, Punam Mangtani, Vincent J. Munster, Javier Guitian

After the first detection of Middle East respiratory syndrome coronavirus (MERS-CoV) in camels in Jordan in 2013, we conducted 2 consecutive surveys in 2014–2015 and 2017–2018 investigating risk factors for MERS-CoV infection among camel populations in southern Jordan. Multivariate analysis to control for confounding demonstrated that borrowing of camels, particularly males, for breeding purposes was associated with increased MERS-CoV seroprevalence among receiving herds, suggesting a potential route of viral transmission between herds. Increasing age, herd size, and use of water troughs within herds were also associated with increased seroprevalence. Closed herd management practices were found to be protective. Future vaccination strategies among camel populations in Jordan could potentially prioritize breeding males, which are likely to be shared between herds. In addition, targeted management interventions with the potential to reduce transmission between herds should be considered; voluntary closed herd schemes offer a possible route to achieving disease-free herds.

Middle East respiratory syndrome (MERS) coronavirus (MERS-CoV) represents 1 of 3 major zoonotic coronaviruses to have emerged with global impact in the past 2 decades, alongside severe acute

Author affiliations: The Royal Veterinary College, Hatfield, UK (P. Holloway, J.M. Cardwell, J. Guitian); Glasgow University, Glasgow, Scotland, UK (M. Gibson); National Institute of Allergy and Infectious Diseases, National Institutes of Health, Hamilton, Montana, USA (N. van Doremalen, M. Letko, V.J. Munster); London School of Hygiene and Tropical Medicine, London, UK (S. Nash, T. Holloway, P. Mangtani); Jordan University of Science and Technology, Irbid, Jordan (B. Al Omari, A. Al-Majali, E. Abu-Basha)

respiratory syndrome coronavirus (SARS-CoV-1) in 2002–2003 and severe acute respiratory syndrome coronavirus 2 (SARS-CoV-2) from 2019 onward (1). The earliest known outbreak of MERS-CoV began in a hospital in Zarqa, Jordan, in April 2012 (2,3). Since that time, >2,500 cases and 880 deaths (case-fatality rate of 34%) have been reported across 27 countries worldwide (4). The first detection of positive MERS-CoV by serologic testing in camels was also from Zarqa, Jordan, in 2013 (5); camels were later confirmed as the reservoir for MERS-CoV infection in humans (6) and bats the likely ancestral host (7).

Most confirmed MERS-CoV cases have occurred within the Arabian Peninsula; Saudi Arabia, the location of ≈80% of all human cases, is the epicenter (8). Phylogenetic analyses of viral sequences isolated from camels and humans suggest that multiple camel-to-human spillover events have occurred since the initial MERS outbreaks in 2012 (9). Although humans sometimes represent a dead-end host, secondary human-to-human infection does occur, leading in some cases to large-scale outbreaks in hospital settings, such as those seen in Saudi Arabia and South Korea in recent years (10,11). Whereas infection in camels might be subclinical or cause mild upper respiratory symptoms (12,13), infection in humans can range from asymptomatic to severe acute respiratory disease or death (14).

The World Health Organization has declared MERS-CoV a priority disease in its Research and Development Blueprint program as a public health risk of epidemic potential (15); vaccination of camels is a potential key component of future disease control strategies (16). Although MERS-CoV is widespread among camel populations in Africa, the Middle East,

and South Asia, its epidemiology within these populations remains poorly understood, particularly with regard to viral transmission routes and risk factors for infection (*17*). Such knowledge is urgently needed if camel vaccines currently in development are to be deployed effectively (*18–21*) and if management interventions with the potential to contribute to disease control are to be identified. We addressed these key knowledge gaps through 2 large-scale, consecutive epidemiologic surveys among camel populations in southern Jordan, close to the border of Saudi Arabia.

Methods

Study Design and Study Population
We conducted 2 distinct studies during February 2014–December 2015 and October 2017–October 2018. Both studies were conducted in Aqaba and Ma'an governorates of southern Jordan, an area with ≈8,000 camels (according to Jordanian Ministry of Agriculture [MoA] data) and 550 km of desert border with Saudi Arabia to the south and east (Figure 1).

In the 2014–2015 study, because of the absence of an adequate sampling frame, we conducted nonprobabilistic sampling among clients of a centrally located private veterinary practice in Al Quwayrah (Aqaba governorate). During the study period, the Al Quwayrah clinic closed (February 2015); the final 53 herds included in the study were recruited through local contacts of government veterinarians working

in the study area. We collected serum samples from the onset, whereas collection of nasal swab specimens began in March 2015 and occurred in the final 53 herds only.

In the 2017–2018 study, we conducted multistage cross-sectional random sampling by using MoA-supplied lists of camel owners for Aqaba and Ma'an governorates organized by 4 local administrative areas (Aqaba East, Aqaba West, Ma'an East, and Ma'an West). We collected serum samples and nasal swab specimens from the onset.

In both studies, to encourage owner compliance, we sampled ≤12 camels per herd; in herds of <12, we sampled all camels, subject to accessibility and owner permissions. A structured questionnaire regarding potential risk factors for MERS-CoV infection was administered in the local dialect on paper (2014–2015 study) or on Android tablets using the application Open Data Kit (2017–2018 study) (https://getodk.org) to herd owners face-to-face at the time of sampling or by telephone after sampling. A veterinary surgeon clinically examined all camels included in the study to assess general health before sampling.

Sample Storage and Laboratory Methods
Blood samples were collected in 8 mL serum vacutainer tubes and centrifuged at 2,000 RPM for 10 min, followed by serum collection and storage at −20°C. Nasal swab specimens were placed in viral transport medium and chilled before storage at −20°C (2014–2015

Figure 1. Location of camel herds sampled for Middle East respiratory syndrome coronavirus in southern Jordan, February 2014–December 2015 and October 2017–October 2018. A) 2014–2015 study; B) 2017–2018 study. Samples were taken from camels from 97 herds in the 2014–2015 study and from 121 herds in the 2017–2018 study. In the 2017–2018 study, because of local grazing movements, 3 herds selected from the Jordanian Ministry of Agriculture list for Ma'an West were sampled in the neighboring region, Tafilah, and results from these herds attributed to Ma'an West.

study) or −80°C (2017–2018 study). All laboratory testing of samples was performed at the Diagnostic Laboratory, Veterinary Health Centre, Jordan University of Science and Technology (Irbid, Jordan).

ELISA

We tested serum samples in duplicate by using a MERS-CoV spike protein ELISA as previously described by van Doremalen et al. (22). In brief, maxisorp plates were coated overnight with S1 protein (Sino Biological, https://www.sinobiological.com) before blocking with 1% milk. MERS-CoV S1-specific antibodies were detected by using anti-llama IgG horseradish peroxidase-conjugated antibodies (Agrisera, https://www.agrisera.com) and subsequently developed with peroxidase-substrate reagent (KPL). Optical densities were measured at 405 nm and positivity at 3 times mean negative camel serum samples collected from United States–bred dromedary camels confirmed to be MERS-CoV–free. This assay does not cross-react with antibodies to bovine coronavirus, OC43, or SARS-CoV-1 (23).

Viral RNA Extraction and MERS-CoV Detection

RNA was extracted from nasal swab specimens by using the QiaAmp Viral RNA kit (QIAGEN, https://www.qiagen.com) according to the manufacturer's instructions ≤18 months after sample collection. Extracted RNA was used in a 1-step real-time reverse transcription PCR (rRT-PCR) UpE MERS-CoV assay performed on a QIAGEN Rotor-Gene instrument, with positivity set at a cycle threshold value of <40, on the basis of standard operating procedures as described in Corman et al. (24).

Statistical Analysis

In each study, we separately calculated seroprevalence estimates weighted according to sample size relative to the estimated camel population (based on MoA data) and ran regression models for identification of risk factors. Because of the differences in sampling strategy, weighting was conducted by region for the 2014–2015 study and by subregion for the 2017–2018 study. In both studies, we excluded camels ≤6 months of age from analyses because of the potential influences of maternally derived immunity.

We conducted univariate analyses by using mixed-effects regression with herd as a random effect and camel serologic status considered a binary outcome. All potential risk factors were analyzed as categorical variables, with the exception of camel age and herd size, which were analyzed as continuous variables. Variables were herd level with the exception of

age, sex, racing camel, and nasal discharge. For the 2017–2018 study (data were missing in the 2014–2015 study), we constructed a composite variable "closed herd," which we defined as herds in which no borrowing, lending, purchasing, racing, or contact with local or distant herds occurred.

We considered variables with a p value of <0.2 for inclusion in the multivariate models, with the exception of any variables missing >10% of their values. We used the Pearson R coefficient and a threshold of 0.4 to compare collinearities between variables; we excluded colinear variables from the same multivariate model and tested in separate models. We conducted multivariate models by using mixed-effects regression with herd as a random effect and constructed using a backward stepwise method, removing the least significant variable at each step while p>0.1, unless the variable was considered an a priori factor (region, sex, and age) or the removal of the variable demonstrated a significant effect on the other variables (a change in log odds of >10%). We repeated model creation by using a forward stepwise method, beginning with a priori variables and adding new variables in order of significance, keeping variables if they showed significance of p<0.1 or changed the log odds of other risk factors by >10%. We performed all statistical analyses in R version 3.5.1 (https://cran.r-project.org) and generated mixed-effects models by using the glmer function of the R package lme4 version 1.1–21.

Ethics Statement

Informed consent was obtained from all participating camel owners at the time of sampling, and institutional and national guidelines for care, use, and handling of animals were followed at all times. Studies were conducted with institutional review board approval by the Royal Veterinary College and London School of Hygiene and Tropical Medicine, National Institute of Allergy and Infectious Diseases, and Jordan University of Science and Technology and MoA.

Results

Study Results for 2014–2015

For 2014–2015, we included 433 camels with a median age of 6 years (interquartile range [IQR] 3–9 years) representing 97 herds (median herd size 11 [IQR 5–22]). We obtained blood samples from an average of 4.5 camels/herd and collected nasal swab specimens from 65% of included camels. The questionnaire was completed for 93 of 97 herds; we excluded 4 herds (17 camels) that lacked questionnaire data from the

analysis of risk factors. A total of 21 questionnaires were completed at the time of sampling, and 72 were completed subsequently by telephone.

In total, 128 sampled camels (from 22 herds) were from Ma'an region and 305 (from 75 herds) were from Aqaba region. MoA records indicated an estimated population of 4,436 camels (317 herds) in Ma'an region and 3,314 camels (265 herds) in Aqaba region; we weighted adjusted seroprevalence accordingly. Of 433 camels sampled, 381 were seropositive for MERS-CoV, an unadjusted seroprevalence of 88.0% and adjusted seroprevalence of 86.8% (95% CI 82.8–90.3). Of these, 9 camels were ≤6 months of age, of which 4 were seropositive (44.4%). After we excluded these calves from the dataset, the adjusted seroprevalence was 88.0% (95% CI 84.1–91.4). No nasal swab specimens tested positive for MERS-CoV RNA on rRT-PCR.

Of 97 herds sampled, 93 had >1 seropositive camel (including calves <6 months of age), resulting in an unadjusted herd-level seroprevalence of 95.9% and adjusted herd-level seroprevalence of 92.3% (95% CI 83.3–97.1); median herd sample seroprevalence was 100% (IQR 80%–100%) (Figures 2, 3). Highest weight-adjusted seasonal seroprevalence was in summer (93%) and lowest was in fall (84%); winter and spring results were both 88%.

In univariate analysis, age, sex, herd size, number of herds nearby, quarantine >3 days after purchase, borrowing of breeding males, and water source were all found to be associated with seropositivity at p<0.2, although we identified no significant correlations for these variables (Table 1, https://wwwnc.cdc.gov/EID/article/27/9/20-3508-T1.htm; Table 2; Figures 4, 5). Quarantine was excluded from the multivariate models because of a high number of missing values (62%).

Variables in the final multivariate model results were age, herd size, borrowing of males for breeding purposes, and water source (Table 3). We noted evidence of an association between camel seropositivity and borrowing of males for breeding purposes (adjusted OR [aOR] 4.18 (95% CI 1.45–12.09); p = 0.01), age per year (aOR 1.24 [95% CI 1.08–1.42]; p<0.01), and herd size per additional camel (aOR 1.04 [95% CI 1.01–1.08]; p = 0.02).

Study Results for 2017–2018

Blood samples and nasal swab specimens were collected from 404 camels (median age 5 years [IQR 3–8 years]) in 121 herds; an average of 3.3 camels were sampled per herd (median herd size 9 [IQR 4–17]). The questionnaire was administered to all 121 herd owners; 114 questionnaires were completed at the time of sampling, and 7 were completed subsequently by telephone. In total, 90 camels (29 herds) were sampled from Ma'an East, 70 (21 herds) Ma'an West, 152 camels (36 herds) from Aqaba East, and 92 (35 herds) from Aqaba West. MoA records described an estimated 1,909 camels (138 herds) in Aqaba East, 1,405 camels (127 herds) in Aqaba West, 3,563 camels (198 herds) in Ma'an East, and 873 camels (119 herds) in Ma'an West; we weighted adjusted seroprevalence accordingly.

Of 404 camels sampled, 264 were seropositive for MERS-CoV, for an unadjusted seroprevalence of 65.3% and an adjusted seroprevalence of 70.2% (95% CI 65.6–74.7). Of these, 26 of 39 camels ≤6 months of age were seropositive (66.7%), which compares with 18 (22.8%) of 79 among camels >6 months–2 years of age (OR 20.8 [95% CI 4.8–226.3]; p<0.01). After removal of calves ≤6 months from the dataset, the adjusted seroprevalence was 70.2% (95% CI 65.0–75.2) among 119 herds.

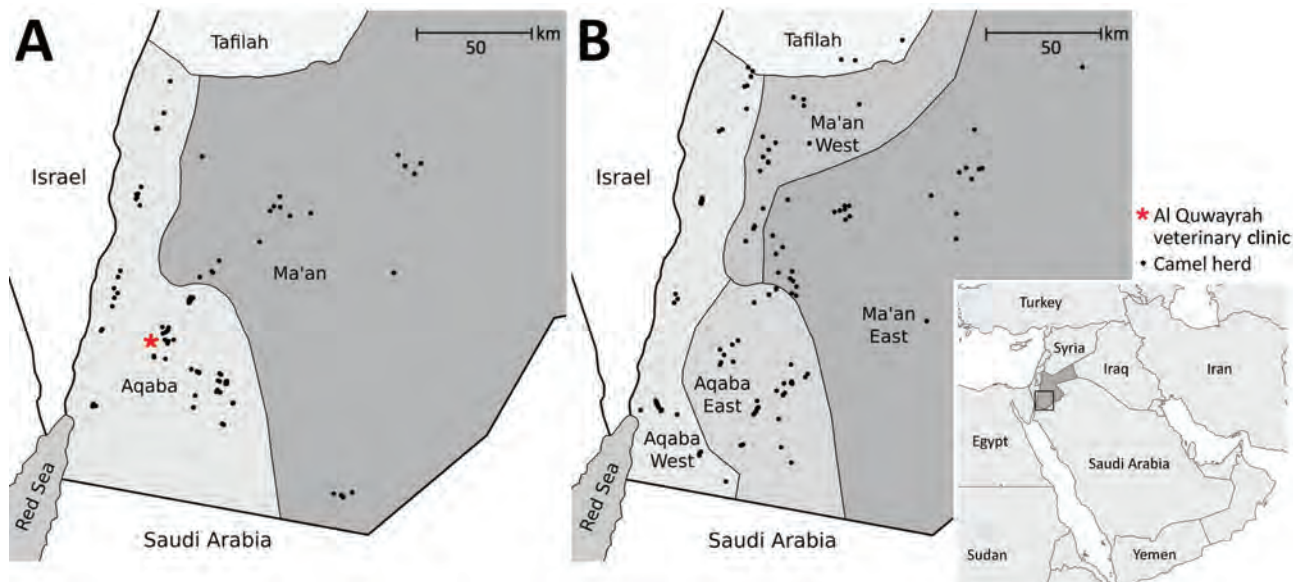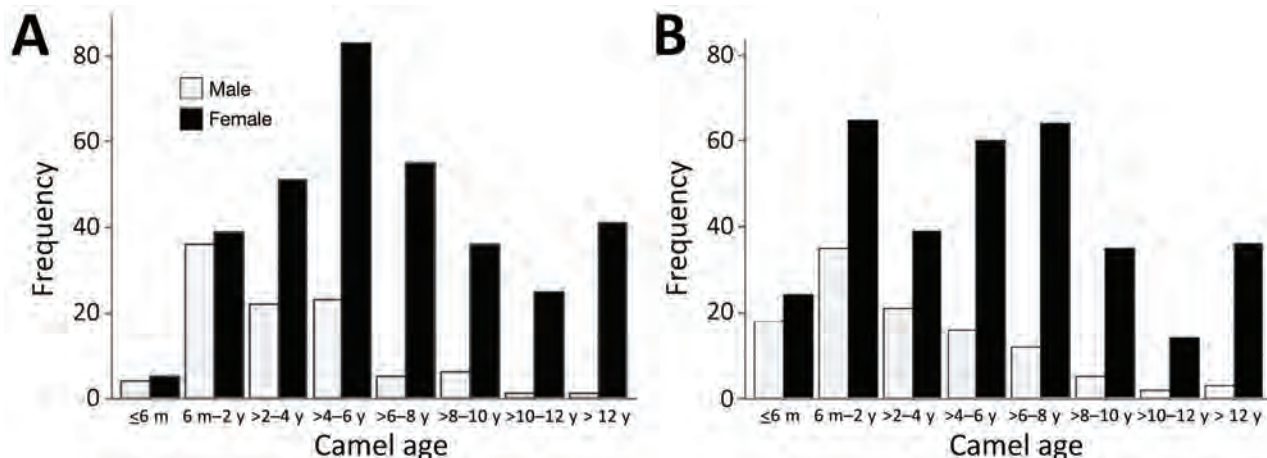**Figure 2.** Frequency distribution of camels sampled for Middle East respiratory syndrome coronavirus in southern Jordan, February 2014–December 2015 and October 2017–October 2018, stratified by age. A) 2014–2015 study; B) 2017–2018 study.

Table 2. Univariate associations between potential risk factors and Middle East respiratory syndrome coronavirus seropositivity in camel populations, Jordan, February 2014–December 2015 and October 2017–October 2018*

Variable	2014–2015 study		2017–2018 study	
	OR (95% CI)	p value	OR (95% CI)	p value
Region				
Aqaba	Referent	0.53	Referent	0.01
Ma'an	0.68 (0.18–2.30)		3.95 (1.42–12.85)	
Age, per y†	1.22 (1.08–1.39)	<0.01	1.63 (1.39–2.01)	<0.01
Sex†				
F	2.48 (0.90–6.70)	0.07	3.02 (1.28–7.09)	0.01
Herd size				
Per individual no. camels	1.05 (1.01–1.09)	0.01	1.02 (1.00–1.04)	0.08
No. camel herds within a 15 min drive				
>20	2.42 (0.72–9.07)	0.16	2.24 (0.70–7.86)	0.18
Herd kept together as single group throughout the year	0.84 (0.13–5.04)	0.85	2.88 (1.04–8.93)	0.05
Herd has contact with other local herds	1.43 (0.30–6.64)	0.63	2.97 (1.07–9.17)	0.04
Herd has contact with distant herds	0.55 (0.13–2.00)	0.36	1.86 (0.67–5.34)	0.23
New camels are purchased‡	0.77 (0.19–2.94)	0.70	1.51 (0.53–4.71)	0.44
Quarantine >3 d after purchase before joining herd	0.23 (0.03–1.55)	0.10	0.42 (0.02–6.88)	0.52
Camels borrowed for breeding purposes§	2.96 (0.87–11.42)	0.08	3.94 (1.45–12.32)	0.01
Herd-level borrowing of males	2.96 (0.87–11.42)	0.08	NR	NR
Herd-level borrowing of females	2.45 (0.49–16.62)	0.30	NR	NR
Camels loaned for breeding	NR	NR	3.28 (1.19–10.44)	0.03
Camels in herd are used for racing	0.49 (0.07–3.26)	0.44	0.89 (0.29–2.66)	0.83
Camel is a racing camel†	NR	NR	0.37 (0.09–1.44)	0.15
Water source¶				
Open ad lib	Referent	0.13	Referent	0.15
Household only	1.89 (0.05–72.38)		2.81 (0.59–14.25)	
Trough only	7.15 (0.95–70.49)		4.07 (1.01–18.88)	
Spring	0.13 (0.01–0.98)	0.05	0.20 (0.04–0.80)	0.03
Irrigation reservoir	0.05 (0.00–0.91)	0.05	0.36 (0.06–2.22)	0.27
Tanker	1.24 (0.31–5.11)	0.75	0.77 (0.25–2.37)	0.64
Tap	0.82 (0.20–3.94)	0.78	0.99 (0.35–2.86)	0.99
Well	0.57 (0.08–3.57)	0.54	0.44 (0.13–1.41)	0.16
Water source not shared with herd, household use only	0.30 (0.01–7.54)	0.45	0.96 (0.29–3.00)	0.94
Closed herd#	NR	NR	0.09 (0.01–0.39)	<0.01

*Variables reference the 1-year period before sampling, with the exception of herd size, camel is a racing camel, and a priori variables: age, sex, and region. Because of the potential influence of maternal immunity, camels ≤6 m of age have been excluded from all variables except age. NR, not recorded.
†Individual camel–level variables (all other variables being herd-level).
‡Camels purchased are locally bred; Jordanian Ministry of Agriculture Camel Import Regulations and Conditions allow import only for live camels for direct slaughter.
§In the 2014–15 study, results for camels are borrowed for breeding purposes (male and/or female) and camels are borrowed for breeding purposes (male) were the same (i.e., all herds that borrowed camels for breeding borrowed males, and some of these herds also borrowed females). In the 2017–18 study, the sex of camels borrowed or loaned for breeding was not recorded.
¶Open ad lib indicates irrigation reservoir or spring water sources were used; household only indicates water source was not shared between household and herd; trough only indicates only tanker, tap, or well sources were used.
#Closed herd indicates herd owners answered no to all of the following variables: borrowing, lending, purchasing, racing, and contact with local or distant herds (2017–2018 study only, missing data 2014–2015).

Of 119 herds sampled, 92 had >1 seropositive camel (including calves <6 months of age), resulting in an unadjusted herd-level seroprevalence of 77.3% and adjusted herd-level seroprevalence of 77.0% (95% CI 69.8–83.0); median herd sample seroprevalence was 75% (IQR 25%–100%) (Figures 2, 3). The highest weight-adjusted seasonal seroprevalence was in spring (75%) and the lowest in winter (63%); seroprevalence in fall was 70% (because of logistical constraints, no samples were collected during the summer).

No nasal swab specimens tested positive for MERS-CoV RNA on rRT-PCR. Nasal discharge was noted in 8 camels (2.6% [95% CI 1.4%–4.8%]) at the time of sampling (ages 3, 5, 6, 7, 7, 12, 14 and 15 years).

In the univariate analysis, the following 12 variables were found to be associated with seropositivity at p<0.2: region, age, sex, herd size, number of herds nearby, herd being kept as a single group throughout the year, contact with local herds, borrowing of camels for breeding purposes, lending of camels for breeding purposes, use of camels for racing, water source, and closed herd status (Tables 1, 2; Figures 4, 5). We identified correlations between contact with local herds and lending for breeding purposes (Pearson R coefficient = 0.46) and between borrowing for breeding purposes and lending for breeding purposes (Pearson R coefficient = 0.46).

Variables in the final multivariate model results were region, sex, age, herd size, borrowing
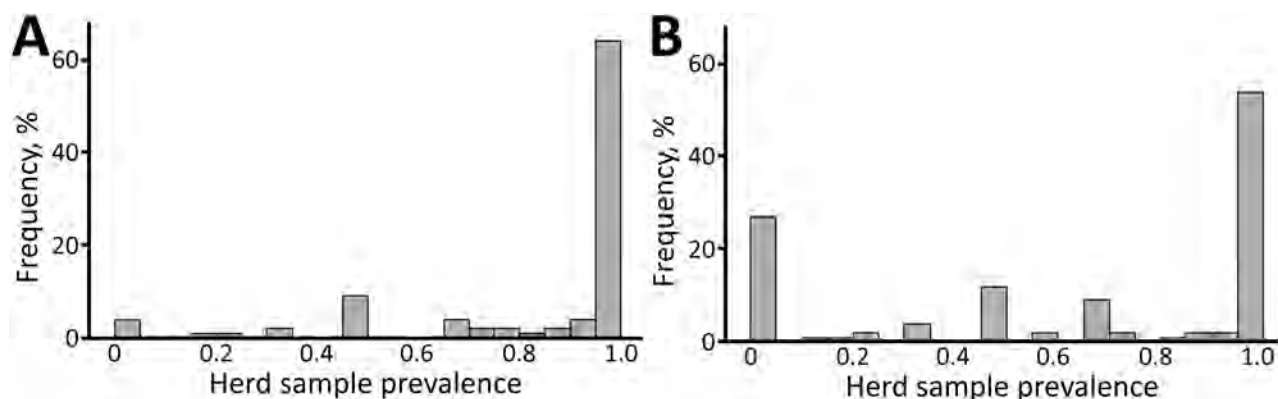
Figure 3. Frequency distribution of camel herd sample Middle East respiratory syndrome coronavirus seroprevalence, southern Jordan, February 2014–December 2015 and October 2017–October 2018. A) 2014–2015 study; B) 2017–2018 study

for breeding purposes, water source, and closed herd status (Table 4). Evidence of an association was noted between camel MERS-CoV seropositivity and drinking from water trough sources only, as compared with open ad lib sources (aOR 9.48 [95% CI 1.54–58.24]; p = 0.05); borrowing camels for breeding purposes (aOR 5.07 [95% CI 1.37–18.75]; p = 0.02); location in Ma'an region (aOR 3.83 [95% CI 1.01–14.51]; p = 0.05); and increasing age per year (aOR 1.60 [95% CI 1.34–1.92]; p<0.01). We investigated the variable of lending camels for breeding purposes in a separate model, in place of camels being borrowed for breeding purposes, but did not find evidence of a significant association with seropositivity. The composite variable closed herd demonstrated evidence of a protective association with MERS-CoV seropositivity (aOR 0.08 [95% CI 0.01–0.55]; p = 0.02) when included in a separate

model adjusted for the same confounders, although excluding constituent variables for closed herd, borrowing, and lending for breeding purposes.

Discussion

Previous studies have described MERS-CoV seroprevalence among camel populations worldwide; however, substantial knowledge gaps remain, in particular with regard to factors associated with higher risk for infection, which might provide insights into viral transmission routes between and within camel herds (16,17). Such knowledge is essential if effective disease control strategies, such as targeted vaccination programs and camel management interventions, are to be appropriately designed and implemented.

Our findings suggest that borrowing male camels for breeding might serve as a transmission route for

Table 3. Multivariate associations between potential risk factors and Middle East respiratory syndrome coronavirus seropositivity in camel populations, southern Jordan, February 2014–December 2015*

Variable	A priori adjusted OR (95% CI)†	p value	Fully adjusted OR (95% CI)‡	p value
Age, per y§	1.21 (1.07—1.40)	<0.01	1.24 (1.08—1.42)	<0.01
Male camels borrowed for breeding purposes	3.44 (1.09—12.25)	0.04	4.18 (1.45—12.09)	0.01
Herd size				
Increasing individual camel nos.	1.05 (1.01—1.09)	<0.01	1.04 (1.01—1.08)	0.02
Water source¶				
Open ad lib	Referent	0.19	Referent	0.08
Household only	0.52 (0.01—21.39)		0.90 (0.05—16.46)	
Trough only	4.02 (0.51—40.84)		4.74 (0.93—24.08)	
Region				
Ma'an	0.56 (0.16—1.79)	0.33	0.37 (0.12—1.14)	0.08
Sex§				
F	1.35 (0.45—3.86)	0.58	1.12 (0.38—3.26)	0.84
Number of camel herds within a 15-min drive				
>20	2.24 (0.68—7.99)	0.18	–	–

*Variables reference the 1-year period before sampling, with the exception of herd size, camel is a racing camel, and a priori variables: age, sex, and region. Because of the potential influence of maternal immunity, camels ≤6 m of age have been excluded. OR, odds ratio.
†Adjusted for a priori variables: age, sex, and region.
‡2014–2015 study was adjusted for a priori variables and number of camels nearby (within a 15 min drive).
§Individual camel–level variables (all other variables being herd-level).
¶Open ad lib indicates irrigation reservoir or spring water sources were used; household only indicates water source was not shared between household and herd; trough only indicates only tanker, tap, or well sources were used.
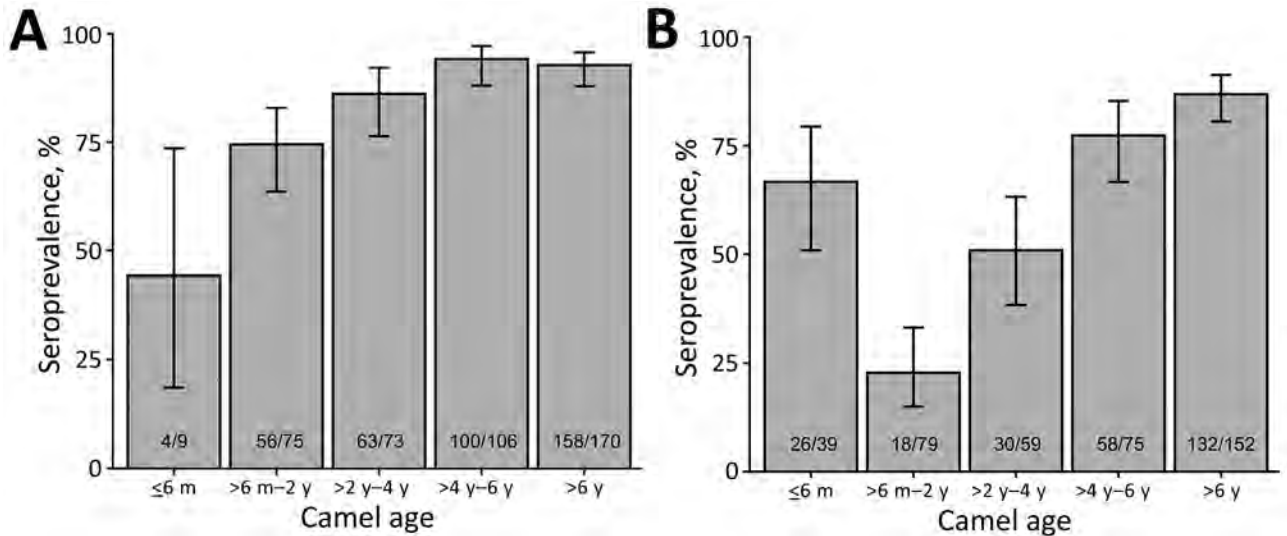
Figure 4. Middle East respiratory syndrome coronavirus seroprevalence among camel population in southern Jordan, stratified by age, February 2014–December 2015 and October 2017–October 2018. A) 2014–2015 study, B) 2017–2018 study. Error bars indicate 95% CIs. Numbers within gray boxes depict seropositive camels and total number of camels per age group.

MERS-CoV between infected and uninfected camel herds in Jordan. Both studies demonstrated that borrowing camels for breeding was associated with an increase in MERS-CoV seropositivity in receiving herds. In addition, the 2014–2015 study demonstrated that the borrowing of breeding males was a significant risk, whereas the borrowing of breeding females was not (we did not record sex of camels borrowed for breeding in 2017–2018).

In Jordan, as in other countries in the region, many herd owners do not own a breeding male camel because of cost or ease of management; instead, they borrow stud bulls from neighboring herds or send

breeding females to herds that have a bull. These practices serve to provide spatial connectivity between infected and uninfected herds; this effect is potentially compounded by the immunosuppressive stresses of transport and joining a new herd and by the effects of male rutting behavior, in which oronasal secretions are sprayed over, or close to, breeding females (25,26).

Given evidence for the potential risk posed by borrowing breeding males, vaccination of male camels shared between herds for breeding could be prioritized when effective camel vaccines become available (18), particularly among small-scale extensively
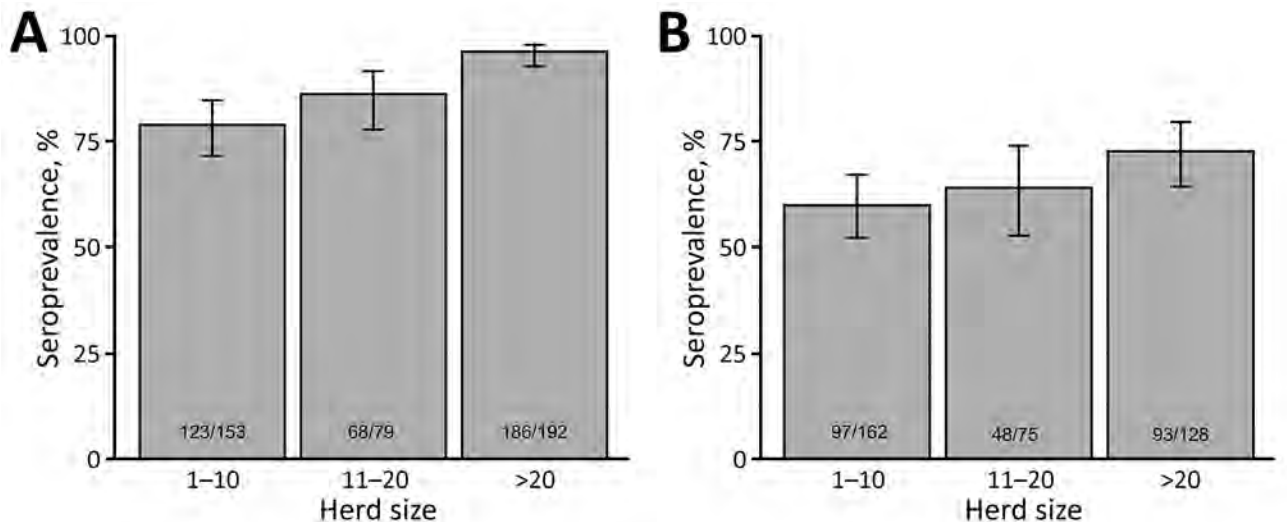
Figure 5. Middle East respiratory syndrome coronavirus seroprevalence among camel population in southern Jordan, stratified by herd size, February 2014–December 2015 and October 2017–October 2018. A) 2014–2015 study; B) 2017–2018 study. Error bars indicate 95% CIs. Numbers within gray boxes depict seropositive camels and total camels per herd size range.

Table 4. Multivariate associations between potential risk factors and Middle East respiratory syndrome coronavirus seropositivity in camel populations, southern Jordan, October 2017–October 2018

Variable*	A priori adjusted OR (95% CI)†	p value	Fully adjusted OR (95% CI)‡	p value
Age, per y§	1.60 (1.35—1.99)	<0.01	1.60 (1.34—1.92)	<0.01
Camels borrowed for breeding purposes	4.46 (1.29—21.68)	0.03	5.07 (1.37—18.75)	0.02
Water source¶		0.07		0.05
Open ad lib	Referent		Referent	
Household only	3.17 (0.44—25.78)		3.33 (0.51—21.71)	
Trough only	7.93 (1.41—65.04)		9.48 (1.54—58.24)	
Region				
Ma'an	3.28 (0.92—14.94)	0.08	3.83 (1.01—14.51)	0.05
Herd size				
Increasing individual camel nos.	1.02 (1.00—1.05)	0.05	1.00 (1.00—1.05)	0.10
Sex§				
F	1.70 (0.59—4.88)	0.32	1.38 (0.48—3.97)	0.54
No. camel herds within a 15-min drive				
>20	3.33 (0.77—17.53)	0.11	2.40 (0.53—10.84)	0.25
Herd is kept together as single group throughout the year	2.24 (0.61. 9.85)	0.23	–	–
Herd has contact with other local herds	2.34 (0.65—9.85)	0.19	–	–
Camel is a racing camel§	0.73 (0.13—4.33)	0.72	–	–
Camels are lent for breeding purposes	2.39 (0.66—10.70)	0.19	–	–
Closed herd#	0.07 (0.01—0.43)	0.01	0.08 (0.01—0.55)	0.02

*Variables reference the 1-year period before sampling, with the exception of herd size, camel is a racing camel, and a priori variables: age, sex, and region. Because of the potential influence of maternal immunity, camels <6 m of age have been excluded.
†Adjusted for a priori variables: age, sex, and region.
‡2017–2018 study was adjusted for a priori variables and number of camels nearby (within a 15 min drive), herd is kept as a single group throughout the year, herd has contact with other local herds, and camel is a racing camel.
§Individual camel–level variables (all other variables being herd-level).
¶Open ad lib indicates irrigation reservoir or spring water sources were used; household only indicates water source was not shared between household and herd; trough only indicates only tanker, tap, or well sources were used.
#Closed herd indicates herd owners answered no to all of the following variables: borrowing, lending, purchasing, racing, and contact with local or distant herds (2017–2018 study only, missing data 2014–2015). Because of collinearity with constituent variables, the variable closed herd was included in a separate multivariate model from camels are borrowed for breeding purposes and camels are lent for breeding purposes. In this model, all variables listed continued to demonstrate significant association (p<0.05) with Middle East respiratory syndrome coronavirus seropositivity, with the exception of water source (p = 0.07).

managed herds, such as those in Jordan. In addition, despite the challenges of artificial insemination in camelids, the introduction of an affordable artificial insemination service, where feasible, could mitigate the transmission of MERS-CoV between infected and uninfected herds (27). Other potential control measures could be introducing rRT-PCR testing schemes using nasal swab samples before movement between herds and quarantining of positive animals (28). In view of the current understanding that MERS-CoV transmission in camels occurs primarily through upper respiratory droplet, evidence for possible sexual transmission remains inconclusive, and further research is required (12,29).

Closed herd management practices were found to be significantly protective, offering a potentially valuable tool in controlling MERS-CoV among camels; voluntary closed herd schemes are a possible route to achieving disease-free herds (30). Where such practices would be impractical, our findings suggest that quarantining animals before introduction to the herd offers a protective effect. On the basis of current evidence of viral shedding patterns in camels, quarantine periods of ≥2 weeks should be employed.

Increasing herd size was found to be associated with increased MERS-CoV seroprevalence; larger herds are thought to provide a greater host reservoir capable of sustaining viral transmission between infected and uninfected animals (16,17). In addition, the use of water troughs within herds, as opposed to open ad lib water sources, was associated with increased herd seroprevalence (although only in the 2017–2018 multivariate model when the variable borrowing for breeding was included). Although crowded troughs might be a potential route of viral transmission within herds, further research is required (31).

As described in other studies, seroprevalence increased significantly with age in both studies, likely associated with the increased probability of disease exposure over time and boosting of antibody levels by repeat infections (16,17). Results of the 2017–2018 study strongly suggest the presence of maternally derived immunity among calves ≤6 months of age, which could have relevance for future vaccination strategies (18). This association was less evident in the 2014–2015 study; however, only 9 camels ≤6 months of age were sampled in 2014–2015, compared with 39 in 2017–2018. Associations between sex and seropositive status have been previously described, but

no significant associations were identified in either study (*16*,*17*,*32*).

The difference in adjusted seroprevalence observed between studies (together with differences in regional associations with seropositivity) might be explained by several factors. Those factors include differences in sampling strategy (nonprobabilistic vs. probabilistic), an absence of sample collection during the 2017–2018 summer period (with seroprevalence highest in summer 2014–2015), and a possibly limited introduction of new MERS-CoV variants into the population between the study periods, with geographic spread over time (*33*). Importing of foreign camels into Jordan is strictly regulated by MoA and permitted only for animals going directly to slaughter (*34*).

The first limitation of this study is that no nasal swab specimens tested positive for MERS-CoV RNA on rRT-PCR; evidence for potential viral transmission routes were therefore suggestive instead of definitive. Possible explanations include the narrow window of nasal shedding reported in camels ($\leq$2 weeks) (*12*) and the low prevalence of nasal discharge observed, potentially reflecting a limited genetic diversity of MERS-CoV variants circulating among camels in Jordan with rapid seroconversion and clearance (*35*). Second, limited sample size resulted in considerable uncertainty on strength of associations. Third, data at the level of individual camels, particularly regarding history of movement for purchase and breeding, were limited. Such data could have supported herd-level findings and identified camels potentially infected outside the herd (depending on duration of detectable antibodies) (*36*). Fourth, in detecting an association between seropositivity and potential risk factors, assumptions were made regarding persistence of detectable antibodies (>1 year), meaning that estimates of association are potentially conservative (*37*,*38*).

In conclusion, borrowing male camels for breeding and closed herd management practices were associated with MERS-CoV infection prevalence among camel populations in Jordan, suggesting possible useful interventions to reduce transmission. In addition, older age, larger herd size, and use of water troughs within herds were also associated with seropositivity. In view of this finding, future MERS-CoV vaccination strategies among camel populations in Jordan could potentially prioritize breeding males, which are likely to be shared between herds for breeding purposes. In addition, several targeted management interventions should be considered: measures to reduce the number of camels, particularly males, shared between herds for breeding purposes

(including, if feasible, introducing an affordable camel artificial insemination service at a regional or national level); maintaining a closed herd where possible, including the potential for voluntary closed herd management schemes; and quarantine practices of $\geq$2 weeks before introducing new animals to the herd. The implementation of such interventions among herds in Jordan and the wider region, alongside targeted vaccination, could reduce the prevalence of MERS-CoV among camel populations and confer a vitally protective effect on human populations associated with these herds (*39*).

About the Author

Dr. Holloway is a researcher with the Royal Veterinary College, London. His primary research interest is the epidemiology and control of camel zoonoses.

References

1. Peeri NC, Shrestha N, Rahman MS, Zaki R, Tan Z, Bibi S, et al. The SARS, MERS and novel coronavirus (COVID-19) epidemics, the newest and biggest global health threats: what lessons have we learned? Int J Epidemiol. 2020;49:717–26. https://doi.org/10.1093/ije/dyaa033
2. European Centre for Disease Prevention and Control. Severe respiratory disease of unknown origin—Jordan—outbreak in ICU. Communicable Disease Threats Report, Week 18, 29 April–5 May, 2012 [cited 2021 May 19]. https://www.ecdc.europa.eu/sites/default/files/media/en/publicationsPublications/CDTR%20online%20version%204%20May%202012.pdf
3. Lucey DR. Editorial commentary: still learning from the earliest known MERS outbreak, Zarqa, Jordan, April 2012. Clin Infect Dis. 2014;59:1234–6. https://doi.org/10.1093/cid/ciu638
4. World Health Organization. Middle East respiratory syndrome [cited 2021 May 19]. http://www.emro.who.int/health-topics/mers-cov/mers-outbreaks.html
5. Reusken CB, Ababneh M, Raj VS, Meyer B, Eljarah A, Abutarbush S, et al. Middle East Respiratory Syndrome

coronavirus (MERS-CoV) serology in major livestock species in an affected region in Jordan, June to September 2013. Euro Surveill. 2013;18:20662. https://doi.org/10.2807/1560-7917. ES2013.18.50.20662

6. Azhar EI, El-Kafrawy SA, Farraj SA, Hassan AM, Al-Saeed MS, Hashem AM, et al. Evidence for camel-to-human transmission of MERS coronavirus. N Engl J Med. 2014;370:2499–505. https://doi.org/10.1056/NEJMoa1401505

7. Lau SKP, Zhang L, Luk HKH, Xiong L, Peng X, Li KSM, et al. Receptor usage of a novel bat lineage C betacoronavirus reveals evolution of Middle East respiratory syndrome-related coronavirus spike proteins for human dipeptidyl peptidase 4 binding. J Infect Dis. 2018;218:197–207. https://doi.org/10.1093/infdis/jiy018

8. World Health Organization. Middle East respiratory syndrome coronavirus (MERS-CoV) [cited 2021 May 19]. https://www.who.int/news-room/fact-sheets/detail/middle-east-respiratory-syndrome-coronavirus-(mers-cov)

9. Dudas G, Carvalho LM, Rambaut A, Bedford T. MERS-CoV spillover at the camel-human interface. [Erratum in: Elife. 2018;7:e37324]. eLife. 2018;7:e31257.

10. Assiri A, McGeer A, Perl TM, Price CS, Al Rabeeah AA, Cummings DA, et al.; KSA MERS-CoV Investigation Team. Hospital outbreak of Middle East respiratory syndrome coronavirus. N Engl J Med. 2013;369:407–16. https://doi.org/10.1056/NEJMoa1306742

11. Cho SY, Kang JM, Ha YE, Park GE, Lee JY, Ko JH, et al. MERS-CoV outbreak following a single patient exposure in an emergency room in South Korea: an epidemiological outbreak study. Lancet. 2016;388:994–1001. https://doi.org/10.1016/S0140-6736(16)30623-7

12. Adney DR, van Doremalen N, Brown VR, Bushmaker T, Scott D, de Wit E, et al. Replication and shedding of MERS-CoV in upper respiratory tract of inoculated dromedary camels. Emerg Infect Dis. 2014;20:1999–2005. https://doi.org/10.3201/eid2012.141280

13. Alnaeem A, Kasem S, Qasim I, Al-Doweriej A, Al-Houfufi A, Alwazan A, et al. Some pathological observations on the naturally infected dromedary camels (Camelus dromedarius) with the Middle East respiratory syndrome coronavirus (MERS-CoV) in Saudi Arabia 2018–2019. Vet Q. 2020;40:190–7. https://doi.org/10.1080/01652176.2020.1781350

14. Hui DS, Azhar EI, Kim YJ, Memish ZA, Oh MD, Zumla A. Middle East respiratory syndrome coronavirus: risk factors and determinants of primary, household, and nosocomial transmission. Lancet Infect Dis. 2018;18:e217–27. https://doi.org/10.1016/S1473-3099(18)30127-0

15. World Health Organization. Prioritizing diseases for research and development in emergency contexts [cited 2021 May 19]. https://www.who.int/activities/prioritizing-diseases-for-research-and-development-in-emergency-contexts

16. Dighe A, Jombart T, Van Kerkhove MD, Ferguson N. A systematic review of MERS-CoV seroprevalence and RNA prevalence in dromedary camels: implications for animal vaccination. Epidemics. 2019;29:100350. https://doi.org/10.1016/j.epidem.2019.100350

17. Sikkema RS, Farag EABA, Islam M, Atta M, Reusken CBEM, Al-Hajri MM, et al. Global status of Middle East respiratory syndrome coronavirus in dromedary camels: a systematic review. Epidemiol Infect. 2019;147:e84. https://doi.org/10.1017/S095026881800345X

18. Alharbi NK, Qasim I, Almasoud A, Aljami HA, Alenazi MW, Alhafufi A, et al. Humoral immunogenicity and efficacy of a single dose of ChAdOx1 MERS vaccine candidate in dromedary camels. Sci Rep. 2019;9:16292. https://doi.org/10.1038/s41598-019-52730-4

19. Rodon J, Okba NMA, Te N, van Dieren B, Bosch BJ, Bensaid A, et al. Blocking transmission of Middle East respiratory syndrome coronavirus (MERS-CoV) in llamas by vaccination with a recombinant spike protein. Emerg Microbes Infect. 2019;8:1593–603. https://doi.org/10.1080/22221751.2019.1685912

20. Adney DR, Wang L, van Doremalen N, Shi W, Zhang Y, Kong WP, et al. Efficacy of an adjuvanted Middle East respiratory syndrome coronavirus spike protein vaccine in dromedary camels and alpacas. Viruses. 2019;11:212. https://doi.org/10.3390/v11030212

21. Mubarak A, Alturaiki W, Hemida MG. Middle East respiratory syndrome coronavirus (MERS-CoV): infection, immunological response, and vaccine development. J Immunol Res. 2019;2019:6491738. https://doi.org/10.1155/2019/6491738

22. van Doremalen N, Hijazeen ZS, Holloway P, Al Omari B, McDowell C, Adney D, et al. High prevalence of Middle East respiratory coronavirus in young dromedary camels in Jordan. Vector Borne Zoonotic Dis. 2017;17:155–9. https://doi.org/10.1089/vbz.2016.2062

23. Falzarano D, Kamissoko B, de Wit E, Maïga O, Cronin J, Samaké K, et al. Dromedary camels in northern Mali have high seropositivity to MERS-CoV. One Health. 2017;3:41–3. https://doi.org/10.1016/j.onehlt.2017.03.003

24. Corman VM, Eckerle I, Bleicker T, Zaki A, Landt O, Eschbach-Bludau M, et al. Detection of a novel human coronavirus by real-time reverse-transcription polymerase chain reaction [Erratum in: Euro Surveill. 2012;17:pii/20288]. Euro Surveill. 2012;17:20285. https://doi.org/10.2807/ese.17.39.20285-en

25. Saeb M, Baghshani H, Nazifi S, Saeb S. Physiological response of dromedary camels to road transportation in relation to circulating levels of cortisol, thyroid hormones and some serum biochemical parameters. Trop Anim Health Prod. 2010;42:55–63. https://doi.org/10.1007/s11250-009-9385-9

26. Padalino B, Monaco D, Lacalandra G. Male camel behaviorand breeding management strategies: how to handle a camel bull during the breeding season? Emir J Food Agric. 2015;27:338–49. https://doi.org/10.9755/ejfa.v27i4.19909

27. Skidmore JA, Morton KM, Billah M. Artificial insemination in dromedary camels. Anim Reprod Sci. 2013;136:178–86. https://doi.org/10.1016/j.anireprosci.2012.10.008

28. Al Hammadi ZM, Chu DK, Eltahir YM, Al Hosani F, Al Mulla M, Tarnini W, et al. Asymptomatic MERS-CoV infection in humans possibly linked to infected dromedaries imported from Oman to United Arab Emirates, May 2015. Emerg Infect Dis. 2015;21:2197–200. https://doi.org/10.3201/eid2112.151132

29. Hemida MG, Waheed M, Ali AM, Alnaeem A. Detection of the Middle East respiratory syndrome coronavirus in dromedary camel's seminal plasma in Saudi Arabia 2015–2017. Transbound Emerg Dis. 2020;67:2609–14. https://doi.org/10.1111/tbed.13610

30. Sayers RG, Sayers GP, Mee JF, Good M, Bermingham ML, Grant J, et al. Implementing biosecurity measures on dairy farms in Ireland. Vet J. 2013;197:259–67. https://doi.org/10.1016/j.tvjl.2012.11.017

31. Fèvre EM, Bronsvoort BM, Hamilton KA, Cleaveland S. Animal movements and the spread of infectious diseases. Trends Microbiol. 2006;14:125–31. https://doi.org/10.1016/j.tim.2006.01.004

32. Kandeil A, Gomaa M, Nageh A, Shehata MM, Kayed AE, Sabir JSM, et al. Middle East respiratory syndrome coronavirus (MERS-CoV) in dromedary camels in Africa and Middle East. Viruses. 2019;11:717. https://doi.org/10.3390/v11080717

33. Wernery U, Woo PCY. Middle East respiratory syndrome: making the case for surveillance of transboundary coronaviruses in the Middle East. Rev Sci Tech. 2019;38:61–9. https://doi.org/10.20506/rst.38.1.2941

34. Abutarbush S, Hijazeen Z, Doodeen R, Hawawsheh M, Ramadneh W, Al Hanatleh M. Analysis, description and mapping of camel value chain in Jordan. Glob Vet. 2018;20:144–52.

35. Seifert SN, Schulz JE, Ricklefs S, Letko M, Yabba E, Hijazeen ZS, et al. Limited genetic diversity detected in Middle East respiratory syndrome-related coronavirus variants circulating in dromedary camels in Jordan. Viruses. 2021;13:592. https://doi.org/10.3390/v13040592

36. Ali MA, Shehata MM, Gomaa MR, Kandeil A, El-Shesheny R, Kayed AS, et al. Systematic, active surveillance for Middle East respiratory syndrome coronavirus in camels in Egypt. Emerg Microbes Infect. 2017;6:e1. https://doi.org/10.1038/emi.2016.130

37. Hemida MG, Alnaeem A, Chu DK, Perera RA, Chan SM, Almathen F, et al. Longitudinal study of Middle East Respiratory Syndrome coronavirus infection in dromedary camel herds in Saudi Arabia, 2014–2015. Emerg Microbes Infect. 2017;6:e56. https://doi.org/10.1038/emi.2017.44

38. Wernery U, Corman VM, Wong EY, Tsang AK, Muth D, Lau SK, et al. Acute Middle East respiratory syndrome coronavirus infection in livestock dromedaries, Dubai, 2014. Emerg Infect Dis. 2015;21:1019–22. https://doi.org/10.3201/eid2106.150038

39. Al-Ahmadi K, Alahmadi M, Al-Zahrani A. Spatial association between primary Middle East respiratory syndrome coronavirus infection and exposure to dromedary camels in Saudi Arabia. Zoonoses Public Health. 2020;67:382–90. https://doi.org/10.1111/zph.12697

Address for correspondence: Peter Holloway, Veterinary Epidemiology, Economics and Public Health Group, The Royal Veterinary College, Royal College St, London NW1 0TU, UK; email: pholloway3@rvc.ac.uk

May 2021

COVID-19

EMERGING INFECTIOUS DISEASES

To revisit the May 2021 issue, go to:
https://wwwnc.cdc.gov/eid/articles/issue/27/5/table-of-contents

Estimating the Impact of Statewide Policies to Reduce Spread of Severe Acute Respiratory Syndrome Coronavirus 2 in Real Time, Colorado, USA

Andrea G. Buchwald,[1] Jude Bayham, Jimi Adams, David Bortz, Kathryn Colborn, Olivia Zarella, Meghan Buran, Jonathan Samet, Debashis Ghosh, Rachel Herlihy, Elizabeth J. Carlton

The severe acute respiratory syndrome coronavirus 2 (SARS-CoV-2) pandemic necessitated rapid local public health response, but studies examining the impact of social distancing policies on SARS-CoV-2 transmission have struggled to capture regional-level dynamics. We developed a susceptible-exposed-infected-recovered transmission model, parameterized to Colorado, USA–specific data, to estimate the impact of coronavirus disease–related policy measures on mobility and SARS-CoV-2 transmission in real time. During March–June 2020, we estimated unknown parameter values and generated scenario-based projections of future clinical care needs. Early coronavirus disease policy measures, including a stay-at-home order, were accompanied by substantial decreases in mobility and reduced the effective reproductive number well below 1. When some restrictions were eased in late April, mobility increased to near baseline levels, but transmission remained low (effective reproductive number <1) through early June. Over time, our model's parameters were adjusted to more closely reflect reality in Colorado, leading to modest changes in estimates of intervention effects and more conservative long-term projections.

Mathematical transmission models are useful tools for predicting the magnitude, duration, and severity of the severe acute respiratory coronavirus 2 (SARS-CoV-2) pandemic. However, widely used national-level models might not capture regional heterogeneity. The coronavirus disease (COVID-19) outbreak in Colorado, USA, has been the subject of numerous discrepant projections from the Institute for Health Metrics and Evaluation and other modeling groups (1), which might have structural and data source explanations, highlighting the need for ensuring that models are fit to local epidemiologic data (2–4).

We report on our experience using a locally tailored model to inform policy in Colorado. Social distancing policies, intended to decrease contact rates, have been cornerstone public health tools for pandemic control, and these strategies have been adopted to control SARS-CoV-2 globally (2,5). Until recently, evidence of the effects of social distancing has come primarily from studies of the consequences of school and transit closures on influenza transmission (3,4,6). Early evidence suggests that social distancing policies can suppress transmission of SARS-CoV-2 (7,8), and recent evidence suggests a strong correlation between mobility and transmission reduction (9). However, these studies largely focused on periods when social distancing policies were in place, leaving critical questions unanswered regarding how long populations will comply with such measures and what happens when policies are relaxed.

One of the defining characteristics of the COVID-19 pandemic is the need for rapid response in the face of imperfect and incomplete information. Mathematical models of infectious disease transmission can be used in real-time to estimate parameters, such as the effective re-

Author affiliations: Colorado School of Public Health, Aurora, Colorado, USA (A.G. Buchwald, O. Zarella, M. Buran, J. Samet, D. Ghosh, E.J. Carlton); Colorado State University, Fort Collins, Colorado, USA (J. Bayham); University of Colorado, Denver, Colorado, USA (J. Adams); University of Colorado, Boulder, Colorado, USA (D. Bortz); University of Colorado School of Medicine, Aurora (K. Colborn); Colorado Department of Public Health and Environment, Denver (R. Herlihy)

[1]Current affiliation: University of Maryland School of Medicine, Baltimore, Maryland, USA.

productive number (R_e) and the efficacy of current and future intervention measures, providing time-sensitive data to policy-makers (*10*). We describe development of such a model, in close collaboration with the Colorado Department of Health and Environment and the Governor's office, to gauge the current and future effects of early policies to decrease social contacts and, later, the gradual relaxing of stay-at-home orders.

We developed a compartmental susceptible-exposed-infected-recovered (SEIR) model calibrated to statewide COVID-19 case and hospitalization data to estimate changes in the contact rate and the R_e after emergence of SARS-CoV-2 and the implementation of statewide social distancing policies in Colorado. We supplemented model estimates with an analysis of mobility by using mobile-device location data. Estimates were generated in near real time, at multiple time-points, with a rapidly evolving understanding of SARS-CoV-2. At each time point, we generated projections of the possible course of the outbreak under future social distancing scenarios. Findings were regularly provided to key Colorado decision-makers. We present estimates generated at multiple time points to document how our model, estimates and projections evolved over time. Although our analysis is specific to Colorado, our experience highlights the need for locally calibrated transmission models to inform public health preparedness and policymaking, along with ongoing analyses of the impact of policies to slow the spread of SARS-CoV-2.

Methods

COVID-19 Timeline and Policies

The first SARS-CoV-2 case was reported in Colorado on March 5, 2020, and a rapid succession of policies to control transmission followed (Table 1). The Colorado governor formally declared a disaster emergency on March 11. During March 14–April 16, a total of 35 executive orders were mandated to curb SARS-CoV-2 transmission, including school closures, reduction in workforce percentages, and shelter-in-place (stay-at-home) orders. In conjunction with state executive orders, the Colorado Department of Health and Environment issued orders closing restaurants, bars, and other congregate environments on March 17 and prohibiting gatherings of >10 persons on March 19. A state-wide stay-at-home order was in effect during March 26–April 26. Transition to a less restrictive phase, safer-at-home, began on April 27, which enabled some businesses to reopen with restrictions. The metropolitan Denver counties, comprising ≈50%

of the population of Colorado, were under extended stay-at-home orders until May 8.

Reported Case and Hospitalization Data

Hospitalization data are a robust indicator of transmission trends compared with reported case data because reported case data are sensitive to testing capacity. However, because COVID-19 hospitalization data were sparse early in the epidemic, we initially fit models to reported COVID-19 cases from the Colorado Electronic Disease Reporting System (CEDRS). We fit models to the daily number of symptom onsets to reflect a biologically meaningful process (report date can be sensitive to testing lags). Missing onset dates were imputed as report date minus 7 days, the median onset-to-report lag. In May, we began fitting models to the daily number of hospitalized COVID-19 patients because we suspected that reported cases captured a variable proportion of infections over time because of increases in testing capacity. Daily hospital census records were obtained from EMResource (https://emresource.juvare.com). Because EMResource appeared to underreport COVID-19 hospitalizations during March, we inferred COVID-19 hospitalizations by using CEDRS before April 8 (Appendix Figure 1, https://wwwnc.cdc.gov/EID/article/27/9/20-4167-App1.pdf).

Model Description

We used a deterministic age-structured SEIR model with 3 age groups (<30, 30–59, and ≥60 years of age) to estimate key model parameters and project the number of COVID-19 hospitalizations (Appendix). In the model, we assume a single virus introduction event occurring on January 24, a date extrapolated from the first reported cases in Colorado.

In the model, the probability that an infected person shows development of symptoms (*13*) and needs hospitalization or ICU care is age dependent (*14*) (Appendix Table 1). All persons have an equal probability of exposure and infection, regardless of age. Initially, we used published estimates (*15*) for the proportion of symptomatic case-patients requiring hospitalization and critical care. Starting in May, with sufficient hospitalization data, we generated Colorado-specific estimates of the probability of hospitalization and critical care among case-patients by using model-fitting approaches, which enabled us to better account for underlying health status and patterns of care in Colorado (*16*).

The model includes 3 types of transmission-reducing parameters: social distancing, mask wearing,

Table 1. Key state-level events, executive orders, and policies directed at controlling transmission of SARS-CoV-2, Colorado, USA, 2020*

Policy/event	Description	Date announced	Policy effective date	Policy effective until
First case of COVID-19	First case of infection with SARS-CoV-2 reported	Mar 5	NA	NA
Executive Order D 2020 003	Disaster emergency	Mar 10	Mar 11	Apr 11
Executive Order D 2020 004	Ski resort closure	Mar 14	Mar 15	Mar 22
Executive Order D 2020 006	Extension of ski resort closure	Mar 18	Mar 18	Apr 17
CDPHE Order 20–22	Closure of bars, restaurants, theaters, gymnasiums, and casinos	Mar 16	Mar 17	Apr 16
CDPHE Order 20–23	Prohibition of >10 person gatherings	Mar 19	Mar 19	Apr 19
Executive Order D 2020 007	School closures during Mar 18–Apr 17	Mar 18	Mar 18	Apr 17
Executive Order D 2020 013	Reduction of in-person workforce by 50%	Mar 22	Mar 24	May10
Executive Order D 2020 017	Stay-at-home order: directive to require all residents of Colorado to stay home unless in pursuant of essential items (i.e., food) or working for critical businesses and ordering noncritical businesses to close temporarily.	Mar 25	Mar 26	Apr 11
Executive Order D 2020 021	Extension to school closures until Apr 30	Apr 1	Apr 1	May 1
Executive Order D 2020 024	Stay-at-Home extension	Apr 6	Apr 6	Apr 26
Executive Order D 2020 039	Ordering workers in critical businesses and government functions to wear nonmedical face coverings	Apr 17	Apr 17	May 17
Executive Order D 2020 041	Suspension of school closures until end of school year	Apr 22	Apr 22	May 20
Executive Order D 2020 044	Safer at home: All susceptible persons and those who have COVID-19 instructed to stay at home. State residents directed to limit interactions, only travel for essential needs, and limit gatherings to <10 people in public and private spaces. Nonmedical mask coverings recommended. Retail businesses can open for curbside delivery, elective medical, dental, and veterinary surgeries and procedures resume. Retail businesses and personal services (e.g., salons) can open. Offices can open at 50% capacity.†	Apr 26	Apr 27–May 4	May 27
Executive Order D 2020 058	Disaster emergency extension	May 7	May 7	Jun 6
Executive Order D 2020 067	Extending EO D 2020 039, ordering workers in critical businesses and government, to wear nonmedical face coverings	May 16	May 16	Jun 16
Executive Order D 2020 079	Extension to EO D 2020 044: Safer at Home to permit public places to offer outdoor dining, and limited indoor dining	May 25	May 25	Jun 1

*COVID-19–relevant executive orders are detailed in (11) and CDPHE policies are described in (12). CDPHE, Colorado Department of Public Health and Environment; COVID-19, coronavirus disease; EO, executive order; NA, not applicable; SARS-CoV-2, severe acute respiratory syndrome coronavirus 2.
†Retail business and personal services were permitted to open on May 1, offices were permitted to open at 50% capacity on May 4. All other measures went into effect April 27.

and self-isolation of symptomatic persons. Social distancing was modeled as a reduction in the contact rate between susceptible and infectious persons by multiplying the transmission parameter, β, by (1 – social distancing). We defined contacts as interactions that could enable spread of infections from an infected person to a susceptible person. The term social distancing is used to encompass all contact-reducing behaviors and policies, including working from home, school closures, maintaining physical distancing, socializing outdoors (vs. indoors), and increased hygiene. Social distancing was modeled in phases coinciding with major events and policy measures (Figure 1). Phase 1 (March 17–25) corresponds with mid-March policies and increasing public concern regarding COVID-19, phase 2 (March 26–April 26) corresponds with the state-wide stay-at-home order, phase 3 (April 27–May 8) is the period when half the state transitioned to safer-at-home, and phase 4 (May 9–June 3) is the period when safer-at-home was in effect statewide.

We added mask wearing to the model in May (fits 3 and 4) in response to increasing evidence that masks are effective for controlling transmission (17,18). We modeled the effect of mask wearing as a reduction in the spread of infections from asymptomatic and presymptomatic persons to nonhousehold contacts. More recent evidence suggests that masks might also protect the wearer, an added benefit not considered here (19). The effectiveness of mask wearing depends on the ability of the mask to trap infectious particles and the proportion of the population

wearing masks. We assume in the model that masks made from household materials are ≈50% effective in trapping infectious particles when worn properly (*17,18*). Previous studies estimated that ≈23% of contacts occur at home (*20*). Because persons spent more time at home during the pandemic, we assumed that 67% of the contact of an individual is with nonhousehold members. We assumed that mask wearing was uniform across asymptomatic and presymptomatic persons and fit the proportion of the population wearing masks beginning on April 4, the date of the governor's press conference advising persons living in Colorado to wear masks. Because some transmission might also occur by fomites, we modeled mask effectiveness as a net 27% reduction in infectiousness among asymptomatic persons wearing masks. In addition, we assume mask wearing decreases transmission by presymptomatic persons (*21,22*); this is modeled as a 3.4% reduction in infectiousness for symptomatic persons wearing masks (assuming that symptomatic persons are asymptomatic on 1 of 8 infectious days). This model does not account for potential reduction in infectiousness by symptomatic persons who are assumed to isolate (*23*).

We modeled self-isolation assuming that a proportion of symptomatic case-patients self-isolate 24 hours after the onset of symptoms, and that self-isolation reduces transmission by symptomatic persons to nonhousehold contacts. This assumption is modeled as a 59% reduction in contacts by symptomatic persons who self-isolate. Self-isolation begins in the model on March 5 and the proportion of symptomatic persons who self-isolate is fit to the data.

Estimating Social Distancing and Other Transmission-Reducing Interventions

We inferred the effect of social distancing and other interventions on transmission by using an algorithm-based optimization procedure at 4 different time points from April through June. We used the same approaches to estimate parameters that might vary regionally or for which there was considerable uncertainty in the literature (Table 2). We identified best-fitting parameter values by using a least-squares cost function that minimized difference between the model-estimated and observed number of reported SARS-CoV-2 cases in Colorado (fits 1 and 2) and the observed number of COVID-19 hospitalizations (fits 3 and 4). When fitting to cases (fits 1 and 2), it was necessary to also fit a parameter for the estimated probability that cases would be detected by state surveillance. We minimized the cost function by using a 2-stage fitting algorithm in R (*27*) and used the FME package (*28*) by first applying a pseudo-random optimization algorithm (*29*) to find a
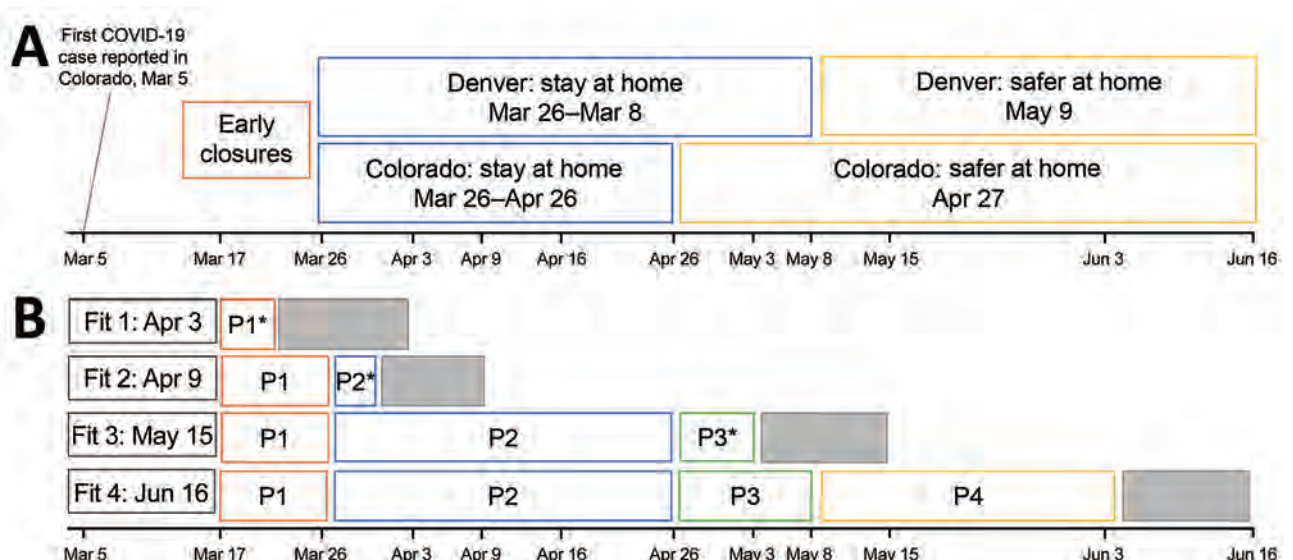
Figure 1. Emergence of COVID-19, Colorado, USA, 2020, showing policy-based responses (A) and definition of 4 distinct social distancing phases (B) corresponding with early closures (phase 1, March 17–25); statewide stay-at-home (phase 2, March 26–April 26), statewide partial transition to safer-at-home (phase 3, April 27–May 8); statewide safer-at-home (phase 4, May 5–June 3). Social distancing parameters were estimated at 4 points during March–June by using model fitting procedures and reported case data (fits 1 and 2) and hospital census data (fits 3 and 4). In light of the 5.1 day mean incubation period, the ≈7-day lag between symptom onset and case report, and the ≈8-days between symptom onset and hospitalization based on state records, there are ≈12 and 13 day lags between infection and case report, and infection and hospitalization, respectively (gray boxes). Thus, at each model fit, we could estimate social distancing parameters reflecting transmission conditions up to 12 (fits 1 and 2) or 13 (fits 3 and 4) days before the fit date. Asterisks (*) indicate estimate generated for only part of the period. COVID-19, coronavirus disease; P, phase.

Table 2. Model-estimated levels of social distancing, mask wearing and other parameter values at 4 time points over the course of the SARS-CoV-2 epidemic, Colorado, USA, 2020*

Characteristic	Range of possible values and sources (ref.)	Fitted value as of Apr 3† (95% CI)	Fitted value as of Apr 16† (95% CI)	Fitted value as of May 15† (95% CI)	Fitted value as of Jun 16† (95% CI)
Estimated effectiveness of social distancing					
Phase 1: early closures, Mar 17–25, %‡	10–70	45 (42–53)	65 (63–72)	52 (49–66)	52 (52–53)
Phase 2: state-wide stay-at-home, Mar 26–Apr 26, %	50–99	NA	76 (72–77)	80 (80–83)	81 (80–82)
Phase 3: half of state under stay-at-home, half transitioned to safer at home, Apr 27–May 8, %	45–99	NA	NA	80 (78–84)	85 (83–90)
Phase 4: statewide safer at home, May 9–Jun 3, %§	NA	NA	NA	NA	90 (85–93)
Proportion of population wearing masks starting Apr 4	0.1–0.8	NA	NA	0.4 (0.11–0.64)	0.40 (0.15–0.76)
Other parameter values					
Rate of infection	0.2–0.6 (24)	0.41 (0.39–0.42)	0.50 (0.49–0.51)	0.48 (0.46–0.49)	0.48 (0.48–0.48)
Reduction in infectious contacts due to symptomatic persons who self-isolate after March 5	0.3–0.8 (15)	0.38 (0.22–0.43)	0.47 (0.34–0.50)	0.30 (0.29–0.31)	0.32 (0.32–0.32)
Ratio of infectiousness for symptomatic vs. asymptomatic persons	1.0–4.0 (25,26)	2.27 (2.22–2.29)	1.50 (1.35–1.56)	1.65 (1.60–1.77)	1.68 (1.67–1.69)
Probability that symptomatic cases are identified by state surveillance	0.05–0.6 (24)	0.28 (0.16–0.45)	0.33 (0.27–0.44)	NA	NA

*COVID-19, coronavirus disease; NA, not available; ref, reference; SARS-CoV-2, severe acute respiratory syndrome coronavirus 2.
†Fit 1 uses all reported SARS-CoV-2 cases as of Apr 3 with an onset date of Mar 26 or earlier; fit 2 uses all reported cases as of Apr 16 with an onset date of Apr 8 or earlier; fit 3 uses COVID-19 hospital census through May 15; fit 4 uses hospital census data through Jun 16.
‡For the purpose of model fitting, phase 1 social distancing was modeled by using a start date of Mar 17, which corresponded with the closure of bars, restaurants, casinos, and many public schools in the state.
§The statewide Safer at Home policy remained in effect through the summer, but because of the ≈5.1-d mean incubation period and the 8-d lag between symptom onset and hospitalization, we were able to generate transmission estimates through Jun 3.

region of minimum difference between the model and the data. The second phase used least-squares optimization applying the Levenberg-Marquardt algorithm (30). We calculated 95% CIs by using a Markov Chain Monte Carlo simulation with an adaptive Metropolis algorithm with 1,500 iterations (28). This method obtains 95% CIs by sampling from a Gaussian distribution around the mean trajectory of the ordinary differential equation model. By the end of March, the differential sensitivity matrix was full rank, and thus all 6 parameters were identifiable for all datasets used (Appendix Figure 3).

Because of the median 7-day lag between symptom onset and reporting, on April 3 (fit 1), we included cases that had a symptom onset date through March 26 for model fitting, which enabled us to generate a preliminary estimate of phase 1 social distancing. On April 16 (fit 2), we included cases that had an onset date through April 9 for model fitting, which enabled us to refine estimates of social distancing during phase 1 and generate preliminary estimates of social distancing during phase 2. We generated a preliminary estimate of phase 3 social distancing on May 15 (fit 3) and then re-estimated on June 16 (fit 4), when social distancing during phase 4 was estimated. We estimated the proportion of the population wearing masks in fits 3 and 4 with the effectiveness assumptions

defined and estimated the effective reproduction number (R_e) from the model output (Appendix). We additionally estimated the overall number of hospitalizations prevented as a result of decreasing contacts by comparing the fitted model on June 16 with a reference scenario assuming no reduction of the contact rate (social distancing = 0%).

Projections of COVID-19 Hospitalizations and ICU Need
We used the fitted parameters to generate projections of future hospital and critical care needs under different scenarios. Changes in social distancing were implemented beginning 2 weeks after the date of model fitting to account for lags in policy implementation. All other parameters were held fixed as estimated from the model. Preparing for and meeting ICU load was a critical decision-making issue.

Population Mobility
We used SafeGraph (https://www.safegraph.com) data to examine changes in mobility in Colorado from March through June. Specifically, we used an aggregated and anonymized measure of time away from home reported at the census block group. We calculated changes in mobility as a percent decrease in time away from home relative to pre-epidemic baseline: January 29–February 15 (mean 2.3 hours).

We examined the relationship between mobility and transmission by calibrating the transmission parameter, β, conditional on time away from home at baseline. We then projected the model forward, enabling the parameter for the daily time away from home to change according to observed mobility data. These projections assume no other transmission reducing behavior (i.e., no mask wearing or self-isolation) to avoid conflating parametric assumptions with changes in observed mobility, nor changes to any other aspects of the model.

Results

Estimating Efficacy of Social Distancing and Other Transmission-Reducing Interventions

On April 3 (fit 1), we generated a preliminary estimate of social distancing during phase 1, which equated to a ≈45% decrease in the contact rate (Table 2; Figure 2), and R_e decreased from 5.3 to 2.4 (Figure 3). Because of the ≈12-day lag between infection and case report, this preliminary estimate was through March 21. On April 16 (fit 2), with more complete case data, the updated estimate of social distancing during phase 1 was greater: a 65% decrease in the contact rate. At this point, we generated a preliminary estimate of the level of social distancing during the first 2 weeks of phase 2 (March 26–April 4): 76%. R_e was estimated to

be 0.9. Incorporating increasing data and using CO-VID-19 hospitalizations instead of case reports, on May 15 (fit 3), we re-estimated phase 1 and phase 2 parameters, which indicated transmission reduction had been more moderate initially (social distancing = 52% for phase 1), and greater for phase 2 (social distancing = 80%). On May 15, which was 18 days after the end of the stay-at-home order, there was no evidence of an increase in hospitalizations or contact rate due to decreased restrictions, noting that because of the ≈13-day lag between infection and hospitalization, this estimate reflects transmission through May 2. A month later on June 16 (fit 4), a greater decrease in transmission was estimated for phase 3 (social distancing = 85%), and the estimated decrease in contact rates during safer-at-home (phase 4) was 90%. Estimated R_e decreased to 0.6 during phase 4.

Estimated Reduction in Hospitalizations from Decreased Contacts

As of June 16, a total of 5,272 COVID-19 hospitalizations in Colorado had been reported to CEDRS, and EMResource data strongly suggested under-reporting of COVID-19 hospitalizations to CEDRS during April and May. Using CEDRS and EMResource data, we found that the SEIR model estimated a cumulative of 5,344 COVID-19 hospitalizations in Colorado by Jun 16 (Figure 2, panel D).
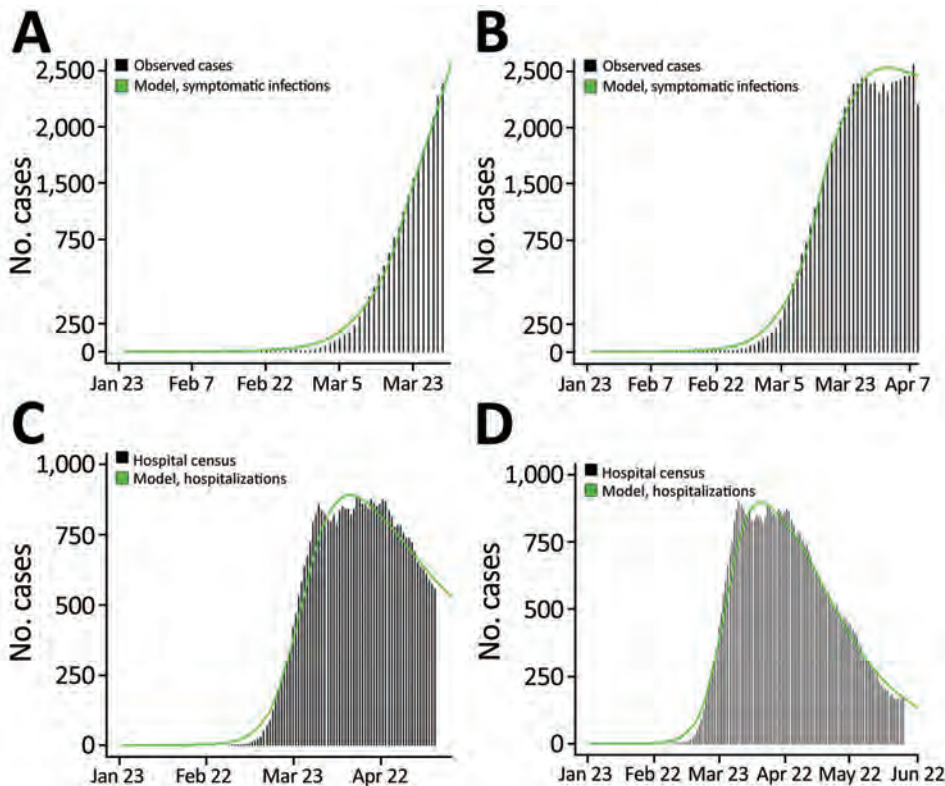
Figure 2. Observed (black bars) versus model-estimated (green line) number of reported coronavirus disease cases (panels A, B) and hospitalizations (panels C, D), Colorado, USA, 2020, based on models calibrated at 4 points in the early months of the epidemic. Model-based estimates were generated by using an age-structured susceptible-exposed-infected-recovered model, and best-fit parameter values were estimated based on observed data shown. Reported cases are shown by using symptom onset date or report date minus 7 days if onset date was missing, in accordance with onset to report lags for Colorado during this period.
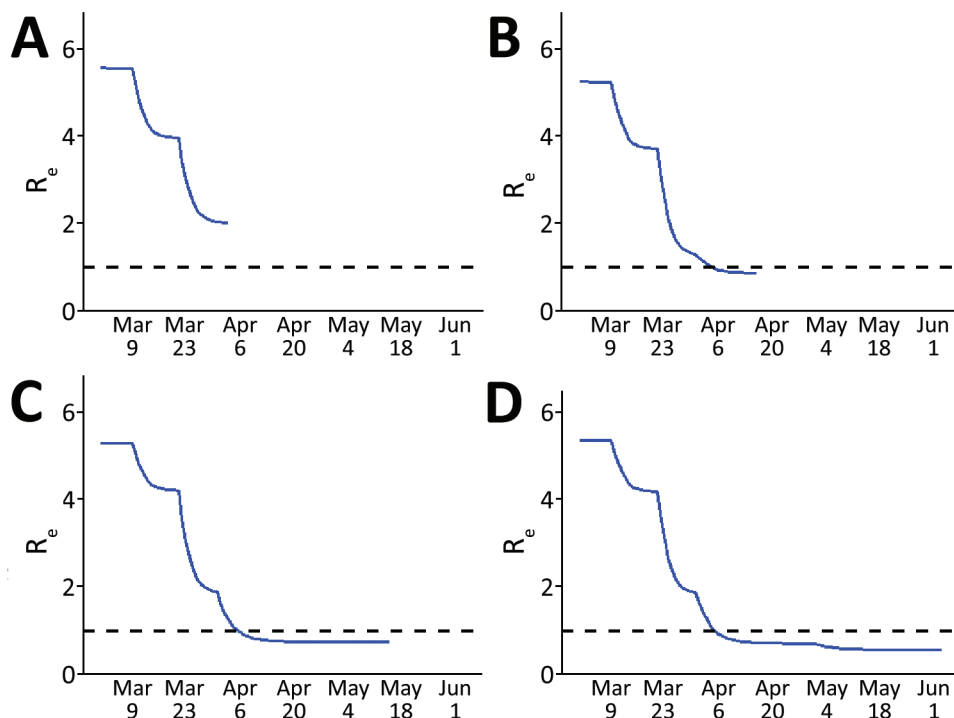
Figure 3. Estimated R_e over time, Colorado, USA 2020, based on susceptible-exposed-infected-recovered models fit to data at 4 time points in the early months of the epidemic. The reproductive number was estimated from model output at the time of each fit. A) Fit 1 on April 3; B) fit 2 on April 16; C) fit 3 on May 15; D) fit 4 on June 16. Dashed lines indicate an R_e of 1, below which the rate of new infections decreases and above which the rate of new infections increases. R_e, effective reproductive number.

Assuming that no measures had been taken to alter individual behavior or risk perception (social distancing 0% throughout), we estimate that >173,000 hospitalizations would have occurred by that same date, suggesting that ≈97% of potential hospitalizations were avoided as a result of decreases in effective contacts.

Projecting Hospitalizations and ICU Need

We provide projected hospitalizations (Figure 4) and ICU need (Figure 5) that were generated from each of the 4 model fits. Fit 1, produced with the least available data, substantially overestimated hospitalizations and ICU need compared with later fits and predicted that ICU capacity would be exceeded even if 80% contact reduction was achieved. As data accumulated and transmission slowed in the state, the estimated peaks under all possible levels of social distancing decreased and shifted later in the year, and projections indicated contact reduction would need to remain at or above ≈70% to prevent exceeding ICU capacity.

Association between Changes in Mobility and Contact Rates

Residents of Colorado decreased activity outside the home starting in early March (Figure 6, panel A). The trends in mobility data suggest that, on average, the time spent away from home decreased by ≈60% from

February to mid-April. Time away from home began to increase in late April, before the end of statewide stay-at-home orders, and increased steadily through June. Mobility metrics initially reinforced estimated social distancing levels, and percent reduction in time away from home coincided with estimated transmission reduction resulting from social distancing (Figure 6, panel B). However, increased time away from home in late April contrasted with estimated infectious contact reduction, which remained high through June. We compared hospitalizations simulated from mobility data to observed and observed a relatively strong association up until late April (Figure 6, panel C). After that, the modeled and observed trends decoupled, indicating that other behaviors or interventions not captured by mobility played a major role in transmission reduction.

Discussion

We used an SEIR transmission model, calibrated to local COVID-19 case and hospital data, to estimate the collective impact of individual behaviors and public policy measures in reducing COVID-19 transmission in Colorado during 2020, providing time-sensitive estimates of the pandemic trajectory to policy-makers to assist in decision-making. COVID-19 policies introduced during March and April were followed by substantial decreases in contact rates and suppression of the R_e well below 1, in agreement with other

studies of nonpharmaceutical interventions to decrease SARS-CoV2 transmission (*31–34*). These values remained low after the stay-at-home order was lifted and mobility increased.

The continued suppression of transmission might be explained, in part, by transmission control policies that remained in effect and/or were implemented after stay-at-home ended: outbreak prevention and control strategies in long-term care facilities persisted, capacity limits were implemented for businesses and restaurants, and mass gatherings were banned. Moreover, the state reopened slowly during April and May. Given the typical lags between infection and hospitalization, the estimates do not capture the impact of reopening measures implemented during or after late May (e.g., restaurant openings).

Mobility, assessed by using mobile-device data, generally reflected state-level policy during March–June but mirrored transmission only in the early months of the pandemic. Mobility decreased rapidly in March in concert with early transmission control policies and the statewide stay-at-home order, and mobility increased as social distancing policies were relaxed. Consistent with our findings, others have found that US population mobility was reactive to policy during March: greater perceived disease prevalence and governmental stay-at-home orders resulted in less mobility and social interaction (*35–37*). However, in Colorado, lifting stay-at-home orders

and concurrent increases in mobility do not appear to have led to increased transmission, indicating the limitations in using mobility data to predict transmission. These results warrant further investigation in other contexts to help clarify the utility of mobility data in SARS-CoV-2 forecasting, particularly during reopening phases.

Mobility data can be used to estimate when and where persons are congregating, a precondition for transmission, but do not sufficiently capture behaviors such as mask wearing, physical distancing, or moving activities outside. Those individual behaviors can play a critical role in spreading infections, and understanding what drives those behaviors can improve epidemic response. Public perception of and reaction to perceived risk is multifactorial, and, although clearly influenced by policy, in a time of heightened fear, local policy probably plays only a partial role in determining risk-reducing behavior. Rapid and frequent introduction of COVID-19–related policy measures and public communication by government officials at the national, state, and local scales probably increased fear and public risk perception regarding COVID-19 transmission, and contributed to adoption of transmission-reducing behaviors before the start of and beyond the end of stay-at-home orders (*38*). Conversely, persons might perceive decreased risks and abandon risk-reducing behaviors when transmission control policies are relaxed, a

Figure 4. Projected coronavirus disease hospitalizations, Colorado, USA, 2020, if current trajectory continued (black line) and for a range of social distancing scenarios (colored lines) generated by models calibrated at 4 time points during April–June (fit 1: Apr 3; fit 2: April 16; fit 3: May 15; fit 4: June 16). Current trajectory was based on estimated parameters generated for each fit. Social distancing is modeled as a percent reduction in the contact rate (from baseline), and changes in social distancing are introduced 2 weeks after model fitting date. All other fitted parameters are held at the estimated values for each fit. Because peak hospitalization estimates from fit 1 were substantially higher than estimated for later fits, the y-axis is scaled to 50,000 as opposed to 25,000 for fits 2–4. Numbers in parentheses are current values.
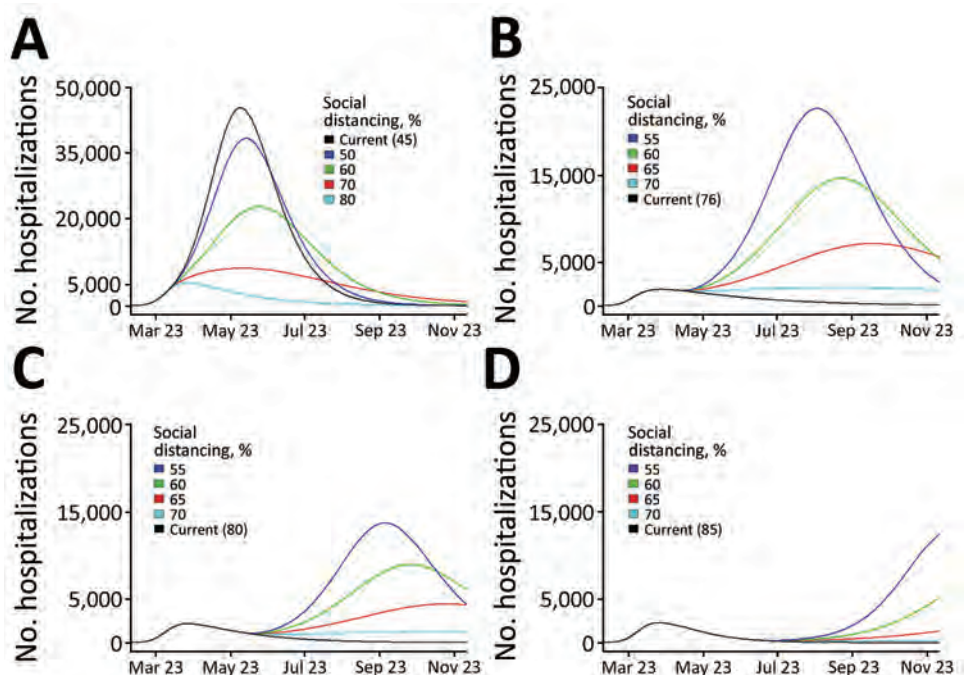
Figure 5. Projected coronavirus disease ICU needs, Colorado, USA, 2020, if current trajectory continues (black line) and for a range of social distancing scenarios (colored lines) generated by using models calibrated at 4 time points during April– June (fit 1: Apr 3; fit 2: April 16; fit 3: May 15; fit 4: June 16). Current trajectory was based on estimated parameters generated for each fit. Social distancing is modeled as a percent reduction in the contact rate from baseline, and changes in social distancing are introduced 2 weeks after model fitting date. All other fitted parameters are held at the estimated values for each fit. Because ICU estimates from fit 1 were substantially higher than for later fits, the y-axis is scaled to 20,000 as opposed to 10,000 for fits 2–4. Colorado estimated ICU capacity (1,800 beds) is indicated by the dashed gray horizontal line. ICU, intensive care unit. Numbers in parentheses are current values.
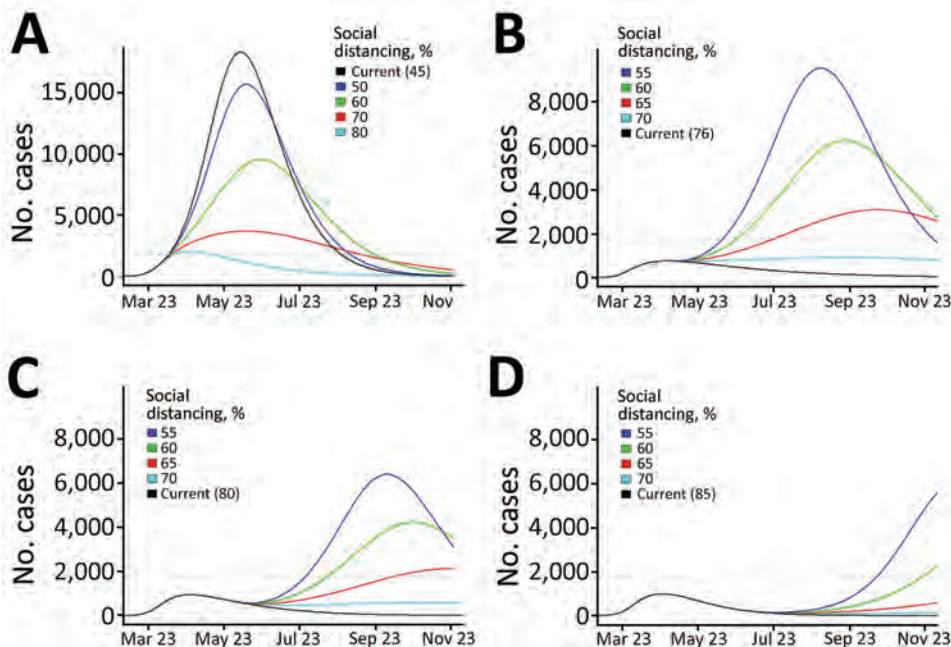
phenomenon we suspect contributed to an increase in COVID-19 transmission in Colorado during July 2020 (*39*). Research on how risk perception and behavior fluctuates in relationship to the epidemic trajectory can improve communication and policy making.

Real-time estimation of contact reduction enabled us to respond to urgent requests to actively inform rapidly changing public health policy amidst a pandemic. In early stages, the urgent need was to flatten the curve (Figure 4, panels A, B; Figure 5, panels A, B). Policymakers used initial projections to support

decision making on the timing and scope of proposed social distancing policies and to compare potential healthcare need and existing capacity under different scenarios. Once infections began to decrease, there was interest in the degree of increased social contact that could be tolerated as the economy reopened without leading to overwhelmed hospitals (Figure 4, panels C, D; Figure 5, panels C, D). Model estimates were used to evaluate the impact of past policies and to forecast the impact of future proposed interventions, including permutations of layered policies or
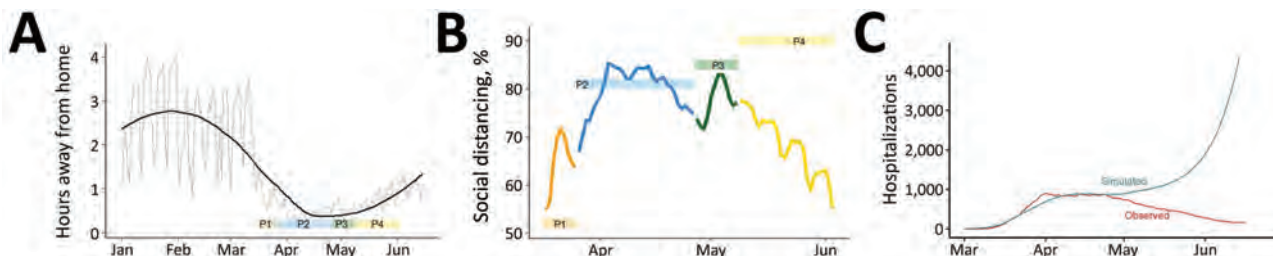
Figure 6. Changes in population mobility before and after emergence of coronavirus disease, Colorado, USA, 2020, and comparison between mobility and estimated social distancing. A) Changes in mobility measured by the number hours spent away from home per day (source: SafeGraph, https://www.safegraph.com). Gray line indicates daily observations, and black line indicates a smoothed line using locally estimated scatterplot smoothing in R (https://www.r-project.org). The ribbon at the bottom indicates the 4 social distancing phases. B) Comparison between susceptible-exposed-infected-recovered model-estimated social distancing (colored boxes) and reduction in mobility relative to the preintervention period, January 29–February 15 (colored lines). Colors correspond to the 4 social distancing phases. Reductions in mobility are calculated as percentage decreases in time away from home relative to pre-epidemic baseline. C) Observed hospitalization data (red) and the simulated hospitalizations based on time away from home relative to a baseline mean during January 29–February 15. In the simulation, it is assumed there is no self-isolation of symptomatic infectious, no mask wearing, and no other transmission reduction to highlight the role of the mobility data in the simulation. P, phase.

interventions. Using locally derived estimates enabled policymakers to evaluate potential disease control strategies that were relevant to the current transmission trends in Colorado. For example, as the age distribution shifted within the epidemic in Colorado, estimates with contact rates that varied by age group were produced and used to evaluate policies or interventions targeted to specific age groups, such as return to school and alcohol last call policies.

A key challenge we faced was generating projections of hospital and critical care needs with limited data and rapidly evolving science. Early model estimates were imprecise because data were sparse and poor quality, leading projections to overestimate hospital needs. Estimates and, consequently, projections improved with greater data quantity and quality. Another challenge was the need to generate estimates under extreme time constraints. We designed a preliminary model in a matter of days and adapted it regularly to accommodate new data streams and science. The need for efficiency led to tradeoffs: for example, we did not account for age-specific contact rates (*40*). We present this material not as a finished work but to illustrate how models can be constructed and adapted in real time to inform critical policy questions.

The model findings were provided weekly to decision-makers in Colorado by written reports and briefings. These collaborative interactions provided an opportunity to review findings and define projection scenarios useful for decision-making. The rapidly developed, locally calibrated transmission model provided timely evidence of a moderate decrease in transmission in Colorado after an early transmission control policy began and a substantial decrease in the contact rate after stay-at-home orders that persisted after these policies were partially relaxed. Decreases in transmission mirrored changes in mobility through the end of stay-at-home, at which point mobility ceased to be a clear proxy for transmission. Locally calibrated models have local credibility and can be used to provide time-sensitive, tailored information to policymakers to assist their decision-making.

About the Author

At the time of this study, Dr. Buchwald was a research associate at the Colorado School of Public Health, University of Colorado, Aurora, CO. She is currently a research associate at the University of Maryland School of Medicine, Baltimore, MD. Her primary research interests include transmission of asymptomatic infections and vector-borne diseases.

References

1. Centers for Disease Control and Prevention. Observed and forecasted new and total reported COVID-19 deaths as of August 10, 2020 [cited 2021 Jun 2]. https://www.cdc.gov/coronavirus/2019-ncov/covid-data/forecasting-us.html#state-forecasts
2. Bell D, Nicoll A, Fukuda K, Horby P, Monto A, Hayden F, et al.; World Health Organization Writing Group. Non-pharmaceutical interventions for pandemic influenza, national and community measures. Emerg Infect Dis. 2006;12:88–94.
3. Cauchemez S, Valleron A-J, Boëlle P-Y, Flahault A, Ferguson NM. Estimating the impact of school closure on influenza transmission from Sentinel data. Nature. 2008;452:750–4. https://doi.org/10.1038/nature06732
4. Ferguson NM, Cummings DA, Fraser C, Cajka JC, Cooley PC, Burke DS. Strategies for mitigating an influenza pandemic. Nature. 2006;442:448–52. https://doi.org/10.1038/nature04795
5. Fineberg HV. Rapid expert consultation on social distancing for the COVID-19 pandemic. Washington (DC): National Academies Press; 2020 Mar 19 [cited 2021 Jun 22]. https://www.nap.edu/read/25753/chapter/1
6. Jackson C, Vynnycky E, Hawker J, Olowokure B, Mangtani P. School closures and influenza: systematic review of epidemiological studies. BMJ Open. 2013;3:e002149. https://doi.org/10.1136/bmjopen-2012-002149
7. Hsiang S, Allen D, Annan-Phan S, Bell K, Bolliger I, Chong T, et al. The effect of large-scale anti-contagion policies on the COVID-19 pandemic. Nature. 2020;584:262–7. https://doi.org/10.1038/s41586-020-2404-8
8. Matrajt L, Leung T. Evaluating the effectiveness of social distancing interventions to delay or flatten the epidemic curve of coronavirus disease. Emerg Infect Dis. 2020;26:1740–8. https://doi.org/10.3201/eid2608.201093
9. Klein B, LaRock T, McCabe S, Torres L, Friedland L, Privitera F, et al. Reshaping a nation: mobility, commuting, and contact patterns during the COVID-19 outbreak, 2020 [cited 2021 Jun 2]. https://www.mobs-lab.org/uploads/6/7/8/7/6787877/covid19mobility_report2.pdf
10. Buchwald AG, Adams J, Bortz DM, Carlton EJ. Infectious disease transmission models to predict, evaluate, and improve understanding of SARS-COV-2 trajectory and interventions. Ann Am Thorac Soc. 2020;17:1204–6. https://doi.org/10.1513/AnnalsATS.202005-501PS
11. Colorado Governor Jared Polis. Executive orders, 2020 [cited 2021 Jun 2]. https://www.colorado.gov/governor/2020-executive-orders
12. Colorado Department of Public Health and Environment. Public health and executive orders, 2020 [cited 2021 Jun 2]. https://covid19.colorado.gov/prepare-protect-yourself/prevent-the-spread/public-health-executive-orders
13. Davies NG, Klepac P, Liu Y, Prem K, Jit M, Eggo RM; CMMID COVID-19 working group. Age-dependent effects

in the transmission and control of COVID-19 epidemics. Nat Med. 2020;26:1205–11. https://doi.org/10.1038/s41591-020-0962-9

14. Verity R, Okell LC, Dorigatti I, Winskill P, Whittaker C, Imai N, et al. Estimates of the severity of coronavirus disease 2019: a model-based analysis. Lancet Infect Dis. 2020;20:669–77. https://doi.org/10.1016/S1473-3099(20)30243-7

15. Ferguson N, Laydon D, Nedjati-Gilani G, Imai N, Ainslie K, Baguelin M, et al. Report 9: impact of non-pharmaceutical interventions (NPIs) to reduce COVID-19 mortality and healthcare demand, 2020. [cited 2021 Jun 2]. https://www.imperial.ac.uk/media/imperial-college/medicine/sph/ide/gida-fellowships/Imperial-College-COVID19-NPI-modelling-16-03-2020.pdf

16. Williamson EJ, Walker AJ, Bhaskaran K, Bacon S, Bates C, Morton CE, et al. Factors associated with COVID-19-related death using OpenSAFELY. Nature. 2020;584:430–6. https://doi.org/10.1038/s41586-020-2521-4

17. Tian L, Li X, Qi F, Tang QY, Tang V, Liu J, et al. Harnessing peak transmission around symptom onset for non-pharmaceutical intervention and containment of the COVID-19 pandemic. Nat Commun. 2021;12:1147. https://doi.org/10.1038/s41467-021-21385-z

18. Howard J, Huang A, Li Z, Tufekci Z, Zdimal V, van der Westhuizen HM, et al. An evidence review of face masks against COVID-19. Proc Natl Acad Sci U S A. 2021; 118:e2014564118. https://doi.org/10.1073/pnas.2014564118

19. Clapp PW, Sickbert-Bennett EE, Samet JM, Berntsen J, Zeman KL, Anderson DJ, et al. Evaluation of cloth masks and modified procedure masks as personal protective equipment for the public during the COVID-19 pandemic. JAMA Intern Med. 2020;181:463–9. https://doi.org/10.1001/jamainternmed.2020.8168

20. Mossong J, Hens N, Jit M, Beutels P, Auranen K, Mikolajczyk R, et al. Social contacts and mixing patterns relevant to the spread of infectious diseases. PLoS Med. 2008;5:e74. https://doi.org/10.1371/journal.pmed.0050074

21. He X, Lau EH, Wu P, Deng X, Wang J, Hao X, et al. Temporal dynamics in viral shedding and transmissibility of COVID-19. Nat Med. 2020;26:672–5. https://doi.org/10.1038/s41591-020-0869-5

22. Huff HV, Singh A. Asymptomatic transmission during the COVID-19 pandemic and implication for public health strategies. Clin Infect Dis. 2020;71:2752–6. https://doi.org/10.1093/cid/ciaa654

23. Leung NH, Chu DK, Shiu EY, Chan KH, McDevitt JJ, Hau BJ, et al. Respiratory virus shedding in exhaled breath and efficacy of face masks. Nat Med. 2020;26:676–80. https://doi.org/10.1038/s41591-020-0843-2

24. Models of Infectious Disease Agent Study. MIDAS online COVID-19 portal, 2020 [cited 2021 Jun 2]. https://github.com/midas-network/COVID-19/tree/master/parameter_estimates/2019_novel_coronavirus

25. Li R, Pei S, Chen B, Song Y, Zhang T, Yang W, et al. Substantial undocumented infection facilitates the rapid dissemination of novel coronavirus (SARS-CoV-2). Science. 2020;368:489–93. https://doi.org/10.1126/science.abb3221

26. Zou L, Ruan F, Huang M, Liang L, Huang H, Hong Z, et al. SARS-CoV-2 viral load in upper respiratory specimens of infected patients. N Engl J Med. 2020;382:1177–9. https://doi.org/10.1056/NEJMc2001737

27. R Core Team. R: A language and environment for statistical computing. Vienna: R Foundation for Statistical Computing; 2019.

28. Soetaert K, Petzoldt T. Inverse modelling, sensitivity and Monte Carlo analysis in R using package FME. J Stat Softw. 2010;33:1–28. https://doi.org/10.18637/jss.v033.i03

29. Price WL. A controlled random search procedure for global optimisation. The Computer Journal. 1977;20:367–70. https://doi.org/10.1093/comjnl/20.4.367

30. Moré JJ. The Levenberg-Marquardt algorithm: implementation and theory. In: Watson GA, editor. Numerical analysis. Heidelberg (Germany): Springer; 1978. p. 105–16.

31. Flaxman S, Mishra S, Gandy A, Unwin HJT, Mellan TA, Coupland H, et al.; Imperial College COVID-19 Response Team. Estimating the effects of non-pharmaceutical interventions on COVID-19 in Europe. Nature. 2020;584:257–61. https://doi.org/10.1038/s41586-020-2405-7

32. Brauner JM, Mindermann S, Sharma M, Johnston D, Salvatier J, Gavenciak T, et al. Inferring the effectiveness of government interventions against COVID-19. Science. 2020.

33. Courtemanche C, Garuccio J, Le A, Pinkston J, Yelowitz A. Strong social distancing measures in the United States reduced the COVID-19 growth rate. Health Aff (Millwood). 2020;39:1237–46. https://doi.org/10.1377/hlthaff.2020.00608

34. Hsiang S, Allen D, Annan-Phan S, Bell K, Bolliger I, Chong T, et al. The effect of large-scale anti-contagion policies on the COVID-19 pandemic. Nature. 2020;584:262–7. https://doi.org/10.1038/s41586-020-2404-8

35. Wellenius GA, Vispute S, Espinosa V, Fabrikant A, Tsai TC, Hennessy J, et al. Impacts of state-level policies on social distancing in the United States using aggregated mobility data during the COVID-19 pandemic. Nat Commun. 2021;12:3118. https://doi.org/10.1038/s41467-021-23404-5

36. Engle S, Stromme J, Zhou A. Staying at home: mobility effects of COVID-19. COVID Economics. 2020;4:86–102. https://cepr.org/sites/default/files/news/CovidEconomics4.pdf

37. Abouk R, Heydari B. The immediate effect of COVID-19 policies on social-distancing behavior in the United States. Public Health Rep. 2021;136:245–52. https://doi.org/10.1177/0033354920976575

38. Albright E, Banacos N, Birkland T, Crow D, DeLeo R, Dickinson KL, et al. COVID-19 technical report wave one, June 22, 2020 [cited 2021 June 2]. https://www.riskandsocialpolicy.org/our-work

39. Yan Y, Bayham J, Richter A, Fenichel EP. Risk compensation and face mask mandates during the COVID-19 pandemic. Sci Rep. 2021;11:3174. https://doi.org/10.1038/s41598-021-82574-w

40. Mistry D, Litvinova M, Pastore Y Piontti A, Chinazzi M, Fumanelli L, Gomes MFC, et al. Inferring high-resolution human mixing patterns for disease modeling. Nat Commun. 2021;12:323. https://doi.org/10.1038/s41467-020-20544-y

Address for correspondence: Elizabeth J. Carlton, Department of Environmental and Occupational Health, Colorado School of Public Health, 17001 E 17th Pl, B119, Aurora, CO 80045, USA; email: elizabeth.carlton@cuanschutz.edu

Patterns of Virus Exposure and Presumed Household Transmission among Persons with Coronavirus Disease, United States, January–April 2020

Rachel M. Burke, Laura Calderwood, Marie E. Killerby, Candace E. Ashworth, Abby L. Berns,
Skyler Brennan, Jonathan M. Bressler, Laurel Harduar Morano, Nathaniel M. Lewis,
Tiffanie M. Markus, Suzanne M. Newton, Jennifer S. Read, Tamara Rissman, Joanne Taylor,
Jacqueline E. Tate, Claire M. Midgley, for the COVID-19 Case Investigation Form Working Group

We characterized common exposures reported by a convenience sample of 202 US patients with coronavirus disease during January–April 2020 and identified factors associated with presumed household transmission. The most commonly reported settings of known exposure were households and healthcare facilities; among case-patients who had known contact with a confirmed case-patient compared with those who did not, healthcare occupations were more common. Among case-patients without known contact, use of public transportation was more common. Within the household, presumed transmission was highest from older (≥65 years) index case-patients and from children to parents, independent of index case-patient age. These findings may inform guidance for limiting transmission and emphasize the value of testing to identify community-acquired infections.

Author affiliations: Centers for Disease Control and Prevention, Atlanta, Georgia, USA (R.M. Burke, M.E. Killerby, L. Harduar Morano, N.M. Lewis, S.M. Newton, J. Taylor, J.E. Tate, C.M. Midgley) Cherokee Nation Assurance, Arlington, Virginia, USA (L. Calderwood), Virginia Department of Health, Richmond, Virginia, USA (C.E. Ashworth); Rhode Island Department of Health, Providence, Rhode Island, USA (A.L. Berns); Georgia Department of Health, Atlanta (S. Brennan); Alaska Department of Health and Social Services, Anchorage, Alaska, USA (J.M. Bressler); Pennsylvania Department of Health, Harrisburg, Pennsylvania, USA (L. Harduar Morano); Vanderbilt University Medical Center, Nashville, Tennessee, USA (T.M. Markus); Vermont Department of Health, Burlington, Vermont, USA (J. Read); University of Vermont, Burlington (J.S. Read); Yale School of Public Health, New Haven, Connecticut, USA (T. Rissman)

Coronavirus disease (COVID-19) was first identified in Wuhan, China, in December 2019 (*1*). The first reported case in the United States was identified in January 2020 (*2*); by mid-March, cases had been reported in all 50 states (*3*). On March 16, 2020, the White House Coronavirus Task Force published guidance for curbing community spread of COVID-19 (*4*); soon after, states began to enact stay-at-home orders (*5*). By late May 2020, all 50 states had begun easing restrictions; reported cases reached new peaks in the summer and then winter months of 2020 (*6,7*). As restrictions further ease with increased availability of vaccine, and as pandemic fatigue may cause persons to adhere less consistently to recommended guidance such as masking and distancing, it may be informative to look back at exposures and within-household transmission during a period when few mitigation measures were in place. We characterized exposures common among persons with the earliest reported confirmed COVID-19 cases in the United States (onset mid-January through early April 2020) and identified factors associated with presumed household transmission.

This activity was reviewed by the Centers for Disease Control and Prevention (CDC) and was conducted consistent with applicable federal law and CDC policy. Forms were approved under the Office of Management and Budget (no. 0920–1011).

Methods

Data Source

The case investigation form (CIF; Appendix 1, https://wwwnc.cdc.gov/EID/article/27/9/20-4577-App1.

pdf) is a supplemental questionnaire designed by CDC in January 2020 to collect detailed demographic and epidemiologic information about a convenience sample of US COVID-19 case-patients reported by participating states. This purposive nonprobability sample was selected at the state level from persons identified through care-seeking, surveillance, or contact tracing as having COVID-19; infection with severe acute respiratory coronavirus 2 (SARS-CoV-2) was confirmed by reverse transcription PCR. CDC provided guidance for selection of case-patients across a range of ages and symptom severities (i.e., hospitalized and nonhospitalized), but states individually controlled sampling. The CIF was completed by state or local health department personnel or by CDC staff through case-patient or proxy interviews, along with medical record reviews (when relevant).

Case-patient demographic information included age, sex, race, ethnicity, and occupation. Workplace settings were classified according to 2012 census industry codes (Appendix 2, https://wwwnc.cdc.gov/EID/article/27/9/20-4577-App2.pdf). Clinical information included underlying conditions, symptoms, symptom onset date, dates of medical visits, and outcome (death or survival). For hospitalized case-patients, information was requested about whether the patient had been admitted to an intensive care unit, whether oxygen was received, admission and discharge dates, diagnosis, and location. Questions about exposure included whether in the 14 days before illness onset the case-patient had known exposure to a case-patient with laboratory-confirmed COVID-19 (COVID-19 contact) and, if so, the relationship and setting of the exposure. Case-patients were also asked about their exposure risks (activities and possible exposures in the 14 days before illness onset) including travel; friends, acquaintances, coworkers, or family members with fever or respiratory symptoms; close contact with (e.g., caring for, speaking with, or touching) any ill persons; attendance at a mass gathering (e.g., religious event, concert, sports event); public transportation use; attendance or work at a school or daycare; school or daycare attendance by household members; close contact with a contact of a laboratory-confirmed case-patient; close contact with someone with fever, acute respiratory illness, or both who had traveled internationally in the previous 14 days; and time in a healthcare setting as an employee, patient, or visitor.

The CIF also collected data on the case-patient's household members, defined as anyone who stayed overnight in the same residence as the case-patient during the 14 days before the case-patient's illness onset until the date of interview. Case-patients were asked for household members' age, sex, relationship to the case-patient, and whether each person had "experienced fever or respiratory symptoms (e.g., cough, sore throat, etc.) within 14 days before or after the COVID-19 patient's illness"; if yes, date of illness onset was collected. When the CIF was designed in January 2020, the most commonly reported COVID-19 signs and symptoms were fever and respiratory symptoms, and guidance for mitigation measures within households had not been widely distributed.

Analysis of Exposures

We compared exposures between those reporting known close contact with a COVID-19 case-patient in the 14 days before illness onset and those reporting no known contact. Categorical variables were compared by using χ^2 or Fisher exact tests, as appropriate. Continuous variables were compared by using t tests for normally distributed data and Wilcoxon rank sum tests otherwise. $p<0.05$ was considered significant. Analyses were conducted in SAS version 9.4 (https://www.sas.com) and R (https://www.r-project.org).

Analysis of Presumed Household Transmission

We separately assessed presumed household transmission by using information about household members provided by the interviewed COVID-19 case-patient (CIF subject). In the absence of SARS-CoV-2 testing data for all household members, we used reported signs and symptoms (i.e., fever or respiratory symptoms) as a proxy for symptomatic COVID-19 infection (i.e., household transmission). We analyzed households of ≥ 2 members (including the CIF subject) if the CIF subject had experienced ≥ 1 symptom (to enable identification of the first ill person [index case-patient] in the household), and symptom status was provided for ≥ 1 other household member. We required that the earliest symptom onset date in the household be ≥ 1 calendar day before symptom onset in subsequent case-patients (to limit effect of co-exposures outside the home) and that the earliest onset date in the household be ≥ 3 days (our median serial interval) before the interview (to allow time for symptoms to develop in exposed household members). We considered presumed household transmission to have occurred if ≥ 1 household member, in addition to the CIF subject, was reported as having fever or respiratory symptoms. The person with the earliest symptom onset date in a household was considered the index case-patient, regardless whether SARS-CoV-2 testing had been performed. Any members of a given household

not identified as the index case-patient are hereafter referred to as household contacts.

We calculated the overall household attack rate for symptoms as the number of symptomatic household contacts divided by the total number of household contacts with reported symptom status, with Wilson score 95% CI, and the serial interval as the time from symptom onset in the index case-patient to first symptom onset in a household contact. We investigated age and sex of the index case-patients and their contacts, household size, and relationship of the contact to the index case-patient as possible correlates of contact symptom status by using generalized estimating equation logistic regression with households as the cluster and individual symptom status as the outcome; we used an exchangeable correlation matrix and robust SEs. We excluded household contacts missing symptom status from this analysis. We examined models for collinearity and reduced if necessary. We did not include hospitalization status of the index case-patient in models because of collinearity with index case-patient age. We dichotomized contact age (<18 or $\geq$18 years) to avoid collinearity with familial relationship and index case-patient age.

To explore the validity of using reported symptom status to estimate household symptomatic attack rates, we calculated sensitivity and specificity by using a subset of households for which complete reverse transcription PCR and serologic testing data were available (8). We conducted a sensitivity analysis by reclassifying data according to a range of plausible misclassification rates (Appendix 2).

Results

Overview of the Analysis Population

Data were collected from 16 states (Alaska, Arizona, California, Connecticut, Georgia, Hawaii, Illinois, Minnesota, Pennsylvania, Rhode Island, Tennessee, Utah, Virginia, Vermont, Washington, and Wisconsin) with 202 laboratory-confirmed COVID-19 case-patients with symptom onset during January 14–April 4, 2020. Age of COVID-19 case-patients in the sample ranged from <1 to 95 years, almost all were symptomatic (195; 97%), and 1 in 3 was hospitalized for management of COVID-19 symptoms (Appendix 2 Table 3). Of the 202 case-patients, 34 (17%) reported having diabetes mellitus and 48 (24%) reported hypertension.

Exposures

A total of 82 (41%) case-patients reported known contact with a laboratory-confirmed COVID-19 case-

patient in the 14 days before symptom onset. The most commonly reported exposure setting was the household (44/82; 54%); within the household setting, the most frequently reported source of COVID-19 exposure was the spouse or partner of the COVID-19 case-patient (16/44; 36%). The second most reported exposure setting was healthcare (20/82; 24%); 14 of the 20 persons exposed in the healthcare setting were healthcare workers, 4 were seeking care for unrelated medical issues, and 2 were visitors.

Among persons reporting no known COVID-19 contact, 20/84 (24%) reported having close contact with an ill person. Persons with no known COVID-19 contact worked in a variety of industries, most commonly healthcare (10/90; 11%); professional/office settings (10/90; 11%); education (9/90; 10%); and accommodation, food, or other services (9/90; 10%) (Table 1). In comparison, 28% (20/72) of persons with known COVID-19 contact reported working in healthcare. Persons with no known COVID-19 contact were significantly less likely than those with known contact to report spending time in a healthcare setting (p = 0.004). However, they were somewhat more likely to report travel (38% vs. 26%) or attendance at a mass gathering (36% vs. 21%) and significantly more likely to report use of public transportation (44% vs. 16%), compared with persons reporting known COVID-19 contact (p = 0.005)

Of the 202 case-patients, 23 (11.3%) reported no known contact with a confirmed case-patient, no travel within 14 days before illness onset, and none of the exposure risks assessed. These persons ranged in age from 21 to 88 years and were significantly older than those reporting $\geq$1 possible exposure (median age 52 vs. 49 years; p<0.0001). They required hospitalization more frequently than those reporting $\geq$1 possible exposure (52% [12/23] vs. 30% [54/179]; p = 0.10), and were significantly more likely to report $\geq$1 underlying medical condition (87% [20/23] vs. 58% [104/179]; p = 0.029). They were much more likely to report having diabetes mellitus (43% [10/23] vs. 14% [24/176]; p = 0.002).

Analysis of Presumed Household Transmission

A total of 69 case-patients provided data on the symptom status of $\geq$1 household members and were included in our household analysis; in 48 (70%) households, the CIF subject was the first or only symptomatic person in the household (i.e., was identified as the index case-patient; Figure 1). In half (34/69; 49%) of included households, $\geq$1 household member, in addition to the CIF subject, was symptomatic (i.e., virus transmission was presumed). Included households ranged in size

Table 1. Reported exposures of 179 COVID-19 case-patients with submitted case investigation forms by known contact with a laboratory-confirmed COVID-19 case-patient, United States, January–April 2020*

Exposure	No known contact, no. (%), n = 97	Known contact, no. (%), n = 82	p value†
Workplace setting‡			0.10
Accommodation, food, and other services§	9 (10.0)	2 (2.8)	
Construction	4 (4.4)	1 (1.4)	
Education¶	9 (10.0)	5 (6.9)	
Healthcare	10 (11.1)	20 (27.8)	
Manufacturing	2 (2.2)	1 (1.4)	
Professional or office setting	10 (11.1)	7 (9.7)	
Transportation and warehousing and utilities	8 (8.9)	3 (4.2)	
Wholesale or retail trade	3 (3.3)	7 (9.7)	
Other	7 (7.8)	6 (8.3)	
Insufficient information	5 (5.6)	6 (8.3)	
Not currently in the workforce	23 (25.6)	14 (19.4)	
Other exposure risks in previous 14 d			
Spent time in a healthcare setting			0.0044
Yes	24 (26.1)	39 (48.1)	
No	68 (73.9)	42 (51.9)	
Close contact with a contact of a confirmed case			0.0002
Yes	3 (3.6)	17 (25.4)	
No	81 (96.4)	50 (74.6)	
Attended a mass gathering**			0.07
Yes	29 (35.8)	16 (21.3)	
No	52 (64.2)	59 (78.7)	
Used public transportation			0.0048
Yes	23 (44.2)	8 (16.3)	
No	29 (55.8)	41 (83.7)	
Attended or worked at a school or daycare			1.00
Yes	8 (14.3)	7 (14.3)	
No	48 (85.7)	42 (85.7)	
Had a household member who attended school or daycare			0.51
Yes	15 (18.3)	9 (13.0)	
No	67 (81.7)	60 (87.0)	
Travel away from home			0.14
International, with or without domestic	18 (18.9)	8 (10.0)	
Domestic only	18 (18.9)	13 (16.3)	
None	59 (62.1)	59 (73.8)	

*A total of 23 persons did not know or did not report whether they had known contact with a person with laboratory-confirmed COVID-19 in the 14 d before their own illness onset. Denominators differ because some questions had incomplete responses. All complete responses are presented for each question. COVID-19, coronavirus disease.
†χ² or Fisher exact test.
‡Based on 2012 census industry codes. Mapping shown in Appendix 2 (https://wwwnc.cdc.gov/EID/article/27/9/20-4577-App2.pdf).
§Not including public administration services.
¶Includes persons ≥18 y of age who are pursuing higher education.
**Examples given in the questionnaire included religious event, wedding, party, dance, concert, banquet, festival, sports event, or other event.

from 2 to 16 persons (median 4 persons) and comprised a variety of household types (e.g., couples, nuclear families, roommates, multigenerational); household size and members' ages, sexes, and relationships were interrelated. Presumed transmission was more frequently observed in larger households (78% of households with ≥5 members vs. 39% of households with <5 members; p = 0.005) (Figure 2). Within households with more members, a larger number of household contacts reported symptoms (Figure 2).

Among 201 household contacts, 193 had data on symptom status, of which 62 (32%; 95% CI 26%–39%) were symptomatic. Sensitivity analysis results showed a similar plausible range of attack rates (21%–39%; Appendix 2 Results and Table 1). The median serial interval was 3 days (range 1–10 days).

Although our sample did not have large numbers of index case-patients at the age extremes, household contacts were more likely to be symptomatic if the index case-patient was <5 (5 households) or ≥65 years of age (9 households) (Figure 3, panel A); trends were similar, but the point estimates were significant only for index case-patients ≥45 years of age (vs. index case-patients 18–44 years of age) after adjustment for contact age, contact sex, household size, and relationship of the contact to the index case-patient (Table 2). Adult contacts were symptomatic more often than contacts <18 years of age (Figure 3, panel B), but this association was not significant in adjusted analyses (Table 2). The symptom status of household contacts was also associated with their relationship to the index case-patient (Table 2). Among

the contacts of 9 index case-patients <18 years of age, 11/16 (69%) parents, 6/13 (46%) siblings, and 2/5 (40%) other household contacts later became symptomatic. Among contacts of the 60 adult index case-patients, 12/44 (27%) children (range 2–49 years of age), 12/45 (27%) spouses/partners, 7/16 (44%) parents, and 11/42 (26%) other household contacts became symptomatic. When we restricted the analysis to households in which the CIF subject was the index case-patient, overall trends were similar to those reported above, but small sample sizes precluded adjusted analyses (Appendix 2 Table 2).

Illness severity of the index case-patient could not be assessed in multivariable models because of low sample size and correlation with age. However, among 12 household contacts of 10 index case-patients requiring hospitalization (three 18–44, five 45–64, and two index case-patients ≥65 years of age), only 2 were symptomwatic.

Discussion

In this convenience sample of 202 early laboratory-confirmed COVID-19 case-patients, predominantly identified before widespread mitigation measures in the United States, the most commonly reported settings of known exposure were households and healthcare facilities (primarily as a workplace). Within the household, presumed transmission by age of index case-patient followed a U-shaped pattern and was significantly higher among contacts of older (≥65 years of age) index case-patients than among contacts of index case-patients 18–44 years of age. Independent of index case-patient age, parents of index case-patients were significantly more likely than other household members to report development of symptoms consistent with COVID-19.

Previous research has also found healthcare workplaces and households to be commonly reported settings of COVID-19 acquisition in the United States (9,10). In our analysis, the presumed secondary symptomatic attack rate among household members was 32%, somewhat high but consistent with estimates from previous studies, ranging from 10% to 38% (11–16; J.B. Lopez et al., unpub data, https://www.medrxiv.org/content/10.1101/2020.08.19.20177188v1). We found that presumed transmission was highest among contacts of older index case-patients (≥65 years of age), even when controlling for contact age category, relationship, and household size; however, our sample size was insufficient to control for underlying conditions or hospitalization status of the index case-patient or for detailed age category of the household contact, which may have confounded
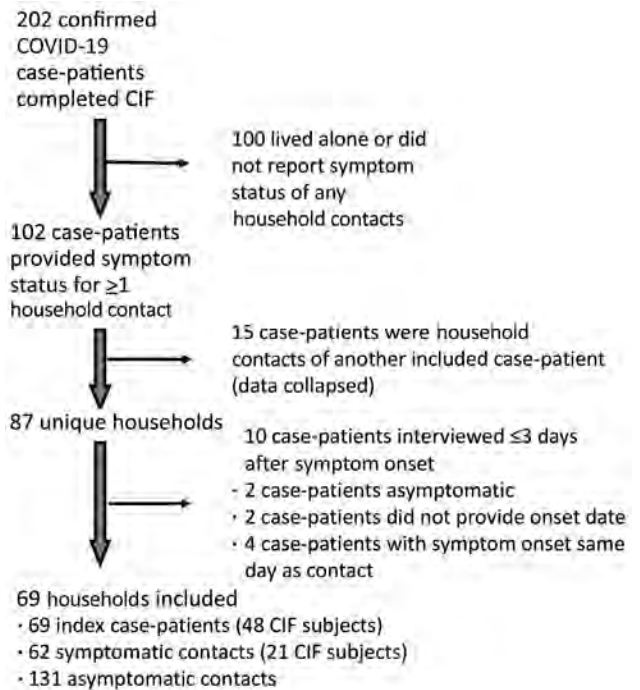
Figure 1. Households included in the analysis population for study of presumed household transmission among persons with COVID-19, United States, January–April 2020. CIF, case investigation form; CIF subject, interviewed COVID-19 case-patient; COVID-19, coronavirus disease.

this relationship because evidence suggests that older adults are more susceptible to COVID-19 (17). Although results were not statistically significant in adjusted analyses, we also found that contacts of index case-patients <18 years of age (especially index case-patients <5 years of age) were more likely than contacts of index case-patients 18–44 years of age to be symptomatic. Further, symptoms were significantly more likely to develop in parents of index case-patients than in other household members. This relationship was independent of index case-patient age; however, in 8 households of adult case-patients with parental household members, 6 index case-patients were <30 years of age. Higher secondary transmission to the household contacts of younger versus adult or older COVID-19 case-patients has also been reported in analyses from the United Kingdom, South Korea, and Canada (16; B.J. Lopez et al., unpub. data, https://www.medrxiv.org/content/10.1101/2020.08.19.20177188v1; L.A. Paul, unpub. data, https://www.medrxiv.org/content/10.1101/2021.03.29.21254565v1). These findings may be explained by the fact that SARS-CoV-2–infected children may have similar or higher viral loads than adults (18) and that they may have closer interaction with family members,

Figure 2. Proportion of households with presumed severe acute respiratory syndrome coronavirus 2 transmission, by household size (including index case-patient), United States, January–April 2020. Shading indicates percentage of households with the specified number of symptomatic household contacts (i.e., excluding index case-patient); households with zero symptomatic contacts (in white) are those in which presumed household transmission did not occur. n = no. households in each stratum.
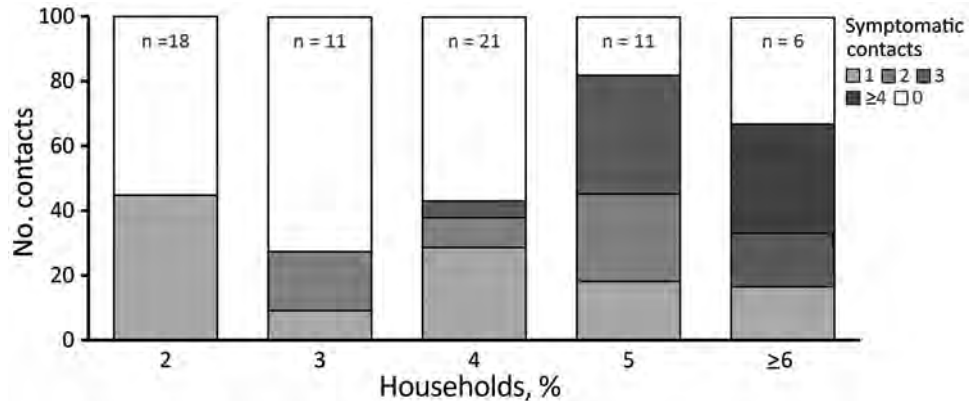
especially parents. Parents, compared with other household members, may also play a greater role in caregiving to index case-patients, even for young adults. Conversely, in multigenerational households, adult children may act as caregivers for elderly parents, possibly exposing them before symptom onset.

A substantial proportion (60%) of case-patients in our sample did not report contact with a laboratory-confirmed COVID-19 case-patient in the 14 days before illness onset. Among case-patients without known COVID-19 contact, travel and public activities were more common, although only public transportation use was significantly higher when this group was compared with case-patients with known COVID-19 contact. Public transportation has not been identified as a major source of SARS-CoV-2 transmission (19–21), although transmission on buses, trains, and commercial flights has been reported (19,22–26). However, in our analysis, public transportation use might also have been more common among essential workers, those living in densely populated areas, or those with a history of travel—factors that could also increase opportunity for exposure to SARS-CoV-2 (27). Case-patients

reporting no known source of infection, travel, or any other exposure risk factor tended to be older and to have more underlying medical conditions—particularly diabetes mellitus. Persons with concurrent conditions may be not only more susceptible to severe outcomes from COVID-19 (28,29) but also more susceptible to infection, as suggested by other analyses of SARS-CoV-2 (8,30) and Middle East respiratory syndrome coronavirus (31); however, more investigation is warranted.

The first limitation of our study was that the COVID-19 case-patients for whom the CIF was completed are a convenience sample of case-patients reported by 16 states during January–April 2020. Given restricted testing practices in the United States during January–March 2020, these case-patients are not representative of all US COVID-19 case-patients in terms of demographics, clinical characteristics, or exposures. Furthermore, common exposures have varied in time and geography over the course of the epidemic, and it is not possible to exclude the possibility that persons without known COVID-19 exposure had contact with an asymptomatic friend, co-worker, or
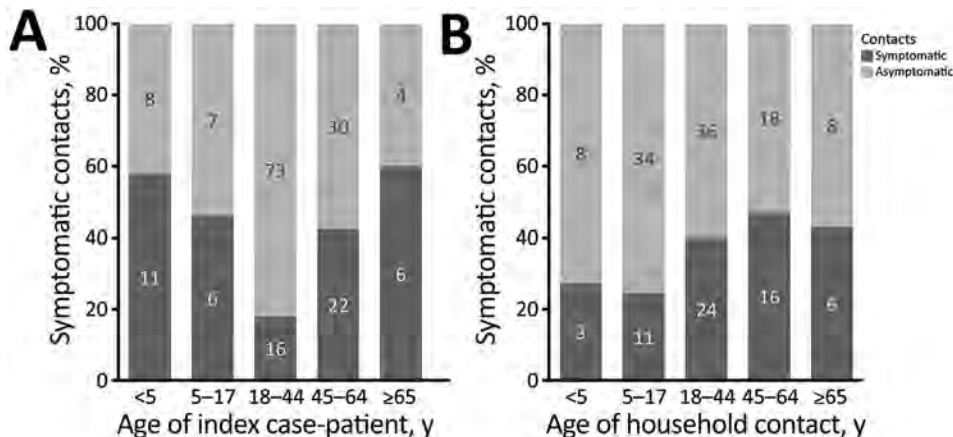
Figure 3. Symptom status of household contacts, by age group of index coronavirus disease case-patient (n = 192) and age group of household contact (n = 173), United States, January–April 2020. Age group missing for 20 contacts; age of index case-patient missing for 1 contact.

Table 2. Factors associated with symptom status of 172 household contacts of 64 symptomatic index case-patients in households with presumed COVID-19 transmission, United States, January–April 2020*

Factor	Unique households	No. with symptoms/no. total contacts (%)	aOR (95% CI)†	p value‡
Contact sex				0.73
F	50	28/85 (32.9)	Referent	
M	46	29/87 (33.3)	0.90 (0.49–1.64)	
Contact age, y				0.73
<18	25	13/50 (26.0)	Referent	
>18	63	44/115 (38.3)	1.15 (0.53–2.47)	
Household size, persons				0.006
<5	48	23/92 (25.0)	Referent	
>5	16	34/80 (42.5)	3.56 (1.45–8.74)	
Index case-patient age, y				0.035
<5	5	11/19 (57.9)	3.69 (0.65–20.95)	
5–17	4	6/13 (46.2)	2.09 (0.39–11.05)	
18–44	26	15/82 (18.3)	Referent	
45–64	21	20/49 (40.8)	4.61 (1.45–14.66)	
>65	8	5/9 (55.6)	15.43 (2.28–104.17)	
Relationship of contact to index case-patient				0.070
Spouse	43	11/44 (25.0)	Referent	
Child	21	11/39 (28.2)	1.78 (0.58–5.45)	
Parent	17	18/31 (58.1)	4.55 (1.22–17.00)	
Other§	23	17/58 (29.3)	1.47 (0.42–5.11)	

*A total of 21 contacts from 5 households (i.e., 5 index case-patients) are excluded because of missing data: only relationship data for 7, only sex data for 2, only index case-patient's age for 1; only contact's age for 5, relationship and contact age for 6. Households with presumed transmission indicates households of laboratory-confirmed COVID-19 case-patients where >1 household member exhibited symptoms; index case-patient indicates household /member with first reported onset of symptoms (regardless of laboratory confirmation); household contact indicates household member of the index case-patient. aOR, adjusted odds ratio (adjusted for all variables in the table); COVID-19, coronavirus disease.
†Calculated using robust SEs.
‡Generalized Wald test.
§Includes siblings, grandparents, grandchildren, friends, and any household relationship or contact other than spouse, child, or parent.

family member. Our observed secondary attack rates (symptomatic persons) may also have been affected by the timing of the investigation because public awareness regarding measures to mitigate within-household transmission (e.g., isolation and mask-wearing within the home) was probably lower in the early stages of the US epidemic. Information was not collected on the specifics of known COVID-19 exposure, such as mask wearing or social distancing in the home or other exposure settings, because these were not common practices during survey design. The use of a convenience sample may have also affected findings regarding presumed household transmission, such as if selection were biased toward inclusion of more severe cases or larger investigations.

A second limitation is that SARS-CoV-2 infection in most household members was not laboratory-confirmed, so household members with other causes of illness could have been misclassified as COVID-19 case-patients and those with asymptomatic SARS-CoV-2 infections misclassified as non–case-patients. The possibility of misclassification of children may have been higher, given that young children frequently experience respiratory symptoms (32) and are less likely to show symptoms of SARS-CoV-2 infection (33–35). However, overall patterns were similar when analysis was restricted to laboratory-confirmed index case-patients, and the point estimate

for odds of presumed symptomatic infection among contacts of index case-patients <5 years of age versus contacts of those 18–44 years of age was similar when contacts of unconfirmed index case-patients <5 years of age were excluded. In addition, 4 of 5 households with index case-patients <5 years of age reported that >1 household member attended school or daycare in the 14 days before illness onset in the CIF subject, suggesting a possible outside source of infection. Of note, similar methods are frequently used for studies of influenza (36), and our observed overall symptomatic attack rate and serial interval are consistent with previous knowledge of SARS-CoV-2 transmission (37,38). It is also possible that symptoms developed in some household members after the date of interview. To limit this possibility, we excluded households in which the interview took place <3 days (median serial interval in our data) after the CIF subject's symptom onset. Similarly, some presumed secondary case-patients may have actually been index case-patients or were co-exposed to the index case-patient; we tested exclusion of contacts with a 1-day lag in symptom onset and found similar trends, although the sample size precluded adjusted models. Previous research showing longer incubation periods for older patients suggests that households with older index patients would be less affected by such misclassification (39,40).

Last, our sample size was limited by state capacity for participation and data completeness. We did not have sufficient sample size to control for all possible confounders, such as index case-patient signs/symptoms, clinical characteristics, or detailed contact age category, so residual confounding is possible. The lower sample size also limited the precision of our estimates.

Our findings underline the exposure risk associated with work in a healthcare setting and within the household, as previously documented (*9,10*). However, most case-patients in the analysis did not have known contact with a laboratory-confirmed COVID-19 case-patient, reflecting unrecognized transmission and highlighting the need for widespread testing in addition to community mitigation measures such as masking, hand hygiene, physical distancing, and limiting nonessential travel, as well as vaccination (*41–43*). When going out in public, persons should take preventive actions and consider the risks associated with public activities by taking into account local orders, their ability to maintain physical distance during the activity, and whether they or their household members are at risk for severe illness from COVID-19 (*41*). Everyday preventive actions also protect at-risk household members. In this analysis, presumed household transmission was common, especially from the oldest index case-patients and from children to their parents. These findings are especially relevant to the context of in-person schooling because children exposed at schools or daycare centers may introduce COVID-19 into the home. Special care must be taken to mitigate exposure risks outside the home and to protect household members at high risk for severe COVID-19, such as older persons and those with concurrent conditions. Persons with COVID-19 should follow recommendations to reduce the risk for within-household transmission, such as staying in a separate room, wearing a mask around others, practicing hand and cough hygiene, and frequently cleaning high-touch surfaces (*44*).

About the Author

Dr. Burke is an epidemiologist in the Division of Viral Diseases, National Center for Immunization and Respiratory Diseases, Centers for Disease Control and Prevention. Her research interests include infectious diseases and epidemiology.

References

1. World Health Organization. Novel coronavirus (2019-nCoV): situation report—1 [cited 2020 Jul 29]. https://www.who.int/docs/default-source/coronaviruse/situation-reports/20200121-sitrep-1-2019-ncov.pdf?sfvrsn=20a99c10_4
2. Holshue ML, DeBolt C, Lindquist S, Lofy KH, Wiesman J, Bruce H, et al.; Washington State 2019-nCoV Case Investigation Team. First case of 2019 novel coronavirus in the United States. N Engl J Med. 2020;382:929–36. https://doi.org/10.1056/NEJMoa2001191
3. Bialek S, Bowen V, Chow N, Curns A, Gierke R, Hall A, et al.; CDC COVID-19 Response Team. Geographic differences in COVID-19 cases, deaths, and incidence—

United States, February 12–April 7, 2020. MMWR Morb Mortal Wkly Rep. 2020;69:465–71. https://doi.org/10.15585/mmwr.mm6915e4

4. US Department of Justice. 15 Days to slow the spread [cited 2020 Jul 29]. https://www.whitehouse.gov/articles/15-days-slow-spread

5. Kates J, Michaud J, Tolbert J. Stay-at-home orders to fight COVID-19 in the United States: the risks of a scattershot approach [cited 2020 Jul 29]. https://www.kff.org/coronavirus-policy-watch/stay-at-home-orders-to-fight-covid19

6. Chappell B. All 50 U.S. states have now started to reopen, easing COVID-19 shutdown [cited 2020 Jul 29]. https://www.npr.org/sections/coronavirus-live-updates/2020/05/20/859723846/all-50-u-s-states-have-now-started-to-reopen-easing-covid-19-shutdown

7. Centers for Disease Control and Prevention. COVID data tracker [cited 2021 Apr 21]. https://covid.cdc.gov/covid-data-tracker/#datatracker-home

8. Lewis NM, Chu VT, Ye D, Conners EE, Gharpure R, Laws RL, et al. Household transmission of SARS-CoV-2 in the United States. Clin Infect Dis. 2020 Aug 16 [Epub ahead of print].https://doi.org/10.1093/cid/ciaa1166

9. Tenforde MW, Billig Rose E, Lindsell CJ, Shapiro NI, Files DC, Gibbs KW, et al.; CDC COVID-19 Response Team. Characteristics of adult outpatients and inpatients with COVID-19—11 academic medical centers, United States, March–May 2020. MMWR Morb Mortal Wkly Rep. 2020;69:841–6. https://doi.org/10.15585/mmwr.mm6926e3

10. Marshall K, Vahey GM, McDonald E, Tate JE, Herlihy R, Midgley CM, et al.; Colorado Investigation Team. Exposures before issuance of stay-at-home orders among persons with laboratory-confirmed COVID-19—Colorado, March 2020. MMWR Morb Mortal Wkly Rep. 2020;69:847–9. https://doi.org/10.15585/mmwr.mm6926e4

11. Li W, Zhang B, Lu J, Liu S, Chang Z, Peng C, et al. The characteristics of household transmission of COVID-19. Clin Infect Dis. 2020;71:1943–6. https://doi.org/10.1093/cid/ciaa450

12. Rosenberg ES, Dufort EM, Blog DS, Hall EW, Hoefer D, Backenson BP, et al.; New York State Coronavirus 2019 Response Team. COVID-19 testing, epidemic features, hospital outcomes, and household prevalence, New York State–March 2020. Clin Infect Dis. 2020;71:1953–9. https://doi.org/10.1093/cid/ciaa549

13. Wang Z, Ma W, Zheng X, Wu G, Zhang R. Household transmission of SARS-CoV-2. J Infect. 2020;81:179–82. https://doi.org/10.1016/j.jinf.2020.03.040

14. Wu J, Huang Y, Tu C, Bi C, Chen Z, Luo L, et al. Household transmission of SARS-CoV-2, Zhuhai, China, 2020. Clin Infect Dis. 2020;71:2099–108. https://doi.org/10.1093/cid/ciaa557

15. Jing QL, Liu MJ, Zhang ZB, Fang LQ, Yuan J, Zhang AR, et al. Household secondary attack rate of COVID-19 and associated determinants in Guangzhou, China: a retrospective cohort study. Lancet Infect Dis. 2020;20:1141–50. https://doi.org/10.1016/S1473-3099(20)30471-0

16. Park YJ, Choe YJ, Park O, Park SY, Kim YM, Kim J, et al.; COVID-19 National Emergency Response Center, Epidemiology and Case Management Team. Contact tracing during coronavirus disease outbreak, South Korea, 2020. Emerg Infect Dis. 2020;26:2465–8. https://doi.org/10.3201/eid2610.201315

17. Goldstein E, Lipsitch M, Cevik M. On the effect of age on the transmission of SARS-CoV-2 in households, schools, and the community. J Infect Dis. 2021;223:362–9. https://doi.org/10.1093/infdis/jiaa691

18. Heald-Sargent T, Muller WJ, Zheng X, Rippe J, Patel AB, Kociolek LK. Age-related differences in nasopharyngeal severe acute respiratory syndrome coronavirus 2 (SARS-CoV-2) levels in patients with mild to moderate coronavirus disease 2019 (COVID-19). JAMA Pediatr. 2020;174:902–3. https://doi.org/10.1001/jamapediatrics.2020.3651

19. Hu M, Lin H, Wang J, Xu C, Tatem AJ, Meng B, et al. The risk of COVID-19 transmission in train passengers: an epidemiological and modelling study. Clin Infect Dis. 2021;72:604–10.

20. Luo L, Liu D, Liao X, Wu X, Jing Q, Zheng J, et al. Contact settings and risk for transmission in 3410 close contacts of patients with COVID-19 in Guangzhou, China: a prospective cohort study. Ann Intern Med. 2020;173:879–87. https://doi.org/10.7326/M20-2671

21. Heald AH, Stedman M, Tian Z, Wu P, Fryer AA. Modelling the impact of the mandatory use of face coverings on public transport and in retail outlets in the UK on COVID-19-related infections, hospital admissions and mortality. Int J Clin Pract. 2021;75:e13768. https://doi.org/10.1111/ijcp.13768

22. Shen Y, Li C, Dong H, Wang Z, Martinez L, Sun Z, et al. Community outbreak investigation of SARS-CoV-2 transmission among bus riders in eastern China. JAMA Intern Med. 2020;180:1665–71. https://doi.org/10.1001/jamainternmed.2020.5225

23. Luo K, Lei Z, Hai Z, Xiao S, Rui J, Yang H, et al. Transmission of SARS-CoV-2 in public transportation vehicles: a case study in Hunan Province, China. Open Forum Infect Dis. 2020;7:ofaa430.

24. Hoehl S, Karaca O, Kohmer N, Westhaus S, Graf J, Goetsch U, et al. Assessment of SARS-CoV-2 transmission on an international flight and among a tourist group. JAMA Netw Open. 2020;3:e2018044. https://doi.org/10.1001/jamanetworkopen.2020.18044

25. Khanh NC, Thai PQ, Quach HL, Thi NH, Dinh PC, Duong TN, et al. Transmission of SARS-CoV 2 during long-haul flight. Emerg Infect Dis. 2020;26:2617–24. https://doi.org/10.3201/eid2611.203299

26. Yang N, Shen Y, Shi C, Ma AHY, Zhang X, Jian X, et al. In-flight transmission cluster of COVID-19: a retrospective case series. Infect Dis (Lond). 2020;52:891–901. https://doi.org/10.1080/23744235.2020.1800814

27. Figueroa JF, Wadhera RK, Mehtsun WT, Riley K, Phelan J, Jha AK. Association of race, ethnicity, and community-level factors with COVID-19 cases and deaths across U.S. counties. Healthc (Amst). 2021;9:100495. https://doi.org/10.1016/j.hjdsi.2020.100495

28. Mahumud RA, Kamara JK, Renzaho AMN. The epidemiological burden and overall distribution of chronic comorbidities in coronavirus disease-2019 among 202,005 infected patients: evidence from a systematic review and meta-analysis. Infection. 2020;48:813–33. https://doi.org/10.1007/s15010-020-01502-8

29. Yang J, Zheng Y, Gou X, Pu K, Chen Z, Guo Q, et al. Prevalence of comorbidities and its effects in patients infected with SARS-CoV-2: a systematic review and meta-analysis. Int J Infect Dis. 2020;94:91–5. https://doi.org/10.1016/j.ijid.2020.03.017

30. de Lusignan S, Dorward J, Correa A, Jones N, Akinyemi O, Amirthalingam G, et al. Risk factors for SARS-CoV-2 among patients in the Oxford Royal College of General Practitioners Research and Surveillance Centre primary care network: a cross-sectional study. Lancet Infect Dis. 2020;20:1034–42. https://doi.org/10.1016/S1473-3099(20)30371-6

31. Khudhair A, Killerby ME, Al Mulla M, Abou Elkheir K, Ternanni W, Bandar Z, et al. Risk factors for MERS-CoV seropositivity among animal market and slaughterhouse workers, Abu Dhabi, United Arab Emirates, 2014–2017. Emerg Infect Dis. 2019;25:927–35. https://doi.org/10.3201/eid2505.181728

32. Troeger C, Blacker B, Khalil IA, Rao PC, Cao J, Zimsen SRM, et al.; GBD 2016 Lower Respiratory Infections Collaborators. Estimates of the global, regional, and national morbidity, mortality, and aetiologies of lower respiratory infections in 195 countries, 1990-2016: a systematic analysis for the Global Burden of Disease Study 2016. Lancet Infect Dis. 2018;18:1191–210. https://doi.org/10.1016/S1473-3099(18)30310-4

33. Castagnoli R, Votto M, Licari A, Brambilla I, Bruno R, Perlini S, et al. Severe acute respiratory syndrome coronavirus 2 (SARS-CoV-2) infection in children and adolescents: a systematic review. JAMA Pediatr. 2020; 174:882–9. https://doi.org/10.1001/jamapediatrics.2020.1467

34. Ludvigsson JF. Systematic review of COVID-19 in children shows milder cases and a better prognosis than adults. Acta Paediatr. 2020;109:1088–95. https://doi.org/10.1111/apa.15270

35. Zimmermann P, Curtis N. COVID-19 in children, pregnancy and neonates: a review of epidemiologic and clinical features. Pediatr Infect Dis J. 2020;39:469–77. https://doi.org/10.1097/INF.0000000000002700

36. Cauchemez S, Donnelly CA, Reed C, Ghani AC, Fraser C, Kent CK, et al. Household transmission of 2009 pandemic influenza A (H1N1) virus in the United States. N Engl J Med. 2009;361:2619–27. https://doi.org/10.1056/NEJMoa0905498

37. Park M, Cook AR, Lim JT, Sun Y, Dickens BL. A systematic review of COVID-19 epidemiology based on current evidence. J Clin Med. 2020;9:E967. https://doi.org/10.3390/jcm9040967

38. Madewell ZJ, Yang Y, Longini IM Jr, Halloran ME, Dean NE. Household transmission of SARS-CoV-2: a systematic review and meta-analysis of secondary attack rate. JAMA Netw Open. 2020;3:e2031756. https://doi.org/10.1001/jamanetworkopen.2020.31756

39. Quesada JA, Lopez-Pineda A, Gil-Guillen VF, Arriero-Marin JM, Gutierrez F, Carratala-Munuera C. Período de incubación de la COVID-19: revisión sistemática y metaanálisis. Rev Clin Esp. 2021;221:109–17. https://doi.org/10.1016/j.rce.2020.08.005

40. Tan WYT, Wong LY, Leo YS, Toh MPHS. Does incubation period of COVID-19 vary with age? A study of epidemiologically linked cases in Singapore. Epidemiol Infect. 2020;148:e197. https://doi.org/10.1017/S0950268820001995

41. Centers for Disease Control and Prevention. Deciding to go out [cited 2020 Sep 1]. https://www.cdc.gov/coronavirus/2019-ncov/daily-life-coping/deciding-to-go-out.html

42. Centers for Disease Control and Prevention. How to protect yourself & others [cited 2020 Sep 1]. https://www.cdc.gov/coronavirus/2019-ncov/prevent-getting-sick/prevention.html.

43. Centers for Disease Control and Prevention. Vaccines for COVID-19 [cited 2020 Sep 1]. https://www.cdc.gov/coronavirus/2019-ncov/vaccines/index.html

44. Centers for Disease Control and Prevention. What to do if you are sick [cited 2020 Sep 1]. https://www.cdc.gov/coronavirus/2019-ncov/if-you-are-sick/steps-when-sick.html.

Address for correspondence: Rachel M. Burke, Centers for Disease Control and Prevention, 1600 Clifton Rd NE, Mailstop H24-5, Atlanta, GA 30329-4027, USA; email: rburke@cdc.gov

EID Podcast
Oral HPV Infection in Children, Finland

Image credit: Wikimedia Commons, Deposition authors: Bishop, B., Dasgupta, J., Chen, X.S.; http://www.rcsb.org/structure/2r5k

Human papillomavirus (HPV) is usually thought of as a sexually transmitted infection.

However, HPV also can spread through other forms of contact. New research indicates that it might even be common for mothers to transmit the virus to their children before, during, and after birth.

In this EID podcast, Dr. Stina Syrjänen, a professor and chairman emerita at the University of Turku and chief physician in the Department of Pathology at Turku University Hospital in Finland, describes her findings on nonsexual transmission of HPV among young children and families.

Visit our website to listen:
https://go.usa.gov/xHKGj

EMERGING INFECTIOUS DISEASES®

Severe Acute Respiratory Syndrome Coronavirus 2 in Farmed Mink (*Neovison vison*), Poland

Lukasz Rabalski, Maciej Kosinski, Teemu Smura, Kirsi Aaltonen,
Ravi Kant, Tarja Sironen, Bogusław Szewczyk, Maciej Grzybek

Severe acute respiratory syndrome coronavirus 2 (SARS-CoV-2) is the etiologic agent of coronavirus disease and has been spreading worldwide since December 2019. The virus can infect different animal species under experimental conditions, and mink on fur farms in Europe and other areas are susceptible to SARS-CoV-2 infection. We investigated SARS-CoV-2 infection in 91 mink from a farm in northern Poland. Using reverse transcription PCR, antigen detection, and next-generation sequencing, we confirmed that 15 animals were positive for SARS-CoV-2. We verified this finding by sequencing full viral genomes and confirmed a virus variant that has sporadic mutations through the full genome sequence in the spike protein (G75V and C1247F). We were unable to find other SARS-CoV-2 sequences simultaneously containing these 2 mutations. Country-scale monitoring by veterinary inspection should be implemented to detect SARS-CoV-2 in other mink farms.

Identifying possible pathogen hosts and studying transmission dynamics of hosts in their populations are crucial steps in controlling zoonotic diseases. The origin of severe acute respiratory syndrome coronavirus 2 (SARS-CoV-2) is probably bats (*1*), but the potential intermediate host has not yet been confirmed. SARS-CoV-2 seems to readily jump from humans to other animal species, particularly carnivores (i.e., dogs, cats, ferrets, lions, pumas) (*2,3*), raising concerns about new animal sources of coronavirus disease (COVID-19) (*4,5*).

SARS-CoV-2 infections in mink were reported from farms in Denmark and the Netherlands and later in other regions (*6–9*) (Figure 1). Because of SARS-CoV-2 outbreaks in mink farms and their appearance

Author affiliations: University of Gdansk, Gdansk, Poland
(L. Rabalski, M. Kosinski, B. Szewczyk); University of Helsinki,
Helsinki, Finland (T. Smura, K. Aaltonen, R. Kant, T. Sironen)
Medical University of Gdansk, Gdansk, Poland (M. Grzybek)

in the surrounding communities, the European Centre for Disease Prevention and Control and the World Health Organization have emphasized the need for surveying the host–animal interface by collaboration among virologists and epidemiologists to track and characterize viral mutations (*11*). After SARS-CoV-2 infections in mink in the Netherlands, the Dutch Ministry of Agriculture decided to cull the mink from all farms. In Denmark, the Danish National Institute of Public Health announced the culling of all 17 million mink in the country after the virus had passed back from the mink farms into the human community. The data available for Denmark on these mink-associated SARS-CoV-2 variants suggest that these variants can spread rapidly on mink farms and in nearby human communities (*12*). However, humans infected with the mink-related variants do not appear to have more severe clinical symptoms than those infected with non–mink-related variants (*9*).

Poland is the second-largest producer of mink pelts in Europe. Poland has 810 fur animal farms, including those for foxes, mink, raccoons, dogs, and chinchillas. The 354 active mink farms in Poland contain ≈6.3 million mink. During 2019, mink farmers in Poland sold 8.5 million mink pelts (*13,14*).

As of May 5, 2021, Poland had recorded 2,838,180 COVID-19 cases and 70,336 total related deaths (*15*). Considering the recent reports of SARS-CoV-2 infections in mink in other countries in Europe and the high incidence of human SARS-CoV-2 infections in Poland, we monitored SARS-CoV-2 in mink on 1 farm in Pomorskie Voivodeship in northern Poland.

Materials and Methods

Material Collection

We collected throat swab (BIOCOMA, http://www.biocomma.com) specimens from 91 mink culled for pelting at a mink farm in Pomorskie Voivodeship in
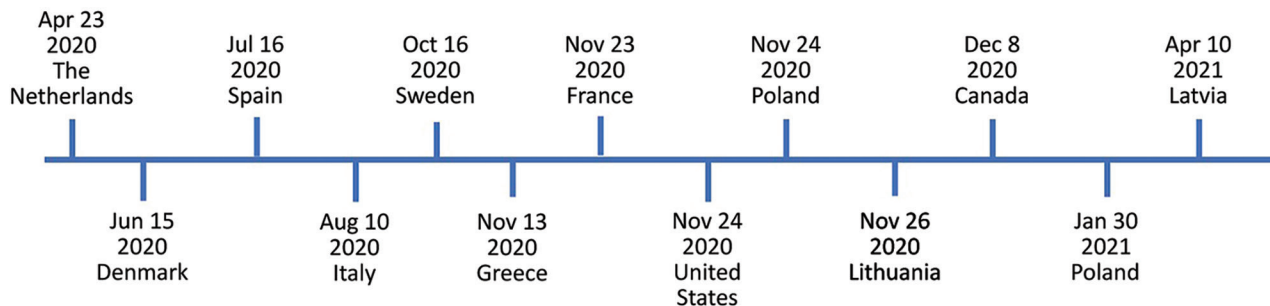
Figure 1. Timeline of severe acute respiratory syndrome coronavirus 2 (SARS-CoV-2) infections in mink farms, Europe, according to the World Organisation for Animal Health (*10*). We investigated SARS-CoV-2 in mink sampled on November 24, 2020, in Pomorskie Voivodeship, northern Poland. The Polish National Veterinary Research Institute, as a national unit responsible for reporting to the World Organisation for Animal Health, detected SARS-CoV-2 infection in the same mink farm on January 30, 2021.

northern Poland on November 17, 2020. The farm owner reported no respiratory symptoms in the animals. We collected blood samples directly from the heart by using cardiac puncture and a sterile 5-mL syringe immediately after death of the mink. After separation of the blood clot, we centrifuged samples at 5,000 rpm for 10 min by using an MPW High-Speed Brushless Centrifuge (MPW Med Instruments, https://mpw.pl). We collected serum and stored it at −80°C until the samples could be analyzed.

RNA Isolation
We added 150 μL of each swab specimen sample in inactivation buffer to 300 μL of RLT lysis buffer (RNeasy Mini Kit; QIAGEN, https://www.qiagen.com). We then mixed samples vortexing and incubated them for 10 min at room temperature. After incubation, we added 400 μL of 70% ethanol to each sample and mixed them by pipetting. We transferred lysates to RNeasy Mini spin columns with collection tubes (QIAGEN) and centrifuged them at 13,000 rpm for 1 min. We then washed the columns once with 700 μL of RW1 buffer and twice with 500 μL of RPE buffer. Between every wash, we centrifuged the columns and discarded the flow-through. We performed elution by adding 50 μL of PCR-grade water to the columns and incubating them for 2 min. We placed the columns into new tubes and centrifuged them at 13,000 rpm for 1 min. After isolation, we stored the samples for <2 hours at 4°C. No human-origin samples were processed at the same time.

SARS-CoV-2 Case Definition
We defined SARS-CoV-2–positive animals as suggested by the World Organisation for Animal Health (*10*). We considered mink to be SARS-CoV-2 positive if SARS-CoV-2 was isolated from a sample taken directly from an animal (nasal or oropharyngeal swab

sample) or if viral nucleic acid was identified in a sample taken directly from an animal, giving cause for suspicion of previous association or contact with SARS-CoV-2, by targeting ≥2 specific genomic regions at a level indicating presence of infectious virus or by targeting 1 genomic region, followed by sequencing of a secondary target.

Real-Time Reverse Transcription PCR
For each sample, we prepared the reaction mixture by using a TaqPath 1-Step quantitative RT-PCR (reverse transcription PCR) Master Mix (ThermoFisher Scientific, https://www.thermofisher.com), polymerase, diethyl pyrocarbonate–treated water (EURx, https://eurx.com.pl) and primers and probes for the RNA-dependent RNA polymerase (RdRp) and envelope (E) genes (*16*) in white, 8-well, quantitative PCR strips with optical clear caps (Applied Biosystems, https://www.thermofisher.com). We also prepared positive control plasmids made in-house containing the RdRp and E genes and a no-template control containing diethyl pyrocarbonate–treated water instead of template reactions. We mixed reactions and loaded them into a Light Cycler 480 (Applied Biosystems, https://www.thermofisher.com). Cycling conditions were incubation with uracil N-glycosylase for 2 min at 25°C, reverse transcription for 15 min at 50°C, and enzyme activation for 2 min at 95°C, followed by 40 amplification cycles consisting of 3 s at 95°C and 30 s at 60°C. After each amplification cycle, we measured the signal from each sample in both the FAM (RdRp gene) and HEX (E gene) channels. Samples with a crossing point (Cp) <35 for any gene were considered positive for SARS-CoV-2.

SARS-CoV-2 Antigen Detection in Mink
We performed 2 different antigen tests to confirm the presence of viral antigen in either the swab or serum

samples. Antigen tests were conducted on samples positive by quantitative PCR. We used 3 negative samples from the same batch as the positive samples as controls. A total of 150 µL of transport medium from each swab specimen was transferred to tubes from a COVID-19 Antigen Detection Kit (Zhuhai Lituo Biotechnology Co., Ltd., https://www.lituo.com.cn) containing extraction buffer. This antigen test was in the form of a cassette with a lateral flow assay that targets the nucleocapsid protein of SARS-CoV-2. Samples were mixed and incubated for 1 min at room temperature. We added 2 drops of each sample to the sample window on the test cassettes. Results consisted of 2 bands: 1 for the control and 1 for the target. If both bands showed a burgundy line, the test result was considered positive. We read results after 12 min.

We tested 91 mink serum samples by using a SARS-CoV-2 antigen ELISA (COV-04-S; Salofa Oy, https://www.salofa.com) according to the kit instructions. This test is a double-antibody sandwich ELISA. The results were obtained according to the formula based on the concentration standards provided in the kit. The cutoff value for this test was 2.97 pg/mL. The tests were repeated twice, and additional dilutions were performed to determine the final concentration as suggested in the kit instructions.

Full SARS-CoV-2 Genome Sequencing and Classification
We performed SARS-CoV-2 genome sequencing at University of Gdansk in Poland and the University of Helsinki in Finland by using only samples containing RNA isolated from virus-positive swab specimens (amplification of target gene in an RT-PCR; this gene has a Cp <35) or that were inconclusive (only 1 target gene amplification with Cp <35). Samples with positive results in the SARS-CoV-2 antigen detection assays were also sequenced.

At Gdansk, 2 independent protocols were used for SARS-CoV-2 genome sequencing. The first protocol was an Illumina (https://www.illumina.com) RNA preparation with enrichment for respiratory virus oligos panel V2, followed by an Illumina MiniSeq medium output run that produced 150-nt paired-end reads. The second protocol was an ARTIC version 3 amplicon generation (https://bmcgenomics.biomedcentral.com), followed by an Oxford Nanopore Technology MinIONB run (https://nanoporetech.com). No human origin samples were processed at the same time. No DNA/rRNA depletion methods were used. Reads were base called, debarcoded, and trimmed to remove adaptor, barcode, and PCR primer sequences. Oxford Nanopore Technology reads were used for SARS-CoV-2 genome

assembly in ARTIC-nCoV-bioinformaticsSOP-v1.1.0 (https://artic.network/ncov-2019).

Illumina paired reads were used to prepare contigs by de novo assembly by using Geneious Prime 2020.2 (https://www.geneious.com) software suite with integrated tools for variant calling (minimum coverage = 100, minimum variant frequency = 0.25) and consensus sequence generation. The fasta files generated by the Illumina procedure were further analyzed in Kraken2 2.1.1 software (https://www.ccb.jhu.edu/software/kraken2) to classify every read to the reference database containing viral and American mink genomes (17).

In Helsinki, the sequencing libraries were prepared by using the Illumina DNA Prep Kit (New England BioLabs, https://www.neb.com). We measured library fragment sizes by using agarose gel electrophoresis and concentrations by using the Qubit dsDNA HS Assay Kit (Life Technologies, https://www.thermofisher.com) and the NEBNext Library Quant Kit for Illumina (New England BioLabs). Sequencing was conducted by using the MiSeq V3 Reagent Kit (Illumina) with 250-bp reads. We trimmed raw sequence reads and removed low-quality (quality score <30) and short (<50 nt) sequences by using Trimmomatic (18). Trimmed sequence reads were mapped against the SARS-CoV-2 reference sequence (GenBank accession no. NC_045512.2) by using BWA-MEM version 0.7.17 (19), followed by sorting and removal of duplicate reads by using SAMTools version 1.10 (20).

Phylogenetic Analysis of SARS-CoV-2 Isolates
The dataset consisted of all genetic sequences of SARS-CoV-2 from this study (Poland, Germany, Lithuania, Latvia, Estonia, Russia, and Ukraine), which was completed as the representative pool Europe by Nextstrain (https://nextstrain.org/ncov/europe) and resulted in 5,778 entries. We performed phylogenetic analysis by using the procedure recommended by Nextstrain with modifications in the subsampling region filtering procedure, in which the number of sequences per country was 40 (21). We used Augur toolkit version 10.1.1 (Nextstrain) for phylogenetic analysis and Auspice version 2.10.1 (Nextstrain) for visualization. Possible time of divergence for samples was inferred by using the TreeTime pipeline (https://www.treetime.com) implemented in the Nextstrain analysis and presented in the phylogenetic tree (22).

Statistical Analysis and Ethics
We calculated 95% CIs by using published procedures (23,24). This study was conducted with due regard for European Union Principles and the Polish

Law on Animal Protection. No permit from the Local Bioethical Committee for Animal Experimentation was obtained because animals were culled by the owner for production of pelts. Samples were collected postmortem.

Results

Prevalence of SARS-CoV-2

We confirmed that 15 mink (16.5%, 95% CI 8.4%–28.6%) were positive for SARS-CoV-2. We summarized and provide the diagnostic results (Table 1).

SARS-CoV-2 Antigen Detection in Mink

Samples mink_4, mink_5, mink_48, mink_50, mink_77, and mink_83 had highly visible signals in both the control and test lines. Samples mink_20, mink_36, mink_42, mink_46, mink_49, mink_67, mink_76, and mink_88 had a highly visible control line and a much less pronounced test line. In all other samples, only the test line was visible. All 8 real-time RT-PCR–positive samples were also positive by the antigen test. In addition, 5 E gene–positive samples were also positive in the antigen test, but 4 were negative. The sample from mink_20 was positive in the antigen test, but SARS-CoV-2 RNA was not detected by RT-PCR.

Read Classification and SARS-CoV-2 Genome Sequences

The final validation of detection of SARS-CoV-2 in the mink was classification of the next-generation sequencing reads on the basis of the database containing reference viral, human, and American mink genomes. We used 3 independent approaches to obtain full viral genomes (Table 2). Only samples that had a complete SARS-CoV-2 genome sequence are shown. The number of Illumina reads generated for samples mink_4, mink_42, mink_49, mink_76, and mink_88 was not enough to produce full SARS-CoV-2 genomes. For these samples, the genomes were obtained by using the ARTIC procedure.

Phylogenetic Analysis of SARS-CoV-2 in Farmed Mink

We checked the 12 mink-originated SARS-CoV-2 sequences for mink-specific mutations detected earlier in mink from the Netherlands and Denmark, but found none. This finding suggested recent and separate introduction of SARS-CoV2 into mink from Poland (Figure 2). Alignment of full-genome sequences from 12 samples showed multiple polymorphisms at different nucleotide sites. Many of these polymorphisms gave rise to changes in amino acids when compared with the reference Wuhan-Hu-1 sequence (GenBank accession no. MN908947). Two specific mutations present in all samples were found in the spike protein: G75V and C1247F. The G75V mutation is present in 199 isolates published in GISAID (https://www.gisaid.org), and the C1257F mutation in 83 isolates. Other rare amino acid variants present in every SARS-CoV-2 isolate from mink in Poland were found in 5 additional proteins: nonstructural protein (nsp) 2, nsp3, nsp14, nsp15, and nucleocapsid protein.

Table 1. Detection of SARS-CoV-2 by different techniques in samples collected from 19 farmed mink, Poland*

Sample name	Cp for RdRP gene†	Cp for E gene†	Antigen in swab specimens	Antigen in serum, concentration of N protein, pg/mL	Sequence obtained
mink_4	ND	34.99	Strong positive	46.85	Full
mink_5	24.36	16.88	Strong positive	3.39	Full
mink_6	ND	34.88	Negative	ND	Partial
mink_20	ND	ND	Positive	132.24	Partial
mink_27	ND	35.62	Negative	ND	Partial
mink_36	ND	ND	Positive	271.30	Partial
mink_39	ND	ND	Negative	35.59	Partial
mink_42	ND	25.62	Positive	ND	Full
mink_46	34.93	22.75	Positive	ND	Full
mink_48	23.83	22.52	Strong positive	ND	Full
mink_49	ND	27.73	Positive	ND	Full
mink_50	32.33	21.61	Strong positive	ND	Full
mink_63	–	–	Negative	19.30	Partial
mink_67	36.30	20.34	Positive	ND	Full
mink_70	ND	34.48	Positive	ND	Partial
mink_76	32.53	22.73	Positive	ND	Full
mink_77	32.87	28.39	Strong positive	ND	Full
mink_83	15.39	21.77	Strong positive	51.57	Full
mink_88	ND	33.55	Positive	ND	Full
NTC	ND	ND	ND	ND	ND
Positive control	16.91	23.31	ND	ND	ND

*Samples in bold are considered positive for SARS-CoV-2 by nucleic acid amplification, serologic analysis, or next-generation sequencing. Cp, crossing point; E, envelope; N, nucleocapsid; ND, not detected; NTC, no template control; RdRp, RNA-dependent RNA polymerase; SARS-CoV-2, severe acute respiratory coronavirus 2.
†By reverse transcription quantitative PCR.

Table 2. Total mean coverage for each sample from 12 mink with a full SARS-CoV-2 genome, Poland*

Sample name	Mean coverage of SARS-CoV-2 genome (ONT plus Illumina)	Total Illumina reads†	Total Illumina SARS-CoV-2 reads†	Total Illumina mink reads†
mink_4	949.6	152,608	37	131,204
mink_5	2,776	395,259	159,484	184,135
mink_42	847.8	66,515	868	34,968
mink_46	1,039.5	387,282	25,975	241,768
mink_48	1,151	125,329	9,526	64,363
mink_49	394.6	487,771	1,711	348,017
mink_50	1,839.6	425,333	79,589	246,546
mink_67	882.1	167,963	10,634	114,163
mink_76	723.0	99,660	2,105	77,945
mink_77	16,078.5	2,434,311	1,609,172	662,301
mink_83	111,976.9	13,495,934	12,730,431	611,926
mink_88	1,205.2	1,071,003	2,822	611,707

*ONT, Oxford Nanopore Technology (https://www.nanoporetech.com); SARS-CoV-2, severe acute respiratory syndrome coronavirus 2.
†These columns indicate how many Illumina (https://www.illumina.com) reads were generated for each sample and how many of them were classified as SARS-CoV-2 or American mink genomes.

On the basis of the dataset, we inferred a phylogenetic relationship by estimating the divergence times between each isolate (Figure 2). The analysis estimated that the most recent common ancestor for SARS-CoV-2 from mink in Poland and the 2 most similar sequences (German/NW-HHU-340/2020 and Norway/4235/2020) diverged on approximately September 31, 2020. We recognized mutations in amino acid sequences. If the molecular evolution started after virus introduction into the farm, this incident is estimated to have occurred on approximately October 4, 2020. Complete genome sequences of SARS-CoV-2 isolated from farmed mink in Poland have been deposited in GISAID (accession nos. EPI_ISL_732948–59).

Discussion

Identifying new species that can serve as animal sources of SARS-CoV-2 and predicting where novel outbreaks are most likely to occur are crucial steps for preventing and minimizing the extent of SARS-CoV-2 infections among humans (25). Recent reports confirmed the presence of SARS-CoV-2 in different animal species, including fur animals (i.e., mink and racoon dogs) (26,27). We report a 16.5% prevalence of SARS-CoV-2 in mink tested at a fur farm in northern Poland, confirming the presence of SARS-CoV-2 in farmed mink in Poland.

During our study, we used 2 different sequencing technologies to sequence the SARS-CoV-2 genomes. We found that amplicon-based nanopore sequencing gave better results than the bed-based enrichment Illumina approach. Conversely, Illumina reads showed a broader context because we were able to classify background reads that do not map to the SARS-CoV-2 genome as being of host origin. Therefore, these reads can be used as proof of sample origin. We also showed that the RdRp target for the quantitative PCR is less effective than the E gene in our experiment settings. The full genome of SARS-CoV-2 was assembled when both target genes were detected or the E gene was detected by a pair of positive signals in the antigenic assay.

Poland is one of the largest fur producers in Europe. Considering the number of farmed mink in the country and the large number of persons employed in this sector, we seek to increase awareness in the scientific community and mink industry that mink are susceptible to SARS-CoV-2 infection. Previous studies reported viral RNA detection in airborne inhalable dust in mink farms (8). Moreover, close contact of farmworkers with animals during feeding, culling, and dehiding increases their risk for exposure. We believe that a country-scale biomonitoring program should be activated as soon as possible to prevent the fur production sector from being a reservoir for future spillover of SARS-CoV-2 to humans. Samples for molecular diagnostics should be obtained from all farms in Poland following the highest standards for material collection, sample handling, and molecular detection of SARS-CoV-2.

We report a possible new genotype of SARS-CoV-2 that has sporadic mutations throughout the full genome sequence. Two mutations located in the spike protein (G75V and C1247F) were present in all isolates reported in this study. The G75V mutation is localized in the N terminal domain and could be responsible for interactions with host receptors or stabilizing the spike protein in a constrained prefusion state (28). To date, no other SARS-CoV-2 sequences deposited in GISAID have these 2 mutations simultaneously (29). We have recently detected possible zoonotic spillover of SARS-CoV-2 in worker employed at the farm described in this study (L. Rabalski et al., unpub. data). Preliminary genome analysis showed that the newly described isolates carry the combination of mutations typical of viruses isolated in November 2020, but additional new changes have accumulated since that time. We believe
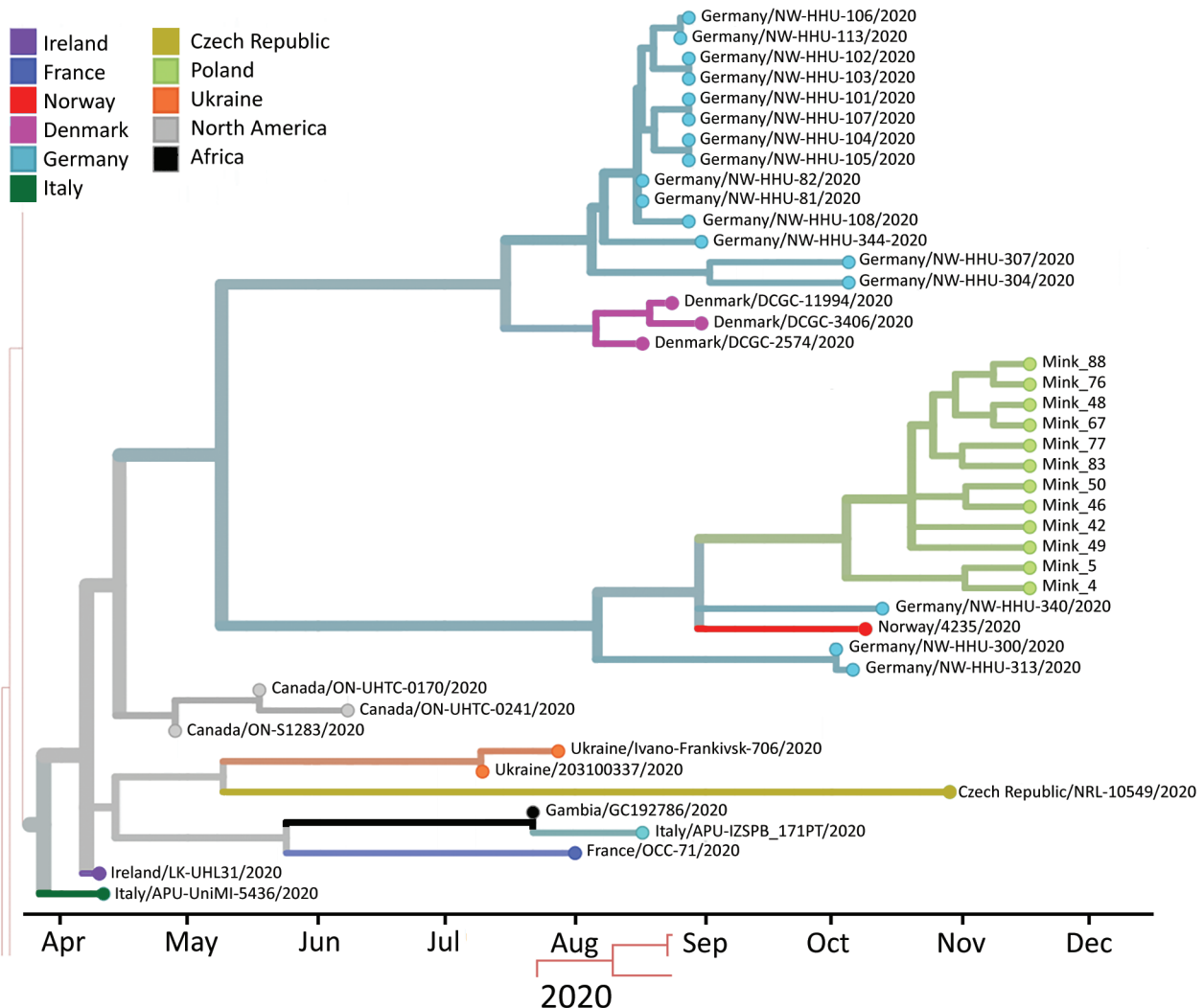
Figure 2. Phylogenetic tree estimating the divergence time for severe acute respiratory syndrome coronavirus 2, Europe. Sequences from mink sampled on November 24, 2020, in Pomorskie Voivodeship, northern Poland, are shown on green branches. Only closely related isolates that were included in the dataset are presented. Visualization was achieved by using Nextstrain (https://nextstrain.org/ncov/europe).

that wide monitoring of humans living near the mink farm should be performed to search for possible spillover and presence of new virus variants. Constant epizootiology monitoring is a crucial step in preventing new outbreaks of zoonotic diseases.

About the Author

Dr. Rabalski is a virologist and assistant professor in the Laboratory of Recombinant Vaccines, Intercollegiate Faculty of Biotechnology of University of Gdansk and Medical University of Gdansk, Gdansk, Poland. His research interests include virology, epidemiology of viral pathogens, virus genomics, novel tools in molecular virology, and next-generation sequencing.

References

1. Zhou P, Yang X-L, Wang X-G, Hu B, Zhang L, Zhang W, et al. A pneumonia outbreak associated with a new coronavirus of probable bat origin. Nature. 2020;579:270–3. https://doi.org/10.1038/s41586-020-2012-7
2. Jo WK, de Oliveira-Filho EF, Rasche A, Greenwood AD, Osterrieder K, Drexler JF. Potential zoonotic sources of SARS-CoV-2 infections. Transbound Emerg Dis. 2020;10:1111.
3. Mallapaty S. The search for animals harbouring coronavirus and why it matters. Nature. 2021;591:26–8. https://doi.org/10.1038/d41586-021-00531-z
4. Alexander MR, Schoeder CT, Brown JA, Smart CD, Moth C, Wikswo JP, et al. Predicting susceptibility to SARS-CoV-2 infection based on structural differences in ACE2 across species. FASEB J. 2020;34:15946–60. https://doi.org/10.1096/fj.202001808R
5. Damas J, Hughes GM, Keough KC, Painter CA, Persky NS, Corbo M, et al. Broad host range of SARS-CoV-2 predicted by comparative and structural analysis of ACE2 in vertebrates. Proc Natl Acad Sci U S A. 2020;117:22311–22. https://doi.org/10.1073/pnas.2010146117
6. Hammer AS, Quaade ML, Rasmussen TB, Fonager J, Rasmussen M, Mundbjerg K, et al. SARS-CoV-2 transmission between mink (Neovison vison) and humans, Denmark. Emerg Infect Dis. 2021;27:547–51. https://doi.org/10.3201/eid2702.203794
7. Koopmans M. SARS-CoV-2 and the human-animal interface: outbreaks on mink farms. Lancet Infect Dis. 2020;21:18–9. https://doi.org/10.1016/S1473-3099(20)30912-9
8. Oreshkova N, Molenaar RJ, Vreman S, Harders F, Oude Munnink BB, Hakze-van der Honing RW, et al. SARS-CoV-2 infection in farmed minks, the Netherlands, April and May 2020. Euro Surveill. 2020;25:200105. https://doi.org/10.2807/1560-7917.ES.2020.25.23.2001005
9. Oude Munnink BB, Sikkema RS, Nieuwenhuijse DF, Molenaar RJ, Munger E, Molenkamp R, et al. Transmission of SARS-CoV-2 on mink farms between humans and mink and back to humans. Science. 2021;371:172–7. https://doi.org/10.1126/science.abe5901
10. World Organisation for Animal Health. COVID-19, 2021 [cited 2021 Jan 12]. https://www.oie.int/en/scientific-expertise/specific-information-and-recommendations/questions-and-answers-on-2019novel-coronavirus/events-in-animals
11. World Health Organization. WHO-convened global study of the origins of SARS-CoV-2, 2020 [cited 2020 Dec 13]. https://www.who.int/publications/m/item/who-convened-global-study-of-the-origins-of-sars-cov-2
12. Boklund A, Hammer AS, Quaade ML, Rasmussen TB, Lohse L, Strandbygaard B, et al. SARS-CoV-2 in Danish mink farms: course of the epidemic and a descriptive analysis of the outbreaks in 2020. Animals (Basel). 2021;11:164. https://doi.org/10.3390/ani11010164
13. European Union Fur Association. Sustainable fur, 2020 [cited 2020 Dec 13]. https://www.sustainablefur.com
14. Związku Przedsiębiorców i Pracodawców. Facts about breeding fur animals in Poland [in Polish]. Warsaw; 2020 [cited 2021 Jun 17]. https://zpp.net.pl/wp-content/uploads/2020/09/Raport-ZPP_Fakty-o-hodowli-zwierząt-futerkowych-w-Polsce.pdf
15. European Centre for Disease Prevention and Control. COVID-19 situation update for the EU/EEA and the UK, 2021 [cited 2021 May 12]. https://www.ecdc.europa.eu/en/cases-2019-ncov-eueea
16. Corman VM, Landt O, Kaiser M, Molenkamp R, Meijer A, Chu DK, et al. Detection of 2019 novel coronavirus (2019-nCoV) by real-time RT-PCR. Euro Surveill. 2020;25:2000045. https://doi.org/10.2807/1560-7917.ES.2020.25.3.2000045
17. Wood DE, Lu J, Langmead B. Improved metagenomic analysis with Kraken 2. Genome Biol. 2019;20:257. https://doi.org/10.1186/s13059-019-1891-0
18. Bolger AM, Lohse M, Usadel B. Trimmomatic: a flexible trimmer for Illumina sequence data. Bioinformatics. 2014; 30:2114–20. https://doi.org/10.1093/bioinformatics/btu170
19. Li H. Aligning sequence reads, clone sequences and assembly contigs with BWA-MEM, 2013 [cited 2021 May 13]. http://github.com/lh3/bwa
20. Li H, Handsaker B, Wysoker A, Fennell T, Ruan J, Homer N, et al.; 1000 Genome Project Data Processing Subgroup. The sequence alignment/map format and SAMtools. Bioinformatics. 2009;25:2078–9. https://doi.org/10.1093/bioinformatics/btp352
21. Hadfield J, Megill C, Bell SM, Huddleston J, Potter B, Callender C, et al. Nextstrain: real-time tracking of pathogen evolution. Bioinformatics. 2018;34:4121–3. https://doi.org/10.1093/bioinformatics/bty407
22. Sagulenko P, Puller V, Neher RA. TreeTime: maximum-likelihood phylodynamic analysis. Virus Evol. 2018;4:vex042. https://doi.org/10.1093/ve/vex042
23. Sokal RR, Rohlf FJ. Biometry: the principles and practices of statistics in biological research. New York: W. H. Freeman; 1995.
24. Grzybek M, Bajer A, Bednarska M, Al-Sarraf M, Behnke-Borowczyk J, Harris PD, et al. Long-term spatiotemporal stability and dynamic changes in helminth infracommunities of bank voles (Myodes glareolus) in NE Poland. Parasitology. 2015;142:1722–43. https://doi.org/10.1017/S0031182015001225
25. Hemida MG, Ba Abduallah MM. The SARS-CoV-2 outbreak from a one health perspective. One Health. 2020;10:100127. https://doi.org/10.1016/j.onehlt.2020.100127
26. Abdel-Moneim AS, Abdelwhab EM. Evidence for SARS-CoV-2 infection of animal hosts. Pathogens. 2020;9:529. https://doi.org/10.3390/pathogens9070529
27. Freuling CM, Breithaupt A, Müller T, Sehl J, Balkema-Buschmann A, Rissmann M, et al. Susceptibility of raccoon dogs for experimental SARS-CoV-2 infection. Emerg Infect Dis. 2020;26:2982–5. https://doi.org/10.3201/eid2612.203733
28. Arya R, Kumari S, Pandey B, Mistry H, Bihani SC, Das A, et al. Structural insights into SARS-CoV-2 proteins. J Mol Biol. 2021;433:166725. https://doi.org/10.1016/j.jmb.2020.11.024
29. Shu Y, McCauley J. GISAID: global initiative on sharing all influenza data - from vision to reality. Euro Surveill. 2017;22:30494. https://doi.org/10.2807/1560-7917.ES.2017.22.13.30494

Address for correspondence: Maciej Grzybek, Department of Tropical Parasitology, Institute of Maritime and Tropical Medicine, Medical University of Gdansk, Powstania Styczniowego 9B, 81-519 Gdynia, Poland; email: maciej.grzybek@gumed.edu.pl

Risk for Acquiring COVID-19 Illness among Emergency Medical Service Personnel Exposed to Aerosol-Generating Procedures

Aubrey Brown, Leilani Schwarcz, Catherine R. Counts, Leslie M. Barnard, Betty Y. Yang, Jamie M. Emert, Andrew Latimer, Christopher Drucker, John Lynch, Peter J. Kudenchuk, Michael R. Sayre, Thomas Rea

We investigated the risk of coronavirus disease (COVID-19) patients transmitting severe acute respiratory syndrome coronavirus 2 (SARS-CoV-2) to emergency medical service (EMS) providers, stratified by aerosol-generating procedures (AGP), in King County, Washington, USA, during February 16–July 31, 2020. We conducted a retrospective cohort investigation using a statewide COVID-19 registry and identified 1,115 encounters, 182 with ≥1 AGP. Overall, COVID-19 incidence among EMS personnel was 0.57 infections/10,000 person-days. Incidence per 10,000 person-days did not differ whether or not infection was attributed to a COVID-19 patient encounter (0.28 vs. 0.59; p>0.05). The 1 case attributed to a COVID-19 patient encounter occurred within an at-risk period and involved an AGP. We observed a very low risk for COVID-19 infection attributable to patient encounters among EMS first responders, supporting clinical strategies that maintain established practices for treating patients in emergency conditions.

Dynamic circumstances, time sensitivity, limited information about widely variable scenes encountered, and heterogeneous patient characteristics make emergency medical service (EMS) responses inherently challenging. The global coronavirus disease (COVID-19) pandemic, caused by severe acute respiratory syndrome coronavirus 2 (SARS-CoV-2), has now forced EMS providers to also consider how best to manage their own potential exposure, particularly when a patient's infection status is unknown (1,2).

During outbreaks of severe acute respiratory syndrome in 2003 and Middle East respiratory syndrome in 2012, many healthcare workers became infected while caring for patients (3–5). There is an evolving understanding of the risk of patients transmitting COVID-19 to healthcare workers, but less is known about transmitting it to emergency medical first responders or about the specific etiology of infection (6–10).

Respiratory exposure is the primary mode of COVID-19 transmission (11,12). Clinical guidelines have evolved to mitigate risk for transmission, especially through aerosolizing procedures used for cardiopulmonary resuscitation (CPR) or airway management. A better understanding of the risks related to patient care itself could further inform clinical practice approaches, therapeutic choices, and personal protective equipment (PPE) strategies in an effort to balance risks and benefits for providers and patients while striving to maintain best practices for patient care (4,12,13). Therefore, we investigated the risk for COVID-19 transmission from patient to provider and how use of aerosol-generating procedures (AGP) during the encounter might affect risk levels.

Methods

Study Design, Population, and Setting

We conducted a retrospective cohort study to evaluate the risk for COVID-19 infection among EMS providers caring for patients in King County, Washington, USA, during February 16–July 31, 2020. When determining risk for COVID-19, we considered all EMS provider-patient encounters and individual EMS providers involved in those encounters. The investigation was designed and reported with consideration of the Strengthening the Reporting of

Author affiliations: University of Washington, Seattle, Washington, USA (A. Brown, C.R. Counts, B.Y. Yang, A. Latimer, J. Lynch, P.J. Kudenchuk, M.R. Sayre, T. Rea); Public Health Seattle and King County Division of Emergency Medical Services, Seattle (L. Schwarcz, L.M. Barnard, J.M. Emert, C. Drucker)

Observational Studies in Epidemiology (STROBE) reporting guidelines (*14*) and approved by the University of Washington and Seattle and King County Public Health and University of Washington public health review boards.

King County is a large metropolitan region encompassing the city of Seattle and covering ≈2,300 square miles with ≈2.3 million residents living in urban, suburban, and rural areas. The EMS system is 2-tiered, the first tier comprising 27 firefighter and emergency medical technician departments and the second tier 5 paramedic departments serving multiple emergency medical technician departments for responding to more serious medical emergencies. EMS teams of 2–7 providers respond to calls based on dispatcher-determined acuity. In general, fire department or private basic life support ambulance units transport medically stable patients to hospitals and advanced life support paramedic units transport patients needing more acute care.

EMS COVID-19 Protocols

Seattle and King County EMS management developed protocols for screening and care of patients at risk for having COVID-19 (*15*). EMS PPE protocols include wearing a mask, eye protection, gloves, and a gown. Surgical masks were considered sufficient for treating patients not requiring AGP, but an N95 respirator was required when patients underwent AGPs. HEPA (high efficiency particulate air) filters were added to ventilation bags. Otherwise, clinical protocols did not change in response to the pandemic. For example, the EMS system continued to support the use of endotracheal intubation and manual CPR to treat out-of-hospital cardiac arrest (*13*).

Data Sources, Linkages, and Abstraction

The Seattle and King County EMS Division of Public Health maintains an encounter-level electronic health record of each EMS response using software from ESO Solutions Inc. (https://www.eso.com). The EMS record for each incident contains information about patient and EMS provider identities, chief complaints, signs and symptoms, EMS care, and PPE use by providers. The state of Washington Disease Reporting System (WDRS) contains names, dates of birth, test dates, and results for all persons who have been tested for SARS-CoV-2 within the state. Seattle and King County Public Health administers the EMS system, enabling identification of EMS encounters with patients who have COVID-19 (*15*). To obtain patient COVID-19 status, we linked WDRS with EMS electronic health records using a

multistep algorithm including the patient's first and last names and date of birth; identification through this linkage was followed by human confirmation of the potential link.

In addition to the linking process for COVID-19 status, we determined the health-related vital status of patients with COVID-19 by linking those patients with Washington State Department of Health vital records available through December 1, 2020, All study information for COVID-19 patient encounters was abstracted into a secure Research Electronic Data Capture (REDCap, https://www.project-redcap.org) platform by using a uniform data abstraction form supported by a data dictionary (*16*). The abstract recorded a review of the narrative and discrete data fields from the dispatch and EMS records.

Exposure and Data Definitions

COVID-19 Patient Classification

A provider was considered to have encountered a patient with COVID-19 if the patient had a positive SARS-CoV-2 swab sample result determined by using real-time reverse transcription PCR (rRT-PCR) ≤10 d before or ≤3 d after an EMS encounter, on the basis of data from the linked EMS and WDRS records. We chose ≤10 d as a criterion on the basis of the 10-day infectious window after onset of symptoms. We used ≤3 d as a criterion after the EMS encounter recognizing that not all patients had been tested upon hospital arrival, especially in the first few months of the pandemic. In addition, a minority of patients were not transported by EMS and had subsequent follow-up for testing even though the EMS encounter appeared to be for illness consistent with COVID-19 (*2*).

AGP Definition and Classification

For this study, we classified endotracheal intubation, supraglottic airway insertion, bag-valve-mask (BVM) ventilation, continuous positive airway pressure nonrebreather mask oxygen, and nebulizer medication therapy as AGPs (*4*). Although the standards for AGP are not fully defined, nonrebreather masks routinely involve using higher-flow oxygen (15 L/min) and require applying and manipulating face masks, which may increase transmission risk (*4,17,18*). We did not classify use of low-flow nasal cannula oxygen as an AGP. In an EMS patient-encounter setting, CPR always involves both chest compressions and BVM ventilation, which constitutes an AGP. We identified AGP procedure usage from the EMS records by searching electronic text records for key phrases

in the narratives or discrete electronic data elements that recorded AGP procedures. We evaluated the accuracy of this method to identify AGP by manually reviewing records of all EMS encounters with COVID-19 patients.

Classifying EMS Provider Person-Days at Risk

For each day of the study period, each EMS provider's day was classified into 1 of 4 mutually exclusive cohorts based on the time interval after COVID-19 patient encounters, if any, and whether or not AGPs were used. Person-days were classified into cohort 1 for COVID-19 patient encounters that involved ≥1 AGPs during the 2–14 d incubation period, cohort 2 for COVID-19 patient encounters that did not involve AGPs during the 2–14 d incubation period, cohort 3 for COVID-19 patient encounters before or after the 2–14 d incubation period, or cohort 4 if the provider had no COVID-19 patient encounters during the study period. Individual EMS providers could contribute discrete person-days to different cohorts, except for cohort 4.

We considered EMS providers at risk for transmission from a patient for 2–14 d after an encounter with a COVID-19 patient (Figure 1), because the biology of transmission and illness indicates that the COVID-19 incubation period is 2–14 d (19). If an EMS provider tested positive for SARS-CoV-2 in the 2–14 d incubation period after treating a COVID-19–positive patient, the infection was attributed to the encounter.

For classification, once an EMS provider completed the 14 d incubation period without SARS-CoV-2 infection, the provider's person-days for subsequent days would transition from cohort 1 or 2 to cohort 3 until the provider was involved with another patient with COVID-19.

For days when a provider had multiple COVID-19 patient encounters and ≥1 involved an AGP, the provider's person-hours for that day were classified into cohort 1, given that AGP use is considered to possess greater intrinsic transmission risk. EMS providers could be diagnosed with COVID-19 on a person-day in any of the 4 cohorts. After a provider's first rRT-PCR–positive SARS-CoV-2 swab result, they were censored from the analysis and did not contribute additional person-days to any cohort. SARS-CoV-2 reinfection was not diagnosed in any provider.

Outcome Measures

We used COVID-19 infections among EMS providers as determined from the WDRS registry during February 15–August 14, 2020, as the primary outcome measure. We extended the period for assessing COVID-19 to August 14, two weeks beyond the final day for recording person-days, to ensure we captured infections identified ≥14 d after COVID-19 patient encounters within the study period.

As part of COVID-19 surveillance, EMS implemented a screening process for potential COVID-19
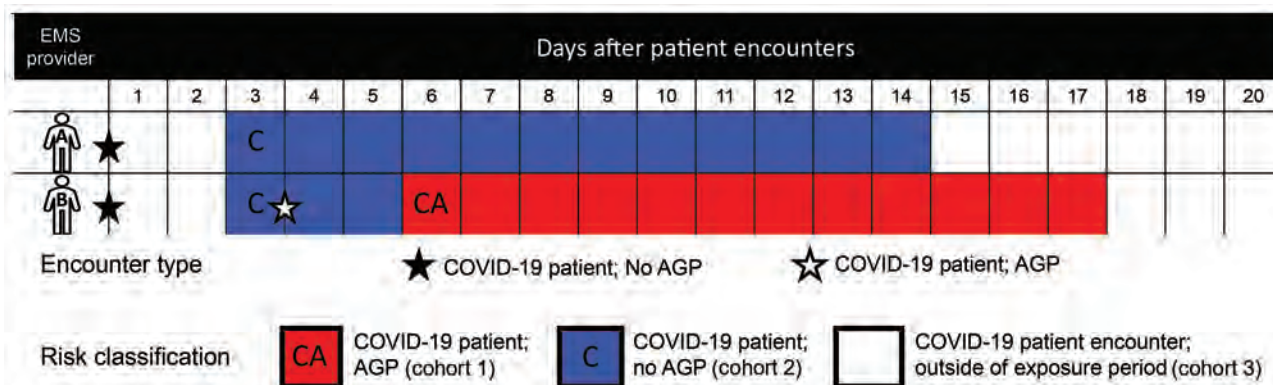
Figure 1. Examples of classification of EMS provider person-days at risk within 2–14 d after COVID-19 patient encounters, King County, Washington, February 16–July 31, 2020. The boxes correspond to the number of person-days an emergency medical services provider contributes to each mutually exclusive risk group. The first row (provider A) demonstrates a COVID-19 patient encounter without an AGP. The provider is classified at risk for COVID-19 transmission because of a patient treated without AGP within 2–14 d after encounter. After the incubation window ends, the EMS provider transitions back to person-days classification of COVID-19 patient outside the incubation period (cohort 3). The second row (provider B) demonstrates classification of person-days from COVID-19 patient without AGP and then with AGP. Person-days transitions from COVID-19 patient encounter without AGP (cohort 2) to patient encounter with AGP (cohort 1). The example illustrates the classification hierarchy that classified the patient into the AGP incubation period when a provider had overlap of person-days following distinct encounters caring for COVID-19 patients without an AGP and then with an AGP. After the incubation window, the EMS provider will transition back to person-days classification of COVID-19 patient outside the incubation period (group 3). AGP, aerosol-generating procedure; COVID-19, coronavirus disease; EMS, emergency medical service.
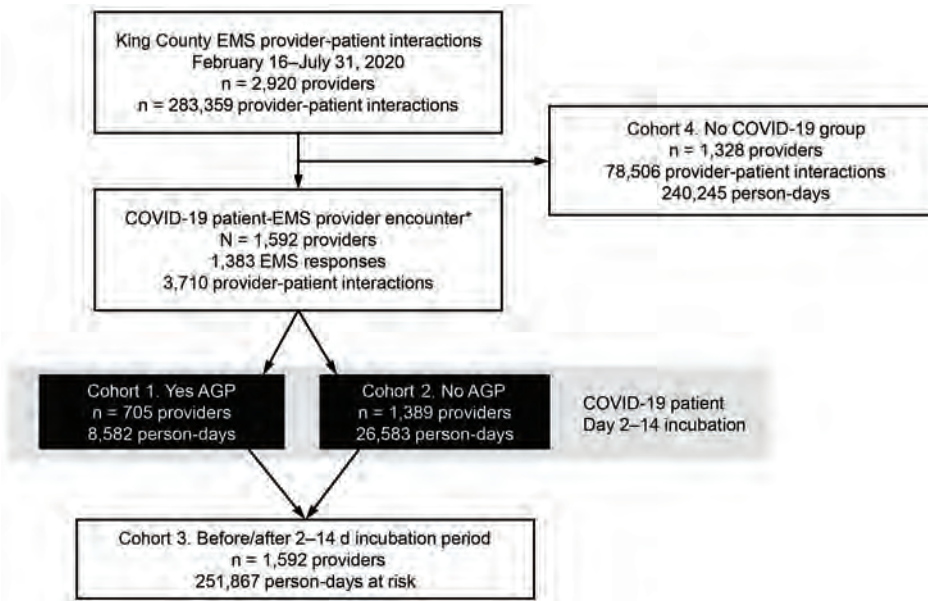
Figure 2. Flow diagram of emergency medical service provider encounters with COVID-19 patients and person-days at risk for transmission, King County, Washington, February 16–July 31, 2020. Individual provider's person-days may transition among cohorts 1–3. AGP, aerosol generating procedure; COVID-19, coronavirus disease; EMS, emergency medical services.

illness among EMS personnel at the outset of each shift comprising a temperature check and observation for symptoms of medical illness. EMS personnel were guided by a return-to-work algorithm that recommended COVID-19 rRT-PCR testing for any acute illness acquired on or off duty in an effort to limit the risk of provider-to-provider transmission and maintain workplace safety (*15*).

Analysis

We performed descriptive analyses at the encounter, patient, and EMS provider levels. We stratified provider encounters and classified person-days according to patient COVID-19 status and whether or not treatment included ≥1 AGPs. EMS providers were censored from the study on the date they were diagnosed with COVID-19 or at the end of the follow-up period (August 15, 2020) if never diagnosed with COVID-19. We then calculated the incidence of COVID-19 infection among EMS providers on the basis of person-days at risk from COVID-19 patient encounters. We calculated the incidence rate ratio using the collective person-days from cohort 3, the cohort including person-days before or after the 2–14 d incubation period of a COVID-19 patient encounter, as the referent group because this approach enabled providers to serve as their own controls when evaluating the risk attributable to COVID-19 patient encounters. In a post hoc analysis, we combined the person-days from cohorts 1 and 2 to evaluate the overall COVID-19 incidence among EMS providers attributed to a COVID-19 patient encounter regardless of AGP use.

Results

Encounters with COVID-19 Patients

During the February 16–July 31, 2020, study period, 1,592 different EMS providers cared for 946 unique COVID-19 patients as part of 1,115 EMS responses, resulting in 3,710 provider-patient COVID-19 encounters. Over that period, 1,328 EMS providers did not care for any patients in whom COVID-19 had been diagnosed. Cohorts 1–3 encompassed a total of 287,032 person-days in which there were COVID-19 patient encounters, and cohort 4 encompassed a total of 240,245 person-days in which there were no COVID-19 patient encounters (Figure 2). Among the 1,592 EMS providers with ≥1 COVID-19 patient encounter, 655 (41%) had 1 encounter, 417 (26%) had 2, and 520 (33%) had ≥3.

We recorded details from the 1,115 encounters involving ≥1 provider and ≥1 COVID-19 patient, overall and stratified by AGP status (Table 1). An AGP was performed in 182 (16%) patient encounters involving 787 EMS providers (567 different providers). Overall, half of the EMS responses were for female patients; the average patient age was 68 years. About half of EMS responses were to private residences and 41% to long-term care or assisted living facilities. Responders reported ≥1 clinical signs of shortness of breath (42%), cough (36%), or fever (42%) in 67% of patients. In the cohort of provider person-days when using AGPs (cohort 1) compared with the cohort of person-days when not using AGPs (cohort 2), patient encounters were more often characterized by tachypnea (63% vs. 28%), hypoxemia (70% vs. 18%), abnormal heart rate (48%

vs. 38%), systolic blood pressure <90 mm Hg (17% vs. 4%), and Glasgow coma scale ≤12 (25% vs. 6%). The most common EMS provider-recorded impression of patient illness overall among the 1,115 responses was respiratory distress (n = 417, 37%), 24% (n = 101) of those among patients needing AGPs and 76% (n = 316) among patients not needing AGPs. Twenty-two patients had out-of-hospital cardiac arrests, comprising 12.1% of the provider person-days in cohort 1 (Table 1). The most common AGP provided was nonrebreather mask oxygen (n = 139) (Table 2). Other common AGPs included BVM ventilation (n = 42) and endotracheal in-

tubation (n = 29). Among patient encounters grouped in the first cohort, 44 (24%) involved >1 AGP during a single encounter, most often nonrebreather oxygen followed by BVM ventilation, then intubation. Overall, 34% of COVID-19 patients, 57% of those receiving AGPs and 29% of those not receiving AGPs, died during follow-up from the time of encounter through December 31, 2020.

EMS Provider Risk

The 2,920 EMS providers followed over the 181-day study period produced 525,154 person-days at

Table 1. Encounter characteristics by aerosol generating procedure status among COVID-19 patients, King County, Washington, February 16–July 31, 2020*

Characteristic	All encounters	AGP encounters	Non–AGP encounters
Unique encounters	1,115 (100.0)	182 (16.3)	933 (83.7)
Patient age, mean (SD)	68.1 (19.8)	69.4 (18.4)	67.8 (20.1)
Sex			
M	563 (50.5)	100 (54.9)	463 (49.6)
F	552 (49.5)	82 (45.1)	470 (50.4)
Location			
Home	529 (47.4)	78 (42.9)	451 (48.3)
Long-term care	458 (41.1)	87 (47.8)	371 (39.8)
Public outdoors	50 (4.5)	3 (1.6)	47 (5.0)
Medical clinic or office	38 (3.4)	11 (6.0)	27 (2.9)
Public indoors	21 (1.9)	1 (0.5)	20 (2.1)
Homeless shelter	19 (1.7)	2 (1.1)	17 (1.8)
Other	Unknown	Unknown	Unknown
Documented signs and symptoms			
Fever	467 (41.9)	74 (40.7)	393 (42.1)
Cough	401 (36.0)	65 (35.7)	336 (36.0)
Shortness of breath	472 (42.3)	133 (73.1)	339 (36.3)
Fever/cough/shortness of breath	751 (67.4)	147 (80.8)	604 (64.7)
Sore throat/nasal congestion	79 (7.1)	8 (4.4)	71 (7.6)
GI symptoms	160 (14.3)	23 (12.6)	137 (14.7)
Body aches	175 (15.7)	27 (14.8)	148 (15.9)
Altered mental status	188 (16.9)	39 (21.4)	149 (16.0)
Fatigue/weakness	354 (31.7)	38 (20.9)	316 (33.9)
Headache	37 (3.3)	6 (3.3)	31 (3.3)
Chest pain	75 (6.7)	11 (6.0)	64 (6.9)
Vital signs			
Any abnormal vital sign	936 (83.9)	179 (98.4)	757 (81.1)
Heart rate ≥100 bpm	438 (39.3)	87 (47.8)	351 (37.6)
Temperature ≥38°C	573 (51.4)	94 (51.6)	479 (51.3)
Respirations ≥24 breaths/min	378 (33.9)	114 (62.6)	264 (28.3)
Oxygen saturation ≤90 SpO_2	292 (26.2)	127 (69.8)	165 (17.7)
Systolic blood pressure ≤90 mm Hg	69 (6.2)	30 (16.5)	39 (4.2)
Glasgow coma scale <12	97 (8.7)	46 (25.3)	51 (5.5)
Glasgow coma scale 13–14	58 (5.2)	20 (11.0)	38 (4.1)
Glasgow coma scale = 15	534 (47.9)	76 (41.8)	458 (49.1)
Patient with cardiac arrest	22 (2.0)	22 (12.1)	Unknown
Initial EMS response type			
Respiratory	417 (37.4)	101 (55.5)	316 (33.9)
Fatigue/weakness/malaise	157 (14.1)	8 (4.4)	149 (16.0)
Infection	128 (11.5)	13 (7.1)	115 (12.3)
Behavioral/psychological/intoxication	114 (10.2)	19 (10.4)	95 (10.2)
Other medical	72 (6.5)	2 (1.1)	70 (7.5)
Cardiovascular	64 (5.7)	29 (15.9)	35 (3.8)
Trauma	64 (5.7)	5 (2.7)	59 (6.3)
Abdominal/GU/endocrine	60 (5.4)	3 (1.6)	57 (6.1)
Neurological	39 (3.5)	2 (1.1)	37 (4.0)

*Values are no. (%) except as indicated. AGP, aerosol generating procedure; COVID-19, coronavirus disease; EMS, emergency medical service; GI, gastrointestinal; GU, genitourinary.

Table 2. Patient outcome emergency medical service care and by aerosol generating procedure status among COVID-19 patients, King County, Washington, February 16–July 31, 2020*

Characteristic	All encounters	AGP encounters	Non–AGP encounters
Unique EMS providers	1,592	567	1,025
EMS encounters	1,115	182	933
ALS unit dispatched	171 (15.3)	98 (53.8)	73 (7.8)
EMS suspicion of COVID-19	715 (64.1)	132 (72.5)	583 (62.5)
Low-flow oxygen	188 (16.9)	34 (18.7)	154 (16.5)
AGP types			
Nonrebreather	139 (12.5)	139 (76.4)	NA
Simple face mask	5 (0.4)	5 (2.7)	NA
Medication therapy	13 (1.2)	13 (7.1)	NA
Metered dose inhaler	4 (0.4)	4 (2.2)	NA
Nebulizer	9 (0.8)	9 (4.9)	NA
NiPPV	48 (4.3)	48 (26.4)	NA
CPAP	6 (0.5)	6 (3.3)	NA
Bag-valve-mask ventilation	42 (3.8)	42 (23.1)	NA
Suction	4 (0.4)	4 (2.2)	NA
Advanced airways	32 (2.9)	32 (17.6)	NA
Supraglottic airway	3 (0.3)	3 (1.6)	NA
Endotracheal intubation	29 (2.6)	29 (15.9)	NA
AGP frequency per encounter			
0	933 (83.7)	0	933 (100)
1	138 (12.4)	138 (75.8)	NA
≥2	44 (3.9)	44 (24.2)	NA
Disposition			
Not transported	245 (22.0)	21 (11.5)	224 (24.0)
BLS transport	759 (68.1)	108 (59.3)	651 (69.8)
ALS transport	86 (7.7)	53 (29.1)	33 (3.5)
Private vehicle	17 (1.5)	0	17 (1.8)
Air ambulance	1 (0.1)	1 (0.5)	0
Patient mortality as of 2020 Dec 1	373 (33.5)	103 (56.6)	270 (28.9)

*Values are no. (%). AGP, aerosol generating procedure; ALS, advanced life support; COVID-19, coronavirus disease; CPAP, continuous positive airway pressure; EMS, emergency medical service; NA, not applicable; NiPPV, noninvasive positive-pressure ventilation.

risk: 8,582 person-days from 705 providers treating COVID-19 patients using AGP within the incubation period (cohort 1); 26,583 person-days from 1,389 providers treating COVID-19 patients without AGP within the incubation period (cohort 2); 252,867 person-days from 1,592 providers treating COVID-19 patients outside the incubation period (cohort 3); and 240,245 person-days from 1,328 providers who never treated a COVID-19 patient during the study period (cohort 4). Thirty EMS providers had positive rRT-PCR COVID-19 test results (Table 3). The median interval between COVID-19 patient encounter and EMS provider positive rRT-PCR test was 73 days (IQR 30–105 days). Only 1 infection occurred within the 2–14-d window after

an encounter with a COVID-19 patient; during that period, the provider encountered >1 COVID-19 patient with ≥1 involving AGP use, so transmission was attributed to a patient encounter in which an AGP was provided. An additional 18 EMS providers cared for COVID-19 patients and acquired COVID-19. However, their COVID-19–positive tests were outside the 2–14-d incubation period after caring for a patient with COVID-19. Eleven EMS providers who never cared for a patient with COVID-19 tested positive for COVID-19.

Overall, the incidence of rRT-PCR positive tests among EMS providers was 0.57/10,000 person-days (30 positive tests in 525,154 person-days). The relative risk associated with COVID-19 patient encounters,

Table 3. Incidence of COVID-19 among EMS providers by COVID-19 patient encounter and AGP status cohort, King County, Washington, February 16–July 31, 2020*

Cohort	COVID-19 patient encounter	2–14 d exposure window	AGP status	EMS provider COVID-19 infection	Person-days at risk	Incidence/10,000 person-days (95% CI)	IRR (95% CI)
1	Yes	Yes	Yes	1	8,582	1.17 (0.03–6.49)	1.64 (0.22–12.26)
2	Yes	Yes	No	0	26,583	0 (0.0–1.39)	0 (0.0–1.50)
3	Yes	No	NA	18	252,867	0.71 (0.42–1.13)	Referent
4	Never	NA	NA	11	240,245	0.46 (0.23–0.82)	0.64 (0.30–1.36)
Post hoc							
1 and 2	Yes	Yes	Y/N	1	35,165	0.28 (0.01–1.58)	0.40 (0.05–2.99)

*AGP, aerosol generating procedure; COVID-19, coronavirus disease; EMS, emergency medical service; IRR, incidence rate ratio; NA, not available.

with or without AGP use, did not differ compared with those without any COVID-19 patient encounters (Table 3). Finally, we found no difference in incidence between aggregated person-days attributed to COVID-19 patient encounters, 0.28/10,000 person-days (1 positive test in 35,165 person-days), and person-days not attributed to COVID-19 patient encounters, 0.59/10,000 person-days (29 positive tests in 489,989 person-days; p>0.05).

Discussion

In this observational study of a populous US metropolitan region, encounters with patients with COVID-19 accounted for 1% of all 911 EMS responses, involving nearly 1,200 unique COVID-19 patients and several thousand patient-provider encounters during the study period. Approximately 16% of these COVID-19 patient encounters involved treatment with AGPs, typically for patients with more severe illness based on field assessment and underscored by subsequent all-cause death rates. However, risk for the first responder workforce primarily originated from nonpatient sources; 29 of 30 COVID-19 illnesses among EMS providers were not directly attributed to COVID-19 patient encounters. Collectively, the results suggest that PPE provides protection against acquiring COVID-19 during prehospital emergency patient care, which supports maintenance of established practices.

Although the results indicate that risk of transmission from patients is low, the findings also highlight potential for concern. COVID-19 patients comprised only 1% of EMS responses, but that small fraction translated to thousands of calls involving ≈55% of the region's first-responder workforce over the 6 months of our investigation. One third of COVID-19 patients did not display any common symptoms, such as fever, coughing, or shortness of breath (2), and about one sixth of all COVID-19 patient encounters involved a prehospital AGP. Collectively, the involvement of such a large proportion of the first responder workforce, the heterogeneous nature of patient characteristics, and the time-pressured need among some patients for AGP intervention could pose major COVID-19 risk to public safety personnel and infrastructure. This reality needs to be considered not only with regard to COVID-19 but also to future infectious disease risks, including as part of pandemics.

In our study, however, we found a low overall risk of EMS provider infection from patient care; COVID-19 occurred in a single provider in 1 of 3,710 provider-patient encounters, representing an incidence of 0.28 cases/10,000 person-days at risk. The low incidence occurred under circumstances in which ample PPEs were available for EMS providers and public health management provided active oversight to support guideline-directed PPE field practices (15,20). The low infection rate attributed to patient care covered 182 COVID-19 patient encounters when AGPs were used, including the spectrum of high-flow oxygen, advanced airway maneuvers, and attempted resuscitation. Although data from larger numbers of patient encounters with use of different AGPs could perhaps help researchers refine the overall estimate and potentially determine treatment-specific risk, the overarching inference is that PPE provides excellent protection under these prehospital circumstances. The findings should reassure first responders that emergency care in general and specifically when using AGPs can be delivered safely to treat patients as long as PPE are properly deployed and that, in general, EMS personnel and management should not change evidence-based practice solely to mitigate transmission risk.

Our results also highlight the realities of the COVID-19 pandemic. Sources of infectious risk for EMS personnel are not confined to patients. We observed that the large majority of COVID-19 illness was a consequence of encounters not with patients but in the community or occupational settings. These findings support efforts to screen workplaces for provider symptoms or initiate point-of-care provider testing to limit on-the-job exposure as well as to practice guideline-directed social distancing, masking, and hygiene recommendations outlined for the general public, acknowledging that vaccination may affect these directives (21).

The study leveraged linking electronic records to establish EMS provider–COVID-19 patient encounters, but the data platforms or linkages may not have been comprehensive. Specifically, the registry of persons positive for COVID-19 requires a test, so we could have underestimated the risk attributable to encounters with untested patients. However, in the study methodology we attributed a priori an EMS provider's COVID-19 infection to a patient encounter if it occurred within 2–14 days after the encounter, even though the transmission could have originated from another source. Conversely, this design approach could have overestimated the risk attributable to the COVID-19 patient encounter because the study did not specifically evaluate non-patient sources of SARS-CoV-2 provider infection (including transmission among co-workers). We

defined AGP on the basis of prior research. Although the results from our study were clinically encouraging, the small number of patient encounters limited our ability to compare encounters with patients by whether AGPs were used and by the different types of AGPs.

This active evaluation in the context of the region's EMS operational structure and the profile of experienced EMS providers may influence the generalizability of the results. For example, each year the Seattle and King County EMS system's providers are required to review and be tested on the topic of occupational infectious diseases. As part of the standard approach to patient care before the pandemic, EMS personnel routinely wore gloves and eyewear and were regularly fit-tested for N95 masks, so PPE use was to some extent already common practice at the outset of the pandemic. Moreover, the EMS system has been able to ensure PPE supply to achieve guideline-directed practices during the pandemic. These study-specific characteristics should be considered in balance with the study's broader strengths: innovative linking across EMS records and with the SARS-CoV-2 test registry, reviewing and classifying AGP status for each COVID-19 patient encounter, and undertaking a population-based regional evaluation.

In summary, we observed a very low overall risk for COVID-19 infection among the EMS first-responder workforce attributed to COVID-19 patient encounters, although the small number of EMS provider infections prevented definitive inference regarding AGP-specific risk. These findings support clinical strategies that maintain established, evidence-based practices for emergency conditions. Future efforts should continue to evaluate care settings, patient medical characteristics, provider behaviors, specific treatments, and systemwide PPE availability and status to establish risk and refine prevention practices.

Acknowledgments

About the Author

Ms. Brown is a senior medical student at the University of Washington who is interested in high acuity medicine. She plans to continue quality improvement and patient-oriented outcomes research throughout her career.

References

1. McMichael TM, Currie DW, Clark S, Pogosjans S, Kay M, Schwartz NG, et al.; Public Health–Seattle and King County, EvergreenHealth, and CDC COVID-19 Investigation Team. Epidemiology of Covid-19 in a Long-Term Care Facility in King County, Washington. N Engl J Med. 2020;382:2005–11. https://doi.org/10.1056/NEJMoa2005412

2. Yang BY, Barnard LM, Emert JM, Drucker C, Schwarcz L, Counts CR, et al. Clinical characteristics of patients with coronavirus disease 2019 (COVID-19) receiving emergency medical services in King County, Washington. JAMA Netw Open. 2020;3:e2014549. https://doi.org/10.1001/jamanetworkopen.2020.14549

3. Centers for Disease Control and Prevention (CDC). Cluster of severe acute respiratory syndrome cases among protected health-care workers—Toronto, Canada, April 2003. MMWR Morb Mortal Wkly Rep. 2003;52:433–6.

4. Tran K, Cimon K, Severn M, Pessoa-Silva CL, Conly J. Aerosol generating procedures and risk of transmission of acute respiratory infections to healthcare workers: a systematic review. PLoS One. 2012;7:e35797. https://doi.org/10.1371/journal.pone.0035797

5. Zumla A, Hui DS. Infection control and MERS-CoV in health-care workers. Lancet. 2014;383:1869–71. https://doi.org/10.1016/S0140-6736(14)60852-7

6. Moscola J, Sembajwe G, Jarrett M, Farber B, Chang T, McGinn T, et al.; Northwell Health COVID-19 Research Consortium. Prevalence of SARS-CoV-2 antibodies in health care personnel in the New York City area. JAMA. 2020;324:893–5. https://doi.org/10.1001/jama.2020.14765

7. Lumley SF, O'Donnell D, Stoesser NE, Matthews PC, Howarth A, Hatch SB, et al.; Oxford University Hospitals Staff Testing Group. Antibody status and incidence of SARS-CoV-2 infection in health care workers. N Engl J Med. 2021;384:533–40. https://doi.org/10.1056/NEJMoa2034545

8. Tarabichi Y, Watts B, Collins T, Margolius D, Avery A, Gunzler D, et al. SARS-CoV-2 infection among serially tested emergency medical services workers. Prehosp Emerg Care. 2021;25:39–45. https://doi.org/10.1080/10903127.2020.1831668

9. Schneider S, Piening B, Nouri-Pasovsky PA, Krüger AC, Gastmeier P, Aghdassi SJS. SARS-Coronavirus-2 cases in healthcare workers may not regularly originate from patient care: lessons from a university hospital on the underestimated risk of healthcare worker to healthcare worker transmission. Antimicrob Resist Infect Control. 2020;9:192. https://doi.org/10.1186/s13756-020-00848-w

10. Abbas M, Robalo Nunes T, Martischang R, Zingg W, Iten A, Pittet D, et al. Nosocomial transmission and outbreaks of coronavirus disease 2019: the need to protect both patients and healthcare workers. Antimicrob Resist Infect Control. 2021;10:7. https://doi.org/10.1186/s13756-020-00875-7

11. Meyerowitz EA, Richterman A, Gandhi RT, Sax PE. Transmission of SARS-CoV-2: a review of viral, host, and environmental factors. Ann Intern Med. 2021;174:69–79. https://doi.org/10.7326/M20-5008

12. Centers for Disease Control and Prevention. Scientific brief: SARS-CoV-2 transmission. Summary of recent changes, May 7, 2021 [cited 2021 May 10]. https://www.cdc.gov/coronavirus/2019-ncov/science/science-briefs/sars-cov-2-transmission.html

13. Edelson DP, Sasson C, Chan PS, Atkins DL, Aziz K, Becker LB, et al.; American Heart Association ECC Interim COVID Guidance Authors. Interim guidance for basic and advanced life support in adults, children, and neonates with

suspected or confirmed COVID-19: from the Emergency Cardiovascular Care Committee and Get with the Guidelines-Resuscitation Adult and Pediatric Task Forces of the American Heart Association. Circulation. 2020; 141:e933–43. https://doi.org/10.1161/CIRCULATIONAHA.120.047463

14. von Elm E, Altman DG, Egger M, Pocock SJ, Gøtzsche PC, Vandenbroucke JP; STROBE Initiative. STROBE Initiative. STROBE Initiative. The Strengthening the Reporting of Observational Studies in Epidemiology (STROBE) statement: guidelines for reporting observational studies. Int J Surg. 2014;12:1495–9. https://doi.org/10.1016/j.ijsu.2014.07.013

15. Murphy DL, Barnard LM, Drucker CJ, Yang BY, Emert JM, Schwarcz L, et al. Occupational exposures and programmatic response to COVID-19 pandemic: an emergency medical services experience. Emerg Med J. 2020;37:707–13. https://doi.org/10.1136/emermed-2020-210095

16. Harris PA, Taylor R, Minor BL, Elliott V, Fernandez M, O'Neal L, et al.; REDCap Consortium. The REDCap consortium: Building an international community of software platform partners. J Biomed Inform. 2019;95:103208. https://doi.org/10.1016/j.jbi.2019.103208

17. Centers for Disease Control and Prevention. Clinical questions about COVID-19: questions and answers [cited 2021 May 12]. https://www.cdc.gov/coronavirus/2019-ncov/hcp/faq.html#Infection-Control

18. Brewster DJ, Chrimes N, Do TB, Fraser K, Groombridge CJ, Higgs A, et al. Consensus statement: Safe Airway Society principles of airway management and tracheal intubation specific to the COVID-19 adult patient group. Med J Aust. 2020;212:472–81. https://doi.org/10.5694/mja2.50598

19. Lauer SA, Grantz KH, Bi Q, Jones FK, Zheng Q, Meredith HR, et al. The incubation period of coronavirus disease 2019 (COVID-19) from publicly reported confirmed cases: estimation and application. Ann Intern Med. 2020;172:577–82. https://doi.org/10.7326/M20-0504

20. Sayre MR, Barnard LM, Counts CR, Drucker CJ, Kudenchuk PJ, Rea TD, et al. Prevalence of COVID-19 in out-of-hospital cardiac arrest: implications for bystander cardiopulmonary resuscitation. Circulation. 2020;142:507–9. https://doi.org/10.1161/circulationaha.120.048951

21. Centers for Disease Control and Prevention. First responders: interim recommendations for emergency medical services (EMS) systems and 911 public safety answering points/emergency communication centers (PSAP/ECCs) in the United States during the coronavirus disease (COVID-19) pandemic [cited 2021 Jan 26]. https://www.cdc.gov/coronavirus/2019-ncov/hcp/guidance-for-ems.html

Address for Correspondence: Thomas Rea, University of Washington, 401 5th Ave, Ste 1200, Seattle, WA 98104, USA; email: rea123@uw.edu

Multicenter Epidemiologic Study of Coronavirus Disease–Associated Mucormycosis, India

Atul Patel,[1] Ritesh Agarwal,[1,2] Shivaprakash M. Rudramurthy, Manoj Shevkani, Immaculata Xess,
Ratna Sharma, Jayanthi Savio, Nandini Sethuraman, Surabhi Madan, Prakash Shastri,
Deepak Thangaraju, Rungmei Marak, Karuna Tadepalli, Pratik Savaj, Ayesha Sunavala,
Neha Gupta, Tanu Singhal, Valliappan Muthu, Arunaloke Chakrabarti,[2] MucoCovi Network[3]

During September–December 2020, we conducted a multi-center retrospective study across India to evaluate epidemiology and outcomes among cases of coronavirus disease (COVID-19)–associated mucormycosis (CAM). Among 287 mucormycosis patients, 187 (65.2%) had CAM; CAM prevalence was 0.27% among hospitalized COVID-19 patients. We noted a 2.1-fold rise in mucormycosis during the study period compared with September–December 2019. Uncontrolled diabetes mellitus was the most common underlying disease among CAM and non-CAM patients. COVID-19 was the only underlying disease in 32.6% of CAM patients. COVID-19–related hypoxemia and improper glucocorticoid use independently were associated with CAM. The mucormycosis case-fatality rate at 12 weeks was 45.7% but was similar for CAM and non-CAM patients. Age, rhino-orbital-cerebral involvement, and intensive care unit admission were associated with increased mortality rates; sequential antifungal drug treatment improved mucormycosis survival. The COVID-19 pandemic has led to increases in mucormycosis in India, partly from inappropriate glucocorticoid use.

Author affiliations: Sterling Hospital, Ahmedabad, India
(A Patel); Postgraduate Institute of Medical Education &
Research, Chandigarh, India (R. Agarwal, S.M. Rudramurthy,
V. Muthu, A. Chakrabarti); Avaron Hospital, Ahmedabad
(M. Shevkani); All India Institute of Medical Science, New Delhi,
India (I. Xess); Apollo Hospital, Hyderabad, India (R. Sharma);
St. John's Medical College, Bengaluru, India (J. Savio); Apollo
Hospital, Chennai, India (N. Sethuraman); Care Institute of
Medical Sciences, Ahmedabad (S. Madan); Sir Ganga Ram
Hospital, New Delhi (P. Shastri); Kovai Medical Centre and
Hospital, Coimbatore, India (D. Thangaraju); Sanjay Gandhi
Postgraduate Institute of Medical Sciences, Lucknow, India
(R. Marak); All India Institute of Medical Sciences, Bhopal, India
(K. Tadepalli); Venus Hospital, Surat, India (P. Savaj); Hinduja
Hospital, Mumbai, Maharashtra, India (A. Sunavala); Medanta
The Medicity, Gurgaon, India (N. Gupta); Kokilaben Hospital,
Mumbai, Maharashtra, India (T. Singhal)

Secondary infections are known to complicate the clinical course of coronavirus disease (COVID-19). Bacterial infections are the most common secondary infections, but increasing reports of systemic fungal infections are causing concern. In the early part of the COVID-19 pandemic, <1% of secondary infections reported in COVID-19 patients were fungal (*1,2*). Pre-existing conditions, indiscriminate use of antimicrobial and glucocorticoid drugs, and lapses in infection control practices are putative factors contributing to the emergence of systemic fungal infections in severe COVID-19 cases (*3*). After incidence of candidemia and invasive aspergillosis in COVID-19 patients increased (*4,5*), awareness of possible fungal co-infections increased among clinicians and microbiologists. One study reported invasive fungal infections in ≈6% of hospitalized COVID-19 patients (*6*). Occasional reports of COVID-19–associated mucormycosis (CAM) from various centers (*7,8*) and a series of 18 cases from a city in South India increased our concerns about CAM (*9*).

India has a high burden of mucormycosis among patients with uncontrolled diabetes mellitus, and many severe COVID-19 patients have diabetes (*8,10*). India also is one of the countries worst affected by the COVID-19 pandemic. Thus, we would expect India to have many CAM cases. We conducted a nationwide multicenter study to evaluate the epidemiology and outcomes of CAM and compare the results with cases of mucormycosis unrelated to COVID-19 (non-CAM).

Methods

Study Design and Setting

We conducted a retrospective observational study involving 16 healthcare centers across India (Figure 1).

---

[1]These first authors contributed equally to this article.

[2]These senior authors contributed equally to this article.

[3]Members are listed at the end of this article.

Figure 1. Locations of 16 healthcare centers participating in MucoCovi Network study on coronavirus disease–associated mucormycosis, India. AIIMS, All India Institute of Medical Sciences; CIMS, Care Institute of Medical Sciences; PD Hinduja, Parmanand Deepchand Hinduja; PGIMER, Post Graduate Institute of Medical Education & Research; SGPI, Sanjay Gandhi Postgraduate Institute

We collected data for all confirmed mucormycosis cases among patients with and without COVID-19 reported during September 1–December 31, 2020. The ethics committees of the respective centers approved the study protocol.

Study Subjects and Definitions

We defined a case of mucormycosis as compatible clinical and radiologic manifestations and demonstration of fungi in the tissue or sterile body fluids of a patient by either direct microscopic visualization of broad ribbon-like aseptate hyphae or isolation of Mucorales. COVID-19 diagnosis was made in patients who tested positive for severe acute respiratory syndrome coronavirus 2 (SARS-CoV-2, the causative agent of COVID-19) RNA in respiratory specimens by reverse transcription PCR (RT-PCR) or a positive rapid antigen test. We defined CAM as the occurrence of proven mucormycosis in COVID-19 patients.

Seven participating centers provided additional data on hospitalized COVID-19 patients and number of diagnosed CAM cases during the study pe-

riod. The prevalence of CAM was calculated as the total number of CAM cases divided by the number of COVID-19 patients treated at the 7 participating centers during the study period. Similarly, the prevalence of CAM cases in the intensive care unit (ICU) was calculated as the total number of patients developing mucormycosis among COVID-19 patients who received treatment in the ICU. We classified CAM cases as early when mucormycosis was diagnosed ≤ 7 days after COVID-19 diagnosis and late when mucormycosis was diagnosed ≥ 8 days after COVID-19 diagnosis. We also collected the number of mucormycosis cases reported at the participating centers during the same months (September–December) of 2019. For patients who left the hospital against medical advice, we considered a worst-case scenario for mortality analysis and assumed the patients died.

Study Procedure

We developed a standard case-record form that we circulated to all the centers for data collection. We extracted the following information from the patient

records: demographic characteristics; underlying diseases, such as diabetes mellitus, hematological malignancy, organ transplantation, and others; days to the diagnosis of mucormycosis before or after COVID-19 diagnosis; anatomic site of mucormycosis involvement; diagnostic modalities for mucormycosis, including microscopy, culture, or histopathology; treatment details, including antifungal drug therapy, surgical therapy, and other treatments; site of case management, including home, hospital ward, or ICU; immunosuppressive treatment received, such as glucocorticoid and other drugs; and outcome at 6 and 12 weeks. We classified multiple underlying diseases by using a hierarchical model. For instance, if a patient had hematologic malignancy and then diabetes mellitus developed due to the patient's therapy, we considered hematologic malignancy as the primary risk factor. On the other hand, for patients with COVID-19 and preexisting uncontrolled diabetes, we regarded diabetes as the primary underlying disease.

Treatment Details

All patients received treatment for COVID-19 and mucormycosis according to protocol at the respective treating institution. We recorded the information regarding the type, dose, and duration of glucocorticoid drugs used for managing COVID-19, where available, by using dexamethasone-equivalent dose; 0.75 mg dexamethasone is equivalent to 4 mg methylprednisolone or 5 mg prednisolone. We classified glucocorticoid use as not indicated when any steroid was used for managing nonhypoxemic COVID-19, appropriate when dexamethasone-equivalent doses of 6 mg/day were used for 10 days, or indicated but inappropriate when dexamethasone-equivalent doses >6 mg/day were used for >10 days. To treat mucormycosis, patients received liposomal amphotericin B (5 mg/kg 1×/d for 4–6 weeks, or, if the patient had economic constraints, amphotericin B deoxycholate 1 mg/kg 1×/d for 6–8 weeks). Duration of induction therapy was dependent on how well patients tolerated amphotericin B infusion. Oral triazoles were given for variable duration depending on the site of mucormycosis, radiologic resolution, and clinical response. Patients with intracranial extension received higher doses of amphotericin B for longer periods. We classified antifungal therapy as combination when the patient received both classes of antifungals in any formulation of amphotericin B and posaconazole or isavuconazole, concurrent when both amphotericin B and triazoles were used simultaneously, and sequential when triazole was used after amphotericin B.

Study Objectives

Our primary objective was to compare the epidemiology of mucormycosis between CAM and non-CAM groups during the study period, including the prevalence, underlying diseases, relationship to COVID-19, site of infection, and outcomes. Our secondary objectives were to compare CAM versus non-CAM and ascertain whether COVID-19 is a risk factor for mucormycosis death.

Sample Processing

Tissue biopsies from mucormycosis-affected anatomical sites were used for conventional microscopy, culture, and histopathology, as appropriate, at the respective health centers. Microscopy was performed by using potassium hydroxide mount with or without calcofluor stain. The samples were inoculated on 2 sets of Sabouraud dextrose agar and incubated at 25°C and 37°C. Positive cultures were identified by macroscopic and microscopic characteristics. Tissue samples submitted for histopathology were examined by using hematoxylin and eosin, periodic acid Schiff, or Gomori methenamine silver stain.

Statistical Methods

We performed data analysis using SPSS Statistics 21.0 (IBM, Inc, https://www.ibm.com). We provide descriptive statistics as frequencies, mean (SD), or median (interquartile range [IQR]), as appropriate. We compared categorical variables by using χ^2 or Fischer exact test and analyzed differences between continuous data by using Mann-Whitney U tests. We performed multivariate logistic regression analyses to identify factors predicting development of late CAM and mucormycosis mortality rates. We considered $p < 0.05$ statistically significant.

Results

During the study period, a total of 295 consecutive mucormycosis cases were diagnosed at the 16 participating centers. We excluded 8 cases because of incomplete data. Of the remaining 287 cases, 187 (65.2%) had CAM. The mean age of the entire study population was 53.4 years (SD 17.1 years); 74.6% were men and 25.4% were women (Table 1). Patients with CAM were older (mean age 56.9 years), and a higher proportion (80.2%) were men than for the non-CAM patients.

CAM Prevalence

Among participating centers, 7 provided information needed to estimate the prevalence of CAM. During the study period, CAM patients accounted for

Table 1. Baseline characteristics among patients with mucormycosis, with and without COVID-19, India*

Variables	CAM, n = 187	Non-CAM, n = 100	p value
Mean age, y (SD)	56.9 (12.5)	46.9 (16.4)	0.0001
Sex			0.003
M	150 (80.2)	64 (64.0)	
F	37 (19.8)	36 (36.0)	
Underlying disease			0.0001
None	0	19 (19.0)	
COVID-19 only	61 (32.6)	0	
Glucocorticoids for COVID-19	48/61 (78.7)	NA	
Diabetes mellitus	113 (60.4)	67 (67.0)	
Traumatic inoculation (dental surgery, trauma, and burns)	3 (1.6)	9 (9.0)	
Hematological malignancy	2 (1.1)	2 (2)	
Renal transplantation	3 (1.6)	0	
Other†	5 (2.7)	3 (3)	
Glucocorticoids	146 (78.1)	6 (6.0)	0.0001
Site of involvement			
Rhino-orbital	117 (62.6)	50 (50.0)	0.07
Rhino-orbito-cerebral	44 (23.5)	34 (34.0)	0.07
Pulmonary	16 (8.6)	6 (6.0)	0.42
Renal	1 (0.5)	1 (1.0)	0.66
Other (e.g., cutaneous, stomach)	5 (2.7)	9 (9.0)	0.03
Disseminated	4 (2.1)	0	0.41
Microscopy			0.10
Negative smear	30 (16.0)	10 (10.0)	
Aseptate hyphae	153 (81.8)	84 (84.0)	
Septate hyphae	1 (0.5)	0	
Septate and aseptate hyphae	3 (1.6)	6 (6.0)	
Culture			0.04
No growth	87 (46.5)	61 (61.0)	
Mucorales	99 (52.9)	37 (37.0)	
Mucorales and *Aspergillus* species	1 (0.5)	1 (1.0)	
Aspergillus species	0	1 (1.0)	
Histopathology diagnostic of mucormycosis‡	143/155 (92.3)	37/44 (84.1)	0.10
Management and outcome			
Hypoxemia during hospitalization	74 (39.6)	12 (12.0)	0.0001
Admission to the intensive care unit	58 (31.0)	9 (9.0)	0.0001
Treatment			
Liposomal amphotericin B	136 (72.7)	84 (84)	0.002
Amphotericin D deoxycholate	31 (16.6)	5 (5.0)	0.005
Posaconazole	73 (39.0)	14 (14.0)	0.0001
Isavuconazole	19 (10.2)	2 (2.0)	0.01
Combined antifungal therapy			0.0001
Single antifungal drug	95 (50.8)	88 (88.0)	
Concurrent	13 (7.0)	1 (1.0)	
Sequential	79 (42.5)	11 (11.0)	
Combined medical and surgical therapy	131 (70.1)	73 (73.0)	0.60
Outcome			
Death ≤6 weeks	70 (37.4)	40 (40.0)	0.67
Death ≤12 weeks (n = 256)	75/170 (44.1)	42/86 (48.8)	0.51

*Values are no. (%) except as indicated. CAM, COVID-19–associated mucormycosis; COVID-19, coronavirus disease; NA, not applicable.
†Includes liver cirrhosis, immunosuppression, and malignancies.
‡Histopathological examination was performed in 199 cases, 155 in the CAM group and 44 non-CAM groups.

28/10,517 COVID-19 patients managed in general wards and 25/1,579 in ICUs. The overall prevalence of CAM was 0.27% (range 0.05%–0.57%); prevalence of CAM in ICUs was 1.6% (range 0.65%–2.0%). More mucormycosis cases were identified during the 2020 study period (231 cases) than during the same time range in 2019 (112 cases). The number of mucormycosis cases unrelated to COVID-19 did not differ much during both the study periods (112 cases in 2019 vs. 92 cases in 2020), indicating the increase in 2020 was chiefly attributed to CAM (Figure 2).

Predisposing Factors

The most common underlying disease among both CAM and non-CAM groups was uncontrolled diabetes mellitus (62.7%). Of note, newly detected diabetes mellitus was more frequent during the evaluation of mucormycosis among CAM (39/187 [20.9%]) than non-CAM (10/100 [10%]; p = 0.02) patients. Diabetic ketoacidosis was seen less often in CAM patients (16/187 [8.6%]) than in non-CAM patients (27/100 [27%]; p = 0.0001). COVID-19 was the only underlying disease in 61/187 (32.6%) CAM patients, among

whom 48 (78.7%) received glucocorticoid treatment for COVID-19 management. Other risk factors, including hematologic malignancy and solid organ transplantation, were noted in few among the study population (Table 1).

Clinical Manifestations and Site of Involvement

A greater percentage of patients with CAM had hypoxemia requiring ICU admission during hospitalization than the non-CAM group (Table 1). The rhino-orbital region was the most common mucormycosis site (58.2%), followed by rhino-orbital-cerebral, pulmonary, and other sites (Table 1). However, site of involvement was similar in both the CAM and the non-CAM groups. Toothache, loosening of teeth, and radiologic involvement of the jaw were noted in many CAM patients (Figure 3) but were not seen in non-CAM patients. One participating center reported jaw involvement in 10/47 (21.3%) contributed CAM cases (Figure 3). The common form of pulmonary involvement was cavitary lung disease (Figure 4).

Diagnosis

Mucormycosis diagnosis was made by direct microscopy in 237/287 (82.6%) patients. Histopathology demonstrated aseptate hyphae in 180/199 (90.5%) patients. Culture identified the etiologic agent in 138/287 (48.1%) cases (Table 1). The isolated Mucorales included *Rhizopus arrhizus*, *Rhizomucor pusillus*, *Apophysomyces variabilis*, *Lichtheimia corymbifera*, and others. We did not note association of any species with any anatomic infection site.
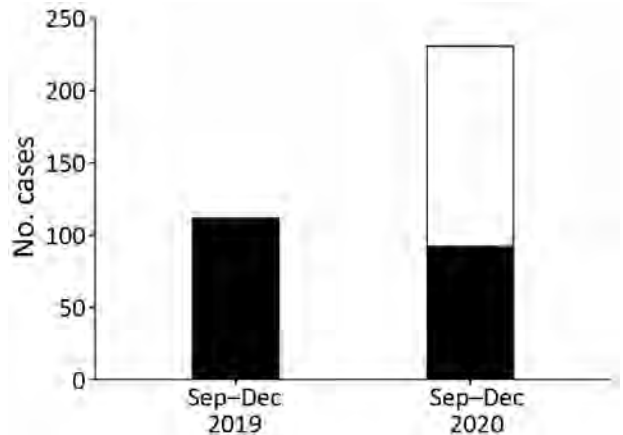
Figure 2. Cumulative number of mucormycosis cases during September–December 2019 and September–December 2020 in 10 health centers, India. White bar section indicates coronavirus disease–associated mucormycosis (CAM); black bar sections indicate non-CAM cases. During 2019, 112 cases of mucormycosis were detected, but a total of 231 cases, 92 non-CAM and 139 CAM, were detected in 2020.

Treatment

Liposomal amphotericin B was the most used antifungal agent in both groups. However, the use of liposomal amphotericin B was much lower in the CAM group (72.7%) compared with the non-CAM group (84%). Posaconazole and isavuconazole were more frequently used in CAM patients than in the non-CAM group. A combination of antifungal therapy, such as amphotericin B plus triazoles, either concurrent or sequential, was used much more often in CAM patients (49.5%) than in non-CAM (12%) patients. Combined medical and surgical management was performed in
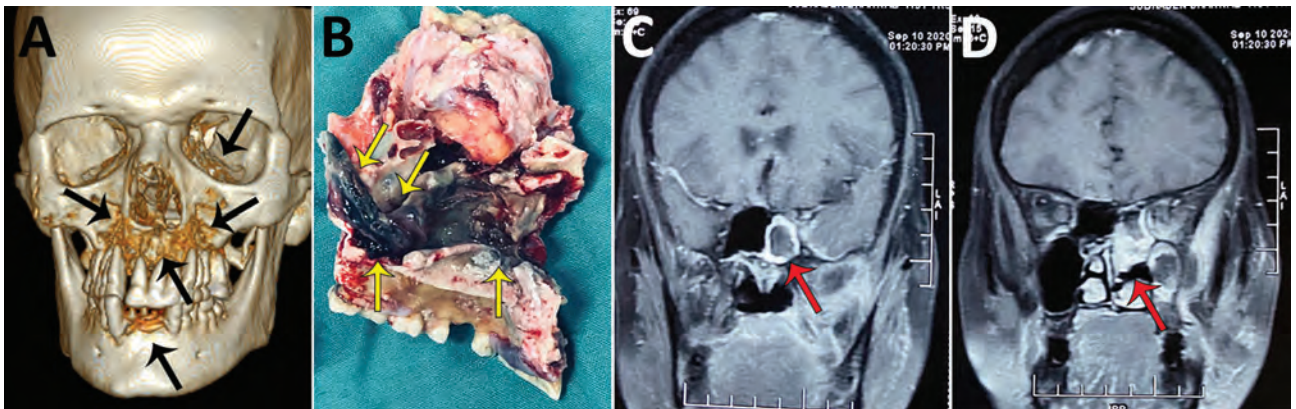
Figure 3. Radiographic images and surgical specimens demonstrating rhino-orbital-cerebral coronavirus disease–associated mucormycosis in patients from India, 2020. A) Three-dimensional reconstruction of computed tomography scan of 54-year-old male patient. Black arrows indicate patchy osteonecrosis involving the upper jaw, right orbital wall, and paranasal sinuses. B) Surgical specimen from the maxilla of 54-year-old male patient showing black necrotic paranasal sinus with palatal involvement indicated by yellow arrows. C, D) Magnetic resonance imaging (MRI) of coronal section of paranasal sinus and brain of 51-year-old female patient. Red arrow in panel C indicates enhancing cavernous sinus lesion; D) red arrow in panel D indicates right ethmoid and maxillary sinusitis. Scale bar indicates 7 cm.
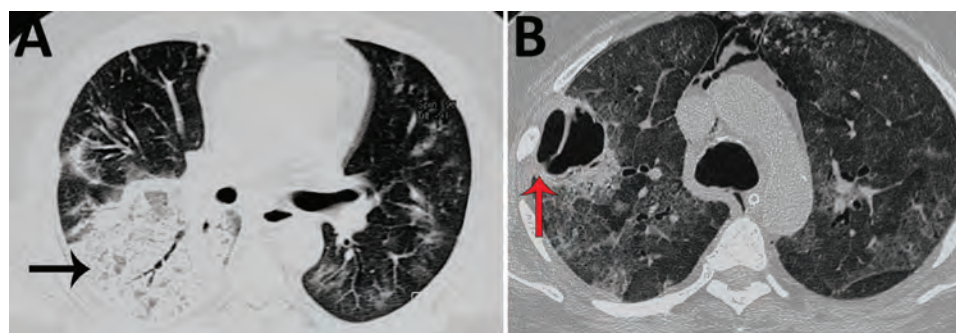
Figure 4. Noncontrast computed tomography scan of the thorax of a patient with coronavirus disease–associated mucormycosis, India, 2020. A) Pulmonary mucormycosis demonstrated as a large area of consolidations with patchy air trapping (black arrow), patchy ground-glass opacities, and septal thickening; B) large thick-walled cavity (red arrow) with surrounding ground-glass opacities.

71.1% (204/287) of patients and was similar in the 2 groups. Major resection of the affected site was performed in 59/284 patients; the remaining patients underwent partial resection or debridement.

Outcomes

Mortality rates were similar between CAM and non-CAM groups; the combined 6-week mortality rate was 38.3% (110/287 patients) and the 12-week mortality rate was 45.7% (117/256 patients) (Table 1). Univariate analysis showed that combined medical and surgical management improved survival in the rhino-orbital-cerebral group but did not improve outcomes for patients with infections at other sites (Appendix Table 1, https://wwwnc.cdc.gov/EID/article/27/9/21-0934-App1.pdf). On multivariate logistic regression analysis, we found age, site of involvement (rhino-orbital-cerebral or pulmonary), and ICU admission were associated with increased mortality rates. In contrast, sequential treatment with a combination of antifungal drugs was independently

associated with better survival at 6 and 12 weeks (Table 2; Appendix Table 2).

Subgroup Analysis of CAM

The median time to CAM diagnosis was 18 (IQR 11–27) days (Figure 5). Among 187 CAM patients, 158 (84.2%) were classified as late CAM (Table 3). Some (33/187; 17.6%) patients were managed for COVID-19 at home before developing CAM. Among 187 CAM patients, 74 (55.6%) were hypoxemic. Glucocorticoid drugs were administered in various doses; the median cumulative dexamethasone-equivalent dose was 84 mg (range 18–1,343 mg). Of note, only 49/146 (33.6%) patients received steroids at appropriate levels (Table 3). Tocilizumab was administered to 5 (2.7%) patients for COVID-19 management.

The demographic characteristics, underlying diseases, and site of involvement were similar among patients with early and late CAM. However, we saw diabetic ketoacidosis more often in patients with early CAM (28%) than late CAM (5%). A higher

Table 2. Multivariate analysis of factors predicting death at 6 weeks among patients with mucormycosis, India*

Variables	Survivors, n = 177	Non-survivors, n = 110	Odds ratio (95% CI)	p value
Mean age, y (SD)	52.6 (15.1)	54.7 (14.0)	1.02 (1.00–1.04)	**0.03**
Underlying disease				
None	10 (5.6)	9 (8.2)	Referent	Referent
Isolated COVID-19	42 (23.7)	19 (17.3)	0.56 (0.17–1.83)	0.34
Diabetes mellitus	109 (61.6)	71 (64.5)	0.92 (0.32–2.64)	0.88
Traumatic inoculation	8 (4.5)	4 (3.6)	1.30 (0.25–6.80)	0.76
Others	5 (2.8)	3 (2.7)	1.20 (0.18–7.81)	0.85
Renal transplantation	1 (0.6)	2 (1.8)	6.87 (0.42–113.19)	0.18
Hematological malignancy	2 (1.1)	2 (1.8)	1.60 (0.14–18.72)	0.71
Site of involvement				
Rhino-orbital	117 (66.1)	50 (45.5)	Referent	Referent
Rhino-orbito-cerebral	39 (22)	39 (35.5)	2.39 (1.30–4.40)	**0.005**
Pulmonary	8 (4.5)	14 (12.7)	3.26 (1.05–10.11)	**0.04**
Other†	13 (7.3)	7 (6.4)	1.29 (0.43–3.86)	0.64
Admission to the intensive care unit	32 (18.1)	35 (31.8)	2.87 (1.43–5.75)	**0.003**
Combined medical surgical therapy	135 (76.3)	69 (62.7)	0.77 (0.41–1.45)	0.41
Combination of antifungals				
Single antifungal drug	95 (53.7)	88 (80)	Referent	Referent
Concurrent	9 (5.1)	5 (4.5)	0.37 (0.09–1.44)	0.15
Sequential	73 (41.2)	17 (15.5)	0.17 (0.87–0.35)	**0.0001**

*Values are no. (%) except as indicated. Bold text indicates statistical significance. COVID-19, coronavirus disease.
†Includes cutaneous, stomach, disseminated, or other.

proportion of patients with late CAM received glucocorticoid treatment (Table 3). Whereas amphotericin B remained the most common antifungal drugs used in both groups, posaconazole, isavuconazole, or a sequential use of antifungal agents (i.e., amphotericin B followed by posaconazole or isavuconazole) was more often seen in patients with late CAM. We saw no statistically significant difference in 6- and 12-week mortality rates between the early and late CAM groups (Table 3).

We also explored factors associated with late CAM development (Table 4). After adjusting for age, sex, and underlying risk factors, we found hypoxemia due to COVID-19 and inappropriate glucocorticoid administration were associated with development of late CAM.

Discussion

In our study, the prevalence of CAM was 0.27% in patients managed in hospital wards and 1.6% in patients managed in ICUs. We found a 2.1-fold increase in mucormycosis cases during September–December 2020 than the same months of 2019; we attribute the increase to COVID-19. Most CAM cases were diagnosed ≥8 days after COVID-19 diagnoses. Hypoxemia due to COVID-19 and inappropriate use of glucocorticoid drugs were independently associated with development of late CAM. The mortality rate for CAM patients was high (44%) but was comparable to rates for non-CAM (49%) patients. Older age (>54 years), admission to an ICU, and pulmonary or brain involvement by Mucorales were independently associated with a higher risk for death. The sequential use of antifungal drugs at any site was associated with improved survival at 6 and 12 weeks, irrespective of anatomical site of mucormycosis.

In our study, 74.6% of patients affected by mucormycosis were men, as observed in previous studies (*11–13*). We found diabetes mellitus was the most common underlying disease for both CAM and non-CAM patients. SARS-CoV-2 has been shown to affect the beta cells of the pancreas, resulting in metabolic derangement, possibly causing diabetes mellitus (*14,15*). Whether more frequent diagnosis (20%) of diabetes mellitus during the evaluation for CAM compared with non-CAM (10%) is related to SARS-CoV-2 infection, glucocorticoid therapy, or a chance occurrence remains unclear. Unfortunately, we do not have glycated hemoglobin values taken at admission for all newly detected diabetes cases in our study, so we cannot determine if these patients had diabetes mellitus before CAM developed.

We found inappropriate glucocorticoid use was independently associated with late CAM. Among
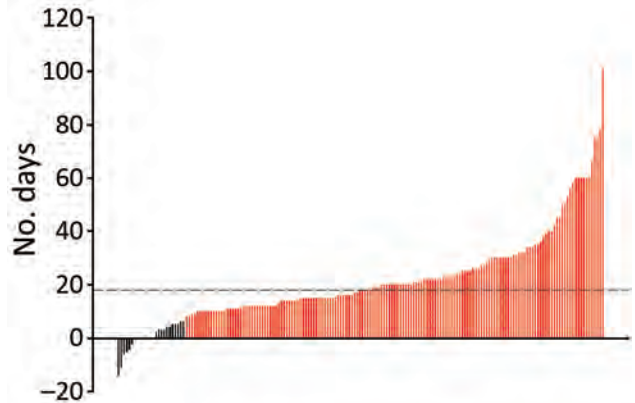
Figure 5. Waterfall plot showing the number of days between the diagnosis of coronavirus disease (COVID-19) and COVID-19–associated mucormycosis (CAM). Each vertical line represents a case-patient. Red indicates late CAM (mucormycosis developing ≥8 days after COVID-19 diagnosis); black indicates early CAM (mucormycosis developing ≤7 days of COVID-19 diagnosis). Among early CAM cases, mucormycosis was diagnosed before (n = 8), concurrently with (n = 8), or after (n = 13) COVID-19 diagnosis. Dotted line represents the median duration (18 days) after COVID-19 diagnosis for the diagnosis of CAM.

187 CAM cases, 61 (32.6%) had COVID-19 as the only underlying disease; 13 of those cases were not treated with glucocorticoid or other immunomodulatory therapies. Whether COVID-19 itself causes immune dysregulation and predisposes patients to invasive mucormycosis remains an unproven possibility (*16–18*). We did not find that COVID-19 was an independent predictor of late CAM, possibly because of the lower numbers of patients in our cohort with COVID-19 as the only underlying disease without any other risk factor. Lymphopenia is common in COVID-19, and progressive lymphopenia has been shown to correlate with COVID-19 severity (*19*). The persisting immune dysregulation during the recovery phase of COVID-19 infection also confers additional risk. Unfortunately, we have not evaluated the effect of lymphopenia on the development or outcome of CAM. Tocilizumab use in COVID-19 has been reported as a risk factor for invasive candidiasis (*20*). However, only 2.7% of the CAM patients in this study received tocilizumab.

The high mortality rate for CAM is a major concern (*7*). Patients with CAM were older (56.9 years) than non-CAM patients (46.9 years). Evidence suggests that older age imparts increased risk for hospitalization, respiratory failure, ICU admission, and attendant glucocorticoid therapy in COVID-19 (*21,22*). Further, age >54 years also was associated with an increased risk for death among our cohort. The site of mucormycosis involvement and the survival at 6 and 12 weeks was

Table 3. Characteristics of early and late CAM among patients with COVID-19, India*

Variables	Early CAM, n = 29†	Late CAM, n = 158‡	p value
Mean age, y (SD)	51.8 (14.2)	57.8 (11.9)	0.015
Sex			0.10
F	9 (31.0)	28 (17.7)	
M	20 (69.0)	130 (82.3)	
Glucocorticoids	8 (27.6)	138 (87.3)	0.0001
Tocilizumab	0	5 (3.2)	0.33
Underlying diseases			0.52
COVID-19 only	11 (37.9)	50 (31.6)	
Diabetes mellitus	16 (55.2)	97 (61.4)	
Diagnosed during current illness	6	33	
Diabetic ketoacidosis§	8	8	
Traumatic inoculation: dental surgery, trauma, and burns	0	3 (1.9)	
Hematological malignancy	0	2 (1.3)	
Renal transplantation	0	3 (1.9)	
Other: liver cirrhosis, immunosuppression, and others	2 (6.9)	3 (1.9)	
Site of involvement			0.88
Rhino-orbital	17 (58.7)	100 (63.3)	
Rhino-orbito-cerebral	8 (27.6)	36 (22.8)	
Pulmonary	3 (10.3)	13 (8.2)	
Renal	0	1 (0.6)	
Other: e.g., cutaneous, stomach	0	5 (3.2)	
Disseminated	1 (3.4)	3 (1.9)	
Hypoxemia during hospitalization	9 (31.0)	65 (41.1)	0.19
ICU admission	12 (41.4)	46 (29.1)	0.31
Glucocorticoid treatment for COVID-19	N = 17	N = 133	
Appropriate	11 (64.7)	44 (33.1)	
Not indicated	4 (23.5)	46 (34.6)	
Indicated, but inappropriately high dose	2 (11.8)	43 (32.3)	
Treatment			
Liposomal amphotericin B	26 (89.7)	110 (71.9)	0.06
Amphotericin D deoxycholate	3 (10.3)	28 (17.7)	0.33
Posaconazole	4 (13.8)	69 (43.7)	0.02
Isavuconazole	0	19 (12.0)	0.049
Combined antifungal therapy			0.004
Single antifungal drug	23 (79.4)	72 (45.6)	
Concurrent	1 (3.4)	12 (7.6)	
Sequential	5 (17.2)	74 (46.8)	
Combined medical and surgical therapy	18 (62.1)	113 (71.5)	0.31
Outcomes			
Death at 6 weeks	12 (41.4)	58 (36.7)	0.63
Death at 12 weeks, n = 170	13/22 (59.1)	62/148 (41.9)	0.17

*Values are no. (%) except as indicated. CAM, COVID-19–associated mucormycosis; COVID-19, coronavirus disease; ICU, intensive care unit.
†Early CAM is considered mucormycosis diagnosed ≤7 days of COVID-19 diagnosis.
‡Late CAM is mucormycosis diagnosed ≥8 days of COVID-19 diagnosis.
§Diabetic ketoacidosis was more frequent among patients with early CAM (p = 0.0001).

similar in CAM and non-CAM groups. We expected a higher proportion of pulmonary mycosis because respiratory viral infections, such as influenza, often are associated with secondary invasive aspergillosis (*8*). However, we did not observe an increased occurrence of pulmonary mucormycosis compared with infections in other sites among the CAM group. Considering the low rate of pulmonary involvement, we believe that CAM can be attributed to the systemic effects of COVID-19 or its treatment, rather than a sole alteration in the lungs. Several pulmonary mucormycosis cases also might have remained undiagnosed because of challenges in obtaining diagnostic respiratory samples among critically ill COVID-19 patients.

Appropriate and timely antifungal therapy and surgical resection, when feasible, are considered es-

sential in mucormycosis management. Liposomal amphotericin B is the drug of choice, but isavuconazole also is recommended in primary therapy. Triazoles, including posaconazole and isavuconazole, commonly are used in the consolidation phase or as salvage therapy (*23*). The role of combination antifungal treatment in mucormycosis is not clearly supported by evidence (*24*). The combination of surgery and antifungal therapy was associated with better survival in the rhino-orbital-cerebral group in this study, conforming with previous experiences (*6,11,25*). However, the same was not true for mucormycosis in other anatomic sites. Early diagnosis of mucormycosis and the more frequent use of consolidation therapy or combination of antifungals in this study could be one explanation; another could be fewer surgeries

performed in patients with other than rhino-orbital mucormycosis.

We found the sequential use of antifungal drugs, amphotericin B then posaconazole or isavuconazole, was independently associated with improved survival among mucormycosis patients. However, the lack of randomization, possibility of case selection, and chance survival are potential biases. In addition, the optimal duration and dose of amphotericin B and posaconazole are not clear. The usefulness of antifungal combination administered simultaneously could not be ascertained due to the small number of patients receiving concurrent therapy in our study. A randomized controlled trial could affirm the role of a combination of antifungals or maintenance therapy in mucormycosis.

We expected better survival for the CAM patients in this study. Contrary to the prevailing practices (11,24), a combination of antifungal agents was more frequently used (50%) in CAM patients than in non-CAM patients (12%). Also, hospitalized CAM patients were closely monitored. The treatment practices used for the CAM group, especially those with late CAM, were distinct from those for the non-CAM group and those for patients with early CAM. The occurrence of a mold infection and the apprehension associated with the COVID-19 pandemic could have resulted in more frequent use of combination therapy in CAM. However, we saw no difference in mortality rates between CAM and non-CAM patients. Of course, increased risk for death due to COVID-19 itself cannot be ruled out for these CAM patients.

Our study's first limitation is that we collected data from a single country. The predominant risk factor for mucormycosis in our study was diabetes, which is also the case in some countries, including Bangladesh, China, Iran, Mexico, and Pakistan, from which data on mucormycosis are still limited (26). Further studies should compare data from countries with high rates of diabetes and mucormycosis with that of data from the United States and Europe, where mucormycosis predominantly is encountered in hematological malignancies and organ transplantation. Given the large number of late CAM cases, healthcare-associated mucormycosis remains a distinct possibility (27,28). Contaminated ventilation systems, air conditioners, and ongoing construction in hospitals have been reported to cause outbreaks of mucormycosis in the past (28). However, we did not estimate the burden of Mucormycetes spores in the hospital environment (29). We also do not have data on the timing of amphotericin B use, timing of surgery, or duration of sequential antifungal therapy, which are critical factors that have a bearing on mucormycosis outcomes; hence, we could not analyze these factors. Other unexplored factors, including genetic predisposition, might explain the high prevalence of CAM and non-CAM in India. Thus, prospective studies from the rest of the world, especially those severely affected by the COVID-19 pandemic, would be needed to ascertain the epidemiology of CAM. The strength of our study is the large number of patients, which lends credibility to our observations.

In conclusion, mucormycosis is a rare but critical problem complicating the later part of the clinical course of COVID-19 in India, possibly due to improper glucocorticoid usage. We found no difference in the risk factors, site of involvement, and outcome of mucormycosis complicating COVID-19 cases compared with non–COVID-19 cases. Nevertheless, the prevalence of mucormycosis has increased greatly in

Table 4. Multivariate analysis of factors predicting the development of late CAM among COVID-19 patients, India*

Variables	Early CAM, n = 29†	Late CAM, n = 158‡	Odds ratio (95% CI)	p value
Mean age, y (SD)	51.8 (14.2)	57.8 (11.9)	1.02 (0.96–1.07)	0.62
Sex				
M	20 (69.0)	130 (82.3)	0.25 (0.06–1.10)	0.07
F	9 (31.0)	28 (17.7)	Referent	
Underlying disease				
Isolated COVID-19	11 (23.7)	50 (17.3)	1.71 (0.25–11.96)	0.59
Diabetes mellitus	16 (61.6)	97 (64.5)	5.84 (0.70–48.89)	0.10
Others§	2 (4.5)	11 (3.6)	Referent	
Hypoxemia due to COVID-19	9 (31.0)	65 (41.1)	11.84 (1.43–98.06)	**0.02**
Glucocorticoid usage	N = 17	N = 133		
Appropriate	11 (64.7)	44 (33.1)	Referent	
Not indicated	4 (23.5)	46 (34.6)	66.93 (7.05–635.19)	**0.0001**
Indicated, but inappropriately high dose	2 (11.8)	43 (32.3)	9.91 (1.39–70.77)	**0.02**

*Values are no. (%) except as indicated. Bold text indicates statistical significance. CAM, COVID-19–associated mucormycosis; COVID-19, coronavirus disease.
†Early CAM is considered mucormycosis diagnosed ≤7 days of COVID-19 diagnosis.
‡Late CAM is mucormycosis diagnosed ≥8 days of COVID-19 diagnosis.
§Includes traumatic inoculation, cirrhosis, immunosuppression, renal transplantation, and hematological malignancy.

India, coinciding with the country's COVID-19 epidemic. Clinicians should be vigilant for mucormycosis in the patients recovering from COVID-19 illness, especially among patients with new or previously diagnosed diabetes mellitus and clinical manifestations of facial or orbital pain or black or blood-stained nasal discharge. In addition, we found improper glucocorticoid use for the COVID-19 treatment to be an additional risk factor in CAM. Therefore, treating physicians should ensure they use appropriate drugs and doses in treating COVID-19 patients.

Acknowledgments

About the Authors

Dr. Patel is an infectious disease specialist at the Sterling Hospital, Ahmedabad, India, and a fellow of the Infectious Disease Society for America. His research interests include fungal infections. Dr. Agarwal is a pulmonologist at Postgraduate Institute of Medical Education & Research, Chandigarh, India. His research interests include allergic and chronic lung aspergillosis.

References

1. Baiou A, Elbuzidi AA, Bakdach D, Zaqout A, Alarbi KM, Bintaher AA, et al. Clinical characteristics and risk factors for the isolation of multi-drug-resistant Gram-negative bacteria from critically ill patients with COVID-19. J Hosp Infect. 2021;110:165–71. https://doi.org/10.1016/j.jhin.2021.01.027
2. Ripa M, Galli L, Poli A, Oltolini C, Spagnuolo V, Mastrangelo A, et al.; COVID-BioB study group. Secondary infections in patients hospitalized with COVID-19: incidence and predictive factors. Clin Microbiol Infect. 2021;27:451–7. https://doi.org/10.1016/j.cmi.2020.10.021
3. Seaton RA, Gibbons CL, Cooper L, Malcolm W, McKinney R, Dundas S, et al. Survey of antibiotic and antifungal prescribing in patients with suspected and confirmed COVID-19 in Scottish hospitals. J Infect. 2020;81:952–60. https://doi.org/10.1016/j.jinf.2020.09.024
4. Nucci M, Barreiros G, Guimarães LF, Deriquehem VAS, Castiñeiras AC, Nouér SA. Increased incidence of candidemia in a tertiary care hospital with the COVID-19 pandemic. Mycoses. 2021;64:152–6. https://doi.org/10.1111/myc.13225
5. van Arkel ALE, Rijpstra TA, Belderbos HNA, van Wijngaarden P, Verweij PE, Bentvelsen RG. COVID-19–associated pulmonary aspergillosis. Am J Respir Crit Care Med. 2020;202:132–5. https://doi.org/10.1164/rccm.202004-1038LE
6. Chong WH, Saha BK, Ananthakrishnan Ramani, Chopra A. State-of-the-art review of secondary pulmonary infections in patients with COVID-19 pneumonia. Infection. 2021 Mar 11 [Epub ahead of print]. https://doi.org/10.1007/s15010-021-01602-z
7. Garg D, Muthu V, Sehgal IS, Ramachandran R, Kaur H, Bhalla A, et al. Coronavirus disease (Covid-19) associated mucormycosis (CAM): case report and systematic review of literature. Mycopathologia. 2021;186:289–98. https://doi.org/10.1007/s11046-021-00528-2
8. Ahmadikia K, Hashemi SJ, Khodavaisy S, Getso MI, Alijani N, Badali H, et al. The double-edged sword of systemic corticosteroid therapy in viral pneumonia: a case report and comparative review of influenza-associated mucormycosis versus COVID-19 associated mucormycosis. Mycoses. 2021 Feb 16 [Epub ahead of print]. https://doi.org/10.1111/myc.13256
9. Moorthy A, Gaikwad R, Krishna S, Hegde R, Tripathi KK, Kale PG, et al. SARS-CoV-2, uncontrolled diabetes and corticosteroids—an unholy trinity in invasive fungal infections of the maxillofacial region? A retrospective, multi-centric analysis. J Maxillofac Oral Surg. 2021 Mar 6 [Epub ahead of print]. https://doi.org/10.1007/s12663-021-01532-1
10. Joshi SR, Das AK, Vijay VJ, Mohan V. Challenges in diabetes care in India: sheer numbers, lack of awareness and inadequate control. J Assoc Physicians India. 2008;56:443–50.
11. Patel A, Kaur H, Xess I, Michael JS, Savio J, Rudramurthy S, et al. A multicentre observational study on the epidemiology, risk factors, management and outcomes of mucormycosis in India. Clin Microbiol Infect. 2020;26:944.e9–15. https://doi.org/10.1016/j.cmi.2019.11.021
12. Jeong W, Keighley C, Wolfe R, Lee WL, Slavin MA, Kong DCM, et al. The epidemiology and clinical manifestations of mucormycosis: a systematic review and meta-analysis of case reports. Clin Microbiol Infect. 2019;25:26–34. https://doi.org/10.1016/j.cmi.2018.07.011
13. Prakash H, Ghosh AK, Rudramurthy SM, Singh P, Xess I, Savio J, et al. A prospective multicenter study on mucormycosis in India: epidemiology, diagnosis, and treatment. Med Mycol. 2019;57:395–402. https://doi.org/10.1093/mmy/myy060
14. Müller JA, Groß R, Conzelmann C, Krüger J, Merle U, Steinhart J, et al. SARS-CoV-2 infects and replicates in cells of the human endocrine and exocrine pancreas. Nat Metab. 2021;3:149–65. https://doi.org/10.1038/s42255-021-00347-1
15. Accili D. Can COVID-19 cause diabetes? Nat Metab. 2021;3:123–5. https://doi.org/10.1038/s42255-020-00339-7
16. Files JK, Boppana S, Perez MD, Sarkar S, Lowman KE, Qin K, et al. Sustained cellular immune dysregulation in individuals recovering from SARS-CoV-2 infection. J Clin

Invest. 2021;131:e140491. https://doi.org/10.1172/JCI140491

17. Potenza L, Vallerini D, Barozzi P, Riva G, Forghieri F, Zanetti E, et al. Mucorales-specific T cells emerge in the course of invasive mucormycosis and may be used as a surrogate diagnostic marker in high-risk patients. Blood. 2011;118:5416–9. https://doi.org/10.1182/blood-2011-07-366526

18. Ghuman H, Voelz K. Innate and adaptive immunity to mucorales. J Fungi (Basel). 2017;3:48. https://doi.org/10.3390/jof3030048

19. Zhang X, Tan Y, Ling Y, Lu G, Liu F, Yi Z, et al. Viral and host factors related to the clinical outcome of COVID-19. Nature. 2020;583:437–40. https://doi.org/10.1038/s41586-020-2355-0

20. Antinori S, Bonazzetti C, Gubertini G, Capetti A, Pagani C, Morena V, et al. Tocilizumab for cytokine storm syndrome in COVID-19 pneumonia: an increased risk for candidemia? Autoimmun Rev. 2020;19:102564. https://doi.org/10.1016/j.autrev.2020.102564

21. Levin AT, Hanage WP, Owusu-Boaitey N, Cochran KB, Walsh SP, Meyerowitz-Katz G. Assessing the age specificity of infection fatality rates for COVID-19: systematic review, meta-analysis, and public policy implications. Eur J Epidemiol. 2020;35:1123–38. https://doi.org/10.1007/s10654-020-00698-1

22. Pijls BG, Jolani S, Atherley A, Derckx RT, Dijkstra JIR, Franssen GHL, et al. Demographic risk factors for COVID-19 infection, severity, ICU admission and death: a meta-analysis of 59 studies. BMJ Open. 2021;11:e044640. https://doi.org/10.1136/bmjopen-2020-044640

23. Cornely OA, Alastruey-Izquierdo A, Arenz D, Chen SCA, Dannaoui E, Hochhegger B, et al.; Mucormycosis ECMM MSG Global Guideline Writing Group. Global guideline for the diagnosis and management of mucormycosis: an initiative of the European Confederation of Medical Mycology in cooperation with the Mycoses Study Group Education and Research Consortium. Lancet Infect Dis. 2019;19:e405–21. https://doi.org/10.1016/S1473-3099(19)30312-3

24. Jeong W, Keighley C, Wolfe R, Lee WL, Slavin MA, Chen SC, et al. Contemporary management and clinical outcomes of mucormycosis: a systematic review and meta-analysis of case reports. Int J Antimicrob Agents. 2019;53:589–97. https://doi.org/10.1016/j.ijantimicag.2019.01.002

25. Muthu V, Agarwal R, Dhooria S, Sehgal IS, Prasad KT, Aggarwal AN, et al. Has the mortality from pulmonary mucormycosis changed over time? A systematic review and meta-analysis. Clin Microbiol Infect. 2021;27:538–49. https://doi.org/10.1016/j.cmi.2020.12.035

26. Prakash H, Chakrabarti A. Global Epidemiology of mucormycosis. J Fungi (Basel). 2019;5:26. https://doi.org/10.3390/jof5010026

27. Rammaert B, Lanternier F, Zahar JR, Dannaoui E, Bougnoux ME, Lecuit M, et al. Healthcare-associated mucormycosis. Clin Infect Dis. 2012;54:S44–54. https://doi.org/10.1093/cid/cir867

28. Walther G, Wagner L, Kurzai O. Outbreaks of mucorales and the species involved. Mycopathologia. 2020;185:765–81.

29. Prakash H, Singh S, Rudramurthy SM, Singh P, Mehta N, Shaw D, et al. An aero mycological analysis of *Mucormycetes* in indoor and outdoor environments of northern India. Med Mycol. 2020;58:118–23. https://doi.org/10.1093/mmy/myz031

Address for correspondence: Arunaloke Chakrabarti, Department of Medical Microbiology, Postgraduate Institute of Medical Education & Research, Sector-12, Chandigarh 160012, India; email: arunaloke@hotmail.com

etymologia

Paracoccidioides [pʼa ɾə kok-sid"e-oiʼ dʼez]

Lucas Nojosa Oliveira, Patrícia de Sousa Lima

From the Greek (*para/*παρά + *kokkis* [coccidia]), Adolpho Lutz described *Paracoccidioides* in 1908. After analysis of oral and cervical lymph node lesions from infected patients, Lutz initially believed that he had detected *Coccidioides*. However, more extensive analysis showed that he had detected another fungus. Because of morphologic and clinical

Figure 1. Adolfo Lutz (1855–1940). Unknown author, Wikimedia Commons.

disease similarities, the name *Paracoccidioides* was suggested. The prefix para (near) indicates its similarity with *Coccidioides*.

   Paracoccidioides is a thermally dimorphic fungus. It grows as an infective mycelium form (at 18°C–23°C) or a parasitic multibudding yeast form (at 35°C–37°C). It is composed of 2 species:
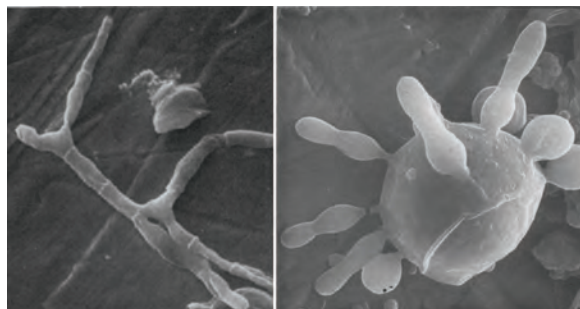
Figure 2. *Paracoccidioides brasiliensis* mycelium cells (left) and multibudding yeasts (right) by scanning electron microscopy. Original magnifications ×1,500 for the left panel and ×3,000 for the right panel. Image adapted from Vieira e Silva et al. 1974.

P. brasiliensis and *P. lutzi*. They are the etiologic agents of paracoccidioidomycosis. This systemic infection is endemic to Latin America (southern Mexico to northern Argentina). The highest number of cases are found in Brazil, Colombia, and Venezuela. *Paracoccidioides* conidia and mycelia are found in soil and transmitted by inhalation.

Sources

1. Bocca AL, Amaral AC, Teixeira MM, Sato PK, Shikanai-Yasuda MA, Soares Felipe MS. Paracoccidioidomycosis: eco-epidemiology, taxonomy and clinical and therapeutic issues. Future Microbiol. 2013;8:1177–91. https://doi.org/10.2217/fmb.13.68
2. Chaves AF, Navarro MV, de Barros YN, Silva RS, Xander P, Batista WL. Updates in *Paracoccidioides* biology and genetic advances in fungus manipulation. J Fungi (Basel). 2021;7:116. https://doi.org/10.3390/jof7020116
3. Lutz A. A pseudococcidic mycose located in the mouth and observed in Brazil: contribution to the knowledge of American hypoblatomycoses [in Portuguese]. Revista Semanal de Medicina e Cirurgia. 1908;22:121–4.
4. Turland NJ, Wiersema JH, Barrie FR, Greuter W, Hawksworth DL, Herendeen PS, et al., editors. International code of nomenclature for algae, fungi, and plants (Shenzhen code) adopted by the Nineteenth International Botanical Congress Shenzhen, China, July 2017. Regnum Vegetabile 159. Glashütten (Germany): Koeltz Botanical Books; 2018 [cited 2021 May 17]. https://www.iapt-taxon.org/nomen/pages/intro/citation.html
5. Viera e Silva CR, de Mattos MC, Fujimore K. Scanning electron microscopy of *Paracoccidioides brasiliensis*. Study with and without pre-treatment with pooled sera from patients with 'South American blastomycosis'. Mycopathol Mycol Appl. 1974;54:235–51.

Address for correspondence: Lucas Nojosa Oliveira, Faculdade Estácio de Sá de Goiás, Avenida Goiás 2151, Setor Central, Goiânia, Goiás, CEP 74063-010, Brazil; email: nojosalucas@gmail.com

Real–Time Genomics for Tracking Severe Acute Respiratory Syndrome Coronavirus 2 Border Incursions after Virus Elimination, New Zealand

Jordan Douglas, Jemma L. Geoghegan, James Hadfield, Remco Bouckaert,
Matthew Storey, Xiaoyun Ren, Joep de Ligt, Nigel French, David Welch

Since severe acute respiratory syndrome coronavirus 2 was first eliminated in New Zealand in May 2020, a total of 13 known coronavirus disease (COVID-19) community outbreaks have occurred, 2 of which led health officials to issue stay-at-home orders. These outbreaks originated at the border via isolating returnees, airline workers, and cargo vessels. Because a public health system was informed by real-time viral genomic sequencing and complete genomes typically were available within 12 hours of community-based positive COVID-19 test results, every outbreak was well-contained. A total of 225 community cases resulted in 3 deaths. Real-time genomics were essential for establishing links between cases when epidemiologic data could not do so and for identifying when concurrent outbreaks had different origins.

Early in the coronavirus disease (COVID-19) pandemic, New Zealand (Aotearoa in Māori language) adopted a disease elimination approach. Elimination was first achieved in May 2020 (*1,2*), and through April 30, 2021, only 13 community outbreaks (Table) had occurred, comprising a total of 225 recorded community cases. We define a community case as illness in someone who has either been in

contact with the wider community while potentially infectious or who was infected after being put into a dedicated managed isolation and quarantine (MIQ) facility because of one of the outbreaks discussed here. In contrast, we consider MIQ case-patients (i.e., returnees or MIQ workers) as those who acquired their infection through a chain of transmission that had not entered New Zealand.

The public health response to community outbreaks differed according to the extent of the outbreak. Two outbreaks resulted in Auckland, New Zealand's largest city, moving to alert level 3, which mandates stay-at-home-orders for most persons. The alert level system comprises levels 1–4; the most stringent is level 4 (*4*).

A core part of the COVID-19 elimination strategy is a strictly controlled border where nearly every person entering the country is required to isolate for 14 days at an MIQ facility and be tested for severe acute respiratory syndrome coronavirus 2 (SARS-CoV-2) on days 0, 3, and 12 of their stay (*4,5*). The MIQ facilities are repurposed hotels, more than half of which are located in Auckland. With an operational capacity of 4,000 returnees, the returnees (135,451 as of May 1, 2021) (*6*) and the considerable workforce required to service them present a possible transmission route into the community. Of the 13 known border incursions, 7 originated in MIQ facilities (4 from MIQ workers and 3 from returnees who tested positive after leaving the facility), 3 were from airline workers, and 1 was from an infection on a visiting ship; the sources of the remaining 2, which both led to stay-at-home orders, remain unknown.

Since April 19, 2021, travel between New Zealand and Australia has been open. Australia has also pursued an elimination strategy (although it is typically referred to as aggressive suppression) (7) and uses a hotel-based MIQ system although with notably fewer but larger outbreaks detected from their MIQ facilities (L.M. Grout et al., unpub. data, https://www.medrxiv.org/content/10.1101/2021.02.17.21251946v1) (8).

Viral genomic sequencing has played a crucial role in tracing and delineating all community outbreaks in New Zealand (3,9,10), complementing border controls, the alert level system, and contact tracing. There has been an effort to sequence the virus from every case-patient. Infected returnees in MIQ facilities are sequenced weekly, and community case-patients are sequenced more urgently; complete genomes are typically available to inform health officials within 12 hours of the first positive test result. Real-time genomic surveillance has been indispensable for confirming or disproving links between cases, particularly when epidemiologic data were lacking. We recount the events surrounding the 13 community outbreaks as of April 30, 2021, and demonstrate how genomic sequencing technologies have played vital roles in delineating these outbreaks.

Materials and Methods

We constructed a multiple sequence alignment (11) containing 225 genomes from New Zealand community outbreaks and another 663 from the rest of the world, downloaded from GISAID (12). For each New Zealand outbreak, we sampled up to 50 global sequences from the same pangolin lineage(s) (13) as those of the outbreak, uniformly through time between the date of the first case in the outbreak and 60 days before. To reduce the effect of geographic sampling biases, global sequences were weighted proportionally to the number of sequences from the same country. For example, to sample the Pullman MIQ outbreak, we considered all B.1.351 global genomes collected up to 60 days before the outbreak and sampled 50 genomes from this pool, where the probability of sampling genome X was inversely proportional to the number of genomes in the pool from the same country as X. Our tree is the maximum-clade credibility tree summarizing a posterior distribution of trees inferred by BEAST 2 (14). Genomic sites were partitioned into the 3 codon positions, plus noncoding, as described (3)

For each partition, we modeled evolution with an HKY (Hasegawa-Kishino-Yano) substitution model with log-normal($\mu = 1$, $\sigma = 1.25$) prior on κ, frequencies estimated with Dirichlet (1,1,1,1) prior, and relative substitution rates with Dirichlet (1,1,1,1). We used a strict clock model with log-normal($\mu = -7$, $\sigma = 1.25$) prior on mean clock rate, and for the tree prior we used a Bayesian skyline model (15) with Markov chain distribution on population sizes and log-normal($\mu = 0$, $\sigma = 2$) on the first population size. We established convergence of the analysis by running multiple analyses (8) and using Tracer (16) to ensure that effective sample sizes were sufficient and that all individual analyses converged to the same distribution (supplemental information available at https://zenodo.org/record/5093838#.YOy_YDqxU5k).

Outbreaks

We reconstructed the phylogenetic tree for New Zealand's border incursions by using complete viral genomes from New Zealand and, for context, from the rest of the world (12) (Figure; Appendix Figure, https://wwwnc.cdc.gov/EID/article/27/9/21-1097-App1.pdf). As of April 30, 2021, complete genomes (>90% recovery) have been obtained from 1,288 (57%) of 2,243 case-patients total and from 583 (57%) of 1,030 case-patients since June 1, 2020. For some case-patients without a full genome sequence, genomes were of lower quality, which was sufficient to assign them to a lineage, but for many case-patients, viral material was insufficient for any meaningful analysis. For the community outbreaks considered here, we had high-quality genomes for 225 (85%) of 265 case-patients (Table).

Compassionate Exemption

After 24 days without any recorded cases in the community or at the border and 1 week after all of New Zealand had been moved down to alert level 1, two cases were found in the community. These case-patients had arrived on June 7 and were granted a compassionate exemption to exit MIQ early to attend a funeral on June 13. The conditions of the exemption required them to self-isolate as much as possible while traveling and to get tested. They were both positive for COVID-19 on June 16. Within 1 day, complete viral genome sequencing confirmed that virus from the 2 case-patients shared a single origin. Although there were no secondary infections, concern for public health led to the New Zealand Defence Force being put in charge of managing MIQ facilities, no returnees being allowed to leave MIQ without having a negative test result, and ending compassionate exemptions from most of the MIQ requirements.

Auckland August 2020 Lockdown

On August 11, 2020, a 102-day period with no recorded community transmission ended when 4 cases of COVID-19 were found among workers at an Auckland cold storage facility. The city was sent into an immediate lockdown (alert level 3), and lower level restrictions were introduced for the rest of the country (alert level 2). Elevated restrictions remained until October 7 as the cluster grew to a total of 179 cases, including 3 deaths. This COVID-19 cluster was the largest in New Zealand.

All genomes were closely related; 44 segregating sites were found across 155 genomes (Table). The single origin gave public health officials confidence that it was a single outbreak despite several cases having no clear epidemiologic links with other cases (*17*). The cluster included a healthcare worker who was infected during work at an MIQ facility where community case-patients were sent to quarantine (*18*). Although the index case-patients worked at a cold chain supply facility linked to the border, the source of the outbreak was never established (*19*). Complete genomes were available for 87% of cases in this outbreak, which we believe makes it one of the most comprehensively sampled large COVID-19 outbreaks.

Rydges MIQ Facility

During the Auckland outbreak in August, there was an unusual case of COVID-19 in a maintenance worker at the Rydges MIQ facility with no known epidemiologic link to the ongoing community outbreak. Sequencing confirmed that the source of infection was not related to the main community cluster but rather to an overseas returnee under managed isolation at the Rydges MIQ facility. A follow-up investigation suggested that transmission probably occurred when
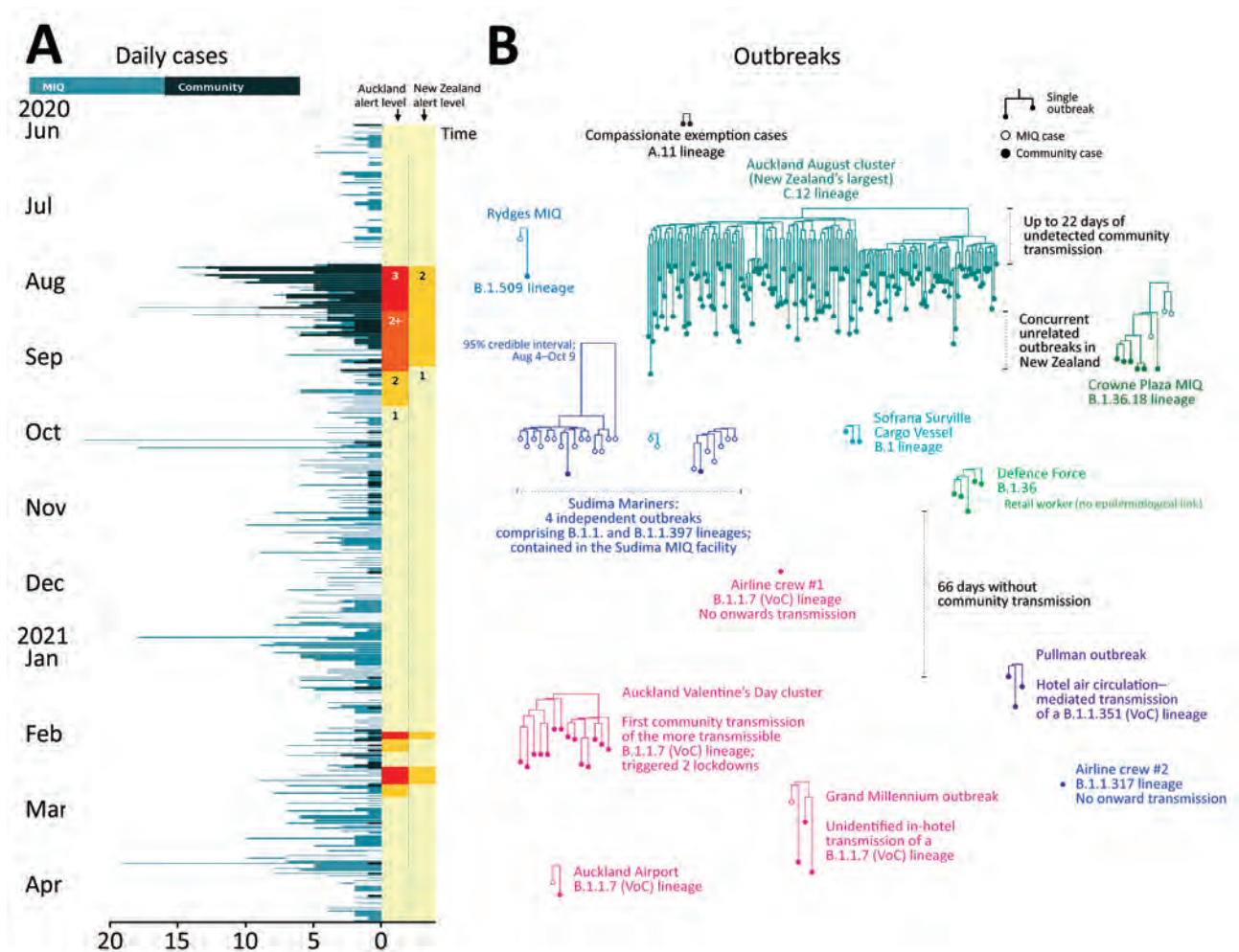
Figure. Outbreaks of coronavirus disease (COVID-19) after initial elimination in New Zealand. A) Daily COVID-19 cases, June 2020–April 2021. Alert levels in the Auckland region and across the wider country are indicated. B) Phylogenetic trees of all 13 COVID-19 postelimination community outbreaks. VoCs are indicated. Each subtree displayed is part of the larger phylogenetic tree built from genomes around the world. MIQ, managed isolation and quarantine; VoC, variant of concern.

Table. Summary of all coronavirus disease community cases in New Zealand since elimination was first achieved*

Outbreak	First case report date	Last case report date	Genomes	Community	Lineage(s)	No. unique genomes	No. segregating sites	Origin
Compassionate Exemption	2020 Jun 16	2020 Jun 16	2/2	2	A.11	1	0	MIQ
Auckland August 2020 Lockdown	2020 Aug 11	2020 Oct 20	155/179	179	C.12	40	44	Unknown
Rydges MIQ	2020 Aug 1	2020 Aug 16	2/2	1	B.1.509	1	0	MIQ
Crowne Plaza MIQ	2020 Aug 30	2020 Sep 22	9/9	6	B.1.36.18	4	4	MIQ
Sudima MIQ	2020 Oct 10	2020 Nov 3	24/33	2	B.1.1, B.1.1.397	1, 2, 7	0, 1, 14	MIQ
Sofrana Surville	2020 Oct 17	2020 Oct 22	3/4	4	B.1	1	0	Cargo vessel
Defence Force	2020 Nov 6	2020 Nov 18	5/8	6	B.1.36	1	0	MIQ
Airline Crew 1	2020 Dec 12	2020 Dec 12	1/1	1	B.1.1.7	1	0	Airline/ abroad
Pullman MIQ	2021 Jan 13	2021 Feb 4	3/5	4	B.1.351	2	1	MIQ
Auckland February 2021 Lockdown	2021 Feb 13	2021 Feb 28	14/15	15	B.1.1.7	4	3	Unknown
Airline Crew 2	2021 Mar 7	2021 Mar 7	1/1	1	B.1.1.317	1	0	Airline/ abroad
Grand Millennium MIQ	2021 Mar 13	2021 Apr 11	4/4	3	B.1.1.7	1	0	MIQ
Auckland Airport	2021 Apr 15	2021 Apr 20	2/2	1	B.1.1.7	1	0	Airport
Total	NA	NA	225/265	225	NA	NA	NA	NA

*Pangolin lineages are specified (version 2.3.9) (3) as well as the number of complete genomes/no. confirmed cases and no. community cases. No. unique genomes and no. segregating sites (i.e., no. genome positions that differ) within each cluster are counted, or within the 3 subclusters of the Sudima outbreak. All dates are the dates of report for the laboratory test. MIQ, managed isolation and quarantine; NA, not applicable.

the 2 case-patients used the same elevator minutes apart from each other (20) and that transmission was most likely airborne (21,22), although fomite transmission (e.g., through elevator buttons) cannot be ruled out.

Crowne Plaza MIQ Facility

The complete Crowne Plaza outbreak has been thoroughly analyzed (23), so we provide only brief detail here. In September 2020, symptoms developed in a returnee who tested positive in Auckland 4 days after leaving the Crowne Plaza MIQ facility in Christchurch. Genomic sequencing showed that this case-patient (case-patient G) and 2 household contacts were not linked to the ongoing Auckland cluster in August. Rather, they were linked to other returnees under managed isolation at the Crowne Plaza. Epidemiologic investigations show that the chain probably started with case-patients A and B, who were seated close to case-patient C on a repatriation flight from India. Case-patient C then infected case-patient D in the MIQ facility via airborne transmission between a hotel room and its adjacent hallway. Case-patient D is then thought to have infected case-patient G on a domestic flight from Christchurch to Auckland. This outbreak illustrates the power of genome sequencing—when coupled with detailed epidemiologic investigations—for identifying cryptic transmission events such as those on flights or airborne transmission between MIQ guests. The genomic evidence here is complete; all sequences in the cluster are available, and the tree is relatively well-resolved, showing 4 distinct genomes among its 9 cases.

Sudima MIQ Facility

On October 16, 2020, a group of 235 international mariners arrived in New Zealand on a charter flight from Moscow and began self-isolation at the Sudima MIQ facility in Christchurch. In the ensuing period, 31 of the mariners tested positive for COVID-19, as did 2 workers at the MIQ facility (24). Genomic sequencing produced full genomes for 24 case-patients and indicated $\geq$4 independent origins for the 33 cases; the viruses fell into 3 distinct phylogenetic clades (Figure). The 3 clades accounted for 2, 7, and 15 cases. We estimate the date of origin of the largest clade as between August 4 and October 9 (95% credible interval), but the mariners arrived on October 16, suggesting $\geq$2 separate introductions of this variant into the facility. The 2 MIQ workers were infected with 2 different variants of the virus; public health officials concluded that the 2 transmission events occurred via regular interactions with the mariners where protocols were followed but were insufficient to prevent transmission (25).

Sofrana Surville

In mid-October, routine testing indicated that a border worker was positive for COVID-19. Extensive

surveillance testing found 3 others who were positive: 2 were household contacts and 1 was a mariner who worked on the same cargo vessel, the Sofrana Surville (26). Genomic testing confirmed that virus isolates from the 4 case-patients shared the same origin and were part of a lineage that was novel to New Zealand, thus making residual community transmission an unlikely explanation. International crew members on the Sofrana Surville were confirmed as the source of infection when the ship arrived in Australia, and crew were tested by health officials in Queensland. One crew member tested positive, and the virus sequence reportedly matched that of the New Zealand case-patients.

Defence Force

After visiting several public locations in the Auckland central business district, a New Zealand Defence Force member tested positive for COVID-19 (November 2020). Genomic sequencing confirmed that his infection was acquired from the quarantine facility where he worked. Contact tracing identified 3 additional cases in Wellington (500 km from Auckland, where the Defence Force member's close contact resided), and surveillance testing identified 1 community case in the Auckland central business district. The only known connection to the rest of the outbreak was that this case-patient worked at a retail outlet ≈50 m from one of the locations visited by the index case-patient (27). The case was quickly linked to the rest of the cluster through whole-genome sequencing, providing reassurance that widespread undetected community transmission was unlikely (28). The circumstances of the transmission event remain unknown. Because the genomic link was established, the alert level was not changed. However, the general public was asked to avoid the Auckland central business district, if possible, for ≈3 days.

Airline Crew 1

In December 2020, an airline crew member tested positive for COVID-19. The worker was self-isolating at an airline hotel-based facility (as opposed to a dedicated MIQ facility) because of return from a high-risk country (United States). The crew member tested positive within the first 48 hours of self-isolation, and there were no recorded secondary infections (29). Genomic sequencing indicated that the infection had been acquired abroad. Although this case meets our definition of a community case in that it occurred outside one of the MIQ facilities, the wider community was at little risk, and the case was managed according to aircrew protocols (30).

Pullman MIQ Facility

A returnee (case-patient A) tested positive for COVID-19 1 week after completing managed isolation at the Pullman MIQ facility (January 2021). Despite extensive travel across the Northland region while infected with the B.1.351 lineage (Beta variant) of SARS-CoV-2 (H. Tegally et al., unpub. data, https://www.medrxiv.org/content/10.1101/2020.12.21.20248640v) (31), no secondary infections were reported, including in case-patient A's traveling companion. Shortly thereafter, 2 additional cases (case-patients B and C) with the same variant (and their household contact) were found in the community; case-patients B and C had completed self-isolation at Pullman (32). The outbreak was successfully limited to these 4 community cases, which were genomically linked to a returnee under isolation at Pullman. Case-patient A had occupied a room on the same floor as the source case-patient and may have been infected through the air circulation system; whereas, case-patient B was most likely infected from using an elevator 3 minutes after the source case-patient, despite their use of face masks (33). New arrivals at the MIQ facility were suspended, and its air filtration systems were improved.

Auckland February 2021 Lockdowns

On February 13, 2021, a total of 3 household members in Auckland tested positive for SARS-CoV-2. The genomes were identical and of the highly transmissible B.1.1.7 (Alpha) variant (34,35). Although 1 case-patient worked at an airline services company, that person had no obvious contact with persons coming through the border. Auckland was immediately sent into its third alert level 3 lockdown for 3 days, and widescale surveillance testing commenced. Other cases with closely related virus genomes were found; however, the epidemiologic links were not always strong (36). A fourth alert level 3 lockdown followed shortly after, when another case was found that could not immediately be linked to the cluster.

The known outbreak was restricted to 4 households and 15 cases, although epidemiologic gaps suggest that there may have been undetected cases. Genetic evidence showed 4 distinct genomes among 14 cases, which was not informative beyond confirming a single origin; the B.1.1.7 variant's global overrepresentation presented further difficulties at pinpointing an overseas origin. The outbreak has not been traced back beyond the original 3 cases, and its origin remains unknown.

Airline Crew 2

During the Auckland February outbreak, an airline crew member tested positive 1 week after arriving

from Japan (*37*). Self-isolation was not required because the worker did not arrive from a high-risk location. There were no known secondary infections, including household contacts. Genomic sequencing suggested that the infection was most likely acquired overseas.

Grand Millennium MIQ Facility

In late March 2021, a cleaner at the Grand Millennium MIQ facility tested positive. Despite this person being infected with the more transmissible B.1.1.7 lineage, there were no known secondary infections in the community. Two weeks later, 2 other workers from the same facility tested positive. All 3 cases were genomically linked back to a returnee isolating at the Grand Millennium.

Auckland Airport

A worker at Auckland International Airport tested positive for the B.1.1.7 variant in April 2020. No onward transmission was detected. Genomic sequencing linked the case to a recent returnee, and a follow-up investigation showed that the infected worker had cleaned the airplane on which the returnee had arrived, so it was likely a case of fomite or airborne transmission, despite the worker wearing personal protective equipment (*38*).

Discussion

Real-time genomic sequencing has been used to investigate each of the 13 COVID-19 community outbreaks after the initial elimination in New Zealand. Sequencing has been essential, not only for establishing links between cases when epidemiologic links could not (e.g., the Defence Force outbreak and both Auckland lockdowns) but also for identifying when multiple outbreaks had different origins (e.g., decoupling the Rydges outbreak from the ongoing Auckland outbreak and the second airline crew case from the February 2021 outbreak). These efforts have been instrumental in clearly delineating outbreaks and informing the public health response. Genomic sequencing has also elucidated cryptic modes of transmission, such as airborne transmission (*23*) and in-flight transmission (*39*), which have brought about policy changes (e.g., revision of filtration systems in MIQs).

When paired with routine genomic sequencing from within MIQ facilities and around the world, genomics can identify the origins of community outbreaks and rule out the possibility of undetected widespread community transmission. However, as exemplified by the 2 community outbreaks that led to lockdowns, the ability of this strategy to identify outbreak origins when there is no closely matched genome with a plausible epidemiologic link is limited (*18*).

A wide range of lineages have been imported into New Zealand over the course of the pandemic (Table) (*8*). The fact that the 4 outbreaks of locally acquired infection in 2021 were all caused by variants of concern (VoC)—pangolin lineages B.1.1.7 and B.1.351 (*13,40*) (P. Wang et al., unpub data, https://www.biorxiv. org/content/10.1101/2021.03.01.433466v1)—reflects the lineages that are arriving at the border. A total of 83 of the 142 genomes from overseas returnees found during January 1–April 30, 2021, were from those 2 lineages or other VoCs. However, data are too scarce to make any link between these outbreaks and the reported higher transmissibility of the VoCs.

New Zealand's ability to rapidly generate SARS-CoV-2 genomes has greatly improved over the past year, to the point where new genomes are routinely available within hours of positive community test results. Although the potential of the techniques described here has been well characterized in academia (*41*), the pandemic has facilitated their widespread adoption in New Zealand and other places (e.g., Singapore and Australia) (*42,43*); the term "whole-genome sequencing" is becoming commonplace in public health announcements. Combined with epidemiologic investigation, those data have increased public knowledge of the outbreak and have driven policy change. Although the techniques described here of real-time sequencing and analysis coupled with epidemiologic investigation have come to the fore during the COVID-19 pandemic, they are not limited to pandemic situations. These technologies can be integrated into regular surveillance of other pathogens, such as seasonal influenza viruses, which have been largely absent from many countries over the past year (*44*).

About the Author

Dr. Douglas is a research fellow at the School of Computer Science, University of Auckland. His research interests lie in computational biology and phylogenetics, including viral phylodynamics.

References

1. Cousins S. New Zealand eliminates COVID-19. Lancet. 2020; 395:1474. https://doi.org/10.1016/S0140-6736(20)31097-7
2. Baker M, Kvalsvig A, Verrall AJ, Telfar-Barnard L, Wilson N. New Zealand's elimination strategy for the COVID-19 pandemic and what is required to make it work. N Z Med J. 2020;133:10–4.
3. Douglas J, Mendes FK, Bouckaert R, Xie D, Jimenez-Silva CL, Swanepoel C, et al. Phylodynamics reveals the role of human travel and contact tracing in controlling the first wave of COVID-19 in four island nations. Virus Evolution. 2021 Jun 8 [Epub ahead of print]. https://doi.org/10.1093/ve/veab052
4. Jefferies S, French N, Gilkison C, Graham G, Hope V, Marshall J, et al. COVID-19 in New Zealand and the impact of the national response: a descriptive epidemiological study. Lancet Public Health. 2020;5:e612–23. https://doi.org/10.1016/S2468-2667(20)30225-5
5. New Zealand Government. Additional COVID-19 tests for returnees from higher risk countries [cited 2021 Apr 10]. https://covid19.govt.nz/updates-and-resources/latest-updates/additional-covid-19-tests-for-returnees-from-higher-risk-countries
6. Ministry of Business, Innovation and Employment. Managed isolation and quarantine: daily 14 day forecast [cited 2021 Apr 10]. https://www.mbie.govt.nz/dmsdocument/14219-miq-daily-update-2021-05-01
7. Baker MG, Wilson N, Blakely T. Elimination could be the optimal response strategy for covid-19 and other emerging pandemic diseases. BMJ. 2020;371:m4907. https://doi.org/10.1136/bmj.m4907
8. Smith P. Covid-19 in Australia: most infected health workers in Victoria's second wave acquired virus at work. BMJ. 2020;370:m3350. https://doi.org/10.1136/bmj.m3350
9. Geoghegan JL, Ren X, Storey M, Hadfield J, Jelley L, Jefferies S, et al. Genomic epidemiology reveals transmission patterns and dynamics of SARS-CoV-2 in Aotearoa New Zealand. Nat Commun. 2020;11:6351. https://doi.org/10.1038/s41467-020-20235-8
10. Geoghegan JL, Moreland NJ, Le Gros G, Ussher JE. New Zealand's science-led response to the SARS-CoV-2 pandemic. Nat Immunol. 2021;22:262–3. https://doi.org/10.1038/s41590-021-00872-x
11. Katoh K, Standley DM. MAFFT multiple sequence alignment software version 7: improvements in performance and usability. Mol Biol Evol. 2013;30:772–80. https://doi.org/10.1093/molbev/mst010
12. Shu Y, McCauley J. GISAID: Global initiative on sharing all influenza data - from vision to reality. Euro Surveill. 2017;22:30494. https://doi.org/10.2807/1560-7917.ES.2017.22.13.30494
13. Rambaut A, Holmes EC, O'Toole Á, Hill V, McCrone JT, Ruis C, et al. A dynamic nomenclature proposal for SARS-CoV-2 lineages to assist genomic epidemiology. Nat Microbiol. 2020;5:1403–7. https://doi.org/10.1038/s41564-020-0770-5
14. Bouckaert R, Vaughan TG, Barido-Sottani J, Duchêne S, Fourment M, Gavryushkina A, et al. BEAST 2.5: an advanced software platform for Bayesian evolutionary analysis. PLOS Comput Biol. 2019;15:e1006650. https://doi.org/10.1371/journal.pcbi.1006650
15. Drummond AJ, Rambaut A, Shapiro B, Pybus OG. Bayesian coalescent inference of past population dynamics from molecular sequences. Mol Biol Evol. 2005;22:1185–92. https://doi.org/10.1093/molbev/msi103
16. Rambaut A, Drummond AJ, Xie D, Baele G, Suchard MA. Posterior summarization in Bayesian phylogenetics using Tracer 1.7. Syst Biol. 2018;67:901–4. https://doi.org/10.1093/sysbio/syy032
17. New Zealand Ministry of Health. 9 new cases of COVID-19 [cited 2021 Apr 10]. https://www.health.govt.nz/news-media/media-releases/9-new-cases-covid-19-2
18. New Zealand Ministry of Health. 1 new case of COVID-19 [cited 2021 Apr 10]. https://www.health.govt.nz/news-media/media-releases/1-new-case-covid-19-18
19. Geoghegan JL, Douglas J, Ren X, Storey M, Hadfield J, Silander OK, et al. Use of genomics to track coronavirus disease outbreaks, New Zealand. Emerg Infect Dis. 2021;27:1317–22. https://doi.org/10.3201/eid2705.204579
20. New Zealand Ministry of Health. 11 new cases of COVID-19 [cited 2021 Apr 10]. https://www.health.govt.nz/news-media/media-releases/11-new-cases-covid-19-0
21. van Rijn C, Somsen GA, Hofstra L, Dahhan G, Bem RA, Kooij S, et al. Reducing aerosol transmission of SARS-CoV-2 in hospital elevators. Indoor Air. 2020;30:1065–6. https://doi.org/10.1111/ina.12744
22. Dbouk T, Drikakis D. On airborne virus transmission in elevators and confined spaces. Phys Fluids (1994). 2021;33:011905.
23. Eichler N, Thornley C, Swadi T, Devine T, McElnay C, Sherwood J, et al. Transmission of severe acute respiratory syndrome coronavirus 2 during border quarantine and air travel, New Zealand (Aotearoa). Emerg Infect Dis. 2021;27:1274–8. https://doi.org/10.3201/eid2705.210514
24. New Zealand Ministry of Health. International mariners to leave managed isolation [cited 2021 Apr 10]. https://www.health.govt.nz/news-media/media-releases/international-mariners-leave-managed-isolation
25. Ministry of Business, Innovation and Employment. Lessons learned review [cited 2021 Apr 10]. https://www.mbie.govt.nz/dmsdocument/12887-lessons-learned-review-international-mariners
26. New Zealand Ministry of Health. Confirmed cases of COVID-19 on Sofrana Surville [cited 2021 Apr 10]. https://www.health.govt.nz/news-media/media-releases/confirmed-cases-covid-19-sofrana-surville
27. New Zealand Ministry of Health. 3 new cases of COVID-19 [cited 2021 Apr 10]. https://www.health.govt.nz/news-media/media-releases/3-new-cases-covid-19-12
28. New Zealand Ministry of Health. 4 cases of COVID-19 - none in the community [cited 2021 Apr 10]. https://www.health.govt.nz/news-media/media-releases/4-cases-covid-19-none-community.
29. New Zealand Ministry of Health. 1 new case of COVID-19 [cited 2021 Apr 10]. https://www.health.govt.nz/news-media/media-releases/1-new-case-covid-19-23
30. New Zealand Ministry of Health. COVID-19: Aviation sector [cited 2021 Apr 10]. https://www.health.govt.nz/our-work/diseases-and-conditions/covid-19-novel-coronavirus/covid-19-information-specific-audiences/covid-19-resources-border-sector/covid-19-aviation-sector
31. Cele S, Gazy I, Jackson L, Hwa S-H, Tegally H, Lustig G, et al. Escape of SARS-CoV-2 501y.v2 variants from neutralization by convalescent plasma. Nature.2021; 593:142–6.
32. New Zealand Ministry of Health. 3 new cases of COVID-19 at the border and an update on border-related cases in Auckland [cited 2021 Apr 10]. https://www.health.govt.nz/news-media/media-releases/3-new-cases-covid-19-border-and-update-border-related-cases-auckland
33. Andrew P, Freeman J. MIQ COVID-19 case incident report [cited 2021 Apr 10]. https://www.miq.govt.nz/assets/MIQ-documents/case-incident-review-pullman-march-2021.pdf

34. Volz E, Mishra S, Chand M, Barrett JC, Johnson R, Geidelberg L, et al.; COVID-19 Genomics UK (COG-UK) Consortium. Assessing transmissibility of SARS-CoV-2 lineage B.1.1.7 in England. Nature. 2021;593:266–9. https://doi.org/10.1038/s41586-021-03470-x

35. Davies NG, Abbott S, Barnard RC, Jarvis CI, Kucharski AJ, Munday JD, et al.; CMMID COVID-19 Working Group; COVID-19 Genomics UK (COG-UK) Consortium. Estimated transmissibility and impact of SARS-CoV-2 lineage B.1.1.7 in England. Science. 2021;372:eabg3055. https://doi.org/10.1126/science.abg3055

36. New Zealand Ministry of Health. 5 border cases and 1 new community case [cited 2021 Apr 10]. https://www.health.govt.nz/news-media/media-releases/5-border-cases-and-1-new-community-case

37. New Zealand Ministry of Health. Confirmed case at the border [cited 2021 Apr 10]. https://www.health.govt.nz/news-media/media-releases/confirmed-case-border

38. New Zealand Ministry of Health. No new community cases; 1 new case of COVID-19 in managed isolation [cited 2021 Apr 10]. https://www.health.govt.nz/news-media/media-releases/no-new-community-cases-1-new-case-covid-19-managed-isolation

39. Swadi T, Geoghegan JL, Devine T, McElnay C, Sherwood J, Shoemack P, et al. Genomic evidence of in-flight transmission of SARS-CoV-2 despite predeparture testing. Emerg Infect Dis. 2021;27:687–93. https://doi.org/10.3201/eid2703.204714

40. Wang P, Nair MS, Liu L, Iketani S, Luo Y, Guo Y, et al. Antibody resistance of SARS-CoV-2 variants B.1.351 and B.1.1.7. Nature. 2021;593:130–5. https://doi.org/10.1038/s41586-021-03398-2

41. Gardy JL, Loman NJ. Towards a genomics-informed, real-time, global pathogen surveillance system. Nat Rev Genet. 2018;19:9–20. https://doi.org/10.1038/nrg.2017.88

42. Pung R, Chiew CJ, Young BE, Chin S, Chen MI, Clapham HE, et al.; Singapore 2019 Novel Coronavirus Outbreak Research Team. Investigation of three clusters of COVID-19 in Singapore: implications for surveillance and response measures. Lancet. 2020;395:1039–46. https://doi.org/10.1016/S0140-6736(20)30528-6

43. Seemann T, Lane CR, Sherry NL, Duchene S, Gonçalves da Silva A, Caly L, et al. Tracking the COVID-19 pandemic in Australia using genomics. Nat Commun. 2020;11:4376. https://doi.org/10.1038/s41467-020-18314-x

44. Olsen SJ, Azziz-Baumgartner E, Budd AP, Brammer L, Sullivan S, Pineda RF, et al. Decreased influenza activity during the COVID-19 pandemic–United States, Australia, Chile, and South Africa, 2020. Am J Transplant. 2020;20:3681–5. https://doi.org/10.1111/ajt.16381

Address for correspondence: Jordan Douglas, The University of Auckland, Private Bag 92019, Auckland 1142, New Zealand; email: jordan.douglas@auckland.ac.nz

Genomic Epidemiology of Azithromycin-Nonsusceptible *Neisseria gonorrhoeae*, Argentina, 2005–2019

Ricardo Ariel Gianecini, Tomas Poklepovich, Daniel Golparian, Noelia Cuenca,
Ezequiel Tuduri, Magnus Unemo, Josefina Campos, Patricia Galarza,
Gonococcal Antimicrobial Susceptibility Surveillance Programme—Argentina[1]

Azithromycin-nonsusceptible *Neisseria gonorrhoeae* strains are an emerging global public health threat. During 2015–2018, the prevalence of azithromycin-nonsusceptible gonococcal infection increased significantly in Argentina. To investigate the genomic epidemiology and resistance mechanisms of these strains, we sequenced 96 nonsusceptible isolates collected in Argentina during 2005–2019. Phylogenomic analysis revealed 2 main clades, which were characterized by a limited geographic distribution, circulating during January 2015–November 2019. These clades included the internationally spreading multilocus sequence types (STs) 1580 and 9363. The ST1580 isolates, which had MICs of 2–4 µg/mL, had mutations in the 23S rRNA. The ST9363 isolates, which had MICs of 2–4 or ≥256 µg/mL, had mutations in the 23S rRNA, a mosaic *mtr* locus, or both. Identifying the geographic dissemination and characteristics of these predominant clones will guide public health policies to control the spread of azithromycin-nonsusceptible *N. gonorrhoeae* in Argentina.

Gonorrhea, caused by infection with the bacterium *Neisseria gonorrhoeae*, is the second most prevalent bacterial sexually transmitted infection (STI) globally (*1,2*). The World Health Organization (WHO) estimated that in 2016, a total of 86.9 million incident gonorrhea cases occurred among persons 15–49 years of age, including 13.8 million cases in the WHO Region of the Americas (*1*). Researchers have documented antimicrobial resistance (AMR) to all drugs used to treat gonorrhea (*2,3*). Ceftriaxone, an extended-spectrum cephalosporin, is the last option for first-line empirical treatment, but the emergence of ceftriaxone resistance has raised concerns about future treatments (*2,4*). Consequently, WHO guidelines and national guidelines of many countries now recommend a combination of ceftriaxone (250 mg–1 g) and azithromycin (1–2 g) as first-line treatment for uncomplicated gonorrhea (*5,6*). However, in 2016 Fifer et al. (*7*) reported the failure of dual therapy. Two years later, a gonococcal strain with ceftriaxone resistance and high-level azithromycin resistance was isolated in Australia and England (*8–10*). In recent years, international reports of azithromycin-resistant *N. gonorrhoeae* have substantially increased (*2,3,11,12*). The WHO Global Gonococcal Antimicrobial Surveillance Program showed that in 2016, a total of 48.4% of reporting countries had an >5% increase in rates of azithromycin resistance (*3*).

Argentina has reported low azithromycin resistance levels since the early 2000s (*13*). In Argentina, the proportion of azithromycin-nonsusceptible isolates (i.e., requiring MICs >1 µg/mL) increased from 0.1% in 2015 to 4.3% in 2018 (p<0.01) (*14*). The Clinical and Laboratory Standards Institute currently states a susceptible-only breakpoint for azithromycin (*15*); for simplicity, we refer to these isolates as resistant. High-level azithromycin-resistant isolates requiring MICs ≥256 µg/mL have emerged in several countries, including Argentina (*16–20*). Azithromycin resistance threatens the effectiveness of dual antimicrobial gonorrhea treatment.

[1]Members of this group are listed at the end of the article.

Whole-genome sequencing (WGS) provides higher resolution and accuracy than other typing methods, making it an ideal method to study the dissemination and transmission dynamics of *N. gonorrhoeae* strains on a national and international level (*21,22*). Furthermore, WGS data offer insights into AMR determinants, thereby enabling prediction, enhanced detection, and characterization of high-risk clones (*22,23*). Several studies have found *N. gonorrhoeae* lineages and clones driving AMR transmission among *N. gonorrhoeae* strains within local, national, and international networks (*16,17,24–26*). Genomic surveillance provides information on current and emerging trends of circulating strains. Phenotypic, epidemiologic, and genomic surveillance data are critical for designing public health interventions and treatment strategies. Genomic approaches, including molecular epidemiology and detection of AMR determinants, are crucial for monitoring resistance to first-line drugs. We examined the genomic background of azithromycin-resistant *N. gonorrhoeae* isolates with MICs ≥2 µg/mL collected throughout Argentina during 2005–2019.

Materials and Methods

We examined 96 azithromycin-resistant *N. gonorrhoeae* isolates (MICs ≥2 µg/mL) from male and female patients treated at STI hospitals throughout Argentina. We selected 95 isolates from 8,002 consecutive isolates collected through the Gonococcal Antimicrobial Susceptibility Surveillance Programme—Argentina during January 2005–November 2019; we also included an isolate with high-level azithromycin resistance cultured in 2001 (*20*). We confirmed the *N. gonorrhoeae* species by culture on selective agar media, microscopic analysis using Gram staining, rapid oxidase positivity, superoxol test, carbohydrate utilization test, and matrix-assisted laser desorption/ionization time-of-flight mass spectrometry (microflex LT/SH; Bruker Daltonik, https://www.bruker.com) (*27*). The study was approved by the Research Ethics Committee of the Hospital General de Agudos "Bernardino Rivadavia" (Buenos Aires, Argentina). MIC determinations and whole-genome sequencing for all isolates were conducted using methods previously described (Appendix, https://wwwnc.cdc.gov/EID/article/27/9/20-4843-App1.pdf).

WGS Analysis

We identified AMR determinants (i.e., the *mtrR*-35A, *mtr*$_{120}$, and mosaic *N. meningitidis*–like *mtrR* mutations) in addition to the MtrR A39T and G45D amino acid mutations in silico from WGS data, as described (*26,28*). We aligned and compared the *mtr* locus and *rplD*, *rplV*, and *macAB* sequences with the *N. gonorrhoeae* FA1090 reference genome (GenBank accession no. AE004969). To identify the frequency of 23S rRNA A2059G and C2611T mutations (named using *Escherichia coli* numbering), we mapped sequence reads against a single copy of the FA1090 23S rRNA gene using Burrow-Wheeler Aligner version 0.7.17 (http://bio-bwa.sourceforge.net) with the default settings. We determined base counts using a custom script, enabling the estimation of the proportion of copies with the A2059G, C2611T, or both mutations. We examined additional macrolide resistance genes (e.g., *ereA*, *ereB*, *ermA*, *ermB*, *mefA*, *mefB*, *msrA*, and *msrC*) using ARIBA version 2.14.4 and the ResFinder (https://cge.cbs.dtu.dk/services/ResFinder) and CARD (https://card.mcmaster.ca) databases (*29*). We identified alleles in silico from WGS data using *N. gonorrhoeae* multiantigen sequence typing (NG-MAST), multilocus sequence typing (MLST), and *N. gonorrhoeae* sequence typing for antimicrobial resistance (NG-STAR). We used the MLST (https://pubmlst.org/neisseria), NG-MAST (http://www.ng-mast.net), and NG-STAR (https://ngstar.canada.ca) databases to assign allele numbers and sequence types (ST)s (*30,31*). We grouped closely related NG-MAST STs using a previously described genogroup definition (*28*).

For phylogenetic analysis, we identified single-nucleotide polymorphisms (SNPs) in sequence reads mapped against the WHO P reference genome using the variant calling tool Snippy version 4.4.5 (https://github.com/tseemann/snippy). We identified and filtered recombinant regions using Gubbins version 2.1.0 (Sanger, https://sanger-pathogens.github.io/gubbins); the resulting core SNP alignment consisted of 9,415 sites. We used IQ-tree version 1.6.1 (http://www.iqtree.org) to infer a maximum-likelihood tree from the whole-genome SNP alignment with a generalized time-reversible model of evolution using gamma correction for among-site rate variation with 4 rate categories; branch support was estimated by bootstrap analysis of 10,000 replicates (*32*). We visualized the resulting phylogeny with Figtree version 1.4.4 (http://tree.bio.ed.ac.uk/software/figtree) and phandango (*33*). We clustered sequences using RAMI with a branch length threshold of 0.01 (*34*). For comparison, we selected international isolates and publicly available genomic data on the basis of MICs, MLST STs (i.e., ST9363 and ST1580), and NG-MAST genogroups (i.e., G470 and G12302) from the National Center for Biotechnology Information (https://www.ncbi.nlm.nih.gov), European Molecular Biology

Laboratory (https://www.embl.org), and the DNA Data Bank of Japan (https://www.ddbj.nig.ac.jp). We found 17 genomes from the United Kingdom, 3 from Canada, 3 from Scotland, 17 from Australia, 28 from the United States, 7 from Brazil, and 11 from Norway (*16,17,24,25,35–37*). We generated a phylogenetic tree of 86 international and 96 isolates from Argentina as described for domestic isolates and visualized the tree in Figtree version 1.4.4. Sequence reads are available from the European Nucleotide Archive (accession no. PRJEB41007).

Results

Patient Data
The 96 *N. gonorrhoeae* isolates were collected from male (90.6%) and female (6.3%) patients; sex was unreported for 3.1% of patients. Patient age was reported for 88 (91.7%) isolates. Patients were 4–47 years of age (mean 24.3 years of age); 79.5% were <30 years of age. In total, 72 isolates were cultured from the urethra, 11 from urine, 3 from the cervix, 2 from the vagina (in children 4 and 6 years of age), 1 from the pharynx, and 7 from an unreported site.

The isolates were collected in 7/24 provinces. Among these, Córdoba and Ciudad Autónoma de Buenos Aires (CABA), 2 of the most populated provinces in Argentina, had the highest percentage of isolates (Córdoba had 47.9%; CABA had 39.6%) (Figure 1). We observed a lower percentage of isolates from the provinces of Buenos Aires (5.2%), Rio Negro (3.1%), Neuquén (2.1%), La Pampa (1.0%), and Santa Fe (1.0%).

Antimicrobial Susceptibility of *N. gonorrhoeae* Isolates
Overall, 78 (81.3%) isolates had azithromycin MICs of 2–4 µg/mL, 13 (13.5%) had MICs of 8–16 µg/mL, and 5 (5.2%) had MICs of ≥256 µg/mL (Table 1). Among 5 isolates with MICs ≥256 µg/mL, 3 were collected in CABA in 2001 (n = 1) and 2019 (n = 2); the other 2 isolates were collected in Buenos Aires in 2018 and Córdoba in 2019. All 96 azithromycin-resistant isolates were susceptible to ceftriaxone, cefixime, and spectinomycin. However, 2 isolates collected in 2016 from Córdoba, each had a MIC of 4 µg/mL, showed decreased susceptibility to ceftriaxone (MIC = 0.06 µg/mL) and cefixime (MIC = 0.125 µg/mL) (Table 2).

Molecular AMR Determinants
All 5 isolates with MICs of ≥256 µg/mL had the A2059G mutation in all 4 23S rRNA alleles, whereas none of the 91 isolates with MICs of 2–16 µg/mL had this SNP (Table 1). Most (72; 75%) isolates with MICs of 2–16 µg/

mL had the 23S rRNA C2611T mutation. Nearly all (70; 97.2%) of these isolates had the C2611T mutation in all 4 23S rRNA alleles, except for 2 isolates: 1 with a single mutated allele that had a MIC of 4 µg/mL and 1 with 3 mutated alleles that had a MIC of 8 µg/mL. Interspecies mosaics in the *mtr* locus (which encodes the tripartite MtrCDE efflux pump), as well as mutations in the *mtrR* promoter, coding region, or both, have been associated with increased azithromycin MICs (*38–40*). Among the 80 (83.3%) isolates with *mtrR* mutations, 17 (17.7%) had an *mtrR*-35A promoter deletion, 44 (45.8%) had an MtrR G45D amino acid mutation, 1 (1.0%) had an *mtrR*-35A deletion and MtrR G45D substitution, and 18 (18.8%) had a mosaic *N. meningitidis*–like *mtrR* promoter. We did not identify any isolates with the mtr_{120} mutation. Eighteen isolates, all of which had MICs of 2–4 µg/mL, had no 23S rRNA mutations; however, 13 contained a mosaic *mtrR* promoter and 5 had a *mtrR*-35A deletion. Among 18 isolates with mosaic *mtrR* promoters, 100% also had mosaic sequences in the *mtrD*, 100% in *mtrC*, and 94.4% in *mtrE* loci. Fifteen isolates with a mosaic *mtrD* allele had sequences identical to the *N. meningitidis*–like mosaic previously described (*39,40*); 2 isolates had sequences sharing 97.8% identity and 1 had a sequence sharing 97.3% identity with the *N. meningitidis*–like mosaic (Appendix Figure 1). Isolates containing a mosaic-like *mtr* locus had MICs of ≥2 to ≥256 µg/mL. Isolates with MICs of ≥256 µg/mL also contained the 23S rRNA A2059G mutation.

We did not find any mutations associated with macrolide resistance in the *rplD* gene, which encodes ribosomal protein L4, or the *rplV* gene, which encodes ribosomal protein L22 (*23*). In addition, we did not find AMR mutations in *macAB*, which encodes the MacA-MacB efflux pump, or the acquired macrolide resistance genes, *ere*, *mef*, *erm*, *mph*, and *msr* (*38*). An isolate that had a MIC of 2 µg/mL had an unclear resistance mechanism.

Molecular Epidemiology and Phylogenomic Analysis
Among the 96 *N. gonorrhoeae* isolates, we observed 42 NG-MAST STs, including 21 new STs and 25 STs represented by single isolates. We found 24 isolates belonging to ST470, 7 belonging to ST20102, 6 belonging to ST696, 4 belonging to ST12302, and 4 belonging to ST20104. We found 3 NG-MAST genogroups comprising ≥3 isolates: 33 belonged to G470, 10 belonged to G12302, and 10 belonged to G20102. We also documented 14 MLST STs, including 2 new STs and 8 STs represented by single isolates. We found 43 isolates belonging to ST1580, 14 belonging to ST1901, 14 belonging to ST9363, and 10 belonging to ST1584. NG-STAR showed 32 types, of which 11 were new and 20 were represented by single isolates.
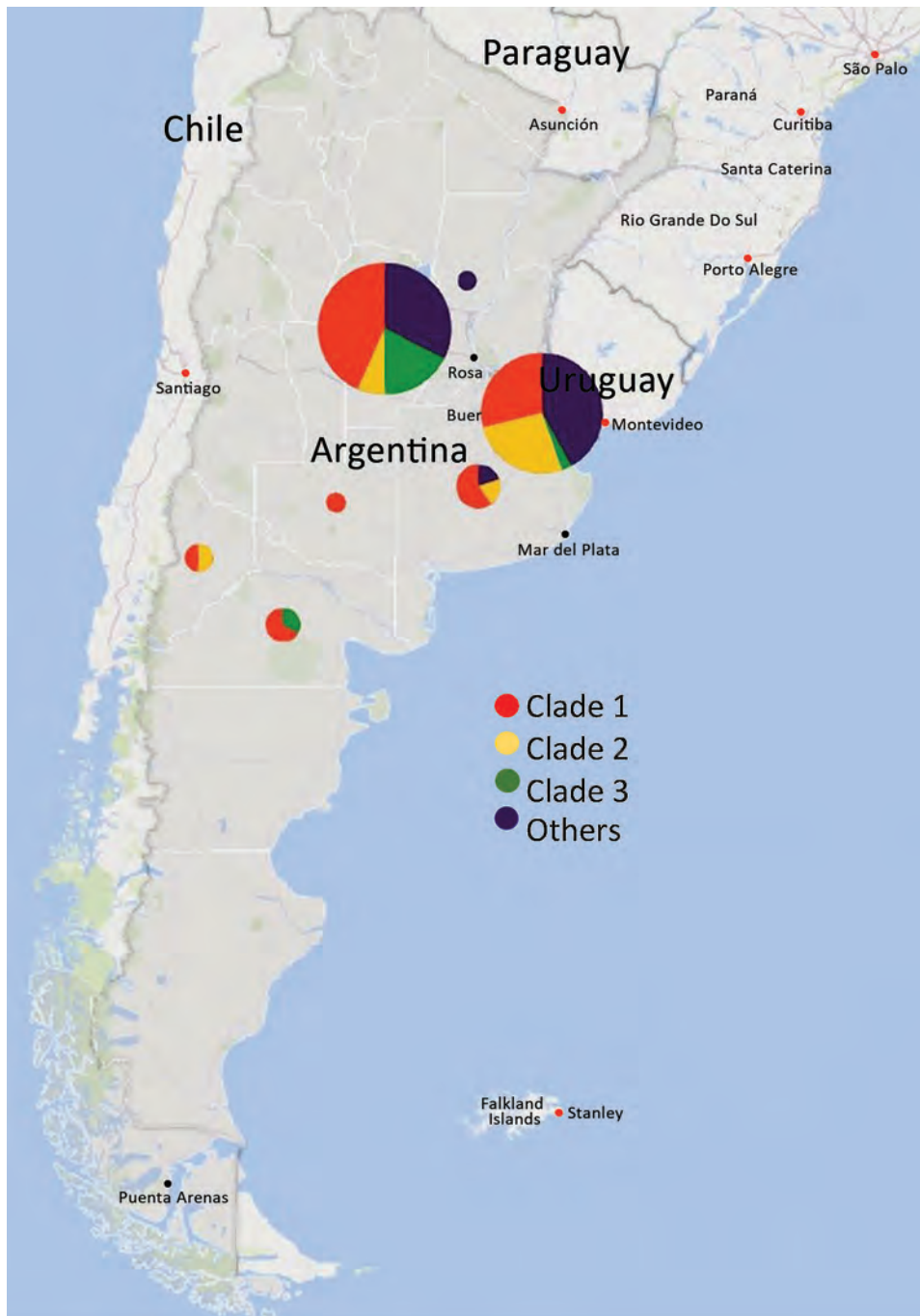
Figure 1. Geographic distribution of *Neisseria gonorrhoeae* isolates with azithromycin MICs of >2 μg/mL, Argentina, January 2005–November 2019. Circle size corresponds to the number of isolates in each location. Circle colors indicate the proportion of isolates belonging to the 3 main genomic clades compared with other clades.

We found 32 isolates belonging to NG-STAR type 1038, 10 belonging to type 179, 5 belonging to type 168, and 5 belonging to type 3200.

Analysis of the phylogenomic tree revealed 14 clades. In total, 63 (65.6%) isolates were grouped into 3 clades, each containing 10–38 isolates (Figure 2) (https://microreact.org/project/AZM_Project/006b822d). The remaining 33 isolates were singletons or belonged to smaller clonal groups of 2–6 isolates each.

Clade 1 comprised 38 isolates, most of which belonged to NG-MAST G470 (86.8%), MLST ST1580 (97.4%), or NG-STAR ST1038 (84.2%). Clade 1 isolates had mean SNP difference of 8.5 (range 0–39). The isolates required MICs of 2–16 μg/mL; most (76.3%; 29/38) required an MIC of 4 μg/mL. The oldest isolate in clade 1 was identified in CABA in 2013. The proportion of clade 1 isolates increased significantly from 1.0% (1/96) in 2013 to 11.4% (11/96) in 2019 ($p < 0.05$). Clade 1 was

Table 1. Characteristics of 96 azithromycin-resistant *Neisseria gonorrhoeae* isolates, Argentina, January 2005–November 2019*

Characteristics	MICs for azithromycin, μg/mL		
	2–4	8–16	>256
Total	78	13	5
Province	Buenos Aires, CABA, Córdoba, Neuquén, La Pampa, Río Negro, Santa Fe	CABA, Córdoba	Buenos Aires, CABA, Córdoba
Resistance determinants			
23S rRNA (no. mutated alleles; total no. isolates)	C2611T (4; 58); C2611T (1; 1)	C2611T (4; 12); C2611T (3; 1)	A2059G (4; 5)
MtrR protein (no. isolates)	A-deletion (12)†; *N. meningitidis*–like (14); G45D (41); mtr_{120} (0)‡	A-deletion (6); G45D (3); mtr_{120} (0)	*N. meningitidis*–like (4); G45D (1); mtr_{120} (0)
Mosaic *mtr* locus (no. isolates)	*mtrC* (14); *mtrD* (14); *mtrE* (13)	*mtrC* (0); *mtrD* (0); *mtrE* (0)	*mtrC* (4); *mtrD* (4); *mtrE* (4)
ST			
N. gonorrhoeae multiantigen sequence typing (no. isolates)	ST470 (23); ST20102 (7); ST696 (4); ST12302 (4); ST11062 (3); other STs (37)	ST18761 (3); ST20104 (3); singleton STs (7)	ST3935 (2); ST20106 (2); ST696 (1)
Multilocus sequence typing (no. isolates)	ST1580 (39); ST1584 (10); ST9363 (10); ST1901 (8); other STs (11)	ST1901 (6); ST1580 (3); ST13844 (3); ST13594 (1)	ST9363 (4); ST1580 (1)
N. gonorrhoeae sequence typing for antimicrobial resistance (no. isolates)	ST1038 (30); ST179 (10); ST168 (5); ST3200 (4); other STs (29)	ST27 (4); ST2728 (3); ST1038 (2); singleton STs (4)	ST1993 (2); ST2906 (1); ST3194 (1); ST3199 (1)

*CABA, Ciudad Autónoma de Buenos Aires; ST, sequence type.
†Deletion of A in 13-bp inverted repeat sequence of the *mtrR* gene.
‡C-to-T transition mutation 120 bp upstream of the *mtrC* start codon.

dominated by isolates from Córdoba (52.6%; 20/38) and CABA (28.9%; 11/38) but also included isolates obtained in 4 additional provinces. In total, 92.1% of the clade 1 isolates were from male patients and 7.9% were from female patients. Clade 1 isolates were characterized by the 23S rRNA C2611T mutation in all 4 alleles and the MtrR G45D amino acid mutation.

Clade 2 comprised 15 isolates that mainly belonged to NG-MAST G12302 (66.7%) and MLST ST9363 (93.3%). Clade 2 isolates had a mean SNP difference of 13.1 (range 0–33). All clade 2 isolates were cultured from men. Most (73.3%; 11/15) required an MIC of 2 μg/mL, and 26.7% (4/15) required MICs of >256 μg/mL. The first clade 2 isolate was detected in Córdoba in 2016; during 2017–2019, isolates were mainly detected in CABA (71.4%; 10/14), except for 2 isolates detected in Córdoba, 1 in Neuquén, and 1 in Buenos Aires. Clade 2 isolates did not have the 23S rRNA C2611T mutation but possessed the mo-saic *mtrR* promoter and *mtrCDE* locus. In addition, isolates requiring MICs of >256 μg/mL had the 23S rRNA A2059G mutation in all 4 alleles.

Clade 3 was composed of 10 isolates belonging to NG-MAST G20102 and MLST ST1584. Clade 3 isolates had a mean SNP difference of 1.1 (range 0–2). Eight isolates were collected in Córdoba, 1 in CABA, and 1 in Río Negro during 2017–2019; of these, 8 were from men. All isolates required an MIC of 4 μg/mL and possessed the 23S rRNA C2611T mutation in all 4 alleles.

To investigate the international context of the 2 major MLST STs in Argentina, including azithromycin-resistant ST1580 and ST9363, we conducted a phylogenomic analysis using SNPs (Figure 3) (https://microreact.org/project/AZM_Project_2/7a2032e2). The ST1580 isolates from Argentina clustered with isolates from the United States, the United Kingdom (particularly Scotland), Australia, and Brazil. The mean pairwise SNP differences between ST1580

Table 2. Antimicrobial susceptibility of 96 azithromycin-resistant *Neisseria gonorrhoeae* isolates, Argentina, January 2005–November 2019*

	Azithromycin MICs, μg/mL (no. isolates)					
	2–16 (91)				>256 (5)	
Antimicrobial drug	MIC_{50}	MIC_{90}	Range	Resistance, %	MIC	Resistance, %
Ciprofloxacin	0.004	16	0.001–32	28.6	0.002–4	20
Tetracycline	1	2	0.125–4	25.3	0.5–2	20
Benzylpenicillin	1	2	0.25–8	14.3	0.5–1	0
Ceftriaxone	0.004	0.03	0.002–0.06	0	0.004–0.016	0
Cefixime	0.016	0.03	0.004–0.125	0	0.008–0.03	0
Spectinomycin	32	32	16–32	0	32	0
Gentamicin	8	8	4–16	0	8–16	0

*MIC_{50}, MIC for 50% of isolates; MIC_{90}, MIC for 90% of isolates.
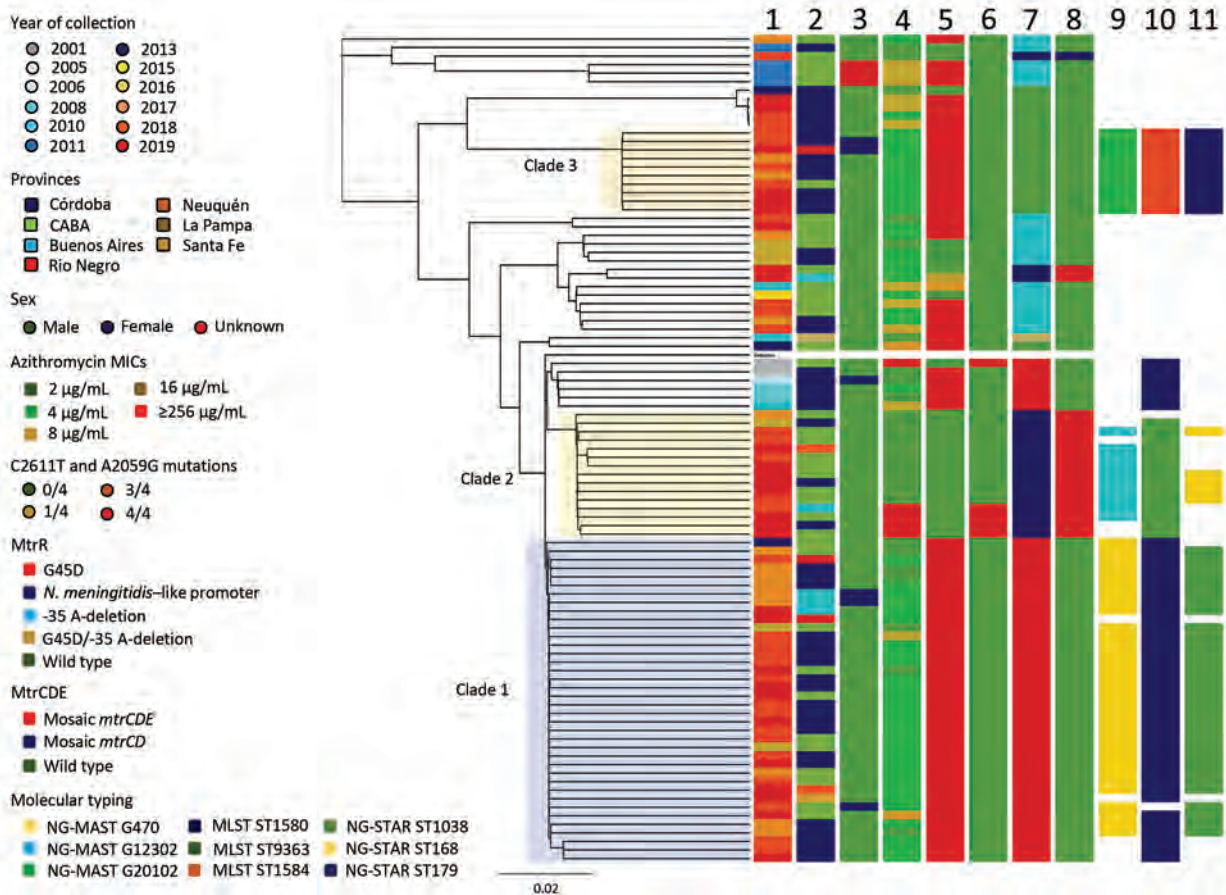
Figure 2. Phylogenomic tree of 96 *Neisseria gonorrhoeae* isolates with azithromycin MICs of ≥2 μg/mL, Argentina, January 2005–November 2019. Lane 1, year; lane 2, province; lane 3, sex; lane 4, azithromycin MICs; lane 5, 23S C2611T; lane 6, 23S A25059G; lane 7, MtrR; lane 8, MtrCDE; lane 9, NG-MAST; lane 10, MLST; lane 11, NG-STAR. Scale bar indicates substitutions per site. CABA, Ciudad Autónoma de Buenos Aires; MLST, multilocus sequence typing; NG-MAST, *N. gonorrhoeae* multiantigen sequence typing; NG-STAR, *N. gonorrhoeae* sequence typing for antimicrobial resistance; ST, sequence type.

isolates from Argentina and other countries were 6.8 (range 1–23) for the isolates from the United States, 6.9 (range 1–22) for isolates from Australia, 7.9 (range 4–22) for isolates from Scotland, 11.4 (range 4–28) for isolates from Brazil, and 16.8 (range 13–31) for isolates from the United Kingdom (excluding Scotland). Isolates from Scotland and the United Kingdom had MICs of ≥256 μg/mL whereas isolates from the United States, Australia, and Brazil had MICs of 2–8 μg/mL. All isolates with MICs of 2–8 μg/mL had the 23S rRNA C2611T mutation and all isolates with MICs of ≥256 μg/mL had the A2059G mutation. In addition, 2 isolates from Brazil had mosaic *mtrD* alleles, but no mutations in the 23S rRNA gene; these isolates had MICs of 2 μg/mL. The ST9363 isolates from Argentina clustered with other ST9363 isolates from the United States, Australia, Canada, Brazil, and Norway. ST9363 isolates

from Argentina had a mean pairwise SNP difference of 7.7 (range 0–20) with isolates from Brazil, 10.1 (range 1–23) with isolates from Norway, 12.5 (range 5–25) with isolates from Canada, 13.1 (range 2–42) with isolates from the United States, and 14.8 (range 2–35) with isolates from Australia. All isolates had mosaic *mtrR* promoters and *mtrD* alleles. All isolates with MICs of ≥256 μg/mL had the 23S rRNA A2059G mutation and 4 isolates with MICs of 8–16 μg/mL had the 23S rRNA C2611T mutation.

Conclusion

We characterized the genomes of azithromycin-resistant *N. gonorrhoeae* isolates collected in Argentina during 2005–2019. Phylogenomic analysis showed that isolates from Argentina clustered into distinct clades, including 3 clades comprising 63 (65.6%) isolates collected during 2016–2019. All isolates also were

resistant to benzylpenicillin, tetracycline, ciprofloxacin or some combination, but susceptible to ceftriaxone and cefixime.

In Argentina, dual therapy is recommended as first-line treatment for uncomplicated gonorrhea, according to the WHO guidelines (*6*). The Argentine Ministry of Health and the Sociedad Argentina de Infectología recommend a single 1-g dose of azithromycin monotherapy for the treatment of *Chlamydia trachomatis* and *Mycoplasma genitalium* infections (*41,42*). These guidelines also recommend antimicrobial treatment for suspected infections. Azithromycin has a long half-life, resulting in detectable drug concentrations in human plasma for up to 14 days (*43*). Undiagnosed *N. gonorrhoeae* infections concurrent with the treatment of *C. trachomatis* and *M. genitalium* infections might lead to prolonged exposure to subinhibitory concentrations of azithromycin, thereby prompting the induction of or selection for resistance genes. In the United States and United Kingdom, dual therapy is no longer the first-line treatment. Instead, high-dose ceftriaxone monotherapy (500 mg in the United States or 1 g in the United Kingdom) is now recommended for treatment of uncomplicated gonorrhea (*44,45*). Moreover, additional treatment with doxycycline (100 mg 2×/d for 7 d) is recommended if

chlamydial infection has not been excluded (*44*). Similar empirical antimicrobial therapies for gonorrhea and chlamydial infections might be of benefit in Argentina to reduce patient exposure to azithromycin and avoid the emergence of resistant gonococcal strains.

Azithromycin resistance (i.e., MICs of ≥ 2 μg/mL) in *N. gonorrhoeae* has been mainly associated with mutations in the 23S rRNA target (*38*). The 23S rRNA A2059G mutation causes high-level resistance (i.e., MICs of ≥ 256 μg/mL) and the C2611T mutation causes low-level resistance (i.e., MICs of 2–16 μg/mL) (*38*). We found that 75% of isolates had the C2611T mutation. These isolates were phylogenetically diverse; however, clade 1, which was predominated by MLST ST1580 and NG-MAST G470, comprised 38 (52.8%) isolates. NG-MAST ST470 has been associated with high-level resistance to azithromycin in Scotland (*18*). In addition, NG-MAST ST470 has >99% similarity to ST9768, which caused an outbreak of high-level azithromycin-resistant *N. gonorrhoeae* in the United Kingdom (*16*). Previous gonococcal evolution studies have estimated that ≈4 (range 0–14) SNPs occur per year per genome, enabling phylogenetic analysis (*21*). Isolates from Argentina differed from isolates from Scotland by ≥ 4 (mean 7.9) SNPs and the United Kingdom by 13 (mean 16.8) SNPs. In addition,
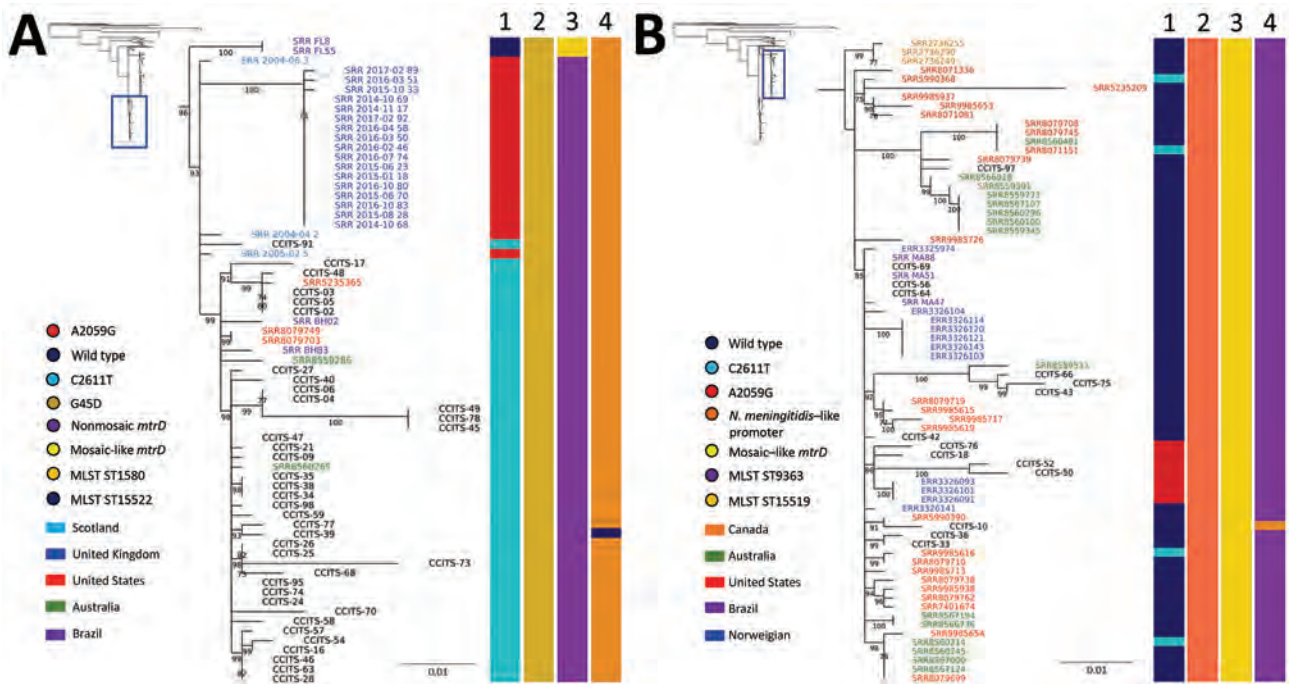
Figure 3. Phylogenomic tree of *Neisseria gonorrhoeae* isolates with azithromycin MICs of ≥ 2 μg/mL, 2004–2017. A) MLST ST1580 and NG-MAST genogroup 470 isolates from Argentina in the context of selected isolates from Scotland (2004–2005), the United States (2016), Australia (2017), Brazil (2015–2016), and the United Kingdom (2014–2017). B) MLST ST9363 and NG-MAST genogroup G12302 isolates from Argentina in the context of selected isolates from Australia (2017), the United States (2014–2017), Brazil (2015–2016), Norway (2017), and Canada (2013–2014). Lane 1, 23S rRNA; lane 2, *mtrR*; lane 3, *mtrD*; lane 4, MLST. Labels indicate isolate identity; font colors indicate country of isolation. Bar colors indicate distribution of mutations. Insets indicate relationship of sequences to larger phylogenetic tree. Scale bar indicates substitutions per site. MLST, multilocus sequence typing; NG-MAST, *N. gonorrhoeae* multiantigen sequence typing.

NG-MAST ST470 isolates from the United States, Brazil, and Australia, all of which showed low-level resistance to azithromycin, were closely related to isolates from Argentina (mean 7–11 SNPs). These findings support the hypothesis that NG-MAST G470 strains from Argentina might be descended from 1 lineage of the ST470 clone, which has spread internationally and can develop high-level and low-level resistance to azithromycin. Previous research, especially that of Unemo et al. (*38*), hypothesized that gonococcal antimicrobial-resistant strains emerge through genetic events, such as horizontal gene transfer or spontaneous mutations; these strains can spread quickly within a geographic region through sexual networks. Furthermore, compensatory mutations or gene exchange might have preserved this lineage in Argentina. The presence of additional STs, such as the co-circulation of MLST ST1584 and MLST ST1580 (NG-MAST G470), suggests that novel introductions also have occurred.

The *mtr* locus recently has been described as a hotspot for genetic recombination; mosaic-like *mtr* loci are associated with decreased susceptibility to azithromycin (i.e., MICs of 1–4 µg/mL) and contribute to the survival and transmission of *N. gonorrhoeae* (*39,40*, *46*). Most clade 2 isolates were associated with MLST ST9363 and had a mosaic-like *mtr* locus. MLST ST9363 was the predominant strain type of isolates with MICs of 2–4 µg/mL identified in Australia during 2017 and the United States during 2014–2017 (*24,25,35*). We found that MLST ST9363 isolates from Argentina shared a high level of genomic similarity with the ST9363 clones reported in Australia, the United States, Canada, Norway, and Brazil, indicating that importation and dissemination has occurred. Those data further support the hypothesis that *N. gonorrhoeae* isolates carrying a mosaic-like *mtr* locus contribute to the emergence of isolates with low-level resistance to azithromycin in many countries (*24,25*). Isolates with MICs of ≥256 µg/mL have recently re-emerged in Argentina (*20*). Those isolates belonged to clade 2 and were distinguished by the mosaic-like *mtr* locus and the A2059G mutation in all 4 23S rRNA gene alleles. The phylogenetic tree showed that these isolates were closely related to isolates from Norway (mean 10.2 SNPs) that also had MICs of ≥256 µg/mL, suggesting that strains carrying a mosaic-like *mtr* locus and 23S rRNA A2059G mutation can disseminate internationally. Previous studies have suggested that isolates carrying the A2059G mutation or mosaic *mtr* locus have enhanced fitness; elucidating the effects of both mechanisms on *N. gonorrhoeae* evolution might help predict the emergence and spread of azithromycin resistance (*39,46,47*).

Because we received a small number of isolates from some provinces, our dataset might have been limited by selection bias. In addition, we did not have access to therapy strategies and treatment success rates, which might have provided insight into the generation of resistance or the selection of azithromycin-resistant isolates. Finally, we obtained limited data regarding patients' sexual orientation and HIV status, but found that clade 2 strains were slightly more associated with male patients, including men who have sex with men, than clade 1 strains (100.0% vs. 92.1%). In addition, 3 patients who had infections caused by clade 2 strains were HIV-positive (data not shown). Increased awareness of the transmission dynamics of azithromycin-resistant gonococcal strains within sexual networks is crucial to confirming these observations. Continuing surveillance of the prevalence and distribution of azithromycin-resistant strains in addition to genomic monitoring using individual-level epidemiologic data should provide a more complete picture of azithromycin-resistant gonococcal strains. These data will inform public health strategies to control azithromycin-resistant *N. gonorrhoeae*.

In conclusion, the recent increase in the prevalence of azithromycin-resistant *N. gonorrhoeae* isolates in Argentina was mainly the result of the introduction and expansion of 2 clones belonging to MLST ST1580 and ST9363. The integration of appropriate STI diagnosis and antimicrobial prescription into health services combined with genomic, phenotypic, and epidemiologic gonococcal surveillance data will be critical in preventing the dissemination of gonococcal clones resistant to azithromycin, ceftriaxone, or both, and preserving the current available therapeutic option for gonorrhea.

Acknowledgments

About the Author

Mr. Gianecini is a microbiologist at the Instituto Nacional de Enfermedades Infecciosas—Administración Nacional de Laboratorios e Institutos de Salud Dr. Carlos G. Malbrán in la Ciudad Autónoma de Buenos Aires, Argentina. His primary research interests include public health and antimicrobial resistance.

References

1. Rowley J, Vander Hoorn S, Korenromp E, Low N, Unemo M, Abu-Raddad LJ, et al. Chlamydia, gonorrhoea, trichomoniasis and syphilis: global prevalence and incidence estimates, 2016. Bull World Health Organ. 2019;97:548–562P. https://doi.org/10.2471/BLT.18.228486
2. Wi T, Lahra MM, Ndowa F, Bala M, Dillon JR, Ramon-Pardo P, et al. Antimicrobial resistance in *Neisseria gonorrhoeae*: global surveillance and a call for international collaborative action. PLoS Med. 2017;14:e1002344. https://doi.org/10.1371/journal.pmed.1002344
3. Unemo M, Lahra MM, Cole M, Galarza P, Ndowa F, Martin I, et al. World Health Organization Global Gonococcal Antimicrobial Surveillance Program (WHO GASP): review of new data and evidence to inform international collaborative actions and research efforts. Sex Health. 2019;16:412–25. https://doi.org/10.1071/SH19023
4. Unemo M. Current and future antimicrobial treatment of gonorrhoea—the rapidly evolving *Neisseria gonorrhoeae* continues to challenge. BMC Infect Dis. 2015;15:364. https://doi.org/10.1186/s12879-015-1029-2
5. Unemo M, Ross J, Serwin AB, Gomberg M, Cusini M, Jensen JS. 2020 European guideline for the diagnosis and treatment of gonorrhoea in adults. Int J STD AIDS. 2020;2020:956462420949126.
6. World Health Organization. WHO guidelines for the treatment of *Neisseria gonorrhoeae*. 2016 [cited 2020 Dec 4]. http://www.who.int/reproductivehealth/publications/rtis/gonorrhoea-treatment-guidelines/en
7. Fifer H, Natarajan U, Jones L, Alexander S, Hughes G, Golparian D, et al. Failure of dual antimicrobial therapy in treatment of gonorrhoea. N Engl J Med. 2016;374:2504–6. https://doi.org/10.1056/NEJMc1512757
8. Whiley DM, Jennison A, Pearson J, Lahra MM. Genetic characterisation of *Neisseria gonorrhoeae* resistant to both ceftriaxone and azithromycin. Lancet Infect Dis. 2018;18:717–8. https://doi.org/10.1016/S1473-3099(18)30340-2
9. Eyre DW, Sanderson ND, Lord E, Regisford-Reimmer N, Chau K, Barker L, et al. Gonorrhoea treatment failure caused by a *Neisseria gonorrhoeae* strain with combined ceftriaxone and high-level azithromycin resistance, England, February 2018. Euro Surveill. 2018;23:1800323. https://doi.org/10.2807/1560-7917.ES.2018.23.27.1800323
10. Jennison AV, Whiley D, Lahra MM, Graham RM, Cole MJ, Hughes G, et al. Genetic relatedness of ceftriaxone-resistant and high-level azithromycin resistant *Neisseria gonorrhoeae* cases, United Kingdom and Australia, February to April 2018. Euro Surveill. 2019;24:1900118. https://doi.org/10.2807/1560-7917.ES.2019.24.8.1900118
11. Williamson DA, Fairley CK, Howden BP, Chen MY, Stevens K, De Petra V, et al. Trends and risk factors for antimicrobial-resistant *Neisseria gonorrhoeae*, Melbourne, Australia, 2007 to 2018. Antimicrob Agents Chemother. 2019;63:e01221–19. https://doi.org/10.1128/AAC.01221-19
12. US Centers for Disease Control and Prevention. Sexually transmitted disease surveillance 2017. 2018 [cited 2020 Dec 4]. https://www.cdc.gov/std/stats17/2017-STD-Surveillance-Report_CDC-clearance-9.10.18.pdf
13. Thakur SD, Araya P, Borthagaray G, Galarza P, Hernandez AL, Payares D, et al. Resistance to ceftriaxone and azithromycin in *Neisseria gonorrhoeae* isolates from 7 countries of South America and the Caribbean: 2010–2011. Sex Transm Dis. 2017;44:157–60. https://doi.org/10.1097/OLQ.0000000000000587
14. Ministerio de Salud y Desarrollo Social. Bulletin on HIV/AIDS and STIS in Argentina no. 36 [in Spanish]. 2019 [cited 2020 Dec 4]. https://bancos.salud.gob.ar/recurso/boletin-sobre-el-vih-sida-e-its-en-la-argentina-ndeg-36
15. Clinical and Laboratory Standards Institute. 2019. Performance standards for antimicrobial susceptibility testing: twenty-ninth informational supplement (M100–S29). Wayne (PA): The Institute; 2019.
16. Fifer H, Cole M, Hughes G, Padfield S, Smolarchuk C, Woodford N, et al. Sustained transmission of high-level azithromycin-resistant *Neisseria gonorrhoeae* in England: an observational study. Lancet Infect Dis. 2018;18:573–81. https://doi.org/10.1016/S1473-3099(18)30122-1
17. Demczuk W, Martin I, Peterson S, Bharat A, Van Domselaar G, Graham M, et al. Genomic epidemiology and molecular resistance mechanisms of azithromycin-resistant *Neisseria gonorrhoeae* in Canada from 1997 to 2014. J Clin Microbiol. 2016;54:1304–13. https://doi.org/10.1128/JCM.03195-15
18. Palmer HM, Young H, Winter A, Dave J. Emergence and spread of azithromycin-resistant *Neisseria gonorrhoeae* in Scotland. J Antimicrob Chemother. 2008;62:490–4. https://doi.org/10.1093/jac/dkn235
19. Jacobsson S, Golparian D, Cole M, Spiteri G, Martin I, Bergheim T, et al. WGS analysis and molecular resistance mechanisms of azithromycin-resistant (MIC >2 mg/L) *Neisseria gonorrhoeae* isolates in Europe from 2009 to 2014. J Antimicrob Chemother. 2016;71:3109–16. https://doi.org/10.1093/jac/dkw279
20. Galarza PG, Alcalá B, Salcedo C, Canigia LF, Buscemi L, Pagano I, et al. Emergence of high level azithromycin-resistant *Neisseria gonorrhoeae* strain isolated in Argentina. Sex Transm Dis. 2009;36:787–8. https://doi.org/10.1097/OLQ.0b013e3181b61bb1
21. De Silva D, Peters J, Cole K, Cole MJ, Cresswell F, Dean G, et al. Whole-genome sequencing to determine transmission of *Neisseria gonorrhoeae*: an observational study. Lancet Infect Dis. 2016;16:1295–303. https://doi.org/10.1016/S1473-3099(16)30157-8
22. Harris SR, Cole MJ, Spiteri G, Sánchez-Busó L, Golparian D, Jacobsson S, et al.; Euro-GASP study group. Public health surveillance of multidrug-resistant clones of *Neisseria gonorrhoeae* in Europe: a genomic survey. Lancet Infect Dis. 2018;18:758–68. https://doi.org/10.1016/S1473-3099(18)30225-1

23. Grad YH, Harris SR, Kirkcaldy RD, Green AG, Marks DS, Bentley SD, et al. Genomic epidemiology of gonococcal resistance to extended-spectrum cephalosporins, macrolides, and fluoroquinolones in the United States, 2000–2013. J Infect Dis. 2016;214:1579–87. https://doi.org/10.1093/infdis/jiw420

24. Williamson DAF, Chow EPF, Gorrie CL, Seemann T, Ingle DJ, Higgins N, et al. Bridging of *Neisseria gonorrhoeae* lineages across sexual networks in the HIV pre-exposure prophylaxis era. Nat Commun. 2019;10:3988. https://doi.org/10.1038/s41467-019-12053-4

25. Gernert KM, Seby S, Schmerer MW, Thomas JC IV, Pham CD, St Cyr S, et al.; Antimicrobial-Resistant *Neisseria gonorrhoeae* Working Group. Azithromycin susceptibility of *Neisseria gonorrhoeae* in the USA in 2017: a genomic analysis of surveillance data. Lancet Microbe. 2020;1:e154–64. https://doi.org/10.1016/S2666-5247(20)30059-8

26. Gianecini RA, Zittermann S, Oviedo C, Galas M, Pardo PR, Allen VG, et al. Use of whole genome sequencing for the molecular comparison of *Neisseria gonorrhoeae* isolates with decreased susceptibility to extended spectrum cephalosporins from 2 geographically different regions in America. Sex Transm Dis. 2019;46:548–55. https://doi.org/10.1097/OLQ.0000000000001011

27. World Health Organization. Laboratory diagnosis of sexually transmitted infections, including human immunodeficiency virus. 2013 [cited 2020 Dec 4]. http://apps.who.int/iris/bitstream/10665/85343/1/9789241505840_eng.pdf

28. Gianecini RA, Golparian D, Zittermann S, Litvik A, Gonzalez S, Oviedo C, et al.; Gonococcal Antimicrobial Susceptibility Surveillance Programme—Argentina Working Group. Genome-based epidemiology and antimicrobial resistance determinants of *Neisseria gonorrhoeae* isolates with decreased susceptibility and resistance to extended-spectrum cephalosporins in Argentina in 2011-16. J Antimicrob Chemother. 2019;74:1551–9. https://doi.org/10.1093/jac/dkz054

29. Hunt M, Mather AE, Sánchez-Busó L, Page AJ, Parkhill J, Keane JA, et al. ARIBA: rapid antimicrobial resistance genotyping directly from sequencing reads. Microb Genom. 2017;3:e000131. https://doi.org/10.1099/mgen.0.000131

30. Martin IM, Ison CA, Aanensen DM, Fenton KA, Spratt BG. Rapid sequence-based identification of gonococcal transmission clusters in a large metropolitan area. J Infect Dis. 2004;189:1497–505. https://doi.org/10.1086/383047

31. Demczuk W, Sidhu S, Unemo M, Whiley DM, Allen VG, Dillon JR, et al. *Neisseria gonorrhoeae* sequence typing for antimicrobial resistance, a novel antimicrobial resistance multilocus typing scheme for tracking global dissemination of *N. gonorrhoeae* strains. J Clin Microbiol. 2017;55:1454–68. https://doi.org/10.1128/JCM.00100-17

32. Nguyen LT, Schmidt HA, von Haeseler A, Minh BQ. IQ-TREE: a fast and effective stochastic algorithm for estimating maximum-likelihood phylogenies. Mol Biol Evol. 2015;32:268–74. https://doi.org/10.1093/molbev/msu300

33. Hadfield J, Croucher NJ, Goater RJ, Abudahab K, Aanensen DM, Harris SR. Phandango: an interactive viewer for bacterial population genomics. Bioinformatics. 2018;34:292–3.

34. Pommier T, Canbäck B, Lundberg P, Hagström A, Tunlid A. RAMI: a tool for identification and characterization of phylogenetic clusters in microbial communities. Bioinformatics. 2009;25:736–42. https://doi.org/10.1093/bioinformatics/btp051

35. Thomas JC, Seby S, Abrams AJ, Cartee J, Lucking S, Vidyaprakash E, et al.; Antimicrobial-Resistant Neisseria gonorrhoeae Working Group. Evidence of recent genomic evolution in gonococcal strains with decreased susceptibility to cephalosporins or azithromycin in the United States, 2014–2016. J Infect Dis. 2019;220:294–305. https://doi.org/10.1093/infdis/jiz079

36. Golparian D, Bazzo ML, Golfetto L, Gaspar PC, Schörner MA, Schwartz Benzaken A, et al.; Brazilian—GASP Network. Genomic epidemiology of *Neisseria gonorrhoeae* elucidating the gonococcal antimicrobial resistance and lineages/sublineages across Brazil, 2015–16. J Antimicrob Chemother. 2020;75:3163–72. https://doi.org/10.1093/jac/dkaa318

37. Alfsnes K, Eldholm V, Olsen AO, Brynildsrud OB, Bohlin J, Steinbakk M, et al. Genomic epidemiology and population structure of *Neisseria gonorrhoeae* in Norway, 2016–2017. Microb Genom. 2020;6:e000359. https://doi.org/10.1099/mgen.0.000359

38. Unemo M, Shafer WM. Antimicrobial resistance in *Neisseria gonorrhoeae* in the 21st century: past, evolution, and future. Clin Microbiol Rev. 2014;27:587–613. https://doi.org/10.1128/CMR.00010-14

39. Wadsworth CB, Arnold BJ, Sater MRA, Grad YH. Azithromycin resistance through interspecific acquisition of an epistasis-dependent efflux pump component and transcriptional regulator in *Neisseria gonorrhoeae.* MBio. 2018;9:e01419–18. https://doi.org/10.1128/mBio.01419-18

40. Rouquette-Loughlin CE, Reimche JL, Balthazar JT, Dhulipala V, Gernert KM, Kersh EN, et al. Mechanistic basis for decreased antimicrobial susceptibility in a clinical isolate of *Neisseria gonorrhoeae* possessing a mosaic-like *mtr* efflux pump locus. MBio. 2018;9:e02281–18. https://doi.org/10.1128/mBio.02281-18

41. Ministerio de salud y ambiente de la nación. Management guide for sexually transmitted infections [in Spanish]. Buenos Aires: El Ministerio; 2004.

42. Sociedad Argentina de Infectología. First consensus on the diagnosis, treatment, and prevention of sexually transmitted infections [in Spanish]. 2011 [cited 2020 Dec 4]. https://drive.google.com/file/d/1VqW7USdEyO5FkJXwB239f8pudQ9MbDUr/view

43. Kong FYS, Horner P, Unemo M, Hocking JS. Pharmacokinetic considerations regarding the treatment of bacterial sexually transmitted infections with azithromycin: a review. J Antimicrob Chemother. 2019;74:1157–66. https://doi.org/10.1093/jac/dky548

44. St Cyr S, Barbee L, Workowski KA, Bachmann LH, Pham C, Schlanger K, et al. Update to CDC's treatment guidelines for gonococcal infection, 2020. MMWR Morb Mortal Wkly Rep. 2020;69:1911–6. https://doi.org/10.15585/mmwr.mm6950a6

45. Fifer H, Saunders J, Soni S, Sadiq ST, FitzGerald M. 2018 UK national guideline for the management of infection with *Neisseria gonorrhoeae.* Int J STD AIDS. 2020;31:4–15. https://doi.org/10.1177/0956462419886775

46. Handing JW, Ragland SA, Bharathan UV, Criss AK. The MtrCDE efflux pump contributes to survival of *Neisseria gonorrhoeae* from human neutrophils and their antimicrobial components. Front Microbiol. 2018;9:2688. https://doi.org/10.3389/fmicb.2018.02688

47. Zhang J, van der Veen S. *Neisseria gonorrhoeae* 23S rRNA A2059G mutation is the only determinant necessary for high-level azithromycin resistance and improves in vivo biological fitness. J Antimicrob Chemother. 2019;74:407–15. https://doi.org/10.1093/jac/dky438

Address for correspondence: Patricia Galarza, National Institute of Infectious Diseases—ANLIS Dr. Carlos G. Malbrán, Velez Sarsfield 563, C1282AFF, Ciudad Autónoma de Buenos Aires, Argentina; email: pgalarza@anlis.gob.ar.

Development and Clinical Evaluation of a CRISPR-Based Diagnostic for Rapid Group B *Streptococcus* Screening

Lingxiao Jiang,[1] Weiqi Zeng,[1] Wanting Wu,[1] Yingying Deng, Fusheng He, Wenli Liang, Mingyao Huang, Hong Huang, Yongjun Li, Xiaorui Wang, Hang Su, Shilei Pan, Teng Xu[1]

Vertical transmission of group B *Streptococcus* (GBS) is among the leading causes of neonatal illness and death. Colonization with GBS usually is screened weeks before delivery during pregnancy, on the basis of which preventive measures, such as antibiotic prophylaxis, were taken. However, the accuracy of such an antenatal screening strategy has been questionable because of the intermittent nature of GBS carriage. We developed a simple-to-use, rapid, CRISPR-based assay for GBS detection. We conducted studies in a prospective cohort of 412 pregnant women and a retrospective validation cohort to evaluate its diagnostic performance. We demonstrated that CRISPR-GBS is highly sensitive and offered shorter turnaround times and lower instrument demands than PCR-based assays. This novel GBS test exhibited an overall improved diagnostic performance over culture and PCR-based assays and represents a novel diagnostic for potential rapid, point-of-care GBS screening.

Group B *Streptococcus* (GBS) is a common commensal bacteria of vaginal flora with reported carriage rates of 4%–40% (*1–3*). Vertical transmission of (GBS) through fetal aspiration of infected amniotic fluid or during birth canal passage has been considered one of the most important causes of neonatal illness and death (*3,4*). GBS colonization during pregnancy has been a leading cause of severe neonatal

Author affiliations: Zhujiang Hospital, Southern Medical University, Guangzhou, China (L. Jiang, Y. Deng, W. Liang, M. Huang); Vision Medicals Center for Medical Research, Shenzhen, China (W. Zeng, W. Wu, H. Huang, Y. Li, X. Wang, H. Su, T. Xu); Key Laboratory of Animal Gene Editing and Animal Cloning in Yunnan Province and College of Veterinary Medicine, Yunnan Agricultural University, Kunming, China (W. Zeng, T. Xu); Zhujiang Hospital, Southern Medical University, Guangzhou (S. Pan)

infectious diseases, including sepsis, pneumonia, and meningitis (*5,6*). Early onset neonatal infections can be prevented in most cases by providing intrapartum antibiotic prophylaxis to the colonized mother (*7*). However, GBS carriages are often intermittent, and the rate of GBS colonization varies during pregnancy (*1,8*). On the other hand, use of antibiotic prophylaxis solely relying on risk assessment leads to unnecessary treatment in many women. Therefore, determination of colonization at the time of delivery is crucial for the prevention of neonatal infection (*9*).

Culture-based methods remain the most commonly used screening practice and the standard for GBS detection; however, because of technical limitations, including turnaround time, pregnant women are usually screened for GBS at 35–37 weeks of gestation (*6*). As many studies have pointed out, the predictive value of GBS decreases as the interval time increases between screening and delivery (*10,11*). These studies underlie the needs for a more rapid and sensitive diagnostic for intrapartum GBS screening.

CRISPR/Cas has been widely used as a programmable tool for gene editing and other in vivo applications since 2013 (*12–14*). However, recently, the collateral, promiscuous cleavage activities of a unique group of Cas enzymes were discovered and harnessed for in vitro nucleic acid detection (*15–17*).

To address the unmet clinical needs for GBS screening, we developed CRISPR-GBS, a novel CRISPR/Cas13-based in vitro diagnostic assay, and conducted a prospective cohort study and a validation study in >400 clinical cases to evaluate its diagnostic performance among different technology platforms, including culture and PCR-based methods. Our findings demonstrate that CRISPR-GBS is rapid and easy-

to-use, having a low instrument requirement and a level of sensitivity that surpasses PCR-based assays.

Materials and Methods

Study Participants and Sample Collection

A total of 426 pregnant women were prospectively admitted into Zhujiang Hospital (Guangzhou, China) for antenatal care during March 7–November 22, 2019. We excluded 14 from this cohort study because of insufficient samples for testing, incomplete clinical or experimental data, or invalid test results attributable to internal control failures. We included the remaining 412 samples in the prospective cohort study, in which direct culture, direct clinically validated PCR, and CRISPR-GBS tests were performed for each patient.

We conducted the validation cohort retrospectively, where we performed direct culture and CRISPR-GBS. For the purpose of validation, we included for enrichment culture 31 samples consisting of about one third each of dual-positive, dual-negative and discordant samples, according to the results of direct culture and CRISPR-GBS.

We collected vaginal–rectal swab specimens from the enrolled patients. Sample collection was reviewed and approved by the Zhujiang Hospital Ethics Committee Review Board. Informed consents were signed by patients or their surrogates.

Cas13a Protein

After codon optimization, we synthesized the open reading frame (ORF) of Cas13a and cloned it by using Gene Services (Genscript Biotech, https://www.genscript.com). The Cas13a ORF expression vector was transfected into *Escherichia coli* BL21. We first grew transfected cells at 37°C and then incubated them with isopropyl β-d-1-thiogalactopyranoside at 16°C. We purified proteins from lysed bacteria by using the Ni-NTA protocol (*18*) and stored aliquots of purified protein at −80°C.

Strains and Human DNA

We purchased the *S. agalactiae* (group B *Streptococcus*) strain from the American Type Culture Collection (ATCC13813). *S. pneumoniae*, *S. pyogenes*, *S. mitis*, *Enterococcus faecalis*, *Acinetobacter baumannii*, and *Pseudomonas aeruginosa* strains were donated by China's National Institutes for Food and Drug Control. We purchased another 2 species of bacteria, *E. coli* and *Staphylococcus aureus*, from China's General Microbiological Culture Collection Center. We purchased pure human DNA from Solarbio (http://www.solarbio.net), which we eluted in nuclease-free water.

Oligos and gRNA

Primer with an appended T7 promoter used in the recombinase polymerase amplification (RPA) for *atoB* amplification were forward primer 5′-TAAT ACGA CTCA CTAT AGGG AATT GAAT GGAA TGAA CCAT TTGC AGCG AT-3′ and reverse primer 5′-AATA ATTC CTGA GCAG GCAT AAGG GTGT C-3′. We used sgRNA for Cas13 (5′-GGGG AUUU AGAC UACC CCAA AAAC GAAG GGGA CUAA AACU CUCU CUUC AGGA UAAU AAUG AUUA AAU-3′) and ssRNA probe (5′-6-FAM-UUUUUC-BHQ1) for CRISPR detection after RPA amplification. Primer used in the nested PCR amplification for *atoB* amplification for round 1 were forward primer 5′-ACGG AAAA ACTA TTAA CAGA AACT CATA CT-3′ and reverse primer 5′-AATA ATTC CTGA GCAG GCAT AAGG GTGT C-3′ and for round 2 were forward primer 5′-CTCA TACT AAAA TATC GGAT TATG ATGC-3′ and reverse primer 5′-AGGC ATAA GGGT GTCC GTAA GC-3′.

DNA Rapid Extraction

We eluted swabs with 1 mL of saline. We transferred 200 µL of eluate to a new sterile, nuclease-free 1.5-mL tube. After a 5-minute centrifugation at 10,000 × *g*, we resuspended the pellet in lysis buffer consisting of 0.1% sodium dodecyl sulfate and 1% NP40. We added glass microbeads and used a Crystal Industries vortex mixer (https://crystalindustries.com) to disrupt the bacterial cell walls. We then heated samples at 99°C for 10 min and centrifuged them again at 14,000 × *g*. We used 2 µL of supernatant as template for each subsequent assay for GBS detection.

CRISPR-GBS

The CRISPR-GBS test combines an RPA step and a subsequent T7 transcription and Cas13 detection step, as described previously (*17*). In brief, we incubated reactions containing 2 µL of sample, 0.4 µM of each primer, 1 × reaction buffer, 14 mM of magnesium acetate, and the RPA enzyme mix at 37°C for 30 min. Then we added the amplification product to the CRISPR reaction mix, consisting of 33.3 nM of gRNA, 66.7 nM of Cas13, 5 mmol/L of each nucleotide triphosphate, 1 µL of T7 RNA polymerase (New England Biolabs, https://www.neb.com) and 166 nM of ssRNA reporter. We incubated the final reaction mix at 37°C and monitored it for fluorescence signal. We collected fluorescent signals by using an ABI7500 qPCR machine (ThermoFisher Scientific, https://www.thermofisher.com) for 20 min.

Evaluation of Limit of Detection

For the evaluation of limit of detection by the number of genomic copies, we purified DNA of the GBS strain (ATCC13813) and determined the concentration by using Qubit (ThermoFisher Scientific). We calculated the number of genomic copies by using the formula

$$\text{copies} = \frac{(6.02 \times 10^{23}) \times (\text{concentration of DNA} \times 10^{-9})}{(\text{length of DNA} \times 660)}$$

We performed serial dilution with nuclease-free water to achieve desired concentrations. For the evaluation of limit of detection by CFU per mL, we serially diluted a reference ATCC strain with known CFU with a negative sample to the desired titer before subjecting it to DNA extraction. Although accurate conversion is challenging, our and others' observations comparing DNA quantity and CFU counts showed that 1 CFU equaled ≈3–5 genome copies (data not shown) (19).

We used 2 μL of extracted DNA at each titer as templates. We performed 10 replicates at each data point.

Direct Culture and Enrichment Culture

We eluted each swab with 1 mL of saline. For direct culture, we inoculated 200 μL of eluate onto selective chromogenic GBS screening media (CHROMID Strepto B; bioMérieux, https://www.biomerieux-diagnostics.com) and incubated it at 37°C for 24 h aerobically. We incubated negative plates for another 24 h before the final plate reading. For enrichment culture, we first inoculated 200 μL of swab eluate into selective Todd Hewitt broth and incubated it at 37°C aerobically overnight. We then inoculated the enriched broth onto chromogenic Brilliance GBS agar (bioMérieux) by using the same experimental procedures as direct culture. We subjected all suspect colonies to Lancefield streptococcal grouping to confirm GBS.

PCR and Nested PCR

We performed the regular PCR testing by using a validated commercial GBS PCR kit (BEC, http://www.biochainbj.com) according to the manufacturer's instructions. We performed the nested PCR assay in 2 successive rounds of amplification. The first round amplified a larger fragment of the *atoB* gene for 35 cycles. We then subjected 2 μL of the primary PCR product to the second amplification by using a nested set of primers targeting a shorter fragment as part of the first amplicon. We then purified the amplicons from the second round and subjected them to Sanger sequencing for validation. We considered positive only those samples that both yielded PCR products after the second round of amplification and had sequences validated by Sanger.

Statistical Analysis

We conducted comparative analysis by using Pearson χ^2 test, Fisher exact test, or the Student *t*-test, where appropriate. We performed data analyses by using SPSS Statistics 22.0 (IBM, https://www.ibm.com). We considered p values <0.05 as statistically significant. All tests were 2-tailed unless indicated otherwise.

Results

Development of CRISPR-GBS

To address the challenges in clinical GBS screening, we aimed to develop a rapid, highly sensitive, and simple-to-use GBS assay by combining an RPA reaction with a CRISPR/Cas13 step for target detection (17). We established a rapid extraction method for high efficiency GBS DNA extraction by combining chemical, heat, and bead beating-based cell wall disruption, which eliminated the need for any column and organic solvents (Figure 1; Appendix Figure 1, https://wwwnc.cdc.gov/EID/article/27/9/20-0091-App1.pdf). This strategy takes advantage of both the polymerase-mediated DNA amplification and the CRISPR/Cas-mediated enzymatic signal amplification for greater sensitivity. Moreover, the rapid extraction and isothermal nature of such an assay eliminated the demand for sophisticated instruments such as thermal cyclers.

We chose the thiolase (*atoB*) gene as the target region in this assay because it is highly conserved and specific for the GBS genome (20). We screened multiple sets of RPA primers and CRISPR gRNAs targeting different regions within *atoB* (Appendix Table 2, Figure 2). The set that showed the best overall performance of sensitivity and specificity was then used in this study for assay optimization and clinical diagnostic evaluation.

We then sought to determine the analytical sensitivity by serial dilutions of GBS with negative swabs at various counts of CFU per mL. CRISPR-GBS managed to detect samples at 30 CFU/mL in 6 of 10 runs and at 60 CFU/mL in all 10 replicates (Figure 2, panel A). We further assessed the limit of detection of CRISPR-GBS by titrations of copies per reaction. The CRISPR assay consistently detected 5 copies of GBS in 10 of 10 runs and 2 copies in 4 of 10 replicates (Figure 2, panel B). These data indicate that CRISPR-GBS could detect a low number of genome copies or ≈50 CFU/mL and
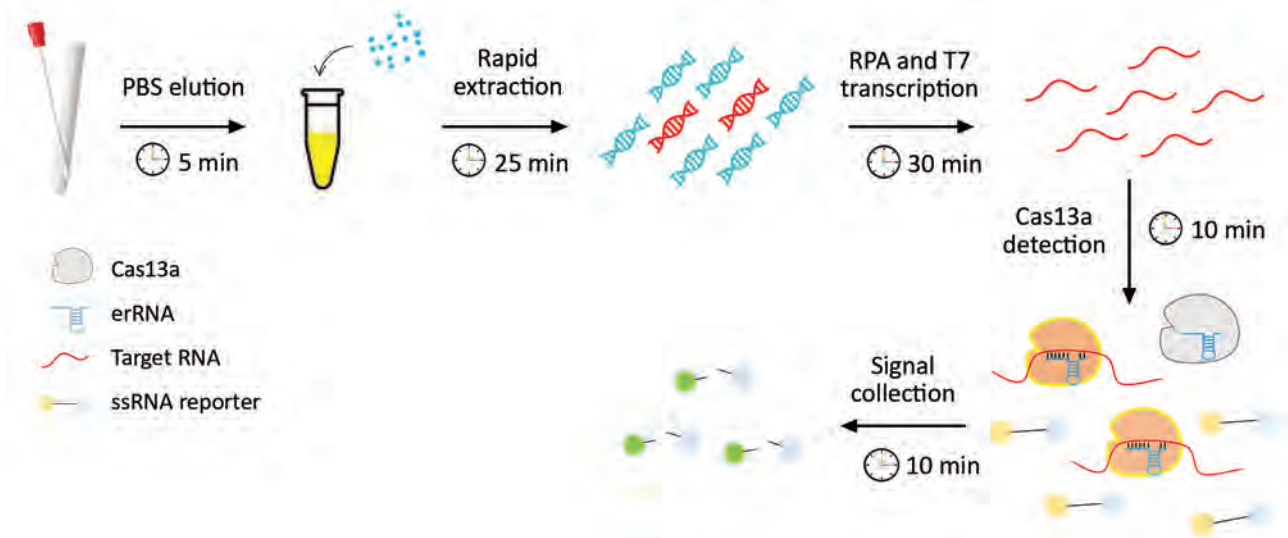
Figure 1. Schematic diagram of CRISPR-based diagnostic for rapid GBS screening. Swab samples are first eluted and followed by a rapid DNA extraction step where the bacterial cell walls are disrupted by a combination of chemical, physical, and heating effects. The extracted DNA is then subjected to the CRISPR/Cas reaction. The collateral nuclease activity of Cas proteins are activated upon specific binding of gRNA to the *atoB* gene. Fluorescent signal produced from cleaved probes is captured and indicates the presence of GBS. GBS, group B *Streptococcus.* gRNA, guide RNA; ssRNA, single-stranded RNA.

is more sensitive than most of the commercially available US Food and Drug Administration–approved GBS assays, such as GeneXpert GBS (300 CFU/mL) (Cepheid, https://www.cepheid.com), BD Max GBS (1,000 CFU/mL) (BD, https://www.bd.com), Quidel Solana GBS (2.6×10^5 CFU/mL) (Quidel, https://www.quidel.com), and AmpliVue GBS (1.4×10^6 CFU/mL) (Quidel) (*20–22*).

With such a high sensitivity of CRISPR-GBS, we set out to confirm its specificity. For this purpose, we assayed DNA from humans and a panel of bacteria, including bacteria in the same genus (e.g., *S. pneumonia*, *S. pyogenes*, and *S. mitis*), microbes commonly found in vaginal swabs (e.g., *E. coli*, *Staphylococcus aureus*, and *Enterococcus faecalis*), and bacteria commonly found in nosocomial infections (e.g., *Acinetobacter baumannii* and *Pseudomonas aeruginosa*) (*23*). Of note, none of these interference samples triggered a false-positive reaction (Figure 2, panel C). Altogether, these analytical evaluations suggest that CRISPR-GBS, with its great sensitivity and specificity, is a promising molecular assay for GBS detection.

Clinical Diagnostic Evaluation of CRISPR-GBS
After the analytical study, we further assessed the diagnostic potential of CRISPR-GBS in settings of clinical screening. A total of 426 pregnant women with a median age of 29 years (20–47 years) were enrolled in this cohort study. Sample collection was performed at 34–38 weeks of gestation. Among these patients,

14 were excluded because of invalid test results, an insufficient specimen, or both. The remaining 412 patients were tested for GBS by culture, PCR, and CRISPR-GBS on their direct swab samples. We found no significant differences between patients who were negative or positive for GBS on the basis of patient age or weeks of gestation (Appendix Table 1).

When we conducted the CRISPR-GBS assay, we included a positive control of GBS DNA and a no-template control in parallel for each run. We used a fluorescent signal from no-template control normalize the signal of other samples in the same run to calculate the corresponding fold changes. We noticed clear distinctions in signal patterns of the reactions. Specifically, the fluorescent signal curve either remained flat (e.g., the no-template control runs) or had a distinguishable takeoff from the baseline (e.g., the positive control runs) (Figure 3, panel A). To determine the cutoff value as fold-changes for the CRISPR-GBS results, we first separated all the runs into a tentatively positive group and a tentatively negative group according to these distinct patterns. We then analyzed the cutoff values. The tentatively positives had fold changes ranging from 3.9 to 90.3 (median 26.3), whereas the tentatively negatives ranged from 0.5 to 2.9 (median 1.5) (Figure 3, panel B; Appendix Figure 3). Therefore, we were able to set the cutoff value at 3.5 for complete separation of the 2 groups. Consistently, this cutoff was further confirmed by the receiver operating characteristic analysis for optimal sensitivity and specificity (data not shown).

To evaluate the diagnostic performances of different methodologies for GBS detection, we began by comparing direct culture and PCR. We found a concordance of 97.1% between these 2 traditional methods. Specifically, only 5 (1.2%) of 412 culture-positive and 7 (1.7%) of 412 PCR-positive cases were missed by the other test. When culture was used as the reference standard, PCR demonstrated a sensitivity of 90.9% (50/55 results) and specificity of 98.0% (350/357 cases).

We further assessed the CRISPR-GBS test in comparison with direct culture and the PCR-based assay (Table; Figure 4). When the comparison was made separately, CRISPR-GBS was able to detect most of the positive samples by either reference method, with a sensitivity of 94.5% (52/55 cases) compared with culture and 94.7% (54/57 cases) compared with PCR. When we included only the 400 cases with concordant culture and PCR results in the analysis, CRISPR identified 94.0% (47/50) of the positive results and offered a negative predictive value of 99.1% (320/323 cases).

Among the cases reported negative by culture, PCR, or both, we also found ≈10% of them to be positive by CRISPR, which included 37 of 357 culture-negative cases, 35 of 355 PCR-negative cases, and 30 of 350 dual-negative cases (i.e., by culture and PCR). These data indicate a greater sensitivity or a lower specificity of CRISPR-GBS.
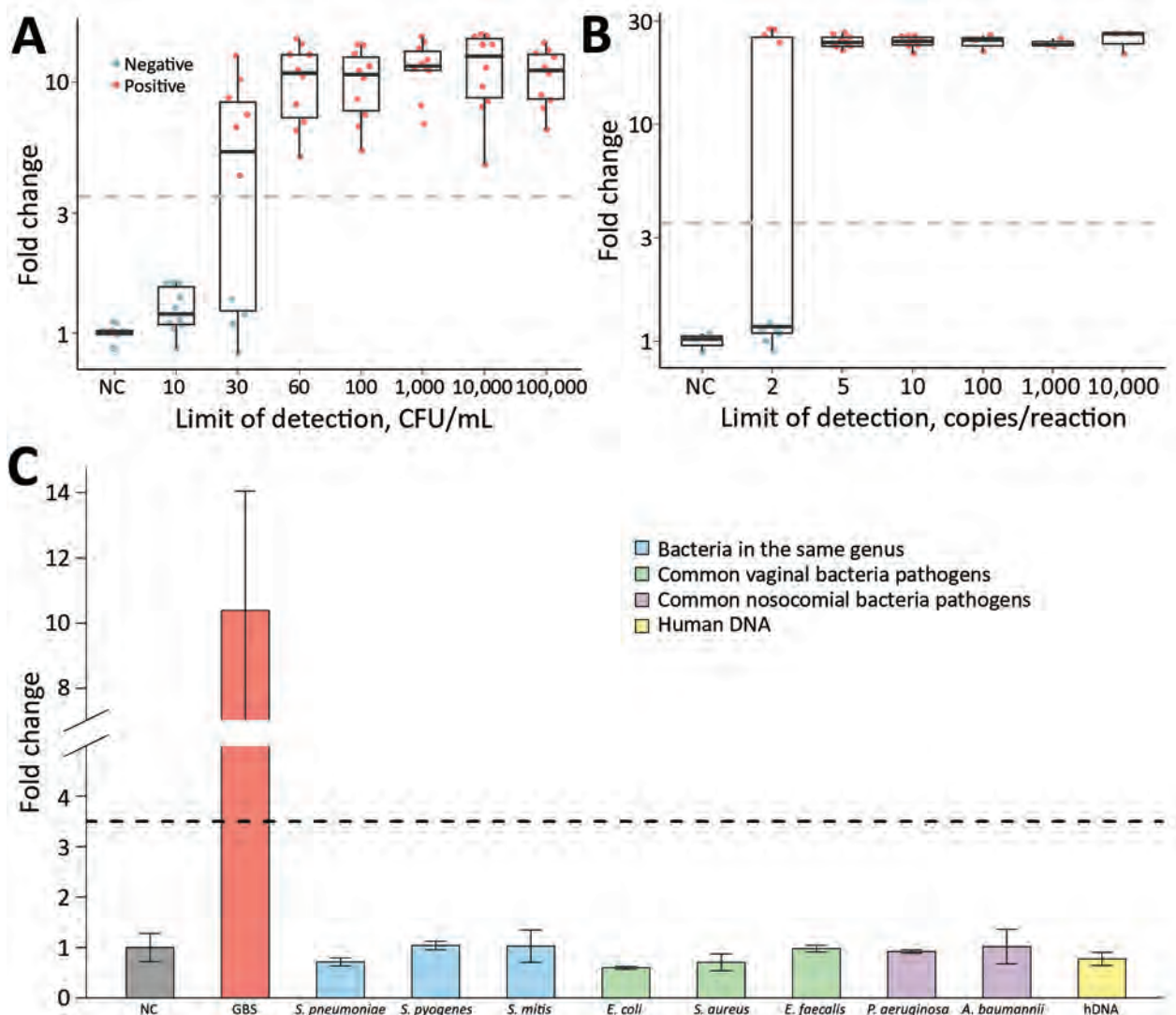
Figure 2. Analytical assessment of the sensitivity and specificity of CRISPR-based diagnostic for rapid GBS screening. Evaluation was performed by testing contrived negative swab samples with indicated CFUs of GBS (A), different copy numbers of GBS genomic DNA (B), and various microbes as interfering materials (C). GBS, group B *Streptococcus*. A. baumannii, *Acinetobacter baumannii*; *E. coli, Escherichia coli*; *E. faecalis*, *Enterococcus faecalis*; hDNA, human DNA; *P.aeruginosa, Pseudomonas aeruginosa*; *S. aureus, Staphylococcus aureus*; *S. mitis*, *Streptococcus mitis*; *S. pneumoniae, Streptococcus pneumoniae*; *S. pyogenes, Streptococcus pyogenes*.
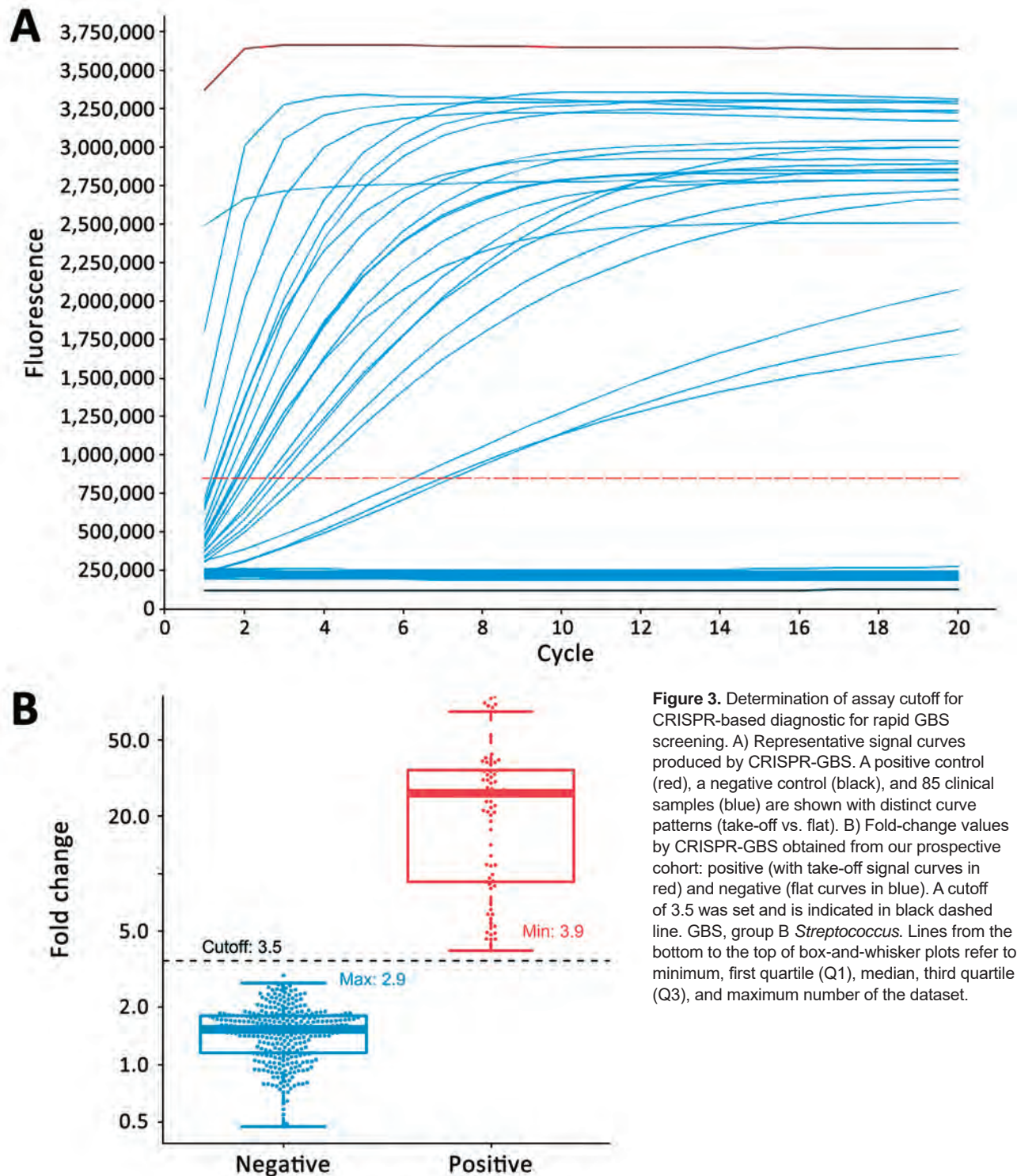
Figure 3. Determination of assay cutoff for CRISPR-based diagnostic for rapid GBS screening. A) Representative signal curves produced by CRISPR-GBS. A positive control (red), a negative control (black), and 85 clinical samples (blue) are shown with distinct curve patterns (take-off vs. flat). B) Fold-change values by CRISPR-GBS obtained from our prospective cohort: positive (with take-off signal curves in red) and negative (flat curves in blue). A cutoff of 3.5 was set and is indicated in black dashed line. GBS, group B *Streptococcus*. Lines from the bottom to the top of box-and-whisker plots refer to minimum, first quartile (Q1), median, third quartile (Q3), and maximum number of the dataset.

We designed and conducted additional validation studies in an attempt to validate the improved sensitivity of CRISPR-GBS. We developed a nested PCR–Sanger assay targeting the *atoB* gene, in which we performed 2 successive rounds of PCR in a nested manner to achieve greater amplification sensitivity compared with regular single-round PCR reactions. We then subjected the amplicons to Sanger sequencing for further validation. With this nested PCR assay, we tested the 30 specimens that were only positive by

Table. Positive and negative agreement of CRISPR-based diagnostic for rapid group B *Streptococcus* screening versus different reference standards*

| Assay and result | CRISPR-GBS | | | % (95% CI) | | | |
	Positive	Negative	Total	Sensitivity	Specificity	Positive predictive value	Negative predictive value
Direct culture							
Positive	52	3	55	94.5 (83.9–98.6)	89.6 (85.9–92.5)	58.4 (47.5–68.6)	99.1 (97.1–99.8)
Negative	37	320	357				
Total	89	323	412				
PCR							
Positive	54	3	57	94.7 (84.5–98.6)	90.1 (86.4–92.9)	60.7 (49.7–70.7)	99.1 (97.1–99.8)
Negative	35	320	355				
Total	89	323	412				
Direct culture and PCR							
Positive	47	3	50	94.0 (82.5–98.4)	91.4 (87.9–94.0)	61.0 (49.2–71.7)	99.0 (97.1–99.8)
Negative	30	320	350				
Total	77	323	400				
Enriched culture							
Positive	22	0	22	100 (81.5–100.0)	100 (62.9–100.0)	100 (81.5–100.0)	100 (62.9–100.0)
Negative	0	9	9				
Total	22	9	31				

CRISPR-GBS but negative by both direct culture and regular PCR in our cohort. We were able to confirm 15 of 30 discordant cases (Figure 4, panel A). These data supported the previous findings and again indicate higher sensitivity of CRISPR-GBS compared with direct culture or PCR.

To further rule out the possibility of false-positive results, we set up a retrospective validation study and compared the sensitivity of CRISPR-GBS with enrichment culture, which had been shown to be more sensitive than direct culture (*5,24*). The validation cohort

of 31 patients consisted of 13 CRISPR-positive and direct culture–positive, 10 CRISPR-positive and direct culture–negative, and 8 CRISPR-negative and direct culture–negative samples. We tested each sample by direct culture, enriched culture, and CRISPR-GBS both before and after broth enrichment. We performed enriched culture by overnight culture in selective broth, followed by inoculation onto blood agar. We found that the samples that were negative by both direct culture and CRISPR originally would remain negative even after broth enrichment. However, of the 10
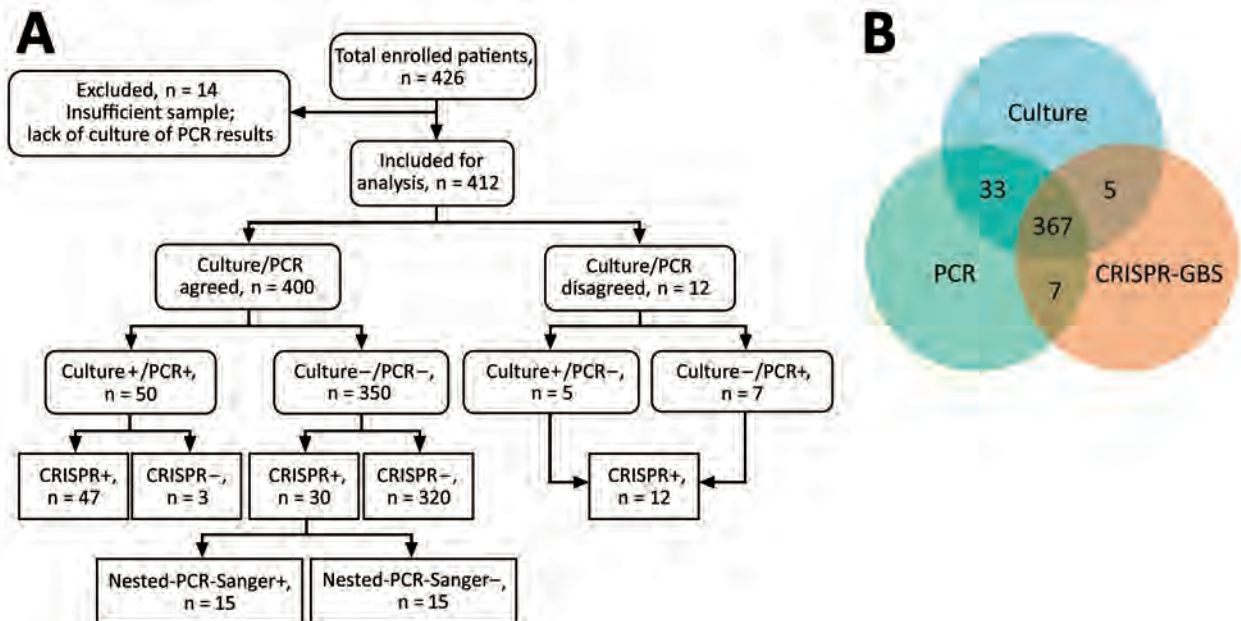
Figure 4. Overview and summary of the prospective cohort study assessing CRISPR-GBS. A) Study enrollment and result summary as categorized by agreements between different tests. B) Venn diagram demonstrating the overall concordance and discordance among direct culture, regular PCR, and CRISPR-GBS in the cohort. CRISPR-GBS, CRISPR-based diagnostic for rapid group B *Streptococcus* screening.

cases that were positive by CRISPR but negative by direct culture, adding the broth enrichment step yielded positive results in 90% of those cases (Figure 5). These results validated the greater sensitivity of CRISPR and suggested that the testing direct swabs by CRISPR-GBS conferred comparable sensitivity as enrichment culture. In our antepartum cohort of 412 pregnant women, the prevalence of GBS carriage was the highest by CRISPR at 21.6% (89/412) and was similar by culture (13.3% [55/412]), and PCR (13.8% [57/412]).

When we compared turnaround time, we found that the CRISPR-GBS test required an average of <1.5 hours, which includes 30 minutes of rapid DNA extraction, 30 minutes for DNA amplification by RPA, and 20 minutes for Cas13 detection. This turnaround time is a considerable advantage over those for conventional culture-based (24–60 hours) and PCR-based (≈2.5 hours for a regular PCR assay and much longer for nested PCR–Sanger) methods.

Discussion

We developed and demonstrated a CRISPR-based assay that offered short turn-around time and great sensitivity, which makes it a potential rapid, point-of-care assay for intrapartum GBS diagnosis, even in low-resource settings. Debates have occurred over approaches of preventing neonatal diseases caused by GBS infection (25). However, both of the 2 commonly used conventional strategies (i.e., risk-based screening or late antenatal microbiologic testing) have their own limitations (3,26). A point-of-care, rapid intrapartum GBS diagnosis at the onset of labor or membrane rupture is highly desired clinically because it would enable more accurate antibiotic prophylaxis and better antimicrobial stewardship (5). Successful development of such a diagnostic has been hindered by its requirement for a combination of short turnaround time, high diagnostic performance, low technical complexity, and low instrument requirement. In our study, we took advantage of the programmable

CRISPR/Cas system for GBS detection. The CRISPR-GBS assay as established and demonstrated in our study takes <1.5 hours to complete, has a sensitivity comparable to enriched culture, and does not require any sophisticated instruments. These features illustrate its great potential to be an onsite, rapid diagnostic for intrapartum GBS screening. Given the low complexity of the CRISPR-GBS assay established in our study, integration of the entire testing into a compact desktop instrument for an automated sample-in-report-out assay is highly feasible.

In our prospective study, we found the prevalence of GBS in our cohort to be slightly higher than 20% by CRIPSR. Although studies have shown differential prevalence between rectal and vaginal screening, the question of whether this could be caused by a lack of assay sensitivity for detecting borderline bacterial level remains controversial (1,24,27). In current clinical practice, vaginal–rectal swab specimens are commonly collected for optimized GBS detection, despite reported discomfort or even pain associated with rectal swabs (28,29). Determining whether patients could be spared the discomfort of rectal specimens without compromising the results with a more sensitive assay would be worthwhile. With this sensitive and rapid CRISPR assay, further studies are also warranted to evaluate its diagnostic and clinical value as an intrapartum assay by comparing it to antepartum culture (30).

Apart from GBS diagnosis, obtaining the information on drug susceptibility is also of great clinical value. For instance, recent reports have showed a trend of increased erythromycin and clindamycin resistance internationally (31–33). Genotypic analysis has been proven to have great predictive value for drug resistance. Given the highly sensitive nature of this CRISPR diagnostic technology, it holds the potential to simultaneously detect genes related to drug susceptibility (34). An expanded CRISPR-GBS assay would be able to not only diagnose GBS colonization
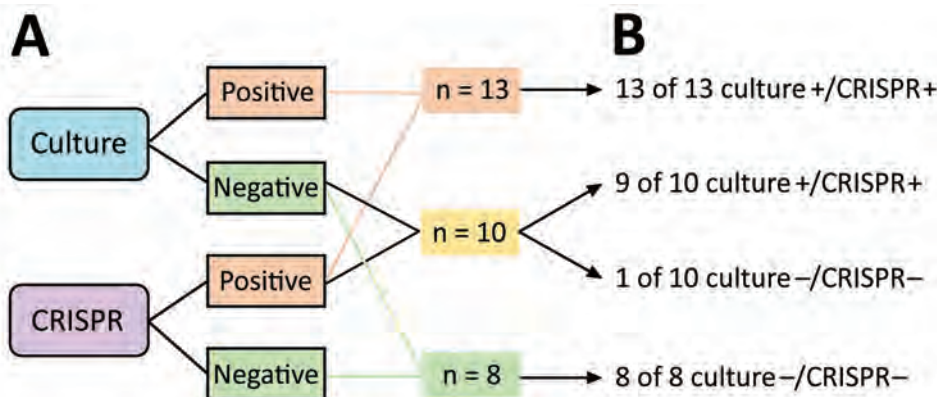
Figure 5. Overview of the validation study with enrichment culture for CRISPR-based diagnostic for rapid group B *Streptococcus* screening. Testing results by culture and CRISPR before (left) and after (right) broth enrichment are shown.

but also provide genetic insight into drug susceptibility for first-line antibiotics. On the basis of the proof-of-principle demonstrated in our study for direct-from-swab testing, rapid CRISPR detection of both pathogen and drug sensitivities would permit the precise approach to identification of GBS colonization and prevention of related neonatal diseases.

Because GBS is an important infection agent for multiple invasive infectious diseases such as meningitis, CRISPR-GBS could also be a promising tool for potentially much wider applications. A future multicenter study with a larger cohort would provide a more thorough evaluation of its diagnostic value, including its performance under different clinical settings.

In summary, the CRISPR-based rapid GBS assay we established in this study exhibits great diagnostic performance for GBS colonization under analytical and clinical settings. This novel test offers improved diagnostic performance over culture- and PCR-based assays and represents a novel option for potential rapid, point-of-care GBS screening.

About the Author

Dr. Jiang is Senior Technologist at Zhujiang Hospital, Southern Medical University, Guangzhou, China. His primary research interests are pathogenic mechanisms of clinical pathogens and the development of novel rapid diagnostic assays.

Reference

1. Dillon HC Jr, Gray E, Pass MA, Gray BM. Anorectal and vaginal carriage of group B streptococci during pregnancy. J Infect Dis. 1982;145:794–9. https://doi.org/10.1093/infdis/145.6.794
2. American Academy of Pediatrics Committee on Infectious Diseases and Committee on Fetus and Newborn. Guidelines for prevention of group B streptococcal (GBS) infection by chemoprophylaxis. Pediatrics. 1992;90:775–8.
3. Melin P. Neonatal group B streptococcal disease: from pathogenesis to preventive strategies. Clin Microbiol Infect. 2011;17:1294–303. https://doi.org/10.1111/j.1469-0691.2011.03576.x
4. Phares CR, Lynfield R, Farley MM, Mohle-Boetani J, Harrison LH, Petit S, et al.; Active Bacterial Core surveillance/Emerging Infections Program Network. Epidemiology of invasive group B streptococcal disease in the United States, 1999–2005. JAMA. 2008;299:2056–65. https://doi.org/10.1001/jama.299.17.2056
5. Verani JR, McGee L, Schrag SJ; Division of Bacterial Diseases, National Center for Immunization and Respiratory Diseases, Centers for Disease Control and Prevention. Prevention of perinatal group B streptococcal disease—revised guidelines from CDC, 2010. MMWR Recomm Rep. 2010;59(RR-10):1–36.
6. The Royal Australian and New Zealand College of Obstetricians and Gynaecologists. Maternal group B Streptococcus in pregnancy: screening and management (C-Obs 19). 2019 [cited 2021 Jul 19]. https://ranzcog.edu.au/RANZCOG_SITE/media/RANZCOG-MEDIA/Women%27s%20Health/Statement%20and%20guidelines/Clinical-Obstetrics/Maternal-Group-B-Streptococcus-in-pregnancy-screening-and-management-(C-Obs-19).pdf
7. Schrag SJ, Zywicki S, Farley MM, Reingold AL, Harrison LH, Lefkowitz LB, et al. Group B streptococcal disease in the era of intrapartum antibiotic prophylaxis. N Engl J Med. 2000;342:15–20. https://doi.org/10.1056/NEJM200001063420103
8. Hansen SM, Uldbjerg N, Kilian M, Sørensen UB. Dynamics of Streptococcus agalactiae colonization in women during and after pregnancy and in their infants. J Clin Microbiol. 2004;42:83–9. https://doi.org/10.1128/JCM.42.1.83-89.2004
9. Valkenburg-van den Berg AW, Houtman-Roelofsen RL, Oostvogel PM, Dekker FW, Dörr PJ, Sprij AJ. Timing of group B streptococcus screening in pregnancy: a systematic review. Gynecol Obstet Invest. 2010;69:174–83. https://doi.org/10.1159/000265942
10. Boyer KM, Gadzala CA, Kelly PD, Burd LI, Gotoff SP. Selective intrapartum chemoprophylaxis of neonatal group B streptococcal early-onset disease. II. Predictive value of prenatal cultures. J Infect Dis. 1983;148:802–9. https://doi.org/10.1093/infdis/148.5.802
11. Yancey MK, Schuchat A, Brown LK, Ventura VL, Markenson GR. The accuracy of late antenatal screening cultures in predicting genital group B streptococcal colonization at delivery. Obstet Gynecol. 1996;88:811–5. https://doi.org/10.1016/0029-7844(96)00320-1
12. Hwang WY, Fu Y, Reyon D, Maeder ML, Tsai SQ, Sander JD, et al. Efficient genome editing in zebrafish using a CRISPR-Cas system. Nat Biotechnol. 2013;31:227–9. https://doi.org/10.1038/nbt.2501
13. Wu Y, Liang D, Wang Y, Bai M, Tang W, Bao S, et al. Correction of a genetic disease in mouse via use of CRISPR-Cas9. Cell Stem Cell. 2013;13:659–62. https://doi.org/10.1016/j.stem.2013.10.016
14. Knott GJ, Doudna JA. CRISPR-Cas guides the future of genetic engineering. Science. 2018;361:866–9. https://doi.org/10.1126/science.aat5011
15. Chen JS, Ma E, Harrington LB, Da Costa M, Tian X, Palefsky JM, et al. CRISPR-Cas12a target binding unleashes indiscriminate single-stranded DNase activity. Science. 2018;360:436–9. https://doi.org/10.1126/science.aar6245
16. Harrington LB, Burstein D, Chen JS, Paez-Espino D, Ma E, Witte IP, et al. Programmed DNA destruction by miniature CRISPR-Cas14 enzymes. Science. 2018;362:839–42. https://doi.org/10.1126/science.aav4294
17. Myhrvold C, Freije CA, Gootenberg JS, Abudayyeh OO, Metsky HC, Durbin AF, et al. Field-deployable viral

diagnostics using CRISPR-Cas13. Science. 2018;360:444–8. https://doi.org/10.1126/science.aas8836

18. Crowe J, Döbeli H, Gentz R, Hochuli E, Stüber D, Henco K. 6xHis-Ni-NTA chromatography as a superior technique in recombinant protein expression/purification. Methods Mol Biol. 1994;31:371–87.

19. Parham NJ, Picard FJ, Peytavi R, Gagnon M, Seyrig G, Gagné PA, et al. Specific magnetic bead based capture of genomic DNA from clinical samples: application to the detection of group B streptococci in vaginal/anal swabs. Clin Chem. 2007;53:1570–6. https://doi.org/10.1373/clinchem.2007.091389

20. Miller SA, Deak E, Humphries R. Comparison of the AmpliVue, BD Max System, and Illumigene molecular assays for detection of group B *Streptococcus* in antenatal screening specimens. J Clin Microbiol. 2015;53:1938–41. https://doi.org/10.1128/JCM.00261-15

21. Park JS, Cho DH, Yang JH, Kim MY, Shin SM, Kim EC, et al. Usefulness of a rapid real-time PCR assay in prenatal screening for group B *streptococcus* colonization. Ann Lab Med. 2013;33:39–44. https://doi.org/10.3343/alm.2013.33.1.39

22. Berry GJ, Zhang F, Manji R, Juretschko S. Comparison of the Panther Fusion and BD MAX Group B *Streptococcus* (GBS) assays for detection of GBS in prenatal screening specimens. J Clin Microbiol. 2019;57:e01034–19. https://doi.org/10.1128/JCM.01034-19

23. Ke D, Ménard C, Picard FJ, Boissinot M, Ouellette M, Roy PH, et al. Development of conventional and real-time PCR assays for the rapid detection of group B streptococci. Clin Chem. 2000;46:324–31. https://doi.org/10.1093/clinchem/46.3.324

24. Platt MW, McLaughlin JC, Gilson GJ, Wellhoner MF, Nims LJ. Increased recovery of group B *streptococcus* by the inclusion of rectal culturing and enrichment. Diagn Microbiol Infect Dis. 1995;21:65–8. https://doi.org/10.1016/0732-8893(95)00022-3

25. Davies HD. Preventing group B streptococcal infections: new recommendations. Can J Infect Dis. 2002;13:232–5. https://doi.org/10.1155/2002/352613

26. Puopolo KM, Lynfield R, Cummings JJ; Committee on Fetus and Newborn; Committee on Infectious Diseases. Management of infants at risk for group B streptococcal disease. Pediatrics. 2019;144:e20191881. https://doi.org/10.1542/peds.2019-1881

27. Philipson EH, Palermino DA, Robinson A. Enhanced antenatal detection of group B streptococcus colonization. Obstet Gynecol. 1995;85:437–9. https://doi.org/10.1016/0029-7844(94)00412-7

28. Jamie WE, Edwards RK, Duff P. Vaginal-perianal compared with vaginal-rectal cultures for identification of group B streptococci. Obstet Gynecol. 2004;104:1058–61. https://doi.org/10.1097/01.AOG.0000144120.20312.ed

29. Orafu C, Gill P, Nelson K, Hecht B, Hopkins M. Perianal versus anorectal specimens: is there a difference in group B streptococcal detection? Obstet Gynecol. 2002;99:1036–9. https://doi.org/10.1097/00006250-200206000-00015

30. Iams JD, O'Shaughnessy R. Antepartum versus intrapartum selective screening for maternal group B streptococcal colonization. Am J Obstet Gynecol. 1982;143:153–6. https://doi.org/10.1016/0002-9378(82)90645-7

31. Guo Y, Deng X, Liang Y, Zhang L, Zhao GP, Zhou Y. The draft genomes and investigation of serotype distribution, antimicrobial resistance of group B *Streptococcus* strains isolated from urine in Suzhou, China. Ann Clin Microbiol Antimicrob. 2018;17:28. https://doi.org/10.1186/s12941-018-0280-y

32. Gao K, Guan X, Zeng L, Qian J, Zhu S, Deng Q, et al. An increasing trend of neonatal invasive multidrug-resistant group B s*treptococcus* infections in southern China, 2011–2017. Infect Drug Resist. 2018;11:2561–9. https://doi.org/10.2147/IDR.S178717

33. Tsai MH, Hsu JF, Lai MY, Lin LC, Chu SM, Huang HR, et al. Molecular characteristics and antimicrobial resistance of group b *Streptococcus* strains causing invasive disease in neonates and adults. Front Microbiol. 2019;10:264. https://doi.org/10.3389/fmicb.2019.00264

34. Campisi E, Rosini R, Ji W, Guidotti S, Rojas-López M, Geng G, et al. Genomic analysis reveals multi-drug resistance clusters in group B *Streptococcus* CC17 hypervirulent isolates causing neonatal invasive disease in southern mainland China. Front Microbiol. 2016;7:1265. https://doi.org/10.3389/fmicb.2016.01265

Address for correspondence: Teng Xu, Vision Medicals Center for Medical Research, 31 Kefeng Ave, Bldg G10, Unit 301, Guangzhou 510000, China; email: txu@visionmedicals.com; Shilei Pan, Department of Prenatal Diagnosis, Zhujiang Hospital, Southern Medical University, 253 Middle Gongye Ave, Guangzhou 510282, China; email: 13602882918@163.com

Geographically Targeted Interventions versus Mass Drug Administration to Control *Taenia solium* Cysticercosis, Peru

Seth E. O'Neal, Ian W. Pray, Percy Vilchez, Ricardo Gamboa, Claudio Muro,
Luz Maria Moyano, Viterbo Ayvar, Cesar M. Gavidia, Robert H. Gilman,
Armando E. Gonzalez, Hector H. Garcia, for the Cysticercosis Working Group in Peru

Optimal control strategies for *Taenia solium* taeniasis and cysticercosis have not been determined. We conducted a 2-year cluster randomized trial in Peru by assigning 23 villages to 1 of 3 geographically targeted intervention approaches. For ring screening (RS), participants living near pigs with cysticercosis were screened for taeniasis; identified cases were treated with niclosamide. In ring treatment (RT), participants living near pigs with cysticercosis received presumptive treatment with niclosamide. In mass treatment (MT), participants received niclosamide treatment every 6 months regardless of location. In each approach, half the villages received targeted or mass oxfendazole for pigs (6 total study arms). We noted significant reductions in seroincidence among pigs in all approaches (67.1% decrease in RS, 69.3% in RT, 64.7% in MT; p<0.001), despite a smaller proportion of population treated by targeted approaches (RS 1.4%, RT 19.3%, MT 88.5%). Our findings suggest multiple approaches can achieve rapid control of *T. solium* transmission..

*T*aenia solium is a zoonotic cestode that infects both humans and pigs (Figure 1). Human brain infection, neurocysticercosis, is a major cause of preventable epilepsy across much of Asia, Africa, and Latin America (*1*); ≈1.35 million persons in Latin America and ≈3 million persons in Africa have epilepsy thought to be secondary to neurocysticercosis (*2,3*). Porcine cysticercosis is a food safety hazard and source of economic harm in rural regions where the parasite is endemic and of increasing public health concern because of the rapidly growing global demand for pork (*4*). The United Nations Food and Agriculture Organization (https://www.fao.org) ranks *T. solium* as a major foodborne parasite on the basis of global likelihood of exposure and potential severity of infection (*5*). In the United States, hospitalizations for cysticercosis exceed those for all other neglected tropical diseases combined (*6*).

One of the targets of the 2011 World Health Organization roadmap to overcome neglected tropical diseases is to validate *T. solium* control and elimination strategies and scale up taeniasis and cysticercosis interventions (*7*). Several different interventions to control transmission have been attempted, including mass treatment for taeniasis (*8–10*), combined mass treatment for taeniasis and porcine cysticercosis (*8,11*), targeted screening and treatment for taeniasis (*12*), pig vaccination (*13*), improvements in sanitation (*14*), and various education interventions (*15,16*). However, most studies have been limited by small scale or inconsistent monitoring, making conclusions regarding effectiveness and generalizability uncertain. No clear indication has yet determined which control strategies will be feasible and effective.

We previously completed a pilot study in Peru to evaluate a targeted ring approach to control transmission of *T. solium*, which exhibits spatial clustering (*12*). The premise of this approach is that selective treatment for taeniasis among high-risk subgroups within villages might reduce transmission and limit the number of persons treated (*17*). We offered screening and treatment for taeniasis within groups of households located near pigs that had visible cyst infection during periodic surveillance. We noted a 50% relative reduction

Author affiliations: Oregon Health & Science University–Portland State University School of Public Health, Portland, Oregon, USA (S.E. O'Neal, I.W. Pray); Universidad Peruana Cayetano Heredia, Lima, Peru (S.E. O'Neal, P. Vilchez, R. Gamboa, C. Muro, L.M. Moyano, H.H. Garcia); Universidad Nacional Mayor de San Marcos, Lima (V. Ayvar, C.M. Gavidia, A.E. Gonzalez); Johns Hopkins University, Baltimore, Maryland, USA. (R.H. Gilman)
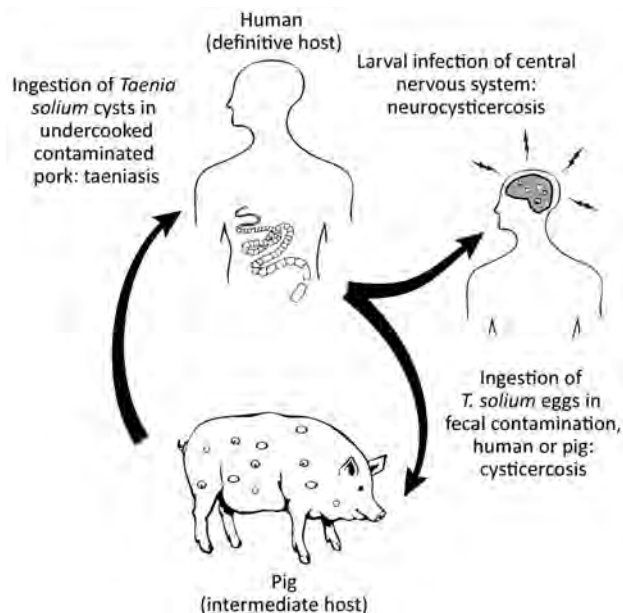
Figure 1. Lifecycle of the *Taenia solium* tapeworm in humans and pigs.

in transmission within the intervention village compared with the negative control village (*12*), but a larger randomized trial could help validate this approach. We conducted a follow-up study to compare effectiveness of 2 ring approaches and mass treatment, and to explore whether including treatment for cysticercosis in pigs provided additional control benefits.

Methods

Study Design
We conducted a community cluster randomized trial with a 3 × 2 factorial design. We randomly assigned 23 villages (total population 10,551) to 1 of 6 study arms (Figures 2, 3). Each study arm corresponded to a unique intervention comprised of an approach to deliver the antiparasitic drug niclosamide, for human taeniasis. The 6 study arms were ring screening (RS), ring treatment (RT), or mass treatment (MT), with or without antiparasitic drug treatment with oxfendazole for cysticercosis in pigs.

Outcome Measures
The primary outcome was seroincidence of *T. solium* antibodies in all pigs born into the villages during the 2-year study period. The secondary outcome was prevalence of human taeniasis at study end.

Study Sites and Participants
We conducted the study during 2015–2017 in Piura, Peru, an agricultural region where *T. solium* is endemic. Outdoor defecation is common among humans and pigs roam free, a combination that places pigs at high risk for cysticercosis. Villages of 50–500 residents were eligible to participate; 43 villages met this criterium. We selected 23 villages because they were accessible year-round and had no history of control interventions for taeniasis or cysticercosis (Appendix, https://wwwnc.cdc.gov/EID/article/27/9/20-3349-App1.pdf). All residents >2 years of age were eligible to participate. The study was approved by the institutional review boards for human (approval no. IRB00010117) and animal (approval no. IP00000617) research at Oregon Health & Science University–Portland State University, Portland, Oregon, USA, and Universidad Peruana Cayetano Heredia, Lima, Peru (approval no. 62206).

Baseline Census
We conducted a door-to-door census in villages to collect information on demographics, household sanitation, and pig husbandry. We used global positioning system receivers (Trimble, https://www.trimble.com) with post-processed differential correction to collect coordinates of each house, then created a georeferenced map of each village by using ArcMAP10 (Environmental Systems Research Institute, https://www.esri.com) and a 100-m buffer around each household to define extent of future intervention rings (*12*).

Randomization
We randomly assigned the 23 villages to 1 of 6 study arms, repeating the allocation sequence until the human population in all 6 arms was approximately equal, within 10% of the study population divided by 6 (Appendix). We considered no other factors in assigning villages.

Interventions
In the MT approach, we returned to each village every 6 months and went door-to-door to offer residents >2 years of age presumptive treatment for taeniasis with a single oral dose of niclosamide. Persons who weighed 11–34 kg received 1 g niclosamide, persons who weighed 35–50 kg received 1.5 g, and persons weighing >50 kg received 2 g. We chose the 6-month interval to be consistent with the frequency of mass drug administration (MDA) recommended by the World Health Organization for other helminths (*18*). During each treatment cycle, we returned to households >1 additional time to locate persons who were absent when treatment initially was offered. We did not collect stool samples in the MT approach.

In the RT approach, we returned to each village every 4 months to perform active surveillance for heavily infected pigs. Surveillance included visiting all households, catching all pigs, and examining pigs' tongues for visible or palpable cysts (*19*). We returned to households >1 additional time if any pigs evaded capture or were otherwise unaccounted for during the first visit. When we identified a pig with cysticercosis of the tongue, we opened a treatment ring comprising all households within a 100-m radius of the house where the tongue-positive pig was raised. We offered all persons >2 years of age living within the treatment ring the standard oral niclosamide dose for taeniasis and a second oral dose 15 days later. We used 2 doses because single-dose treatment failure is common in this region (*20*). We

did not collect stool samples in the RT approach. We offered to purchase all cysticercosis tongue-positive pigs and remove these pigs from the village; if the owner did not agree to sell the pig, we treated it with a single 30 mg/kg dose of oxfendazole, as recommended (*21*).

In the RS approach, we conducted active surveillance for heavily infected pigs as described in the RT approach. When we identified a cysticercosis tongue-positive pig, we requested a single stool sample from each person >2 years of age living in a 100-m radius of the house where the infected pig was raised. We tested stool samples for *Taenia* sp. eggs or antigens and only offered niclosamide single-dose treatment to persons with diagnosed taeniasis. We collected a follow-up stool sample from taeniasis-positive persons
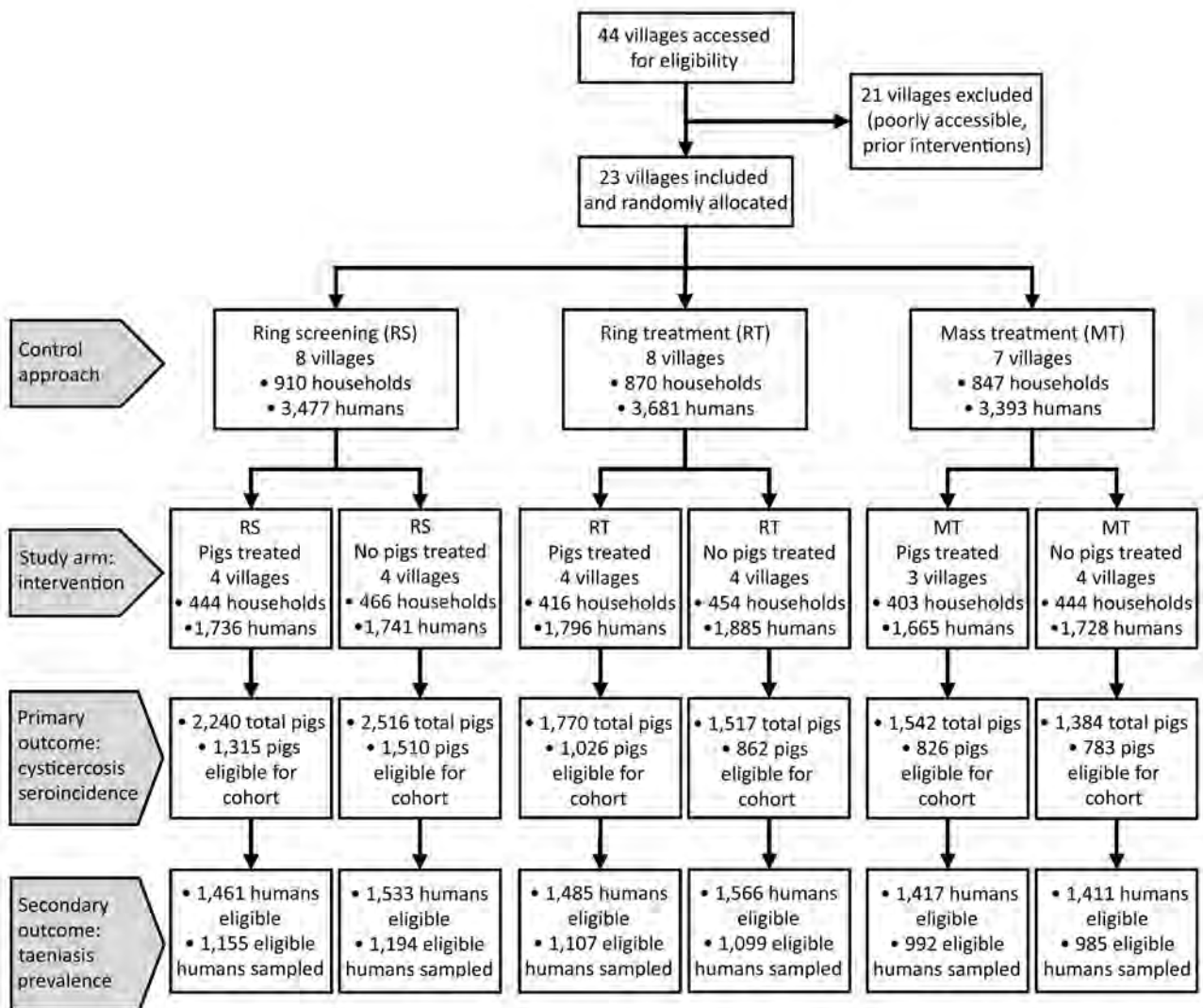
Figure 2. Flowchart of participating villages, humans, and pigs in a study of *Taenia solium* intervention strategies, Peru. Humans were treated with niclosamide, pigs (when treated) with oxfendazole. MT, mass treatment; RS, ring screening; RT, ring treatment.

		Study month								
		0	4	6	8	12	16	18	20	24
Ring screening Pig treatment	Humans	SCR_r/NSM_r	SCR_r/NSM_r	NA	SCR_r/NSM_r	SCR_r/NSM_r	SCR_r/NSM_r	NA	SCR_r/NSM_r	SCR_r/NSM_r
	Pigs	OXF_r	OXF_r	NA	OXF_r	OXF_r	OXF_r	NA	OXF_r	OXF_c
Ring screening No pig treatment	Humans	SCR_r/NSM_r	SCR_r/NSM_r	NA	SCR_r/NSM_r	SCR_r/NSM_r	SCR_r/NSM_r	NA	SCR_r/NSM_r	SCR_r/NSM_r
	Pigs	NA	NA	NA	NA	NA	NA	NA	NA	NA
Ring treatment Pig treatment	Humans	NSM_r	NSM_r	NA	NSM_r	NSM_r	NSM_r	NA	NSM_r	NSM_r
	Pigs	OXF_r	OXF_r	NA	OXF_r	OXF_r	OXF_r	NA	OXF_r	OXF_r
Ring treatment No pig treatment	Humans	NSM_r	NSM_r	NA	NSM_r	NSM_r	NSM_r	NA	NSM_r	NSM_r
	Pigs	NA	NA	NA	NA	NA	NA	NA	NA	NA
Mass treatment Pig treatment	Humans	NSM_m	NA	NSM_m	NA	NSM_m	NA	NSM_m	NA	NSM_m
	Pigs	OXF_m	OXF_m	NA	OXF_m	OXF_m	OXF_m	NA	OXF_m	OXF_m
Mass treatment No pig treatment	Humans	NSM_m	NA	NSM_m	NA	NSM_m	NA	NSM_m	NA	NSM_m
	Pigs	NA	NA	NA	NA	NA	NA	NA	NA	NA

Figure 3. Timeline showing interventions in humans and pigs during a study of *Taenia solium* tapeworms, Peru. NSM_m, presumptive treatment with niclosamide for humans; NA, not applicable; NSM_r, presumptive treatment with niclosamide for humans only in rings; OXF_m, presumptive treatment with oxfendazole for pigs; OXF_r, presumptive treatment with oxfendazole for pigs only in rings; SCR_r/NSM_r, stool screening and treatment with niclosamide for humans with diagnosed taeniasis only in rings.

30 days after treatment to verify cure and retreated persistent infections. We purchased cysticercosis tongue-positive pigs or treated with oxfendazole as described in the RT approach.

In half of the villages in each approach, we treated pigs ≥6 weeks of age for cysticercosis by using a single oral dose of 30 mg/kg of oxfendazole. In the MT approach, we treated all pigs in the village at 4-month intervals. In the RT and RS approaches, we treated only pigs owned by households within a 100-m ring of a cysticercosis tongue-positive pig. Owners were instructed not to slaughter pigs within 21 days after treatment so that the drug would clear from tissues before human consumption (*22*).

Measurement of Primary Outcome

We conducted serosurveys of the pig population every 4 months in all 23 villages to determine seroincidence of antibodies against cysticercosis. During each serosurvey, veterinary staff visited each household, captured all pigs ≥6 weeks of age, collected a 5-mL blood sample, placed an ear tag with a unique identifier on new pigs, and updated the pig census. Pigs 6 weeks–4 months of age when first captured were placed into a cohort for incidence calculations. We followed the serologic antibody response of every pig in this cohort through subsequent serosurveys until an antibody response developed in the pig (primary outcome) or the pig was lost to follow-up because it died, was sold, evaded capture or other reasons. The seroincidence reported at each sampling point reflects the risk for exposure during the preceding 4-month interval.

Measurement of Secondary Outcome

At study end (month 24), we determined the prevalence of taeniasis in all 23 villages. We offered presumptive treatment with niclosamide to all residents ≥2 years of age, requested collection of the first post-treatment stool in a 500-mL plastic container, and collected stool samples for testing within 24 hours.

Laboratory Procedures

We centrifuged pig blood samples to separate serum, froze serum at −20°C, and later processed it for antibodies against porcine cysticercosis by using lentil-lectin glycoprotein enzyme-linked immunoelectrotransfer blot, as previously described (*23*), except we considered results positive when a reaction occurred to any of the 6 glycoprotein (GP) antigens, GP39/42, GP24, GP21, GP18, GP14, or GP13. We excluded the GP50 antigen because recent studies have shown this band cross-reacts with *T. hydatigena*, a cestode that infects pigs and is coendemic in the region (*24*). We examined human stool samples macroscopically for *Taenia* sp. scoleces or proglottids, then prepared fecal aliquots in 5% formol-phosphate buffered saline (Appendix). We used ELISA to detect *Taenia* sp. coproantigens in aliquots, as previously described (*25*).

Statistical Analysis

We analyzed data in Stata SE14.2 (StataCorp LLC, https://www.stata.com). To evaluate pig seroincidence, we used binomial family generalized estimating equations with log-link and exchangeable correlation structure. We aggregated individual

pig-level data into panel format to reflect the hierarchical structure of study arm, village, house, and intervention round, then further stratified by age category (0–4, 5–8, 9–12, and ≥13 months). We set village as the panel variable and used robust sandwich-type errors to account for intrahousehold clustering. We used quasilikelihood information criteria to select variables for the final model and retained variables that decreased criteria value relative to the saturated model. The final model variables were study arm, intervention round, baseline village seroprevalence, presence or absence of household latrine and pig corral, pig age, and oxfendazole treatment for pigs. We included 2- and 3-way interactions for study arm × intervention round × oxfendazole to evaluate any additional effect of including pig treatment in interventions. We considered p<0.05 statistically significant. We then used margins command to estimate predicted probabilities (cumulative seroincidence) and absolute differences within each study arm over time and between study arms. For the taeniasis prevalence, we used a separate binomial family generalized estimating equation with log-link that included participant age, number of pigs in village, and baseline village seroprevalence.

Results

Village Assignment and Characteristics
The total population of all 23 villages was 10,551; 10,094 (95.7%) persons were ≥2 years and eligible to participate (Table 1; Figure 2). Compared with other study approaches, the MT approach had more latrines, fewer pigs, and a lower baseline seroprevalence.

Interventions Applied
In MT, we conducted 5 rounds of MDA with niclosamide to an age-eligible population of 3,329 persons (Table 2); 1,240 (37.3%) participants received all 5 rounds, 583 (17.5%) in 4 rounds, 411 (12.4%) in 3 rounds, 354 (10.6%) in 2 rounds, 359 (10.8%) in 1 round, and 382 (11.5%) were not treated. We treated 88.5% (2,641/3,329) of the age-eligible population with ≥1 dose.

In RT, we conducted 7 rounds of surveillance and examined tongues of 5,764 pigs (Table 3). We identified 37 tongue-positive pigs, resulting in 37 distinct screening rings. We purchased and removed 20 (54.1%) pigs; 17 (45.9%) pigs were treated with oxfendazole and remained with their owners. A total of 803/3,525 (22.8%) age-eligible persons in 183/870 (21.0%) households were included in a treatment ring in ≥1 surveillance round; 538 (67.0%) persons were offered niclosamide in 1 round, 202 (25.2%) in 2 rounds, 48 (6.0%) in 3 rounds, and 15 (1.9%) in 4 rounds. We treated 19.3% (680/3,525) of the overall age-eligible population with ≥1 dose.

In RS, we conducted 7 rounds of surveillance and examined tongues of 7,885 pigs (Table 4). We identified 74 tongue-positive pigs, resulting in 65 distinct screening rings, but 9 rings completely overlapped with others. We purchased and removed 57 (77.0%) pigs, 15 (20.3%) were treated and remained, and 2 (2.7%) were reported slaughtered and buried by the owner. A total of 1,475/3,328 (44.3%) age-eligible persons in 397/910 (43.6%) households were included in a screening ring in ≥1 surveillance round; 972 (65.9%) were included in 1 round, 455 (31.8%) in 2 rounds, and 48 (3.3%) in 3 rounds. We collected ≥1 stool sample from 1,231/1,475 (83.5%) participants; 51 (4.1%) persons tested positive. We screened 37.0% (1,231/3,328) of the overall age-eligible population and treated 1.4% (46) with niclosamide.

The primary reasons eligible persons did not receive niclosamide in all study arms included not being in the village at the time of intervention and participant refusal. The main reasons eligible pigs did not receive oxfendazole were pregnancy and inability to capture the animal.

Table 1. Village and household characteristics at baseline in each arm of a study on control of *Taenia solium* cysticercosis, Peru*

Characteristics	Ring screening		Ring treatment		Mass treatment	
	Pig treatment	No pig treatment	Pig treatment	No pig treatment	Pig treatment	No pig treatment
No. villages	4	4	4	4	3	4
Human residents	1,736 (16.5)	1,741 (16.5)	1,796 (17.0)	1,885 (17.9)	1,665 (15.8)	1,728 (16.4)
Residents ≥2 y of age	1,662 (16.5)	1,666 (16.5)	1,736 (17.2)	1,789 (17.7)	1,594 (15.8)	1,647 (16.3)
No. pigs at baseline	457	556	349	395	369	305
Seropositive pigs	194 (42.5)	224 (40.3)	148 (42.4)	190 (48.1)	141 (38.2)	96 (31.5)
Households	444 (16.9)	466 (17.7)	416 (15.8)	454 (17.3)	403 (15.3)	444 (16.9)
Latrine	249 (58.1)	346 (74.3)	249 (59.9)	311 (68.5)	330 (81.9)	341 (76.8)
Treated water source	394 (88.7)	427 (91.6)	291 (70.0)	352 (77.5)	357 (88.6)	350 (78.8)
Raise pigs	230 (51.8)	251 (53.9)	217 (52.2)	241 (53.1)	178 (44.2)	253 (57.0)
Corral for pigs	146 (63.5)	132 (52.6)	82 (37.8)	118 (49.0)	114 (64.0)	107 (42.3)

*Values are no. (%), except as indicated.

Table 2. Summary of participation in mass treatment intervention in a study on control of *Taenia solium* cysticercosis, Peru*

| Characteristics | Study month | | | | | Total |
	0	6	12	18	24	
No. eligible households	799	794	816	804	815	4,028
No. eligible participants	2,994	2,973	3,021	2,956	2,998	14,942
Not treated, no. (%)	709 (23.7)	743 (25.0)	819 (27.1)	755 (25.5)	730 (24.4)	3,756 (25.1)
Took ≥1 dose of NSM, no. (%)	2,285 (76.3)	2,230 (75.0)	2,202 (72.9)	2,201 (74.5)	2,268 (75.7)	11,186 (74.9)

*Distinct households and participants might be counted more than once in the totals column. NSM, niclosamide.

Porcine Seroincidence

We captured 10,969 distinct pigs over the 24-month study, of which 6,322 (57.6%) were eligible for seroincidence monitoring; 2,825 (44.7%) in RS, 1,888 (29.9%) in RT, and 1,609 (25.5%) in MT. We collected 11,165 blood samples from the eligible cohort. Some pigs were sampled during ≥1 round; 3,132 (49.5%) had 1 sample, 1,938 (30.7%) had 2 samples, and 1,252 (19.8%) had ≥3 samples.

The 4-month cumulative seroincidence at baseline was 42.1% (95% CI 36.6%–47.6%) in RS, 45.8% (95% CI 37.1%−54.4%) in RT, and 36.2% (95% CI 30.3%–42.1%) in MT. We saw a strong control effect in all 3 approaches with statistically significant (p<0.001) reduction in seroincidence from baseline to study end. In RS, the relative decrease was 66.4% and the absolute decrease was 28.0 (95% CI 22.5–33.4) percentage points. In RT, the relative decrease was 69.4% and the absolute decrease was 31.8 (95% CI 20.1–43.4) percentage points. In MT, the relative decrease was 64.9% and the absolute decrease was 23.5 (95% CI 15.2–31.7) percentage points (Figure 4). The most rapid decrease occurred with RS, in which maximum effect was reached after 8 months, and remained stable thereafter. We did not see a significant difference in reduction of seroincidence between any 2 pairs of study approaches during the 24 month-study (RT vs. MT, p = 0.27; RT vs. RS, p = 0.55; RS vs. MT, p = 0.40).

Prevalence of Taeniasis

At study end, 81.7% (7,248/8,873) of age-eligible persons accepted treatment for taeniasis; 6,537 (73.6%) provided a posttreatment stool sample. The unadjusted prevalence of taeniasis was 0.72% (17/2,349) in RS, 1.31% (29/2,206) in RT, and 0.40% (8/1,977)

in MT. After adjusting for number of pigs in the village, baseline village seroprevalence, participant age, and the clustered study design, the model-estimated prevalence of taeniasis was 0.74% (95% CI 0.14%–3.81%) in RS, 1.09% (95% CI 0.21%–5.61%) in RT, and 0.62% (95% CI 0.11%–3.46%) in MT (Table 5). In villages that received a targeted strategy, most (78.2%; 36/46) persons who had taeniasis at study end lived in households that were not identified for intervention by using the ring approach.

Antiparasitic Treatment for Pigs

Adding oxfendazole treatment for pigs did not provide additional benefit and did not decrease overall pig seroincidence in any of the 3 approaches (Figure 5). We saw no statistically significant interaction between study arm and oxfendazole treatment; treatment was not a statistically significant covariate in the full model. The model-estimated seroincidence was 20.9% (95% CI 19.0%– 22.8%) in nontreated pigs compared with 21.9% (95% CI 20.2%–23.7%) in treated pigs.

Discussion

We found that targeted delivery of niclosamide to treat and prevent human taeniasis in a ring strategy and uniform delivery in MDA both effectively reduced *T. solium* transmission. All 3 tested intervention approaches achieved >65% reduction in porcine *T. solium* seroincidence during the 2-year study, and all 3 were accepted broadly within study communities.

Ideal control approaches for taeniasis and cysticercosis might vary across regions, and such approaches should consider which resources and infrastructure are available locally. Niclosamide MDA

Table 3. Summary of surveillance and participation in ring treatment intervention in a study of *Taenia solium* cysticercosis, Peru*

| Characteristics | Study month | | | | | | | Total |
	0	4	8	12	16	20	24	
No. pigs examined	748	625	783	751	937	931	989	5,764
Tongue-positive pigs, no. (%)	7 (0.9)	6 (1.0)	6 (0.8)	4 (0.5)	2 (0.2)	9 (1.0)	4 (0.4)	38 (0.7)
No. screening rings	7	6	7	3	2	9	3	37
No. eligible households	43	39	58	15	13	71	10	249
No. eligible participants	193	187	261	72	66	338	36	1,153
Not treated, no. (%)	14 (7.3)	35 (18.7)	32 (12.3)	10 (13.9)	14 (21.1)	56 (16.6)	13 (36.1)	174 (15.1)
Took 1 dose of NSM, no. (%)	23 (11.9)	36 (19.3)	31 (11.9)	4 (5.6)	4 (6.1)	67 (19.8)	2 (5.6)	167 (14.5)
Took 2 doses of NSM, no. (%)	156 (80.8)	116 (62.0)	198 (75.9)	58 (80.6)	48 (72.7)	215 (63.6)	21 (58.3)	812 (70.4)

*Distinct households, participants, and pigs might be counted more than once in the totals column. NSM, niclosamide.

Table 4. Summary of surveillance and participation in ring screening intervention in a study of *Taenia solium* cysticercosis, Peru*

Characteristics	Study month							Total*
	0	4	8	12	16	20	24	
No. pigs examined	1,015	875	1,010	1,075	1,174	1,424	1,312	7,885
Tongue-positive pigs, no. (%)	23 (2.3)	3 (0.3)	0 (0)	12 (1.1)	17 (1.5)	5 (0.4)	14 (1.1)	74 (1.0)
No. screening rings	21	3	0	9	15	5	12	65
No. eligible households	170	24	0	53	150	25	124	546
No. eligible participants	625	90	0	220	532	107	452	2026
Provided stool (%)	548 (87.7)	73 (81.1)	0	185 (84.1)	422 (79.3)	83 (77.6)	352 (77.9)	1,663 (82.1)
Suspect taeniasis (%)	24 (4.4)	2 (2.7)	NA	5 (2.7)	18 (4.3)	0 (0)	12 (3.4)	61 (3.7)
Accepted NSM (%)	22 (91.7)	2 (100)	NA	5 (100)	15 (83.3)	NA	12 (100)	56 (91.8)

*Distinct households, participants, and pigs might be counted more than once in the totals column. NA, not applicable; NSM, niclosamide.

might be the easiest strategy to implement because of the extensive worldwide experience with this approach for other neglected tropical diseases. Primary benefits of MDA include operational simplicity and familiarity. In our study, *T. solium* transmission decreased steadily over time during repeated rounds of niclosamide at 6-month intervals. Niclosamide is safe for the general population (*8*) because it does not provoke brain inflammation in persons with neurocysticercosis, which is a concern in using the alternative drug, praziquantel (*26*). On the other hand, MDA is particularly inefficient for treating taeniasis. Unlike other neglected tropical diseases for which MDA is used, endemic *T. solium* transmission is sustained by a low prevalence of taeniasis, typically 1%–3%. Therefore, MDA for taeniasis applies most drugs to persons who are not infected and who might have limited risk for disease. Other drawbacks of MDA include more of the population exposed to possible adverse events, declining participation over time, and mixed evidence of sustained effect of MDA on transmission (*27*).

Ring strategy is applied on the premise that targeting high-risk subpopulations with niclosamide can achieve taeniasis control by treating fewer persons than in MDA, which ignores known spatial risk heterogeneity (*17*). Although only 19.3% of our study population received niclosamide through RT whereas 88.5% of persons received it through MDA, we saw no difference in reduction of transmission between the 2 approaches. The main disadvantage

of ring strategy is operational complexity; this strategy requires surveillance to detect heavily infected pigs and identify focal areas for intervention. We used centralized active surveillance in which dedicated veterinary teams screened the pig population every 4 months. This approach might be difficult to implement on a large scale, particularly in impoverished rural regions isolated from government resources and attention.

For programmatic application of ring strategy, passive community surveillance with incentives for reporting could be more pragmatic. In this strategy, residents would report meat visibly contaminated with cysts at time of slaughter or animals found to be tongue-positive during sale, thus prompting RT with niclosamide by community health workers. We pilot tested this approach in Peru and found that passive surveillance without incentives did not achieve sufficient reports and drug delivery to reduce parasite transmission (*28*). Pigs provide cash income to villagers who sell their animals to offset unanticipated economic needs. Loss of income at these crucial moments was a strong disincentive to report and often resulted in consuming or selling contaminated meat. However, in another pilot study in the same region, strong community engagement with incentives resulted in sufficient reporting to control transmission (S. O'Neal, unpub. data). We are conducting implementation research for programmatic application of RT in Peru.

Screening for taeniasis followed by treatment for diagnosed cases is an alternative to presumptive

Table 5. Taeniasis frequency and prevalence by study arm after 24 months of *Taenia solium* intervention, Peru

Study arm	No. taeniasis cases	No. stool samples tested	Prevalence, %	
			Crude	Adjusted* (95% CI)
Ring screening				
Pig treatment	3	1,155	0.26	0.32 (0.07–1.45)
No pig treatment	14	1,194	1.17	0.89 (0.22–3.56)
Ring treatment				
Pig treatment	14	1,107	1.26	0.55 (0.09–3.23)
No pig treatment	15	1,099	1.36	1.54 (0.37–6.51)
Mass treatment				
Pig treatment	4	992	0.40	0.69 (0.16–2.86)
No pig treatment	4	985	0.41	0.46 (0.09–2.33)

*Adjusted for number of pigs in the village, baseline village seroprevalence, participant age, and the clustered study design.
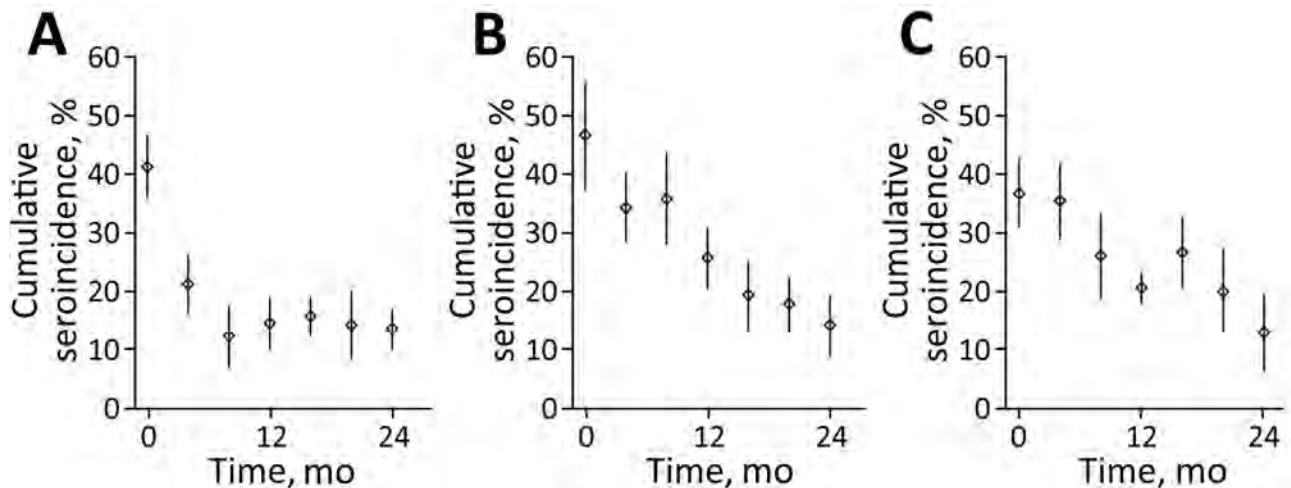
Figure 4. Cumulative *Taenia solium* seroincidence among pigs by study approach over time, Peru. A) Ring screening; B) ring treatment; C) mass treatment. In ring screening, human participants living near pigs with cysticercosis were screened for taeniasis using stool coproantigen; identified cases were treated with niclosamide. In ring treatment, human participants living near pigs with cysticercosis received presumptive treatment with niclosamide. In mass treatment, human participants received treatment with niclosamide every 6 months regardless of location. Diamonds indicate point estimates; vertical bars indicate 95% CIs.

treatment. Mass stool screening is infeasible on a large scale because of cost and operational complexity, but ring strategy enables targeted application of screening resources. In our study, screening reduced the proportion of the population receiving niclosamide to 1.4% in RS versus 19.3% in RT while maintaining control effectiveness but did so at additional cost and complexity due to collection and processing of stool samples. A screening approach for taeniasis using the most sensitive test, coproantigen ELISA, might not be possible in regions without laboratory infrastructure or access to reagents, which remains a barrier to screening in most endemic areas (*29*).

In regions with robust veterinary infrastructure, control interventions in the pig population, such as treatment with oxfendazole or immunization with highly effective vaccines (*13*), could be applied as a standalone program or in combination with treatment for taeniasis. All the strategies we tested had treatment for taeniasis as the core intervention because taeniasis is the most prolific *T. solium* life stage and direct cause of cysticercosis in humans and pigs. Of note, we saw no additional reduction in transmission in any study approach when we added oxfendazole treatment for pigs. This finding suggests that when sustained control pressure is applied to humans as the definitive
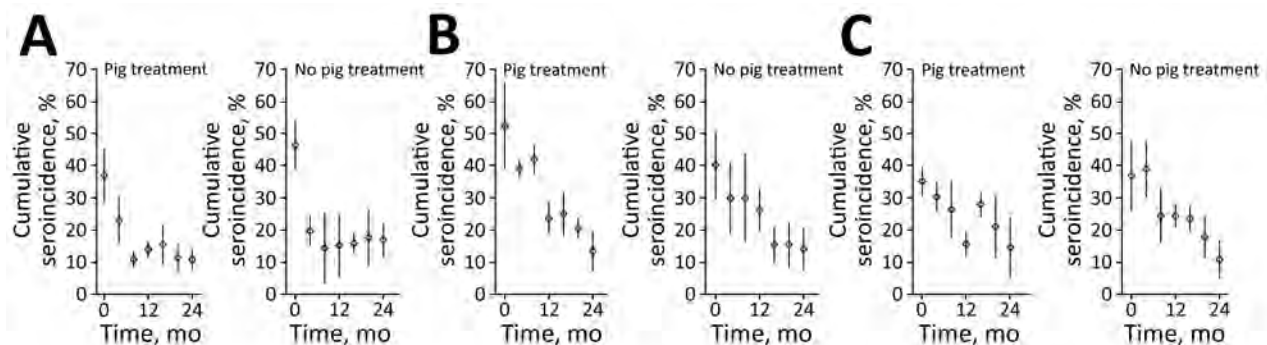
Figure 5. Comparison of cumulative *Taenia solium* seroincidence among pigs by study arm over time, Peru. A) Ring screening; B) ring treatment; C) mass treatment. Each intervention approach used niclosamide for human taeniasis in villages. Each approach included 2 arms: 1 with oxfendazole treatment of pigs for cysticercosis and 1 without pig treatment. In ring screening, participants living near pigs with cysticercosis were screened for taeniasis using stool coproantigen; identified cases were treated with niclosamide. In ring treatment, participants living near pigs with cysticercosis received presumptive treatment with niclosamide. In mass treatment, participants received treatment with niclosamide every 6 months regardless of location. Diamonds indicate point estimates; vertical bars indicate 95% CIs.

host, additional interventions in the intermediate pig host might not be necessary. We did not test oxfendazole in the absence of treatment for taeniasis; therefore, we cannot draw conclusions on the effectiveness of treatment interventions exclusively in pig versus human populations. We also did not apply vaccines against porcine cysticercosis, but this option could be considered in both mass and targeted approaches (*30*).

The strengths of our study were cluster-randomized design, head-to-head evaluation of interventions, and 2-year duration of the intervention. Limitations include that the small number of clusters in each study arm limited precision of outcome estimates, which could have affected our ability to distinguish true differences between arms. However, results and interpretations were consistent using multiple methods for determining SEs with small numbers of clusters, and we reported results using the most conservative method. The factorial design and large number of pigs in each cluster also benefited study efficiency. We randomly assigned villages to interventions, but the groups differed with respect to the proportion of households with pig corrals and latrines and the baseline seroprevalence of porcine cysticercosis. We controlled for these factors in the analysis, but residual confounding or differences in other unmeasured risk factors might have contributed to observed differences in outcomes. Participation in the studied interventions likely would differ across regions and cultures. In addition, ring interventions likely are dependent on geographic features, such as terrain and housing density. Thus, the results of this study might not be the same in regions where these factors differ. Finally, the secondary outcome measure of taeniasis prevalence at study end should be interpreted with caution because a baseline measurement was not taken. Diagnosis of taeniasis obligates treatment, so baseline measurement of taeniasis was not done because it would have confounded the interventions under evaluation.

In conclusion, our findings clearly demonstrate that substantial and rapid *T. solium* control can be achieved by using existing technology. Government control programs for taeniasis and cysticercosis can be initiated and scaled in accordance with the World Health Organization roadmap for overcoming neglected tropical diseases (*7*).

About the Author

Dr. O'Neal is an associate professor of epidemiology at Oregon Health & Science University, Portland, Oregon, USA. His primary research interest is the epidemiology and control of *Taenia solium* infection.

References

1. Ndimubanzi PC, Carabin H, Budke CM, Nguyen H, Qian Y-J, Rainwater E, et al. A systematic review of the frequency of neurocyticercosis with a focus on people with epilepsy. PLoS Negl Trop Dis. 2010;4:e870. https://doi.rg/10.1371/journal.pntd.0000870
2. Coyle CM, Mahanty S, Zunt JR, Wallin MT, Cantey PT, White AC, et al. Neurocysticercosis: neglected but not forgotten. PLoS Negl Trop Dis. 2012;6:e1500. https://doi.org/10.1371/journal.pntd.0001500
3. Winkler AS. Neurocysticercosis in sub-Saharan Africa: a review of prevalence, clinical characteristics, diagnosis, and management. Pathog Glob Health. 2012;106:261–74. https://doi.org/10.1179/2047773212Y.0000000047
4. Godfray HCJ, Aveyard P, Garnett T, Hall JW, Key TJ, Lorimer J, et al. Meat consumption, health, and the environment. Science. 2018;361:eaam5324. https://doi.org/10.1126/science.aam5324
5. Torgerson PR, Devleesschauwer B, Praet N, Speybroeck N, Willingham AL, Kasuga F, et al. World Health Organization estimates of the global and regional disease burden of 11 foodborne parasitic diseases, 2010: a data synthesis. PLOS Med. 2015;12:e1001920. https://doi.org/10.1371/journal.pmed.1001920
6. O'Neal SE, Flecker RH. Hospitalization frequency and charges for neurocysticercosis, United States, 2003-2012. Emerg Infect Dis. 2015;21:969–76. https://doi.org/10.3201/eid2106.141324
7. World Health Organization. Accelerating work to overcome the global impact of neglected tropical diseases: a roadmap for implementation. Geneva; The Organization: 2012 [cited 2020 Jul 18]. https://www.who.int/neglected_diseases/NTD_RoadMap_2012_Fullversion.pdf
8. Garcia HH, Gonzalez AE, Tsang VCW, O'Neal SE, Llanos-Zavalaga F, Gonzalvez G, et al.; Cysticercosis Working Group in Peru. Elimination of *Taenia solium* transmission in northern Peru. N Engl J Med. 2016;374:2335–44. https://doi.org/10.1056/NEJMoa1515520
9. Allan JC, Velasquez-Tohom M, Fletes C, Torres-Alvarez R, Lopez-Virula G, Yurrita P, et al. Mass chemotherapy for intestinal *Taenia solium* infection: effect on prevalence in humans and pigs. Trans R Soc Trop Med Hyg. 1997;91:595–8. https://doi.org/10.1016/S0035-9203(97)90042-0
10. Sarti E, Schantz PM, Avila G, Ambrosio J, Medina-Santillán R, Flisser A. Mass treatment against human taeniasis for the control of cysticercosis: a population-based intervention study. Trans R Soc Trop Med Hyg. 2000;94:85–9. https://doi.org/10.1016/S0035-9203(00)90451-6
11. Garcia HH, Gonzalez AE, Gilman RH, Moulton LH, Verastegui M, Rodriguez S, et al.; Cysticercosis Working Group in Peru. Combined human and porcine mass chemotherapy for the control of *T. solium*. Am J Trop Med Hyg. 2006;74:850–5. https://doi.org/10.4269/ajtmh.2006.74.850
12. O'Neal SE, Moyano LM, Ayvar V, Rodriguez S, Gavidia C, Wilkins PP, et al. Ring-screening to control endemic transmission of *Taenia solium*. PLoS Negl Trop Dis. 2014;8:e3125. https://doi.org/10.1371/journal.pntd.0003125

13. Assana E, Kyngdon CT, Gauci CG, Geerts S, Dorny P, De Deken R, et al. Elimination of *Taenia solium* transmission to pigs in a field trial of the TSOL18 vaccine in Cameroon. Int J Parasitol. 2010;40:515–9. https://doi.org/10.1016/j.ijpara.2010.01.006

14. Bulaya C, Mwape KE, Michelo C, Sikasunge CS, Makungu C, Gabriel S, et al. Preliminary evaluation of community-led total sanitation for the control of *Taenia solium* cysticercosis in Katete District of Zambia. Vet Parasitol. 2015;207:241–8. https://doi.org/10.1016/j.vetpar.2014.12.030

15. Carabin H, Millogo A, Ngowi HA, Bauer C, Dermauw V, Koné AC, et al. Effectiveness of a community-based educational programme in reducing the cumulative incidence and prevalence of human *Taenia solium* cysticercosis in Burkina Faso in 2011–14 (EFECAB): a cluster-randomised controlled trial. Lancet Glob Health. 2018;6:e411–25. https://doi.org/10.1016/S2214-109X(18)30027-5

16. Mwidunda SA, Carabin H, Matuja WBM, Winkler AS, Ngowi HA. A school based cluster randomised health education intervention trial for improving knowledge and attitudes related to *Taenia solium* cysticercosis and taeniasis in Mbulu district, northern Tanzania. PLOS ONE. 2015;10:e0118541. https://doi.org/10.1371/journal.pone.0118541

17. Anderson RM, May RM. Population dynamics of human helminth infections: control by chemotherapy. Nature. 1982;297:557–63. https://doi.org/10.1038/297557a0

18. World Health Organization. Guideline: preventive chemotherapy to control soil-transmitted helminth infections in at-risk population groups. Geneva; the Organization: 2017 [cited 2018 Nov 19]. http://www.ncbi.nlm.nih.gov/books/NBK487927

19. Gonzalez AE, Cama V, Gilman RH, Tsang VCW, Pilcher JB, Chavera A, et al. Prevalence and comparison of serologic assays, necropsy, and tongue examination for the diagnosis of porcine cysticercosis in Peru. Am J Trop Med Hyg. 1990;43:194–9. https://doi.org/10.4269/ajtmh.1990.43.194

20. Bustos JA, Rodriguez S, Jimenez JA, Moyano LM, Castillo Y, Ayvar V, et al.; Cysticercosis Working Group in Peru. Detection of *Taenia solium* taeniasis coproantigen is an early indicator of treatment failure for taeniasis. Clin Vaccine Immunol. 2012;19:570–3. https://doi.org/10.1128/CVI.05428-11

21. Gonzales AE, Garcia HH, Gilman RH, Gavidia CM, Tsang VC, Bernal T, et al. Effective, single-dose treatment or porcine cysticercosis with oxfendazole. Am J Trop Med Hyg. 1996;54:391–4. https://doi.org/10.4269/ajtmh.1996.54.391

22. Moreno L, Lopez-Urbina MT, Farias C, Domingue G, Donadeu M, Dungu B, et al. A high oxfendazole dose to control porcine cysticercosis: pharmacokinetics and tissue residue profiles. Food Chem Toxicol. 2012;50:3819–25. https://doi.org/10.1016/j.fct.2012.07.023

23. Tsang VCW, Pilcher JA, Zhou W, Boyer AE, Kamango-Sollo EIO, Rhoads ML, et al. Efficacy of the immunoblot assay for cysticercosis in pigs and modulated expression of distinct IgM/IgG activities to *Taenia solium* antigens in experimental infections. Vet Immunol Immunopathol. 1991;29:69–78. https://doi.org/10.1016/0165-2427(91)90053-F

24. Muro C, Gomez-Puerta LA, Flecker RH, Gamboa R, Barreto PV, Dorny P, et al.; for the Cysticercosis Working Group In Peru. Porcine cysticercosis: possible cross-reactivity of *Taenia hydatigena* to GP50 antigen in the enzyme-linked immunoelectrotransfer blot assay. Am J Trop Med Hyg. 2017;97:1830–2. https://doi.org/10.4269/ajtmh.17-0378

25. Guezala M-C, Rodriguez S, Zamora H, Garcia HH, Gonzalez AE, Tembo A, et al. Development of a species-specific coproantigen ELISA for human *Taenia solium* taeniasis. Am J Trop Med Hyg. 2009;81:433–7. https://doi.org/10.4269/ajtmh.2009.81.433

26. Flisser A, Madrazo I, Plancarte A, Schantz P, Allan J, Craig P, et al. Neurological symptoms in occult neurocysticercosis after single taeniacidal dose of praziquantel. Lancet. 1993;342:748. https://doi.org/10.1016/0140-6736(93)91743-6

27. Smits HL. Prospects for the control of neglected tropical diseases by mass drug administration. Expert Rev Anti Infect Ther. 2009;7:37–56. https://doi.org/10.1586/14787210.7.1.37

28. Beam M, Spencer A, Fernandez L, Atto R, Muro C, Vilchez P, et al.; for the Cysticercosis Working Group in Peru. Barriers to participation in a community-based program to control transmission of *Taenia solium* in Peru. Am J Trop Med Hyg. 2018;98:1748–54. https://doi.org/10.4269/ajtmh.17-0929

29. Donadeu M, Fahrion AS, Olliaro PL, Abela-Ridder B. Target product profiles for the diagnosis of Taenia solium taeniasis, neurocysticercosis and porcine cysticercosis. PLoS Negl Trop Dis. 2017;11:e0005875. https://doi.org/10.1371/journal.pntd.0005875

30. Lightowlers MW. Eradication of Taenia solium cysticercosis: a role for vaccination of pigs. Int J Parasitol. 2010;40:1183–92. https://doi.org/10.1016/j.ijpara.2010.05.001

Address for correspondence: Dr. Seth O'Neal, School of Public Health, Oregon Health & Science University–Portland State University, 3181 SW Sam Jackson Park Rd, Portland, OR 97239, USA; email: oneals@ohsu.edu

Risk Areas for Influenza A(H5) Environmental Contamination in Live Bird Markets, Dhaka, Bangladesh

Shovon Chakma, Muzaffar G. Osmani, Holy Akwar, Zakiul Hasan, Tanzinah Nasrin,
Md Rezaul Karim, Mohammed Abdus Samad, Mohammad Giasuddin, Peter Sly,
Zahir Islam, Nitish Chandra Debnath, Eric Brum, Ricardo Soares Magalhães

We evaluated the presence of influenza A(H5) virus environmental contamination in live bird markets (LBMs) in Dhaka, Bangladesh. By using Bernoulli generalized linear models and multinomial logistic regression models, we quantified LBM-level factors associated with market work zone–specific influenza A(H5) virus contamination patterns. Results showed higher environmental contamination in LBMs that have wholesale and retail operations compared with retail-only markets (relative risk 0.69, 95% 0.51–0.93; p = 0.012) and in March compared with January (relative risk 2.07, 95% CI 1.44–2.96; p<0.001). Influenza A(H5) environmental contamination remains a public health problem in most LBMs in Dhaka, which underscores the need to implement enhanced biosecurity interventions in LBMs in Bangladesh.

Live bird markets (LBMs) have long been identified as major sites for the maintenance, transmission, amplification, and dissemination of influenza A(H5) virus (*1,2*). Studies in the United States, China, Indonesia, and Vietnam have shown that LBMs can pose a public health risk for zoonotic spill-over to humans through environmental contamination (*2–8*). In Bangladesh, the first evidence of zoonotic transmission of influenza A(H5) virus emerged in 2012; LBMs in Dhaka were considered the main source of exposure for all 3 human cases reported (*9,10*). The relatively low level of influenza A(H5) endemicity found in studies

conducted in LBMs in Bangladesh since 2012 (e.g., ≤10% prevalence at live bird sampling level) (*11–13*) have contributed to a false sense of security regarding contamination risk. Indeed, since 2013, several influenza A(H5) outbreaks in poultry (9 outbreaks), wild birds (5 outbreaks), and humans (2 outbreaks) have occurred in Bangladesh (*14,15*). During March 2007–December 2020, Bangladesh reported 556 outbreaks of influenza A(H5) virus in poultry (*14*) and 8 cases in humans (*15*).

Environmental sampling in LBMs for the purposes of avian influenza virus surveillance was first introduced in the United States in 1986 (*16*). A recent study evaluated the effectiveness of environmental sampling for influenza A surveillance and described multiple sampling sites in an LBM (*17*). Earlier studies from Bangladesh primarily focused on collecting samples from market environment sites (such as market floor, stall floor, slaughter area, waste bin, poultry cage, water, fecal material on or underneath the poultry cage, blood, and poultry offal) to understand the LBM environment status for influenza A (*11,12,18–25*).

Few studies to date—1 in Indonesia and 3 in Guangdong, China—have performed simultaneous sampling in different LBM work zones, such as the poultry delivery, poultry holding, poultry slaughter, poultry sale, and waste disposal zones (*26–29*). These studies indicated that the poultry slaughter and sale zones were the 2 most contaminated LBM work zones for influenza A(H5N1) in Indonesia (*27*) and influenza A(H7N9), (H5), and (H9) in China (*26,28,29*). To date, no studies have been performed in Bangladesh on influenza A environmental contamination within different LBM work zones. The results from China and Indonesia have provided additional justification to evaluate the influenza A surveillance program of

the Food and Agriculture Organization of the United Nations (FAO) in Bangladesh. Given the costs of maintaining influenza surveillance programs, epidemiologic evidence on within-market risk areas for contamination would help fine-tune current surveillance approaches in Bangladesh.

Implementing biosecurity practices in LBMs reduces environmental contamination with influenza A (*30*). For example, weekly market closures (>1 day) and everyday cleaning and disinfecting interventions were reported to reduce market contamination with avian influenza virus (H7N2) in the United States and influenza (H7N9) and (H9N2) in China (*5,31,32*). In Bangladesh, improved biosecurity practices at the market level have not effectively reduced environmental contamination for influenza A(H5) virus in Dhaka and Chittagong LBMs during 2012–2014 (*22,25*). Since 2014, no study has comprehensively reported the effect of market-level biosecurity practices on the probability of influenza A(H5) environmental contamination in Dhaka. Although the 2 administrative areas of the Dhaka metropolitan area (Dhaka North City Corporation [DNCC] and Dhaka South City Corporation [DSCC]) are known for their distinct demographic and urban features (*33*), no studies to date have investigated how biosecurity practices and influenza A(H5) contamination rates differ in relation to market-level characteristics of LBMs located in different parts of Dhaka. To inform the development of effective environmental sampling strategies for influenza surveillance in LBMs, our study sought to characterize the differences in the proportion of influenza A(H5) environmental contamination in markets in DNCC and DSCC, to identify and quantify market-level factors associated with the probability of influenza A(H5) contamination in specific work zones (i.e., arrival, slaughtering and processing, and consumer exposure or sales), and to identify and quantify market-level factors associated with work zone–specific contamination patterns within LBMs.

Materials and Methods

Study Design for Influenza A(H5) Virus Surveillance in LBMs in Dhaka Metropolitan

We focused our investigation on the Dhaka metropolitan area, which has the highest population density (30,551 residents/km^2) of all metropolitan areas in Bangladesh (*34*). We selected 104 LBMs within metropolitan Dhaka (Figure 1), which were part of the influenza surveillance initiative of the FAO and Department of Livestock Services (DLS) (Appendix, https://wwwnc.cdc.gov/EID/article/27/9/20-4447-App1.pdf) (*35*). Sampling targeted

the months of January–March, which are known for a higher level of circulation of influenza A(H5) virus in poultry in Bangladesh (*36*).

We used data on market-level characteristics collected during the Dhaka LBM census to quantify the association between influenza A(H5) environmental contamination in LBMs and within specific market work zones adjusted for market-level characteristics (Appendix). Three market work zones (poultry arrival [A], poultry slaughtering and processing [S], and consumer exposure or sales [E]) and environmental sites in each work zone were selected for sampling on the basis of the findings from Indrani et al. (Appendix) (*27*).

Collection, Preservation, and Transportation of Environmental Samples

Sample collectors from DLS, DNCC, and DSCC performed monthly collection of environmental samples from the selected LBMs. In a given visit, a pool of 6 samples were collected from each work zone using standard polyester-tipped swabs and stored separately in a 3 mL viral transport medium (Becton Dickinson, https://www.bd.com). Pooled samples were kept in ice boxes and transported to the DLS Central Disease Investigation Laboratory and Livestock Research Institute laboratory for temporary storage at 4°C. All samples were then transported in ice boxes to the National Reference Laboratory for Avian Influenza at Bangladesh Livestock Research Institute (Savar, Dhaka) and stored at −80°C before testing.

Laboratory Testing

We tested for influenza A(H5) virus 18-swab pools from each selected market (i.e., 6 swabs/3 work zones) using real-time reverse transcription PCR (rRT-PCR). When an 18-swab pool of a market tested positive, further testing was carried out using rRT-PCR to confirm influenza A(H5) virus in the 6-swab pool of a specific work zone (Figure 2). We used Mag-MAX viral RNA isolation kit and KingFisher mL Purification System extractor (ThermoFisher Scientific, https://www.thermofisher.com) for RNA extraction. The rRT-PCR testing protocols followed the procedures recommended by the Australian Centre for Disease Preparedness quality assurance manual with influenza A(H5) primers (IVA D148 H5, IVA D149 H5, IVA D204f, and IVA D205r) and probes (IVA H5a and IVA D215P) produced at Australian Animal Health Laboratory and AgPath-ID One-Step RT-PCR Reagents (ThermoFisher Scientific). A pool sample was considered positive for influenza A(H5) if the cycle threshold value was <40 (*37*).

Data Analyses

Our study included markets with information on both infection status and market-level characteristics (n = 97) and those with information on market-level infection status only (n = 7). In our analyses, we considered 2 outcomes of interest: presence or absence of influenza A(H5) virus environmental contamination in specific work zones and LBM–level zone-specific influenza A(H5) environmental contamination patterns. Work zone–specific environmental contamination patterns were classified as negative if all 3 work zones tested negative; ASE–positive when all 3 work zones tested positive; S only–positive when only the slaughtering and processing zone tested positive; SE– or AS–positive when the slaughtering and processing zone and 1 other work zone (E or A) tested positive; and other when the market tested positive for A only, E only, or both A and E.

We summarized DNCC and DSCC market-level biosecurity characteristics by using descriptive statistical analyses. Market-level biosecurity characteristics considered in the investigation included market location, market type, species sold, number of vendors,

number of poultry species sold, dominant species (by comparing the poultry headcount), poultry headcount, electricity in the facility, presence of roof, running water in the facility, sale of poultry to other vendors, weekly market closure (≥1 day), direct sale of poultry to consumers, sale of products other than poultry (i.e., fish, red meat, vegetables, groceries), daily cleaning protocol (at minimum with detergent), poultry slaughtering locations, and number of slaughtering facilities. We used a univariable Fisher exact test with a significance level of $p<0.05$ to identify differences in influenza A(H5) recovery by the geographic location of Dhaka markets. We then ran Bernoulli generalized linear models and multinomial logistic regression models to quantify risk factors associated with the probability of influenza A(H5) environmental contamination and work zone–specific contamination patterns (Appendix). The goodness-of-fit of the final multivariable model was assessed by Akaike information criterion (AIC), and the lowest AIC among all competing models was identified as the best fitting model in the study (38). We used Stata 15 (StataCorp LLC, https://www.stata.com) for statistical analyses.
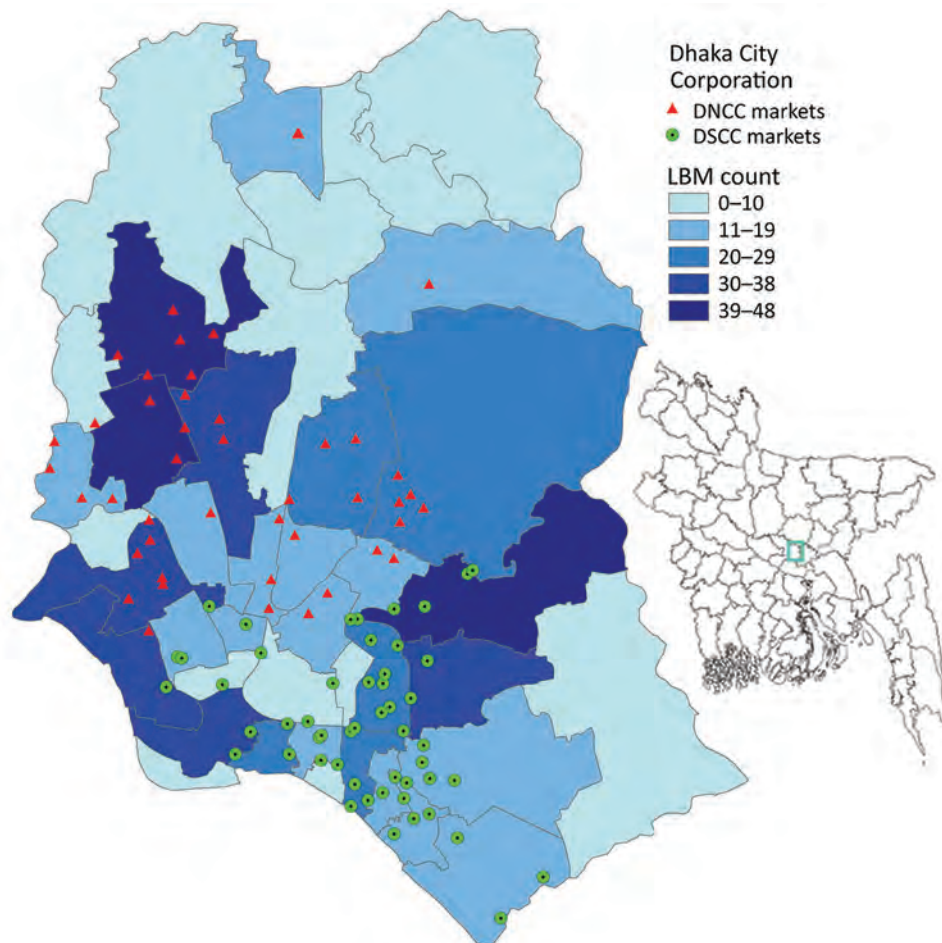
Figure 1. Locations of LBMs in the Dhaka metropolitan area, Bangladesh, January–March 2016. Inset map shows location of Dhaka in Bangladesh. DNCC, Dhaka North City Corporation; DSCC, Dhaka South City Corporation; LBM, live bird market.
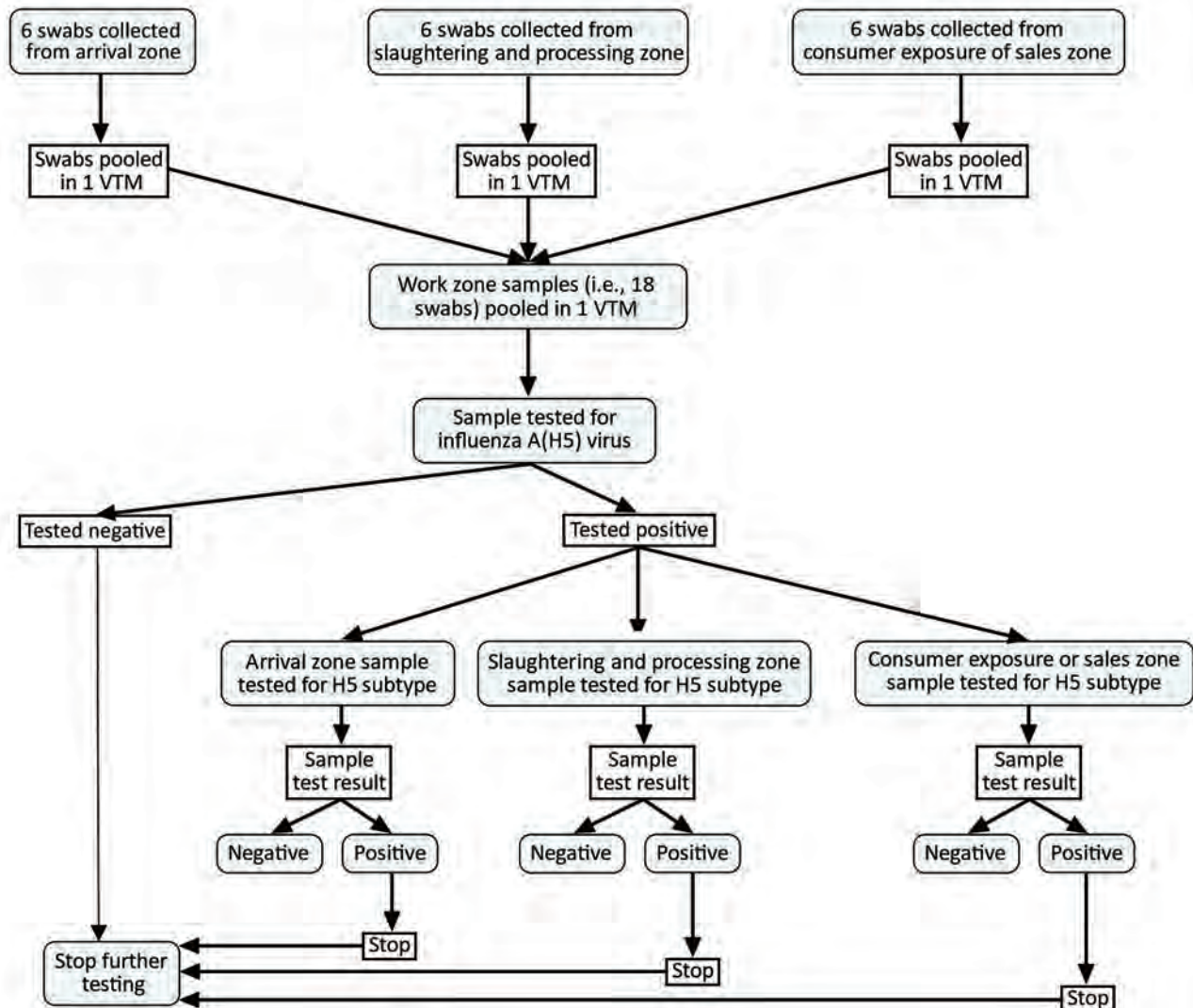
Figure 2. Sampling and laboratory testing protocol for influenza A(H5) in live bird markets, Dhaka, Bangladesh, January–March 2016. VTM, viral transport medium.

Results

Characteristics of LBMs

Of 104 enrolled LBMs, a total of 97 markets (52 from DSCC and 45 from DNCC) had complete questionnaire information on their biosecurity characteristics (Appendix Table 1). The retail type of LBM was predominant in DSCC (84.62%, 45/52) and DNCC (64.44%, 29/45) of Dhaka. Most markets in DSCC (88.46%, 46/52) and DNCC (97.78%, 44/45) sold multiple species of poultry. The broiler chicken was the main species at LBMs in DSCC (69.23%, 36/52) and DNCC (80.00%, 36/45).

Market-level daily cleaning (at minimum with detergent) and weekly market closure (≥1 day)

practices varied among DNCC and DSCC markets. These 2 practices were reported to be more common in DSCC markets (75.00% [39/52] for daily cleaning and 45.15% [24/52] for weekly closure) compared with DNCC markets (31.11% [23/45] and 17.78% [8/45]). Most markets reported slaughtering poultry at vendor stalls (78.85% [41/52] in DSCC and 93.33% [42/45] in DNCC) (Appendix Table 1).

Differences in the Proportion of Influenza A(H5) Virus Environmental Contamination and Market Characteristics

Our analysis indicates that the proportion of influenza A(H5) virus environmental contamination was significantly higher in March than the previous 2 months

(p≤0.001) (Appendix Table 2). The trend of LBM work zone–specific influenza A(H5) environmental contamination was similar in March in DSCC and DNCC markets, and the highest level of environmental contamination was in the slaughtering and processing zone (Figure 3). Of all market-level characteristics, only 3 characteristics were found to be significantly associated with proportions of influenza A(H5) environmental contamination: market type (p = 0.036) and location of poultry slaughtering (p = 0.014) in DNCC markets and weekly market closure of ≥1 day (p = 0.006) in DSCC markets (Appendix Table 2).

Factors Associated with Influenza A(H5) Virus Environmental Contamination within LBMs

Factors Associated with the Probability of LBM Influenza A(H5) Environmental Contamination Risk

We demonstrated by univariable analysis that the probability of influenza A(H5) environmental contamination was significantly higher in slaughtering and processing zones (relative risk [RR] 1.22, 95% CI 1.01–1.49; p = 0.041) than in market arrival zones. The probability of contamination was significantly higher in March (RR 1.90, 95% CI 1.36–2.65; p≤0.001) than January (Table 1).

In the final multivariable analysis (model 2), after adjusting for market-level biosecurity factors, we demonstrated that the probability of influenza A(H5) environmental contamination remained 2-fold significantly higher in March than January (RR 2.07, 95% CI 1.44–2.96; p<0.001). Our findings also demonstrated that slaughtering and processing zones had an increased risk for influenza A(H5) recovery compared to the arrival zone, but this effect was not statistically significant (RR 1.21, 95% CI 0.99–1.49; p = 0.067). In addition, the probability of influenza A(H5) environmental contamination was significantly associated with market type: retail markets were at lower risk than dual-purpose markets (RR 0.69, 95% CI 0.51–0.93; p = 0.012) (Table 1). Model 2 presented a better fit to the data than model 1 (i.e., without adjusting for market-level biosecurity factors). The AIC of model 1 was 1020.6 and in model 2 was 932.9. Effect modification and confounding were not found among pairs of biologically plausible LBM predictor variables.

Factors Associated with Work Zone–Specific Influenza A(H5) Virus Environmental Contamination Patterns

Our univariable and multivariable model of the multinomial analysis showed a significant increased risk in all LBM work zone–specific influenza A(H5) environmental contamination patterns except "slaughtering and processing zone area only" in March (relative risk ratio [RRR] >1; null value not contained within 95% CI) compared with January (Table 2, https://wwwnc.cdc.gov/EID/article/27/9/20-4447-T2.htm). After multivariable adjustment, no market-level factors were significantly associated with work zone–specific influenza A(H5) virus environmental contamination patterns.

Discussion

Our analyses provide the most comprehensive account of the recovery of influenza A(H5) virus in specific LBM work zones over 3 months across a large sample of LBMs (n = 104) within the Dhaka metropolitan area of Bangladesh. This study overcomes many of the limitations seen in previous studies of LBMs in Dhaka in the context of within-market measurement of environmental contamination (11,12,19,20,22,25).

Our descriptive results indicated vulnerabilities in LBMs in Dhaka associated with increased proportions of influenza A(H5) virus environmental contamination. Previous studies have shown that dual-purpose LBMs (i.e., markets conducting both wholesale and retail operations) in Dhaka were at higher risk for influenza A contamination (11). This previous finding suggests that markets in DNCC would be at greater risk for influenza A(H5) contamination. Our analyses confirmed this suggestion, demonstrating a larger proportion of influenza A(H5) recovery in dual-purpose DNCC markets than in retail-only markets. Poultry slaughtering has been consistently found to be a significant risk factor for LBM environmental contamination with influenza A(H5), and studies in Indonesia (2,27) and Bangladesh (19) support this observation. Environmental contamination with influenza A(H5) was significantly higher in DNCC markets without slaughtering facilities than in those reporting poultry slaughtering. Market environmental contamination in the absence of slaughtering facilities could be linked to the sampling procedure, in which sample collectors were instructed to use their sense of perceived risk if suggested sampling sites were not present in the market and other sites had to be chosen. This limitation in the sampling procedure should be corrected in future studies. Biosecurity practices such as cleaning and market closures have been reported to reduce environmental contamination in LBMs and eliminate risk for human infection with influenza A (39). Our results indicate that DSCC markets would benefit from higher rates of closures; a higher proportion of influenza A(H5) contamination was found in DSCC markets that did not perform market closures. In 2017, China established the

1110 policy, which involves daily cleaning, weekly disinfection, monthly closure, and no overnight stay of poultry (*40*). This approach has been successful at reducing the level of contamination within LBMs. This suggests that the implementation of a 1110-type policy in Dhaka's LBMs would strengthen LBM biosecurity, thereby reducing the level of influenza A(H5) contamination. Taken together, the observed differences in environmental contamination between markets in DSCC and DNCC can partly be explained by poultry slaughter and market management activities and less so by trader and poultry demographics.

Risk for influenza A(H5) infection in humans and poultry has been shown to be associated with movement of live poultry during national festive periods (*41–43*). In Bangladesh, demand for poultry products is influenced by traditional customs and rituals, including religious and cultural festivals (*44–46*). Our analysis found a 2-fold increase in the probability of environmental contamination in March compared with January, and market-level covariates did not modify this effect. Our analysis indicates the increased probability of influenza A(H5) environmental contamination in March in urban LBMs of Dhaka is likely related to the Bangla new year festival, which occurs in April and is linked to increased demand for poultry products in urban Dhaka LBMs.

We demonstrated that influenza A(H5) environmental contamination was positively associated with 2 market-level covariates: work zone (slaughtering and processing zone compared with arrival zone) and type of market (dual-purpose markets compared with retail-only markets). The higher probability of influenza A(H5) environmental contamination in the slaughtering and processing zone and in dual-purpose markets could be related to the challenge of maintaining adequate sanitation in LBMs with these characteristics. The risk for environmental contamination is known to be increased when slaughtering equipment is not frequently cleaned throughout the day using adequate disinfection protocols (*47*). Market attributes such as the presence of wholesalers in the market (*11*) and within-market trade of asymptomatic poultry between wholesalers and retailers (*44*) explain the higher levels of influenza A(H5) environmental contamination in dual-purpose markets compared with retail markets. Our analysis uncovered biosecurity characteristics that could partially explain these higher levels of influenza A(H5) environmental contamination. For example, dual-purpose markets have greater heterogeneity in poultry species

Table 1. Risk factors associated with the probability of influenza A(H5) environmental contamination at specific live bird market work zones, Dhaka, Bangladesh, January–March 2016

Risk factor	Univariable analysis			Multivariable model 1			Multivariable model 2		
	RR (95% CI)	p value	Overall p value	RR (95% CI)	p value	Overall p value	RR (95% CI)	p value	Overall p value
Market work zones of sample collection; reference: arrival									
Slaughtering and processing	1.22 (1.01–1.49)	0.041	0.110	1.23 (1.01–1.50)	0.040	0.103	1.21 (0.99–1.49)	0.067	0.180
Consumer exposure or sales	1.05 (0.84–1.31)	0.647		1.05 (0.84–1.32)	0.655		1.09 (0.86–1.37)	0.487	
Month of sample collection; reference: January									
February	1.24 (0.87–1.77)	0.233	<0.001	1.24 (0.87–1.76)	0.239	<0.001	1.33 (0.91–1.94)	0.138	<0.001
March	1.90 (1.36–2.65)	<0.001		1.90 (1.36–2.65)	<0.001		2.07 (1.44–2.96)	<0.001	
Market type; reference: dual-purpose†									
Wholesale	0.79 (0.57–1.10)	0.161	0.042				0.79 (0.571.10)	0.161	0.042
Retail	0.69 (0.51–0.92)	0.012					0.69 (0.510.93)	0.012	
Species being sold (reference: multiple species)†	0.57 (0.30–1.08)	0.084							
Electricity in facility†	1.50 (0.87–2.60)	0.148							
Market sells poultry to other vendors†	1.21 (0.92–1.58)	0.176							
Weekly market closure (≥1 day)†	0.79 (0.55–1.14)	0.207							
Akaike information criterion				1,020.588			932.9017		

*Blank cells indicate variables not included in model. RR, relative risk.
†Univariable results adjusted for month of sample collection and market work zones of sample collection.
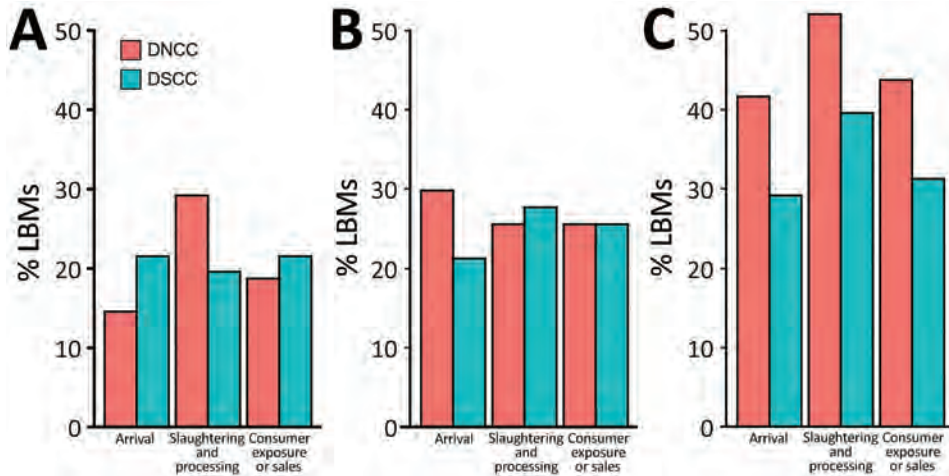
Figure 3. Distribution of influenza A(H5) virus environmental contamination in specific work zones in LBMs of DNCC and DSCC, Dhaka, Bangladesh, January–March 2016. A) January; B) February; C) March. DNCC, Dhaka North City Corporation; DSCC, Dhaka South City Corporation; LBM, live bird market.

than retail-only markets (Appendix Table 3), which could promote virus introduction. Furthermore, our data suggest that the *Sonali* chicken crossbreed was dominant in dual-purpose markets compared with other markets (Appendix Table 3); this crossbreed has previously been shown to have a higher bird-level influenza A(H5) prevalence (*11*).

Our study revealed a significantly increased probability of influenza A(H5) environmental contamination in March in 3 of the 4 site-specific influenza A(H5) environmental contamination patterns. Our results also extend those from a recent study by demonstrating that, outside the month of March, the slaughter area was the environmental site most contaminated with influenza A(H5) in LBMs (*25*). Our findings suggest that to increase the probability of detection of influenza A(H5) environmental contamination, those conducting surveillance should consider the slaughtering and processing zone as the candidate sampling site within LBMs during the months leading up to the increased demand for poultry in April. Furthermore, our results suggest that market-level biosecurity characteristics did not influence the temporal variation in work zone–specific influenza A(H5) environmental contamination patterns (Appendix Figure 1).

Of note, only 1 market-level characteristic (market sells poultry to other traders) was reported to be marginally associated with the probability of S-only environmental contamination pattern. This relationship could be partly explained by the fact that LBM contamination level is not simply the result of continuous introductions of infected birds, but a consequence of virus recirculation and amplification within them (*1*). To further elucidate the market work zone–specific influenza A(H5) environmental contamination patterns identified in this study, follow-up studies into the social network of poultry trade in LBMs are needed to clarify the effect.

The first limitation of our study is that, although we triangulated information on Dhaka LBM characteristics from data collectors with that from market managers through telephone call data validation, the use of secondary data might have introduced undue reporting bias. Second, we focused our analyses on the 3-month period of the winter season (January–March); further analyses should consider expanding the temporal scope of the investigation to better understand the seasonal trends identified in this study. Third, we used a sample pooling strategy (i.e., 18-swab pools collected in 5 mL of viral transport medium), which has not been validated for the presence of serial dilution effect and should be evaluated in future studies. However, despite the 18-swab pooling, we found a significant positivity rate in pooled samples. Fourth, because of budgetary limitations, our study was only conducted in LBMs in the Dhaka metropolitan area without consideration of other cities in Bangladesh. Thus, caution should be taken in interpretation, because the environmental contamination of LBMs in Dhaka might not reflect the local idiosyncrasies of LBMs in other cities in Bangladesh. Finally, despite our efforts to address confounding effects, we could not consider other factors that could be associated with contamination levels, including the poultry trade network between LBMs and source farms and the presence of other infection reservoirs in LBMs.

In conclusion, this study demonstrates that LBMs located in DNCC of Dhaka are qualitatively more vulnerable to influenza A(H5) virus environmental contamination. The probability of influenza A(H5) environmental contamination is equally likely across all within-LBM sites investigated and particularly

higher in the month of March. The slaughtering and processing zones of LBMs could serve as candidate zones for active surveillance programs. Future work also should evaluate the effects of poultry movement and LBM biosecurity in the epidemiology of influenza A (H5) virus. Sanitation practices, market closures, and slaughtering and processing practice interventions within LBMs would help to reduce market-level influenza A contamination.

Acknowledgments

About the Author

Dr. Chakma is a veterinary epidemiologist currently enrolled as a PhD Candidate at the UQ Spatial Epidemiology Laboratory, School of Veterinary Science, University of Queensland. He has expertise in epidemiological research, infectious diseases and AMR surveillance, and One Health issues.

References

1. Fournié G, Guitian FJ, Mangtani P, Ghani AC. Impact of the implementation of rest days in live bird markets on the dynamics of H5N1 highly pathogenic avian influenza. J R Soc Interface. 2011;8:1079–89. https://doi.org/10.1098/rsif.2010.0510

2. Henning J, Hesterberg UW, Zenal F, Schoonman L, Brum E, McGrane J. Risk factors for H5 avian influenza virus prevalence on urban live bird markets in Jakarta, Indonesia—evaluation of long-term environmental surveillance data. PLoS One. 2019;14:e0216984. https://doi.org/10.1371/journal.pone.0216984

3. Trock SC, Gaeta M, Gonzalez A, Pederson JC, Senne DA. Evaluation of routine depopulation, cleaning, and disinfection procedures in the live bird markets, New York. Avian Dis. 2008;52:160–2. https://doi.org/10.1637/7980-040607-Reg

4. Garber L, Voelker L, Hill G, Rodriguez J. Description of live poultry markets in the United States and factors associated with repeated presence of H5/H7 low-pathogenicity avian influenza virus. Avian Dis. 2007;51(Suppl):417–20. https://doi.org/10.1637/7571-033106R.1

5. Bulaga LL, Garber L, Senne DA, Myers TJ, Good R, Wainwright S, et al. Epidemiologic and surveillance studies on avian influenza in live-bird markets in New York and New Jersey, 2001. Avian Dis. 2003;47(Suppl):996–1001. https://doi.org/10.1637/0005-2086-47.s3.996

6. Kung NY, Morris RS, Perkins NR, Sims LD, Ellis TM, Bissett L, et al. Risk for infection with highly pathogenic influenza A virus (H5N1) in chickens, Hong Kong, 2002. Emerg Infect Dis. 2007;13:412–8. https://doi.org/10.3201/eid1303.060365

7. Wang X, Wang Q, Cheng W, Yu Z, Ling F, Mao H, et al. Risk factors for avian influenza virus contamination of live poultry markets in Zhejiang, China during the 2015-2016 human influenza season. Sci Rep. 2017;7:42722. https://doi.org/10.1038/srep42722

8. Tran DT, Hoang BT, Chanachai K, Prarakamawongsai T, Padungtod P, Wongsathapornchai K, et al. Avian influenza outbreaks and surveillance in live bird markets, Quang Ninh Province, Vietnam, 2015–2017. Outbreak, Surveillance, Investigation & Response (OSIR). Journal. 2018;11:1–7.

9. World Health Organization. Influenza at the human-animal interface: summary and assessment as of 5 March 2012. 2012 [cited 2019 Dec 3]. https://www.who.int/influenza/human_animal_interface/Influenza_Summary_IRA_HA_interface_05March12.pdf

10. Hill EM, House T, Dhingra MS, Kalpravidh W, Morzaria S, Osmani MG, et al. Modelling H5N1 in Bangladesh across spatial scales: Model complexity and zoonotic transmission risk. Epidemics. 2017;20:37–55. https://doi.org/10.1016/j.epidem.2017.02.007

11. Kim Y, Biswas PK, Giasuddin M, Hasan M, Mahmud R, Chang YM, et al. Prevalence of avian influenza A (H5) and A (H9) viruses in live bird markets, Bangladesh. Emerg Infect Dis. 2018;24:2309–16. https://doi.org/10.3201/eid2412.180879

12. Khan SU, Gurley ES, Gerloff N, Rahman MZ, Simpson N, Rahman M, et al. Avian influenza surveillance in domestic waterfowl and environment of live bird markets in Bangladesh, 2007-2012. Sci Rep. 2018;8:9396. https://doi.org/10.1038/s41598-018-27515-w

13. Gupta SD, Hoque MA, Fournié G, Henning J. Patterns of avian influenza A (H5) and A (H9) virus infection in backyard, commercial broiler and layer chicken farms in Bangladesh. Transbound Emerg Dis. 2021;68:137–51. https://doi.org/10.1111/tbed.13657

14. World Organisation for Animal Health. World animal health information database (WAHIS interface): quantitative data. 2020 [cited 2019 Jun 16]. https://wahis.oie.int/#/dashboards/qd-dashboard

15. World Health Organization. Cumulative number of confirmed human cases of avian influenza A(H5N1) reported to WHO, 2003–2020 as of 10 July 2020. 2020 [cited 2020 Dec 20]. https://www.who.int/influenza/human_animal_interface/2020_01_20_tableH5N1.pdf

16. Senne D, Pearson J, Panigrahy BJAD. Live poultry markets: a missing link in the epidemiology of avian influenza. Avian Dis. 2003;47:50–8.

17. Hood G, Roche X, Brioudes A, von Dobschuetz S, Fasina FO, Kalpravidh W, et al. A literature review of the use of environmental sampling in the surveillance of avian influenza viruses. Transbound Emerg Dis. 2021;68:110–26. https://doi.org/10.1111/tbed.13633

18. Rahman M, Mangtani P, Uyeki TM, Cardwell JM, Torremorell M, Islam A, et al. Evaluation of potential risk

of transmission of avian influenza A viruses at live bird markets in response to unusual crow die-offs in Bangladesh. Influenza Other Respir Viruses. 2020;14:349–52. https://doi.org/10.1111/irv.12716

19. Chowdhury S, Azziz-Baumgartner E, Kile JC, Hoque MA, Rahman MZ, Hossain ME, et al. Association of biosecurity and hygiene practices with environmental contamination with influenza A viruses in live bird markets, Bangladesh. Emerg Infect Dis. 2020;26:2087–96. https://doi.org/10.3201/eid2609.191029

20. Yang G, Chowdury S, Hodges E, Rahman MZ, Jang Y, Hossain ME, et al. Detection of highly pathogenic avian influenza A(H5N6) viruses in waterfowl in Bangladesh. Virology. 2019;534:36–44. https://doi.org/10.1016/j.virol.2019.05.011

21. Barman S, Turner JCM, Hasan MK, Akhtar S, El-Shesheny R, Franks J, et al. Continuing evolution of highly pathogenic H5N1 viruses in Bangladeshi live poultry markets. Emerg Microbes Infect. 2019;8:650–61. https://doi.org/10.1080/22221751.2019.1605845

22. Biswas PK, Giasuddin M, Chowdhury P, Barua H, Debnath NC, Yamage M. Incidence of contamination of live bird markets in Bangladesh with influenza A virus and subtypes H5, H7 and H9. Transbound Emerg Dis. 2018;65:687–95. https://doi.org/10.1111/tbed.12788

23. Turner JCM, Feeroz MM, Hasan MK, Akhtar S, Walker D, Seiler P, et al. Insight into live bird markets of Bangladesh: an overview of the dynamics of transmission of H5N1 and H9N2 avian influenza viruses. Emerg Microbes Infect. 2017;6:e12. https://doi.org/10.1038/emi.2016.142

24. Sayeed MA, Smallwood C, Imam T, Mahmud R, Hasan RB, Hasan M, et al. Assessment of hygienic conditions of live bird markets on avian influenza in Chittagong metro, Bangladesh. Prev Vet Med. 2017;142:7–15. https://doi.org/10.1016/j.prevetmed.2017.04.009

25. Biswas PK, Giasuddin M, Nath BK, Islam MZ, Debnath NC, Yamage M. Biosecurity and circulation of influenza A (H5N1) virus in live–bird markets in Bangladesh, 2012. Transbound Emerg Dis. 2017;64:883–91. https://doi.org/10.1111/tbed.12454

26. Kang M, He J, Song T, Rutherford S, Wu J, Lin J, et al. Environmental sampling for avian influenza A (H7N9) in live-poultry markets in Guangdong, China. PLoS One. 2015;10:e0126335. https://doi.org/10.1371/journal.pone.0126335

27. Indriani R, Samaan G, Gultom A, Loth L, Irianti S, Adjid R, et al. Environmental sampling for avian influenza virus A (H5N1) in live-bird markets, Indonesia. Emerg Infect Dis. 2010;16:1889–95. https://doi.org/10.3201/eid1612.100402

28. Chen Z, Li K, Luo L, Lu E, Yuan J, Liu H, et al. Detection of avian influenza A(H7N9) virus from live poultry markets in Guangzhou, China: a surveillance report. PLoS One. 2014; 9:e107266. https://doi.org/10.1371/journal.pone.0107266

29. Cheng KL, Wu J, Shen WL, Wong AYL, Guo Q, Yu J, et al. Avian influenza virus detection rates in poultry and environment at live poultry markets, Guangdong, China. Emerg Infect Dis. 2020;26:591–5. https://doi.org/10.3201/eid2603.190888

30. Zhou X, Wang Y, Liu H, Guo F, Doi SA, Smith C, et al. Effectiveness of market-level biosecurity at reducing exposure of poultry and humans to avian influenza: a systematic review and meta-analysis. J Infect Dis. 2018;218:1861–75. https://doi.org/10.1093/infdis/jiy400

31. Yuan J, Lau EH, Li K, Leung YH, Yang Z, Xie C, et al. Effect of live poultry market closure on avian influenza A (H7N9) virus activity in Guangzhou, China, 2014. Emerg

Infect Dis. 2015;21:1784–93. https://doi.org/10.3201/eid2110.150623

32. Kung NY, Guan Y, Perkins NR, Bissett L, Ellis T, Sims L, et al. The impact of a monthly rest day on avian influenza virus isolation rates in retail live poultry markets in Hong Kong. Avian Dis. 2003;47(Suppl):1037–41. https://doi.org/10.1637/0005-2086-47.s3.1037

33. Swapan MSH, Zaman AU, Ahsan T, Ahmed F. Transforming urban dichotomies and challenges of South Asian megacities: rethinking sustainable growth of Dhaka, Bangladesh. Urban Sci. 2017;1:31. https://doi.org/10.3390/urbansci1040031

34. Bangladesh Bureau of Statistics. District statistics. 2019 [cited 2021 Mar 25]. http://www.bbs.gov.bd/site/page/2888a55d-d686-4736-bad0-54b70462afda/-

35. Osmani M, Akwar H, Hasan Z, Chakma S, Hossain MM, Brum E. Sink surveillance, an innovative approach to identify HPAI and other emerging zoonotic pathogens in live bird markets in Bangladesh. Presented at: Prince Mahidol Award Conference (PMAC); 2018 Jan 29–Feb 3; Bangkok, Thailand.

36. Durand LO, Glew P, Gross D, Kasper M, Trock S, Kim IK, et al. Timing of influenza A(H5N1) in poultry and humans and seasonal influenza activity worldwide, 2004–2013. Emerg Infect Dis. 2015;21:202–8. https://doi.org/10.3201/eid2102.140877

37. Heine HG, Trinidad L, Selleck P, Lowther S. Rapid detection of highly pathogenic avian influenza H5N1 virus by TaqMan reverse transcriptase-polymerase chain reaction. Avian Dis. 2007;51(Suppl):370–2. https://doi.org/10.1637/7587-040206R.1

38. Mohammed EA, Naugler C, Far BH. Emerging business intelligence framework for a clinical laboratory through big data analytics. In: Tran QN, Arabnia H, editors. Emerging trends in computational biology, bioinformatics, and systems biology. Boston: Morgan Kaufmann; 2015. p. 577–602.

39. Zhou X, Li Y, Wang Y, Edwards J, Guo F, Clements AC, et al. The role of live poultry movement and live bird market biosecurity in the epidemiology of influenza A (H7N9): A cross-sectional observational study in four eastern China provinces. J Infect. 2015;71:470–9. https://doi.org/10.1016/j.jinf.2015.06.012

40. Zhou X, Gao L, Wang Y, Li Y, Zhang Y, Shen C, et al. Geographical variation in the risk of H7N9 human infections in China: implications for risk-based surveillance. Sci Rep. 2020;10:10372. https://doi.org/10.1038/s41598-020-66359-1

41. Soares Magalhães RJ, Zhou X, Jia B, Guo F, Pfeiffer DU, Martin V. Live poultry trade in Southern China provinces and HPAIV H5N1 infection in humans and poultry: the role of Chinese New Year festivities. PLoS One. 2012;7:e49712. https://doi.org/10.1371/journal.pone.0049712

42. Delabouglise A, Choisy M, Phan TD, Antoine-Moussiaux N, Peyre M, Vu TD, et al. Economic factors influencing zoonotic disease dynamics: demand for poultry meat and seasonal transmission of avian influenza in Vietnam. Sci Rep. 2017;7:5905. https://doi.org/10.1038/s41598-017-06244-6

43. Van Kerkhove MD, Vong S, Guitian J, Holl D, Mangtani P, San S, et al. Poultry movement networks in Cambodia: implications for surveillance and control of highly pathogenic avian influenza (HPAI/H5N1). Vaccine. 2009; 27:6345–52. https://doi.org/10.1016/j.vaccine.2009.05.004

44. Moyen N, Ahmed G, Gupta S, Tenzin T, Khan R, Khan T, et al. A large-scale study of a poultry trading network in Bangladesh: implications for control and surveillance of

avian influenza viruses. BMC Vet Res. 2018;14:12. https://doi.org/10.1186/s12917-018-1331-5

45. Sultana R, Nahar N, Rimi NA, Azad S, Islam MS, Gurley ES, et al. Backyard poultry raising in Bangladesh: a valued resource for the villagers and a setting for zoonotic transmission of avian influenza. A qualitative study. Rural Remote Health. 2012;12:1927.

46. Høg E, Fournié G, Hoque MA, Mahmud R, Pfeiffer DU, Barnett T. Competing biosecurity and risk rationalities in the Chittagong poultry commodity chain, Bangladesh. Biosocieties. 2019;14:368–92. https://doi.org/10.1057/s41292-018-0131-2

47. icddr,b and United Nations Children's Fund. Evaluation of avian influenza communication for development initiative— improving biosecurity in live bird markets: lessons learned report. Dhaka (Bangladesh); United Nations Children's Fund; 2013.

Address for correspondence: Shovon Chakma, School of Veterinary Science, Veterinary Science Building (8114), The University of Queensland, Gatton QLD 4343, Australia; email: shovon.chakma@uq.net.au

EMERGING INFECTIOUS DISEASES®

To revisit the January 2021 issue, go to:
https://wwwnc.cdc.gov/eid/articles/issue/27/1/table-of-contents

Perinatal Outcomes of Asynchronous Influenza Vaccination, Ceará, Brazil, 2013–2018

José Q. Filho, Francisco S. Junior, Thaisy B.R. Lima, Vânia A.F. Viana, Jaqueline S.V. Burgoa, Alberto M. Soares, Álvaro M. Leite, Simone A. Herron, Hunter L. Newland, Kunaal S. Sarnaik, Gabriel F. Hanson, Jason A. Papin, Sean R. Moore, Aldo A.M. Lima

In Ceará, Brazil, seasonal influenza transmission begins before national annual vaccination campaigns commence. To assess the perinatal consequences of this misalignment, we tracked severe acute respiratory infection (SARI), influenza, and influenza immunizations during 2013–2018. Among 3,297 SARI cases, 145 (4.4%) occurred in pregnant women. Statewide vaccination coverage was >80%; however, national vaccination campaigns began during or after peak influenza season. Thirty to forty weeks after peak influenza season, birthweights decreased by 40 g, and rates of prematurity increased from 10.7% to 15.5%. We identified 61 children born to mothers with SARI during pregnancy; they weighed 10% less at birth and were more likely to be premature than 122 newborn controls. Mistiming of influenza vaccination campaigns adversely effects perinatal outcomes in Ceará. Because Ceará is the presumptive starting point for north-to-south seasonal influenza transmission in Brazil, earlier national immunization campaigns would provide greater protection for pregnant women and their fetuses in Ceará and beyond.

Respiratory infections are a leading cause of disease and death worldwide (*1,2*), especially among young children and older adults. However, the adverse effects of respiratory infections on pregnant women and fetal development are understudied, particularly in low- and middle-income countries. Respiratory infections in pregnant women can negatively affect birth outcomes, early childhood growth, and neurodevelopment (*3*).

Influenza epidemics are associated with excess rates of pneumonia, related hospitalizations, and death (*4*). Pregnant women and their infants are at heightened risk for severe influenza (*5,6*). In 2020, Regan et al. (*7*) conducted a retrospective cohort study of pregnant women from Australia, Canada, Israel, and the United States; results showed hospitalizations for acute respiratory or febrile illnesses were associated with low birthweight but not small-for-gestational-age births. A prospective cohort study of pregnant women in India, Peru, and Thailand showed influenza during pregnancy is associated with late pregnancy loss and reduced mean birthweight (*8*). A meta-analysis (*9*) found that during the 2009 pandemic of influenza A(H1N1)pdm09, the risk for influenza hospitalization was 2-fold higher for women who were pregnant than those who were not. Children born to mothers infected during pregnancy face potential adverse consequences for physical and neurocognitive development. These consequences resemble the growth and developmental challenges described in children born to undernourished mothers in global settings with high rates of pneumonia and diarrhea (*10–14*).

In 2018, Almeida et al. (*15*) revealed that 12 of 27 states in Brazil demonstrate annual seasonal influenza activity. States along the coast generally have seasonal influenza patterns, whereas states in the North and Central West regions exhibit no readily identifiable seasonality, probably because landlocked states might have more complex and difficult to detect transmission patterns. In the semiarid state of Ceará, which has a population of ≈8.8 million persons, peak seasonal influenza

activity usually begins in mid-May, before the virus spreads southward (*5*). However, influenza circulation begins as early as mid-March. Fortaleza, the state capital, which has a population of 2.7 million, has seasonal influenza peaks 2–3 months earlier than in South and Southeast Brazil (*16,17*). Despite these well-described epidemiologic differences, the entire country uses the same vaccination schedule, which is usually concurrent with or after peak influenza activity in the semiarid region (Figure 1). Because vaccine-acquired immunity against influenza usually develops 2 weeks after immunization, we hypothesized that pregnant women and their fetuses in the semiarid region might not be adequately protected against influenza.

We analyzed whether severe acute respiratory infection (SARI) during pregnancy correlated with low birthweight and premature birth in Ceará. We also evaluated the timing of national influenza vaccine campaigns relative to statewide patterns of SARI and influenza. Finally, we analyzed whether SARI during pregnancy was correlated with low birthweight and prematurity, after adjusting for known confounding variables.

Methods

Ethics Approval

We conducted this study with approval from the ethics review committees of the Federal University of Ceará (Fortaleza, Brazil) and the State Health Secretariat (Fortaleza) (registered at Coordenadoria de Gestão do Trabalho e Educação em Saúde (CTGTES)/ Nucleo de Negociação, Valorização e Educação em Saúde NUVEN). We used guaranteed public access information according to the terms of Law No. 12,527 of November 18, 2011. We also used aggregated information from deidentified databases in a manner
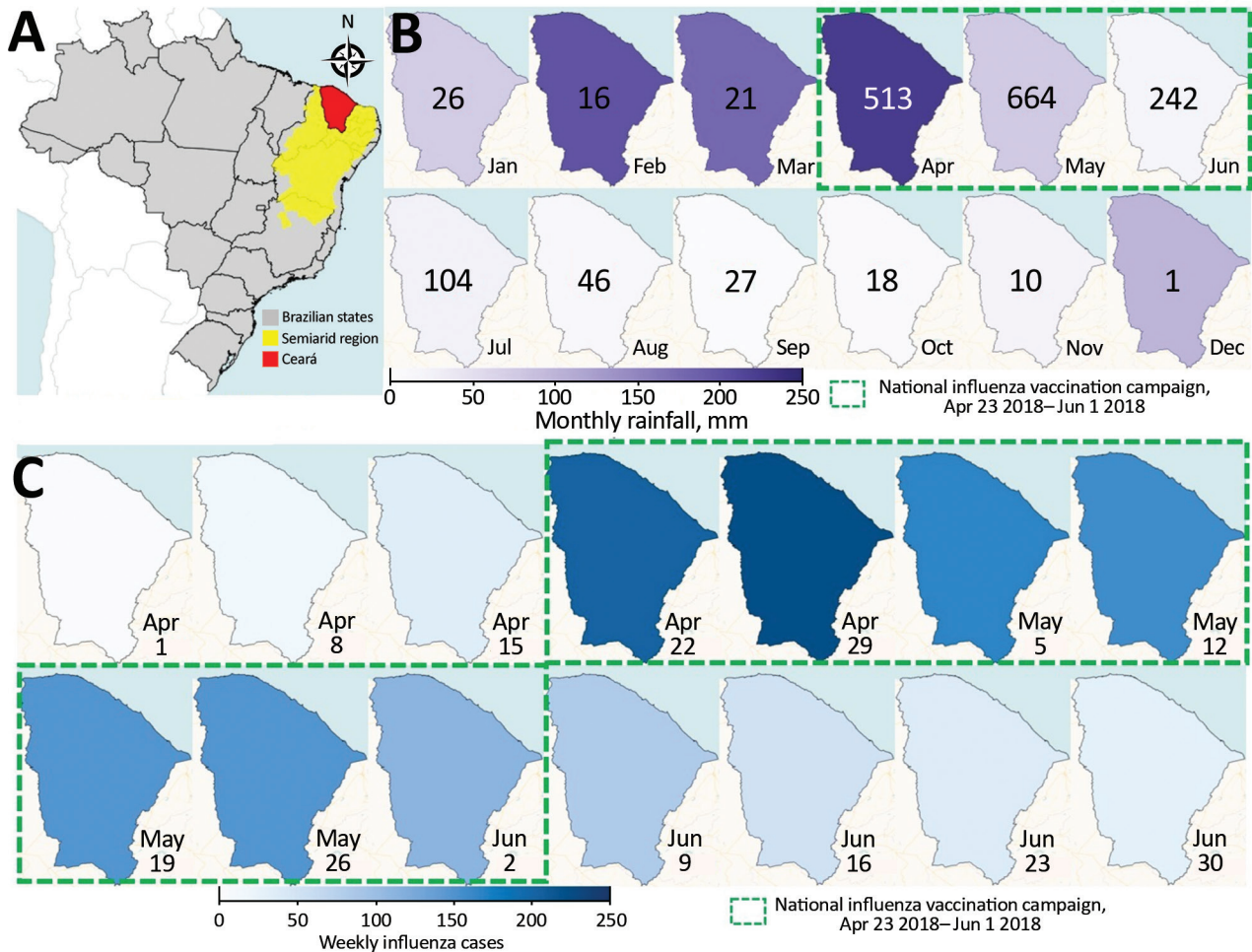
Figure 1. Seasonal patterns in rainfall and influenza and timing of influenza vaccination campaign, Ceará, Brazil, 2018. A) Location of Ceará state in the semiarid region of Brazil. B) Monthly rainfall in Ceará. Numbers indicate total influenza cases each month. C) Weekly influenza cases before, during, and after the annual vaccination campaign in Ceará.
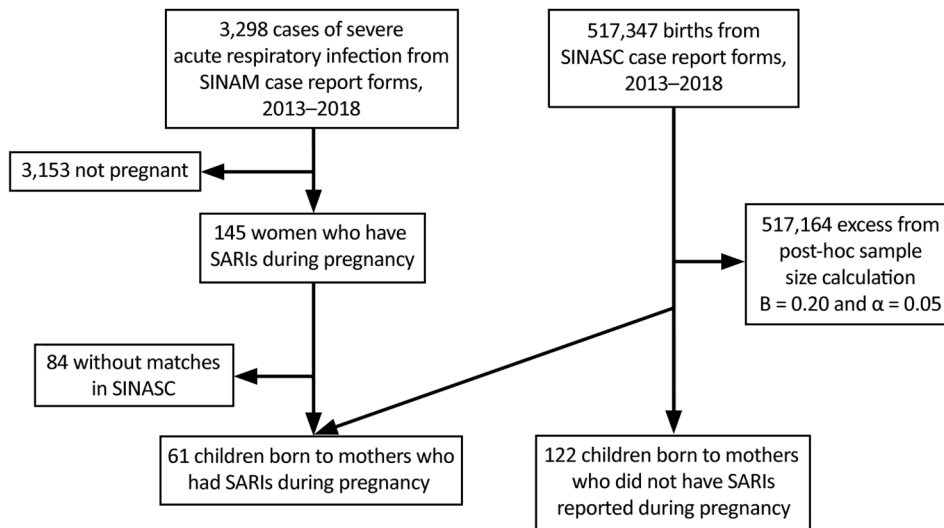
Figure 2. Design of study of SARI during pregnancy, Ceará, Brazil, 2013–2018. SARI, severe acute respiratory infection; SINASC, the Sistema de Informações Sobre Nascidos Vivos (*24*); SINAN, Notifiable Diseases Information System (*19*).

consistent with the provisions of Conselho Nacional de Saúde Resolution No. 510 of April 7, 2016 (http://www.conselho.saude.gov.br/resolucoes/2016/Reso510.pdf).

Study Design and Population

Public and private hospitals are required to report SARI cases to the Ministry of Health to inform epidemic prevention, vaccine development, and vaccination campaigns (*18*). We identified SARI cases registered with the Notifiable Diseases Information System (SINAN–Influenza) in Ceará during 2013–2018 (*19*). We defined SARI as onset of fever (even if subjective) accompanied by cough, sore throat, dyspnea, oxygen saturation <95%, or respiratory discomfort within the preceding 7 days (*20*). Previous studies using multivariate regression analysis have shown that cough and fever are the best predictors of laboratory-confirmed influenza (*21,22*). We collected data on patient demographics, education, clinical signs and symptoms, epidemiologic risk factors, vaccination status, treatments received, samples collected (i.e., nasopharyngeal secretions, bronchial aspirations, tissue, or others), and reverse transcription PCR (RT-PCR) results from SINAN–Influenza case report forms.

Molecular Detection of Influenza

RT-PCR detection of influenza viruses was based on a protocol published by the World Health Organization Global Influenza Surveillance Network (*23*). The RT-PCR was specific for the matrix and hemagglutinin genes of seasonal influenza A; B; H1, including A(H1N1)pdm09 and A(H1N1); H3, including A(H3N2); and avian H5 serotypes. Healthcare

workers collected patient nasal, oropharyngeal, and nasopharyngeal swab samples and extracted nucleic acid using the QIAamp Viral Mini Kit (QIAGEN, https://www.qiagen.com) according to the manufacturer's recommended protocols. Laboratory technicians conducted RT-PCR of the extracted viral RNA, enabling production, amplification, and detection of cDNA (*23*).

Detection of SARI during Pregnancy and Linkage to Birth Data

We constructed a database by linking information from the SINAN–Influenza database with data from the Sistema de Informações Sobre Nascidos Vivos (SINASC) database (*24*). We used MySQL version 5.0.11 (Oracle Corporation, https://www.mysql.com), R version 3.6.2 with the genderBR package 1.1.0 (The R Project for Statistical Computing, https://www.r-project.org), and Stata version 11 (StataCorp LLC, https://www.stata.com) to construct and manage the combined database. We compared SARI case report forms and birth records of pregnant women with documented SARI. Separately, we linked deidentified data from individual pregnant women to birth certificate data for a case–control study. When possible, we also linked influenza test results to these records. We collected each child's birthweight and Apgar score, as well as information concerning demographics, maternal education, previous and current pregnancies, and mode of delivery from birth certificate data.

Maternal and Fetal Effects of SARI

To evaluate the effects of maternal SARI on birthweight and gestational length, we designed an

Table 1. Prevalence of severe acute respiratory infection, Ceará, Brazil, 2013–2018*

Variable	Year					
	2013	2014	2015	2016	2017	2018
Sex†						
M	141 (43)	68 (39)	115 (40)	272 (50)	150 (53)	854 (51)
F	189 (57)	105 (61)	174 (60)	274 (50)	135 (47)	820 (49)
Age, y (range)‡	26.02 (0–96)	26.54 (0–97)	23.11 (0–94)	16.85 (0–100)	1.58 (0–94)	5.26 (0–102)
Age groups at high risk†						
<6 mo	47 (14)	46 (27)	76 (26)	52 (10)	88 (31)	235 (14)
6 mo to 5 y	43 (13)	16 (9)	23 (8)	174 (32)	84 (29)	594 (35)
>60 y	53 (16)	27 (16)	30 (10)	102 (19)	21 (7)	247 (15)
Pregnant women†	38 (12)	13 (8)	32 (11)	17 (3)	10 (4)	35 (2)
SARI cases, total†	330 (100)	173 (100)	289 (100)	546 (100)	285 (100)	1,674 (100)
Influenza	56 (17)	24 (14)	58 (20)	107 (20)	36 (13)	451 (27)
Noninfluenza	61 (18)	22 (13)	36 (12)	64 (12)	101 (35)	21 (1)
Unspecified or unknown	213 (65)	127 (73)	198 (69)	375 (69)	148 (52)	1,202 (72)
Influenza subtypes§	56 (100)	24 (100)	58 (100)	107 (100)	35 (100)	450 (100)
Seasonal A(H1N1)	30 (54)	18 (75)	1 (2)	89 (83)	2 (6)	309 (69)
Other seasonal A(H1)	0	0	45 (78)	0	1 (3)	0
Seasonal A(H3)	2 (4)	0	0	0	25 (71)	23 (5)
A, unknown subtype	22 (39)	1 (4)	4 (7)	16 (15)	0	14 (3)
B	2 (4)	5 (21)	8 (14)	2 (2)	7 (20)	104 (23)
SARI deaths¶	13 (100)	2 (100)	1 (100)	40 (100)	24 (100)	159 (100)
Influenza	9 (69)	1 (50)	0	17 (43)	5 (21)	75 (47)
Death rate of laboratory-certified influenza#	16.1	4.2	0	15.9	20.8	16.6
Other viruses/etiologic agents or unspecified	4 (31)	1 (50)	1(100)	23 (58)	19 (79)	84 (53)
Influenza vaccination coverage**	88	84	83	91	90	NA

*Data from Notifiable Diseases Information System (*19*). Values are no. (%), except as indicated. NA, not available; SARI, severe acute respiratory infection.
†Of total SARI patients.
‡Values are median age (range).
§Of total persons with identified influenza subtype.
¶Of total SARI deaths.
#Of total laboratory-certified influenza deaths.
**Among persons at risk (estimated at ≈2.6 million). Population at risk comprises children <6 mo of age; children 6 mo to <5 y of age; persons ≥60 years of age; pregnant women; postpartum women (≤45 d after delivery); healthcare workers; teachers; indigenous persons; persons who have chronic noncommunicable diseases and other immunocompromising conditions; persons 12–21 y of age experiencing poverty; prisoners; prison system officials; and military police, civilians, firefighters, and armed forces.

observational descriptive study of children born to mothers who did and did not have SARI during pregnancy. The control group was composed of randomly selected children born to mothers matched by age (≤3 months) to mothers who had SARI during pregnancy. We collected birthweights from SINAN data recorded during routine clinical practice.

Annual Periodicity in Birthweight and Gestational Length

To evaluate the effects of seasonal influenza on birth outcomes, we investigated the periodicity associated with birthweight and gestation length in Ceará. We obtained birth outcomes from the SINASC database. SINASC classifies gestational length using a scale of 1–6 in which 1 indicates <22 weeks, 2 indicates 22–27 weeks, 3 indicates 28–31 weeks, 4 indicates 32–36 weeks, 5 indicates 37–41 weeks, and 6 indicates ≥42 weeks of gestation. We defined preterm birth as <37 weeks' gestation. We calculated the average birthweights and gestations by epidemiologic week.

Sample Size and Statistical Analysis

We estimated the sample size needed to detect an effect of SARI on birthweight would be 183 children: 61 born to mothers who did and 122 born to mothers who did not have SARI during pregnancy (Figure 2). This sample size provided a statistical power of 80% at p<0.05 for children who were 10% underweight compared with controls (*21,23*). We compared mean birthweight using the formula $n_1 = (u + v)^2(\sigma_1^2 + \sigma_2^2/K)/(\mu_1 - \mu_2)^2$, where $\mu_1 - \mu_2$ represents the difference between means, σ_1 and σ_2 represent SDs, u represents the 1-sided percentage point of the normal distribution corresponding to 100% (e.g., if power = 80%, then $u = 0.84$), v represents the percentage point of the normal distribution corresponding to the 2-sided significance level (e.g., if significance level = 5%, then $v = 1.96$), and $K = n_2/n_1$. We used ClinCalc.com (https://clincalc.com/Stats/SampleSize.aspx) for sample size calculations.

Data were entered into spreadsheets and checked by 2 independent researchers to ensure accuracy. All data were deidentified. We conducted statistical analysis using SPSS Statistics 20.0 (IBM
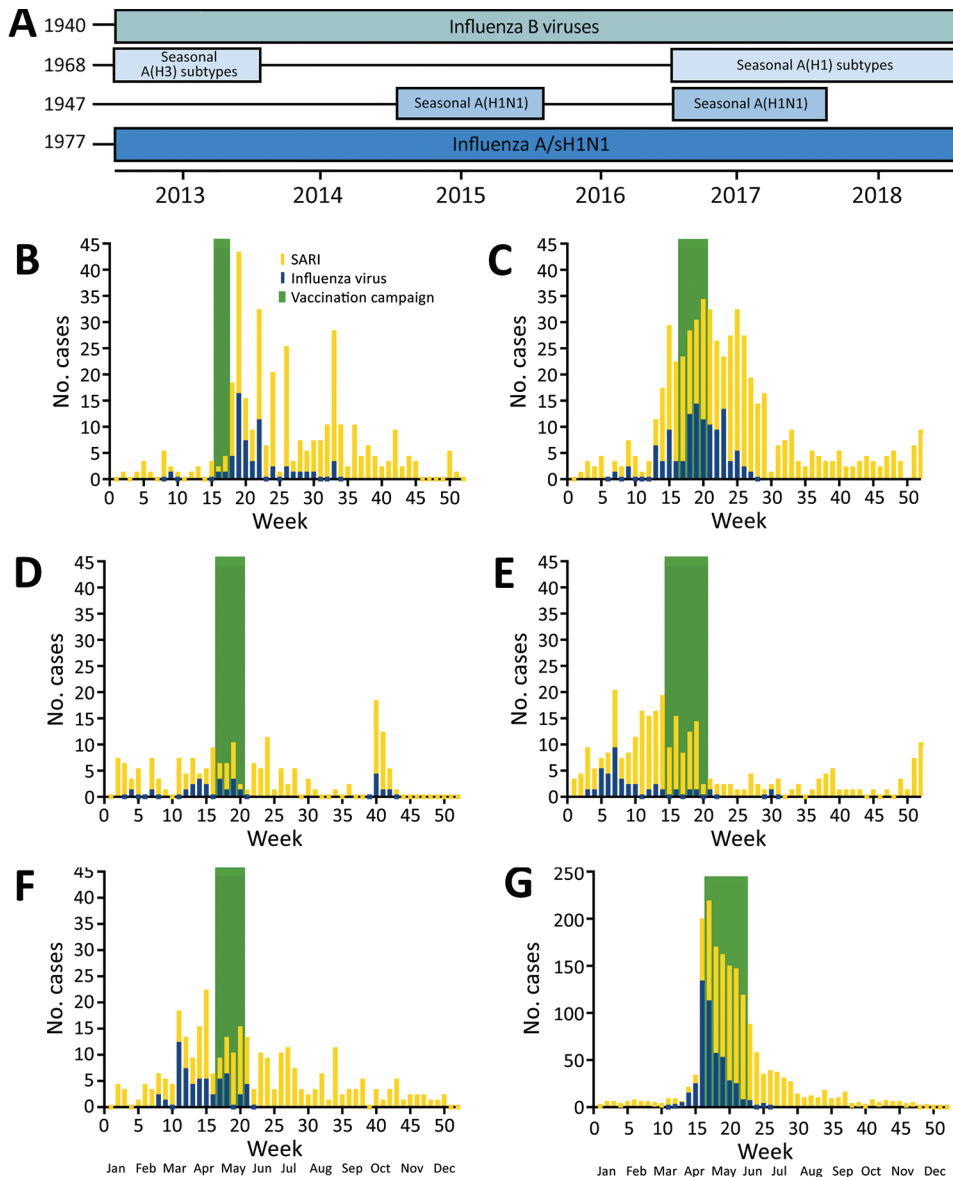
Figure 3. Patterns of influenza and severe acute respiratory infections and timing of influenza vaccination campaigns, Ceará, Brazil, 2013–2018. A) Dominance of various influenza subtypes over time. Years indicate date each strain was first identified. B) Weekly cases of influenza and severe acute respiratory infections.

Corporation, https://www.ibm.com). We used the Shapiro-Wilk test to evaluate normality of quantitative data and the Levene test to evaluate equality of variances. For nonparametric variables, we used the Mann-Whitney test. We analyzed qualitative variables using the χ^2 test or Fisher exact test. We used GraphPad Prism version 3.0 for Windows (GraphPad Software, https://www.graphpad.com) for complementary statistical analysis, table formatting, and figure creation. We used adjusted and nonadjusted multivariate logistic regression models to assess underweight and preterm birth associations. To reduce possible influence from confounding variables, we coadjusted variables measuring sex, maternal education, information

from previous and current pregnancies, and delivery data. We used odds ratios or relative risk ratios with 95% CIs to assess the relationship between a variable and its outcome. All statistical tests were 2-sided with a significance level of $p < 0.05$.

Results

Using the SINAN database, we identified 3,298 SARI cases in Ceará during 2013–2018, including 145 cases among pregnant women (Table 1). We linked the SINAN and SINASC databases to identify 61 children born to mothers who had ≥ 1 SARI during pregnancy. We used the same databases to identify 122 children born to age-matched pregnant women who did not have recorded SARI during pregnancy.

Table 2. Characteristics of pregnant women with SARI, Ceará, Brazil, 2013–2018*

Characteristic	Value
Total SARI cases	3,297 (100)
Among pregnant women	145 (4)
Median age, y (range)	25.95
	(15–44)
SARI cases with etiologic testing	134 (100)
Influenza	43 (32)
Noninfluenza	11 (8)
Unspecified or unknown	80 (60)
% Laboratory-confirmed influenza	32.1
Influenza subtypes†	43 (100)
Seasonal A(H1N1)	18 (42)
Other seasonal A(H1)	0
Seasonal A(H3)	14 (33)
A (unknown subtype)	3 (7)
B	8 (19)
SARI deaths‡	3 (100)
Influenza	0
Death rate of laboratory-certified influenza	0
Other viruses/etiologic agents or unspecified	3 (100)

*Data from Notifiable Diseases Information System (19). Values are no. (%), except as indicated. SARI, severe acute respiratory infection.
†Of total persons with identified influenza subtype.
‡Of total SARI deaths.

We observed equal proportions of SARI cases among male and female patients registered in the SINAN database of 3,298 overall SARI cases in Ceará. Children <5 years of age comprised 27%–61% of patients; children <6 months of age comprised 10%–31% of patients. Older adults (7%–32%) and pregnant women (2%–38%) also comprised large proportions of patients. We observed cases of seasonal H1N1 throughout the study period, notably in 2013 (54%), 2014 (75%), 2016 (83%), and 2018 (69%). The highest number of SARI cases occurred in 2018, mostly caused by seasonal H1N1 and influenza B viruses (23%). We observed sporadic cases of seasonal influenza caused by other H1 subtypes in 2015 and 2017 and seasonal H3 subtypes in 2013 and 2017–2018 (Table 1; Figure 3, panels A, B). Influenza death rates varied from 0%–21%; the peak death rate occurred during a season predominated by H3 subtypes.

The median age of pregnant women who had SARI was 26 years (range 15–44 years). Among 145 pregnant women who had SARI, 43 (32%) had laboratory-confirmed influenza. Among those 43 women, 42% had illnesses caused by H1N1, 33% by H3 subtypes, 7% by influenza A viruses without an identified subtype, and 19% by influenza B subtypes (19%). We identified no deaths caused by SARI in pregnant women (Table 2).

To better visualize the relationship between birth outcomes, SARI, and influenza, we overlaid sets of data for 2018 on the same plot (Figure 4, panel A). We found that average birthweight decreased shortly before influenza season. During 2018, birth-

weight peaked in the first week of the year. By week 15, average birthweight had fallen by ≈40 g (Figure 4, panel A). After the influenza vaccination campaign ended, SARI cases declined and birthweights returned to their yearly averages. For all years of the study, we found lower average gestational scores, which indicates a higher proportion of preterm births, before and during influenza season (Figure 4, panel B).

Each year, average birthweights oscillated by up to 40 g, or 1%–2% of total birthweight (Figure 5). In February, a month associated with worse birth outcomes, 15.5% (8,399/54,311) of children were born prematurely (<37 weeks), whereas in October, a month associated with better birth outcomes, 10.7% (6,552/61,067) of children were born prematurely. These data indicate that circannual oscillations in birth outcomes might be associated with SARI and seasonal influenza in Ceará.

Children born to mothers who had SARI during pregnancy had significantly lower birthweights (p = 0.02), higher risk for prematurity (p = 0.03), shorter gestation times (p<0.01), and lower Apgar scores at 5 minutes after birth than children in the control group (p<0.01). Mothers who had SARI during pregnancy had significantly less formal education than mothers who did not have SARI (p<0.01). Mothers with SARI had a significantly lower number of previous pregnancies (p = 0.01), previous vaginal births (p<0.01), and previous live births (p = 0.01). Mothers with SARI had a higher number of previous cesarean sections (p<0.01). Cesarean deliveries and medical assistance were more frequent in cases versus controls (86.7% vs. 0.8%; p<0.01) (Table 3).

We used multiple logistic regression to identify predictor variables independently associated with SARI during pregnancy. First, we examined 11 significant variables identified by univariate analysis (Table 3), of which 5 showed >40% collinearity. We had an adequate sample size (123 cases) to run a logistic regression for these 5 variables (23,25). The overall model fit showed a χ^2 value of 23.135 (df = 6; p<0.01). The Cox and Snell test and Nagelkerke test indicated variances between 17.1% and 23.2%. Including predictor variables increased model accuracy from 61% to 68%. We found that birthweight (p = 0.03) and attendance of birth by a physician (p = 0.04) were significantly associated with SARI during pregnancy (Table 4; Figure 6).

Discussion

We documented 3,298 SARI cases in Ceará, Brazil, during 2013–2018. Cases occurred predominantly
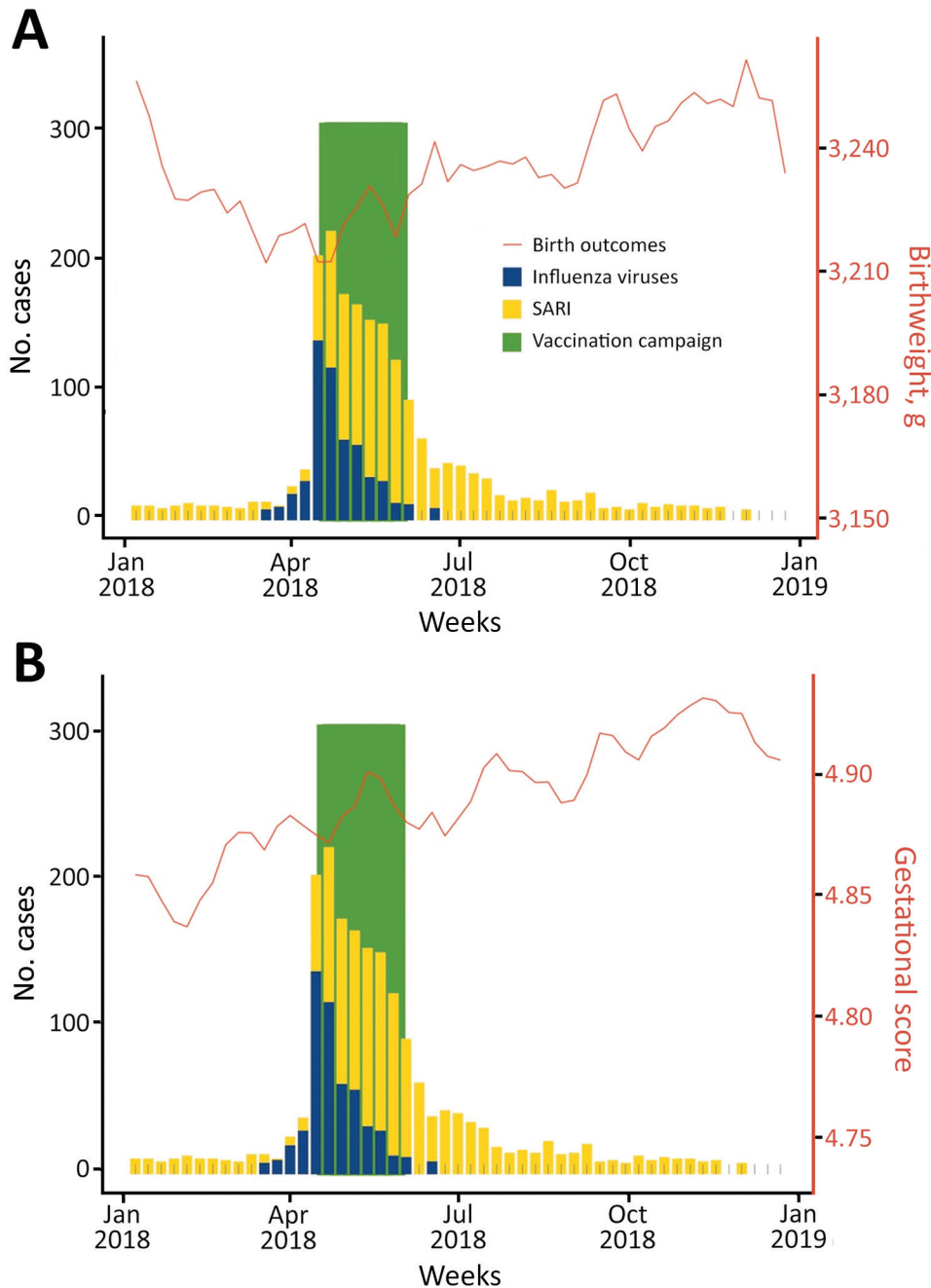
Figure 4. Associations between SARI among pregnant women and birth outcomes, Ceará, Brazil, 2018. A) By birthweight; B) by gestational score. Gestational length scored using a 1–6 scale in which 1 indicates <22 weeks, 2 indicates 22–27 weeks, 3 indicates 28–31 weeks, 4 indicates 32–36 weeks, 5 indicates 37–41 weeks, and 6 indicates >42 weeks of gestation. SARI, severe acute respiratory infection.

in younger children, especially children <6 months of age, as well as older adults and pregnant women. These data are consistent with previous studies showing higher rates of infection among younger populations but increased death rates among older adults (*26*).

H1N1 was the dominant influenza subtype during seasonal epidemic outbreaks, illustrating the capacity of this strain to recirculate and co-circulate with other seasonal influenza strains (Table 1; Figure

3, panel A). H1N1 caused a high death rate throughout the study. However, in 2015, when seasonal H1 strains predominated in Ceará, we observed a lower overall death rate among influenza patients. These data are consistent with prior literature showing more deaths associated with H1N1 (*27*). The mortality rate in our study might be attributable to the mistiming of vaccination campaigns, which occurred during and after peak influenza activity in Ceará. The state has high vaccination coverage, suggesting that

A

B
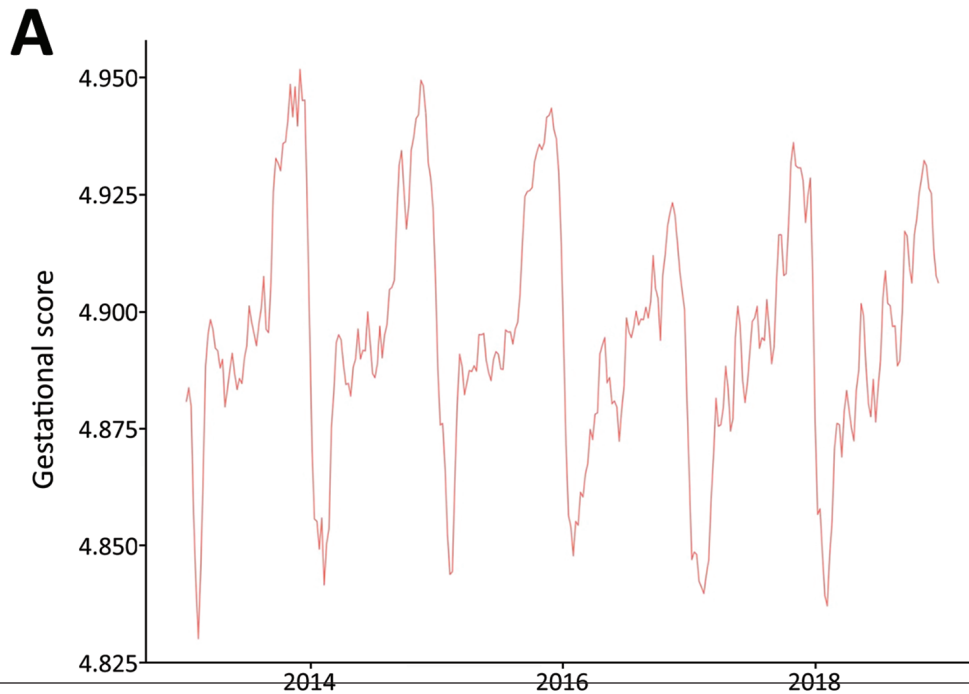
Figure 5. Seasonal periodicity of gestational score (A) and birthweight (B), Ceará, Brazil, 2013–2018. Gestational length scored using a scale of 1–6: 1 indicates <22 weeks, 2 indicates 22–27 weeks, 3 indicates 28–31 weeks, 4 indicates 32–36 weeks, 5 indicates 37–41 weeks, and 6 indicates >42 weeks of gestation.
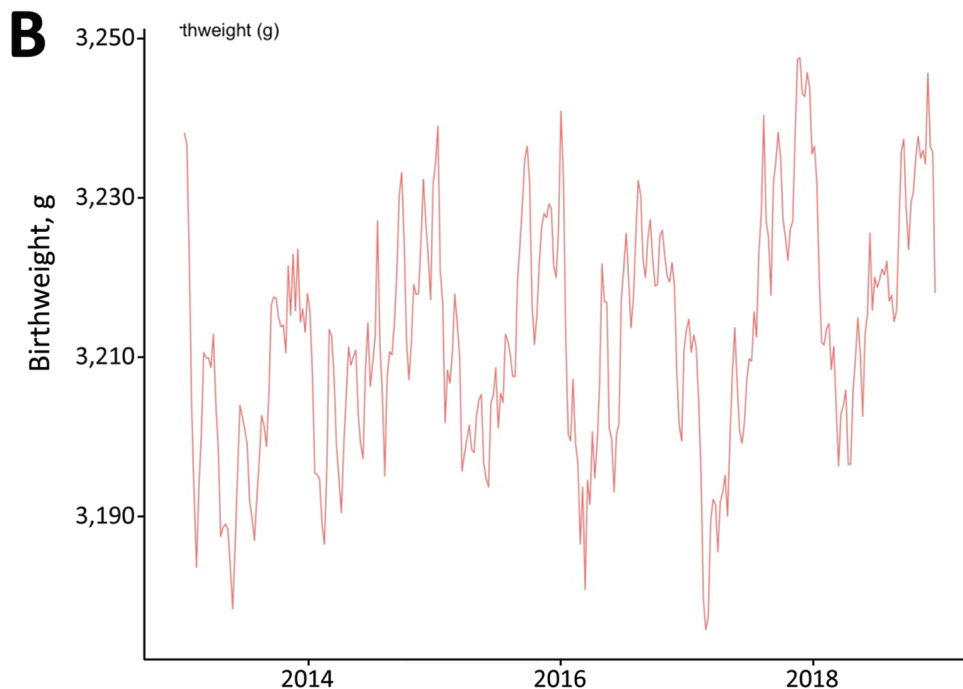
earlier administration of influenza vaccines might reduce death and disease. Mistiming of immunization schedules also might explain the unusually high disease incidence among infants <6 months of age. The World Health Organization does not recommend immunization in this age group. Consequently, immunization of pregnant mothers is especially crucial for passive immunity against influenza during the first 6 months of life.

In this study, we assessed whether SARI during pregnancy was associated with a higher risk for low birthweight or prematurity. We found statewide correlations between peak influenza activity and nadirs in birthweight and gestational length. Furthermore,

we confirmed associations of maternal SARI with low birthweight and preterm birth in matched mother–infant pairs. These associations remained significant when adjusted for confounders by multiple logistic regression. Our findings agree with 2 recently published studies (*7,8*) showing an association of SARI, including influenza, among pregnant women with low birthweights. Pregnant mothers who had SARI were more likely to require medical assistance during labor than those who did not have SARI.

Our study aligns with earlier reports showing the importance of prevention and adjustment of

Table 3. Characteristics of children born to women who did and did not have severe acute respiratory infections during pregnancy, Ceará, Brazil, 2013–2018*

Variables	Total	Born to mothers who had severe acute respiratory infections during pregnancy		p value†
		Yes	No	
Total	183	61	122	
Sex				
M	81 (44)	24 (39)	57 (47)	0.20
F	102 (56)	378 (61)	65 (53)	
Mean birthweight, g (SD)	3,090.1 (665.42)	2,879.1 (783.57)	3,195.6 (572.61)	0.02
Preterm birth (i.e., gestation <37 wks)	26 (14)	16 (27)	10 (13)	0.03
Mean Apgar index (SD)				
At 1 min	8.0 (1.45)	7.9 (1.66)	8.0 (1.32)	0.83
At 5 min	9.0 (0.98)	8.9 (0.75)	9.1 (1.08)	<0.01
Mean maternal age, y (SD)	28.3 (6.65)	28.3 (6.69)	28.3 (6.66)	0.98
Education				<0.01
None	0	0	0	
Elementary I: ≤4th grade	8 (4.6)	1 (1.7)	7 (6.0)	
Elementary II: ≤8th grade	19 (10.9)	1 (1.7)	18 (15.5)	
Secondary: ≤12th grade	60 (34.5)	14 (24.1)	46 (39.7)	
Partial college	73 (42.0)	34 (58.6)	39 (33.6)	
College	14 (8.0)	8 (13.8)	6 (5.2)	
Previous pregnancies				
Median no. previous pregnancies (range)	2 (0–16)	1 (0–7)	2 (0–16)	0.01
Median no. vaginal deliveries (range)	2 (0–12)	0 (0–4)	2 (0–12)	<0.01
Median no. cesarean sections (range)	0 (0–4)	0 (0–4)	0 (0–2)	<0.01
Median no. live births (range)	2 (0–12)	1 (0–7)	2 (0–12)	0.01
Median no. fetal losses or abortions (range)	0 (0–4)	0 (0–2)	0 (0–4)	0.16
Current pregnancy				
Mean gestation length, wks (SD)	37.8 (3.15)	36.9 (3.72)	38.4 (2.50)	<0.01
Mean no. prenatal consultations (SD)	6.9 (3.15)	7.0 (2.55)	6.7 (2.16)	0.56
Mean start of prenatal care started, mo (SD)	2.9 (1.38)	2.8 (1.22)	3.1 (1.48)	0.14
Type of pregnancy				0.11
Single	181 (98.9)	59 (96.7)	122 (100)	
Twins	2 (1.1)	2 (3.3)	0	
Triplets or more	0	0	0	
Fetal presentation at delivery‡				0.09
Cephalic	138 (96.5)	54 (93.1)	84 (98.8)	
Pelvic or podalic	5 (3.5)	4 (6.9)	1 (1.2)	
Transversal	0	0	0	
Induced labor				0.10
Y	5 (3.6)	4 (6.9)	1 (1.2)	
N	134 (96.4)	54 (93.1)	80 (98.8)	
Type of delivery§				<0.01
Vaginal	128 (70.7)	8 (13.3)	120 (99.2)	
Cesarean	53 (29.3)	52 (86.7)	1 (0.8)	
Cesarean section without labor¶				NS
Y	29 (76.3)	29 (76.3)	0	
N	9 (23.7)	9 (23.7)	0	
Birth attendant#				0.01
Doctor	122 (84.1)	59 (98.3)	63 (74.1)	
Obstetric nurse	6 (4.1)	1 (1.7)	5 (5.9)	
Midwife	9 (6.2)	0	9 (10.6)	
Others	8 (5.5)	0	8 (9.4)	

*Data from Sistema de Informações Sobre Nascidos Vivos (*24*). Values are no. (%), except as indicated. NS, not significant.
†Mann-Whitney test was used for variables whose distribution was not normal and χ2 analysis was used for normally distributed data.
‡Of 143 cases with available data.
§Of 181 cases with available data.
¶Of 38 cases with available data.
#Of 135 cases with available data.

Table 4. Odds ratios for characteristics of 61 children born to women who had SARI during pregnancy compared with 122 children born to women who did not have SARI, Ceará, Brazil, 2013–2018*

Variables	Odds ratio (95% CI)	Adjusted odds ratio (95% CI)*
Birthweight, g†	0.999 (0.999–1.000)	0.999 (0.998–1.000)
Preterm birth (i.e., gestation <37 wks)‡	2.944 (1.100–7.879)	0.849 (0.151–4.771)
Mother education	4.320 (1.095–17.051)	1.156 (0.198–6.746)
No. previous pregnancies¶	0.795 (0.659–0.960)	0.894 (0.727–1.099)
No. wks gestation†	0.852 (0.756–0.961)	1.025 (0.794–1.325)
Birth attended	20.603 (2.692–157.697)	9.327 (1.144–76.060)

*Data from Sistema de Informações Sobre Nascidos Vivos (*24*). SARI, severe acute respiratory infection.
*Determined by multivariate logistic regression analysis of variables associated with births requiring the presence of a skilled attendant.
†Analysis of means and SDs.
‡Categories comprise children born at <37 and >37 wks gestation.
§Categories comprise mothers who had attended no schooling, elementary I (1st–4th grade), elementary II (5th–8th grade), secondary school (9th–12th grade), incomplete college, and complete college. Analysis grouped no schooling, elementary I (1st–4th grade), elementary II (5th–8th grade), and secondary school (9th–12th grade), as well as incomplete and complete higher education categories.
¶Analysis of medians and variations.
#Categories comprise births attended by a physician, obstetric nurse, midwife, or other. Analysis grouped obstetric nurse, midwife, and other categories.

influenza vaccine campaign schedules to avoid complications of influenza (*6,28–31*). Previous studies show the importance of the first 1,000 days of life in reducing undernutrition, enteric infections, and risk for metabolic syndrome and cardiovascular diseases (*32,33*). Neurocognitive, physical, and educational deficits have been well-documented among children exposed in utero or during the first months of life to influenza and other diseases such as enteric infections (*10–12,34*).

The first limitation of our study is that we analyzed only cases of influenza associated with SARI and did not include cases of mild-to-moderate influenza. However, our analyses of statewide birth outcomes detected substantial periodicity in birthweights and gestational length; poorer outcomes coincided with influenza season. Maternal influenza also might affect other perinatal outcomes, such as medical necessity for caesarean birth. Second, our nested observational descriptive study cannot infer a causal relationship between maternal SARI and

Figure 6. Comparison of birthweights of children born to mothers who did (cases) and did not (controls) have severe acute respiratory infections during pregnancy, Ceará, Brazil, 2013–2018. Horizontal lines within boxes indicate means; box tops and bottoms indicate 25th and 75th percentiles; whiskers indicate 95% CIs. p = 0.02 by Mann-Whitney test.

adverse birth outcomes. However, the associations were robust to logistic regression adjusted for several potential confounders. In addition, because hospitalization is part of the case definition for SARI, public and private hospitals (but not private clinics) are required to report SARI cases to SINAN. Although many private clinics do report, most reported cases come from public institutions. Thus, we might not have analyzed all SARI cases in Ceará. Finally, our results suggest that asynchronous vaccination schedules might be associated with adverse influenza outcomes in Ceará, but we did not model the extent to which earlier immunization or the use of vaccine strains from the Northern or Southern Hemispheres might mitigate these outcomes. Recent epidemiologic models suggest Ceará is the starting point for influenza transmission from the semiarid region in southern Brazil, hence earlier immunization in Ceará might have substantial benefits for the region and country (*5*). We did not account for infections with Zika virus as a potential confounder of our findings because the reported Zika incidence was 0 during 2013–2016; however, testing for Zika was not routinely performed during this time period. The state had low Zika incidence during the study: 5.6 cases/100,000 persons in 2017 and 0.2 cases/100,000 persons in 2018 (*35*).

In conclusion, our results show that late timing of influenza vaccination in Ceará, a populous semiarid state in Brazil with high vaccination coverage, correlates with adverse perinatal outcomes. In addition, we found that mean birthweight and rates of prematurity followed an annual periodicity, suggesting additional associations with seasonal influenza. Finally, we confirmed a robust association of maternal SARI with poor birth outcomes using an observational descriptive study design. Further work is urgently needed to model and study the

optimal timing, potential impact, logistics, economics, and implementation of such a diversified national influenza vaccine strategy. Because Ceará is the presumptive starting point for an annual north-to-south pattern of seasonal influenza transmission in Brazil (*15*), our data indicate earlier timing of national immunization campaigns, ideally before seasonal influenza circulation in Ceará, might provide substantial benefits not only for women and children in the semiarid region but also for Brazil as a country.

This article was preprinted at https://www.medrxiv.org/content/10.1101/2020.08.24.20180455v2.

About the Author
Mr. Filho is a doctoral student at the Federal University of Ceará in Fortaleza, Brazil. His research interests include infectious disease epidemiology and maternal-child health.

References
1. World Health Organization. The top 10 causes of death. 2020 Dec 9 [cited 2021 Jul 7]. https://www.who.int/news-room/fact-sheets/detail/the-top-10-causes-of-death
2. Wang X, Li Y, O'Brien KL, Madhi SA, Widdowson MA, Byass P, et al.; Respiratory Virus Global Epidemiology Network. Global burden of respiratory infections associated with seasonal influenza in children under 5 years in 2018: a systematic review and modelling study. Lancet Glob Health. 2020;8:e497–510. https://doi.org/10.1016/S2214-109X(19)30545-5
3. Schlaudecker EP, Steinhoff MC, Moore SR. Interactions of diarrhea, pneumonia, and malnutrition in childhood: recent evidence from developing countries. Curr Opin Infect Dis. 2011;24:496–502. https://doi.org/10.1097/QCO.0b013e328349287d
4. Simonsen L, Clarke MJ, Williamson GD, Stroup DF, Arden NH, Schonberger LB. The impact of influenza epidemics on mortality: introducing a severity index. Am J Public Health. 1997;87:1944–50. https://doi.org/10.2105/AJPH.87.12.1944
5. Katz MA, Gessner BD, Johnson J, Skidmore B, Knight M, Bhat N, et al. Incidence of influenza virus infection among pregnant women: a systematic review. [Erratum in: BMC Pregnancy Childbirth. 2017;17:192]. BMC Pregnancy Childbirth. 2017;17:155. https://doi.org/10.1186/s12884-017-1333-5
6. Fell DB, Sprague AE, Liu N, Yasseen AS III, Wen SW, Smith G, et al.; Better Outcomes Registry & Network (BORN) Ontario. H1N1 influenza vaccination during pregnancy and fetal and neonatal outcomes. Am J Public Health. 2012;102:e33–40. https://doi.org/10.2105/AJPH.2011.300606
7. Regan AK, Feldman BS, Azziz-Baumgartner E, Naleway AL, Williams J, Wyant BE, et al. An international cohort study of birth outcomes associated with hospitalized acute respiratory infection during pregnancy. J Infect. 2020;81:48–56. https://doi.org/10.1016/j.jinf.2020.03.057
8. Dawood FS, Kittikraisak W, Patel A, Rentz Hunt D, Suntarattiwong P, Wesley MG, et al. Incidence of influenza during pregnancy and association with pregnancy and perinatal outcomes in three middle-income countries: a multisite prospective longitudinal cohort study. Lancet Infect Dis. 2021;21:97–106. https://doi.org/10.1016/S1473-3099(20)30592-2
9. Mertz D, Geraci J, Winkup J, Gessner BD, Ortiz JR, Loeb M. Pregnancy as a risk factor for severe outcomes from influenza virus infection: A systematic review and meta-analysis of observational studies. Vaccine. 2017;35:521–8. https://doi.org/10.1016/j.vaccine.2016.12.012
10. Black RE, Allen LH, Bhutta ZA, Caulfield LE, de Onis M, Ezzati M, et al.; Maternal and Child Undernutrition Study Group. Maternal and child undernutrition: global and regional exposures and health consequences. Lancet. 2008;371:243–60. https://doi.org/10.1016/S0140-6736(07)61690-0
11. Victora CG, Adair L, Fall C, Hallal PC, Martorell R, Richter L, et al.; Maternal and Child Undernutrition Study Group. Maternal and child undernutrition: consequences for adult health and human capital. Lancet. 2008;371:340–57. https://doi.org/10.1016/S0140-6736(07)61692-4
12. Guerrant DI, Moore SR, Lima AAM, Patrick PD, Schorling JB, Guerrant RL. Association of early childhood diarrhea and cryptosporidiosis with impaired physical fitness and cognitive function four-seven years later in a poor urban community in northeast Brazil. Am J Trop Med Hyg. 1999;61:707–13. https://doi.org/10.4269/ajtmh.1999.61.707
13. MAL-ED Network Investigators. Early childhood cognitive development is affected by interactions among illness, diet, enteropathogens and the home environment: findings from the MAL-ED birth cohort study. BMJ Glob Health. 2018;3:e000752. https://doi.org/10.1136/bmjgh-2018-000752
14. Takeda S, Hisano M, Komano J, Yamamoto H, Sago H, Yamaguchi K. Influenza vaccination during pregnancy and its usefulness to mothers and their young infants. J Infect Chemother. 2015;21:238–46. https://doi.org/10.1016/j.jiac.2015.01.015

15. Almeida A, Codeço C, Luz PM. Seasonal dynamics of influenza in Brazil: the latitude effect. [Erratum in: BMC Infect Dis. 2018;19:225]. BMC Infect Dis. 2018;18:695. https://doi.org/10.1186/s12879-018-3484-z

16. Moura FEA, Perdigão ACB, Siqueira MM. Seasonality of influenza in the tropics: a distinct pattern in northeastern Brazil. Am J Trop Med Hyg. 2009;81:180–3. https://doi.org/10.4269/ajtmh.2009.81.180

17. Instituto Brasileiro de Geografia e Estatística. Fortaleza. 2017 [2021 July 7]. https://cidades.ibge.gov.br/brasil/ce/fortaleza/panorama

18. Ministério da Saúde. Edict no. 1,271, June 6, 2014 [in Portuguese]. 2014 [2021 Jul 9]. https://bvsms.saude.gov.br/bvs/saudelegis/gm/2014/prt1271_06_06_2014.html

19. Sistema de Informação de Agravos de Notificação. SINAN influenza. 2016 [cited 2021 Jul 7]. https://portalsinan.saude.gov.br/sinan-influenza

20. World Health Organization. Global epidemiological surveillance standards for flu. 2014 [cited 2019 Dec 18]. https://apps.who.int/iris/handle/10665/311268

21. Monto AS, Gravenstein S, Elliott M, Colopy M, Schweinle J. Clinical signs and symptoms predicting influenza infection. Arch Intern Med. 2000;160:3243–7. https://doi.org/10.1001/archinte.160.21.3243

22. Yang JH, Huang PY, Shie SS, Yang S, Tsao KC, Wu TL, et al. Predictive symptoms and signs of laboratory-confirmed influenza: a prospective surveillance study of two metropolitan areas in Taiwan. Medicine (Baltimore). 2015;94:e1952. https://doi.org/10.1097/MD.0000000000001952

23. World Health Organization. WHO information for the molecular detection of influenza viruses. 2017 [cited 2021 Jul 7]. https://www.who.int/influenza/gisrs_laboratory/WHO_information_for_the_molecular_detection_of_influenza_viruses_20171023_Final.pdf

24. Global Health Data Exchange. Brazil live birth information system. 2018 [cited 2021 Jul 7]. http://ghdx.healthdata.org/series/brazil-live-birth-information-system-sinasc

25. Kirkwood BR, Sterne JAC. Essential medical statistics. Malden (MA): Wiley-Blackwell; 2003.

26. Tabachnick BG, Fidell LS. Using multivariate statistics. 6th ed. New York: Harper and Row; 2012.

27. Simonsen L, Taylor R, Viboud C, Dushoff J, Miller M. US flu mortality estimates are based on solid science. BMJ. 2006;332:177–8. https://doi.org/10.1136/bmj.332.7534.177-a

28. Glezen WP, Keitel WA, Taber LH, Piedra PA, Clover RD, Couch RB. Age distribution of patients with medically-attended illnesses caused by sequential variants of influenza A/H1N1: comparison to age-specific infection rates, 1978–1989. Am J Epidemiol. 1991;133:296–304. https://doi.org/10.1093/oxfordjournals.aje.a115874

29. Bhat N, Wright JG, Broder KR, Murray EL, Greenberg ME, Glover MJ, et al.; Influenza Special Investigations Team. Influenza-associated deaths among children in the United States, 2003-2004. N Engl J Med. 2005;353:2559–67. https://doi.org/10.1056/NEJMoa051721

30. Omer SB, Goodman D, Steinhoff MC, Rochat R, Klugman KP, Stoll BJ, et al. Maternal influenza immunization and reduced likelihood of prematurity and small for gestational age births: a retrospective cohort study. PLoS Med. 2011;8:e1000441. https://doi.org/10.1371/journal.pmed.1000441

31. Dodds L, MacDonald N, Scott J, Spencer A, Allen VM, McNeil S. The association between influenza vaccine in pregnancy and adverse neonatal outcomes. J Obstet Gynaecol Can. 2012;34:714–20. https://doi.org/10.1016/S1701-2163(16)35336-1

32. Giles ML, Krishnaswamy S, Macartney K, Cheng A. The safety of inactivated influenza vaccines in pregnancy for birth outcomes: a systematic review. Hum Vaccin Immunother. 2019;15:687–99. https://doi.org/10.1080/21645515.2018.1540807

33. Niehaus MD, Moore SR, Patrick PD, Derr LL, Lorntz B, Lima AA, et al. Early childhood diarrhea is associated with diminished cognitive function 4 to 7 years later in children in a northeast Brazilian shantytown. Am J Trop Med Hyg. 2002;66:590–3. https://doi.org/10.4269/ajtmh.2002.66.590

34. Lorntz B, Soares AM, Moore SR, Pinkerton R, Gansneder B, Bovbjerg VE, et al. Early childhood diarrhea predicts impaired school performance. Pediatr Infect Dis J. 2006;25:513–20. https://doi.org/10.1097/01.inf.0000219524.64448.90

35. Governo do Estado do Ceará. Epidemiological Bulletin, Congenital Syndrome Associated with Zika Virus Infection [in Portuguese]. 2018 [cited 2021 Jul 7]. https://www.saude.ce.gov.br/wp-content/uploads/sites/9/2018/06/boletim_microcefalia_30_05_2018.pdf

Address for correspondence: Aldo A.M. Lima, R. Cel. Nunes de Melo, 1315, Rodolfo Teófilo, Fortaleza, Ceará, CEP 60.430-270, Brazil; email: alima@ufc.br; Sean R. Moore, MR-4 Bldg, 409 Lane Rd, Rm 2129, Charlottesville, VA 22908, USA; email: srm5u@virginia.edu

Spatiotemporal Dynamics of Sporadic Shiga Toxin–Producing *Escherichia coli* Enteritis, Ireland, 2013–2017

Eimear Cleary,[1] Martin Boudou,[1] Patricia Garvey,
Coilin Oh'Aiseadha, Paul McKeown, Jean O'Dwyer, Paul Hynds

The Republic of Ireland regularly reports the highest annual crude incidence rates of Shiga toxin–producing *Escherichia coli* (STEC) enteritis in the European Union, ≈10 times the average. We investigated spatiotemporal patterns of STEC enteritis in Ireland using multiple statistical tools. Overall, we georeferenced 2,755 cases of infection during January 2013–December 2017; we found ≥1 case notified in 2,340 (12.6%) of 18,641 Census Small Areas. We encountered the highest case numbers in children 0–5 years of age (n = 1,101, 39.6%) and associated with serogroups O26 (n = 800, 29%) and O157 (n = 638, 23.2%). Overall, we identified 17 space-time clusters, ranging from 2 (2014) to 5 (2017) clusters of sporadic infection per year; we detected recurrent clustering in 3 distinct geographic regions in the west and mid-west, all of which are primarily rural. Our findings can be used to enable targeted epidemiologic intervention and surveillance.

Over the previous decade, the Republic of Ireland has frequently reported the highest incidence rates of symptomatic Shiga toxin–producing *Escherichia coli* (STEC) infection in the European Union (EU) (*1*). The reported national crude incidence rate (CIR) of confirmed STEC infections in Ireland during 2017 was 923 cases (16.6 cases/100,000 population), equating to ≈10 times the EU average (1.66 cases/100,000 population) (*1,2*).

Shiga toxin–producing *E. coli* bacteria, of which there are >100 serotypes, were first discovered in 1977; the most well-known STEC strain, *E. coli* O157:H7,

was first recognized as a pathogen in 1982. The Shiga toxin–producing group of *E. coli* includes serotypes O157, O26, and other enterohemorrhagic *E. coli* bacteria; serotypes are typically categorized by the presence of *stx1* or *stx2* genes (*3*). STEC is associated with a wide range of sequelae, from mild diarrhea to hemorrhagic colitis, hematochezia (bloody diarrhea), thrombotic thrombocytopenic purpura, and hemolytic uremic syndrome (HUS) causing intravascular lysis of red blood cells (*2,4*). Infection is characterized by several transmission routes, including consumption of contaminated food and water, person-to-person contact, or direct contact with infected animals (*4,5*). A recent study found the incidence of confirmed sporadic (i.e., nonoutbreak) STEC O157 infection in Ireland in 2008–2013 significantly elevated in regions characterized by high reliance on private groundwater (odds ratio [OR] 18.727; p<0.001) and high livestock densities (OR 1.001; p = 0.007) (*6*).

Transmission sources, pathways, and source–pathway interactions associated with STEC infection in Ireland are multifaceted, resulting in a complex exposure profile (*7,8*). Sporadic cases of infection are inherently difficult to attribute to specific risk factors for reasons that include the absence of accurate date-of-onset data, underreporting, misdiagnosis, myriad potential exposures, and surveillance limitations (*5,6,7*). Of 2,210 confirmed STEC cases reported in Ireland during 2008–2013, a total of 1,264 (57.2%) were defined as sporadic (*6*).

The high proportion of sporadic STEC infections relative to total annual cases in Ireland, and their association with environmental exposures, has made the spatiotemporal occurrence of STEC particularly important in public health. We used a suite of

[1]These first authors contributed equally to this article.
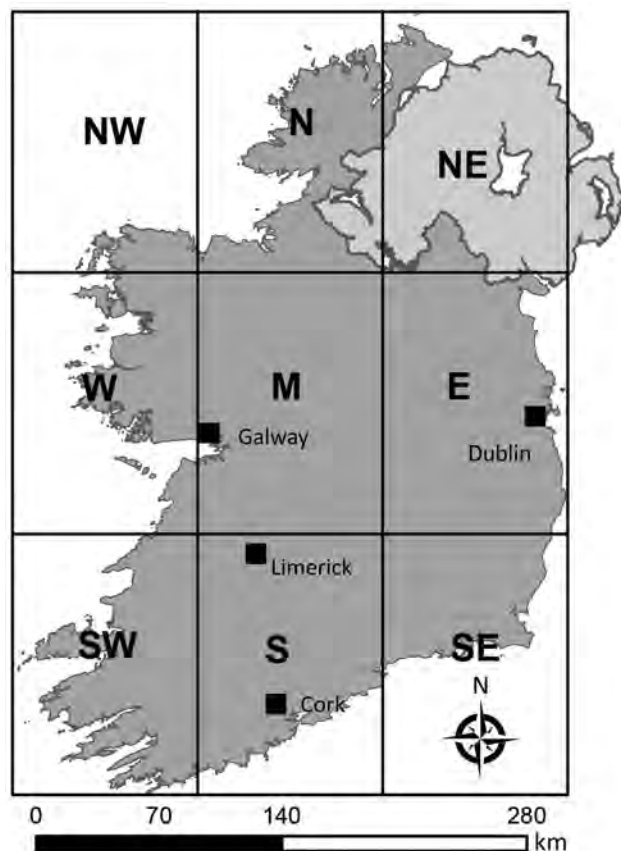
Figure 1. Geographic zones of Ireland. Sections of the grid represent the 8 distinct zones; zone NE, Northern Ireland, was not included in study of primary Shiga toxin–producing *Escherichia coli* enteritis cases. NW, northwest; N, north; W, west; M, midlands; E, east; SW, southwest; S, south; SE, southeast.

geostatistical approaches to explore spatiotemporal analyses of sporadic STEC infection in Ireland, a country characterized by the highest infection CIRs in Europe.

Methods

Data Collection and Processing

Because the primary study objective was to investigate patterns of domestic transmission, we excluded from analyses cases attributed to secondary infection (i.e., person-to-person transmission), and cases originating outside Ireland. We defined primary sporadic infection as a laboratory-confirmed case notified to a Department of Public Health during January 1, 2013–December 31, 2017, that had no reported epidemiological link to another notified case, or as an outbreak index case (i.e., the first documented case within a recognized cluster or outbreak). We obtained irreversibly anonymized case data from the Computerised Infectious Disease Reporting (CIDR) database (http://www.hpsc.ie/CIDR), a national database of notifiable infectious disease events reported by regional departments of public health in accordance with the Infectious Diseases (Amendment) Regulations 2011 (S.I. No. 452 of 2011).

Case confirmations were determined by both clinical and laboratory criteria; clinical criteria are primarily based on symptoms (diarrhea, abdominal pain, and HUS), and laboratory criteria require ≥ 1 of the following: isolation of strains positive for *stx1*, *stx2*, or both; direct detection of *stx1* or *stx2* nucleic acids (in the absence of strain isolation); or direct detection of Shiga toxin in fecal sample. We geographically referenced all confirmed cases to 1 of 18,641 Census Small Areas from the 2011 Central Statistics Office (CSO) census using the Health Atlas Ireland georeferencing tool. Small areas (SAs) are currently the smallest spatially defined area for census reporting in the state and exist as subdivisions within electoral districts (ED) of Ireland; each covers an area of 0.001–163 km² and holds 80–120 dwellings. SAs are thus developed on the basis of household numbers and residential population (i.e., not spatial extent or population density) to report population-based statistics while ensuring personal and household anonymity. We delineated 3 infection subsets for additional analyses based upon epidemiologic and clinical significance: urban/rural classification; STEC serogroup (O157, O26, other); and case-patient age (≤ 5 years, 6–65 years, ≥ 65 years)

We extracted SA-specific human population counts from the 2011 and 2016 (CSO) census datasets

Table 1. Confirmed sporadic verocytotoxin-producing *Escherichia coli* infections in Ireland, 2013–2017*				
Characteristic	VTEC O157	VTEC 026	Other serogroups	Not serotyped/ungroupable
Total	668	714	724	649
Age				
≤ 5 y	231 (34.6)	431 (60.4)	255 (35.2)	184 (28.4)
6–64 y	373 (55.8)	232 (32.5)	314 (43.4)	273 (42.1)
≥ 65 y	64 (9.6)	51 (7.1)	155 (21.4)	192 (29.6)
Setting				
Urban	288 (43.1)	278 (38.9)	329 (45.4)	309 (47.6)
Rural	380 (56.9)	436 (61.1)	395 (54.6)	340 (52.4)

*Values are no. (%) except as indicated. Percentages refer to VTEC serotype column totals vs case age range and Central Statistics Office Urban/Rural classification. VTEC, verocytotoxin-producing *Escherichia coli*.
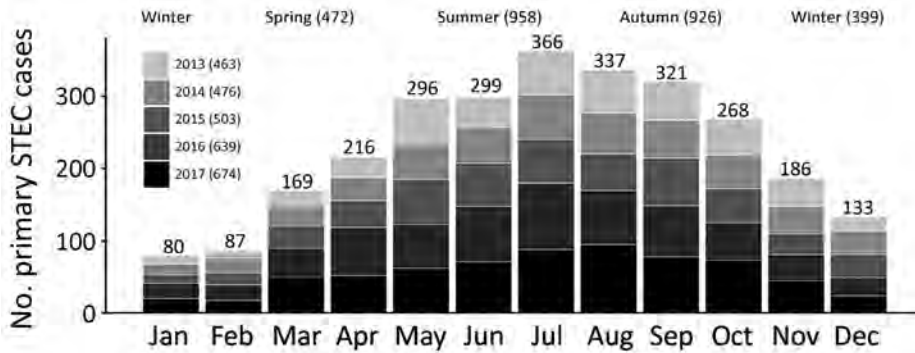
Figure 2. Temporal distribution of primary Shiga toxin–producing *Escherichia coli* (STEC) enteritis cases in Ireland, 2013–2017.

and used those counts to calculate SA-specific STEC incidence rates. We merged the CSO's 14 urban/rural categories to classify each spatial unit as rural or urban, using population density and settlement size used to verify classification. For reporting purposes, we have defined 8 distinct geographic zones in Ireland (Figure 1). Zone NE (Northern Ireland) is located outside CIDR surveillance boundaries and was not included for analyses. The Royal College of Physicians of Ireland Research Ethics Committee granted ethics approval for acquisition and analyses of human infection data (RCPI RECSAF_84).

Seasonal Decomposition
We analyzed seasonal decomposition for monthly incidence rates using the seasonal-trend decomposition by LOESS (locally estimated scatterplot smoothing) (STL) method, which combines multiple regression with k–nearest neighbor meta-modeling (*9*). The STL method decomposes a time series into trend, seasonal, and residual components; we used an additive model for our study because peak values of the seasonal time-series exhibit a relatively

constant trend (*10*). The monthly incidence rate (Yv) is equal to the sum of the trend (Tv), the seasonal variation (Sv), and the residuals (Rv). For the seasonal decompositions, we used the STL() function in R version 3.6.0 (R Foundation for Statistical Computing, https://www.r-project.org).

Spatial Autocorrelation (Anselin Local Moran's *I*)
We used Anselin Local Moran's *I* to examine individual features, specifically disease incidence within individual SAs, and their relationship to nearby features, returning localized clusters that may be correlated based on variance assigned to all individual spatial units (*11*). We calculated Local Moran's I statistics using the cluster/outlier tool in ArcGIS software version 10.6 (ESRI, https://www.esri.com) and maps of resultant high and low spatial clusters generated. We used cluster/outlier analysis to classify statistically significant clusters of high values surrounded by high values; low values surrounded by low values; outliers of high values surrounded by low values; and low values surrounded by high values. We conceptualized spatial relationships using the inverse distance
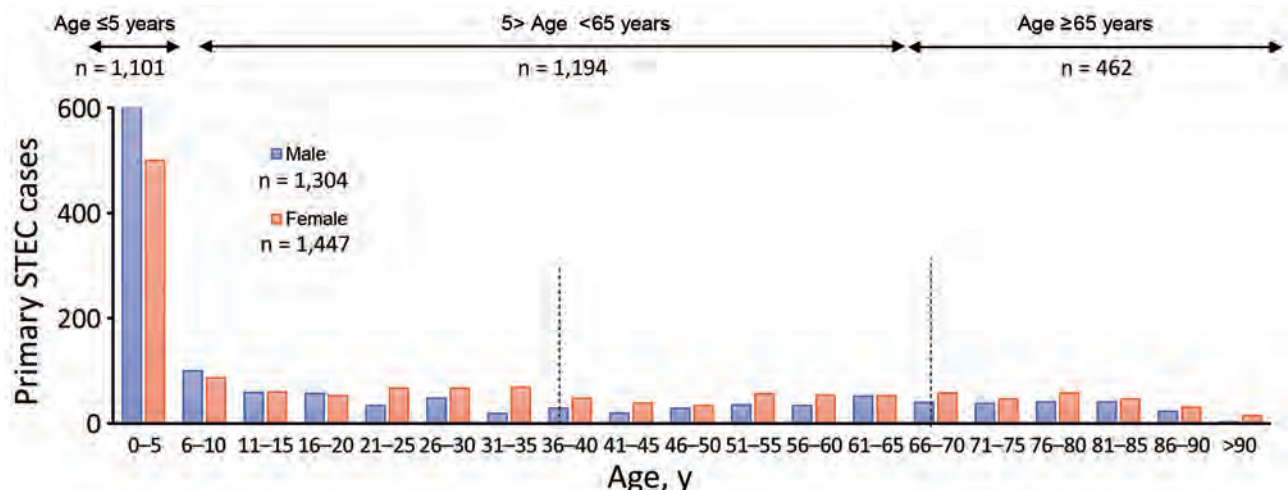
Figure 3. Distributions of primary STEC enteritis cases by age and sex, Ireland, 2013–2017. Dotted vertical lines show the main age-group divisions. STEC, Shiga toxin–producing *Escherichia coli*.

and Euclidean distance methods; we set significance at 95% based on pseudo p-values.

Space-Time Scanning

We used SaTScan version 9.6 space-time cluster detection software (https://www.satscan.org) to identify temporally-specific high- and low-risk regions. We defined the space-time scan statistic by a cylindrical window with a circular (or elliptic) geographic base (e.g., radius unit) of which height corresponded to the time-period of potential clusters (*12*). The null test hypothesis presumes that geographic regions inside and outside the scanning area are characterized by an equal relative risk (RR) of infection during the analyzed time period. We compared RR differences using the log likelihood ratio (i.e., RR within an area is expected to be proportional to population size or population-years) (*13*). We used a discrete Poisson model due to the high level of geographic resolution (SA, n = 18,641) in our study (i.e., high number of SAs with 0 or 1 case over the modeled period). We used the total population of each SA from 2011 national census as a control parameter; we performed multiple scans to optimize parameter selection and
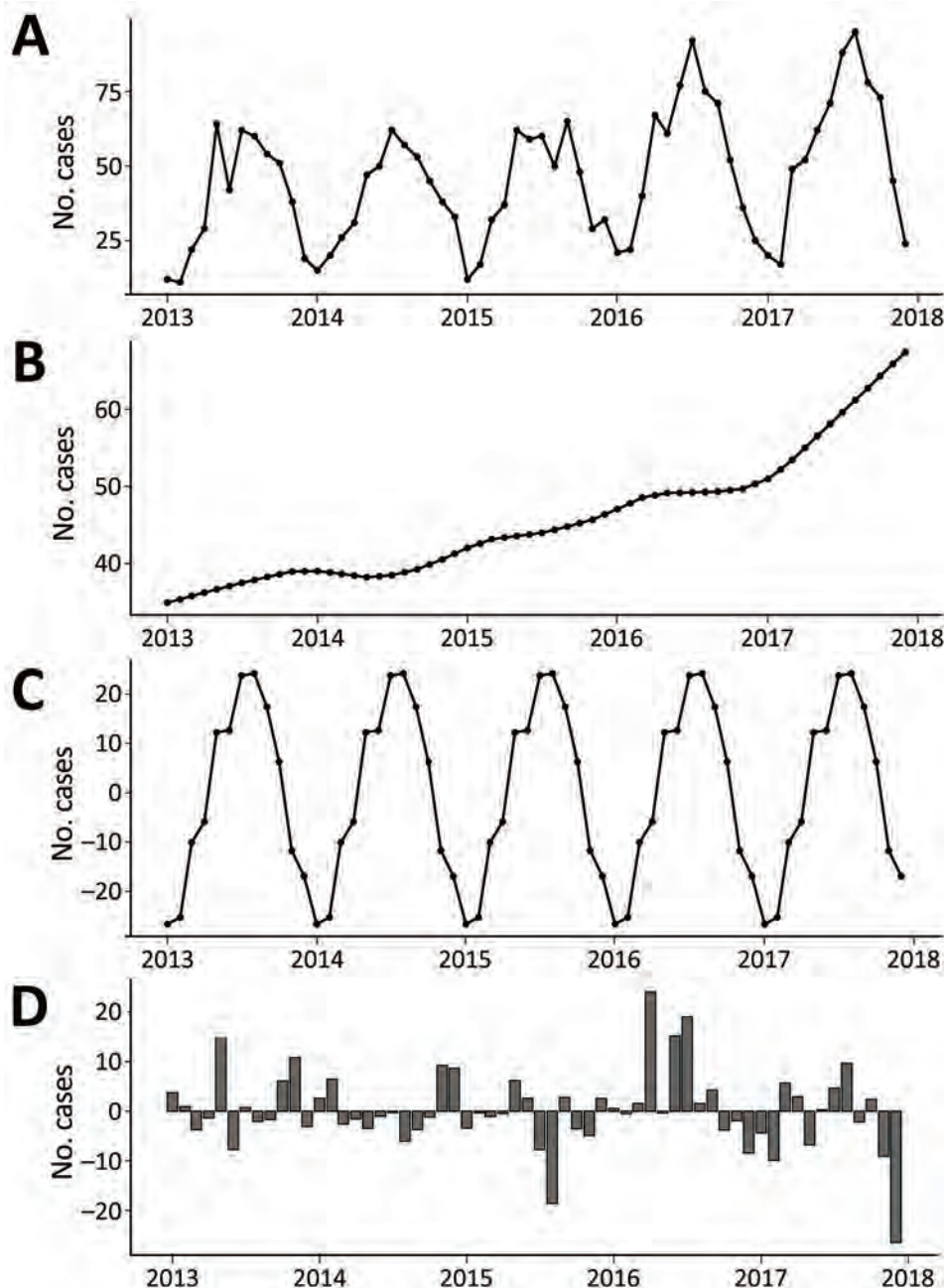
Figure 4. Trends and variations in confirmed primary Shiga toxin–producing *Escherichia coli* enteritis cases, Ireland, 2013–2017. A) all confirmed cases; B) decomposed 5-year trend of confirmed cases; C) seasonal variation in confirmed cases; D) calculated residual trend in confirmed cases.
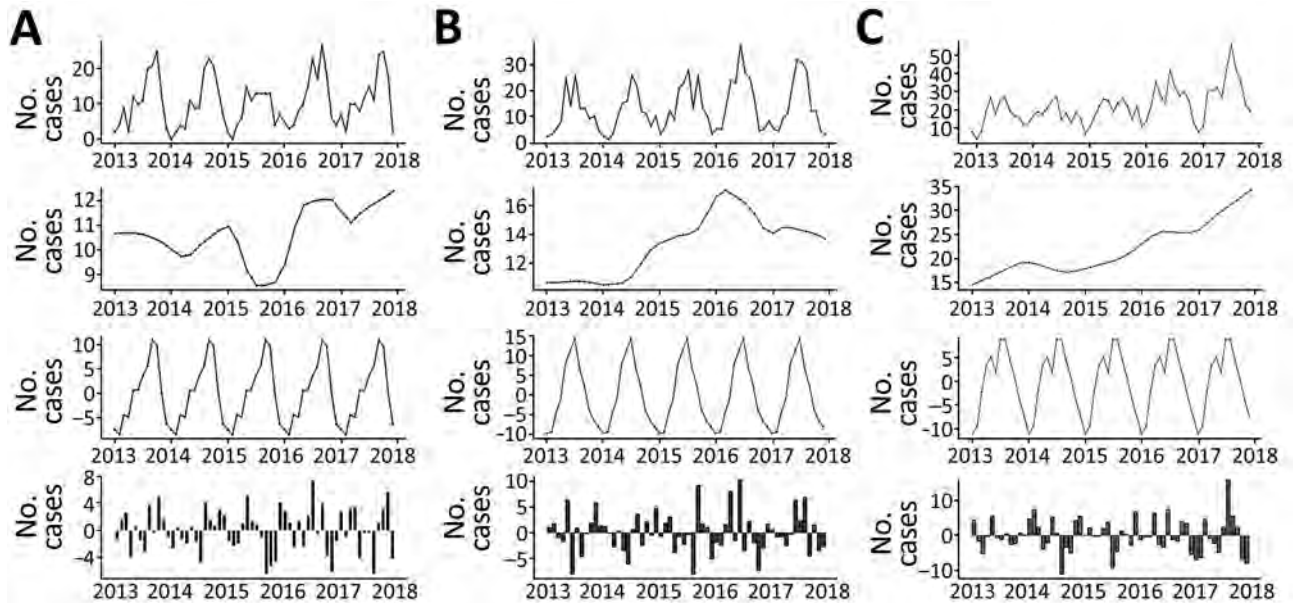
Figure 5. Trends and variations in confirmed cases of primary Shiga toxin–producing *Escherichia coli* enteritis in Ireland, 2013–2017, delineated for serogroup O157 (A), serogroup O26 (B), and other serogroups (C). Shown, top to bottom, are the trend for all confirmed cases, decomposed 5-year trend, seasonal variation, and calculated residual trend..

outcome stability. We chose a maximum geographic cluster size of 10% of the population at risk to account for the low number of reported cases in many areas, in concurrence with a maximum cluster radius of 50 km. We aggregated data monthly; maximum temporal cluster duration was 3 months based on known seasonal effects. Cluster size was ≥10 reported cases to ensure that identified clusters contained enough observed cases.

We used findings from annual space-time scanning to acquire a spatiotemporal picture of recurrent cluster locations by a cluster recurrence index. We mapped each significant space-time cluster (p<0.05) from annual scans in ArcGIS software and attributed a binary cluster location (i.e., cluster membership (0/1) to each spatial unit (SA); the resulting cluster recurrence index value ranged from 0 (no clusters over study period) to 5 (>1 cluster per year over the study period).

Several tools have been developed to detect space-time anomalies, including the spatial varying temporal trend scan, implemented in SaTScan, which is used to identify unusual spatial cluster locations that contribute to substantial increase or decrease in general trends (*14*). The cluster recurrence index we describe aims to shed light on spatially specific, recurrent space-time hot spots of infection by providing an ordinal classification for all spatial units that may be amended over time and used for prospective surveillance purposes.

Results

Occurrence of Sporadic STEC Infection

Of 2,783 confirmed sporadic cases included in the CIDR system during 2013–2017, we successfully geolinked 2,755 (98.9%) to a distinct spatial area. The most frequently confirmed serogroups associated with notified human infection were STEC O26 (n = 800, 29%) and O157 (n = 638, 23.2%) (Table 1; Appendix Table 1). We classified an additional 23.5% of confirmed infections as ungroupable (n = 391) or not serogrouped (n = 255). Of the remaining confirmed infection serogroups, STEC O145 (n = 126), O103 (n = 79), and O146 (n = 59) were the only serogroups associated with >50 confirmed infections. Temporal cumulative incidence rates exhibited an annual peak during late summer and early autumn; maximum peaks typically occurred during July (n = 366) (Figure 2). We observed yearly increase in case numbers between 2013 (463 cases) and 2017 (674 cases).

We observed markedly higher case numbers among children ≤5 years of age (Figure 3); 1,101 confirmed cases (39.6%) occurred within this subpopulation. Older persons (≥65 years) were also disproportionately affected, accounting for 462 cases (16.6%, compared with 11.7% for the national population). A slightly higher rate of occurrence was associated with female patients (52.5%) than male (47.2%). We observed ≥1 cases more frequently

in SAs classified as rural (1,252/6,242 SAs, 20.1%) than urban (n = 1,086/12,246 SAs, 8.9%) (Table 1). Pearson χ^2 tests with Yates' continuity corrections indicate a significant association between cases of STEC O26 infection and the ≤5 year age category (χ^2 = 17.055; p<0.0001); STEC O26 cases were more than twice as likely to occur among this subpopulation than among those >5 years (OR 2.338). No statistical association was found between STEC serogroup and urban/rural classification (p = 0.6005) or the incidence of age-specific cases and urban/rural classification (p = 0.7803).

Seasonal Decomposition

The decomposed 5-year trend indicates a monotonic increase in the occurrence of sporadic infection, with a clear annual peak occurring during late summer (July–August) (Figure 4). Calculated residuals point to a relatively consistent annual and longer-term trend, ranging from a maximum of +24 cases during April 2016 to −26 cases during December 2018. Decomposed trends associated with ≤5 year and 6–64 year subcategories both exhibited an overall (nonmonotonic) increase; higher levels of variability were associated with the ≥65 year subcategory (Appendix
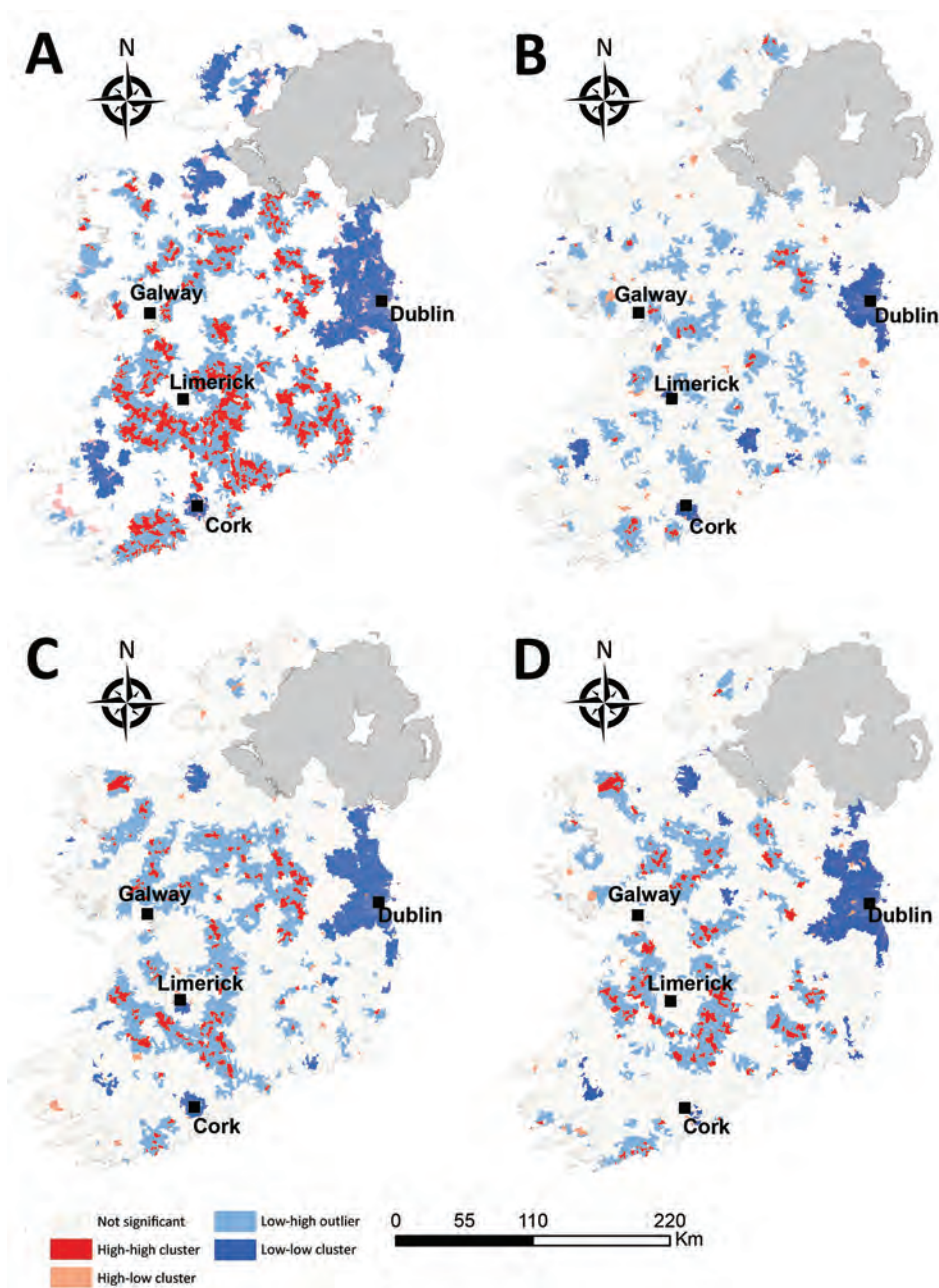
Figure 6. Spatial autocorrelation clusters of Shiga toxin–producing *Escherichia coli* (STEC) enteritis, Ireland, 2013–2017. A) All confirmed STEC infections; B) STEC O157 infections; C) STEC O26 infections; D) STEC infections in children ≤5 years.

Table 2. Results of year on year space-time scanning among all confirmed sporadic VTEC cases in Ireland, 2013–2017

Cluster no.	Population	No. cases	Expected	Observed/ expected	RR	Start date	End date	p value
2013								
1	268,082	32	4.62	6.93	7.37	2013 Jul 1	2013 Aug 31	0.00000000016
2	140,784	27	3.60	7.50	7.90	2013 May 1	2013 Jul 31	0.0000000041
3	147,000	25	3.76	6.65	6.97	2013 May 1	2013 Jul 31	0.00000030
4	154,425	18	3.91	4.61	4.75	2013 Apr 1	2013 Jun 30	0.022
2014								
1	370,743	40	9.72	4.11	4.40	2014 Jul 1	2014 Sep 30	0.00000022
2	75,467	14	1.96	7.15	7.34	2014 Apr 1	2014 Jun 30	0.0041
2015								
1	165,552	14	1.50	9.36	9.60	2015 Sep 1	2015 Sep 30	0.00018
2	245,189	27	6.79	3.97	4.14	2015 May 1	2015 Jul 31	0.00067
3	59,890	13	1.66	7.83	8.02	2015 May 1	2015 Jul 31	0.0037
2016								
1	299,166	42	10.59	3.97	4.18	2016 May 31	2016 Aug 30	0.00000033
2	119,941	21	4.20	5.00	5.14	2016 May 1	2016 Jul 30	0.0017
3	261,375	31	9.25	3.35	3.47	2016 Mar 31	2016 Jun 30	0.0044
2017								
1	345,279	54	12.93	4.18	4.45	2017 Jun 30	2017 Sep 29	0.00000000006
2	190,947	27	7.15	3.78	3.89	2017 Jul 30	2017 Oct 29	0.0042
3	232,749	29	8.71	3.33	3.43	2017 Jun 30	2017 Sep 29	0.015
4	66,817	15	2.47	6.06	6.18	2017 Apr 30	2017 Jul 29	0.017
5	81,564	10	1.00	10.04	10.18	2017 Sep 30	2017 Oct 29	0.027

*RR, relative risk; VTEC, verocytotoxin-producing *Escherichia coli*.

Figure 1). We found substantial variation in seasonal infection peaks (all STEC serogroups) among delineated age categories; infections among the ≤5 year subpopulation peaked from May to July, whereas infections among the older subpopulation occurred in July–August, followed by a smaller secondary peak in October.

The general decomposed trend for STEC O157 infection indicates a relatively modest overall increase over the study period, with a marked decrease during 2015 (Figure 5). Conversely, the incidence of STEC O26 exhibited a greater increase from January 2013–April 2016, followed by a consistent decrease to the end of the study period. Other (non-O157 and non-O26) STEC serogroups exhibited a gradual monotonic increase over the study period. Seasonal signals indicate a notable difference between the 2 main serogroups; STEC O157 infections exhibit highest rates of occurrence during September–October, whereas STEC O26 notifications peak in July. Urban cases exhibited an annual peak from July–September, whereas categorically rural case notifications display a longer but decreasing peak from May–October (Appendix Figure 2).

Spatial Autocorrelation (Local Anselin Moran's *I*)
The spatial distribution of high-high STEC incidence clusters were predominantly situated in zones S (south) and SE (southeast) around counties Clare, Limerick, and Tipperary (Figure 6), interspersed with smaller low-high outlier clusters. We observed

infection cold spots (low-low clusters) around the greater Dublin area (zone E) and Cork city (zone S), in addition to counties Sligo (zone N) and Kerry (zone SW). The occurrence of STEC O157 infection clusters were geographically sparse with small distinct HH clusters (hotspots) observed in zones M, E, and S. We again observed large infection cold spots among the STEC O26 serogroup and the ≤5-year age group for all STEC in the urban centers of Dublin and Cork cities (zones E and S) in addition to counties Kerry, Waterford, and Sligo (zones SW, SE, and N). The spatial distribution of STEC O26 and ≤5-year age group hot spots of infection followed a similar trend to overall STEC clustering patterns: H-H clusters were identified in zones S, M, and E, in addition to 1 unique H-H cluster in zone NW, that we did not observe for STEC O157.

Space-Time Scanning
Overall, we identified 17 distinct space-time clusters, ranging from 2 clusters during 2014 to 5 clusters during 2017 (Table 2; Figure 7). To acquire a clearer picture of hot- and cold spots relative to space-time cluster occurrence, we developed a space-time cluster recurrence index of 0 (SA never located within a space-time cluster) to 5 (SA situated within ≥1 space-time cluster during all study years) and generated maps of clusters (Figure 8). We identified 2 distinct areas situated southeast and southwest of Limerick City (Figure 1, zones M and S), and 1 area northeast of Galway city (zone M) as STEC infection
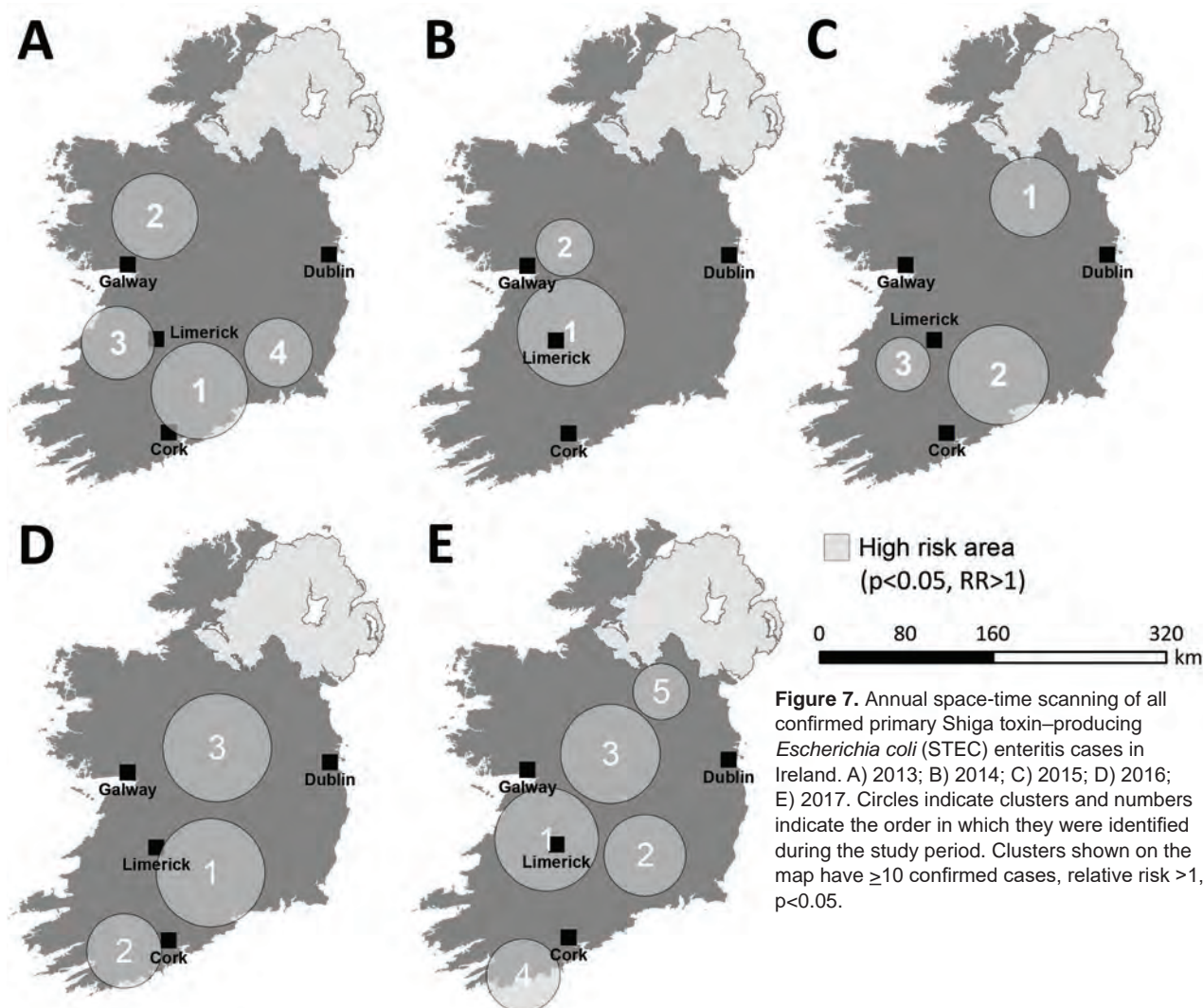
Figure 7. Annual space-time scanning of all confirmed primary Shiga toxin–producing *Escherichia coli* (STEC) enteritis cases in Ireland. A) 2013; B) 2014; C) 2015; D) 2016; E) 2017. Circles indicate clusters and numbers indicate the order in which they were identified during the study period. Clusters shown on the map have ≥10 confirmed cases, relative risk >1, p<0.05.

hotspots during the study period. Of note, no major population centers other than Limerick were located within an identified hot spot; the entire eastern seaboard classified as an infection cold spot on the basis of population-adjusted incidence rates. Space-time clusters occurred from April–September and peaked during July (n = 11) (Figure 8).

We observed much less space-time clustering (i.e., occurrence more geographically distributed) for STEC O157 infection than STEC O26 infection; Most STEC O157 clustering was low (1–2 clusters over the study period) in the south, south-west, and midlands zones (Figure 9). The spatial distribution and recurrence index of STEC O26 clusters mirrored those found for all confirmed STEC infections (Figure 10). The temporal window of serogroup-specific space-time clusters reflected the decomposed seasonal peak for both serogroups; STEC O157 clusters

occurred more frequently in September–December, whereas STEC O26 clusters typically occurred in June–November.

We identified much of the western seaboard as a particularly high incidence region for the ≤5 year subpopulation (zones W, SW, S) (Figure 11), with a notable temporal clustering peak (April–May) and relatively broad temporal baseline (March–September). In contrast, we noted 3 space-time clusters within the ≥65 year subpopulation (Figure 12); all occurred in the south of the country (zone S), with no specific temporal period associated with these clusters.

Discussion

The power of understanding spatial and temporal patterns of infection has long been recognized (*15*); identifying infection hot and cold spots and their

time periods informs targeted surveillance and control interventions and is a precursor to increasingly complex epidemiologic analyses and risk factor attribution (*16–18*). Since approximately 2000, space-time scanning and geostatistical approaches have been increasingly recognized as powerful tools for endemic disease surveillance and early outbreak detection (*19*).

Overall, we identified 17 space-time clusters during the 5-year study period, ranging from 2 clusters during 2014 to 5 clusters during 2017. All analyses were of categorically sporadic infections; thus, the identification of distinct space-time clusters is noteworthy and underlines the potential utility of real-time or prospective space-time scanning as part of ongoing surveillance procedures. For example,

Green et al. reported on the efficacy of using daily space-time statistics for 35 reportable communicable diseases in New York, New York, during 2014–2015 (*20*). The distribution of identified space-time clusters of sporadic STEC enteritis reveals high annual levels of persistence and variation in sporadic STEC infection in Ireland. We identified 3 distinct regions as exhibiting particularly high space-time cluster

Figure 8. Monthly distribution of space-time clusters (A) and cluster recurrence index (0–5) within census small areas (B) for all confirmed primary Shiga toxin–producing *Escherichia coli* (STEC) enteritis cases in Ireland, 2013–2017.

Figure 9. Monthly distribution of space-time clusters (A) and cluster recurrence index (0–5) within census small areas (B) for confirmed primary Shiga toxin–producing *Escherichia coli* (STEC) enteritis cases caused by STEC serogroup O157, Ireland, 2013–2017.

recurrence rates (Figure 6), namely southwest and east of Limerick city (zones SW, S, and SE), and northeast of Galway city (zone M), indicating the presence of persistent STEC reservoirs in these areas that cause regular exposure and transmission.

Spatial autocorrelation of STEC clusters further highlights the disparity between rural and urban living. Sporadic cases were more frequently identified in rural areas where ≈37.3% of the populace reside (20.1% of rural SAs vs. 8.9% of urban) (*21*). We identified low-incidence clusters in major cities, including Cork and the greater Dublin area. These findings emphasize the association of rurality with STEC transmission; increased environmental

Figure 10. Monthly distribution of space-time clusters (A) and cluster recurrence index (0–5) within census small areas (B) for confirmed primary Shiga toxin–producing *Escherichia coli* (STEC) enteritis cases caused by STEC serogroup O26, Ireland, 2013–2017.

Figure 11. Monthly distribution of space-time clusters (A) and cluster recurrence index (0–5) within census small areas (B) for confirmed primary Shiga toxin–producing *Escherichia coli* (STEC) enteritis cases among patients ≤5 years of age, Ireland, 2013–2017.

exposure to pathogen sources coupled with enhanced transport of pathogens through untreated drinking water supplies, extreme weather events, and so on are likely to increase risk for exposure and subsequent infection (*22*).

The relative proximity of large urban centers to the 3 identified high-recurrence regions may also point to narrow transitional zones between urban and populated-rural regions. Rural commuter belts that have inadequate municipal wastewater treatment or drinking supplies, in addition to relatively low levels of acquired immunity among children of young families residing within commuter belt regions, may contribute to this high spatial risk for transmission (*6*). National census statistics predict strongest population growth in peri-urban/commuter belt areas in Ireland (*21*), which are potentially at high risk for STEC infection incidence.

All 3 high-recurrence regions are predominantly underlain by karstified carboniferous limestone aquifers (*23*), which have previously been associated with the presence of STEC in private and small public drinking water supplies (*7*). The lack of space-time clustering found within the Greater Dublin area, which houses ≈39% of the national population (1.9 million persons) and is characterized by a spatially extensive urban commuter belt, consolidated bedrock, and a high level of water and wastewater infrastructure, seems to validate our hypotheses. Boudou et al. (2021) report that rates of space-time cluster recurrence of cryptosporidiosis from 2008 to 2017 followed similar patterns in the same 3 geographically distinct regions we identified; co-occurrence of STEC enteritis and cryptosporidiosis in Ireland requires further study (*24*).

Cumulative incidence rates of STEC infection exhibit a marked seasonal distribution; we identified peaks during late summer and early autumn, reflecting previously noted patterns of STEC shedding from zoonotic reservoirs and subsequent influx to the environment (*25*). Our findings, however, indicate a geographic and temporal disparity between the 2 primary serogroups, STEC O157 and STEC O26, with high-incidence geographic clusters of STEC O157 occurring more frequently in zones E and S. Previous work has identified associations between STEC O157 infection and persons residing in areas characterized by a higher density of cattle, private well usage, and domestic wastewater treatment systems (*6*), all of which are very common within spatial locations identified as HH clusters (*26*).

The ≤5 year age category has been associated with cases of STEC O26 infection, which has been characterized by an earlier annual infection peak in Ireland (*5*), implying age-specific peaks of infection. Garvey et al. (2016) reported a 2-month phase difference between STEC O26 (July) and STEC O157 (September) infections in Ireland; the difference was reported as significant in all (outbreak and sporadic) confirmed STEC infections (p<0.0001) and in sporadic

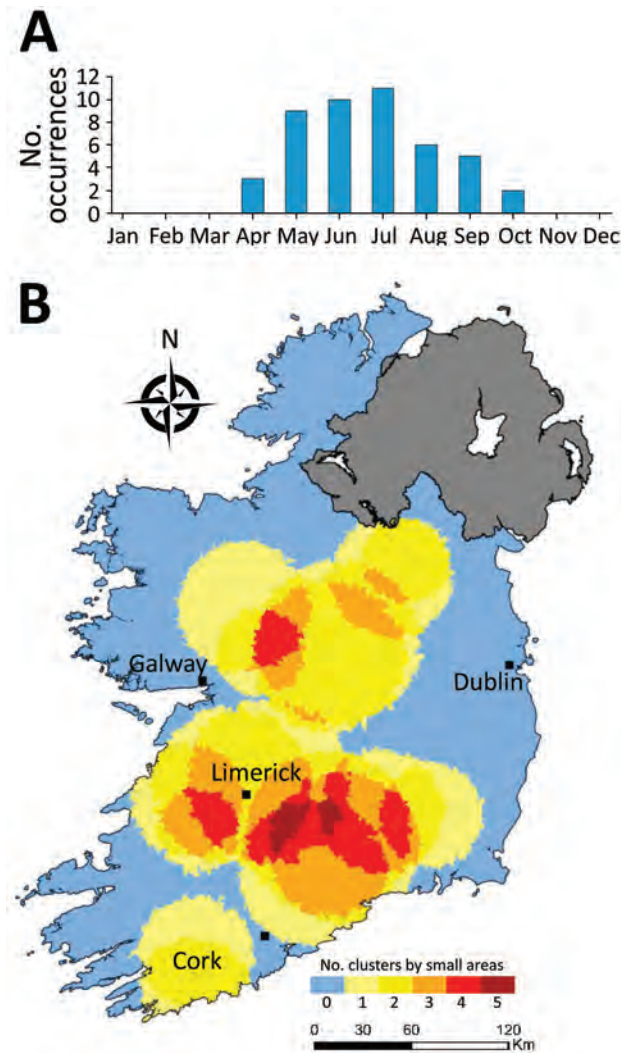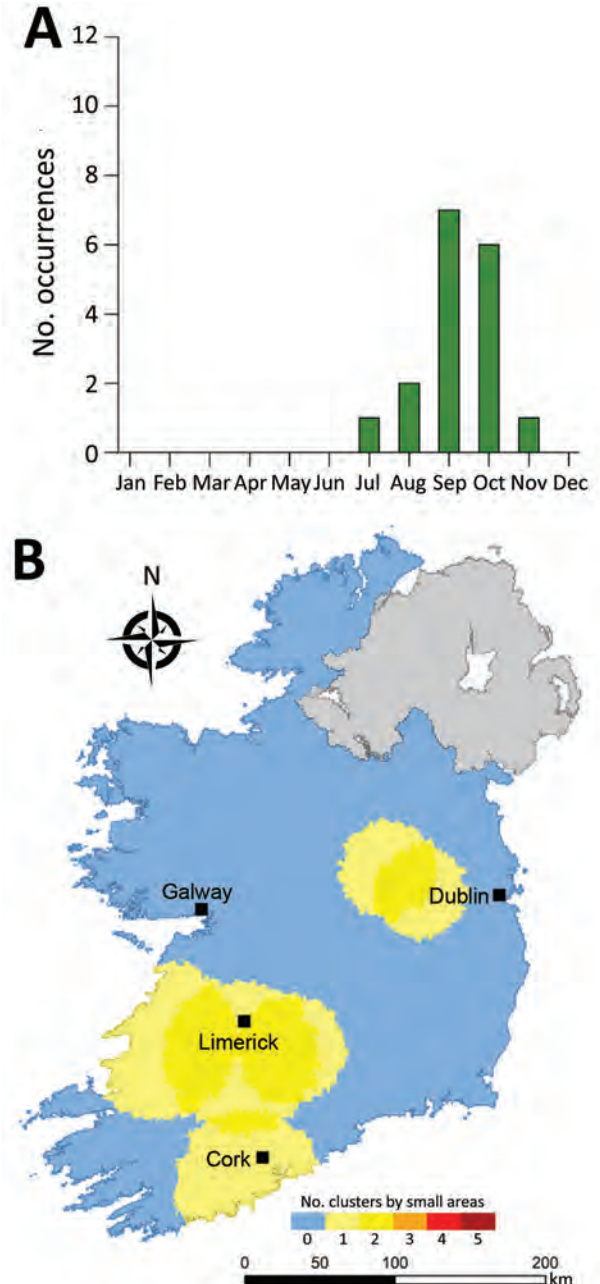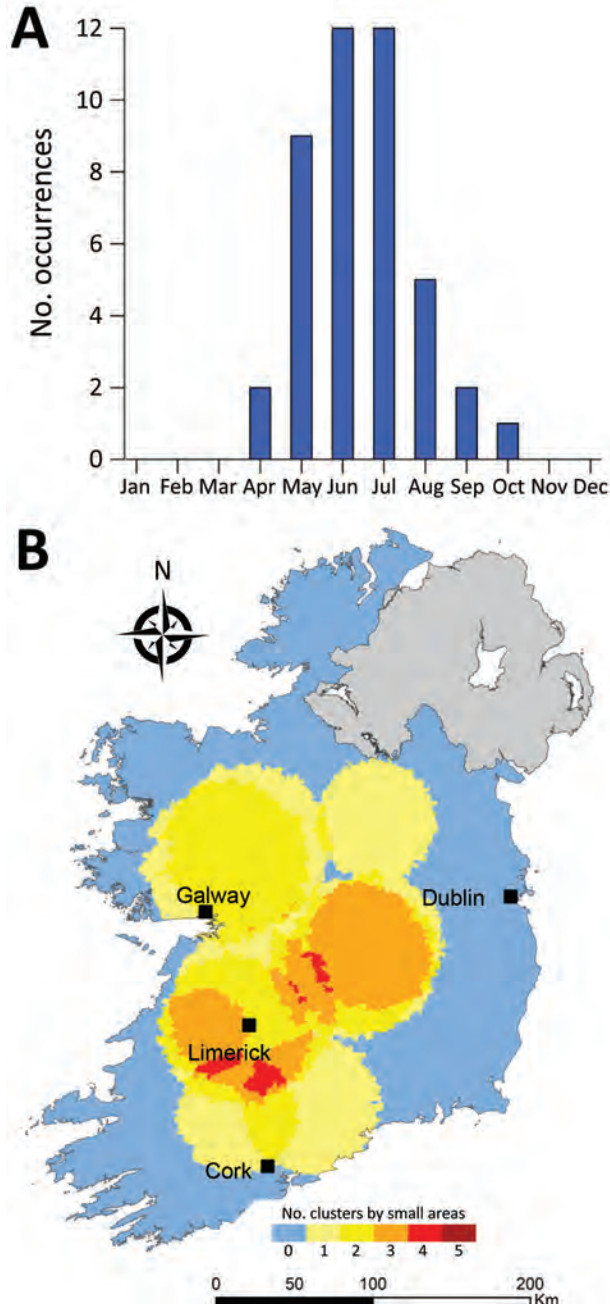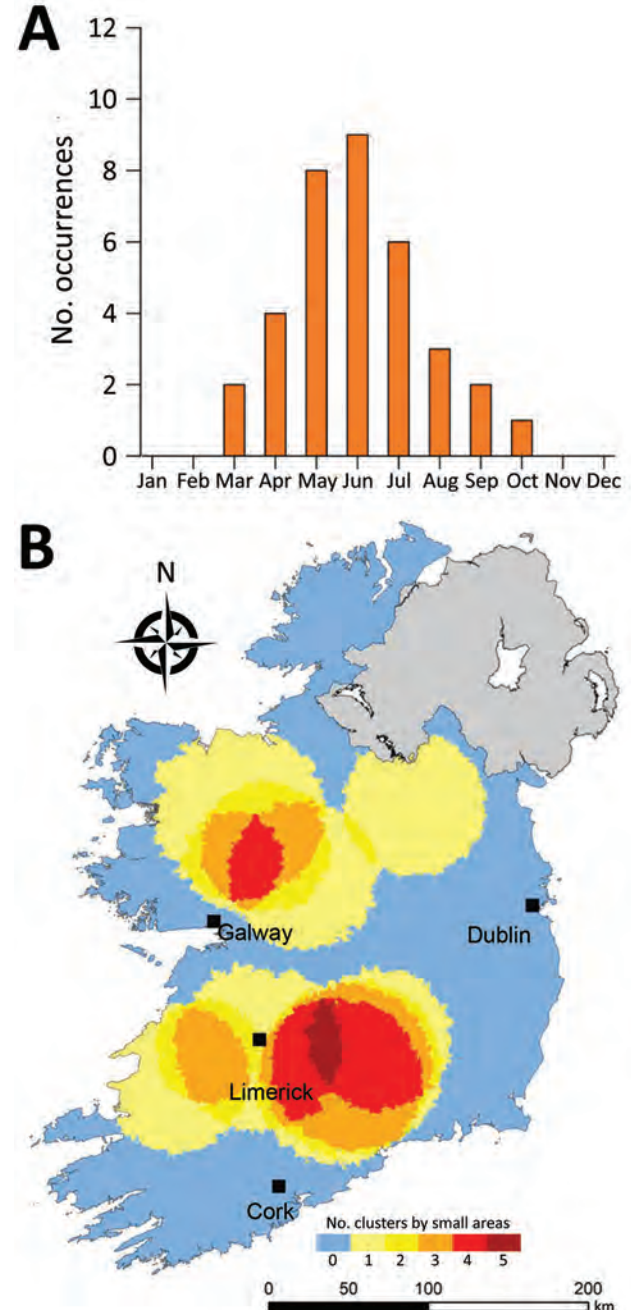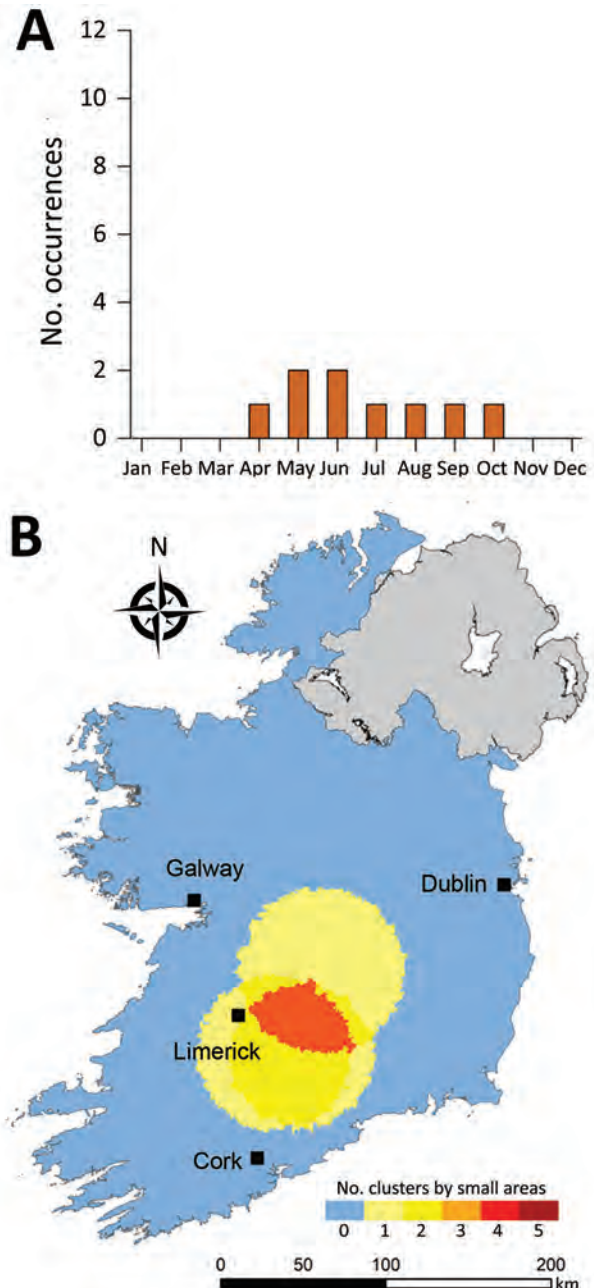**Figure 12.** Monthly distribution of space-time clusters (A) and cluster recurrence index (0–5) within census small areas (B) for confirmed primary Shiga toxin–producing *Escherichia coli* (STEC) enteritis cases among patients ≥65 years of age, Ireland, 2013–2017.

cases only (p<0.0001) and possibly attributed to seasonal variation in infection exposure such as contact with primary animal reservoirs of infection (5). Significantly higher incidence rates were noted in children ≤5 years of age; previous studies attributed this pattern to an increased risk for direct contact with environmental sources of fecal matter (27) and lower standards of hygiene (28) within this subpopulation.

Cumulatively, young children (≤5 years) and the older subpopulation (≥65 years) accounted for 56.7% (n = 1,563) of confirmed sporadic infections. Both of these subpopulations are known to be immunologically vulnerable and exhibit higher incidence rates of infection and severe sequelae (29,30). Younger cohorts especially are at increased risk of infection caused by frequent contact with other children of a similar age, and also pose a risk as a source of infection associated with increased contact with adults, particularly among the 30–39 year age group (31,32). Prominent clustering of infection identified among the ≤5 and ≥65 year age groups, and the relative spatial heterogeneity of infection clusters, underscore the need for enhanced targeted surveillance measures, particularly in geographic areas characterized by a higher proportion of younger and older populations (33).

About the Author

Dr. Cleary is a spatial epidemiologist in the School of Natural Sciences, the National University of Ireland, Galway. Her research interest is the transmission dynamics of infectious diseases.

References

1. HSE Health Protection Surveillance Centre. VTEC infection in Ireland, 2017. Dublin: The Centre; 2019.
2. European Centre for Disease Prevention and Control. Shiga toxin–/verocytotoxin-producing *Escherichia coli* (STEC/VTEC) infection. In: European Centre for Disease Prevention and Control. Annual epidemiological report for 2017. Stockholm: the Centre; 2019.
3. Mead PS, Griffin PM. *Escherichia coli* O157: H7. Lancet. 1998; 352:1207-12. https://doi.org/10.1016/S0140-6736(98)01267-7
4. Karmali, Mohamed A, Gannon V, Sargean JM. Verocytotoxin-producing *Escherichia coli* (VTEC). Vet Microbiol. 2010;140:360–70. https://doi.org/10.1016/j.vetmic.2009.04.011
5. Garvey P, Carroll A, McNamara E, Charlett A, Danis K, McKeown PJ. Serogroup-specific seasonality of verotoxigenic *Escherichia coli*, Ireland. Emerg Infect Dis. 2016;22:742–4. https://doi.org/10.3201/eid2204.151160
6. Óhaiseadha C, Hynds PD, Fallon UB, O'Dwyer J. A geostatistical investigation of agricultural and infrastructural risk factors associated with primary verotoxigenic *E. coli* (VTEC) infection in the Republic of Ireland, 2008–2013. Epidemiol Infect. 2017;145:95–105. https://doi.org/10.1017/S095026881600193X
7. Hynds PD, Gill LW, Misstear BD. A quantitative risk assessment of verotoxigenic *E. coli* (VTEC) in private groundwater sources in the Republic of Ireland. Hum Ecol Risk Assess. 2014;20:1446–68. https://doi.org/10.1080/10807039.2013.862065
8. Brehony C, Cullinan J, Cormican M, Morris D. Shiga toxigenic *Escherichia coli* incidence is related to small area variation in cattle density in a region in Ireland. Sci Total Environ. 2018;637-638:865–70. https://doi.org/10.1016/j.scitotenv.2018.05.038
9. Fox J. Applied regression analysis and generalized linear models. 3rd ed. Los Angeles: SAGE Publications; 2015.
10. Prema V, Rao KU. Development of statistical time series models for solar power prediction. Renew Energy. 2015;83:100–9. https://doi.org/10.1016/j.renene.2015.03.038
11. Anselin L. Local indicators of spatial association—LISA. Geogr Anal. 1995;27:93–115. https://doi.org/10.1111/j.1538-4632.1995.tb00338.x
12. Kulldorff M. Spatial scan statistics: models, calculations, and applications. In: Glaz J, Balakrishnan N, editors. Scan statistics and applications. Boston: Birkhäuser; 1999. p. 303–22.
13. Allévius B. scanstatistics: Space-time anomaly detection using scan statistics. J Open Source Softw. 2018;3:515. https://doi.org/10.21105/joss.00515
14. Kulldorf M. SaTScan user guide for version 9.7. 2021 [cited 2021 Jul 19]. https://satscan.org
15. Cameron D, Jones IG. John Snow, the Broad Street pump and modern epidemiology. Int J Epidemiol. 1983;12:393–6. https://doi.org/10.1093/ije/12.4.393
16. Lau CL, Sheridan S, Ryan S, Roineau M, Andreosso A, Fuimaono S, et al. Detecting and confirming residual hotspots of lymphatic filariasis transmission in American Samoa 8 years after stopping mass drug administration. PLoS Negl Trop Dis. 2017;11:e0005914. https://doi.org/10.1371/journal.pntd.0005914
17. Brown EM, McTaggart LR, Dunn D, Pszczolko E, Tsui KG, Morris SK, et al. Epidemiology and geographic distribution of blastomycosis, histoplasmosis, and coccidioidomycosis, Ontario, Canada, 1990–2015. Emerg Infect Dis. 2018;24:1257–66. https://doi.org/10.3201/eid2407.172063
18. Karunaweera ND, Ginige S, Senanayake S, Silva H, Manamperi N, Samaranayake N, et al. Spatial epidemiologic trends and hotspots of leishmaniasis, Sri Lanka, 2001–2018. Emerg Infect Dis. 2020;26:1–10. https://doi.org/10.3201/eid2601.190971
19. Robertson C, Nelson TA, MacNab YC, Lawson AB. Review of methods for space-time disease surveillance. Spat Spatio-Temporal Epidemiol. 2010;1:105–16. https://doi.org/10.1016/j.sste.2009.12.001
20. Greene SK, Peterson ER, Kapell D, Fine AD, Kulldorff M. Daily reportable disease spatiotemporal cluster detection, New York City, New York, USA, 2014–2015. Emerg Infect Dis. 2016;22:1808–12. https://doi.org/10.3201/eid2210.160097
21. Central Statistics Office. Census 2016 profile 1—town and country. Dublin: Stationery Office; 2018.
22. Andrade L, O'Dwyer J, O'Neill E, Hynds P. Surface water flooding, groundwater contamination, and enteric disease in developed countries: A scoping review of connections and consequences. Environ Pollut. 2018;236:540–9. https://doi.org/10.1016/j.envpol.2018.01.104
23. Woodcock NH, Strachan RA. Geological history of Britain and Ireland. New York: John Wiley & Sons; 2009
24. Boudou M, ÓhAiseadha C, Garvey P, O'Dwyer J, Hynds P. Flood hydrometeorology and gastroenteric infection: the

winter 2015–2016 flood event in the Republic of Ireland. J Hydrol (Amst). 2021;599:126376. https://doi.org/10.1016/j.jhydrol.2021.126376

25. Dewsbury DM, Renter DG, Shridhar PB, Noll LW, Shi X, Nagaraja TG, et al. Summer and winter prevalence of Shiga toxin–producing *Escherichia coli* (STEC) O26, O45, O103, O111, O121, O145, and O157 in feces of feedlot cattle. Foodborne Pathog Dis. 2015;12:726–32. https://doi.org/10.1089/fpd.2015.1987

26. Hynds PD, Misstear BD, Gill LW. Development of a microbial contamination susceptibility model for private domestic groundwater sources. Water Resour Res. 2012;48:W12504. https://doi.org/10.1029/2012WR012492

27. Rechel B, Mahgoub H, Pritchard GC, Willshaw G, Williams C, Rodrigues B, et al. Investigation of a spatiotemporal cluster of verotoxin-producing *Escherichia coli* O157 infections in eastern England in 2007. Euro Surveill. 2011;16:19916. https://doi.org/10.2807/ese.16.28.19916-en

28. Tam CC, O'Brien SJ, Tompkins DS, Bolton FJ, Berry L, Dodds J, et al.; IID2 Study Executive Committee. Changes in causes of acute gastroenteritis in the United Kingdom over 15 years: microbiologic findings from 2 prospective, population-based studies of infectious intestinal disease. Clin Infect Dis. 2012;54:1275–86. https://doi.org/10.1093/cid/cis028

29. Chaisri U, Nagata M, Kurazono H, Horie H, Tongtawe P, Hayashi H, et al. Localization of Shiga toxins of enterohemorrhagic *Escherichia coli* in kidneys of pediatric and geriatric patients with fatal hemolytic uremic syndrome. Microb Pathog. 2001;31:59–67. https://doi.org/10.1006/mpat.2001.0447

30. Adams N, Byrne L, Rose T, Adak B, Jenkins C, Charlett A, et al. Sociodemographic and clinical risk factors for pediatric typical hemolytic uremic syndrome: retrospective cohort study. BMJ Paediatr Open. 2019;3:e000465. https://doi.org/10.1136/bmjpo-2019-000465

31. Xiao X, van Hoek AJ, Kenward MG, Melegaro A, Jit M. Clustering of contacts relevant to the spread of infectious disease. Epidemics. 2016;17:1–9. https://doi.org/10.1016/j.epidem.2016.08.001

32. Hoang T, Coletti P, Melegaro A, Wallinga J, Grijalva CG, Edmunds JW, et al. A systematic review of social contact surveys to inform transmission models of close-contact infections. Epidemiology. 2019;30:723–36. https://doi.org/10.1097/EDE.0000000000001047

33. Bhunia GS, Siddiqui NA, Shit PK, Chatterjee N, Sinha SK. Spatial clustering of *Plasmodium falciparum* in Bihar (India) from 2007 to 2015. Spat Inf Res. 2016;24:639–48. https://doi.org/10.1007/s41324-016-0061-7

Address for correspondence: Paul D. Hynds, Environmental Sustainability & Health Institute, Technological University of Dublin, Greenway Hub, Grangegorman Dublin 7, D07 H6K8, Ireland; email: hyndsp@tcd.ie; Jean O'Dwyer, University College Cork, Distillery Fields, North Mall, Cork T23 N73K, Ireland; email: jean.odwyer@ucc.ie

Reduction in Antimicrobial Use and Resistance to *Salmonella*, *Campylobacter*, and *Escherichia coli* in Broiler Chickens, Canada, 2013–2019

Laura Huber, Agnes Agunos, Sheryl P. Gow, Carolee A. Carson, Thomas P. Van Boeckel

Antimicrobial use contributes to the global rise of antimicrobial resistance (AMR). In 2014, the poultry industry in Canada initiated its Antimicrobial Use Reduction Strategy to mitigate AMR in the poultry sector. We monitored trends in antimicrobial use and AMR of foodborne bacteria (*Salmonella*, *Escherichia coli*, and *Campylobacter*) in broiler chickens during 2013 and 2019. We quantified the effect of antimicrobial use and management factors on AMR by using LASSO regression and generalized mixed-effect models. AMR in broiler chickens declined by 6%–38% after the decrease in prophylactic antimicrobial use. However, the withdrawal of individual compounds, such as cephalosporins and fluoroquinolones, prompted an increase in use of and resistance levels for other drug classes, such as aminoglycosides. Canada's experience with antimicrobial use reduction illustrates the potential for progressive transitions from conventional antimicrobial-dependent broiler production to more sustainable production with respect to antimicrobial use.

In Canada, foodborne pathogens cause an estimated 4 million cases of human illness, 11,600 hospitalizations, and 238 deaths each year (*1*). *Escherichia coli*, *Campylobacter*, and *Salmonella* are the foodborne zoonotic pathogens most frequently associated with infections from poultry products (*2*). Antimicrobial drugs have been used in ovo, feed, or water to pre-

Author affiliations: Auburn University, Auburn, Alabama, USA
(L. Huber); ETH Zürich, Zürich, Switzerland (L. Huber,
T.P. Van Boeckel); Public Health Agency of Canada, Guelph,
Ontario, Canada (A. Agunos, C.A. Carson); Public Health Agency
of Canada, Saskatoon, Saskatchewan, Canada (S.P. Gow);
Center for Disease Dynamics, Economics & Policy, Washington,
DC, USA (T.P. Van Boeckel)

vent or treat commonly occurring diseases of poultry and to enable gains in productivity on farms (*3*,*4*). However, use of antimicrobial drugs contributes to the development of antimicrobial resistance (AMR). In humans, treatment of salmonellosis with antimicrobial drugs is often unnecessary but may be lifesaving in the case of invasive infections (*5*). The rise of AMR progressively reduces the number of antimicrobial drug options available to treat infections, which has important consequences for human health but also for the long-term viability of the production of animals (*6*–*8*).

In 2005, the Canadian Integrated Program for Antimicrobial Resistance Surveillance (CIPARS) reported an increasing frequency of resistance to ceftiofur, a veterinary third-generation cephalosporin (*9*), in *Salmonella enterica* serovar Heidelberg isolates from retail chicken and humans (*10*). In response, broiler chicken producers in Québec Province voluntarily eliminated the extra-label use of ceftiofur through injection (in ovo or subcutaneously) in hatcheries (*11*). By 2006, this measure led to a reduction in prevalence of ceftiofur-resistant *Salmonella* Heidelberg in retail chicken and humans (*8*). In a concerted effort to mitigate AMR and to reduce overall antimicrobial use (AMU), a stewardship program called the Antimicrobial Use Reduction Strategy was initiated in 2014 by the poultry industry. The first objective of this program was the elimination of the preventive use of Health Canada's Veterinary Drugs Directorate' category I antimicrobials (*12*), including third-generation cephalosporins (e.g., ceftiofur) and fluoroquinolones, which was accomplished in 2014 (*13*). Subsequently, the goal was to eliminate the preventive use of category II antimicrobials (e.g., aminoglycosides, lincosamides-aminocyclitols,

macrolides, penicillin, and trimethoprim/sulfonamide combinations), which was accomplished in the end of 2018. The third phase was to include the elimination of the preventive use of category III antimicrobials (e.g., bacitracins and tetracyclines) by the end of 2020 (13). This third step has been postponed pending further consultation with producers, an assessment of overall bird health and welfare from implementation of the first 2 phases, and a more fulsome evaluation of the production outcomes.

In our study, we used farm-level AMU and AMR time series data from CIPARS (2013–2019) to identify how changes in AMU have affected AMR in *E. coli*, *Campylobacter*, and *Salmonella* isolates from broiler chicken farms in Canada. The specific goals were to assess trends in AMR by province during 2013–2019, identify farm-management factors affecting AMU and AMR, and examine the association between route of antimicrobial administration (injections, water, or feed) and the frequency of multidrug resistance (defined as resistance to >2 antimicrobial classes).

Material and Methods

Study Design and Data Collection

We collected AMU and AMR information at the farm level through a network of poultry veterinarians (n = 17) who were assigned to producers (n = 97–147, depending on the year) in the 5 major poultry-producing provinces of Canada: British Columbia, Alberta, Saskatchewan, Ontario, and Québec (14). Participating producers signed an informed consent form, which was administered by the veterinarian. We obtained information on farm-level AMU and farm demographics by using a questionnaire and collected fecal samples for bacterial recovery and antimicrobial-susceptibility testing. We collected samples according to the formula for detection of AMR in a population of >1,000 individuals (n = ln α / ln [1 – minimum expected prevalence]; α = 0.05) (15), according to the routine CIPARS/FoodNet Canada farm sampling strategy. We divided each barn from each farm in 4 quadrants, and we collected 10–15 fresh fecal droppings from each quadrant. We pooled the samples from each quadrant and selected randomly 1 isolate per pooled sample for all *E. coli*, *Salmonella*, and *Campylobacter* for further analysis. Each year, we sampled 1 flock of preharvest broilers (>30 days old) that had been randomly selected from each production unit. We administered questionnaires to record flock characteristics, including hatchery or province and country of origin of the hatching eggs or chicks, breed, production system (conventional or antimicrobial-free), age, and estimated weight of birds at preharvest sampling. We collected detailed AMU information, including the quantity of antimicrobial active ingredients administered, routes of administration (in ovo or subcutaneous injections at the hatchery, feed, and water) and primary reasons for use of antimicrobial (prophylaxis, growth promotion, or disease treatment). We also collected information on biosecurity, health status, and vaccination history (questionnaires were published elsewhere [16] as supplemental material).

Bacteria Isolation and Susceptibility Testing

When an isolate of each bacterial species of interest (*Salmonella*, *E. coli* and *Campylobacter*) was identified, we saved that isolate and tested it for susceptibility. We conducted antimicrobial-susceptibility testing by using routine CIPARS methodology (14). We performed automated broth microdilution by using Sensititre (ThermoFisher Scientific, https://www.thermofisher.com) using the CMV4AGNF panel for *Salmonella* and *E. coli* and the CAMPY plates for *Campylobacter*. Plate configurations were designed by the US National Antimicrobial Resistance Monitoring System. We applied Clinical and Laboratory Standards Institute breakpoint guidelines (17,18) (Appendix Table 1, https://wwwnc.cdc.gov/EID/article/27/9/20-4395-App1.pdf). According to routine CIPARS/National Antimicrobial Resistance Monitoring System methods, we classified isolates with intermediate susceptibility patterns as susceptible. According to CIPARS AMR testing methods, we sued no selective media in this study.

Statistical Analysis

The number of antimicrobial classes each isolate was resistant to (nC) was the main outcome in the regression models. We evaluated the effect of covariates on the nC by using a 2-step procedure. First, we used a LASSO regression to select a subset of risk factors to be included in the generalized models (Appendix Table 2). Second, we ran a mixed-effect model with veterinarian and flock identification as random effects in all models. We cross-validated the models by dividing the dataset into 3 validation sets.

The term "ideal method for cleaning and disinfection" refers to the method recommended by the World Organisation for Animal Health (OIE) (19) aimed at reducing infectious pathogens in animal premises. This method consists of dry cleaning (i.e., removing all equipment and brushing and scraping of all surfaces), followed by a warm water (60°C) wash and application of a disinfectant to reduce

Table 1. Incidence rate ratio of *Salmonella* nC from LASSO-penalized generalized mixed-effects Poisson model in a study of antimicrobial use and in broiler chickens, Canada, 2013–2019*

Variable	Incidence rate ratio	2.5% CI	97.5% CI	p value
Intercept	0.224851	0.1326975	−0.3810016	2.92 × 10⁻⁸†
Production system (referent comparison factor: conventional)				
Antimicrobial-free‡	1.456588	0.9917592	2.1392781	0.05514
Disinfection system (referent comparison factor: no use of the ideal method of disinfection)				
Use of ideal disinfection	0.8947851	0.6969602	1.1487606	0.38316
Continuous variables of antimicrobial use (mg/kg)				
Injections (in ovo or subcutaneous§)	3.3926736	1.1860941	9.704318	0.02271†
Through feed	1.0030552	1.0004128	1.0057047	0.02341†
Through water	1.0005486	0.9947253	1.006406	0.85389
Sample collection year (referent comparison year: 2013)				
2014	0.9904373	0.6355585	1.5434709	0.96614
2015	1.0475486	0.6851365	1.6016635	0.83021
2016	1.0912259	0.7028907	1.6941097	0.69726
2017	0.9097193	0.5821923	1.4215049	0.67777
2018	0.9869455	0.6351112	1.5336864	9.53 × 10⁻¹†
2019	1.548854	1.0091025	2.3773092	0.04534†
Province (referent comparison province: Alberta)				
British Columbia	1.6846635	1.1510546	2.465644	0.00728†
Ontario	1.8199429	1.2502213	2.6492848	0.00177†
Québec	3.7534112	2.4943597	5.6479808	2.24 × 10⁻¹†
Saskatchewan	1.9772529	1.1775379	3.3200878	0.00994†

*nC, number of antimicrobial classes to which each isolate was resistant.
†Statistically significant (p<0.05).
‡Antimicrobial-free flocks were not exposed to medically important antimicrobials through any route of administration.
§Subcutaneous route in young chicks at the hatchery.

microbial populations and carry over of pathogens to the next production cycle. For production system categories, the term "antimicrobial-free"(in contrast with "conventional") refers to farms that were not exposed to nationally defined medically important antimicrobials (*20*) or farms that have a reduced AMU program (i.e., one that may allow use of chemical coccidiostats, according to guidelines [*21*], or ionophores). We estimated AMU at the flock level in milligrams of antimicrobial active ingredient per kilogram broiler chicken biomass (mg/kg) by summing of all antimicrobials reportedly used in the flock from all routes of administration and dividing by the live animal biomass (e.g., birds at risk multiplied by the average preslaughter live weight) (*22*).

Table 2. Incidence rate ratio of *Escherichia coli* nC from LASSO-penalized generalized mixed-effects Poisson model in a study of antimicrobial use and in broiler chickens, Canada, 2013–2019*

Variable	Incidence rate ratio	2.50% CI	97.50% CI	p value
Intercept	1.5740809	1.3050913	1.8985113	2.09 × 10⁻⁶†
Production system (referent comparison factor: conventional)				
Antimicrobial-free‡	1.0275338	0.9170807	1.1512897	0.63969
Ideal disinfection method (referent comparison factor: no use of ideal method)				
Use of ideal disinfection	1.0133377	0.9418401	1.0902627	0.722652
Continuous variables of antimicrobial use (mg/kg)				
Injections (in ovo or subcutaneous§)	1.3588476	0.9911794	1.8628985	0.056785
Through feed	1.0015582	1.0008262	1.0022907	2.99 × 10⁻⁵†
Through water	1.0032516	1.0019576	1.0045473	8.23 × 10⁻⁷†
Sample collection year (referent comparison year: 2013)				
2014	0.8881768	0.7850343	1.0048707	0.05972
2015	0.9555537	0.8431346	1.0829621	0.476499
2016	0.9458207	0.8349598	1.071401	0.381178
2017	0.9144284	0.8066086	1.0366604	0.162256
2018	0.8545609	0.7523902	0.9706058	0.015553†
2019	0.7705043	0.6770116	0.8769079	7.81 × 10⁻⁵†
Province (referent comparison province: Alberta)				
British Columbia	1.2229891	1.0173109	1.4702509	0.032138†
Ontario	0.9922909	0.8315428	1.1841136	0.931604
Québec	1.3924895	1.1564315	1.6767333	0.000477†
Saskatchewan	0.4997466	0.3844197	0.649672	2.20 × 10⁻⁷†

*nC, number of antimicrobial classes to which each isolate was resistant.
†Statistically significant (p<0.05).
‡Antimicrobial-free flocks were not exposed to medically important antimicrobials through any route of administration.
§Subcutaneous route in young chicks at the hatchery.

Table 3. Incidence rate ratio of *Campylobacter* nC from LASSO-penalized generalized mixed-effects Poisson model in a study of antimicrobial use and in broiler chickens, Canada, 2013–2019*

Variable	Incidence rate ratio	2.50% CI	97.50% CI	p value
Intercept	0.277081	0.1054967	0.7277371	0.00919†
Production system (referent comparison factor: conventional)				
Antimicrobial-free‡	0.60892	0.2994255	1.2383169	0.17076
Ideal disinfection method (referent comparison factor: no use of ideal method)				
Use of ideal disinfection	1.3043882	0.7766548	2.190714	0.31513
Continuous variable of antimicrobial use (mg/kg)				
Injections (in ovo or subcutaneous§)	1.7448076	0.1650191	18.4484971	0.64363
Through feed	0.9979396	0.9923108	1.0036003	0.4748
Through water	0.996652	0.9806929	1.0128707	0.68386
Sample collection year (referent comparison year: 2013)				
2014	0.7218903	0.3138241	1.6605658	0.44323
2015	1.7590844	0.8024374	3.8562237	0.15843
2016	0.3714697	0.1493034	0.9242233	0.03322†
2017	0.8334422	0.3732234	1.8611531	0.65669
2018	0.5029853	0.2104181	1.2023406	0.12221
2019	0.6468213	0.2868202	1.4586765	0.29368
Province (referent comparison province: Alberta)				
British Columbia	1.6638783	0.9144055	3.0276404	0.09551
Ontario	1.5284206	0.7983312	2.9261911	0.20045
Québec	2.0744067	0.9336274	4.6090798	0.07323
Saskatchewan	1.8708334	0.5308387	6.5933731	0.32975

*nC, number of antimicrobial classes to which each isolate was resistant.
†Statistically significant (p<0.05).
‡Antimicrobial-free flocks were not exposed to medically important antimicrobials through any route of administration.
§Subcutaneous route in young chicks at the hatchery.

We compared the model fit between models by using the Akaike information criteria and the likelihood ratio test. We performed post hoc pairwise testing of mean flock differences in nC among groups of disinfection method, use of antimicrobials at the hatcheries, year, and province by using Tukey's multiple comparison test.

We quantified the trends of antimicrobial use (Appendix Figures 2–4 for *Salmonella*, 8–10 for *E. coli*, and 14–16 for *Campylobacter*), and the association between resistance for individual antimicrobial classes (Appendix Figures 5–7 for *Salmonella*, 11–13 for *E. coli*, and 17–19 for *Campylobacter*) by using mixed-effect logistic regression models for each bacterial species. We conducted all statistical analysis in RStudio 1.2.5033 (https://www.rstudio.com) and defined statistical significance as p<0.05.

Results

Temporal Differences, Regional Differences, and Factors Associated with AMR

For *Salmonella*, the nC an isolate was resistant to in 2018 was 0.9 times lower than the nC an isolate was resistant to in 2013 (p<0.001); however, the nC an isolate was resistant to in 2019 was 1.6 times higher than in 2013 (p = 0.045), given that other variables were held constant in the model. In individual provinces, compared with the value for Alberta, the nC an isolate was resistant to was 1.7 times higher in British

Columbia (p = 0.007), 1.8 times higher in Ontario (p = 0.002), 3.8 times higher in Québec (p<0.001), and 1.9 times higher in Saskatchewan (p = 0.009). For every 1-unit increase in antimicrobial injected in ovo (mg/kg) in the hatcheries, the national nC an isolate was resistant to increased by 3.4 (p = 0.02). Posthoc (Tukey test) showed that Ontario (p = 0.015) and Québec (p<0.001) had a significantly higher mean nC that an isolate was resistant to compared with Alberta; Québec also had a significantly higher mean nC that an isolate was resistant to than British Columbia and Ontario across all years (p<0.001 for both provinces) (Table 1). The antibiotic-free flocks (n = 286) were not different from conventional flocks (n = 1,612) in the nC an isolate was resistant to (Table 1). However, prevalence of *Salmonella* Heidelberg was statistically significantly higher at conventional farms (Appendix Figure 1). Using the ideal method of disinfection, which that entails dry and wet cleaning followed by the application of a disinfectant, was not a significant factor in the nC a *Salmonella* isolate was resistant to. However, significantly higher prevalence of *Salmonella* Heidelberg and Kentucky (Appendix Figure 1) was found in flocks that did not use the ideal method of disinfection.

For *E. coli*, nationally, during 2018 and 2019, the nC an isolate was resistant to was 0.9 (in 2018, p = 0.015) and 0.8 (in 2019, p<0.001) times lower than the nC an isolate was resistant to in 2013 after controlling for other variables (Table 2). The nC an isolate was

Figure 1. Change in mean proportion of antimicrobial resistance *in Salmonella* (A), *Escherichia coli* (B), and *Campylobacter* (C) in broiler chickens, overall and by drug class, Canada, 2013–2019. Arrows represent directionality of proportion change in resistance from 2013 (gray) to 2019 (red) for each of the antimicrobial classes. Differences in proportion resistance from 2013 to 2019 are presented on the right side of each graph. Asterisks indicate p<0.05 as determined by mixed-effects logistic regression, including year and antimicrobial use (in ovo or through subcutaneous injection, water, and feed) as fixed effects and flock and veterinarian identification as random effects. AMC, amoxicillin/clavulanic acid; AMP, ampicillin; AZM, azithromycin; CHL, chloramphenicol; CIP, ciprofloxacin; CLI, clindamycin; CRO, ceftriaxone; ERY, erythromycin; FLR, florfenicol; FOX, cefoxitin; GEN, gentamycin; NAL, nalidixic acid; SSS, sulfisoxazole; STR, streptomycin; TET, tetracycline; TMS, trimethropim/sulfonamides.

resistant to was 1.2 times higher in British Columbia (p = 0.032) and 1.4 times higher in Québec (p<0.001) than the nC an isolate was resistant to in Alberta; in Saskatchewan, the nC an isolate was resistant to was 0.5 times lower than in Alberta (p<0.001). Posthoc (Tukey test) examination demonstrated that the provinces of British Columbia, Ontario, Québec, and Saskatchewan had a significantly higher mean nC an isolate was resistant to compared with Alberta; Québec also had a significantly higher mean nC an isolate was resistant to than the means for British Columbia and Ontario. In 2019, we observed a significantly lower nC an isolate was resistant to than in 2013 (p = 0.002), 2014 (p = 0.002), 2015 (p = 0.012), and 2016 (p = 0.014) (Table 2). The antibiotic-free status of the flock and ideal method of disinfection were not significant factors in the nC to which an *E. coli* isolate was resistant.

For *Campylobacter*, in 2016, the nC to which an isolate was resistant was 0.4 times lower than the nC for 2013, given that other variables were held constant in the model (p = 0.03). Posthoc (Tukey test) comparison shows that 2016 (p = 0.008) and 2018 (p = 0.037) had a significantly lower mean nC

to which an isolate was resistant than the value for 2015 (Table 3). The antibiotic-free status of the flock and ideal method of disinfection were not significant factors in the nC to which a *Campylobacter* isolate was resistant.

Prevalence of Resistance by Antimicrobial Drug

Prevalence of resistance remained <15% (Appendix Table 1) for 10 of 13 tested antimicrobials for *Salmonella* isolates (n = 1,898), 7 of 13 tested antimicrobials for *E. coli* isolates (n = 3,671), and 5 of 8 tested antimicrobials for *Campylobacter* isolates (n = 769). The prevalence of *Salmonella* isolates resistant to tetracycline was 44.7% (95% CI 42.5%–46.9%) and to streptomycin was 43.6% (95% CI 41.3%–45.8%) (Appendix Table 1). Moreover, prevalence of *E.coli* isolates resistant to tetracycline was 46.8% (95% CI 45.2%–48.4%), to streptomycin was 46.3% (95% CI 44.7%–47.9%), to sulfisoxazole was 39.4% (95% CI 37.8%–41.0%), to ampicillin was 40.5% (95% CI 38.9%–42.1%), to gentamicin was 18.4% (95% CI 17.2%–19.7%), and to trimethoprim/sulfamethoxazole was 16.1% (95% CI 14.9%–17.3%) (Appendix Table 1). The prevalence of *Campylobacter* isolates resistant to tetracycline was 38.8% (95% CI

35.3%–42.2%), to ciprofloxacin was 16.5% (95% CI 13.9%–19.1%), and to nalidixic acid was 16.4% (95% CI 13.8%–19.0%) (Appendix Table 1).

Temporal Trend of AMR by Antimicrobial Class

For *Salmonella*, we observed a significant decrease in the mean resistance rates across all antimicrobial drugs included in the panel (1.8%), as well as individually to to cefoxitin (11.8%), amoxicillin/clavulanic acid (15.3%), ceftriaxone (15.3%), and ampicillin (15.9%) during 2013–2019. However, AMR rose significantly in streptomycin (18.8%) and tetracycline (19.7%) during the same period (Figures 1, 2). For *E. coli*, we observed a significant decrease in resistance overall (11.7%), as well as individually to tetracycline (11.4%), cefoxitin (25.4%), amoxicillin/clavulanic acid (25.7%), ceftriaxone (24.5%), and ampicillin (29.9%), whereas resistance to gentamicin (3.8%) and nalidixic acid (3.6%) increased (Figures 1, 2). For *Campylobacter*, we observed a significant decrease in overall (3.7%) resistance and to tetracycline (37.6%), but we observed a significant increase in nalidixic acid resistance (2.8%) (Figures 1, 2).

Temporal Trend of Antimicrobial Use by Class

In flocks where *Salmonella* was isolated, we observed a significant decrease in overall AMU, use of lincosamide-aminocyclitol combinations, and use of third-generation cephalosporins through injection (in ovo or subcutaneous routes) during 2013–2019 (Figures

3, 4; Appendix Figures 3, 4). For feed, we observed a statistically significant decrease in the use of macrolides, penicillins, streptogramins, but we observed a significant increase in the use of orthosomycins (Figures 3, 4; Appendix Figure 4). In flocks where *E. coli* was isolated, we observed a significant decrease in injectable antimicrobials during 2013–2019 (Figures 3, 4; Appendix Figure 8). We observed a decrease in the use of penicillins and streptogramins and an increase in the use of bacitracins and orthosomycins through feed over time (Figures 3, 4; Appendix Figure 10). In flocks where *Campylobacter* was isolated, we observed a significant decrease in overall injectable antimicrobials during 2013–2019 (Figures 3, 4;, Appendix Figure 14). For feed, we observed a decrease in the use of macrolides, penicillins, streptogramins, and a significant increase in the use of bacitracins and orthosomycins (Figures 3, 4; Appendix Figure 16).

Antimicrobial Use and AMR Analysis by Antimicrobial Class

Flocks from which multidrug-resistant (MDR) *Salmonella* was isolated (n = 79 of 604 total flocks) had significantly higher median overall AMU compared with flocks where no MDR *Salmonella* was identified. Specifically, MDR flocks had significantly higher use of injectable lincosamide-aminocyclitol combinations (Figure 5; Appendix Figure 5), penicillins through water (Figure 5; Appendix Figure 6), and
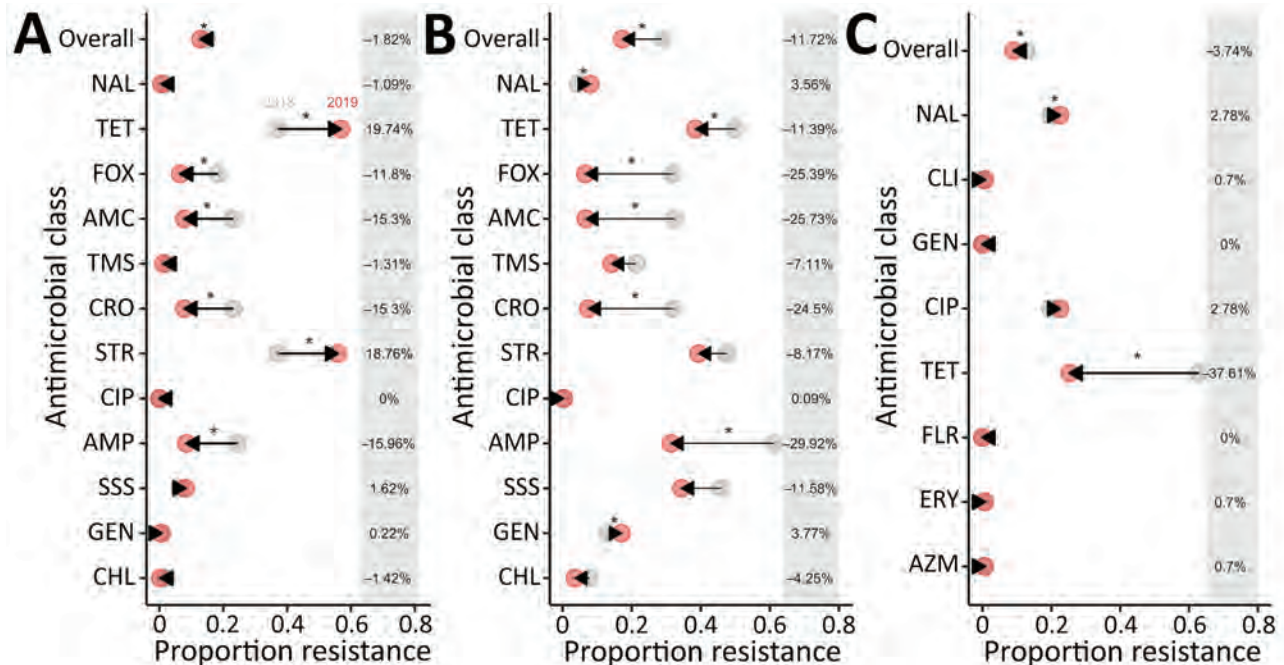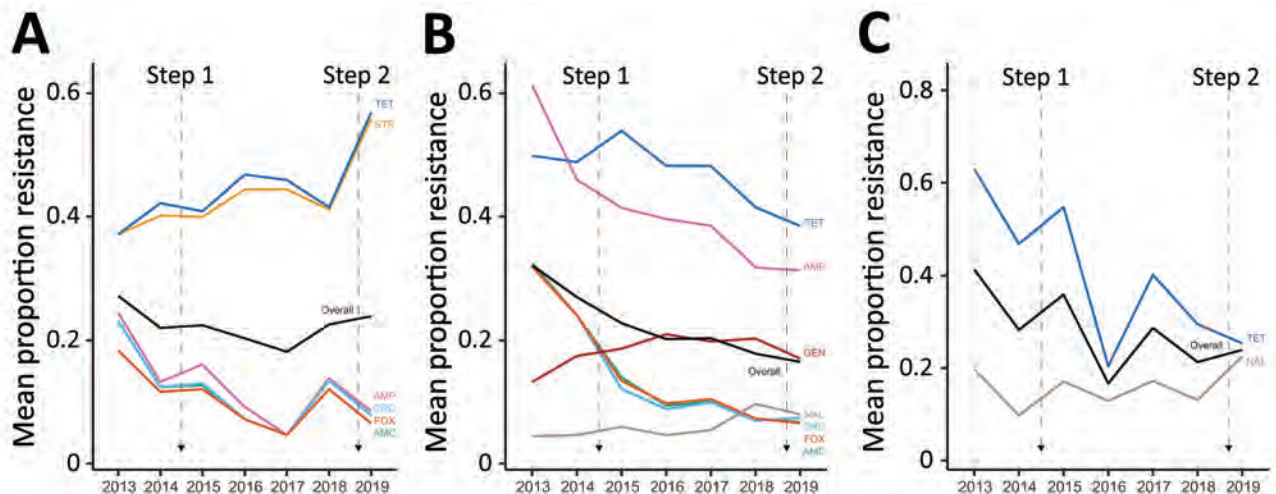

Figure 2. Significant changes (p<0.05) in mean proportion of antimicrobial resistance in *Salmonella* (A), *Escherichia coli* (B), and *Campylobacter* (C) in in broiler chickens, by antimicrobial class, Canada, 2013–2019. Step 1 is the elimination of the preventive use of category I antimicrobials in May 2014 (third-generation cephalosporins and fluoroquinolones) as part of Antimicrobial Use Reduction Strategy stewardship program. Step 2 is the elimination of the preventive use of category II antimicrobials in the end of 2018 (aminoglycosides, lincosamides, macrolides, penicillin, quinolones, streptomycin, and trimethoprim/sulfonamide combinations). Step 3, which was the elimination of the preventive use of category III antimicrobials (e.g., bacitracins and tetracyclines) by the end of 2020, is not represented in the figure. AMC, amoxicillin/clavulanic acid; AMP, ampicillin; CRO, ceftriaxone; FOX, cefoxitin; GEN, gentamycin; NAL, nalidixic acid; STR, streptomycin; TET, tetracycline.
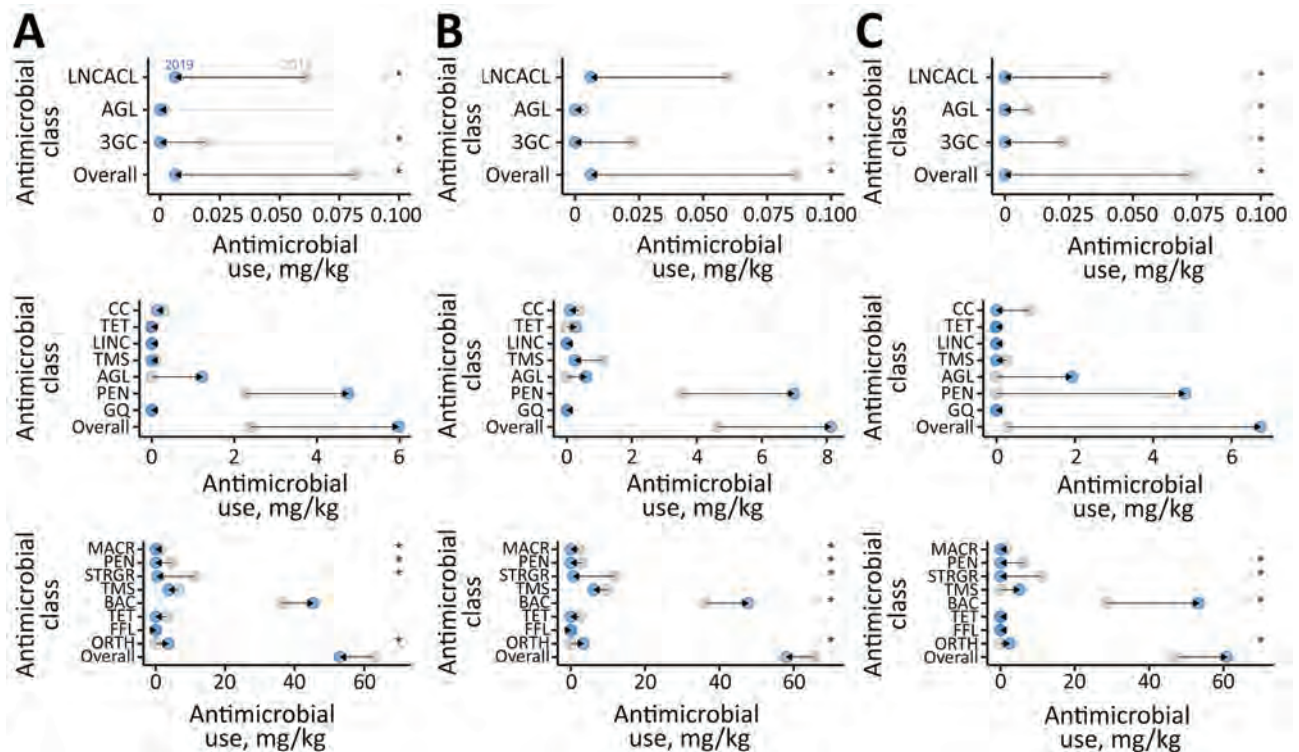
Figure 3. Mean antimicrobial use among broiler chicken flocks by bacterial species and route of administration, Canada, 2013–2019. A) *Salmonella*; B) *Escherichia coli*; C) *Campylobacter*. Route of administration in each panel: top, in ovo or subcutaneous injections; middle, water; bottom, feed. Arrows represent directionality of the antimicrobial use change from 2013 (gray) to 2019 (blue) of each antimicrobial class. Asterisks indicate p<0.05 as determined by a generalized mixed-effects model, including year as fixed effects and flock and veterinarian identification as random effects. AGL, aminoglycoside; BAC, bacitracin; CC, chemical coccidiostats; FFL, flavophospholipid; FQ, fluoroquinolone; LINC, lincomycin; LNCACL, lincosamides; MACR, macrolide; ORTH, orthomycin; PEN, penicillin; STRGR, streptogramin; TET, tetracycline; TMS, trimethropim/sulfonamides; 3GC, third-generation cephalosporin.

penicillins and tetracyclines through feed (Figure 5; Appendix Figure 7). Flocks from which MDR *E. coli* was isolated (n = 444/928) also had significantly higher median overall AMU. Most important, these flocks had significantly higher use of lincosamide-aminocyclitol combinations in ovo or subcutaneously at the hatcheries (Figure 5; Appendix Figure 11); tetracyclines, aminoglycosides, and penicillins through water (Figure 5; Appendix Figure 12); and penicillins, trimethoprim/sulfonamide combinations, bacitracins, and tetracyclines through feed (Figure 5; Appendix Figure 13). Flocks from which MDR *Campylobacter* was isolated (n = 30/218) also had significantly higher median overall AMU. Specifically, these flocks had significantly higher use of injectable lincosamides (Figure 5; Appendix Figure 17); used significantly more aminoglycosides and penicillins through water (Figure 5; Appendix Figure 18); and used significantly more macrolides, penicillins, streptogramins, trimethoprim/sulfonamide combinations, and bacitracins through feed (Figure 5; Appendix Figure 19).

Discussion

Our study examined AMU trends in broiler chicken production in Canada along with AMR trends in important foodborne bacteria. A reduction in both AMR and AMU was observed across most antimicrobials and classes during 2013–2019. The temporal reduction in AMU reflected the implementation of the Chicken Farmers of Canada's AMU Reduction Initiative. This AMU stewardship program involved the elimination of the preventive use of certain antimicrobial classes in a stepwise manner (*13*). Results from this work indicate that a decrease in AMU contributed to a decrease in AMR over time for some antimicrobial drugs; however, increased AMR to streptomycin and tetracycline in *Salmonella* isolates, an increase in AMR to gentamicin and nalidixic acid in *E. coli* isolates, and an increase in AMR to nalidixic acid in *Campylobacter* were observed. We detected an increase in the use of aminoglycosides through water over time, which possibly contributed to the rise in *Salmonella* and *E. coli* aminoglycoside resistance. Historically, the administration of antimicrobials

through water was largely for treatment of diseases such as those associated with avian pathogenic *E. coli* (*14*). Thus, this finding suggests that in addition to the elimination of hatchery-level use, reduced preventive AMU through feed potentially resulted in increased frequency of infectious diseases, thereby increasing the need for AMU through water for disease treatment.

The overall rise the number of classes *Salmonella* isolates were resistant to in 2019 should also be put in perspective with the serotypes identified on farms. The mean proportion of *Salmonella* Kentucky relative to total *Salmonella* isolates increased in 2019 (Appendix Figure 20). Previous work has shown that *Salmonella* Kentucky frequently carries genes conferring resistance to tetracyclines and aminoglycosides (*23*). Therefore, the temporal trends in resistance to these antimicrobial classes could reflect the shift in *S. enterica* serotypes (*24*). Trends in *Salmonella* serotypes and AMR prevalence in poultry in Canada were studied recently (*25*), showing, similar to our results, that different *Salmonella* serotypes carry different resistance profiles that influence the overall prevalence of resistance. In Canada, passive surveillance in poultry frequently detects *Salmonella* Kentucky (*14*). This serotype is 1 of the etiologic

agents of enteric disease and high rates of illness in broiler chickens in Egypt (*26*); however, in Canada, although this serovar was the second-most frequently isolated serovar from passive surveillance, its clinical importance has not yet been determined (*14*). Further studies should estimate whether reduced prophylactic AMU affects serotype diversity and assess whether the *Salmonella* Kentucky lineages circulating in poultry in Canada have clinical impact in broilers. In *Salmonella*-positive flocks, >1 serovar was isolated from a single flock. The serovar isolated from a single sample is generally supposed to represent the most predominant serovar. To reduce potential underestimation of serovar diversity within a flock, CIPARS/FoodNet Canada routinely cultures each sample (4 total).

The study shows that the injection of antimicrobials in ovo or subcutaneously at hatcheries is significantly associated with resistance in foodborne bacteria on the farm. The progressive elimination of AMU administered through injection (ceftiofur in 2014 then gentamicin and lincomycin/spectinomycin at the end of 2018) might have largely contributed to the observed decrease in AMR. In Canada, the injection in ovo or subcutaneously at the hatcheries with ceftiofur was aimed at the prevention of omphalitis caused
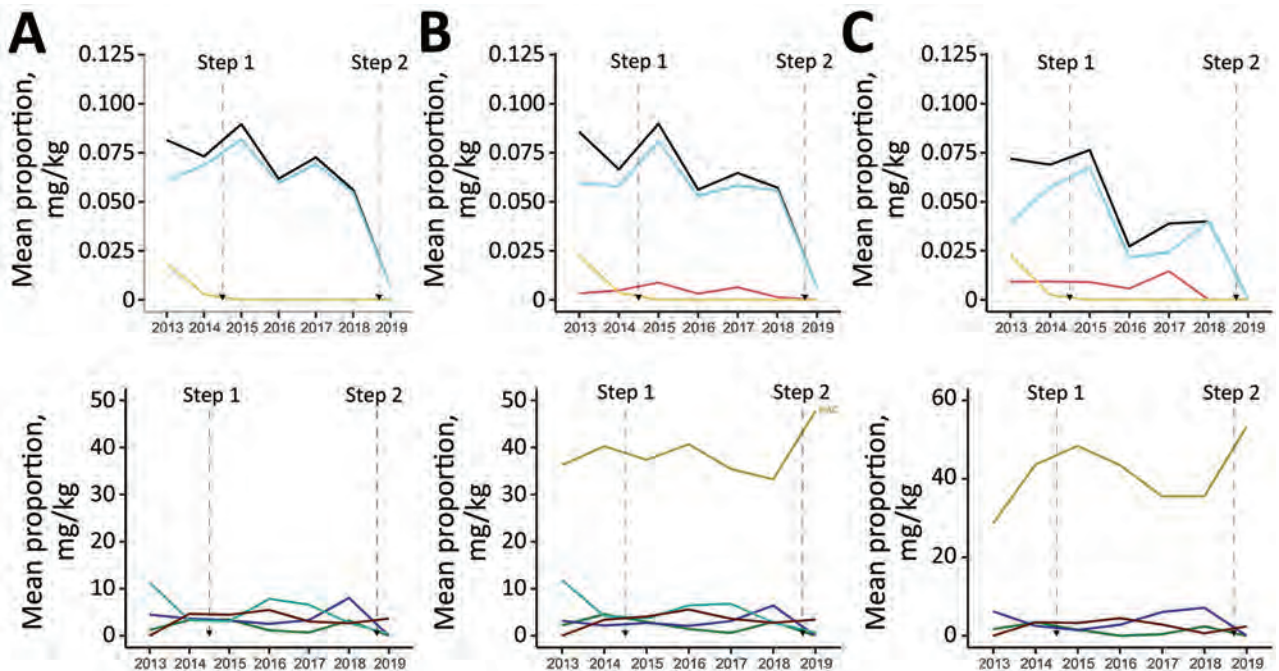
Figure 4. Mean antimicrobial use administered in ovo or subcutaneously at broiler chicken hatcheries or through feed, by isolation of bacterial species, Canada, 2013–2019. A) *Salmonella*; B) *Escherichia coli*; C) *Campylobacter*. Route of administration in each panel: top, in ovo or subcutaneous injections; bottom, feed. Mean antimicrobial use is color coded: lincosamides, in light blue; overall, in black; third-generation cephalosporins, in yellow; orthosomycins, in brown; penicillins, in purple; streptomycin, in cyan; and macrolides, in green. Antimicrobials are represented only if significantly (p<0.05) changing over time. The antimicrobial use trend through water is not represented because no statistically significant differences were found.
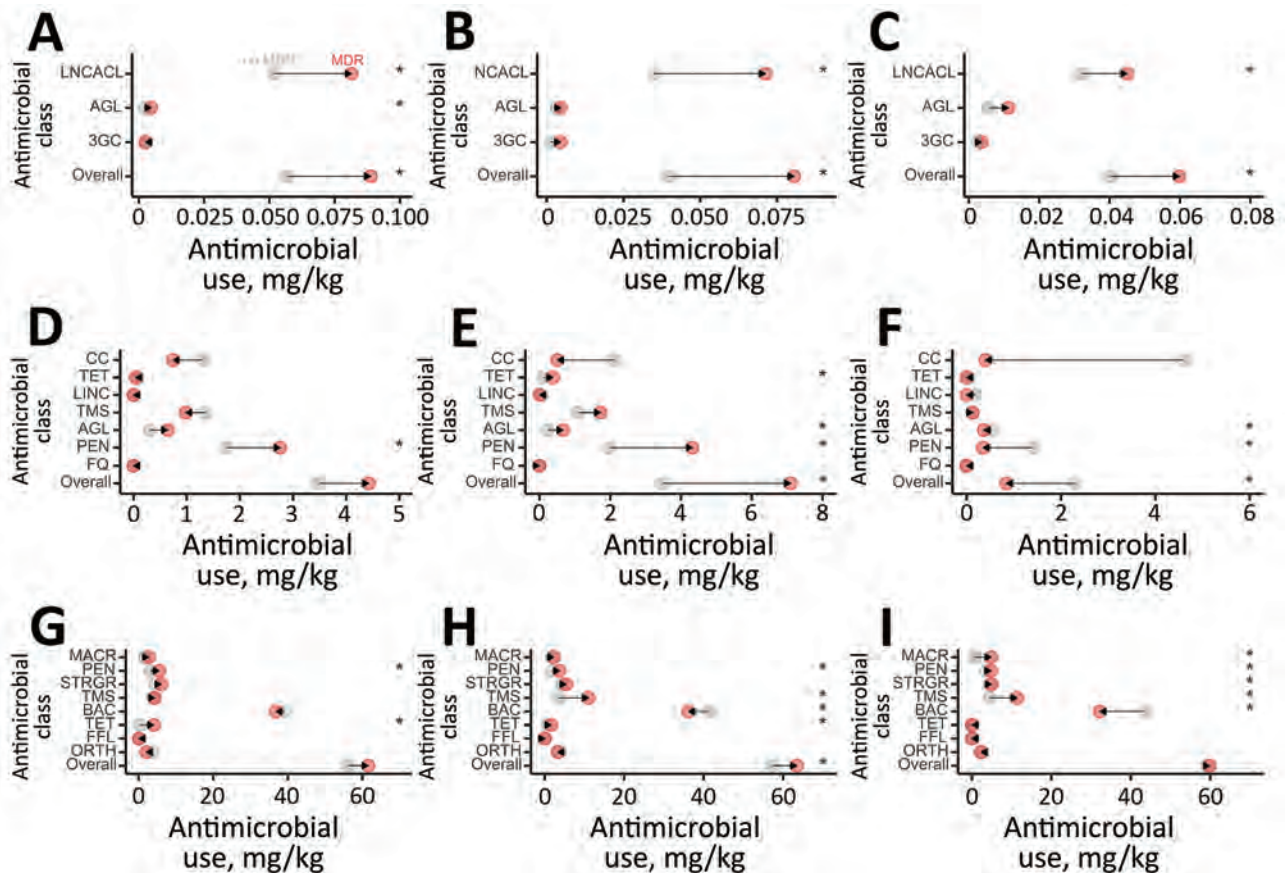
Figure 5. Mean antimicrobial use through injection, water, and feed in broiler chicken flocks where *Salmonella*, *Escherichia coli*, and *Campylobacter* were isolated, Canada, 2013–2019. A) *Salmonella*; B) *Escherichia coli*; C) *Campylobacter.* Route of administration in each panel: top, in ovo or subcutaneous injections; middle, water; bottom, feed. Arrows represent directionality from no multidrug resistance (MDR; gray) to MDR (red). Asterisks (*) indicates p<0.05, obtained from mixed effects logistic regression including antimicrobial use as fixed effect and flock and veterinarian identification as random effects. AGL, aminoglycoside; BAC, bacitracin; CC, chemical coccidiostats; FFL, flavophospholipid; FQ, fluoroquinolone; LINC, lincomycin; LNCACL, lincosamides; MACR, macrolide; ORTH, orthomycin; PEN, penicillin; STRGR, streptogramin; TET, tetracycline; TMS, trimethropim-sulfonamides; 3GC, third-generation cephalosporin.

by *E. coli*. Since 2005, and after the partial voluntary restriction of its use, a decline in the prevalence of third-generation cephalosporin-resistant *Salmonella* Heidelberg isolates in retail chicken was observed (*8*). Moreover, a reduction of AmpC-associated resistance genes was observed in *E. coli* after the elimination of preventive use in 2014, the second cessation of use nationally (*27,28*). We found a decrease not only of cephalosporin resistance (ceftriaxone and cefoxitin) but also ampicillin resistance in *Salmonella* and *E. coli* during 2013–2019. Therefore, decreased use of ceftiofur may have led to a concomitant decrease in resistance to ampicillin.

We did not identify resistance rate differences between antimicrobial-free and conventional farms. Some studies have shown that antimicrobial-free farms have significantly lower resistance rates for

Salmonella (*29*) and *Campylobacter* (*30*) compared with conventional farms, whereas other studies do not report such differences (*7,31*). In our study, although AMR did not differ according to production system, we observed a significantly higher prevalence of *Salmonella* Heidelberg on conventional farms (Appendix Figure 1). Similarly, we observed a small to no effect of using the ideal method for cleaning and disinfection (*19*) on AMR. However, significantly higher prevalence of *Salmonella* Heidelberg and Kentucky (Appendix Figure 1) were found in flocks that did not use the ideal method of disinfection. This finding raises awareness of the larger impact of AMU even when hygiene methods are ideal, but more important, the shift in serotype composition might have affected AMR rate. For example, *Salmonella* Kentucky and Heidelberg have

the highest frequencies of resistance to ciprofloxacin (32) and to cephalosporins (33). The differences in the number of antimicrobial-free (n = 286) and conventional (n = 1,612) farms included in this study may have affected the ability to detect significant differences in AMR levels between farm categories. As more producers transition to alternate production systems, drivers for AMR other than AMU could be further investigated.

In our study, an overall reduction in resistance levels in indicator and zoonotic foodborne bacteria of broiler chicken origin was successfully achieved in response to changes in AMU practices in broiler chickens in Canada during 2013–2019. Resistance to certain antimicrobial classes have emerged or increased; the increases may be associated with use of aminoglycosides through water for disease treatment, the shift in prevalence of different *Salmonella* serotypes over time, or both. Farms that use the ideal method of disinfection and farms classified as antimicrobial free had lower prevalence of *Salmonella* serotypes of higher public health importance, indicating that implementation of sanitation best practices and reduced AMU programs are beneficial. As evidenced by the AMR results, the removal of AMU exposures during the early stages of an animal's life could further reduce AMR. Additional work should address the effect of reduction of AMU on production costs; relevant production indicators including bird morbidity, mortality, and feed-conversion rates; and bird welfare in broiler chicken farms in Canada. The emerging practices on the use of alternatives to antimicrobials (e.g., vaccines against *E. coli*, *Salmonella*, and gut health enhancers) also warrant further investigation. This additional information will provide future guidance for the progressive transition from the current AMU-dependent production systems to alternative and sustainable measures to promote animal health and productivity.

Acknowledgments

About the Author

Dr. Huber is an assistant professor in the Department of Pathobiology, Auburn University. She currently researches the impact of antimicrobial use in animal production and on antimicrobial resistance rates. Her main research interests include using a molecular epidemiologic approach to the spread of antimicrobial resistance between animal, humans, and the environment.

References

1. Government of Canada. Yearly food-borne illness for Canada. 2016 [cited 2020 Jul 1]. https://www.canada.ca/en/public-health/services/food-borne-illness-canada/yearly-food-borne-illness-estimates-canada.html
2. Bagust T. Food and Agriculture Organization of the United Nations: poultry development review. Poultry health and disease control in developing countries. 2013 [cited 2020 Jul 1]. http://www.fao.org/3/al729e/al729e.pdf
3. Page SW, Gautier P. Use of antimicrobial agents in livestock. Rev Sci Tech. 2012;31:145–88. https://doi.org/10.20506/rst.31.1.2106
4. Butaye P, Devriese LA, Haesebrouck F. Antimicrobial growth promoters used in animal feed: effects of less well known antibiotics on gram-positive bacteria. Clin Microbiol Rev. 2003;16:175–88. https://doi.org/10.1128/CMR.16.2.175-188.2003
5. Dunne EF, Fey PD, Kludt P, Reporter R, Mostashari F, Shillam P, et al. Emergence of domestically acquired ceftriaxone-resistant Salmonella infections associated with AmpC beta-lactamase. JAMA. 2000;284:3151–6. https://doi.org/10.1001/jama.284.24.3151
6. Chang Q, Wang W, Regev-Yochay G, Lipsitch M, Hanage WP. Antibiotics in agriculture and the risk to human health: how worried should we be? Evol Appl. 2015;8:240–7. https://doi.org/10.1111/eva.12185
7. Lestari SI, Han F, Wang F, Ge B. Prevalence and antimicrobial resistance of *Salmonella* serovars in conventional and organic chickens from Louisiana retail stores. J Food Prot. 2009;72:1165–72. https://doi.org/10.4315/0362-028X-72.6.1165
8. Dutil L, Irwin R, Finley R, Ng LK, Avery B, Boerlin P, et al. Ceftiofur resistance in *Salmonella enterica* serovar Heidelberg from chicken meat and humans, Canada. Emerg Infect Dis. 2010;16:48–54. https://doi.org/10.3201/eid1601.090729
9. World Health Organization. WHO list of critically important antimicrobials for human medicine. 2018 [cited 2020 Jul 4]. https://apps.who.int/iris/bitstream/handle/10665/325036/WHO-NMH-FOS-FZD-19.1-eng.pdf
10. Avery BP, Parmley EJ, Reid-Smith RJ, Daignault D, Finley RL, Irwin RJ. Canadian integrated program for antimicrobial resistance surveillance: Retail food highlights, 2003–2012. Can Commun Dis Rep. 2014;40(Suppl 2):29–35. https://doi.org/10.14745/ccdr.v40is2a05
11. Government of Canada. Canadian Integrated Program for Antimicrobial Resistance Surveillance annual report. 2003 [cited 2020 Jul 4]. https://publications.gc.ca/collections/Collection/H39-1-3-2003E.pdf
12. Government of Canada. Categorization of antimicrobial drugs based on importance in human medicine. 2009 [cited 2020 Jul 4]. https://www.canada.ca/en/health-canada/services/drugs-health-products/veterinary-drugs/antimicrobial-resistance/categorization-antimicrobial-drugs-based-importance-human-medicine.html

13. Chicken Farmers of Canada. Canadian chicken industry reduces antimicrobial use. 2018 [cited 2020 Jul 8]. https://www.chickenfarmers.ca/wp-content/uploads/2018/10/AMU-Magazine-insides_ENG-Issue2.pdf

14. Government of Canada. Canadian Integrated Program for Antimicrobial Resistance Surveillance annual report. 2018 [cited 2020 July 1]. https://www.canada.ca/en/public-health/services/surveillance/canadian-integrated-program-antimicrobial-resistance-surveillance-cipars/cipars-reports/2018-annual-report-executive-summary.html

15. Dahoo I, Martin W, Stryhn H. Veterinary epidemiologic research. 2nd edition. Charlottetown (CA, USA): VER Inc.; 2014.

16. Agunos A, Gow SP, Léger DF, Deckert AE, Carson CA, Bosman AL, et al. Antimicrobial use indices—the value of reporting antimicrobial use in multiple ways using data from Canadian broiler chicken and turkey farms. Front Vet Sci. 2020;7:567872. https://doi.org/10.3389/fvets.2020.567872

17. Clinical and Laboratory Standards Institute. Performance standards for antimicrobial susceptibility testing (supplement M100). 2019 [cited 2020 Jul 1]. https://clsi.org/media/1930/m100ed28_sample.pdf

18. Clinical and Laboratory Standards Institute. Methods for antimicrobial dilution and disk susceptibility testing of infrequent isolated or fastidious bacteria (supplement M45). 2015 [cited 2020 Jul 1]. https://goums.ac.ir/files/deputy_treat/md_labs_ef39a/files/CLSI-M45ed3e-2018(1).pdf

19. Meroz M, Samberg Y. Disinfecting poultry production premises. Rev Sci Tech. 1995;14:273–91. https://doi.org/10.20506/rst.14.2.839

20. Government of Canada. List A: list of certain antimicrobial active pharmaceutical ingredients. 2013 [cited 2020 Jul 1]. https://www.canada.ca/en/public-health/services/antibiotic-antimicrobial-resistance/animals/veterinary-antimicrobial-sales-reporting/list-a.html

21. Government of Canada. Method of production claims for meat, poultry and fish products. 2019 [cited 2020 Aug 21]. https://www.inspection.gc.ca/food-label-requirements/labelling/industry/method-of-production-claims-on-food-labels/eng/1389379565794/1389380926083?chap=8#s5c8

22. World Organisation for Animal Health. OIE annual report on antimicrobial agents intended for use in animals. Better understanding of the global situation. 2020 [cited 2020 Aug 21]. https://www.oie.int/fileadmin/Home/eng/Our_scientific_expertise/docs/pdf/AMR/A_Fourth_Annual_Report_AMR.pdf

23. Hawkey J, Le Hello S, Doublet B, Granier SA, Hendriksen RS, Fricke WF, et al. Global phylogenomics of multidrug-resistant *Salmonella enterica* serotype Kentucky ST198. Microb Genom. 2019;5:e000269. https://doi.org/10.1099/mgen.0.000269

24. Agunos A, Arsenault RK, Avery BP, Deckert AE, Gow SP, Janecko N, et al. Changes in antimicrobial resistance levels among *Escherichia coli*, *Salmonella*, and *Campylobacter* in Ontario broiler chickens between 2003 and 2015. Can J Vet Res. 2018;82:163–77.

25. Caffrey N, Agunos A, Gow S, Liljebjelke K, Mainali C, Checkley SL. *Salmonella* spp. prevalence and antimicrobial resistance in broiler chicken and turkey flocks in Canada from 2013 to 2018. Zoonoses Public Health. 2021;zph.12769; Epub ahead of print. https://doi.org/10.1111/zph.12769

26. Sorour HK, Gaber AF, Hosny RA. Evaluation of the efficiency of using *Salmonella* Kentucky and *Escherichia coli* O119 bacteriophages in the treatment and prevention of salmonellosis and colibacillosis in broiler chickens. Lett Appl Microbiol. 2020;71:345–50. https://doi.org/10.1111/lam.13347

27. Caffrey N, Nekouei O, Gow S, Agunos A, Checkley S. Risk factors associated with the A2C resistance pattern among *E. coli* isolates from broiler flocks in Canada. Prev Vet Med. 2017;148:115–20. https://doi.org/10.1016/j.prevetmed.2017.11.001

28. Chalmers G, Cormier AC, Nadeau M, Côté G, Reid-Smith RJ, Boerlin P. Determinants of virulence and of resistance to ceftiofur, gentamicin, and spectinomycin in clinical *Escherichia coli* from broiler chickens in Québec, Canada. Vet Microbiol. 2017;203:149–57. https://doi.org/10.1016/j.vetmic.2017.02.005

29. Kassem II, Kehinde O, Kumar A, Rajashekara G. Antimicrobial-resistant *Campylobacter* in organically and conventionally raised layer chickens. Foodborne Pathog Dis. 2017;14:29–34. https://doi.org/10.1089/fpd.2016.2161

30. Noormohamed A, Fakhr MK. Prevalence and antimicrobial susceptibility of *Campylobacter* spp. in Oklahoma conventional and organic retail poultry. Open Microbiol J. 2014;8:130–7. https://doi.org/10.2174/1874285801408010130

31. Roberts T, McEwen S, Reid-Smith R, Sargeant J, Agunos A, Léger D, et al. Prevalence, risk factors and profiles of resistant *Salmonella* isolates obtained from Ontario broiler chicken farms at chick placement and pre-harvest [abstract]. In: Proceedings of the 64th Western Poultry Disease Conference; Sacramento, California, USA; 2015 Mar 22–25. p. 101 [cited 2020 Aug 21]. https://aaap.memberclicks.net/assets/WPDC/wpdc_2015.pdf

32. European Food Safety Authority. EU summary report on antimicrobial resistance in zoonotic and indicator bacteria from humans, animals and food in 2013. 2015 [cited 2020 Aug 21]. http://www.efsa.europa.eu/en/efsajournal/pub/4036

33. Center for Disease Control and Prevention, US Department of Agriculture, USFood and Drug Administration. The National Antimicrobial Resistance Monitoring System (NARMS): the 2012–2013 integrated NARMS report. 2015 [cited 2020 Aug 21]. https://www.fda.gov/media/92766/download

Address for correspondence: Laura Huber, Greene Hall, 1130 Wire Rd, Office 271, Auburn University, Auburn, AL 36832, USA; email: lzh0067@auburn.edu

A Community-Adapted Approach to SARS-CoV-2 Testing for Medically Underserved Populations, Rhode Island, USA

Matthew Murphy, Imshan Dhrolia, Alexandra Zanowick-Marr, Jun Tao, Cassie Sutten Coats, Siena Napoleon, Yelena Malyuta, Emily Adams, Trisha Arnold, Philip A. Chan, Amy Nunn

We developed a testing program for severe acute respiratory syndrome coronavirus 2 in an urban Latinx neighborhood in Providence, Rhode Island, USA. Approximately 11% of Latinx participants (n = 180) tested positive. Culturally tailored, community-based programs that reduce barriers to testing help identify persons at highest risk for coronavirus disease.

As of May 2021, severe acute respiratory syndrome coronavirus 2 (SARS-CoV-2) had infected >154 million globally and caused >3.2 million deaths (*1*). The United States accounts for ≈21% of coronavirus disease (COVID-19) cases and related deaths worldwide (*1*). Vaccines are a highly effective transmission prevention tool. However, SARS-CoV-2 testing, contact tracing, and quarantining are among the few effective prevention measures available to the public that are proven to reduce transmission in the setting of variable vaccine availability and uptake (*2*). The COVID-19 disease burden has disproportionately affected Black and Latinx populations in the United States (*3,4*). These health disparities in racial and ethnic minority populations are driven by complex social and structural factors, such as a paucity of health services, absence of culturally tailored services, and economic barriers that affect adherence to quarantine guidelines (*5,6*). These disparities have been further compounded by fragmented SARS-CoV-2 testing policies in the United States, which have not prioritized testing for medically underserved racial and ethnic minority communities (*2*).

Rhode Island experienced high rates of SARS-CoV-2 infection early in the pandemic and has been recognized for expanding testing early across the state (*5*). Policies in Rhode Island evolved in tandem with the pandemic and availability of testing supplies. In April 2020, faced with limited testing supplies and healthcare personnel, officials in Rhode Island restricted SARS-CoV-2 testing to prescheduled appointments for symptomatic persons with recent travel histories (*7,8*). By June, testing recommendations in Rhode Island had evolved to include populations considered at high risk for COVID-19, and the state has since maintained one of the highest per capita testing rates in the United States (*7,8*). However, most testing locations required appointments and were limited to symptomatic patients, and services were not offered in most urban communities, where infection rates were highest.

As seen elsewhere in the United States, the Latinx community in Rhode Island has been disproportionately affected by COVID-19 (*9*). The Latinx community constitutes just 14% of the population in Rhode Island; the most represented countries and territories are Mexico (35%), Cuba (29%), Spain (11.7%), and Puerto Rico (8.9%). However, the Latinx community accounts for 38% of positive SARS-CoV-2 tests and 33% of COVID-19–related hospitalizations in the state (*1,8*).

The Study

In June 2020, to respond to the unmet need for culturally tailored SARS-CoV-2 testing services, we opened a multilingual, community-based site for testing by PCR in Providence, Rhode Island (*7*). This program

was supported by the Rhode Island Department of Health. We partnered with a local community cultural center to develop a culturally tailored model for SARS-CoV-2 testing in urban neighborhoods with large numbers of Latinx residents and high rates of COVID-19 infection. The cultural center was a well-known space for community gatherings, artist performances, and religious services. The testing site was staffed by trained medical personnel including clinical providers and volunteers. We designed the testing model to accept all walk-ins; offer drive-

through and walk-up testing; provide onsite access to bilingual testing services in English, Spanish, and Portuguese (with additional language services provided by tele-interpretation); offer patients multiple modalities for accessing test results (in person, by telephone, postal mail, or online portal for patients with email addresses); provide testing regardless of insurance status, provider referral, in-state residency, or clinical manifestation; and forego out-of-pocket costs. We also worked with Latinx community leaders to promote our testing program on Latinx

Table 1. Demographic information for patients undergoing testing for severe acute respiratory syndrome coronavirus 2 at Rhode Island Public Health Institute testing site, Rhode Island, USA, June 8–August 8, 2020*

Characteristic	Total, n = 498	SARS-CoV-2–positive patients, n = 26 (5%)	SARS-CoV-2–negative patients, n = 472 (95%)
Median age (range), y	36.9 (7–91)	40.1 (7–91)	36.7 (11–77)
Age group, y			
0–14	13 (3)	1 (4)	12 (3)
15–34	262 (53)	11 (42)	251 (53)
35–64	184 (37)	11 (42)	173 (37)
>65	39 (8)	3 (12)	36 (8)
Race			
White	230 (49)	2 (9)	228 (51)
Other race	123 (26)	14 (61)	109 (24)
Black or African American	86 (18)	4 (17)	82 (18)
Asian	26 (6)	2 (9)	24 (5)
American Indian or Alaskan Native	4 (1)	1 (4)	3 (1)
Unknown or not reported	29 (6)	3 (12)	26 (6)
Ethnicity			
Not Hispanic or Latinx	303 (63)	5 (21)	298 (65)
Hispanic or Latinx	180 (37)	19 (79)	161 (35)
Unknown or not reported	15 (3)	2 (8)	13 (3)
Preferred language			
English	392 (79)	12 (48)	380 (81)
Spanish	102 (21)	12 (48)	90 (19)
Other language	2 (0)	1 (4)	1 (0)
Unknown or not reported	2 (0)	1 (4)	1 (0)
Sex assigned at birth			
F	304 (61)	9 (36)	295 (63)
M	193 (39)	16 (64)	177 (38)
Unknown or not reported	1 (0)	1 (4)	0
Gender identity (grouped)			
Woman	225 (52)	9 (41)	216 (53)
Man	155 (36)	13 (59)	142 (35)
Nonbinary, genderqueer, nonconforming, or agender	46 (11)	0	46 (11)
Not listed or other	5 (1)	0	5 (1)
Unknown or not reported	67 (13)	4 (15)	63 (13)
Sexual orientation			
Straight or heterosexual	260 (60)	20 (91)	240 (59)
Pansexual, queer, asexual, or bisexual	100 (23)	0	100 (24)
Lesbian, gay, or homosexual	57 (13)	1 (5)	56 (14)
Not listed or other	15 (3)	1 (5)	14 (3)
Unknown or not reported	66 (13)	4 (15)	62 (13)
Clinical manifestation			
Asymptomatic	369 (90)	14 (78)	355 (91)
Symptomatic	39 (10)	4 (22)	35 (9)
Unknown or not reported	90 (18)	8 (31)	82 (17)
Insurance package			
Commercial or group policy, e.g., HMO, PPO	307 (62)	10 (40)	297 (63)
No insurance	116 (23)	10 (40)	106 (23)
Medicaid or Medicare Part B	73 (15)	5 (20)	68 (14)
Unknown or not reported	2 (0)	1 (4)	1 (0)

*Values are no. (%) except as indicated. SARS-CoV-2, severe acute respiratory syndrome coronavirus 2.

Table 2. Association between specific sociodemographic characteristics and a positive PCR test result for severe acute respiratory syndrome coronavirus 2, Rhode Island, USA, June 8–August 8, 2020*

Variables	Crude odds ratio (95% CI)	Adjusted odds ratio (95% CI)
Age, y	1.01 (0.99–1.03)	NC
Race		
White	Referent	
Asian	9.5 (1.28–70.52)	NC
Black/African American	5.56 (1.00–30.93)	NC
Other Race	15.27 (3.43–67.92)	NC
Ethnicity		
Non-Hispanic	Referent	
Hispanic	7.03 (2.58–19.19)	NC
Gender		
Female	Referent	
Male	2.96 (1.28–6.84)	NC
Insurance status		
Insured		Referent
Uninsured	NC	1.46 (0.50–4.21)
Medicaid/Medicare Part B	NC	2.57 (0.75–8.75)
Sexual orientation		
Heterosexual		Referent
Same-sex	NC	0.61 (0.07–5.47)
Bisexual	NC	NC
Queer, asexual, or pansexual	NC	NC
Other	NC	0.69 (0.08–5.97)

*In an exploratory analysis, we treated demographics, insurance, and sexual orientations as exposures and identified models for each variable. Because no factors could affect the status of age, race, or ethnicity, we present crude odds ratios for these variables. For insurance and sexual orientation, we identified age, race, and ethnicity as confounding variables on the basis of a priori knowledge and present adjusted odds ratios. NC, not calculable.

radio, Facebook, and other social media; conducted outreach to sexual and gender minority communities on social media platforms; and partnered with established community resources (e.g., cultural centers, churches) to promote testing by word of mouth. All persons who underwent testing were required to provide their legal name and date of birth, proof of identity and address (e.g., state identification card, utility bill, bank statement, etc.), contact information (i.e., address, phone number), and insurance information if applicable. We did not collect information related to immigration or in-state residency status to avoid introducing perceived barriers to testing. A healthcare provider at our facility contacted every person who tested positive for SARS-CoV-2 as soon as results were available. Patients were then connected with available support services, such as food and housing resources. The Department of Health also contacted patients to support additional transmission prevention activities.

During June 8–August 8, 2020, a total of 498 persons in the community underwent testing at this site; 40% of the sample identified as Latinx. Approximately 5% of all persons (Table 1) and 11% of Latinx participants were SARS-CoV-2–positive, compared with a statewide positive rate of 2%–3% (*10*). Furthermore, although 40% of the sample self-identified as Latinx, Latinx persons constituted 80% of positive case-patients. Latinx persons had 7 times higher odds of testing positive (crude odds ratio [OR] 7.03, 95% CI 2.58–19.19) than did non-Latinx persons (Table 2).

Although we designed our program to respond to unmet needs for urban SARS-CoV-2 testing, it attracted persons from throughout the city of Providence and the state of Rhode Island (Figure 1). However, the greatest number of positive SARS-CoV-2 tests were from persons who lived in the surrounding ZIP codes (Figure 2), a geographic area experiencing high rates of community transmission.

Only 39% of all patients in this sample were men, but they represented 59% of all COVID-19 cases. Being male was associated with 2.96 times higher odds of testing positive (crude OR 2.96, 95% CI 1.28–6.84). Sexual minorities accounted for ≈40% of the sample, and gender minorities accounted for 12% of the sample. However, sexual and gender minorities had far lower rates of COVID-19 infection; 90% of persons who tested positive for SARS-CoV-2 were cisgender and heterosexual.

Conclusions

Our experience suggests that SARS-CoV-2 testing models that reduce barriers to care can successfully reach medically underserved communities that have high rates of COVID-19 infection. Culturally tailored approaches might be critical for identifying Latinx populations unaware of their SARS-CoV-2 infection (*10*). Not requiring health insurance or physician orders for testing, not charging
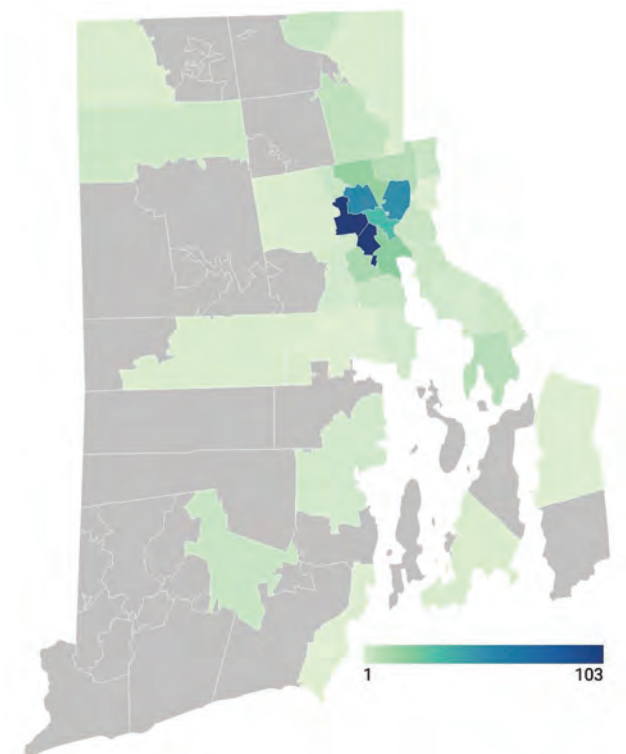
Figure 1. Geographic distribution of 498 persons tested for severe acute respiratory syndrome coronavirus 2 by Rhode Island Public Health Institute staff, Rhode Island, USA, June 8–August 8, 2020. Color scale indicates number of persons tested by ZIP code. Five patients had unknown ZIP codes and 16 were from out of state.
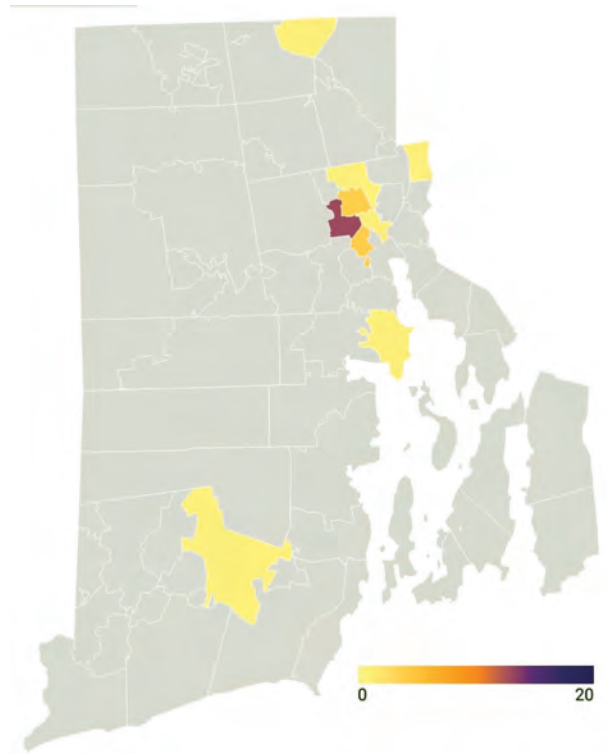
Figure 2. Geographic distribution of 28 persons receiving a positive test result for severe acute respiratory syndrome coronavirus 2 from testing performed by Rhode Island Public Health Institute staff during June 8–August 8, 2020. Color scale indicates number of persons testing positive by ZIP code. One patient had an unknown ZIP code.

payment, and offering walk-up and drive-through testing enabled widespread participation in our testing program. Offering multiple means of bilingual communication, including text, phone, email, traditional mail, and an online portal, also enabled communication with otherwise hard-to-reach patients. Although our findings are notable, they would be strengthened by an increased sample size to better characterize differences observed in the study population. Our outreach strategies were effective, but additional efforts in future initiatives could further improve testing outreach.

Our program provides a useful framework for reducing barriers to SARS-CoV-2 testing services in underserved communities, including sexual and gender minorities and Latinx populations who otherwise might not be tested for SARS-CoV-2. Perhaps the greatest challenge to replicating and sustaining this model is developing a viable funding model. Despite our program's success in enabling testing for persons at elevated risk for COVID-19, the human and financial resources needed to maintain this testing site design might limit its ability to be implemented in resource-

limited environments. The need for culturally tailored testing programs will continue even as vaccination programs are enacted across the country. Currently, reimbursement-based and traditional medical service delivery models often operate at a financial loss; greater public funding support is needed to sustain culturally tailored, low-barrier testing models that address ethnic and racial disparities in SARS-CoV-2 infection.

About the Author

Dr. Murphy is medical director of The Rhode Island Public Health Institute's Open Door Health Clinic (an LGBTQ+-focused primary care clinic in inner-city Providence), and an assistant professor of medicine at Brown University. His research focuses on linkage to community-based HIV prevention, including access to preexposure prophylaxis, for medically underserved populations.

References

1. Dong E, Du H, Gardner L. An interactive web-based dashboard to track COVID-19 in real time. Lancet Infect Dis. 2020;20:533–4. https://doi.org/10.1016/S1473-3099(20)30120-1
2. Robert A. Lessons from New Zealand's COVID-19 outbreak response. Lancet Public Health. 2020;5:e569–70. https://doi.org/10.1016/S2468-2667(20)30237-1
3. Okonkwo NE, Aguwa UT, Jang M, Barré IA, Page KR, Sullivan PS, et al. COVID-19 and the US response: accelerating health inequities. BMJ Evid Based Med. 2020 Jun 3 [Epub ahead of print]. https://doi.org/10.1136/bmjebm-2020-111426
4. Berger ZD, Evans NG, Phelan AL, Silverman RD. Covid-19: control measures must be equitable and inclusive. BMJ. 2020;368:m1141. https://doi.org/10.1136/bmj.m1141
5. Kerkhoff AD, Sachdev D, Mizany S, Rojas S, Gandhi M, Peng J, et al. Evaluation of a novel community-based COVID-19 'Test-to-Care' model for low-income populations. PLoS One. 2020;15:e0239400. https://doi.org/10.1371/journal.pone.0239400
6. Towns R, Corbie-Smith G, Richmond A, Gwynne M, Fiscus L. Rapid deployment of a community-centered mobile COVID-19 testing unit to improve health equity. NEJM Catal. 2020 Oct 22 [cited 2020 Dec 11]. https://catalyst.nejm.org/doi/full/10.1056/CAT.20.0522
7. National Governors Association. Rhode Island—coronavirus state actions. 2020 Mar 9 [cited 2020 Sep 11]. https://www.nga.org/coronavirus-state-actions/rhode-island/
8. Johns Hopkins Coronavirus Resource Center. Impact of opening and closing decisions by state: a look at how social distancing measures have influenced trends in COVID-19 cases and deaths in Rhode Island [cited 2020 Dec 11]. https://coronavirus.jhu.edu/data/state-timeline/new-confirmed-cases/rhode-island
9. Macias Gil R, Marcelin JR, Zuniga-Blanco B, Marquez C, Mathew T, Piggott DA. COVID-19 pandemic: disparate health impact on the Hispanic/Latinx population in the United States. J Infect Dis. 2020;222:1592–5. https://doi.org/10.1093/infdis/jiaa474
10. Rhode Island Department of Health (RIDOH). COVID-19 Rhode Island data [cited 2020 Dec 11]. https://docs.google.com/spreadsheets/d/1c2QrNMz8pIbYEKzMJL7Uh2dtThOJa2j1sSMwiDo5Gz4/edit#gid=31350783

Address for correspondence: Amy Nunn, Rhode Island Public Health Institute, 7 Central St, Providence, RI 02907, USA; email: amycitanunn@gmail.com

September 2020
Coronavirus

- Disparate Effects of Invasive Group A *Streptococcus* on Native Americans
- Seroepidemiologic Study Designs for Determining SARS-COV-2 Transmission and Immunity
- Polyclonal *Burkholderia cepacia* Complex
- Outbreak in Peritoneal Dialysis Patients Caused by Contaminated Aqueous Chlorhexidine
- Severe Acute Respiratory Syndrome Coronavirus 2 Prevalence, Seroprevalence, and Exposure among Evacuees from Wuhan, China, 2020
- Pathology and Pathogenesis of SARS-CoV-2 Associated with Fatal Coronavirus Disease, United States
- Encephalopathy and Encephalitis Associated with Cerebrospinal Fluid Cytokine Alterations and Coronavirus Disease, Atlanta, Georgia, USA, 2020
- Invasive Infections with *Nannizziopsis obscura* Species Complex in 9 Patients from West Africa, France, 2004–2020
- Evaluation of World Health Organization– Recommended Hand Hygiene Formulations
- *Saprochaete clavata* Outbreak Infecting Cancer Center through Dishwasher
- Updated Estimates of Chronic Conditions Affecting Risk for Complications from Coronavirus Disease, United States
- Risk-Based Estimate of Human Fungal Disease Burden, China
- Association of Biosecurity and Hygiene Practices with Environmental Contamination with Influenza A Viruses in Live Bird Markets, Bangladesh
- Q Fever Osteoarticular Infection in Children
- Web-Based Interactive Tool to Identify Facilities at Risk of Receiving Patients with Multidrug-Resistant Organisms
- Isolation, Sequence, Infectivity, and Replication Kinetics of Severe Acute Respiratory Syndome Coronavirus 2
- Retrospective Description of Pregnant Women Infected with Severe Acute Respiratory Syndrome Coronavirus 2, France
- Heterogeneity of Dengue Illness in Community-Based Prospective Study, Iquitos, Peru
- Costs Associated with Nontuberculous Mycobacteria Infection, Ontario, Canada, 2001–2012
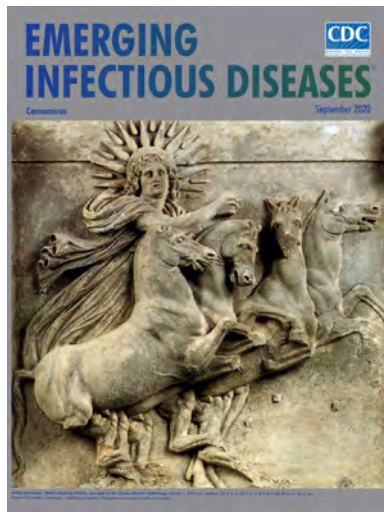
EMERGING INFECTIOUS DISEASES

To revisit the September 2020 issue, go to:
https://wwwnc.cdc.gov/eid/articles/issue/26/9/table-of-contents

Transmission of SARS-CoV-2 from Human to Domestic Ferret

Jožko Račnik, Ana Kočevar, Brigita Slavec, Miša Korva, Katarina Resman Rus, Samo Zakotnik,
Tomaž Mark Zorec, Mario Poljak, Milan Matko, Olga Zorman Rojs, Tatjana Avšič Županc

We report a case of natural infection with severe acute respiratory syndrome coronavirus 2 transmitted from an owner to a pet ferret in the same household in Slovenia. The ferret had onset of gastroenteritis with severe dehydration. Whole-genome sequencing of the viruses isolated from the owner and ferret revealed a 2-nt difference.

Natural infections with severe acute respiratory syndrome coronavirus 2 (SARS-CoV-2) in domestic animals living in infected households have been reported (*1*). Because of their increased popularity as a pet (*2*), domestic ferrets (*Mustela putorius furo*) pose a high risk for transmitting anthropozoonotic infections. A recent study in Spain showed that natural SARS-CoV-2 infections can occur in ferrets kept as working animals for rabbit hunting, especially if a high viral circulation is present in the human population (*3*). Further, ferrets are common laboratory animal models and, at least in experimental conditions, have been shown to be highly susceptible to SARS-CoV-2 infection and likely to transmit the virus to other ferrets without apparent clinical signs (*4*).

The Study

On November 20, 2020, a 5-year-old neutered male domestic ferret had signs of acute gastroenteritis, including apathy, anorexia, vomiting, and profuse mucous diarrhea. Another ferret in the same household appeared healthy. Because the ferret's condition did not improve, the owner took it to a veterinary hospital for clinical examination on November 23. The ferret was lethargic and, on the basis of skin turgor, was

Author affiliations: University of Ljubljana Faculty of Veterinary Medicine, Ljubljana, Slovenia (J. Račnik, B. Slavec, O. Zorman Rojs); Toplica Veterinary Hospital, Topolšica, Slovenia (A. Kočevar, M. Matko); University of Ljubljana Faculty of Medicine, Ljubljana (M. Korva, K. Resman Rus, S. Zakotnik, T.M. Zorec, M. Poljak, T. Avšič Županc)

>5% dehydrated with low body temperature (36.4°C, reference range 37.8–40°C) and slow heart rate (180 beats/min, reference 200–400 beats/min). The body condition of the ferret was good, with a bodyweight of 1.3 kg. Several hematology and serum biochemistry results were elevated: red blood cell count (12.36 × 10^6/μL, reference 7.01–9.65 × 10^6/μL), hemoglobin concentration (21.2 g/dL, reference 12.2–16.5 g/dL), and hematocrit (0.57%, reference 0.36%–0.48%); blood urea nitrogen (>129.94 mg/dL, reference 18–32 mg/dL), hyperproteinemia (8.5 g/dL, reference 4.5–6.2 g/dL), hyperglobulinemia (4.4 g/dL, reference 2.8–3.6 g/dL), and borderline hyperalbuminemia (4.0 g/dL, reference 2.5–4.0 g/dL) were consistent with dehydration and possible infection. The results of all other hematologic and biochemical values were within reference ranges. Whole-body radiographs (Appendix Figure, https://wwwnc.cdc.gov/EID/article/27/9/21-0774-App1.pdf) showed splenomegaly and gas accumulation in intestinal loops. Interstitial and alveolar patterns of cranial lung lobes were present, indicating possible lobar pneumonia. The ferret was hospitalized and initially given fluid therapy, amoxicillin, esomeprazole, maropitant, and dexamethasone. Three days later, the clinical status of the ferret improved, hematologic and biochemical values normalized, and the ferret was scheduled for discharge. However, on the same day, the owner informed the veterinary hospital of having positive results for SARS-CoV-2 RNA tested on November 24, after 9 days of malaise. Additional rectal and oropharyngeal swab specimens and blood samples were taken from the ferret for further diagnostic procedures, and the ferret was discharged from the hospital and put into isolation at the owner's home. Samples were not taken from the other pet ferret at the residence, but the rest of household members tested negative for SARS-CoV-2 RNA on November 25.

We tested the ferret's samples for SARS-CoV-2 RNA (Appendix) and ferret-specific enteric

coronavirus (FERCV) (*5*) by real-time reverse transcription PCR; influenza A and B viruses (*6*) by reverse transcription PCR; and herpesviruses (*7*), adenoviruses (*8*), and circoviruses (*9*) and by PCR. The only positive result was the detection of SARS-CoV-2 RNA in the rectal and oropharyngeal swab specimens. In the oropharyngeal swab specimen, all 3 targeted genes (envelope, cycle threshold [C_t] 27.7; RNA dependent RNA polymerase, C_t 28.5; and nucleocapsid, C_t 32.1) were detected, and in the rectal swab specimen only envelope gene (C_t 35.6) was detected, a finding probably attributable to a lower virus concentration. To compare the SARS-CoV-2 detected in the owner and the ferret, we conducted whole-genome sequencing on Illumina MiSeq (Illumina, https://www.illumina.com) on the basis of the ARTIC protocol (https://artic.network/ncov-2019/ncov2019-bioinformatics-sop.html). The complete genome sequences were deposited in the GISAID database (https://www.gisaid.org; accession nos. EPI_ISL_1490186 and EPI_ISL_1490187). According to the pangolin nomenclature, the sequences belonged to the B.1.258 Pango lineage, which was on the rise in Slovenia in November 2020 (Figure 1). The comparison of both sequences showed ≈100% identity, differing by 2 nucleotides (position/owner/ferret: 2,097/G/T; 22,832/C/A).

We also confirmed the SARS-CoV-2 infection in the ferret on the basis of SARS-CoV-2 IgG seroconversion and development of neutralizing antibodies. We tested the ferret's acute and convalescent serum samples with an in-house immunofluorescent assay (Appendix). The first serum sample obtained on day 6 after disease onset tested negative; however, seroconversion was observed on day 19, when the IgG titer was 1:1,024 (Figure 2, panels A, B). In addition, we detected a high neutralizing antibody titer of 1:320 in the second serum sample (Figure 2, panel C).

Conclusions

SARS-CoV-2 originated in animals, jumped into humans, and is now easily transmitted among humans. In addition to spreading from animals to humans, the virus can be transmitted back into animals, as observed in farmed mink (*Neovison vison*) (*10*). Most experimentally infected ferrets do not exhibit clinical signs or have only mild fever, lethargy, loss of appetite, and occasional cough (*4,11*). Also, among working ferrets naturally infected with SARS-CoV-2 in Spain, no signs of illness were reported (*3*).

In our study, the infected ferret had onset of severe disease with gastroenteritis, pneumonia, and dehydration and required aggressive fluid therapy

and supportive care with antibiotics, antacids, antiemetics, and parenteral dexamethasone. The ferret responded to the therapy promptly and fully recovered in 3 days. Acute epizootic catarrhal enteritis caused
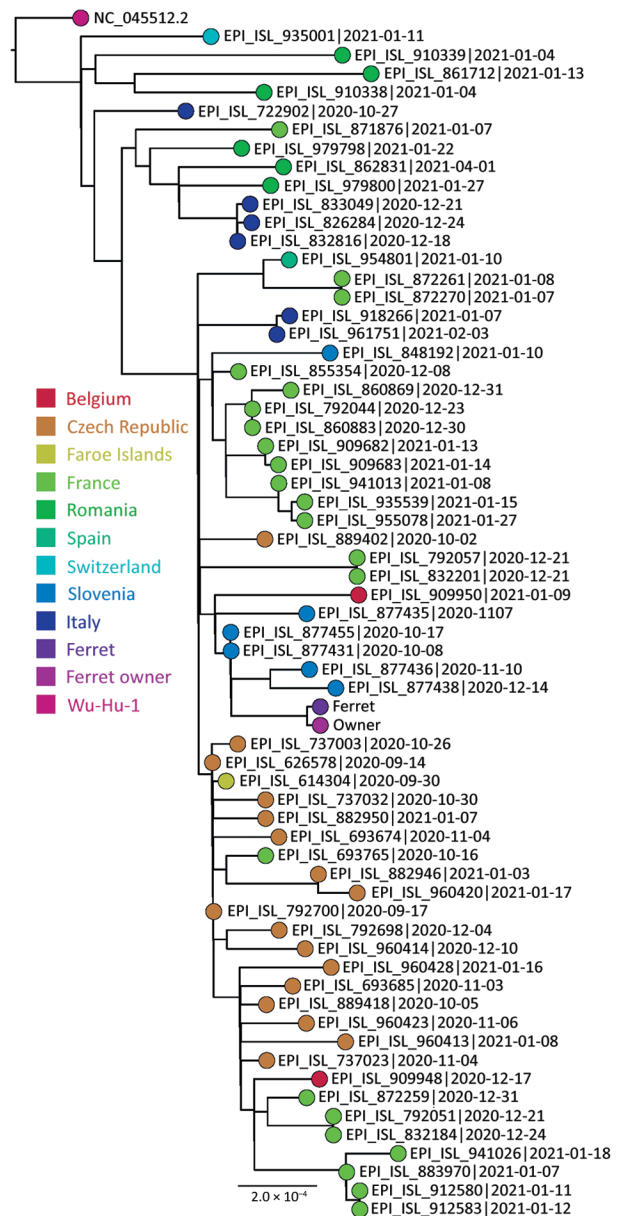
Figure 1. Phylogenetic sequence context consisted of high-quality complete severe acute respiratory syndrome coronavirus 2 genome sequences from a domestic ferret, Slovenia, corresponding to Pango lineage B.1.258. The context sequences were downloaded from GISAID (https://www.gisaid.org) and subsampled to 62 sequences and National Center for Biotechnology Information reference sequence NC_045512.2. The phylogenetic reconstruction using a general time-reversible plus F plus R4 substitution model was built in Figtree (Evomics, http://evomics.org) with 1,000 bootstrap replicates. The reference sequence was used as an outgroup to root the phylogenetic tree. GISAID accession numbers and isolation dates are provided. Scale bar indicates substitutions per site.
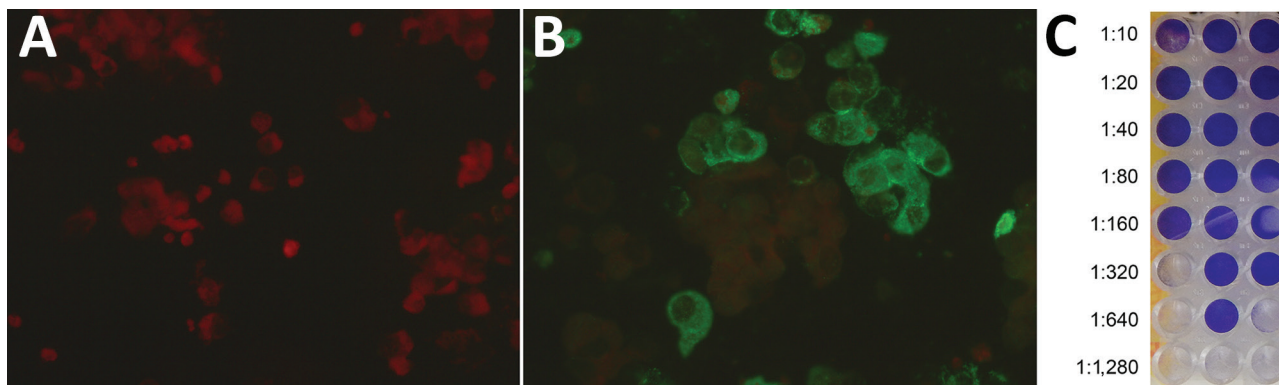
Figure 2. Serological response to infection with severe acute respiratory syndrome coronavirus 2 in a domestic ferret, Slovenia. Immunofluorescent tests showed a negative result in the ferret's acute serum sample obtained on day 6 after disease onset (A) and a positive reaction at titer 1:64 in the ferret's convalescent serum sample obtained on day 19 (B). The neutralization test (C) showed the highest dilution of the ferret's convalescent serum sample that inhibited a cytopathic effect in $\geq$2 of 3 wells to be 1:320.

by FERCV was one of the plausible differential diagnoses in the initial treatment plan for the ferret. For this reason, dexamethasone was used parenterally because additional treatment with a short course of steroids might speed the recovery and reduce future problems of malabsorption attributable to villi destruction caused by fulminate FERCV infection (*12*). In humans, the effective drugs against coronavirus disease are poorly defined, yet dexamethasone in combination with supportive therapy is frequently used (*13*). However, the risk for unnecessary use and adverse effects must be considered before treatment attempts with corticosteroids.

We assume that SARS-CoV-2 likely spread from the infected owner to the ferret living in the same household. Symptoms appeared in the owner 4 days before the ferret became ill. All other household members tested negative for SARS-COV-2 RNA, ruling out asymptomatic infected persons in the family. Another close contact ferret in the same household appeared healthy. Likewise, no disease among staff or animals at the veterinary hospital was reported during or after the hospitalization of the ferret. Nevertheless, ferrets as laboratory models were shown to shed SARS-CoV-2 up to 8 days postinfection in nasal swab, saliva, urine, and fecal samples. Ferrets can effectively transmit the infection to other animals (*14*) or possibly humans, thus highlighting the importance of recognizing the infection in pets early to prevent spread to other animals or humans in the same household or elsewhere (*15*).

In the mink farm outbreak in Denmark, SARS-CoV-2 transmission was shown to spill over from minks to humans accumulating mutations that are resistant to neutralizing antibodies or vaccines along the way (*10*). In our study, whole-genome sequencing of the virus detected in the owner and ferret revealed only a 2-nt difference, and neither of those was present in the spike protein gene. Nonetheless, retaining the One Health approach is crucial for early detection and monitoring of emerging zoonoses in humans.

About the Author

Dr. Račnik is an associate professor at the Faculty of Veterinary Medicine, University of Ljubljana, Slovenia, and diplomate of the European College of Zoological Medicine, wildlife population health specialty. His primary research interests include clinical veterinary medicine and emerging diseases of exotic pets and wild birds.

References

1. Patterson EI, Elia G, Grassi A, Giordano A, Desario C, Medardo M, et al. Evidence of exposure to SARS-CoV-2

in cats and dogs from households in Italy. Nat Commun. 2020;11:6231. https://doi.org/10.1038/s41467-020-20097-0

2. Bixler H, Ellis C. Ferret care and husbandry. Vet Clin North Am Exot Anim Pract. 2004;7:227–55, v. https://doi.org/10.1016/j.cvex.2004.02.002

3. Gortázar C, Barroso-Arévalo S, Ferreras-Colino E, Isla J, de la Fuente G, Rivera B, et al. Natural SARS-CoV-2 infection in kept ferrets, Spain. Emerg Infect Dis. 2021;27(7):1994-1996. https://doi.org/10.3201/eid2707.210096

4. Shi J, Wen Z, Zhong G, Yang H, Wang C, Huang B, et al. Susceptibility of ferrets, cats, dogs, and other domesticated animals to SARS-coronavirus 2. Science. 2020;368:1016–20. https://doi.org/10.1126/science.abb7015

5. Muradrasoli S, Mohamed N, Hornyák A, Fohlman J, Olsen B, Belák S, et al. Broadly targeted multiprobe QPCR for detection of coronaviruses: coronavirus is common among mallard ducks (*Anas platyrhynchos*). J Virol Methods. 2009;159:277–87. https://doi.org/10.1016/j.jviromet. 2009.04.022

6. Boonsuk P, Payungporn S, Chieochansin T, Samransamruajkit R, Amonsin A, Songserm T, et al. Detection of influenza virus types A and B and type A subtypes (H1, H3, and H5) by multiplex polymerase chain reaction. Tohoku J Exp Med. 2008;215:247–55. https://doi.org/10.1620/tjem.215.247

7. VanDevanter DR, Warrener P, Bennett L, Schultz ER, Coulter S, Garber RL, et al. Detection and analysis of diverse herpesviral species by consensus primer PCR. J Clin Microbiol. 1996;34:1666–71. https://doi.org/10.1128/jcm.34.7.1666-1671.1996

8. Wellehan JF, Johnson AJ, Harrach B, Benkö M, Pessier AP, Johnson CM, et al. Detection and analysis of six lizard adenoviruses by consensus primer PCR provides further evidence of a reptilian origin for the atadenoviruses. J Virol. 2004;78:13366–9. https://doi.org/10.1128/JVI.78.23.13366-13369.2004

9. Halami MY, Nieper H, Müller H, Johne R. Detection of a novel circovirus in mute swans (*Cygnus olor*) by using nested broad-spectrum PCR. Virus Res. 2008;132:208–12. https://doi.org/10.1016/j.virusres.2007.11.001

10. Koopmans M. SARS-CoV-2 and the human-animal interface: outbreaks on mink farms. Lancet Infect Dis. 2021;21:18–9. https://doi.org/10.1016/S1473-3099(20)30912-9

11. Abdel-Moneim AS, Abdelwhab EM. Evidence for SARS-CoV-2 infection in animal hosts. Pathogens. 2020;9:529. https://doi.org/10.3390/pathogens9070529

12. Perpiñán D, Johnson Delaney CA. Disorders of the digestive system and liver. In: Johnson Delaney CA, editor. Ferret medicine and surgery. Boca Raton (FL): CRC Press; 2017. p. 159–90.

13. Ledford H. Coronavirus breakthrough: dexamethasone is first drug shown to save lives. Nature. 2020;582:469. https://doi.org/10.1038/d41586-020-01824-5

14. Kim Y-I, Kim S-G, Kim S-M, Kim E-H, Park S-J, Yu K-M, et al. Infection and rapid transmission of SARS-CoV-2 in ferrets. Cell Host Microbe. 2020;27:704–709.e2. https://doi.org/10.1016/j.chom.2020.03.023

15. United Kingdom Animal and Plant Health Agency. Preventative measures regarding SARS-CoV-2 and ferrets in the UK. 2020 [cited 2021 May 8]. http://apha.defra.gov.uk/documents/guidance-sars-cov-2-ferrets.pdf

Address for correspondence: Jožko Račnik, Institute for Poultry, Birds, Small Mammals, and Reptiles, Faculty of Veterinary Medicine, University of Ljubljana, Gerbičeva 60, 1000 Ljubljana, Slovenia; email: josko.racnik@vf.uni-lj.si

Predictors of Nonseroconversion after SARS-CoV-2 Infection

Weimin Liu,[1] Ronnie M. Russell,[1] Frederic Bibollet-Ruche,[1] Ashwin N. Skelly,[1]
Scott Sherrill-Mix,[1] Drew A. Freeman,[1] Regina Stoltz, Emily Lindemuth, Fang-Hua Lee,
Sarah Sterrett, Katharine J. Bar, Nathaniel Erdmann, Sigrid Gouma, Scott E. Hensley, Thomas Ketas,
Albert Cupo, Victor M. Cruz Portillo, John P. Moore, Paul D. Bieniasz, Theodora Hatziioannou,
Greer Massey, Mary-Beth Minyard,[2] Michael S. Saag, Randall S. Davis, George M. Shaw,
William J. Britt, Sixto M. Leal, Jr., Paul Goepfert, Beatrice H. Hahn

Not all persons recovering from severe acute respiratory syndrome coronavirus 2 (SARS-CoV-2) infection develop SARS-CoV-2–specific antibodies. We show that nonseroconversion is associated with younger age and higher reverse transcription PCR cycle threshold values and identify SARS-CoV-2 viral loads in the nasopharynx as a major correlate of the systemic antibody response.

Coronavirus disease (COVID-19) is typically diagnosed by reverse transcription PCR (RT-PCR) amplification of severe acute respiratory syndrome coronavirus 2 (SARS-CoV-2) RNA from nasopharyngeal fluids (*1*). RT-PCR yields cycle threshold (C_t) values that are inversely correlated with viral loads (*2*) and thus provide an estimate of the number of SARS-CoV-2 RNA copies in the sample. Serologic assays complement COVID-19 diagnosis by documenting past infections. In most persons, binding and neutralizing antibodies develop within 1–3 weeks after onset of symptoms (*3*), and titers correlate with disease severity (*4*).

Initial serosurveys identified antibodies in nearly 100% of persons with RT-PCR–confirmed SARS-CoV-2 infection (*5*). However, more recent studies have shown that seroconversion rates are surprisingly variable (*6–10*). For example, a multicenter study from Israel reported that 5% of participants remained seronegative despite a positive test result on a nasal swab specimen (*6*). In contrast, a seroprevalence study from New York found that 20% of persons with a positive RT-PCR test result did not seroconvert (*8*). Another study from Germany reported that 85% of confirmed infected COVID-19 contacts failed to develop antibodies (*9*). To examine the reasons for these differences, we investigated the relationship between seroconversion and demographic, clinical, and laboratory data in a convenience sample of convalescent persons recruited at the University of Alabama at Birmingham (Birmingham, Alabama, USA) in 2020.

The Study

We studied 72 persons, all of whom had a previous positive RT-PCR test but were symptom-free for >3 weeks before blood was collected for testing (Table). Only 2 persons (3%) reported no symptoms, whereas 13 (18%) persons reported mild disease, 48 (67%) reported moderate disease, and 9 (12%) reported severe disease (Appendix Table 1, https://wwwnc.cdc.gov/EID/article/27/9/21-1024-App1.pdf).

We tested plasma samples (n = 144) collected at enrollment and follow-up visits for antibodies to the spike protein by using a validated ELISA (Appendix). Only 46 of the 72 participants had detectable IgG responses, IgA responses, or both (Table); reciprocal endpoint titers ranged from 182 to >312,500 (Appendix Table 2). Analysis of the same samples for receptor-binding domain (RBD) and nucleocapsid (N)

Author affiliations: University of Pennsylvania, Philadelphia, Pennsylvania, USA (W. Liu, R.M. Russell, F. Bibollet-Ruche, A.N. Skelly, S. Sherrill-Mix, R. Stoltz, E. Lindemuth, F.-H. Lee, K.J. Bar, S. Gouma, S.E. Hensley, G.M. Shaw, B.H. Hahn); The University of Alabama at Birmingham, Birmingham, Alabama, USA (D.A. Freeman, S. Sterrett, N. Erdmann, M.S. Saag, R.S. Davis, W.J. Britt, S.M. Leal Jr., P. Goepfert); Weill Cornell Medicine, New York, New York, USA (T. Ketas, A. Cupo, V.M. Cruz Portillo, J.P. Moore); Howard Hughes Medical Institute, New York (P.D. Bieniasz); The Rockefeller University, New York (P.D. Bieniasz, T. Hatziioannou); Assurance Scientific, Vestavia, Alabama, USA (G. Massey, M.-B. Minyard)

[1]These first authors contributed equally to this article.

[2]Current affiliation: MBMicrobio Labs, Birmingham, Alabama, USA.

Table. Demographic, clinical, and laboratory characteristics of serologic responders and nonresponders after SARS-CoV-2 infection*

Characteristic	SARS-CoV-2 antibody positive, n = 46	SARS-CoV-2 antibody negative, n = 26	p value†
Age, y, median (IQR)	49 (37–63)	35 (30–46)	0.03
Sex			0.17
M	30 (65)	10 (38)	
F	16 (35)	16 (62)	
Race/ethnicity			1.00
White	28 (61)	20 (77)	
Black	7 (15)	3 (12)	
Asian	7 (15)	3 (12)	
Latinx	4 (9)	0	
RT-PCR of nasal swabs			
DFOS, d, median (IQR)	5 (3–11)	5 (4–8)	0.95
C_t value, median (IQR)‡	24.5 (22–27)	36 (34–77)	<0.00001
Symptoms§	45 (98)	25 (96)	0.21
Severity 0	1 (2)	1 (4)	
Severity 1	5 (11)	8 (31)	
Severity 2	33 (72)	15 (58)	
Severity 3	7 (15)	2 (8)	
Hospitalization	6 (13)	2 (8)	1.00
Serologic analyses			
DFOS of T1, d, median (IQR)	34 (26–46)	33 (22–43)	0.74
Binding antibodies positive¶			
Spike protein IgG#	46 (100)	0	
Spike protein IgA#	43 (93)	0	
RBD IgG**	44 (96)	0	
RBD IgM**	38 (83)	0	
Nucleocapsid protein IgG††	43 (93)	0	
Neutralizing antibodies positive¶	45 (98)	0	

*Values are no. (%) unless otherwise indicated. Participants were a convenience sample recruited at the University of Alabama at Birmingham (Birmingham, AL, USA) during March–May 2020. C_t, cycle threshold; DFOS, days following onset of symptoms; IQR, interquartile range; RBD, receptor binding domain; RT-PCR, reverse transcription PCR; SARS-CoV-2, severe acute respiratory syndrome coronavirus 2; T1, time of first serologic test.
†Calculated using a likelihood ratio test for a logistic regression predicting seropositivity for the category indicated after Bonferroni correction for multiple comparisons, except for RT-PCR and serologic DFOS, for which p-values were calculated using a Welch's 2-sample t-test.
‡C_t values were only available for a subset of seropositive (n = 34) and seronegative (n = 25) persons (Appendix Table 1, https://wwwnc.cdc.gov/EID/article/27/9/21-1024-App1.pdf).
§Symptom severity was self-reported, with 0 indicating no symptoms, 1 indicating mild symptoms with little impact on daily activities, 2 indicating moderate symptoms with noticeable impact on daily activities, and 3 indicating severe symptoms with a substantial reduction in quality of life (Appendix Table 1).
¶Above assay detection limits (Appendix Table 2 details midpoint and endpoint titers).
#ELISA detection of IgG and IgA binding antibodies to a prefusion stabilized Wuhan-Hu-1 spike protein.
**ELISA detection of IgM and IgG binding antibodies to RBD of the Wuhan-Hu-1 spike protein.
††Detection of IgG binding antibodies to the nucleocapsid protein by the Abbott Architect assay.

antibodies yielded very similar results (Appendix Figure 1). All persons with spike protein antibodies also had detectable RBD (IgG, IgM, or both) or N (IgG) protein responses, except for 1 participant whose spike protein endpoint titers were very low (Appendix Table 2). In contrast, 26 participants remained seronegative, despite the testing of up to 3 samples per person for IgA, IgM, and IgG against multiple antigens as well as neutralizing antibodies. Thus, 36% of our cohort represented serologic nonresponders.

To investigate potential reasons for the lack of seroconversion, we examined available demographic, clinical, and laboratory data. Comparing race/ethnicity, sex, and symptom severity, we failed to find a significant association with serostatus (Table), although we did observe a trend for increasing antibody positivity with increasing symptom severity (Appendix Figure 2). We also found no significant differences in seroconversion between patients reporting or not reporting various symptoms, including symptoms

characteristic of COVID-19 (Appendix Figure 3). However, seronegative persons were on average 10 (95% CI 3–17) years younger than seropositive persons (Figure 1, panel A) and exhibited RT-PCR C_t values that were 11 (95% CI 8–14) cycles higher (Figure 1, panel B). Moreover, logistic regression showed a precipitous decline in the probability of seroconversion at higher C_t values (Figure 2). For example, a C_t of 35 predicted only a 15% (95% CI 5%–37%) probability of seroconversion, which decreased further with increasing C_t values. Thus, low nasopharyngeal viral loads seem insufficient to elicit a systemic antibody response.

For control, we plotted C_t values of serologic responders and nonresponders against the times of RT-PCR and antibody testing relative to symptom onset (Appendix Figure 4). In both cases, the distributions of sampling times were similar for the 2 groups, thus excluding the possibility that seronegative persons had higher C_t values because they were tested too late
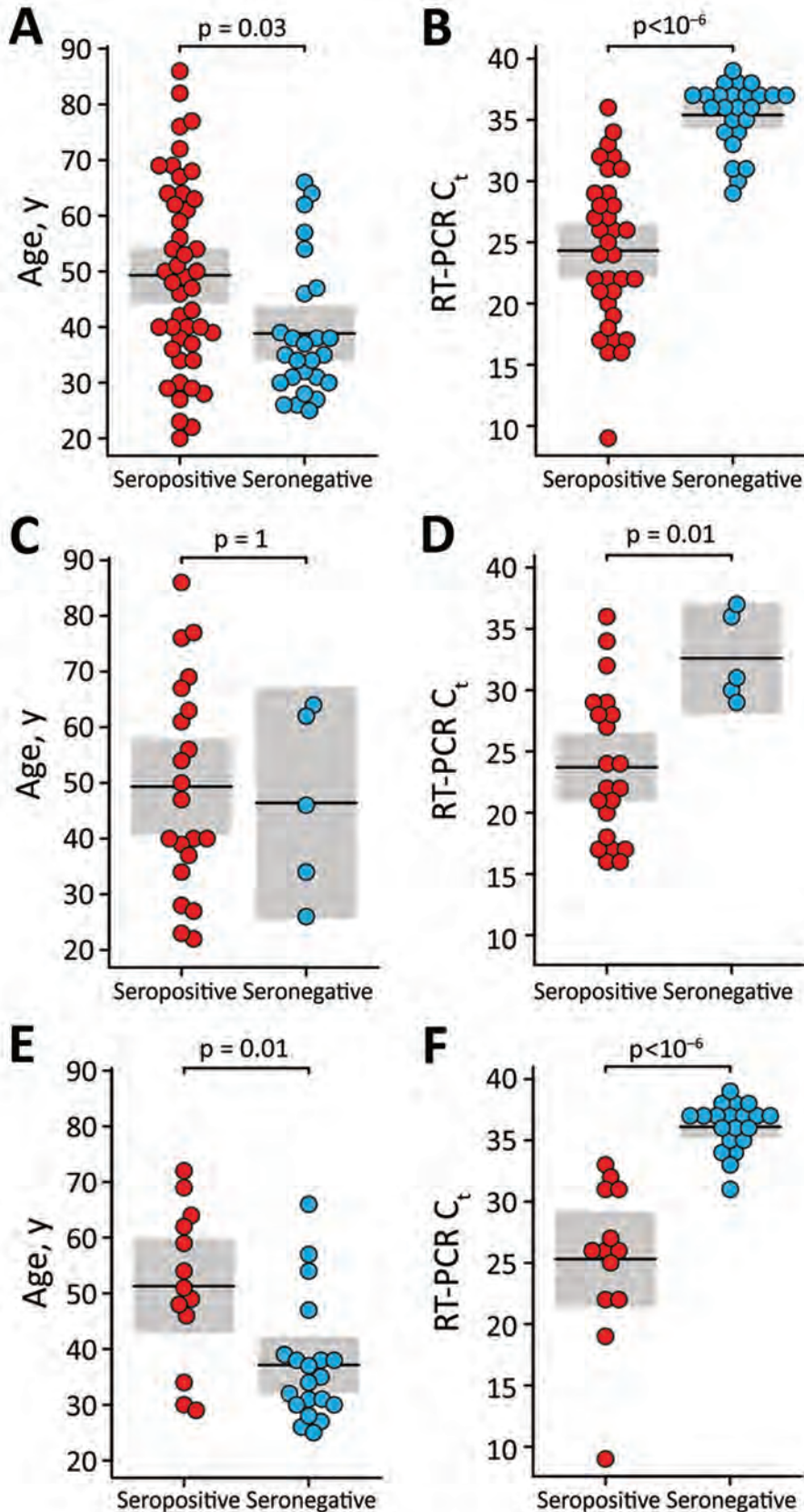
Figure 1. Relationship of age and nasopharyngeal viral loads with SARS-CoV-2 serostatus among convalescent persons after SARS-CoV-2 infection. Participants were a convenience sample of convalescent SARS-CoV-2–infected persons recruited at the University of Alabama at Birmingham, Birmingham, Alabama, USA, 2020. Age (panels A, C, and E) and RT-PCR C_t values (panels B, D, and F) are plotted for seropositive (red) and seronegative (blue) persons. Panels show comparisons of persons tested at all sites (panels A, B), the Assurance Scientific Laboratories site (panels B, C), and the University of Alabama at Birmingham Fungal Reference Laboratory and Children's of Alabama Diagnostic Virology Laboratory sites (panels E, F). The mean (horizontal line) and corresponding 95% CI (shading) are shown; p-values indicate the results of a likelihood ratio test after Bonferroni correction for multiple comparisons. C_t, cycle threshold; RT-PCR, reverse transcription PCR; SARS-CoV-2, severe acute respiratory syndrome coronavirus 2.
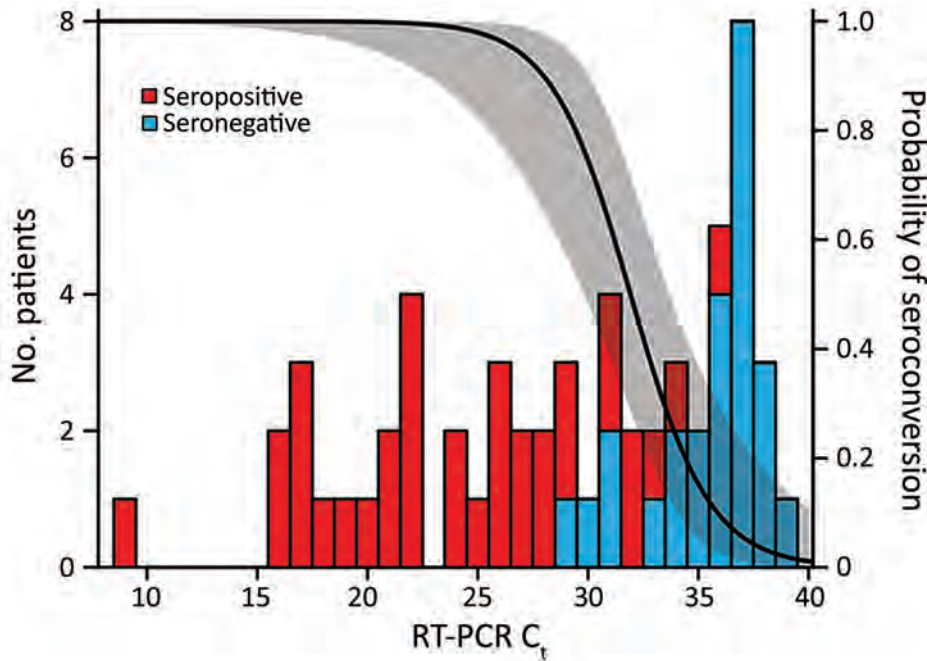
Figure 2. Decreasing probability of SARS-CoV-2 seroconversion with increasing RT-PCR C_t values among persons recovered from SARS-CoV-2 infection. Participants were a convenience sample of convalescent SARS-CoV-2–infected persons recruited at the University of Alabama at Birmingham, Birmingham, Alabama, USA, 2020. The number of serologic responders (red bars) and nonresponders (blue bars) is shown for varying RT-PCR C_t values. A logistic regression was used to estimate the probability of seroconversion for a given C_t (line) and its 95% CI (shaded). C_t, cycle threshold; RT-PCR, reverse transcription PCR; SARS-CoV-2, severe acute respiratory syndrome coronavirus 2.

or that they lacked antibodies because they were tested too early. We also examined remnants of purified RNA used for the initial diagnosis for the presence of SARS-CoV-2 sequences. By analyzing 12 available samples (Appendix Table 1), we were able to amplify full-length intact spike genes from 4 specimens, including 2 from seronegative persons with high C_t values (Appendix Figure 5).

Finally, we asked whether the relationship between seroconversion, age and C_t values was dependent on the diagnostic laboratory. We found that 2 sites with highly sensitive RT-PCR tests (University of Alabama at Birmingham Fungal Reference Laboratory and Children's of Alabama Diagnostic Virology Laboratory in Birmingham) were 6 (95% CI 2–30) times more likely to identify serologic nonresponders than a third site with a less sensitive test (Assurance Scientific Laboratories in Birmingham) (Appendix Methods). However, this difference did not change the relationship between C_t values and seroconversion because seronegative persons had higher C_t values than seropositive persons regardless of the test site (Figure 1, panels D, F). In contrast, we observed little association between age and seroconversion at the Assurance Scientific Laboratories site (Figure 1, panel C), and the difference observed at the other sites was largely driven by young persons who also had high C_t values (Figure 1, panel E). Thus, nasopharyngeal viral loads represent a major correlate of the systemic antibody response, whereas age seems to have only a minor effect.

Conclusions

In summary, we show that patients with low SARS-CoV-2 viral loads in their respiratory tract are less likely to mount a systemic antibody response. Although we cannot formally exclude false-positive RT-PCR results in some participants, PCR contamination is highly unlikely as an explanation for our findings (Appendix). We also show that clinical illness does not guarantee seroconversion and that laboratories with highly sensitive RT-PCR assays are more likely to detect serologic nonresponders. These results provide an explanation for the puzzling variability of seroconversion in different cohorts.

The fact that a considerable fraction of RT-PCR positive persons fail to seroconvert has practical implications. Such persons remain undetected in seroprevalence studies, including in vaccine studies that assess protection from asymptomatic infection by measuring antibodies to antigens not included in the vaccine. Seroconverters and nonseroconverters will probably also respond differently to vaccination. Recent studies revealed that seropositive persons have a heightened antibody response after the first, but not the second, dose of an mRNA vaccine, suggesting that a single dose is sufficient (*11–13*; Samanovic et al., unpub. data, https://doi.org/10.1101/2021.02.07. 21251311). Serologic nonresponders might not exhibit a similarly heightened anamnestic response, but resemble SARS-CoV-2 naive persons, as was observed for 1 previously infected vaccinee who never seroconverted (*14*). Finally, RT-PCR positive persons who

experienced COVID-19 symptoms might be less inclined to seek vaccination, believing they are protected, but our results caution against this assumption.

About the Author

Dr. Liu is a virologist at the University of Pennsylvania. His primary research interests include the evolutionary history and biology of zoonotic pathogens.

References

1. Kevadiya BD, Machhi J, Herskovitz J, Oleynikov MD, Blomberg WR, Bajwa N, et al. Diagnostics for SARS-CoV-2 infections. Nat Mater. 2021;20:593–605. https://doi.org/10.1038/s41563-020-00906-z
2. Pinninti SG, Pati S, Poole C, Latting M, Seleme MC, Yarbrough A, et al. Virological characteristics of hospitalized children with SARS-CoV-2 infection. Pediatrics. 2021 Feb 23 [Epub ahead of print]. https://doi.org/10.1542/peds.2020-037812
3. Sette A, Crotty S. Adaptive immunity to SARS-CoV-2 and COVID-19. Cell. 2021;184:861–80. https://doi.org/10.1016/j.cell.2021.01.007
4. Gaebler C, Wang Z, Lorenzi JCC, Muecksch F, Finkin S, Tokuyama M, et al. Evolution of antibody immunity to SARS-CoV-2. Nature. 2021;591:639–44. https://doi.org/10.1038/s41586-021-03207-w
5. Fafi-Kremer S, Bruel T, Madec Y, Grant R, Tondeur L, Grzelak L, et al. Serologic responses to SARS-CoV-2 infection among hospital staff with mild disease in eastern France. EBioMedicine. 2020;59:102915. https://doi.org/10.1016/j.ebiom.2020.102915
6. Oved K, Olmer L, Shemer-Avni Y, Wolf T, Supino-Rosin L, Prajgrod G, et al. Multi-center nationwide comparison of seven serology assays reveals a SARS-CoV-2 non-responding seronegative subpopulation. EClinicalMedicine. 2020; 29:100651. https://doi.org/10.1016/j.eclinm.2020.100651
7. Masia M, Telenti G, Fernandez M, Garcia JA, Agullo V, Padilla S, et al. SARS-CoV-2 seroconversion and viral clearance in patients hospitalized with COVID-19: viral load predicts antibody response. Open Forum Infect Dis. 2021 Jan 5 [Epub ahead of print].
8. Pathela P, Crawley A, Weiss D, Maldin B, Cornell J, Purdin J, et al. Seroprevalence of SARS-CoV-2 following the largest initial epidemic wave in the United States: findings from New York City, May 13–July 21, 2020. J Infect Dis. 2021 Apr 9 [Epub ahead of print]. PMID 33836067
9. Wellinghausen N, Plonné D, Voss M, Ivanova R, Frodl R, Deininger S. SARS-CoV-2-IgG response is different in COVID-19 outpatients and asymptomatic contact persons. J Clin Virol. 2020;130:104542. https://doi.org/10.1016/j.jcv.2020.104542
10. Thiruvengadam R, Chattopadhyay S, Mehdi F, Desiraju BK, Chaudhuri S, Singh S, et al.; DBT India Consortium for COVID 19 Research. Longitudinal serology of SARS-CoV-2-infected individuals in India: a prospective cohort study. Am J Trop Med Hyg. 2021 May 18 [Epub ahead of print].
11. Krammer F, Srivastava K, Alshammary H, Amoako AA, Awawda MH, Beach KF, et al. Antibody responses in seropositive persons after a single dose of SARS-CoV-2 mRNA vaccine. N Engl J Med. 2021;384:1372–4. https://doi.org/10.1056/NEJMc2101667
12. Stamatatos L, Czartoski J, Wan YH, Homad LJ, Rubin V, Glantz H, et al. mRNA vaccination boosts cross-variant neutralizing antibodies elicited by SARS-CoV-2 infection. Science. 2021 Mar 25 [Epub ahead of print]. https://doi.org/10.1126/science.abg9175
13. Saadat S, Rikhtegaran Tehrani Z, Logue J, Newman M, Frieman MB, Harris AD, et al. Binding and neutralization antibody titers after a single vaccine dose in health care workers previously infected with SARS-CoV-2. JAMA. 2021;325:1467–9. https://doi.org/10.1001/jama.2021.3341
14. Reynolds CJ, Pade C, Gibbons JM, Butler DK, Otter AD, Menacho K, et al.; UK COVIDsortium Immune Correlates Network; UK COVIDsortium Investigators. Prior SARS-CoV-2 infection rescues B and T cell responses to variants after first vaccine dose. Science. 2021 Apr 30 [Epub ahead of print]. https://doi.org/10.1126/science.abh1282

Address for correspondence: Beatrice H. Hahn, Perelman School of Medicine, University of Pennsylvania, 409 Johnson Pavilion, 3610 Hamilton Walk, Philadelphia, PA 19104-6076, USA; email: bhahn@pennmedicine.upenn.edu

Bordetella hinzii Meningitis in Patient with History of Kidney Transplant, Virginia, USA

Joseph Pechacek, Jillian Raybould, Megan Morales

A patient in Virginia, USA, who had previously undergone multiple kidney transplantations showed signs of *Bordetella hinzii* bacteremia and meningitis. This emerging pathogen has been increasingly identified as a clinically significant pathogen in immunosuppressed and, less frequently, immunocompetent patients. This patient was treated and recovered without further issue.

Bordetella is a genus consisting mostly of strictly aerobic, small, gram-negative coccobacilli known to house the causative agent of pertussis and kennel cough in dogs (*Bordetella pertussis*) and cats (*B. bronchiseptica*). Over the past several decades, more human-derived clinical isolates have been identified, causing a range of pathologies. As our ability to rapidly and precisely identify clinical isolates grows, characterizing these rarer causes of human disease and their clinical significance and means of treatment has become vital.

B. hinzii was initially discovered in poultry isolates as a respiratory colonizer and cause of respiratory infection; subsequently, it was discovered to cause clinically significant infection in 1994 in a patient with advanced AIDS (*1*). Since this characterization, *B. hinzii* has been implicated as the cause of a range of clinical symptoms, including bacteremia (*1–3*), pulmonary disease (*4–6*), endocarditis (*7*), chronic cholangitis (*8*), and soft tissue abscess (*9,10*). We describe a case of meningitis in an immunocompromised patient that was caused by *B. hinzii*.

Case Report

A 44-year-old man sought care in the emergency department of Virginia Commonwealth University Medical Center (Richmond, VA, USA) in June 2020 after experiencing 3 days of severe, diffuse headache,

Author affiliation: Virginia Commonwealth University Medical Center, Richmond, Virginia, USA

and subjective fevers; maximum measured temperature was 37.9°C. In 1986, the patient had undergone a living related donor kidney transplant for end-stage renal disease related to focal segmental glomerulosclerosis. He underwent another living related donor transplant in 1999 and a deceased-donor transplant in 2010 after the previous allografts failed. His most recent transplant, which occurred 10 years before the illness documented in this study, was performed with thymoglobulin induction and had been maintained with an immunosuppressive regimen of tacrolimus (goal trough of 5–7 ng/mL at the time of this hospitalization), 180 mg mycophenolic acid (2×/d), and 10 mg prednisone (1×/d). His medical history was further notable for seizure disorder and an allergy to penicillin, which manifested as severe urticaria.

He appeared stable in the emergency department; vital signs were temperature 37.5°C, pulse rate 90 bpm, respiratory rate 17 breaths/min, blood pressure 141/85 mm Hg, and oxyhemoglobin saturation 99% on room air. He reported neck stiffness associated with his headaches. When asked about animal exposures, he noted that he works in a warehouse and was regularly exposed to wild birds and rodents. Physical examination revealed discomfort but no signs of toxicity or neurologic deficits; cranial nerves were intact, and speech, motor abilities, and sensation were unremarkable. Complete blood count revealed a leukocyte count of 8.4×10^9/L, hemoglobin of 11 g/dL, and platelet count of 163×10^9/L. Additional bloodwork showed a glomerular filtration rate of 30 mL/min, which was consistent with the patient's baseline given his history of chronic kidney disease. Noncontrasted computed tomography of the head demonstrated no acute pathology. Cerebrospinal fluid (CSF) was clear and colorless, and analysis indicated neutrophilic pleocytosis (Table 1). The patient was given 2 g intravenous (IV) ceftriaxone, a loading dose of 2 g IV vancomycin, and IV acyclovir. Ceftriaxone was rapidly replaced with 2 g meropenem given the

Table 1. Cerebrospinal fluid sample laboratory results in case of *Bordetella hinzii* meningitis in transplant patient, Virginia, USA*

Characteristic	Hospital admission	Hospital day 9
Leukocytes	852/mm^3	26/mm^3
PMNs	86%	3%
Monocytes	27%	1%
Lymphocytes	5%	96%
Erythrocytes	<1 per mm^3	4 per mm^3
Protein	149 mg/dL†	72 mg/dL†
Glucose	58 mg/dL‡	58 mg/dL§
Opening pressure	ND	39 cm H$_2$O

*ND, not done; PMNs, polymorphonuclear leukocytes.
†No serum protein available for comparison.
‡Serum glucose 108mg/dL.
§Serum glucose 89mg/dL.

patient's immunosuppressed status and to empirically treat for the possibility of *Listeria*.

Additional CSF analysis was negative for cytomegalovirus PCR, enterovirus PCR, adenovirus PCR, herpes simplex virus 1 and 2 PCR, and cryptococcal antigen. Because of concerns about possible viral meningitis, we tested nasopharyngeal swab specimens by using the BioFire FilmArray 2.0 respiratory pathogen PCR panel (bioMérieux, https://www.biomerieux.com); results were negative. Acyclovir was stopped after CSF specimens tested negative for herpes simplex virus by PCR, and the patient continued on vancomycin and meropenem. On the second day of hospitalization, blood cultures taken at admission grew gram-negative rods; CSF culture grew gram-negative rods on the fourth day. Blood cultures drawn after antibiotics were administered showed no growth. Vancomycin was stopped on day 3 after cultures showed growth of only gram-negative organisms, which by that time had been identified by matrix-assisted laser desorption/ionization time-of-flight mass spectrometry as *Bordetella* spp. and subsequently *B. hinzii*. Oral ciprofloxacin (500 mg every 12 h) was added on day 6 of hospitalization because *B. hinzii* isolates have been reported to be sensitive to fluoroquinolones (9).

Around day 6 of hospitalization, the patient again began to experience intermittent headaches, although of lesser intensity than his initial symptoms. He underwent a second lumbar puncture on day 9, which revealed improving neutrophilic pleocytosis (Table 1). CSF cultures from this lumbar puncture remained negative.

The patient was discharged after demonstrating substantial improvement. However, because results of antibiotic sensitivity tests were still pending at that time, he was discharged on renally dosed IV meropenem (2 g every 12 h) and oral ciprofloxacin (500 mg every 12 h) for a planned total antibiotic duration of 21 days. Results of sensitivity testing of the *B. hinzii* isolates from blood and CSF samples returned after the patient was discharged revealed susceptibility to meropenem but only intermediate susceptibility to ciprofloxacin (Table 2). At follow-up 7 days after completion of therapy, the patient felt well and appeared to have clinically recovered.

Conclusions

Since its discovery as a cause of bacteremia in a patient with advanced AIDS in 1994 (1), *B. hinzii* has been implicated in a growing range of clinical syndromes as an opportunistic agent in immunocompromised and immunocompetent persons. It remains an infrequently isolated pathogen; further research and characterization is required. Its relatively recent recognition as an infective agent in humans is likely in part due to the increasingly common use of advanced identification techniques; in the past, *B. hinzii* might have been identified only at the genus level (11) or misidentified as a different, related bacterium (1)

B. hinzii is known to be found in the respiratory tracts of poultry as a colonizer and cause of respiratory infection (12). Exposure to poultry is an established risk factor for *B. hinzii* infection, especially in immunosuppressed populations (6). It is unclear whether this case-patient's exposure to wild birds in his workplace constitutes a similar risk. Although *B. avium* is known to infect a range of wild and domesticated birds (13), whether *B. hinzii* affects birds other than poultry is not known. After the identification of *B. hinzii* from the respiratory tract of laboratory mice (14), rodents have also been proposed as potential reservoirs for this pathogen, and it has been isolated from wild mice (11) and rabbits (12). Definitive evidence of spread from an infected or colonized animal to a human has yet to be discovered.

Table 2. Antibiotic susceptibility of *Bordetella hinzii* isolate from blood and cerebrospinal fluid in transplant patient, Virginia, USA*

Antibiotic	Etest MIC from blood	Etest MIC from CSF
Ceftazidime	4 μg/mL	2 μg/mL
Ciprofloxacin	2 μg/mL	2 μg/mL
Imipenem	2 μg/mL	1 μg/mL
Meropenem	0.125 μg/mL	0.125 μg/mL
Piperacillin	1 μg/mL	1 μg/mL
Tobramycin	8 μg/mL	4 μg/mL
Trimethoprim/sulfamethoxazole	0.125 μg/mL	0.064 μg/mL

*Etest, bioMérieux (https://www.biomerieux.com). CSF, cerebrospinal fluid.

The clinical isolates in this study were notable for sensitivity to carbapenems, piperacillin, and trimethoprim/sulfamethoxazole, which is in accordance with susceptibilities noted in other case reports on this species (9). We further noted an intermediate sensitivity to ciprofloxacin. Previous reports have indicated that levofloxacin might have a more favorable MIC for *B. hinzii* than ciprofloxacin (9).

Because *B. hinzii* is an emerging pathogen, its virulence factors require further research to be fully identified. Although the more classic *B. pertussis* (as well as *B. parapertussis* and *B. bronchiseptica*) rely on filamentous hemagglutinin and adenylate cyclase toxin as virulence factors, these proteins are absent in *B. hinzii* (12). These proteins are thought to assist in tracheal and pulmonary colonization in the more classic *Bordetella* spp. (15), so their absence from *B. hinzii* might begin to explain its propensity to cause syndromes atypical for bacteria of this genus.

In summary, we describe an unusual occurrence of *B. hinzii*–caused meningitis in an immunosuppressed patient. The clinical isolates in this study were sensitive to carbapenems, piperacillin, and trimethoprim/sulfamethoxazole but showed only intermediate sensitivity to ciprofloxacin. Clinicians should be aware of the possibility of human infection with this emerging pathogen, particularly in immunocompromised patients.

About the Author

Dr. Pechacek is an infectious diseases clinical fellow at the National Institute of Allergy and Infectious Diseases, National Institutes of Health. His current research interests include infections in immunodeficient populations, especially with primary immunodeficiency.

References

1. Cookson BT, Vandamme P, Carlson LC, Larson AM, Sheffield JV, Kersters K, et al. Bacteremia caused by a novel Bordetella species, "B. hinzii". J Clin Microbiol. 1994;32:2569–71. https://doi.org/10.1128/jcm.32.10.2569-2571.1994
2. Kattar MM, Chavez JF, Limaye AP, Rassoulian-Barrett SL, Yarfitz SL, Carlson LC, et al. Application of 16S rRNA gene sequencing to identify Bordetella hinzii as the causative agent of fatal septicemia. J Clin Microbiol. 2000;38:789–94. https://doi.org/10.1128/JCM.38.2.789-794.2000
3. Hristov AC, Auwaerter PG, Romagnoli M, Carroll KC. Bordetella hinzii septicemia in association with Epstein-Barr virus viremia and an Epstein-Barr virus-associated diffuse large B-cell lymphoma. Diagn Microbiol Infect Dis. 2008;61:484–6. https://doi.org/10.1016/j.diagmicrobio.2008.03.013
4. Funke G, Hess T, von Graevenitz A, Vandamme P. Characteristics of Bordetella hinzii strains isolated from a cystic fibrosis patient over a 3-year period. J Clin Microbiol. 1996;34:966–9. https://doi.org/10.1128/jcm.34.4.966-969.1996
5. Palacián Ruiz MP, Vasquez Martinez MA, Lopez Calleja AI. Respiratory infection caused by Bordetella hinzii. Arch Bronconeumol. 2013;49:409–10.
6. Fabre A, Dupin C, Bénézit F, Goret J, Piau C, Jouneau S, et al. Opportunistic pulmonary Bordetella hinzii infection after avian exposure. Emerg Infect Dis. 2015;21:2122–6. https://doi.org/10.3201/eid2112.150400
7. González MM, Romano MPC, de Guzmán García Monge MT, Martín BB, García AS. Bordetella hinzii endocarditis, a clinical case not previously described. Eur J Case Rep Intern Med. 2019;6:000994.
8. Arvand M, Feldhues R, Mieth M, Kraus T, Vandamme P. Chronic cholangitis caused by Bordetella hinzii in a liver transplant recipient. J Clin Microbiol. 2004;42:2335–7. https://doi.org/10.1128/JCM.42.5.2335-2337.2004
9. Negishi T, Matsumoto T, Shinagawa J, Kasuga E, Horiuchi K, Natori T, et al. A case of cervical subcutaneous abscess due to Bordetella hinzii. Diagn Microbiol Infect Dis. 2019;95:114865. https://doi.org/10.1016/j.diagmicrobio.2019.07.003
10. Kampmeier S, Rennebaum F, Schmidt H, Riegel A, Herrmann M, Schaumburg F. Peripancreatic abscess supported by Bordetella hinzii. New Microbes New Infect. 2020;34:100650. https://doi.org/10.1016/j.nmni.2020.100650
11. Jiyipong T, Morand S, Jittapalapong S, Raoult D, Rolain J-M. Bordetella hinzii in rodents, Southeast Asia. Emerg Infect Dis. 2013;19:502–3. https://doi.org/10.3201/eid1903.120987
12. Register KB, Kunkle RA. Strain-specific virulence of Bordetella hinzii in poultry. Avian Dis. 2009;53:50–4. https://doi.org/10.1637/8388-070108-Reg.1
13. Harrington AT, Castellanos JA, Ziedalski TM, Clarridge JE III, Cookson BT. Isolation of Bordetella avium and novel Bordetella strain from patients with respiratory disease. Emerg Infect Dis. 2009;15:72–4. https://doi.org/10.3201/eid1501.071677
14. Hayashimoto N, Yasuda M, Goto K, Takakura A, Itoh T. Study of a Bordetella hinzii isolate from a laboratory mouse. Comp Med. 2008;58:440–6.
15. Mattoo S, Cherry JD. Molecular pathogenesis, epidemiology, and clinical manifestations of respiratory infections due to Bordetella pertussis and other Bordetella subspecies. Clin Microbiol Rev. 2005;18:326–82. https://doi.org/10.1128/CMR.18.2.326-382.2005

Address for correspondence: Joseph Pechacek, National Institutes of Health, BG 10-CRC Rm 4-4179, 10 Center Dr, Bethesda, MD 20814, USA; email: joseph.pechacek@gmail.com

Disseminated Cutaneous Leishmaniasis and Alcohol Misuse, Northeast Brazil, 2015–2018

Anastácio Q. Sousa, Pedro D.T. Sindeaux Filho, Diane I.M. Cavalcante,
Mércia S. Frutuoso, Francisco F. Pereira, José W.O. Lima, Laécio P.S. Santos,
José A.N. Queiroz, James H. Maguire, Richard D. Pearson, Margarida M.L. Pompeu

Disseminated cutaneous leishmaniasis (DCL) is an uncommon form of *Leishmania braziliensis* infection. It remains unknown why some people develop this clinical condition. We describe 14 DCL patients in Northeast Brazil during 2015–2018. These patients regularly drank large amounts of alcohol, possibly increasing their risk for DCL.

Leishmaniasis is a parasitic disease caused by infection with *Leishmania* parasites, which are transmitted by the bites of phlebotomine sand flies. Localized cutaneous leishmaniasis (LCL), disseminated cutaneous leishmaniasis (DCL), and mucosal leishmaniasis are clinical manifestations of *L. braziliensis* infection. DCL was initially described in the 1980s (1,2); in 2002, Turetz et al. (2) defined DCL as ≥10 cutaneous lesions (papular, nodular, acneiform, crusted, or ulcerated) on ≥2 anatomic regions of the body (i.e., the head, trunk, upper, and lower extremities). *L. guyanensis*, *L. panamensis*, and *L. peruviana* parasites also cause DCL in the New World, whereas *L. tropica* and *L. major* cause DCL in the Old World (3). DCL is distinct from anergic diffuse cutaneous leishmaniasis caused by *L. amazonensis*, *L. mexicana*, and *L. aethiopica* infections; anergic diffuse cutaneous leishmaniasis causes multiple nonulcerating, nonhealing lesions in immunocompromised persons (3).

In Ceará, a state in Northeast Brazil, only *L. braziliensis* has been isolated from persons who have LCL or DCL (4). We observed that many DCL patients in this region report heavy alcohol use. An excessive intake of alcohol can impair the immune response and increase susceptibility to viral and bacterial infections (5). Carvalho et al. (1) postulated that DCL patients might have a weaker cellular immune response to *Leishmania* spp. than LCL patients. We assessed the association of DCL with heavy alcohol consumption in a region to which *L. braziliensis* is endemic.

The Study

We conducted the case–control study in an outpatient clinic in the Baturité region, Ceará state, Northeast Brazil, during 2015–2018, when 358 LCL and DCL cases were diagnosed. We identified 18 DCL patients and 38 LCL patients matched by sex, age (within ±5 years), and time of diagnosis. All DCL cases fulfilled the criteria set by Turetz et al. (2). Patients with known causes of immunosuppression and pregnant or lactating women were excluded from the study. We collected data on the duration of skin lesions, number and type of lesions, mucosal involvement, underlying conditions (e.g., diabetes, hypertension, etc.) and diagnostic method (i.e., culture, smears, histopathology, or immunohistochemical [IHC] assay). Our histopathological diagnoses were based on inflammatory cell infiltrate patterns and the presence of granulomas and amastigotes. For IHC assays, we used the EnVision FLEX HRP Magenta, High pH (Dako Omnis) kit (Agilent Technologies, https://www.agilent.com) with murine hyperimmune serum from mice infected with *Leishmania braziliensis*. We defined parasite load as the number of intracellular and extracellular amastigotes in 15 high-powered fields (×40) using IHC assays. This work was approved by the Human Ethics Committee of the Federal University of Ceará (Fortaleza, Brazil) (protocol no. 1.552.232 e CAAE 53919816.2.0000.5054).

Participants completed a standardized questionnaire (i.e., the Alcohol Use Disorder Identification Test)

Author affiliations: Hospital São José for Infectious Diseases, Fortaleza, Brazil (A.Q. Sousa); Federal University of Ceará, Fortaleza (A.Q. Sousa, P.D.T. Sindeaux Filho, D.I.M. Cavalcante, M.S. Frutuoso, F.F. Pereira, L.P.S. Santos, J.A.N. Queiroz, M.M.L. Pompeu); State University of Ceará, Fortaleza (J.W.O. Lima); Harvard University, Boston, Massachusetts, USA (J.H. Maguire); University of Virginia, Charlottesville, Virginia, USA (R.D. Pearson)

to estimate the amount of alcohol intake in grams per day (6). We considered ≥28 g/d to be a high level of alcohol consumption (7). Most DCL patients were men 19–77 years of age with a duration of disease ranging from 5–36 weeks at diagnosis of leishmaniasis. Each patient had 13–720 lesions on their trunk, limbs, scalp, face, eyelids, conjunctivae, lips, ears, palms, soles of the feet, or genitalia (Figure). Most (56.3%) patients had lesions in the nasal mucosa. Seventeen patients had ≥1 ulcerated lesion; in patient 5, all lesions were ulcerated (Table 1).

DCL and LCL patients were well-matched by sex and age (Table 2). DCL patients had longer durations of disease before diagnosis than LCL patients (p<0.01). All LCL lesions were ulcerated and found predominantly in exposed skin areas: lower limbs (50%), upper limbs (25%), head (10%), and trunk (5%). In total, 36 (92%) LCL patients had 1–2 lesions; the other 3 (8%) patients had 3, 5, and 6 lesions. We observed nasal mucosa involvement in only 1 LCL patient.

In total, 14 (78%) DCL patients drank alcohol in the form of cachaça, a popular beverage made by distilling fermented sugar cane juice (8). Cachaça has an alcohol content of 40%, similar to that of other distilled spirits such as whiskey, tequila, and vodka. One liter of cachaça or whiskey contains 400 g of pure alcohol. For the 14 patients who drank cachaça, alcohol intake ranged from 45–800 g/d. Twelve (67%) DCL patients drank ≥350 mL of cachaça (140 g of alcohol) daily. The other 4 (22%) DCL patients did not drink alcohol, including 3 patients who had diabetes. LCL patients had a significantly lower alcohol intake than DCL patients (p<0.01). In total, 25 (64%) LCL patients did not drink alcohol. Fourteen (36%) LCL patients reported alcohol consumption, including 4 who had alcohol intakes ≥28 g/d, 3 who had intakes of 28–50 g/d, and 1 who had an intake of 400 g/d. In addition, 3 LCL patients had diabetes. We found an association between alcohol intake and parasite load (Spearman ρ = 0.482; p = 0.03).

Conclusions

The clinical manifestations of DCL in these patients did not differ substantially from those reported previously (2,9). However, we observed 1 patient who had only ulcerated lesions and another with crusted-horny lesions, both uncommon forms of this rare disease (Figure). The duration of skin lesions before diagnosis was longer in persons with DCL than LCL, similar to the observations of Turetz et al. (2). Most DCL lesions were identified by histopathological assays. Our results suggest that DCL is associated with alcohol misuse.

Figure. Lesions of patients with disseminated cutaneous leishmaniasis, Baturité region, Ceará State, Northeast Brazil, 2015–2018. Patient numbers match those given in Table 1. A) Ulcerated, acneiform, and papular lesions on the back of patient 1. B) Ulcerated lesions on the genitalia of patient 2. C–D) Crusted and crusted-horny lesions on the face of patient 3. E) Papular, crusted, and ulcerated lesions on the trunk of patient 3. F) Crusted, ulcerated, and papular lesions on the back of patient 6. G) Ulcer surrounded by zosteriform and papular lesions on the back of patient 11. H) Papular, crusted, and ulcerated lesions on the face as well as an ulcerated and crusted-horny lesion on the superior right eyelid of patient 12.

Table 1. Clinical, diagnostic and alcohol intake data of 18 patients with disseminated cutaneous leishmaniasis, Baturité region, Ceará State, Northeast Brazil, 2015–2018*

Patient ID	Alcohol intake, g/d	Age, y/sex	Duration of lesions, wks†	No. lesions	Lesion type(s)	Mucosal lesions	Diagnostic method
1	800	25/M	NA	79	U, Ac, P	No	H
2	600	41/M	16	184	Cr, U	Yes	H
3	400	36/M	16	167	U, Cr, crusted-horny, P	Yes	C, H, I
4	400	60/M	5	13	U, P	No	H
5	400	41/M	NA	24	U	NA	H
6	400	49/M	16	171	U, N, Ac, P	No	H, I
7	400	44/M	32	720	U, P, Ac	Yes	H, I
8	300	51/M	36	110	U, N	NA	H
9	240	73/M	24	20	U, Cr, N	No	H
10	230	47/M	24	18	U, Cr, P	No	C, H
11	170	39/M	18	37	P, U, zosteriform	Yes	H
12	140	38/M	6	71	P, Cr, U, crusted-horny	Yes	C, H, I
13	60	19/M	12	14	U, Cr, P	No	H, C
14	45	32/M	32	421	U, P, Cr, N	Yes	C, H
15	0	77/M	32	22	U, N, Ac	Yes	H
16	0	34/F	8	41	U, N	Yes	H
17	0	71/F	8	19	U, P	No	H
18	0	42/M	NA	60	U, N, Cr	Yes	C, H

*Ac, acneiform; Cr, crusted; C, culture; H, histopathology; I, immunohistochemical assay; ID, identification; N, nodular; NA, not available; P, papular; U, ulcerated.
†At time of diagnosis.

Alcohol causes dysregulation of the innate and adaptive immune responses (*10*). Persons who misuse alcohol have decreased tissue recruitment of neutrophils during bacterial infections and substantial defects in neutrophil function. In addition, these persons have dendritic cells that are fewer in number and have impaired differentiation and function (*11*), possibly causing an imbalance toward a Th2 profile (*12,13*). Persons who misuse alcohol produce macrophages with decreased phagocytic and microbicidal activity as well as reduced adherence to other cells in the lesion, which increases their migration to the circulatory system (*5,13*). These immune anomalies

could explain the correlation between alcohol misuse and parasite load in DCL patients. Vitamin and micronutrient deficiencies are also common in persons who misuse alcohol (*14*) and might also contribute to risk for DCL.

Other risk factors might also contribute to the pathogenesis of DCL. For example, younger age and male sex are associated with DCL (*2*); we controlled for these variables in our analysis. Different strains of *L. braziliensis* might also account for the differential manifestations of LCL and DCL. Cardoso et al. (*15*) showed that neutrophils from healthy persons had decreased microbicidal activity when infected

Table 2. Comparison of LCL and DCL patients, Baturité region, Ceará State, Northeast Brazil, 2015–2018*

Variable	Localized cutaneous leishmaniasis	Disseminated cutaneous leishmaniasis	Odds ratio†	p value
Total	38 (100.0)	18 (100.0)		
Sex				
M	35 (92.1)	16 (88.9)	1.00	0.7
F	3 (7.9)	2 (11.1)	1.46	
Age, y‡	41 (19–89)	42 (19–77)	1.01	0.64
Diabetes	3 (7.9)	3 (16.7)	2.13	0.39
Disease duration, wks‡	8 (3–26)	16 (5–36)	1.17	<0.01
Mucosal lesion	1 (2.6)	9 (50.0)	43.7	<0.01
Parasite load‡§	3 (1–340)	5 (1–556)	1.002	0.53
Agricultural occupation	22 (57.9)	12 (66.7)	1.45	0.53
Daily alcohol intake, g/d‡	0 (0–400)	325 (0–800)	1.01	<0.01
Days with alcohol intake >28 g	4 (10.5)	14 (77.8)	23	<0.01

*Values are no. (%), except as indicated. DCL, disseminated cutaneous leishmaniasis; LCL, localized cutaneous leishmaniasis.
†Estimated by simple logistic regression.
‡Values are median (range). Load measured as the number of intracellular and extracellular amastigotes in 15 high-powered fields (×40) using immunohistochemical assays.
§Of 6 LCL patients and 7 DCL patients.

with parasites from DCL patients compared with LCL patients.

In summary, we found an association between DCL and heavy alcohol use. Excessive alcohol intake impairs the human immune system. We postulate that alcohol misuse is a risk factor for DCL in persons infected with *L. braziliensis*. Additional studies are needed to determine whether this association is causal, and if so, to elucidate the mechanism(s) of immune dysregulation responsible for development of DCL in persons infected with *L. braziliensis*. Health officials should consider campaigns focused on preventing sand fly bites in persons who misuse alcohol.

About the Author

Dr. Sousa is head of the department of Clinical Medicine at the Federal University of Ceará in Fortaleza, Brazil. His primary research interests are leishmaniasis and other emerging infectious diseases in Northeast Brazil.

References

1. Carvalho EM, Barral A, Costa JM, Bittencourt A, Marsden P. Clinical and immunopathological aspects of disseminated cutaneous leishmaniasis. Acta Trop. 1994;56:315–25. https://doi.org/10.1016/0001-706X(94)90103-1
2. Turetz ML, Machado PR, Ko AI, Alves F, Bittencourt A, Almeida RP, et al. Disseminated leishmaniasis: a new and emerging form of leishmaniasis observed in northeastern Brazil. J Infect Dis. 2002;186:1829–34. https://doi.org/10.1086/345772
3. Hashiguchi Y, Gomez EL, Kato H, Martini LR, Velez LN, Uezato H. Diffuse and disseminated cutaneous leishmaniasis: clinical cases experienced in Ecuador and a brief review. Trop Med Health. 2016;44:2. https://doi.org/10.1186/s41182-016-0002-0
4. Sousa AQ, Parise ME, Pompeu MML, Coelho Filho JM, Vasconcelos IAB, Lima JWO, et al. Bubonic leishmaniasis: a common manifestation of *Leishmania (Viannia) braziliensis* infection in Ceara, Brazil. Am J Trop Med Hyg. 1995;53:380–5. https://doi.org/10.4269/ajtmh.1995.53.380
5. Szabo G, Saha B. Alcohol's effect on host defense. Alcohol Res. 2015;37:159–70.
6. World Health Organization. AUDIT: The Alcohol Use Disorders Identification Test: guidelines for use in primary health care. 2001 [cited 2021 Mar 25]. https://apps.who.int/iris/handle/10665/67205
7. US Centers for Diseases Control and Prevention. Alcohol use and your health. 2021. [cited 2021 Mar 25]. https://www.cdc.gov/alcohol/fact-sheets/alcohol-use.htm
8. Alcarde AR, Souza PA, Belluco AES. Chemical profile of sugarcane spirits produced by double distillation methodologies in rectifying still. Food Sci Technol (Campinas). 2011;31:355–60. https://doi.org/10.1590/S0101-20612011000200012
9. Machado PR, Rosa MEA, Costa D, Mignac M, Silva JS, Schriefer A, et al. Reappraisal of the immunopathogenesis of disseminated leishmaniasis: in situ and systemic immune response. Trans R Soc Trop Med Hyg. 2011;105:438–44. https://doi.org/10.1016/j.trstmh.2011.05.002
10. Pasala S, Barr T, Messaoudi I. Impact of alcohol abuse on the adaptive immune system. Alcohol Res. 2015;37:185–97.
11. Parlet CP, Waldschmidt TJ, Schlueter AJ. Chronic ethanol feeding induces subset loss and hyporesponsiveness in skin T cells. Alcohol Clin Exp Res. 2014;38:1356–64. https://doi.org/10.1111/acer.12358
12. Franchi S, Sacerdote P, Moretti S, Gerra G, Leccese V, Tallone MV, et al. The effects of alcoholism pharmacotherapy on immune responses in alcohol-dependent patients. Int J Immunopathol Pharmacol. 2010;23:847–55. https://doi.org/10.1177/039463201002300320
13. Molina PE, Happel KI, Zhang P, Kolls JK, Nelson S. Focus on: alcohol and the immune system. Alcohol Res Health. 2010;33:97–108.
14. Fuchs J. Alcoholism, malnutrition, vitamin deficiencies, and the skin. Clin Dermatol. 1999;17:457–61. https://doi.org/10.1016/S0738-081X(99)00032-2
15. Cardoso T, Bezerra C, Medina LS, Ramasawmy R, Scheriefer A, Bacellar O, et al. *Leishmania braziliensis* isolated from disseminated leishmaniasis patients downmodulate neutrophil function. Parasite Immunol. 2019;41:e12620. https://doi.org/10.1111/pim.12620

Address for correspondence: Anastácio Q. Sousa, Department of Clinical Medicine, School of Medicine, Federal University of Ceará. Rua Prof. Costa Mendes, 1608–4o. andar–Rodolfo Teófilo, CEP 60.430-140, Fortaleza, Ceará, Brazil; email: aqsousa@gmail.com

Ecologic Determinants of West Nile Virus Seroprevalence among Equids, Brazil

Edmilson F. de Oliveira-Filho,[1] Carlo Fischer,[1] Beatrice Sarah Berneck,
Ianei O. Carneiro, Arne Kühne, Angelica C. de Almeida Campos, Jorge R.L. Ribas,
Eduardo Martins Netto, Carlos Roberto Franke, Sebastian Ulbert, Jan Felix Drexler

Among 713 equids sampled in northeastern Brazil during 2013–2018, West Nile virus seroprevalence was 4.5% (95% CI 3.1%–6.3%). Mathematical modeling substantiated higher seroprevalence adjacent to an avian migratory route and in areas characterized by forest loss, implying increased risk for zoonotic infections in disturbed areas.

West Nile virus (WNV) is a widely distributed arthropodborne flavivirus transmitted predominantly by *Culex* mosquitoes (*1*). Among infected persons, ≈20% show clinical signs, such as mild fever, rash, joint pain, headache, vomiting, and diarrhea (*1,2*); ≈0.7% have severe illness, such as encephalitis, meningitis, acute flaccid paralysis, respiratory failure, and even death (*1*). Beyond vectorborne transmission, transfusion-transmitted WNV infections have endangered blood safety (*3*). Equids are susceptible to WNV and develop severe disease (fatality rate ≤30%), are exposed to WNV vectors outside and in stables, and are spatially distributed near human settlements. Thus, equids can be sentinels for early detection of regional WNV activity (*4*).

In the Americas, WNV gained attention after its rapid spread in the United States beginning in 1999 (*4*). In South America, WNV dispersion is poorly understood. Seropositive horses were found in Colombia in 2004 (*5*) and in Argentina in 2006 (*6*). In Brazil, the largest country in South America, serologic studies from central, southeastern, and northeastern regions suggested WNV circulation among horses since at least 2009 (*7,8*). Human WNV infection was described only once, in 2014, from a patient in northeastern Brazil with encephalitis (*9*). In 2018, a WNV strain was isolated and sequenced during an epizootic in horses in the southeastern coast (*10*). The horse-derived virus from Brazil clustered with strains detected in different birds in the United States in 2002 and 2005 (*10*), indicating that migratory birds could play a role in WNV transmission in Brazil.

Serologic WNV data from equids along avian migratory routes are scarce. In the only available study from northeastern Brazil, 1/88 horses was WNV seropositive with a low neutralization titer (*7*). In the absence of testing for cocirculating flaviviruses, a low WNV antibody titer could be caused by infections with other flaviviruses, eliciting cross-reactive antibodies (*11*). We conducted a seroepidemiologic study among equids to investigate the spread of WNV in northeastern Brazil.

The Study

We collected serum samples from 713 equids, including horses and mules, sampled as part of routine veterinary surveillance activities during 2013–2018 in the state of Bahia in northeastern Brazil. The animal ethics committee of the Federal University of Bahia approved the sampling and analyses (authorization no. 55/2017). Sampling covered a large area that connects the location of the human case from 2014 and the 2018 horse epizootic (*9,10*). The area is adjacent to the Atlantic, northeastern, and central avian migratory routes (Figure 1).

Author affiliations: Charité-Universitätsmedizin Berlin, Berlin, Germany (E.F. de Oliveira-Filho, C. Fischer, A. Kühne, A.C. de Almeida Campos, J.F. Drexler); Fraunhofer Institute for Cell Therapy and Immunology, Leipzig, Germany (B.S. Berneck, S. Ulbert); Federal University of Bahia, Salvador, Brazil (I.O. Carneiro, E.M. Netto, C.R. Franke); Bahia State Agricultural Defense Agency, Salvador (J.R.L. Ribas); Sechenov University, Moscow, Russia (J.F. Drexler); German Centre for Infection Research, Berlin (J.F. Drexler)
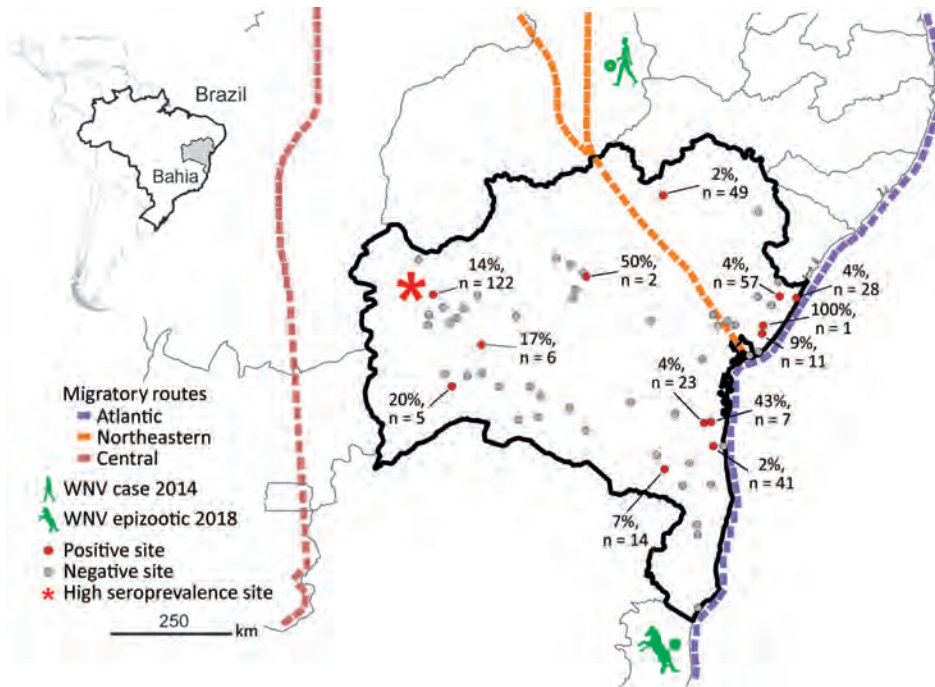
Figure 1. Geographic distribution and PRNT$_{90}$–validated West Nile virus seroprevalence among equids per sampling site in Bahia State, Brazil. Inset shows location of Bahia State in northeastern Brazil. Sample sizes are shown only for locations with seropositive animals. Avian migratory routes are based on the 2016 annual report of the Chico Mendes Institute for Biodiversity and Conservation (https://www.researchgate.net/publication/292980285_Annual_Report_of_Flyways_and_Priority_Areas_for_Migratory_Birds_in_Brazil_Relatorio_anual_de_rotas_e_areas_de_concentracao_de_aves_migratorias_no_Brasil). PRNT$_{90}$, 90% plaque-reduction neutralization tests.

Figure 2. WNV seroprevalence among equids, Brazil. A) ELISA absorbance values displayed as sample to cutoff ratio, as previously described (2). We increased the ELISA cutoff by 10% above which samples were considered positive to maximize specificity because the ELISA was not originally validated for horses in Latin America, which are infected by more Japanese encephalitis serocomplex viruses compared with horses in Europe. Dotted orange line represents the 1.1 positivity cutoff. B) Reciprocal PRNT$_{90}$ titers for WNV and other flaviviruses. Statistical significance levels were inferred by using the Kruskal-Wallis test. Bars indicate mean. Graph created by using Prism (GraphPad software, https://www.graphpad.com). C) Distinction of heterotypic serum samples based on the endpoint titers of various flaviviruses. Triangles indicated endpoint titers ≥4-fold.

titers ≥4-fold. D) Effects of forests and forest loss on WNV seropositivity and seronegativity among equids in municipalities, Brazil. Natural forest is made up of introduced or native tree or vegetation that have reproduced naturally, without help or (human) intervention. Primary forest is made up of intact and nonintact natural forest and refers to areas that reached the final stage of succession during 2013–2018. Data on primary and natural forest were retrieved from Global Forest Watch (http://www.globalforestwatch.org). Right y-axis represents number of total number of equids tested for seroprevalence. Horizontal bars indicate means. Areas below dotted line had no forest loss. BSQV, Bussuquara virus; CPCV, Cacipacoré virus; ha, hectare (10,000 m2); PRNT90, 90% plaque-reduction neutralization test; ROCV, Rocio virus; SLEV, Saint Louis encephalitis virus; WNV, West Nile virus.
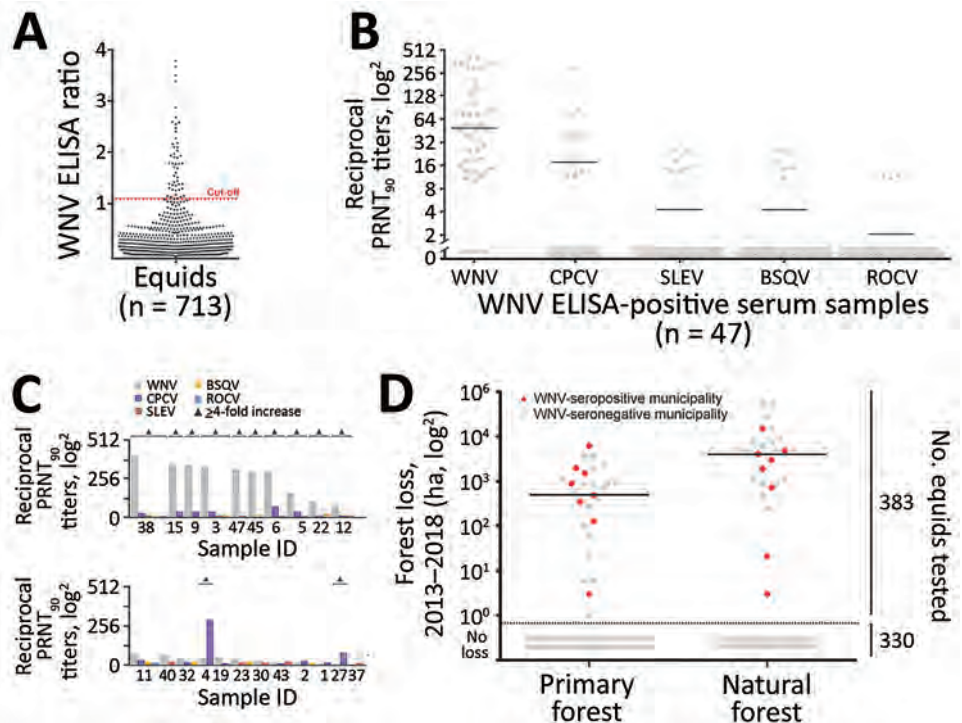
For antibody screening, we used an experimental WNV IgG ELISA based on a fusion loop envelope antigen containing mutations. We chose this ELISA to decrease the chances of cross-reactivity with antibodies elicited by other flaviviruses (2). Among 713 serum samples, 47 (6.6%, 95% CI 4.9%–8.7%) yielded positive ELISA results (Figure 2, panel A). Beyond WNV, horses in Latin America frequently are infected with Saint Louis encephalitis virus (SLEV), Cacipacoré virus (CPCV), Rocio virus (ROCV), and Bussuquara virus (BSQV) (12); and WNV, CPCV, and SLEV all belong to the Japanese encephalitis serocomplex (Appendix Figure 1, https://wwwnc.cdc.gov/EID/article/27/9/20-4706-App1.pdf). Serologic analyses for WNV-specific antibodies in horses could be compromised by cross-reactive antibodies against other flaviviruses, eliciting potentially false-positive test results (11). Therefore, we confirmed ELISA-based WNV antibody detection by comparing the endpoint titers for the 90% plaque-reduction neutralization tests ($PRNT_{90}$), considered the standard for arbovirus serologic testing, for WNV, CPCV, SLEV, BSQV, and ROCV in all 47 ELISA-positive serum samples. Of the 47 samples, 20 (44.7%) neutralized WNV only in $PRNT_{90}$; another 22 (46.8%) showed heterotypic reactions for WNV, CPCV, or SLEV (Figure 2, panel B). Averaged endpoint titers were significantly higher for WNV than for the other flaviviruses (p<0.0001) and exceeded those for CPCV, SLEV, BSQV, or ROCV by $\geq$4-fold in 12/22 heterotypic samples (Figure 2, panel C), a titer difference commonly considered decisive in flavivirus serology. Thus, 68.1% (32/47) of ELISA-positive samples had WNV-specific antibody responses (Figure 2, panel C); 4 samples were seronegative for all 5 flaviviruses by $PRNT_{90}$, potentially because of differential sensitivity of ELISA and PRNT. No samples had higher SLEV-, BSQV-, or ROCV-specific $PRNT_{90}$ titers compared with WNV, but 2 ELISA-positive samples had $\geq$4-fold endpoint titers for CPCV compared with WNV and other flaviviruses (Appendix Table 1). These findings substantiated WNV and CPCV cocirculation among equids in northeastern Brazil, which is consistent with previous data on CPCV circulation in another region of Brazil (12), and high specificity of the ELISA-based screening algorithm.

$PRNT_{90}$ validated the overall WNV seroprevalence of 4.5% (32/713 samples; 95% CI 3.1%–6.3%), which we used for downstream analyses (Table 1). We noted seropositive animals in 11/28 municipalities distributed over ≈900 km², suggesting wide geographic spread of WNV (Table 1; Figure 1). We observed a concentration of positive samples in 2018 (Appendix Figure 2), and in 1 municipality (Figure 1), comprising 9 different seropositive farms with an average seroprevalence of 13.9% (95% CI 8.3%–21.4%). Antibody levels typically decline over time after flavivirus infection (13), which might bias positivity rates of serologic tests. However, WNV-specific $PRNT_{90}$ endpoint titers were significantly lower in 2018 than in the preceding years by Mann-Whitney test (p = 0.002), excluding a bias from hypothetically more recent WNV infection in the animals sampled in 2018 (Appendix Figure 3).

We performed generalized linear model analyses and principal component analysis to compare 12 environmental, ecologic, and demographic factors potentially affecting WNV seroprevalence (Table 2; Appendix Figure 4). Anthropogenic changes of pristine habitats can increase the abundance of zoonotic pathogens (14), potentially including arboviruses like WNV (15). Indeed, the model considering forest loss, but not the model considering tree cover alone, was

Table 1. West Nile virus seroprevalence per municipality, Brazil

Municipalities	Sampling year(s)	No.	% Seroprevalence (95% CI)*
Antonio Cardoso	2015, 2016	10	0
Barreiras	2014, 2017, 2018	17	0
Caatiba	2018	19	0
Conceição do Jacuípe	2013	29	0
Conde	2013	28	3.6 (0.1–18.4)
Cotegipe	2013	11	0
Cristopolis	2013	10	0
Esplanada	2013	57	3.5 (0.4–12.1)
Eunápolis	2013, 2014	21	0
Feira de santana	2013	29	0
Formosa do Rio Preto	2013, 2017	37	0
Gongogi	2018	23	4.3 (0.1–21.9)
Ibotirama	2013	6	0
Igaporã	2013	27	0
Itabela	2013	6	0
Itabuna	2013, 2017	41	2.4 (0.1–12.9)
Itaju do Colônia	2013, 2015	6	0
Itapetinga	2018	14	7.1 (0.2–33.9)
Jaborandi	2017	5	20.0 (0.5–71.6)
Juazeiro	2013, 2017	49	2.0 (0.5–14.0)
Lauro de Freitas	2017	14	0
Mata de São João	2015, 2016, 2017	11	9.1 (0.2–41.3)
Mucuri	2013	13	0
Palmas de Monte Alto	2013	18	0
Riachão das Neves	2017, 2018	122	13.9 (8.3–21.4)
Rio Real	2013	25	0
Serra Dourada	2017	6	16.7 (0.4–64.1)
Ubaitaba	2018	7	42.9 (9.9–81.6)
Others†	2013–2018	52	3.8 (0.5–13.2)
Total	2013–2018	713	4.5 (3.1–6.3)

*Seroprevalence is based on 90% endpoint plaque-reduction neutralization tests.
†Detailed information, including municipalities with >5 serum samples, is available in Appendix Table 2 (https://wwwnc.cdc.gov/EID/article/27/9/20-4706-App2.pdf).

Table 2. Mathematical modeling of ecologic factors potentially affecting West Nile virus seroprevalence, Brazil*

Model	AIC	ΔAIC	AW	p value†	OR (95% CI)	Maximum OR difference among study sites‡	ρ§	Comment#
Distance to bird route, km								
Coastal	248.02	0.00	0.56	0.001	1.002 (1.001–1.004)	4.527	0.09	+
Northeastern	251.41	3.39	0.10	0.009	1.003 (1.001–1.006)	6.813	0.08	+
Central	252.17	4.16	0.07	0.014	0.999 (0.997–1.000)	4.545	−0.08	−
Forest loss, y/n	250.38	2.37	0.17	0.005	5.106 (1.518–31.796)	5.106	0.09	+
Presence of natural or primary forest, y/n	253.39	5.38	0.04	0.029	3.186 (1.111–13.48)	3.186	0.08	+
Altitude, m	255.53	7.51	0.01	0.105	1.002 (1.000–1.004)	3.518	0.06	+
Mean temperature, °C	258.03	10.01	0.00	0.719	0.876 (0.427–0.803)	1.613	−0.04	−
Hottest quarter	255.57	7.55	0.01	0.108	0.617 (0.347–1.113)	5.155	−0.04	−
Human density, no./km^2	255.76	7.74	0.01	0.121	1.000 (1.000–1.001)	3.137	−0.01	+
Tree cover, %	256.87	8.86	0.01	0.257	0.981 (0.941–1.012)	2.618	−0.09	−
Horse density, no./km2	258.10	10.09	0.00	0.817	0.969 (0.741–1.275)	1.170	−0.03	−
Mean precipitation, mm	258.15	10.14	0.00	0.948	1.000 (0.999–1.001)	1.047	−0.01	−

*Models are sorted by AIC, an estimator of the model's quality; models with lower AIC values are superior to models with higher AIC values. Horse and human densities were based on 2018 data available from the Brazilian Institute of Geography and Statistics (https://www.ibge.org.br). Information on precipitation and mean temperature was obtained from WorldClim version 2 (https://www.worldclim.org). Information on tree cover was obtained from Copernicus Global Land Cover (https://lcviewer.vito.be/download). Information on natural or primary forest loss was obtained from Global Forest Watch (https://www.globalforestwatch.org). AIC, Akaike information criterion; AW, Akaike weight; OR, odds ratio; ΔAIC, the difference between a given and the best-supported model in AIC.
†p values were determined by likelihood ratio tests of the different models.
‡Maximum OR difference among study sites indicates the highest OR difference possible for a given variable for better comparability between binary and nonbinary variables.
§ρ, the Spearman correlation coefficient, ranges between −1 for negative correlations and 1 for positive correlations. The closer ρ is to 1 or −1, the greater the correlation between the observed variables.
#Clarification that the observed variable is associated with an increase (+) or a decrease (−) of West Nile virus prevalence.

significantly associated with higher WNV seroprevalence (odds ratio [OR] 5.106, 95% CI 1.318–31.796; p = 0.005) (Table 2). Model results were consistent with a higher proportion of WNV-seropositive sites in disturbed areas compared with pristine areas by χ^2 test (p = 0.009) (Figure 2, panel D). Higher WNV seroprevalence in disturbed areas was not biased by the number of animals living in those sites compared to sites from pristine areas. By Student *t*-test, neither the overall number of animals nor the number of animals per site differed significantly between disturbed (p = 0.9) and pristine areas (p = 0.2894) (Figure 2, panel D; Appendix Figure 5).

Because the geographic distribution of both the 2018 horse epizootic and the only known human case might be linked geographically to the northeastern and coastal avian migratory routes (Figure 1), we included distances to avian routes in model analyses of WNV seroprevalence. Proximity to the central avian migratory route was associated with higher WNV seroprevalence (Table 2; Appendix Figure 4). This finding was consistent with other seroprevalence studies, indicating the presence of WNV in horses in the central region in Brazil (*7,8*), but failed to connect the WNV detections in Brazil to geographically adjacent avian migratory routes. Our data were consistent with prior studies of WNV ecology, but the explicatory power of our models was low despite statistical significance (Table 2; Appendix Figure 4).

Our study was limited by absence of longitudinal samples from individual sampling sites, lack of information on animal trade and animal age, and relatively low numbers of seropositive animals from individual sites. Thus, we cannot exclude biases affecting the accuracy of our modeling approach. However, our large sample and the combination of thorough serologic analyses and mathematical modeling enabled robust estimates of WNV spread that can guide prospective studies.

Conclusions
Our findings of substantial WNV seroprevalence in equids in Brazil warrants WNV surveillance in cases of acute neurologic disease in humans and horses. In addition, blood products should be screened in areas of Latin America with high risk for WNV.

About the Author

Dr. Oliveira-Filho is a virologist at the Institute of Virology, Charité Universitätsmedizin Berlin. His research interests include the epidemiology and evolution of arthropod-borne viruses from animal reservoirs. Dr. Fischer is a virologist at the Institute of Virology, Charité Universitätsmedizin Berlin. His research interests include the epidemiology of arthropod-borne viruses in humans and animal reservoirs.

References

1. Petersen LR, Brault AC, Nasci RS. West Nile virus: review of the literature. JAMA. 2013;310:308–15. https://doi.org/10.1001/jama.2013.8042
2. Rockstroh A, Moges B, Berneck BS, Sattler T, Revilla-Fernández S, Schmoll F, et al. Specific detection and differentiation of tick-borne encephalitis and West Nile virus induced IgG antibodies in humans and horses. Transbound Emerg Dis. 2019;66:1701–8. https://doi.org/10.1111/tbed.13205
3. Dodd RY, Foster GA, Stramer SL. Keeping blood transfusion safe from West Nile virus: American Red Cross experience, 2003 to 2012. Transfus Med Rev. 2015;29:153–61. https://doi.org/10.1016/j.tmrv.2015.03.001
4. Ward MP, Scheurmann JA. The relationship between equine and human West Nile virus disease occurrence. Vet Microbiol. 2008;129:378–83. https://doi.org/10.1016/j.vetmic.2007.11.022
5. Mattar S, Edwards E, Laguado J, González M, Alvarez J, Komar N. West Nile virus antibodies in Colombian horses. Emerg Infect Dis. 2005;11:1497–8. https://doi.org/10.3201/eid1109.050426
6. Morales MA, Barrandeguy M, Fabbri C, Garcia JB, Vissani A, Trono K, et al. West Nile virus isolation from equines in Argentina, 2006. Emerg Infect Dis. 2006;12:1559–61. https://doi.org/10.3201/eid1210.060852
7. Silva JR, Medeiros LC, Reis VP, Chavez JH, Munhoz TD, Borges GP, et al. Serologic survey of West Nile virus in horses from Central-West, Northeast and Southeast Brazil. Mem Inst Oswaldo Cruz. 2013;108:921–3. https://doi.org/10.1590/0074-0276130052
8. Ometto T, Durigon EL, de Araujo J, Aprelon R, de Aguiar DM, Cavalcante GT, et al. West Nile virus surveillance, Brazil, 2008-2010. Trans R Soc Trop Med Hyg. 2013;107:723–30. https://doi.org/10.1093/trstmh/trt081
9. Vieira MACS, Romano APM, Borba AS, Silva EVP, Chiang JO, Eulálio KD, et al. West Nile virus encephalitis: the first human case recorded in Brazil. Am J Trop Med Hyg. 2015;93:377–9. https://doi.org/10.4269/ajtmh.15-0170
10. Martins LC, Silva EVPD, Casseb LMN, Silva SPD, Cruz ACR, Pantoja JAS, et al. First isolation of West Nile virus in Brazil. Mem Inst Oswaldo Cruz. 2019;114:e180332. https://doi.org/10.1590/0074-02760180332
11. Fischer C, de Oliveira-Filho EF, Drexler JF. Viral emergence and immune interplay in flavivirus vaccines. Lancet Infect Dis. 2020;20:15–7. https://doi.org/10.1016/S1473-3099(19)30697-8
12. Pauvolid-Corrêa A, Campos Z, Juliano R, Velez J, Nogueira RM, Komar N. Serological evidence of widespread circulation of West Nile virus and other flaviviruses in equines of the Pantanal, Brazil. PLoS Negl Trop Dis. 2014;8:e2706. https://doi.org/10.1371/journal.pntd.0002706
13. Moreira-Soto A, de Souza Sampaio G, Pedroso C, Postigo-Hidalgo I, Berneck BS, Ulbert S, et al. Rapid decline of Zika virus NS1 antigen-specific antibody responses, northeastern Brazil. Virus Genes. 2020;56:632–7. https://doi.org/10.1007/s11262-020-01772-2
14. Gibb R, Redding DW, Chin KQ, Donnelly CA, Blackburn TM, Newbold T, et al. Zoonotic host diversity increases in human-dominated ecosystems. Nature. 2020;584:398–402. https://doi.org/10.1038/s41586-020-2562-8
15. Swaddle JP, Calos SE. Increased avian diversity is associated with lower incidence of human West Nile infection: observation of the dilution effect. PLoS One. 2008;3:e2488. https://doi.org/10.1371/journal.pone.0002488

Address for correspondence: Dr. Jan Felix Drexler, Helmut-Ruska-Haus, Institute of Virology, Campus Charité Mitte, Charitéplatz 1, 10117 Berlin, Germany; email: felix.drexler@charite.de

Association of Dromedary Camels and Camel Ticks with Reassortant Crimean-Congo Hemorrhagic Fever Virus, United Arab Emirates

Jeremy V. Camp, Pia Weidinger, Sathiskumar Ramaswamy, Dafalla O. Kannan, Babiker Mohammed Osman, Jolanta Kolodziejek, Noushad Karuvantevida, Ahmad Abou Tayoun, Tom Loney, Norbert Nowotny

We previously detected a potentially novel reassortant of Crimean-Congo hemorrhagic fever virus in camels at the largest livestock market in the United Arab Emirates. A broader survey of large mammals at the site indicated zoonotic transmission is associated with dromedaries and camel ticks. Seroprevalence in cattle, sheep, and goats is minimal.

Crimean-Congo hemorrhagic fever virus (CCHFV) is a tickborne nairovirus (order *Bunyavirales*) that is maintained primarily in *Hyalomma* ticks (Ixodidae), and various mammalian livestock serve as amplifying hosts. Humans might become infected from the bite of an infected tick or during slaughter of a viremic animal, and the infection might lead to severe viral hemorrhagic fever and death. In the Arabian Peninsula, human cases are sporadically reported and seem to be primarily associated with abattoir work (*1,2*) or nosocomial human-to-human transmissions (*3*).

CCHFV is genetically diverse and has a relatively wide geographic distribution (*4*). The virus might be introduced into nonendemic regions through commercial trading of livestock (*5*) or through phoretic transport of ticks on migratory birds (*6,7*). Comparatively little is known about the zoonotic transmission of the virus in the United Arab Emirates or whether past outbreaks were only associated with recent importations (*5*).

We previously performed a cross-sectional virologic and serologic survey of CCHFV in dromedary camels (*Camelus dromedarius*) at various sites throughout the United Arab Emirates (*8*). We found the highest transmission activity at a large livestock market, in which viral nucleic acids were detected in camel ticks (*Hyalomma dromedarii*) and camels. On the basis of partial gene sequences from the small and medium (M) RNA gene segments, the virus strain appeared to be a novel reassortant (*8*). We performed a follow-up study at the same market to test whether other livestock are involved in the transmission of CCHFV and to better characterize the virus strain.

The Study

During October 10–24, 2019, we sampled camels, cattle, goats, and sheep upon their entry to a livestock market in the emirate of Abu Dhabi, United Arab Emirates (≈24.16°N, 55.81°E) (Appendix Figure 1, https://wwwnc.cdc.gov/EID/article/27/9/21-0299-App1.pdf). All procedures were conducted as part of standard veterinary inspection required for market entry.

We obtained 5 mL of blood from each animal, separated serum by centrifugation, and stored serum at –80°C. We tested serum for CCHFV-reactive antibodies by using a commercial kit (ID Screen CCHF Double Antigen Multi-species; IDvet, https://www.id-vet.com). Antibodies to CCHFV were found in 72/90 camels, 7/51 cattle, 1/45 goats, and 4/55 sheep (Table). We extracted total nucleic acids from 200 μL of the same serum samples by using a commercial kit (QIAamp Viral RNA Mini Kit; QIAGEN, https://www.qiagen.com) and QIAcube or QIAcube

Author affiliations: Medical University of Vienna, Vienna, Austria (J.V. Camp); University of Veterinary Medicine Vienna, Vienna (J.V. Camp, P. Weidinger, J. Kolodziejek, N. Nowotny); Mohammed Bin Rashid University of Medicine and Health Sciences, Dubai, United Arab Emirates (S. Ramaswamy, N. Karuvantevida, A. Abou Tayoun, T. Loney, N. Nowotny); Al Jalila Children's Hospital, Dubai (S. Ramaswamy, A. Abou Tayoun); Al Ain City Municipality, Al Ain, United Arab Emirates (D.O. Kannan, B.M. Osman)

Table. Evidence of exposure to Crimean-Congo hemorrhagic fever virus in animals at a livestock market, United Arab Emirates, 2019

Species	No. sampled	No. antibody positive	No. virus RNA positive
Camels	90	72	2
Cattle	55	7*	0
Goats	45	1	0
Sheep	55	4	0
*Serum was not available for 4 cattle.			

HT Extraction Robots (QIAGEN). We tested extracts for CCHFV RNA by using a commercially available quantitative reverse transcription PCR (qRT-PCR) assay (RealStar CCHFV RT-PCR Kit 1.0; Altona Diagnostics, https://www.altona-diagnostics.com). Viral nucleic acids were detected in 2 of 90 camels, and in no other species at the market.

During blood collection, we thoroughly searched each animal (≈2 min) and removed attached ticks. Ticks were frozen at −80°C, and adult ticks were morphologically identified by using various keys on an ice cold plate. We collected 210 *H. dromedarii* adults, 4 unidentified *Hyalomma* sp. adults, and 4 *Hyalomma* sp. nymphs from 84/90 camels. No ticks were found on any other animal during this sampling session, and it was later confirmed that topical acaricides were routinely used for all animals except camels, where they were applied only sporadically.

We processed frozen ticks to screen for viral nucleic acids by making a parasagittal section using a sterile scalpel and then made homogenized pools containing half-ticks (≤5 per pool, pooled per tick species, and per individual host) in a bead mill in buffered saline before adding DNA/RNA Shield (ZymoResearch, https://www.zymoresearch.com) and performing nucleic acid extraction and qRT-PCR. We detected CCHFV RNA in 3 pools of *H. dromedarii* ticks taken from 2 camels, 1 of which was seropositive and the other seronegative.

We then extracted nucleic acids from the remaining halves of 3 ticks collected in the previous sampling session (April 2019) (*8*) and 2 ticks collected in this sampling session from pools that were positive by qRT-PCR. After confirming the presence of CCHFV nucleic acid in the individual tick halves, we processed the samples by using a shotgun transcriptomic sequencing approach (Appendix). In brief, we quality-filtered, trimmed, and assembled paired-end reads from Illumina (https://www.illumina.com) sequencing into scaffolds, which we then searched against the National Center for Biotechnology Information nonredundant database using blastn (https://blast.ncbi.nlm.nih.gov).

We identified near-complete genomes of CCHFV, including complete open reading frames of all but 1 gene segment (missing 577 nt from the large segment open reading frame 3′ mRNA end), from all 5 samples (GenBank accession nos. MW548490–504) (Appendix). We aligned the sequences to selected reference sequences representing the major genotypes (*4*). All sequences had high identity to each other (98.8%–100%) and to a recently described CCHFV (98.5%–99.6%) identified in a dromedary from the same livestock market in the emirate of Abu Dhabi, but 4 years earlier, during 2015 (*9*) (Appendix Table). The M segment was the most variable; it had 52–64 nonsynonymous mutations compared with the sample obtained during 2015 from the same place, and 1–40 nonsynonymous mutations among the 5 sequences (Appendix Table).

We constructed phylogenetic trees from the alignments of the respective gene segments by using maximum-likelihood analysis over 500 bootstrap replicates of the general time reversible plus invariant sites plus gamma distribution substitution model and 4 gamma categories. Small segments fit within the previously described genotype from Africa (group III sensu [4] and Africa 3 sensu [9]), and large segments had a common ancestor with sequences from Africa (groups I and III sensu [4], Africa 1/3 sensu [9]), and Europe (group V sensu [4] and Europe 1 sensu [9]) (Appendix Figures 2, 3). The M segment appeared to be a novel lineage of CCHFV (Figure).

Conclusions

We concur with the findings of Khalafalla et al. (*9*), who provided additional serologic and virologic evidence that the CCHFV strain in the United Arab Emirates might be specifically associated with camels and camel ticks. Our study differs from previous studies, in that our sampling was performed directly at entry to a livestock market, but our previous study was performed after camels had entered the market (range 0–77 d, mean 12.2 d). Moreover, all animals were raised in the United Arab Emirates, although some sheep and goats were imported as young animals from India, Saudi Arabia, and Oman. Combined, the evidence suggests that the CCHFV strain has spread throughout the United Arab Emirates, but the livestock market is also a focus of transmission (*8*).

Although this strain of CCHFV appears to be circulating at least since 2015 in the United Arab Emirates (*8,9*), there is additional evidence that it might be more widely distributed (*10*). Evidence of increased exposure of camels to CCHFV at livestock markets in contrast to other locations (e.g., private farms or in tourist/recreational use) increases the potential for the virus to be transported long

distances through the camel trade (*8*). We support the suggestion of Khalafalla et al. to increase efforts to characterize CCHFV from camels, camel ticks, and other livestock in a broader geographic region (*9*). The infection of camels appears to be systemic; virus was detected in blood (*8*; this study) and the respiratory tract (*9*). The low CCHFV-reactive seroprevalence and low tick burden on other livestock

entering the market is probably caused by use of acaricides, which are reportedly used only sporadically on camels. We therefore recommend increased vigilance, including use of acaricides on all livestock, including dromedaries, to limit spillover to humans involved in the camel trade, abattoir workers, and those handling raw meat or consuming raw camel milk.
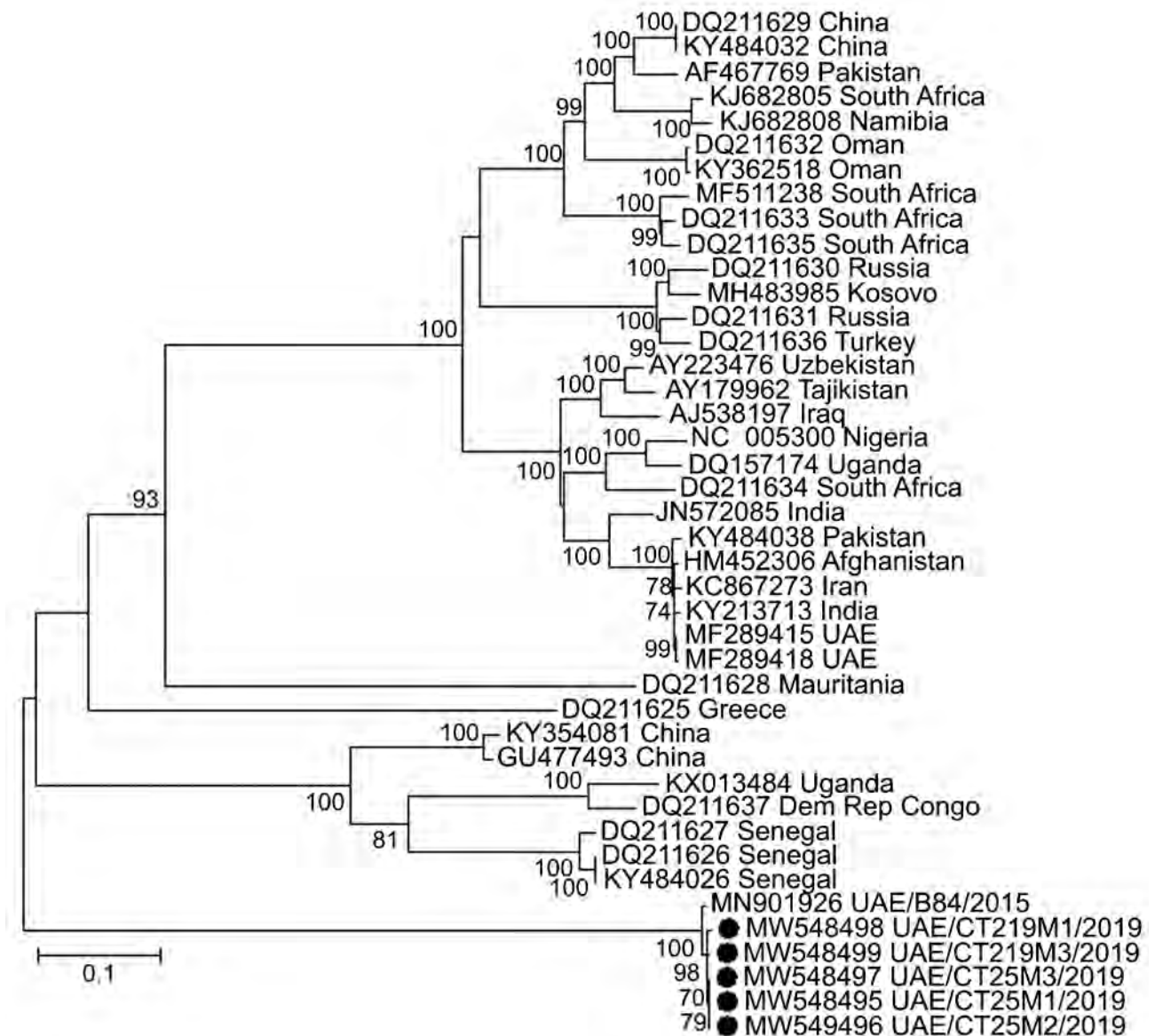
Figure. Molecular phylogeny of Crimean-Congo hemorrhagic fever virus medium RNA segments, United Arab Emirates, 2019 (solid circles), and reference viruses. Viruses from this study were obtained from camel ticks (*Hyalomma dromedarii*) removed from dromedary camels at a large livestock market in the emirate of Abu Dhabi. Other virus sequences included were selected as representatives of the major small and large RNA segment genotypes for which full-length sequences of all 3 viral genomic segments were available. Viruses listed include GenBank accession number and country of origin. Maximum-likelihood analysis of coding-complete sequences was performed by using the general time reversible plus invariant sites plus gamma distribution substitution model and 4 categories with >500 bootstrap replicates. Numbers along branches are percentage support, showing only values >65%, and branch length is relative to the number of substitutions per site, as indicated by the scale bar. Dem Rep Congo, Democratic Republic of the Congo; UAE, United Arab Emirates.

Acknowledgments

About the Author

Dr. Camp is a research virologist at the Medical University of Vienna, Vienna, Austria. His primary research interest is the ecology of emerging zoonotic and vectorborne viruses.

References

1. Al-Abri SS, Hewson R, Al-Kindi H, Al-Abaidani I, Al-Jardani A, Al-Maani A, et al. Clinical and molecular epidemiology of Crimean-Congo hemorrhagic fever in Oman. PLoS Negl Trop Dis. 2019;13:e0007100. https://doi.org/10.1371/journal.pntd.0007100
2. Khan AS, Maupin GO, Rollin PE, Noor AM, Shurie HH, Shalabi AG, et al. An outbreak of Crimean-Congo hemorrhagic fever in the United Arab Emirates, 1994–1995. Am J Trop Med Hyg. 1997;57:519–25. https://doi.org/10.4269/ajtmh.1997.57.519
3. Suleiman MN, Muscat-Baron JM, Harries JR, Satti AG, Platt GS, Bowen ET, et al. Congo/Crimean haemorrhagic fever in Dubai. An outbreak at the Rashid Hospital. Lancet. 1980;2:939–41. https://doi.org/10.1016/S0140-6736(80)92103-0
4. Deyde VM, Khristova ML, Rollin PE, Ksiazek TG, Nichol ST. Crimean-Congo hemorrhagic fever virus genomics and global diversity. J Virol. 2006;80:8834–42. https://doi.org/10.1128/JVI.00752-06
5. Rodriguez LL, Maupin GO, Ksiazek TG, Rollin PE, Khan AS, Schwarz TF, et al. Molecular investigation of a multisource outbreak of Crimean-Congo hemorrhagic fever in the United Arab Emirates. Am J Trop Med Hyg. 1997;57:512–8. https://doi.org/10.4269/ajtmh.1997.57.512
6. Negredo A, de la Calle-Prieto F, Palencia-Herrejón E, Mora-Rillo M, Astray-Mochales J, Sánchez-Seco MP, et al.; Crimean Congo Hemorrhagic Fever@Madrid Working Group. Autochthonous Crimean-Congo hemorrhagic fever in Spain. N Engl J Med. 2017;377:154–61. https://doi.org/10.1056/NEJMoa1615162
7. Capek M, Literak I, Kocianova E, Sychra O, Najer T, Trnka A, et al. Ticks of the *Hyalomma marginatum* complex transported by migratory birds into central Europe. Ticks Tick Borne Dis. 2014;5:489–93. https://doi.org/10.1016/j.ttbdis.2014.03.002
8. Camp JV, Kannan DO, Osman BM, Shah MS, Howarth B, Khafaga T, et al. Crimean-Congo hemorrhagic fever virus endemicity in United Arab Emirates, 2019. Emerg Infect Dis. 2020;26:1019–21. https://doi.org/10.3201/eid2605.191414
9. Khalafalla AI, Li Y, Uehara A, Hussein NA, Zhang J, Tao Y, et al. Identification of a novel lineage of Crimean-Congo haemorrhagic fever virus in dromedary camels, United Arab Emirates. J Gen Virol. 2021;102. https://doi.org/10.1099/jgv.0.001473
10. Chisholm K, Dueger E, Fahmy NT, Samaha HA, Zayed A, Abdel-Dayem M, et al. Crimean-Congo hemorrhagic fever virus in ticks from imported livestock, Egypt. Emerg Infect Dis. 2012;18:181–2. https://doi.org/10.3201/eid1801.111071

Address for correspondence: Norbert Nowotny, Institute of Virology, University of Veterinary Medicine Vienna, Veterinaerplatz 1, 1210 Vienna, Austria; email: norbert.nowotny@vetmeduni.ac.at

Gram-Negative Bacteria Harboring Multiple Carbapenemase Genes, United States, 2012–2019

D. Cal Ham, Garrett Mahon, Sandeep K. Bhaurla, Sam Horwich-Scholefield, Liore Klein,
Nychie Dotson, J. Kamile Rasheed, Gillian McAllister, Richard A. Stanton, Maria Karlsson,
David Lonsway, Jennifer Y. Huang, Allison C. Brown, Maroya Spalding Walters

Reports of organisms harboring multiple carbapenemase genes have increased since 2010. During October 2012–April 2019, the Centers for Disease Control and Prevention documented 151 of these isolates from 100 patients in the United States. Possible risk factors included recent history of international travel, international inpatient healthcare, and solid organ or bone marrow transplantation.

Carbapenems have been standard treatments for multidrug-resistant gram-negative bacilli infections since 1985, when they were approved for clinical use in the United States (https://www.accessdata.fda.gov/drugsatfda_docs/label/2016/050587s074lbl.pdf). Carbapenem-resistant organisms (CROs) are a growing public health concern as carbapenemase-producing CROs become more common (1). Several recent reports describe CROs carrying multiple carbapenemase genes (multi-CPOs) (2–8). We describe multi-CPOs reported to the Centers for Disease Control and Prevention (CDC; Atlanta, GA, USA) during 2012–2019.

The Study

CDC receives reports of carbapenemase-producing CROs from health departments, public health laboratories, healthcare facilities, and isolates sent to CDC for confirmatory testing. In 2016, CDC established

Author affiliations: Centers for Disease Control and Prevention, Atlanta, Georgia, USA (D.C. Ham, G. Mahon, J.K. Rasheed, G. McAllister, R.A. Stanton, M. Karlsson, D. Lonsway, J.Y. Huang, A.C. Brown, M.S. Walters); Los Angeles County Department of Public Health, Los Angeles, California, USA (S.K. Bhaurla); California Department of Public Health, Richmond, California, USA (S. Horwich-Scholefield); Maryland Department of Health, Baltimore, Maryland, USA (L. Klein); Florida Department of Health, Tallahassee, Florida, USA (N. Dotson)

the Antibiotic Resistance Laboratory Network (AR Lab Network), a national network of 55 public health laboratories that test carbapenem-resistant Enterobacterales (CRE), carbapenem-resistant *Pseudomonas aeruginosa* (CRPA), and carbapenem-resistant *Acinetobacter baumannii* (CRAB) isolates for carbapenemase genes.

We reviewed CDC and AR Lab Network reports of multi-CPOs identified during January 1, 2010–April 30, 2019. We defined a multi-CPO case as Enterobacterales, *Pseudomonas* spp., or *A. baumannii* isolated from any specimen source and carrying genes encoding >1 carbapenemase routinely tested for at CDC and the AR Lab Network (CRE, CRPA, and CRAB isolates were tested for *Klebsiella pneumoniae* carbapenemase [KPC], New Delhi metallo-β-lactamase [NDM], Verona integron-encoded metallo-β-lactamase [VIM], active-on-imipenem metallo-β-lactamase [IMP], and oxacillinase [OXA]-48–like β-lactamases; CRAB isolates also were tested for OXA-23, OXA-24/40, and OXA-58–like β-lactamases). Whole-genome sequencing (WGS) was conducted on a subset of isolates (Appendix, https://wwwnc.cdc.gov/EID/article/27/9/21-0456-App1.pdf). We defined an incident case as the first isolation of a unique organism–carbapenemase combination in each patient.

As part of routine public health investigations, health departments reviewed medical records and laboratory reports for patient demographic data and risk factors for exposure. We conducted descriptive analyses using SAS version 9.4 (https://www.sas.com) and calculated Pearson χ^2 score using SPSS Statistics 21.0 (IBM, https://www.ibm.com).

During January 2010–April 2019, a total of 151 multi-CPO isolates, including those from 105 incident cases, were identified in 100 unique patients; the first case was identified in October 2012 (Table 1; Appendix Tables 1,2). Among 89 (84.8%) incident cases

Table 1. Incident cases of gram-negative bacilli harboring multiple carbapenemase genes, United States, January 2012–April 2019*

	Carbapenemase combinations								
Organism	NDM + OXA-48–like	KPC + NDM	KPC + VIM	NDM + VIM	KPC + OXA-48–like	NDM + IMP	NDM + OXA-23	NDM + OXA-48–like + VIM	Total, N = 105
Enterobacterales	64	23	6	0	2	0	0	1	96
Citrobacter freundii	0	0	1	0	1	0	0	0	2
Enterobacter cloacae	0	8	1	0	0	0	0	0	9
Escherichia coli	17	3	0	0	0	0	0	0	20
Klebsiella aerogenes	0	0	1	0	0	0	0	0	1
K. oxytoca	0	0	1	0	0	0	0	0	1
K. pneumoniae	46	12	2	0	1	0	0	1	62
Providencia rettgeri	1	0	0	0	0	0	0	0	1
Pseudomonadales	0	0	1	4	0	2	2	0	9
Pseudomonas aeruginosa	0	0	1	3	0	2	0	0	6
Pseudomonas fluorescens	0	0	0	1	0	0	0	0	1
Acinetobacter baumannii	0	0	0	0	0	0	2	0	2

*IMP, active-on-imipenem metallo-β-lactamase; KPC, *Klebsiella pneumoniae* carbapenemase; NDM, New Delhi metallo-β-lactamase; OXA, oxacillinase; VIM, Verona integron-encoded metallo-β-lactamase.

reported since AR Lab Network testing began in 2017, a total of 15 were reported in 2017, 51 in 2018, and 23 in the first 4 months of 2019. Among the isolates tested through the AR Lab Network during 2017–2019, a total of 111/28,390 (0.391%) CRE, 5/19,609 (0.025%) CRPA, and 2/2,443 (0.082%) CRAB isolates harbored multiple carbapenemase genes; we included CRAB isolates tested only during January 2018–April 2019. Incident cases were reported in 29 US states and the District of Columbia. Enterobacterales accounted for 96 (91.4%) of the incident multi-CPO cases; in addition, 7 (6.7%) were *Pseudomonas* spp. and 2 (1.9%) were *A. baumannii*. Among 96 incident Enterobacterales cases, the most common (46; 47.9%) organism–gene combination was *K. pneumoniae* harboring bla_{NDM} and $bla_{OXA-48–like}$.

WGS was conducted on 46 isolates from incident cases, identifying 6 sequence types of *Enterobacter cloacae*, 9 of *Escherichia coli*, and 11 of *K. pneumoniae*. WGS identified 21 isolates harboring bla_{NDM-1}, 16 harboring bla_{NDM-5}, 16 harboring $bla_{OXA-181}$, and 11 harboring bla_{KPC-3} (Appendix Table 2). In total, 8 incident cases were associated with 2 separate clusters at acute care hospitals.

The median age of patients at the time of multi-CPO identification was 63 years (range 2–94 years). Among 93 incident cases with available data, 62 (66.7%) occurred in patients who had traveled internationally in the 12 months before their incident culture. Among patients with a history of international travel, most (89.5%) had received inpatient healthcare while abroad. Association with international travel varied by carbapenemase combination; among 59 incident cases with available data that harbored bla_{NDM} and $bla_{OXA-48–like}$, 47 (79.7%) occurred in patients who reported international travel; only 5/19 (26.3%; p<0.01) incident cases that harbored bla_{KPC} and bla_{NDM}

occurred in patients who reported international travel. Among the 80 incident cases with available data, 14 (17.5%) occurred in patients with a history of solid organ or bone marrow transplantation before their incident culture (Table 2).

Multi-CPOs in this convenience sample were identified in many states and included diverse organisms, sequence types, and carbapenemase gene combinations and variants, suggesting that clonal spread is not responsible for their emergence. Variants harboring bla_{KPC-4} and bla_{NDM-4}, which are uncommon in the United States, were identified (9–11). Most incident cases of CROs harboring multiple carbapenemase genes occurred in patients who had a recent history of international travel and inpatient healthcare outside the United States; we also identified history of solid organ or bone marrow transplant as a potential risk factor.

Receiving healthcare abroad and, more recently, international travel without medical care are risk factors for acquiring carbapenemase-producing organisms among patients in the United States (9). However, in this study, one third of cases occurred in persons without known recent travel outside the United States. For some carbapenemase combinations, such as isolates harboring bla_{KPC} and bla_{NDM}, most cases occurred in patients who had not recently traveled internationally. In addition, identifying facility clusters raises further concerns about dissemination of these multidrug-resistant organisms among healthcare facilities in the United States.

The emergence of multi-CPOs has clinical, laboratory testing, and public health implications. The ceftazidime/avibactam, meropenem/vaborbactam, and imipenem/cilastatin/relebactam combination therapies have increased treatment options for CREs that produce KPC and OXA-48–like carbapenemases; growth in the proportion of isolates that co-harbor

Table 2. Characteristics and exposures of incident cases of gram-negative bacilli harboring multiple carbapenemase genes, United States, January 2012–April 2019*

Characteristics and exposures	Enterobacterales† NDM + OXA-48§	KPC + NDM	KPC + VIM	KPC + OXA-48	Pseudomonas spp.,‡ KPC + VIM, NDM + VIM, or NDM + IMP	Acinetobacter baumannii, NDM + OXA-23	Total
Total no. (%) cases	65 (100.0)	23 (100.0)	6 (100.0)	2 (100.0)	7 (100.0)	2 (100.0)	105 (100.0)
Region of specimen collection¶							
South	22/65 (33.8)	9/23 (39.1)	2/6 (33.3)	0	3/7 (42.9)	1/2 (50.0)	37/105 (35.2)
West	22/65 (33.8)	3/23 (13.0)	2/6 (33.3)	0	1/7 (14.3)	0	28/105 (26.7)
Northeast	14/65 (21.5)	5/23 (21.7)	0	0	2/7 (28.6)	0	21/105 (20.0)
Midwest	7/65 (10.8)	6/23 (26.1)	2/6 (33.3)	2/2 (100.0)	1/7 (14.3)	1/2 (50.0)	19/105 (18.1)
Location of specimen collection							
Acute care hospital	51/57 (89.5)	18/22 (81.8)	3/4 (75.0)	2/2 (100.0)	5/7 (71.4)	0	79/94 (84.0)
Outpatient facility	5/57 (8.8)	1/22 (4.5)	0	0	2/7 (28.6)	1/2 (50.0)	9/94 (9.6)
Long-term acute care hospital	0	1/22 (4.5)	1/4 (25.0)	0	0	1/2 (50.0)	3/94 (3.2)
Skilled nursing facility	0	2/22 (9.1)	0	0	0	0	2/94 (2.1)
Joint acute care hospital/ inpatient rehabilitation facility	1/57 (1.8)	0	0	0	0	0	1/94 (1.1)
Hospitalization in previous 12 mo, United States#	44/56 (78.6)	19/23 (82.6)	4/5 (80.0)	2/2 (100.0)	4/7 (57.1)	2/2 (100.0)	75/95 (78.9)
International travel in previous 12 mo**							
Yes	47/59 (79.7)††	5/19 (26.3)††	1/4 (25.0)	1/2 (50.0)	7/7 (100.0)	1/2 (50.0)	62/93 (66.7)
International inpatient healthcare‡‡	40/43 (93.0)	3/4 (75.0)	0/1	0/1	6/7 (85.7)	1/1 (100.0)	51/57 (89.5)
India	29/39 (74.4)	1/3 (33.3)		1/1 (100.0)	3/6 (50.0)	1/1 (100.0)	35/50 (70.0)
Other§§	5/39 (12.8)	2/3 (66.7)		0	2/6 (33.3)	0/1	9/50 (18.0)
Pakistan	3/39 (7.7)	0/3		0/1	0/6	1/1 (100.0)	4/50 (8.0)
Egypt	2/39 (5.1)	0/3		0/1	0/6	0/1	2/50 (4.0)
Vietnam	1/39 (2.6)	0/3		0/1	1/6 (16.7)	0/1	2/50 (4.0)
No	12/59 (20.3)	14/19 (73.7)	3/4 (75.0)	1/2 (50.0)	0/7	1/2 (50.0)	31/93 (33.3)
US hospitalization	11/12 (91.7)	12/14 (85.7)	3/3 (100.0)	1/1 (100.0)		1/1 (100.0)	28/31 (90.3)
Transplant recipient¶¶	11/48 (22.9)	4/17 (23.5)	0/5	1/2 (50.0)	1/6 (16.7)	0/2	17/80 (21.3)
Before incident case	8/11 (72.7)	4/4 (100.0)		1/1 (100)	1/1 (100.0)		14/17 (82.4)
Transplant to incident case, d, median (IQR)							44 (15–446)
After incident case	3/11 (27.3)	0/4		0/1	0/1		3/17 (17.6)
Incident case to transplant, d, median (IQR)							96 (28–188)
Type of transplant##							
Solid organ	11/11 (100.0)	2/4 (50.0)		0/1	0/1		13/17 (76.5)
Kidney	7/11 (63.6)	0/2					7/13 (53.8)
Liver	3/11 (27.3)	1/2 (50.0)					4/13 (30.8)
Lung	1/11 (9.1)	1/2 (50.0)					2/13 (15.4)
Bone marrow	0/11	2/4 (50.0)		1/1 (100.0)	1/1 (100.0)		4/17 (23.5)

*Values are no. cases/total no. in category (%) except as indicated. Three incident cases occurred in 3 patients who reported no international travel or hospitalization in the United States during the previous 12 mo (1 case of *E. coli* harboring *bla*NDM and *bla*KPC, 1 case of *K. pneumoniae* harboring *bla*NDM and *bla*KPC, and 1 case of *E. coli* harboring *bla*NDM and *bla*OXA-48-like). Among these patients, 1 was a nursing home resident, 1 did not have additional information provided, and 1 had a spouse who had traveled to India and returned ≈1 mo before their incident case. Exposures are described for the 12 mo before identification of incident case. IMP, active-on-imipenem metallo-β-lactamase; KPC, *Klebsiella pneumoniae* carbapenemase; NDM, New Delhi metallo-β-lactamase; OXA, oxacillinase; VIM, Verona integron-encoded metallo-β-lactamase.
†*Citrobacter freundii*, *Enterobacter cloacae*, *Escherichia coli*, *Klebsiella aerogenes*, *K. oxytoca*, *K. pneumoniae*, and *Providencia rettgeri* isolates.
‡*Pseudomonas aeruginosa* and *Pseudomonas fluorescens* isolates.
§Includes 1 *K. pneumoniae* isolate harboring *bla*NDM, *bla*OXA-48-like, and *bla*VIM.
¶Based on census regions of residence (US Census Bureau, https://www2.census.gov/geo/pdfs/maps-data/maps/reference/us_regdiv.pdf).
#Of 90 unique patients who contributed 95 incident cases with complete data.
**Of 88 unique patients who contributed 93 incident cases with complete data.
††Significant difference; p<0.01. Exclusion of incident cases associated with an outbreak or cluster did not change this association: 47/56 (83.9%) incident cases harboring *bla*NDM and *bla*OXA-48-like occurred in patients who reported international travel, compared with 4/14 (28.6%; p<0.01) with *bla*KPC and *bla*NDM.
‡‡Two patients reported international inpatient healthcare in 2 countries.
§§One hospitalization in Bangladesh, 1 in Columbia, 1 in Iraq, 1 in Mexico, 1 in Nigeria, 1 in Tajikistan, 1 in Thailand, 1 in Turkey, and 1 in Yemen.
¶¶Solid organ or bone marrow transplants; of 75 unique patients who contributed 80 incident cases with complete data.
##Of includes 17 unique patients who contributed 17 incident cases with complete data.

bla_{NDM} jeopardizes the usefulness of these therapies. We noted 1 *P. aeruginosa* isolate harboring bla_{NDM-1} and bla_{IMP-1}; this isolate was panresistant to all antimicrobial drugs tested (*12*). A high proportion (17.5%) of cases occurred among patients with history of solid organ or bone marrow transplantation before their index culture, a population for whom CRO infections are associated with worse outcomes than patients without transplants (*13,14*). In comparison, only 3.1% of patients with CRE reported to the Multi-Site Gram-Negative Surveillance Initiative at CDC during 2012–2019 had a history of transplant before their positive culture (*15*; I. See, CDC, pers. comm., 2021 Jan 19); whether multi-CPOs are emerging in this population requires careful monitoring. Finally, hierarchical testing algorithms, in which testing is halted after detection of an initial carbapenemase, might not identify additional, less common carbapenemases (e.g., hierarchical testing might not identify bla_{VIM} in an isolate with bla_{KPC} and bla_{VIM}).

The first limitation of our analysis is that these data represent a passively reported convenience sample during a period in which multiple changes in testing practices, including the establishment of the AR Lab Network, occurred. For this reason, we cannot determine whether multi-CPOs became more common during the evaluation period. Second, CROs from patients with a history of healthcare abroad might have been selected for mechanism testing, biasing detection toward this risk factor; bias might have been more influential early in the investigation period, when testing resources were limited. Finally, this analysis did not systematically document outpatient healthcare exposures and residence in long-term care facilities, which also might be relevant sources of exposure; 1 case in this analysis was associated with invasive urologic procedures abroad (*7*).

Conclusions

Multi-CPOs in healthcare facilities are an emerging concern in the United States. Although hospitalization outside the United States was the most common risk factor, we found a substantial proportion of cases that were probably acquired in healthcare facilities in the United States. Several measures might slow further spread. First, screening patients who were recently hospitalized outside the United States can help prevent additional introductions of carbapenemase genes not commonly found in the United States. Second, molecular testing to identify carbapenemase genes should not use hierarchical algorithms. Finally, when a multi-CPO is identified, public health officials should assess for potential transmission (https://www.cdc.gov/hai/containment/guidelines.html).

About the Author

Dr. Ham is a public health physician at the National Center for Emerging and Zoonotic Infectious Diseases, Centers for Disease Control and Prevention, Atlanta, Georgia, USA. His primary research focus is antimicrobial resistance among gram-negative and gram-positive bacteria.

References

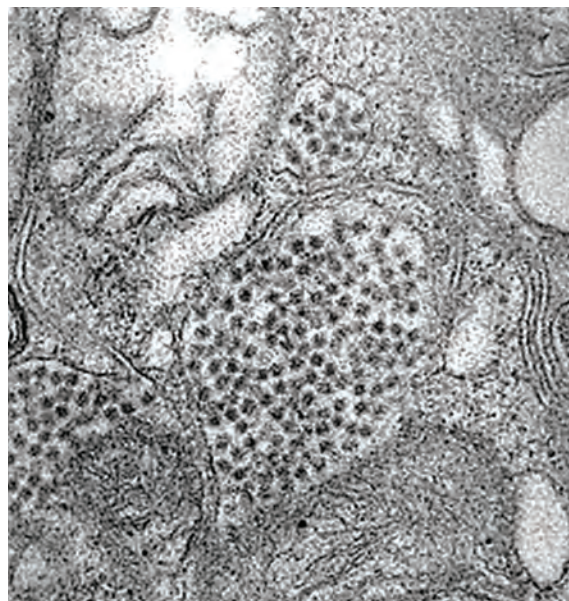1. Centers for Disease Control and Prevention. Biggest threats and data: 2019 AR threats report. 2019 [cited 2020 Oct 7]. https://www.cdc.gov/drugresistance/biggest-threats.html
2. Doi Y, O'Hara JA, Lando JF, Querry AM, Townsend BM, Pasculle AW, et al. Co-production of NDM-1 and OXA-232 by *Klebsiella pneumoniae*. Emerg Infect Dis. 2014;20:163–5. https://doi.org/10.3201/eid2001.130904

3. Jhang J, Wang HY, Yoo G, Hwang GY, Uh Y, Yoon KJ. NDM-5 and OXA-48 co-producing uropathogenic *Escherichia coli* isolate: first case in Korea. Ann Lab Med. 2018;38:277–9. https://doi.org/10.3343/alm.2018.38.3.277

4. Lyman M, Walters M, Lonsway D, Rasheed K, Limbago B, Kallen A. Notes from the field: carbapenem-resistant *Enterobacteriaceae* producing OXA-48-like carbapenemases—United States, 2010–2015. MMWR Morb Mortal Wkly Rep. 2015;64:1315–6. https://doi.org/10.15585/mmwr.mm6447a3

5. Meletis G, Chatzidimitriou D, Malisiovas N. Double- and multi-carbapenemase-producers: the excessively armored bacilli of the current decade. Eur J Clin Microbiol Infect Dis. 2015;34:1487–93. https://doi.org/10.1007/s10096-015-2379-9

6. Politi L, Gartzonika K, Spanakis N, Zarkotou O, Poulou A, Skoura L, et al. Emergence of NDM-1-producing *Klebsiella pneumoniae* in Greece: evidence of a widespread clonal outbreak. J Antimicrob Chemother. 2019;74:2197–202. https://doi.org/10.1093/jac/dkz176

7. Vannice K, Benoliel E, Kauber K, Brostrom-Smith C, Montgomery P, Kay M, et al. Notes from the field: clinical *Klebsiella pneumoniae* isolate with three carbapenem resistance genes associated with urology procedures—King County, Washington, 2018. MMWR Morb Mortal Wkly Rep. 2019;68:667–8. https://doi.org/10.15585/mmwr.mm6830a4

8. Yasmin M, Fouts DE, Jacobs MR, Haydar H, Marshall SH, White R, et al. Monitoring ceftazidime-avibactam and aztreonam concentrations in the treatment of a bloodstream infection caused by a multidrug-resistant *Enterobacter* sp. carrying both *Klebsiella pneumoniae* carbapenemase-4 and New Delhi metallo-β-lactamase-1. Clin Infect Dis. 2020;71:1095–8. https://doi.org/10.1093/cid/ciz1155

9. van Duin D, Doi Y. The global epidemiology of carbapenemase-producing *Enterobacteriaceae*. Virulence. 2017;8:460–9. https://doi.org/10.1080/21505594.2016.1222343

10. Khan AU, Maryam L, Zarrilli R. Structure, genetics and worldwide spread of New Delhi metallo-β-lactamase (NDM): a threat to public health. BMC Microbiol. 2017;17:101. https://doi.org/10.1186/s12866-017-1012-8

11. Stoesser N, Sheppard AE, Peirano G, Anson LW, Pankhurst L, Sebra R, et al. Genomic epidemiology of global *Klebsiella pneumoniae* carbapenemase (KPC)-producing *Escherichia coli*. Sci Rep. 2017;7:5917. https://doi.org/10.1038/s41598-017-06256-2

12. Lonsway DR, Bhatnagar A, Balbuena R, Stanton R, McAllister G, Halpin AL, et al. Characterization of a pan-resistant *Pseudomonas aeruginosa* containing bla_{NDM-1} and bla_{IMP-1}. ASM Microbe 2019; 2019 Jun 22; San Francisco, CA, USA.

13. Pouch SM, Satlin MJ. Carbapenem-resistant *Enterobacteriaceae* in special populations: solid organ transplant recipients, stem cell transplant recipients, and patients with hematologic malignancies. Virulence. 2017;8:391–402. https://doi.org/10.1080/21505594.2016.1213472

14. Smibert O, Satlin MJ, Nellore A, Peleg AY. Carbapenem-resistant *Enterobacteriaceae* in solid organ transplantation: management principles. Curr Infect Dis Rep. 2019;21:26. https://doi.org/10.1007/s11908-019-0679-4

15. Centers for Disease Control and Prevention. Multi-site gram-negative surveillance initiative. 2021 [cited 2021 Jan 19]. https://www.cdc.gov/hai/eip/mugsi.html

Address for correspondence: D. Cal Ham, Centers for Disease Control and Prevention, 1600 Clifton Rd NE, Mailstop A-31, Atlanta, GA 30329-4027, USA; email: ink4@cdc.gov

Hotspot of Crimean-Congo Hemorrhagic Fever Virus Seropositivity in Wildlife, Northeastern Spain

Johan Espunyes, Oscar Cabezón, Lola Pailler-García, Andrea Dias-Alves, Lourdes Lobato-Bailón, Ignasi Marco, Maria P. Ribas, Pedro E. Encinosa-Guzmán, Marta Valldeperes, Sebastian Napp

We conducted a serosurvey for Crimean-Congo hemorrhagic fever virus antibodies in various wildlife species in Catalonia, northeastern Spain. We detected high seroprevalence in southern Catalonia, close to the Ebro Delta wetland, a key stopover for birds migrating from Africa. Our findings could indicate that competent virus vectors are present in the region.

Crimean-Congo hemorrhagic fever virus (CCH-FV) is an arthropodborne *Orthonairovirus* mainly transmitted by ticks. In humans, CCHFV infection can cause severe and even fatal Crimean-Congo hemorrhagic fever (CCHF) disease (*1*). CCHFV also can infect wild and domestic mammalian species, producing viremia but causing a predominantly asymptomatic disease and such species have a role in the maintenance of the virus in the environment (*2*).

CCHFV is endemic in Africa, Asia, and eastern Europe but has more recently emerged in southwestern Europe. In 2010, CCHFV was detected in central-western Spain in *Hyalomma lusitanicum* ticks collected from red deer (*Cervus elaphus*) (*3*). In 2016, 2 autochthonous human CCHF cases were reported in Spain, 1 likely contracted through tick bite and the other caused by nosocomial transmission (*4*). Since then, 6 other CCHF clinical cases, including a retrospectively identified case from 2013, have been reported in the country, all of which are suspected

to be caused by infected ticks (*5,6*). Further surveys on ticks (*7,8*), and serologic studies in humans (*9*) and animals (*10*) have shown evidence of CCHFV circulation in several areas of central and southwestern Spain. The high genetic variability of the CCHFV strains identified in Spain, including genotypes Africa III and IV and Europe V, are indicative of repeated introductions (*7,8*). The area of CCHFV detection coincides with the region where the ecologic conditions are more favorable for the presence of *H. marginatum* and *H. lusitanicum* ticks, the main vectors of the disease. Neither of these species have been reported in northeastern Spain, but ecologic models predict the existence of areas suitable for *H. marginatum* (*11*). To evaluate possible CCHFV circulation in Catalonia, northeastern Spain, we conducted a serosurvey to detect CCHFV antibodies in different susceptible wild animal species.

The Study

Serum samples from different wildlife species were collected during 2014–2020 as part of routine wildlife surveillance in Catalonia from areas representing different ecosystems (Figures 1, 2). We tested for CCHFV antibodies in serum samples from 174 red deer, 84 Iberian ibexes (*Capra pyrenaica*), 79 roe deer (*Capreolus capreolus*), 35 European rabbits (*Oryctolagus cuniculus*), 156 wild boars (*Sus scrofa*), and 4 fallow deer (*Dama dama*) (Table 1). We used the CCHF Double Antigen Multi-species ELISA kit (IDvet, https://www.id-vet.com), which has a sensitivity of 98.9% (95% CI 96.8%–99.8%) and a specificity of 100% (95% CI 99.8%–100%) (*12*).

Because CCHFV might have been introduced in the region via ticks carried by migratory birds (*3*), we selected 226 samples from areas close to the 3 main

Author affiliations: Universitat Autònoma de Barcelona, Bellaterra, Spain (J. Espunyes, O. Cabezón, A. Dias-Alves, L. Lobato-Bailón, I. Marco, M.P. Ribas, P.E. Encinosa-Guzmán, M. Valldeperes); Centre de Recerca en Sanitat Animal, Bellaterra (O. Cabezón, L. Pailler-García, S. Napp)
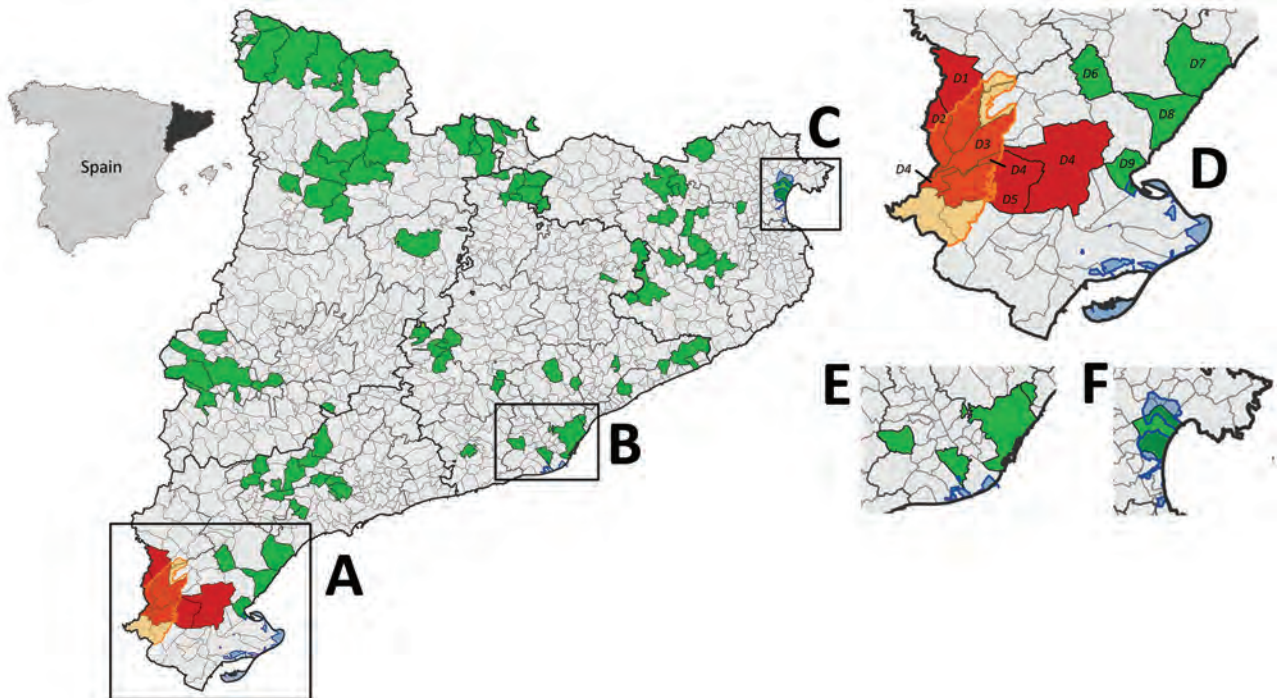
Figure 1. Distribution of areas sampled for detection of antibodies against Crimean-Congo hemorrhagic fever virus (CCHFV) in various species, Catalonia, northeastern Spain. Inset at left shows Catalonia (black) in northeastern Spain. Large map shows distribution of serosurveys throughout Catalonia: A) Ebro Delta; B) Llobregat Delta; C) Aiguamolls de l'Empordà; Enlarged areas represent regions with wetlands (blue shading), which are stopovers for migratory birds from Africa: D) Ebro Delta; E) Llobregat Delta; F) Aiguamolls de l'Empordà. Green shading indicates areas from which all samples were seronegative; red shading indicates ≥1 sample was seropositive; gray shading indicates area was not sampled; yellow shading/outline indicates location of Ports de Tortosa-Beseit National Park. Additional details are provided on CCHFV hotspots in Ebro Delta (D), which are close to and overlap wetlands and Ports de Tortosa-Beseit Natural Park. Among regions in this area, animals tested (no. positive/no. tested) included the following: D1, Iberian ibexes 10/10, wild boar 4/21; D2, Iberian ibexes 17/17, roe deer 1/1, wild boar 1/3; D3, Iberian ibexes 3/3; D4, Iberian ibexes 8/8, European rabbit 0/2; D5, Iberian ibexes 28/28, European rabbit 0/2; D6, European rabbit 0/6; D7, roe deer 0/1; D8, European rabbit 0/1; and D9, European rabbit 0/1.

points of arrival of birds from Africa: the wetlands of the Ebro Delta (n = 101); the Llobregat Delta (n = 82), in close proximity to the urban area of Barcelona; and the Aiguamolls de l'Empordà (n = 43). The remaining 306 samples were collected from municipalities throughout Catalonia.

Of 532 samples tested, CCHFV antibodies were detected in 72 animals, including Iberian ibex (66/84), roe deer (1/79), and wild boar (5/156) (Tables 1, 2). All 72 seropositive samples came from the same area in southern Catalonia, which includes 5 municipalities within or close to the Ports de Tortosa-Beseit Natural Park (Figure 1). This area is composed of rugged terrain, including canyons and ravines, and mainly is covered by a Mediterranean forest dominated by oaks, pines, and dense shrubland. This natural area is located a few kilometers from the Ebro Delta, one of the main wetlands in Spain and a key stopover for birds migrating from Africa to Europe. Thus, CCHFV introduction

via infected ticks transported by migrating birds seems plausible.

The 66 Iberian ibexes tested in the affected area during 2017–2019, and 1/2 roe deer sampled in 2019, were CCHFV-positive, indicating high seroprevalence in the area since at least 2017. A 2018 serosurvey in wild ruminants also found a high seroprevalence (79%) in some areas of central Spain known to have *Hyalomma* ticks but where CCHFV had not been detected previously (*10*). In contrast, of 24 wild boars sampled from affected municipalities during 2017–2020, only 5 (20.8%) were seropositive. Reasons for the difference in seroprevalence between Iberian ibexes and wild boars are not clear and will require additional studies. One possible explanation would be that adult *Hyalomma* ticks feed preferentially on the family Bovidae (*13*); high seroprevalences frequently are observed in Spain among domestic goats (*Capra aegagrus hircus*), a closely related species (*10*). European rabbits tested
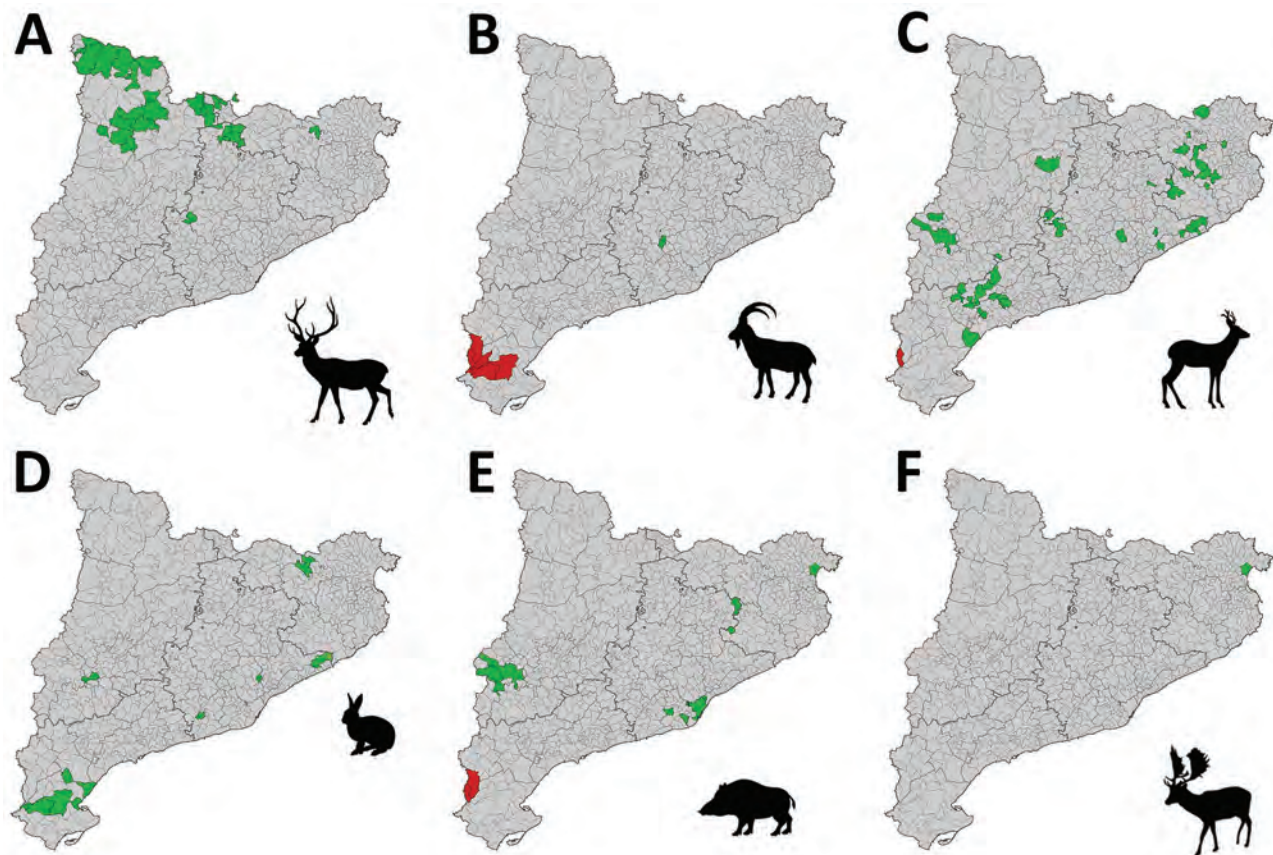
Figure 2. Distribution of areas sampled for detection of antibodies against Crimean-Congo hemorrhagic fever virus CCHFV by species, Catalonia, northeastern Spain. Green indicates all samples were seronegative; red indicates ≥1 sample was seropositive; gray indicates areas not sampled. A) Red deer (*Cervus elaphus*); B) Iberian ibex (*Capra pyrenaica*); C) roe deer (*Capreolus capreolus*); D) European rabbit (*Oryctolagus cuniculus*); E) wild boar (*Sus scrofa*); F) fallow deer (*Dama dama*).

in the affected area were seronegative (Table 2); however, they were sampled in 2016 when CCHFV might not have been introduced or might have been at lower levels. No CCHFV antibodies were detected in red deer or fallow deer, but in the areas where they were sampled, seropositivity was not detected in any of the other susceptible species either (Figure 2).

Conclusions

Detection of CCHFV antibodies among animals in southern Catalonia implies the availability of competent vectors, most likely *H. marginatum* ticks; however, presence of *H. marginatum* ticks in the area and on the host species will need to be confirmed. The range of *H. marginatum* ticks is expanding in Europe; permanent populations have been reported in southern France (*14*). This expansion probably is influenced by the density of wild ungulates, from which adult *H. marginatum* ticks feed, and leporids, from which immature ticks feed. In Catalonia, increasing populations of rabbits and wild ungulates, including wild boar, roe deer, and fallow deer, have

Table 1. Distribution of samples tested for the presence of antibodies against CCHFV among various mammalian species, Catalonia, Spain*

Species	2014–2016	2017	2018	2019	2020	Total
Red deer	0/13 (0%–28%)	0/60 (0%–1%)	0/15 (0%–3%)	0/29 (0%–15%)	0/57 (0%–8%)	0/174 (0%–3%)
Iberian ibex		15/15 (75%–100%)	5/5	46/46 (90%–100%)	0/18 (0%–22%)	66/84 (68%–87%)
Roe deer		0/1	0/1	1/59 (0%–10%)	0/18 (0%–22%)	1/79 (0%–8%)
European rabbit	0/21 (0%–19%)	0/11 (0%–32%)	0/3			0/35 (0%–12%)
Wild boar		1/87 (0%–7%)	3/3		1/48 (0%–13%)	5/156 (1%–8%)
Fallow deer				0/4		0/4
Total	0/34 (0%–13%)	16/174 (6%–15%)	8/27 (15%–50%)	47/156 (23%–38%)	1/141 (0%–5%)	72/532 (11%–17%)

*Data are no. positive/no. tested (95% CI for percentage CCHFV positive). CCHFV, Crimean-Congo hemorrhagic fever virus.

Table 2. Distribution of samples tested for the presence of antibodies against CCHFV among various mammalian species, Ebro Delta area, Spain*

Species	2014–2016	2017	2018	2019	2020	Total
Iberian ibex		15/15 (75%–100%)	5/5	46/46 (90%–100%)		66/66 (93%–100%)
Roe deer				1/2		1/2
European rabbit	0/11 (0%–32%)					0/11 (0%–32%)
Wild boar		1/1	3/3	0/18 (0%–22%)	1/2	5/24 (8%–43%)
Total	0/11 (0%–32%)	16/16 (76%–100%)	8/8 (60%–100%)	47/66 (59%–81%)	1/2	72/103 (60%–78%)

*Data are no. positive/no. tested (95% CI for percentage CCHFV positive). CCHFV, Crimean-Congo hemorrhagic fever virus.

required management measures to control their populations in recent years (*15*).

Besides southern Catalonia, samples from other areas evaluated in this study were seronegative. Whether seronegativity results from the absence of competent vectors or the absence of CCHFV is unclear, but defining seronegative and seropositive areas will be key in assessing risk for CCHFV transmission in the Mediterranean ecologic region. Further serosurveys to identify amplifying hosts and reservoirs of CCHFV in this ecologic region could help determine whether additional prevention measures against zoonotic transmission are needed in the area. Moreover, detecting the virus in hosts or vectors from the affected area and phylogenetic studies could clarify the origin of CCHFV in Catalonia. Risk for further introduction of CCHFV via migratory birds or expansion from the currently affected area to unaffected areas underscore the need for continued CCHF disease surveillance in Catalonia.

About the Author
Dr. Espunyes is a researcher at the Wildlife Conservation Medicine Research Group (WildCoM), Departament de Medicina i Cirurgia Animals, Universitat Autònoma de Barcelona, Spain. His current research focuses on emerging diseases in wildlife species.

References
1. Bente DA, Forrester NL, Watts DM, McAuley AJ, Whitehouse CA, Bray M. Crimean-Congo hemorrhagic fever: history, epidemiology, pathogenesis, clinical syndrome and genetic diversity. Antiviral Res. 2013;100:159–89. https://doi.org/10.1016/j.antiviral.2013.07.006
2. Spengler JR, Estrada-Peña A, Garrison AR, Schmaljohn C, Spiropoulou CF, Bergeron É, et al. A chronological review of experimental infection studies of the role of wild animals and livestock in the maintenance and transmission of Crimean-Congo hemorrhagic fever virus. Antiviral Res. 2016;135:31–47. https://doi.org/10.1016/j.antiviral.2016.09.013
3. Estrada-Peña A, Palomar AM, Santibáñez P, Sánchez N, Habela MA, Portillo A, et al. Crimean-Congo hemorrhagic fever virus in ticks, southwestern Europe, 2010. Emerg Infect Dis. 2012;18:179–80. https://doi.org/10.3201/eid1801.111040
4. Negredo A, de la Calle-Prieto F, Palencia-Herrejón E, Mora-Rillo M, Astray-Mochales J, Sánchez-Seco MP, et al.; Crimean Congo Hemorrhagic Fever@Madrid Working Group. Autochthonous Crimean-Congo Hemorrhagic fever in Spain. N Engl J Med. 2017;377:154–61. https://doi.org/10.1056/NEJMoa1615162
5. Portillo A, Palomar AM, Santibáñez P, Oteo JA. Epidemiological aspects of Crimean-Congo hemorrhagic fever in western Europe: what about the future? Microorganisms. 2021;9:649. https://doi.org/10.3390/microorganisms9030649
6. Negredo A, Sánchez-Ledesma M, Llorente F, Pérez-Olmeda M, Belhassen-García M, González-Calle D, et al. Retrospective identification of early autochthonous case of Crimean-Congo hemorrhagic fever, Spain, 2013. Emerg Infect Dis. 2021;27:1754–6. https://doi.org/10.3201/eid2706.204643
7. Negredo A, Habela MÁ, Ramírez de Arellano E, Diez F, Lasala F, López P, et al. Survey of Crimean-Congo hemorrhagic fever enzootic focus, Spain, 2011–2015. Emerg Infect Dis. 2019;25:1177–84. https://doi.org/10.3201/eid2506.180877
8. Moraga-Fernández A, Ruiz-Fons F, Habela MA, Royo-Hernández L, Calero-Bernal R, Gortazar C, et al. Detection of new Crimean-Congo haemorrhagic fever virus genotypes in ticks feeding on deer and wild boar, Spain. Transbound Emerg Dis. 2021;68:993–1000. https://doi.org/10.1111/tbed.13756
9. Monsalve Arteaga L, Muñoz Bellido JL, Vieira Lista MC, Vicente Santiago MB, Fernández Soto P, Bas I, et al. Crimean-Congo haemorrhagic fever (CCHF) virus-specific antibody detection in blood donors, Castile-León, Spain, summer 2017 and 2018. Euro Surveill. 2020;25:1900507. https://doi.org/10.2807/1560-7917.ES.2020.25.10.1900507
10. Ministry of Health, Consumption and Social Welfare. Report on the situation and evaluation of the risk of transmission of the Crimean-Congo hemorrhagic fever virus in Spain, July 2019 [in Spanish] [cited 2021 May 2]. https://www.mscbs.gob.es/profesionales/saludPublica/ccayes/analisisituacion/doc/ER_FHCC.pdf
11. Fernández-Ruiz N, Estrada-Peña A. Towards new horizons: climate trends in Europe increase the environmental suitability for permanent populations of *Hyalomma marginatum* (Ixodidae). Pathogens. 2021;10:95. https://doi.org/10.3390/pathogens10020095
12. Sas MA, Comtet L, Donnet F, Mertens M, Vatansever Z, Tordo N, et al. A novel double-antigen sandwich ELISA for the species-independent detection of Crimean-Congo hemorrhagic fever virus-specific antibodies. Antiviral Res. 2018;151:24–6. https://doi.org/10.1016/j.antiviral.2018.01.006

13. Spengler JR, Estrada-Peña A. Host preferences support the prominent role of *Hyalomma* ticks in the ecology of Crimean-Congo hemorrhagic fever. PLoS Negl Trop Dis. 2018; 12:e0006248. https://doi.org/10.1371/journal.pntd.0006248

14. Vial L, Stachurski F, Leblond A, Huber K, Vourc'h G, René-Martellet M, et al. Strong evidence for the presence of the tick *Hyalomma marginatum* Koch, 1844 in southern continental France. Ticks Tick Borne Dis. 2016;7:1162–7. https://doi.org/10.1016/j.ttbdis.2016.08.002

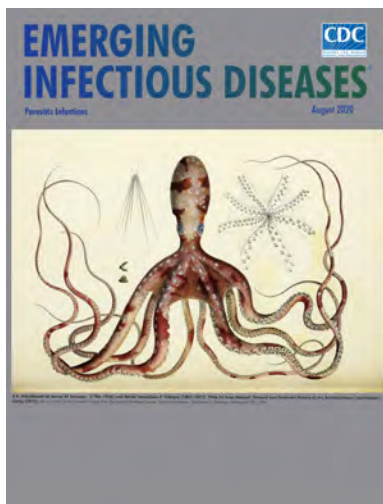15. Department of Agriculture, Livestock, Fisheries and Food. Damage and risk prevention plan originated by hunting fauna (2017–2018) [in Catalan] [cited 2021 May 2]. http://agricultura.gencat.cat/web/.content/01-departament/plans-programes-sectorials/enllacos-documents/fitxers-binaris/pla-prevencio-danys-riscos-originats-fauna-cinegetica-2017-2018.pdf

Address for correspondence: Oscar Cabezón, Wildlife Conservation Medicine Research Group (WildCoM), Departament de Medicina i Cirurgia Animals, Universitat Autònoma de Barcelona, 08193 Bellaterra, Spain; email: oscar.cabezon@uab.cat

August 2020
Parasitic Infections

- Association of Dengue Virus and *Leptospira* Co-Infections with Malaria Severity

- US CDC Real-Time Reverse Transcription PCR Panel for Detection of Severe Acute Respiratory Syndrome Coronavirus 2

- Coronavirus Disease Outbreak in Call Center, South Korea

- Investigation and Serologic Follow-Up of Contacts of an Early Confirmed Case-Patient with COVID-19, Washington, USA

- Characteristics and Outcomes of Coronavirus Disease Patients under Nonsurge Conditions, Northern California, USA, March–April 2020

- Tuberculosis in Internationally Displaced Children Resettling in Harris County, Texas, USA, 2010–2015

- Epidemiology of Legionnaires' Disease, Hong Kong, China, 2005–2015

- Rise in Babesiosis Cases, Pennsylvania, USA, 2005–2018

- Sporadic Creutzfeldt-Jakob Disease among Physicians, Germany, 1993–2018

- Analysis of MarketScan Data for Immunosuppressive Conditions and Hospitalizations for Acute Respiratory Illness, United States

- CrAssphage as a Novel Tool to Detect Human Fecal Contamination on Environmental Surfaces and Hands

- Evaluating the Effectiveness of Social Distancing Interventions to Delay or Flatten the Epidemic Curve of Coronavirus Disease

- Presence of Segmented Flavivirus Infections in North America

- Population Genomic Structure and Recent Evolution of *Plasmodium knowlesi*, Peninsular Malaysia

- Human Outbreak of *Trichinellosis* Caused by *Trichinella papuae* Nematodes, Central Kampong Thom Province, Cambodia

- Increased Sensitivity of *Plasmodium falciparum* to Artesunate/Amodiaquine Despite 14 Years as First-Line Malaria Treatment, Zanzibar

- Factors Associated with Prescription of Antimicrobial Drugs for Dogs and Cats, United Kingdom, 2014–2016

- Linezolid-Associated Neurologic Adverse Events in Patients with Multidrug-Resistant Tuberculosis, France

- Naturally Acquired Human *Plasmodium cynomolgi* and P. knowlesi Infections, Malaysian Borneo

- Characterizing Norovirus Transmission from Outbreak Data, United States

- Imported Monkeypox, Singapore

- Population-Based Estimates of Chronic Conditions Affecting Risk for Complications from Coronavirus Disease, United States

- Prolonged Persistence of SARS-CoV-2 RNA in Body Fluids

- Prognostic Value of Leukocytosis and Lymphopenia for Coronavirus Disease Severity

- SARS-CoV-2 Phylogenetic Analysis, Lazio Region, Italy, February–March 2020

- Plasma-Derived Extracellular Vesicles as Potential Biomarkers in Heart Transplant Patient with Chronic Chagas Disease

- Spread of Multidrug-Resistant Bacteria by Moth Flies from Hospital Waste Water System

- Disseminated *Echinococcus multilocularis* Infection without Liver Involvement in Child, Canada, 2018

- Canine *Dracunculus* Nematode Infection, Toledo, Spain

- *Leishmania donovani* Infection with Atypical Cutaneous Manifestations, Himachal Pradesh, India, 2014–2018

- Doxycycline and Sitafloxacin Combination Therapy for Treating Highly Resistant *Mycoplasma genitalium*

EMERGING INFECTIOUS DISEASES®

To revisit the August 2020 issue, go to:
https://wwwnc.cdc.gov/eid/articles/issue/26/8/table-of-contents

Ongoing High Incidence and Case-Fatality Rates for Invasive Listeriosis, Germany, 2010–2019

Hendrik Wilking, Raskit Lachmann, Alexandra Holzer, Sven Halbedel, Antje Flieger, Klaus Stark

We used 10 years of surveillance data to describe listeriosis frequency in Germany. Altogether, 5,576 cases were reported, 91% not pregnancy associated; case counts increased over time. Case-fatality rate was 13% in non–pregnancy-associated cases, most in adults ≥65 years of age. Detecting, investigating, and ending outbreaks might have the greatest effect on incidence.

Listeria monocytogenes infections are primarily foodborne and cause gastrointestinal disease or invasive syndromes among infected persons (*1*). Because *L. monocytogenes* is an intracellular pathogen and because invasive listeriosis is the primary manifestation in diagnosed listeriosis, persons with deficient cell-mediated immunity are at increased risk for its symptoms, including sepsis and meningitis. In addition, infection during pregnancy can lead to chorioamnionitis and fetal infection that can result in miscarriage and stillbirth even 2 months after the mother is exposed. One study found that 44% of patients with non–pregnancy-associated (NPA) listeriosis in Germany had received immunosuppressive therapy ≤3 months before illness onset and another 28% had a coexistent immunocompromising illness, such as diabetes (*2*). Testing for bacteria in blood cultures or cerebrospinal fluid (CSF) is recommended for diagnosis.

Listeria is ubiquitous in the environment and can produce biofilms in the food production environment and thus contaminate ready-to-eat (RTE) products, which are typically consumed raw or without further processing. *Listeria* species grow during shelf life, even at low temperatures, and multiply to concentration levels that make invasive listeriosis and outbreaks more likely. For these reasons, it is suspected that *L. monocytogenes* exposure is very common but the disease rare. However, in recent years several large outbreaks have been reported in Germany (*3–7*).

The Study

We analyzed mandatory notification data about invasive listeriosis cases in Germany during 2010–2019 to describe time trends, case-fatality rates, demographic distribution, clinical and diagnostic characteristics, and geographic trends (Appendix, https://wwwnc.cdc.gov/EID/article/27/9/21-0068-App1.pdf). In total, 5,576 listeriosis cases were reported during the 10-year study period; 5,064 (91%) of those were NPA and 486 (9%) were pregnancy associated, 241 in mothers and 245 in newborns. Information on disease manifestation was not transmitted for 26 cases. The lowest annual incidence was in 2011 (0.41/100,000 residents) and the highest in 2017 (0.93/100,000 residents); the average for 2010–2019 was 0.69/100,000 residents. We observed a steady increase in cases during 2011–2017, but incidence in 2019 was lower than in previous years. Exceptionally high numbers were reported in the third quarters of 2016, 2017, and 2018 (Figure 1).

Among the 5,064 NPA listeriosis case-patients, 2,032 (40%) were female and 3,855 (76%) were ≥65 years of age (Table 1). Listeriosis among adolescents and children other than newborns is rare (37 cases). Incidence in adults 18–44 years of age is <0.1/100,000 residents, in contrast with incidence among adults ≥85 years of age: 3.99/100,000 residents for men and 2.08/100,000 residents for women. Annual median age of case-patients increased steadily from 72 years of age in 2010 to 77 years of age in 2019.

Sources for testing samples included CSF (657, 13%), blood (4,097, 81%), and material from other usually sterile sites (274, 5%) (Table 2). A significantly higher proportion of *L. monocytogenes* was detected in CSF among adults 18–64 years of age (24%) than among those ≥65 years of age (9%) (p<0.01; for most

Author affiliations: Department for Infectious Disease Epidemiology of the Robert Koch Institute, Berlin, Germany (H. Wilking, R. Lachmann, A. Holzer, K. Stark); Department for Infectious Diseases of the Robert Koch Institute, Wernigerode, Germany (S. Halbedel, A. Flieger)
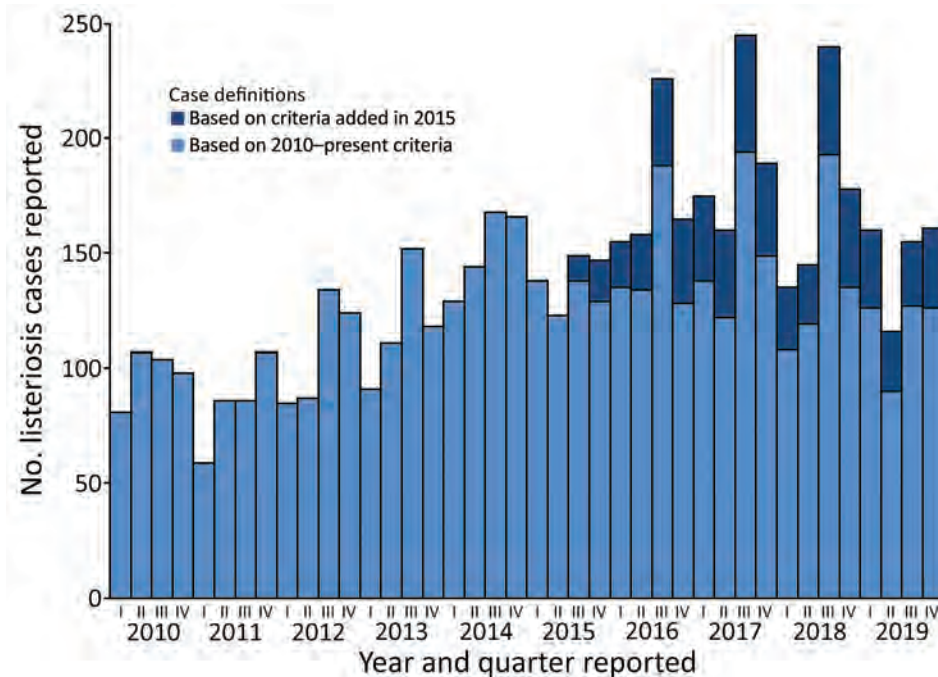
Figure 1. Distribution of pregnancy-associated and non–pregnancy-associated listeriosis cases, by year and quarter, Germany, 2010–2019 (n = 5,576). In the x-axis labels, I corresponds to January–March, II to April–June, III to July–September, and IV to October–December. Before the third quarter of 2015, two groups of patients were not included in the reference definition: those with unknown or unfulfilled clinical criteria and those with nucleic acid detection only. Data from these groups are displayed separately to make the changes in trends over time more apparent.

case-patients ≥65 years of age, the isolate was detected from blood. Most NPA case-patients (95%) were hospitalized; we found no differences among age groups (p = 0.689). Altogether, 658 NPA case-patients have been reported deceased. The case-fatality rate for NPA cases was 13%, significantly higher among patients ≥65 years of age (14%) than among those 18–64 years of age (10%; p<0.001). Listeriosis was the main cause of death for 324 (49%) of NPA case-patients and a contributing factor for 280 (43%). NPA case-fatality rates increased over the 10-year study period, but mainly because of an increase in listeriosis case-patients who died from causes other than listeriosis (Figure 2). For 54 (8%) deceased case-patients, cause-of-death information was missing. Of 301 pregnancy-associated cases, 50% were confirmed from blood

cultures and 54% from samples of newborn, stillborn, or maternal tissues (in some cases, both). A total of 32 fetal losses and 26 neonatal deaths resulted in a case-fatality rate of 19% for pregnancy-associated cases.

Conclusions

The aging of the population of Germany as a result of demographic shifts that will continue in the coming years may partially explain the increase in listeriosis cases and the median age of patients. In addition, factors related to the foodborne nature of the disease and an increase in exposure to *Listeria* must be presumed; it is possible that people eat more RTE food or that RTE food is more likely to become contaminated, although only single-case findings of *L. monocytogenes* >100 CFU/g have been detected in RTE foods in recent years (*8*).

Table 1. Average annual incidence of notified cases of non–pregnancy-associated listeriosis, by age and gender, Germany, 2010–2019*

Patient age, y	No. male case-patients	Incidence among male case-patients	No. female case-patients	Incidence among female case-patients	Overall no. cases	Overall incidence
Total	3,029	0.74	2,032	0.48	5,061	0.61
≤17	15	0.02	22	0.03	37	0.03
18–44	84	0.06	87	0.07	171	0.06
45–49	56	0.21	37	0.14	93	0.18
50–54	120	0.35	68	0.20	188	0.28
55–59	195	0.58	100	0.30	295	0.44
60–64	280	1.01	145	0.51	425	0.75
65–69	389	1.68	207	0.81	596	1.23
70–74	509	2.96	295	1.51	804	2.19
75–79	612	3.53	371	1.73	983	2.54
80–84	452	3.30	369	1.92	821	2.49
≥85	317	3.99	331	2.08	648	2.71

*Incidence is given as no. cases/100,000 residents.

Table 2. Clinical characteristics of notified cases of invasive listeriosis, Germany, 2010–2019*

Characteristic	Pregnancy-associated, no. (%) cases	Non–pregnancy-associated, no. (%) cases			
		Children/adolescents <18 y	Adults 18–64 y	Adults ≥65 y	Total
Total	301 (100)	37 (100)	1,172 (100)	3,855 (100)	5,064 (100)
Sex					
F	301 (100)	22 (59)	437 (37)	1,573 (41)	2,032 (40)
M	0				
Isolate source†					
Cerebrospinal fluid	6 (2)	21 (57)	277 (24)	359 (9)	657 (13)
Blood	152 (50)	15 (41)	800 (68)	3,282 (85)	4,097 (81)
Other sterile site	NA	1 (3)	87 (7)	186 (5)	274 (5)
Birth setting‡	162 (54)	NA	NA	NA	NA
Severity					
Hospitalization§	253 (84)	36 (97)	1,064 (95)	3,535 (95)	4,635 (92)
Death or fetal loss¶	58 (19)	0# (0)	113# (10)	545# (14)	658# (13)

*NA, not applicable
†When *Listeria monocytogenes* is isolated from multiple anatomic sites, only a single site is reported (priority order: cerebral spinal fluid, blood, other sterile site, and birth setting).
‡Either from a newborn, fetus, stillborn or from maternal tissue (placental tissue, uterus, cervix).
§Hospitalizations among singleton neonates for 224 pregnancy-associated cases.
¶26 neonatal deaths, 32 fetal losses. Among all pregnancy-associated cases 161 premature births were recorded.
#Information available for 4,989/5,064 (99%) of notified cases.

The additional case numbers in some quarters of the year (Figure 1) were all associated with large-scale outbreaks (*3,6*). Successfully identifying and controlling large outbreaks, especially after whole-genome sequencing–based surveillance was introduced, possibly explains why the trend in increases ended after 2017 (*9*). Overall listeriosis incidence in Germany is higher than in all neighboring countries except Denmark (*10*). In Europe, incidence is generally higher in countries in Scandinavia and the Baltic region and lower in the United Kingdom and Ireland (*10*).

As is the case for other pathogens, listeriosis surveillance results in underascertainment, although it is difficult to quantify by how much. *Listeria* sepsis cannot be clinically distinguished from other bacterial sepsis, and isolating *Listeria* or detecting DNA from blood samples is often impossible because bacteremia is absent or intermittent. In addition, laboratory diagnostic testing is often not performed after abortions or stillbirths or for persons who are found dead.

Listeriosis has one of the highest case-fatality rates among notifiable infectious diseases. The case-fatality rate for Germany in this study is surprisingly lower than that for Europe overall, 15.6% (*10*), and for the United States, 21% (*11*). A cohort study in France reported a 3-month death rate of 45% for bacteremia from *Listeria* infection and 30% for neurolisteriosis cases (*12*). Lower rates may be partially explained by well-equipped intensive care units, but it is more likely that many deaths occurring long after original disease notifications were not reported to public health departments.

Of interest, surveillance data from the United States indicate more listeriosis among women and higher proportions of pregnancy-associated cases (*11,13*) than in our study. One explanation might be that, in Germany, meat products, more often eaten by men, constitute prominent outbreak vehicles (*3,4,6,7*), whereas in the United States several outbreaks were caused by nonanimal products or cheese (*11*).
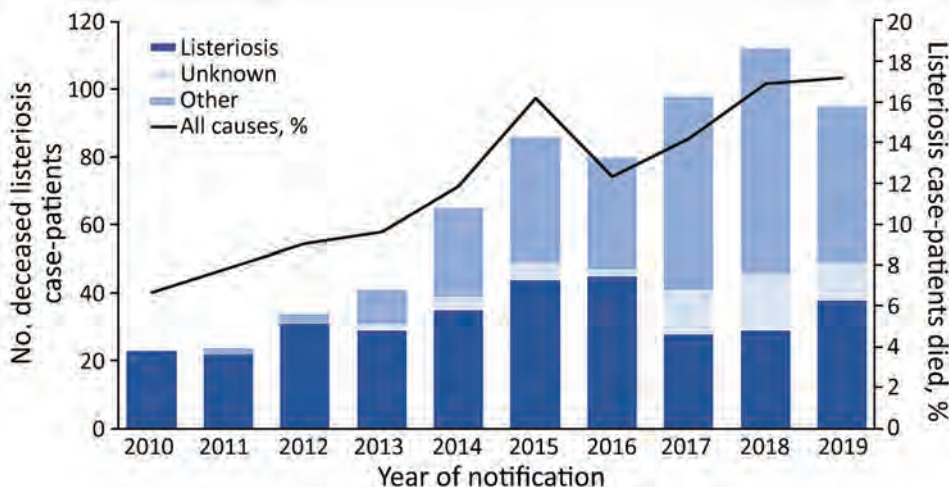

Figure 2. Distribution of non–pregnancy-associated listeriosis cases (n = 5,061) in which the patients died (n = 658) and case-fatalities by year and cause of death, Germany, 2010–2019. Black line indicates percentage of infected persons who died.

Systematic whole-genome sequence typing of *Listeria* isolates from patients would aid in detecting and investigating outbreaks. These molecular data should be integrated into surveillance data from cases notifications and isolates found in food. Combining data from molecular surveillance with epidemiologic investigations would help systematically identify and eliminate contaminated sources, which might have the greatest effect on reducing the overall burden of listeriosis and thus flattening its high incidence curve. Two factors interact to have the greatest influence on personal risk profiles. Listeriosis is highly associated with age, which is affirmed in our study, and strongly associated with documented immunosuppressive conditions (2). Persons with these risk profiles should be targeted in information campaigns about how to safely consume RTE foods and avoid certain types of cheeses, meat products, and smoked or graved (cured) fish products. All food producers, and especially those providing food for immunocompromised patients in healthcare facilities, should take steps to minimize *L. monocytogenes* hazards when producing, selecting, and preparing food.

Acknowledgment

About the Author

Dr. Wilking is an epidemiologist and deputy head of the Unit for Gastrointestinal Infections, Zoonoses and Tropical Infections at Robert Koch Institute in Berlin, Germany. He has a strong interest in foodborne diseases.

References

1. Allerberger F, Wagner M. Listeriosis: a resurgent foodborne infection. Clin Microbiol Infect. 2010;16:16–23. https://doi.org/10.1111/j.1469-0691.2009.03109.x
2. Preußel K, Milde-Busch A, Schmich P, Wetzstein M, Stark K, Werber D. Risk factors for sporadic non-pregnancy associated listeriosis in Germany—immunocompromised patients and frequently consumed ready-to-eat products. PLoS One. 2015;10:e0142986. https://doi.org/10.1371/journal.pone.0142986
3. Halbedel S, Wilking H, Holzer A, Kleta S, Fischer MA, Lüth S, et al. Large nationwide outbreak of invasive listeriosis associated with blood sausage, Germany, 2018–2019. Emerg Infect Dis. 2020;26:1456–64. https://doi.org/10.3201/eid2607.200225
4. Kleta S, Hammerl JA, Dieckmann R, Malorny B, Borowiak M, Halbedel S, et al. Molecular tracing to find source of protracted invasive listeriosis outbreak, southern Germany, 2012–2016. Emerg Infect Dis. 2017;23:1680–3. https://doi.org/10.3201/eid2310.161623
5. Lachmann R, Halbedel S, Adler M, Becker N, Allerberger F, Holzer A, et al. Nationwide outbreak of invasive listeriosis associated with consumption of meat products in health care facilities, Germany, 2014–2019. Clin Microbiol Infect. 2021;27:1035.e1–5. https://doi.org/10.1016/j.cmi.2020.09.020
6. Lüth S, Halbedel S, Rosner B, Wilking H, Holzer A, Roedel A, et al. Backtracking and forward checking of human listeriosis clusters identified a multiclonal outbreak linked to *Listeria monocytogenes* in meat products of a single producer. Emerg Microbes Infect. 2020;9:1600–8. https://doi.org/10.1080/22221751.2020.1784044
7. Ruppitsch W, Prager R, Halbedel S, Hyden P, Pietzka A, Huhulescu S, et al. Ongoing outbreak of invasive listeriosis, Germany, 2012 to 2015. Euro Surveill. 2015;20:20. https://doi.org/10.2807/1560-7917.ES.2015.20.50.30094
8. Bundesamt für Verbraucherschutz und Lebensmittelsicherheit (BVL). Zoonoses monitoring [German]. 2020 [cited 2021 June 8]. https://www.bvl.bund.de/DE/Arbeitsbereiche/01_Lebensmittel/01_Aufgaben/02_AmtlicheLebensmittelueberwachung/06_ZoonosenMonitoring/lm_zoonosen_monitoring_node.html
9. Halbedel S, Prager R, Fuchs S, Trost E, Werner G, Flieger A. Whole-genome sequencing of recent *Listeria monocytogenes* isolates from Germany reveals population structure and disease clusters. J Clin Microbiol. 2018;56:e00119–18. https://doi.org/10.1128/JCM.00119-18
10. European Food Safety Authority and European Centre for Disease Prevention and Control. The European Union One Health 2018 zoonoses report. 2019 [cited 2021 June 8]. https://www.ecdc.europa.eu/en/publications-data/european-union-one-health-2018-zoonoses-report
11. Centers for Disease Control and Prevention (CDC). Vital signs: *Listeria* illnesses, deaths, and outbreaks—United States, 2009-2011. MMWR Morb Mortal Wkly Rep. 2013;62:448–52.
12. Charlier C, Perrodeau É, Leclercq A, Cazenave B, Pilmis B, Henry B, et al.; MONALISA study group. Clinical features and prognostic factors of listeriosis: the MONALISA national prospective cohort study. Lancet Infect Dis. 2017;17:510–9. https://doi.org/10.1016/S1473-3099(16)30521-7
13. European Centre for Disease Prevention and Control. Listeriosis annual epidemiological report for 2017. 2020 [cited 2021 June 8]. https://www.ecdc.europa.eu/sites/default/files/documents/listeriosis-annual-epidemiological-report-2017.pdf

Address for correspondence: Hendrik Wilking, Robert Koch Institute, Seestraße 10, 13353 Berlin, Germany; email: WilkingH@rki.de

Laboratory Exposures from an Unsuspected Case of Human Infection with *Brucella canis*

Jasmine Ahmed-Bentley, Susan Roman, Yazdan Mirzanejad, Erin Fraser,
Linda Hoang, Edward J. Young, Muhammad Morshed, Gregory Deans

We report a case of human infection with a *Brucella canis* isolate in an adult in Canada who was receiving a biologic immunomodulating medication. We detail subsequent investigations, which showed that 17 clinical microbiology staff had high-risk exposures to the isolate, 1 of whom had a positive result for *B. canis*.

A 70 year-old woman came to the emergency department at Abbotsford Regional Hospital (Abbotsford, BC, Canada) after 3 days of chills, headache, nausea, weakness, and urinary frequency. Her medical history included psoriasis and psoriatic arthritis; her medications included ixekizumab. Her vital signs were within reference limits. Initial blood test results were within reference ranges, apart from a mild increase in the monocyte level (0.9×10^9 cells/L, reference range 0.1–0.8×10^9 cells/L) and a high level of C-reactive protein (14.5 mg/L, reference value <7.5 mg/L). Chest radiograph showed no acute findings. The patient, believed to have a urinary tract infection, was discharged and given a 7-day course of oral cefixime.

Four BacT/Alert blood culture bottles (bioMérieux, https://www.biomerieux-usa.com) (3 aerobic and 1 anaerobic) were collected in the emergency department. One aerobic blood culture bottle showed a positive result for *Brucella* sp. after 3.5 days of incubation. A laboratory technologist prepared a slide for Gram staining and subcultured a sample into medium in a biosafety cabinet while wearing a gown and gloves. The result of the Gram stain was difficult to interpret and was initially reported as showing gram-positive cocci. A urine culture result was negative. The patient was readmitted to the emergency department for reassessment. She reported feeling somewhat better and continued using the oral antimicrobial drug while awaiting further information from the laboratory.

Culture plates were examined for growth every 4 hours and after 42 hours of incubation showed faint growth on blood and chocolate agars. Matrix-assisted laser desorption/ionization time-of-flight (MALDI-TOF) mass spectrometry (Bruker Daltonics Instrument; https://www.bruker.com) did not identify the organism, but the highest score was for *Ochrobactrum* spp. At this point, culture examinations and MALDI-TOF mass spectrometry target plate preparations were performed on an open laboratory bench.

The next day, after reviewing the Gram stain result and MALDI-TOF mass spectrometry results, a microbiologist noted that the organisms were pleomorphic, gram-negative coccobacilli, which increased the possibility of *Brucella* spp. The provincial reference laboratory (British Columbia Centre for Disease Control Public Health Laboratory, Vancouver, BC, Canada) was contacted. That evening, molecular testing at that laboratory confirmed the isolate was *Brucella* spp. and the isolate was sent to the National Microbiology Laboratory (Winnipeg, MB, Canada) for species identification. The microbiologist communicated this result to the emergency physician, public health officials, and laboratory leadership; the patient was contacted and returned the same day to initiate outpatient therapy (intravenous gentamicin and oral doxycycline). After 7 days of therapy, the patient was much improved; gentamicin was discontinued, and the patient was transitioned to receiving oral rifampin and doxycycline for 6 weeks of treatment. Blood

Author affiliations: Fraser Health, Surrey, British Columbia, Canada (J. Ahmed-Bentley, S. Roman, Y. Mirzanejad, G. Deans); University of British Columbia, Vancouver, British Columbia, Canada (J. Ahmed-Bentley, Y. Mirzanejad, E. Fraser, L. Hoang, M. Morshed, G. Deans); British Columbia Center for Disease Control Public Health Laboratory, Vancouver (E. Fraser, L. Hoang, M. Morshed); Baylor College of Medicine, Houston, Texas, USA (E.J. Young)

cultures repeated on treatment day 7 had no growth. No focal site of infection was identified after analysis of medical history, physical examination, and computed tomography of the chest, abdomen, and pelvis.

The patient reported a major headache and a depressed mood as she neared the tentative end of her treatment; therapy was extended while investigating for evidence of neurobrucellosis, which would require further prolongation of therapy. Computed tomography of the head and lumbar puncture found no evidence of central nervous system infection; thus, treatment was discontinued (53 days of completed total therapy). The headache and mood changes for the patient resolved within days of treatment discontinuation, and she did not have any symptoms of recurrence after 1 year.

The National Microbiology Laboratory reported the identification as *B. canis*. A public health investigation determined that the patient had helped transport rescue dogs from Mexico and the United States to Canada (*1*). Ten weeks before this patient's onset of symptoms, a pregnant dog from Mexico spontaneously aborted 2 stillborn puppies in the patient's car. After *B. canis* was identified in the human patient, testing of the dog showed that it was positive for *B. canis* by immunofluorescent antibody test. We conducted outreach for *B. canis* detection, prevention, and control of the dog rescue organization and to veterinary and medical professionals in British Columbia.

The patient was seronegative for *B. abortus* (by microagglutination test) and seropositive for *B. canis* (by D-TEC CB Commercial Slide Agglutination Kit; Zoetis, https://www.zoetisus.com). Serologic testing for *B. canis* was performed at Baylor College of Medicine (Houston, TX, USA). This kit is intended for veterinary use; the sensitivity and specificity for human samples is unknown because there are few cases of human *B. canis* infection in North America. Although this kit is not validated for human samples, anecdotal evidence suggests this test provides results that correlate with the clinical picture (E.J. Young, unpub. data). Also, serologic agglutination assays using *B. abortus* antigens do not cross-react with antibodies to *B. canis* (*2*).

As part of the laboratory exposure investigation, we reviewed the workup in the microbiology laboratory and the location of all personnel to identify potential high-risk exposures (≤5 feet from culture manipulation on an open bench) (*3*). A microbiologist performed a risk assessment for all exposed staff (*3*). No aerosol-generating procedures had been performed.

A total of 17 staff had high-risk exposures: 9 were technologists who worked directly on the *Brucella* culture on an open bench and 8 were staff who worked within a 5-foot radius. These staff were referred to an infectious diseases clinic for urgent assessment and consideration of postexposure prophylaxis. Serologic testing for *B. canis* and *B. abortus* was performed at 3 months and 6 months after exposure. One staff member had a positive result for *B. canis* that was detected at 3 months despite taking 3 weeks of postexposure prophylaxis initiated 12 days after a high-risk exposure. All other staff were seronegative. No exposed staff reported symptoms of *Brucella* infection during the 6 months of postexposure follow-up.

This case prompted the following procedure changes to prevent future laboratory exposures. First, *Brucella* spp. are aerobes typically requiring ≥48 hours to grow in automated blood culture systems because the level of bacteremia is usually low (1–5 CFU/mL), doubling time is long (2.5–3.5 hours), and CO_2 production is low (*4–7*). Aerobic blood culture bottles showing a positive result after ≥48 hours of incubation are now processed by using additional personal protective equipment (N95 mask, face shield, gown, and gloves) in a biosafety cabinet, and subculture plates are labeled as containing a possible Risk Group 3 agent. A microbiologist or senior technologist reviews the Gram stain results and guides further workup.

Second, a security-relevant bacterial database was installed on the Bruker instrument. This database contains 1 species of *Brucella*, *B. melitensis*. Using this security-relevant database, we found that the spectra of this organism from the original run was identified as *B. melitensis* (score 2.39). MALDI-TOF mass spectrometry is not routinely performed on suspected Risk Group 3 agents; however, if this process is inadvertently performed in the future, the security-relevant database would help identify the pathogen sooner.

Third, the highest score of *Ochrobactrum* spp. by MALDI-TOF mass spectrometry prompts the technologist to consider *Brucella* spp. Similar to our finding with *B. canis*, it has been reported that *B. melitensis* can be misidentified as *O. anthropi* by MALDI-TOF mass spectrometry by using a library lacking *Brucella* (*8*).

Conclusions

Our investigation shows that humans interacting with dogs from areas to which *B. canis* is endemic are at risk for acquiring human brucellosis (*9*). *B. canis* seropositivity has also been found in dogs within kennels in Canada (*10*). A workup for fever of unknown origin should include a detailed exposure history, including contact with dogs, particularly imported dogs. Laboratory manipulation of *B. canis* isolates from human clinical samples can result in transmission of the organism to laboratory staff. Proactive

measures should be taken to minimize risk for exposure to this potential laboratory hazard.

About the Author

Dr. Ahmed-Bentley is a medical microbiologist at Fraser Health, Surrey, British Columbia, Canada. Her primary research interests include laboratory safety, infection prevention and control, and zoonotic infections.

References

1. Galanis E, Trerise S, Ahmed-Bentley J, Deans G, Fraser E. Brucellosis and other diseases imported with dogs. British Columbia Medical Journal. 2019;61:177–90. https://bcmj.org/bccdc/brucellosis-and-other-diseases-imported-dogs
2. Pappas G, Akritidis N, Bosilkovski M, Tsianos E. Brucellosis. N Engl J Med. 2005;352:2325–36. https://doi.org/10.1056/NEJMra050570
3. Centers for Disease Control and Prevention. Brucellosis reference guide: exposures, testing and prevention, 2017 [cited 2021 Jun 12]. https://www.cdc.gov/brucellosis/pdf/brucellosis-reference-guide.pdf
4. Yagupsky P, Morata P, Colmenero JD. Laboratory diagnosis of human brucellosis. Clin Microbiol Rev. 2019;33:e00073–19. https://doi.org/10.1128/CMR.00073-19
5. Baysallar M, Aydogan H, Kilic A, Kucukkaraaslan A, Senses Z, Doganci L. Evaluation of the BacT/ALERT and BACTEC 9240 automated blood culture systems for growth time of *Brucella* species in a Turkish tertiary hospital. Med Sci Monit. 2006;12:BR235–8.
6. Roiz MP, Peralta FG, Valle R, Arjona R. Microbiological diagnosis of brucellosis. J Clin Microbiol. 1998;36:1819. https://doi.org/10.1128/JCM.36.6.1819-1819.1998
7. Solomon HM, Jackson D. Rapid diagnosis of *Brucella melitensis* in blood: some operational characteristics of the BACT/ALERT. J Clin Microbiol. 1992;30:222–4. https://doi.org/10.1128/jcm.30.1.222-224.1992
8. Poonawala H, Cooner TM, Peaper DR. Closing the brief case: misidentification of *Brucella melitensis* as *Ochrombactrum anthropi* by matrix-assisted laser desorption ionization-time of flight mass spectrometry (MALDI-TOF MS). J Clin Microbiol. 2018;56:e0091914–7. https://doi.org/10.1128/JCM.00918-17
9. Hensel ME, Negron M, Arenas-Gamboa AM. Brucellosis in dogs and public health risk. Emerg Infect Dis. 2018;24:1401–6. https://doi.org/10.3201/eid2408.171171
10. Weese JS, Hrinivich K, Anderson ME. *Brucella canis* in commercial dog breeding kennels, Ontario, Canada. Emerg Infect Dis. 2020;26:3079–80. https://doi.org/10.3201/eid2612.201144

Address for correspondence: Jasmine Ahmed-Bentley, Surrey Memorial Hospital, Microbiology Laboratory, Critical Care Tower, 4th Fl, 13750 96 Ave, Surrey, BC, V3V1Z2, Canada; email: jasmine.ahmedbentley@fraserhealth.ca

EID Podcast:
WWI and the 1918 Flu Pandemic

CDC's Dr. Terence Chorba discusses his EID cover art essay about the 1918 flu pandemic and the WWI painting by John Singer Sargent.

Visit our website to listen:
https://tools.cdc.gov/medialibrary/index.aspx#/media/id/393699
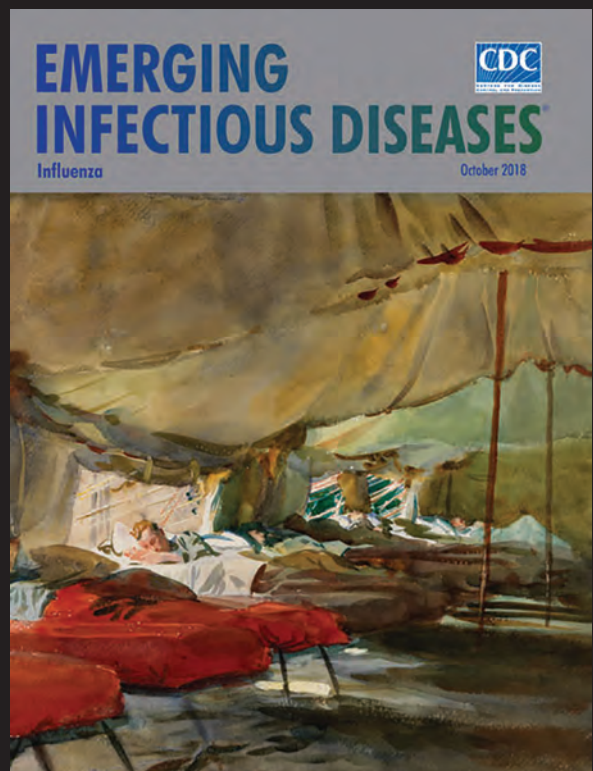
EMERGING INFECTIOUS DISEASES

Highly Pathogenic Avian Influenza A(H5N6) Virus Clade 2.3.4.4h in Wild Birds and Live Poultry Markets, Bangladesh

Jasmine C.M. Turner, Subrata Barman, Mohammed M. Feeroz, M. Kamrul Hasan,
Sharmin Akhtar, Trushar Jeevan, David Walker, John Franks, Patrick Seiler, Nabanita Mukherjee,
Lisa Kercher, Pamela McKenzie, Tommy Lam, Rabeh El-Shesheny, Richard J. Webby

Migratory birds play a major role in spreading influenza viruses over long distances. We report highly pathogenic avian influenza A(H5N6) viruses in migratory and resident ducks in Bangladesh. The viruses were genetically similar to viruses detected in wild birds in China and Mongolia, suggesting migration-associated dissemination of these zoonotic pathogens.

Highly pathogenic avian influenza (HPAI) A(H5) viruses were identified in 1996 in a goose from Guangdong, China, and the evolution of the hemagglutinins (HAs) of these A/goose/Guangdong/1/96 (Gs/GD) lineage viruses has given rise to multiple genetically distinct phylogenetic clades (1). The emergence of HA clade 2.3.4.4 viruses was associated with several different virus subtypes, including H5N6 (2). As of March 2021, a total of 29 laboratory-confirmed human cases of H5N6 viruses have been reported from China, and 9 patients have died (3). Clade 2.3.4.4 H5N6 viruses have subsequently evolved, requiring further clade designations. Clade 2.3.4.4h viruses are found in China, Laos, and Vietnam (4). In December 2019 and January 2020, 2.3.4.4 H5N6 viruses were isolated from dead migratory whooper swans (*Cygnus cygnus*) and mute swans (*Cygnus olor*) in Xinjiang,

western China (5). In April 2021, the same virus was detected in migratory birds in Mongolia (6).

In Bangladesh, HPAI A(H5) viruses have been in circulation since 2008; the predominant clades found are 2.2.2 and 2.3.2.1a. HPAI A(H5N6) clade 2.3.4.4b viruses were identified in domestic poultry in Bangladesh in 2016 (7,8). Although the viruses were detected in live poultry markets (LPMs), they did not replace the H5N1 viruses in circulation, and as of April 2021, there have been no more reports of H5N6 virus detection (9,10). We report a new introduction of clade 2.3.4.4.h viruses that are similar to viruses detected in China (Xinjiang) and Mongolia (5,6), suggesting that migratory birds of the Central Asian flyway introduced this virus into Bangladesh.

The Study

Since 2015, our active surveillance in Bangladesh has been ongoing in both LPMs and Tanguar Haor, a wetlands area where local domestic ducks are reared and where birds winter during the migratory season (Appendix, Table 1, https://wwwnc.cdc.gov/EID/article/27/9/21-0819-App1.pdf). We collected H5N6 virus–positive oropharyngeal and cloacal swabs from 2 apparently healthy wild birds in Baghmara, Tanguar Haor: a ferruginous duck on January 19, 2020, and a common pochard on January 20, 2020. We also obtained positive fecal samples from wild mallard ducks on January 26, 2020, in Puran Gao, Tanguar Haor. The next day, we obtained positive oropharyngeal and cloacal swabs from apparently healthy Khaki Campbell ducks located on various farms in Golabari, Tanguar Haor (Appendix Table 1). On February 18, 2020, ≈3 weeks after detection of H5N6 virus in Tanguar Haor, an apparently healthy mallard duck

located in a Dhaka LPM was also found to be infected with H5N6. Surveillance conducted on February 22, 2020, on various farms in Chitergao, Tanguar Haor, revealed an additional 24 more apparently healthy Khaki Campbell ducks infected with H5N6 virus. During our surveillance study, we identified a total of 40 domestic and wild birds infected with H5N6 virus clade 2.3.4.4h during January–February 2020 (Appendix Table 1).

We determined the complete genome sequences of the 40 HPAI A(H5N6) viruses. The sequence similarity between viruses was 99.4%–100%. As a representative virus, A/Ferruginous duck/Bangladesh/42380/2020 (H5N6) had a high nucleotide identity (99.6%–99.9%) to the HPAI A(H5N6) viruses of clade 2.3.4.4h from China (Xinjiang, January 2020) and Mongolia (April 2020) (Table).

An outbreak of H5N6 virus clade 2.3.4.4h in whooper swans in China (Xinjiang) and Mongolia in early 2020 suggested potential further distribution of these viruses across Asia, especially to areas where poultry is raised along the migration routes of wild birds. We combined genome sequences generated in this study with all sequences of H5N6 viruses available in GenBank and the GISAID database (11). Phylogenetic analysis confirmed that the Bangladeshi A(H5N6) isolates are of clade 2.3.4.4h and clustered with the recent HPAIV A(H5N6) isolates from whooper swans in Xinjiang, western China and in Mongolia (Figure 1, https://wwwnc.cdc.gov/EID/article/27/9/21-0819-F1.htm). The time of most recent common ancestry for HPAI A(H5N6) viruses (Figure 2, https://wwwnc.cdc.gov/EID/article/27/9/21-0819-F2.htm) suggests that the viruses from China, Mongolia, and Bangladesh share

a common ancestor of unknown origin that emerged around mid-2019.

The phylogenetic clustering observed for the H5 gene was also conserved for the remaining 7 genes; the viruses from Bangladesh, China, and Mongolia were of the same genotype, with no evidence of reassortment (Appendix Figure). The A(H5N6) viruses from Bangladesh shared genetic features with their homologs from China, including an HA cleavage site, PLRERRRKR/G, which is characteristic of high pathogenicity in chickens (Appendix Table 2). We also found an amino acid deletion at position 133 in the HA protein (H3 numbering) in all our isolates, a feature common with clade 2.3.4.4.h isolated from humans (Appendix Table 2) and associated with alteration of the H5 HA receptor binding pocket (12). Deletions were also present in both neuraminidase (NA) (an 11-aa deletion in the stalk region) and nonstructural protein 1 (NS1) (deletion from residues 80–84; Appendix Table 2), which are associated with high pathogenicity in avian hosts (13). Postinfection ferret antisera raised to A/duck/Bangladesh/43127/2020 (H5N6) reacted to the World Health Organization's candidate clade 2.3.4.4h vaccine virus, A/Guangdong/18SF020/2018 and, as expected, to all Bangladesh H5N6 viruses tested (Appendix Table 3).

Migratory birds are key in the evolution, maintenance, and spread of avian influenza viruses. We have previously identified viruses in LPMs after their detection in wild birds and domestic ducks in Tanguar Haor (8,14,15). Similarly, detection of the H5N6 virus in an LPM after detection in Tanguar Haor highlights the continuum of migratory birds of the Central Asian flyway and domestic ducks in Tanguar Haor as vectors for viral movement at the wild bird–poultry

Table. Nucleotide sequence identities between the A/Ferruginous duck/Bangladesh/42380/2020 (H5N6) virus from Bangladesh and nearest virus homologs*

Gene	GenBank accession no.	Virus	% Identity
PB2	MT872369.1	A/Whooper swan/Mongolia/25/2020 (H5N6)	99.83
	MW108029.1†	A/duck/Hunan/1.12_YYGK74H3-OC/2018 (H5N6)	98.65
PB1	MT872369.1	A/Whooper swan/Mongolia/25/2020 (H5N6)	99.87
	MW104086.1	A/chicken/Guangdong/7.20_DGCP022-O/2017 (H5N6)	99.04
PA	EPI_ISL_418181	A/Whooper swan/Xinjiang/13/2020 (A/H5N6)	99.9
	EPI_ISL_340825	A/Env/Guangdong/Jieyang/C18289059/2018(H5N6)	99.5
HA	EPI_ISL_418175	A/Whooper swan/Xinjiang/7/2020 (A/H5N6)	99.8
	EPI_ISL_340844	A/Env/Guangdong/C17285752/QY/2017 (H5N6)	98.9
NP	MT872369.1	A/Whooper swan/Mongolia/25/2020 (A/H5N6)	99.65
	MW108029.1	A/duck/Hunan/1.12_YYGK74H3-OC/2018 (H5N6)	99.64
NA	EPI_ISL_418181	A/Whooper swan/Xinjiang/13/2020 (A/H5N6)	99.9
	MW108138.1	A/duck/Hunan/11.30_YYGK63E3-OC/2017 (H5N6)	99.36
M	MT872369.1	A/Whooper swan/Mongolia/25/2020 (H5N6)	99.6
	EPI_ISL_340825	A/Env/Guangdong/Jieyang/C18289059/2018 (H5N6)	99.9
NS	EPI_ISL_418181	A/Whooper swan/Xinjiang/13/2020 (A/H5N6)	99.9
	MW108029.1	A/duck/Hunan/1.12_YYGK74H3-OC/2018 (H5N6)	99.29

*HA, hemagglutinin; MP, matrix protein; NA, neuraminidase; NP, nucleoprotein; NS, nonstructural protein; PA, acidic polymerase; PB1, basic polymerase 1; PB2, basic polymerase 2.
†Nearest virus homologs to A/Ferruginous duck/Bangladesh/42380/2020 (H5N6) excluding the H5N6 viruses from China (Xinjiang), and Mongolia.

interface. We also detected a duck that was co-infected with A/duck/Bangladesh/44500/2020 (H10N7) and A/duck/Bangladesh/44500/2020 (H5N6), raising the possibility of reassortment and highlighting the potential effect of this genetic diversification.

Conclusions

We have identified HPAIV A(H5N6) viruses from migratory birds, domestic duck farms, and LPMs in Bangladesh at a similar time to their detection in China and Mongolia. The wider distribution of this group of viruses with documented zoonotic potential is cause for considerable public health concern. Monitoring for their establishment in South Central Asia must be intensified.

About the Author

Ms. Turner is a lead researcher in the department of infectious diseases at St. Jude Children's Research Hospital, Memphis, Tennessee, USA. Her major research interests are influenza virus ecology and evolution, influenza virus pathogenicity, and diagnosis and surveillance of influenza A viruses and their role in the emergence of new pandemic strains for humans and lower animals.

References

1. Smith GJ, Donis RO; World Health Organization/World Organisation for Animal Health/Food and Agriculture Organization (WHO/OIE/FAO) H5 Evolution Working Group. Nomenclature updates resulting from the evolution of avian influenza A(H5) virus clades 2.1.3.2a, 2.2.1, and 2.3.4 during 2013–2014. Influenza Other Respir Viruses. 2015;9:271–6. https://doi.org/10.1111/irv.12324
2. Yang L, Zhu W, Li X, Bo H, Zhang Y, Zou S, et al. Genesis and dissemination of highly pathogenic H5N6 avian influenza viruses. J Virol. 2017;91:91. https://doi.org/10.1128/JVI.02199-16
3. World Health Organization. Human infections with avian influenza A(H5N6) virus—China. 2020 [cited 2020 Nov 10]. https://wwwwhoint/docs/default-source/wpro—documents/emergency/surveillance/avian-influenza/ai-20201002pdf?sfvrsn=223ca73f_66
4. World Health Organization. Antigenic and genetic characteristics of zoonotic influenza viruses and candidate vaccine viruses developed for potential use in human vaccines. 2021 [cited 2021 Mar 26]. https://www.who.int/influenza/vaccines/virus/202103_zoonotic_vaccinevirus update.pdf
5. Li Y, Li M, Li Y, Tian J, Bai X, Yang C, et al. Outbreaks of highly pathogenic avian influenza (H5N6) virus subclade 2.3.4.4h in swans, Xinjiang, Western China, 2020. Emerg Infect Dis. 2020;26:2956–60. https://doi.org/10.3201/eid2612.201201
6. Jeong S, Otgontogtokh N, Lee DH, Davganyam B, Lee SH, Cho AY, et al. Highly pathogenic avian influenza clade 2.3.4.4 subtype H5N6 viruses isolated from wild whooper swans, Mongolia, 2020. Emerg Infect Dis. 2021;27:1181–3. https://doi.org/10.3201/eid2704.203859
7. Yang G, Chowdury S, Hodges E, Rahman MZ, Jang Y, Hossain ME, et al. Detection of highly pathogenic avian influenza A(H5N6) viruses in waterfowl in Bangladesh. Virology. 2019;534:36–44. https://doi.org/10.1016/j.virol.2019.05.011
8. Barman S, Turner JCM, Hasan MK, Akhtar S, El-Shesheny R, Franks J, et al. Continuing evolution of highly pathogenic H5N1 viruses in Bangladeshi live poultry markets. Emerg Microbes Infect. 2019;8:650–61. https://doi.org/10.1080/22221751.2019.1605845
9. Kwon J-H, Lee D-H, Criado MF, Killmaster L, Ali MZ, Giasuddin M, et al. Genetic evolution and transmission dynamics of clade 2.3.2.1a highly pathogenic avian influenza A/H5N1 viruses in Bangladesh. Virus Evol. 2020;6:veaa046. https://doi.org/10.1093/ve/veaa046
10. Islam K, Ahsan MM, Chakma S, Penjor K, Barua M, Jalal MS, et al. An assessment on potential risk pathways for the incursion of highly pathogenic avian influenza virus in backyard poultry farm in Bangladesh. Vet World. 2020;13:2104–11. https://doi.org/10.14202/vetworld.2020.2104-2111
11. Shu Y, McCauley J. GISAID: Global initiative on sharing all influenza data—from vision to reality. Euro Surveill. 2017;22:22. https://doi.org/10.2807/1560-7917.ES.2017.22.13.30494
12. Watanabe Y, Ibrahim MS, Ellakany HF, Kawashita N, Mizuike R, Hiramatsu H, et al. Acquisition of human-type receptor binding specificity by new H5N1 influenza virus sublineages during their emergence in birds in Egypt. PLoS Pathog. 2011;7:e1002068. https://doi.org/10.1371/journal.ppat.1002068
13. Cui Y, Li Y, Li M, Zhao L, Wang D, Tian J, et al. Evolution and extensive reassortment of H5 influenza viruses isolated from wild birds in China over the past decade. Emerg Microbes Infect. 2020;9:1793–803. https://doi.org/10.1080/22221751.2020.1797542
14. El-Shesheny R, Feeroz MM, Krauss S, Vogel P, McKenzie P, Webby RJ, et al. Replication and pathogenic potential of influenza A virus subtypes H3, H7, and H15 from free-range ducks in Bangladesh in mammals. Emerg Microbes Infect. 2018;7:1–13. https://doi.org/10.1038/s41426-018-0072-7
15. El-Shesheny R, Barman S, Feeroz MM, Hasan MK, Jones-Engel L, Franks J, et al. Genesis of influenza A(H5N8) viruses. Emerg Infect Dis. 2017;23:1368–71. https://doi.org/10.3201/eid2308.170143

Address for correspondence: Richard J. Webby, Department of Infectious Diseases, MS 330, St. Jude Children's Research Hospital, 262 Danny Thomas Pl, Memphis, TN 38105-3678, USA; email: richard.webby@stjude.org

Invasive Meningococcal Disease, 2011–2020, and Impact of the COVID-19 Pandemic, England

Sathyavani Subbarao, Helen Campbell,
Sonia Ribeiro, Stephen A. Clark, Jay Lucidarme,
Mary Ramsay, Ray Borrow, Shamez Ladhani

Author affiliations: Public Health England, London, UK
(S. Subbarao, H. Campbell, S. Ribeiro, M. Ramsay, S. Ladhani);
Manchester Royal Infirmary, Manchester, UK (S.A. Clark,
J. Lucidarme, R. Borrow); St. George's University of London,
London (S. Ladhani)

Invasive meningococcal disease incidence in England declined from 1.93/100,000 persons (1,016 cases) in 2010–11 to 0.95/100,000 (530 cases) in 2018–19 and 0.74/100,000 in 2019–20 (419 cases). During national lockdown for the coronavirus disease pandemic (April–August 2020), incidence was 75% lower than during April–August 2019.

Neisseria meningitidis is a major global cause of bacterial meningitis and septicemia (*1*). Six serogroups (A, B, C, W, X, Y) are responsible for most invasive meningococcal disease (IMD) cases (*1*). In the United Kingdom, implementation of serogroup C (MenC) meningococcal conjugate vaccine in 1999 led to sustained declines in MenC disease (*2*). In August 2015, an emergency adolescent MenACWY immunization program for persons 13–18 years of age and new university students was implemented to control a national outbreak of a hypervirulent MenW strain belonging to sequence type 11 clonal complex (MenW:cc11) (*3*). In September 2015, the United Kingdom became the first country to add a protein-based meningococcal B vaccine, 4CMenB, into the national infant immunization program (*4*). Both programs have reduced IMD caused by the respective vaccine serogroups (*5*).

Since December 2019, the novel coronavirus (COVID-19) pandemic has led to major changes in the epidemiology of bacterial and viral infections worldwide (Brueggemann AB et al., unpub. data, https://www.medrxiv.org/content/10.1101/2020.11.18.20225029v1). We report IMD incidence in England during 2011–2020, including the impact of a national lockdown to control the spread of severe acute respiratory syndrome coronavirus 2 (SARS-CoV-2).

Public Health England (PHE) conducts national surveillance of IMD (*6*) and SARS-CoV-2 (*7*) in England. IMD incidence was highest, 1.93 cases/100,000 population (1,016 total cases), during the 2010–11 academic year (September–August) and declined to 1.15 cases /100,000 population for 2013–14 (617 cases) before increasing to 1.51 cases /100,000 population (825 cases) in 2015–16 (Figure). Adolescent MenACWY and infant 4CMenB immunization programs in 2015 led to additional annual declines in IMD incidence, to 0.95 cases /100,000 population (530 cases) in 2018–19 (incidence rate ratio [IRR] 0.63 [95% CI 0.56–0.70] for 2018–19 vs. 2015–16). Incidence further declined during the 2019–20 pandemic year (419 cases; 0.74 cases /100,000 population; IRR 0.49 [95% CI 0.44–0.56] for 2019–20 vs. 2015–16). IMD cases declined for all serogroups from 2015–16 to 2019–20: MenB by 38% (from 452 to 279 cases), MenC by 41% (41 to 24 cases), MenW by 68% (218 to 70 cases) and MenY by 66% (108 to 37 cases) (Appendix Figure 1, https://wwwnc.cdc.gov/EID/article/27/9/20-4866-App1.pdf).

IMD cases declined after the national COVID-19 lockdown on March 23, 2020, and remained low during April–August 2020 (Appendix Figure 2). During 2018–19, PHE received 12,628 clinical samples from patients with suspected IMD; of these, 462 (4%) tested positive for *N. meningitidis*. These totals were 9,968 specimens, 401 (4%) positive, during 2019–20 (21% fewer cases). During April–August 2020, a total of 50 (1.8%) of 2,808 samples tested positive for *N. meningitidis*, compared
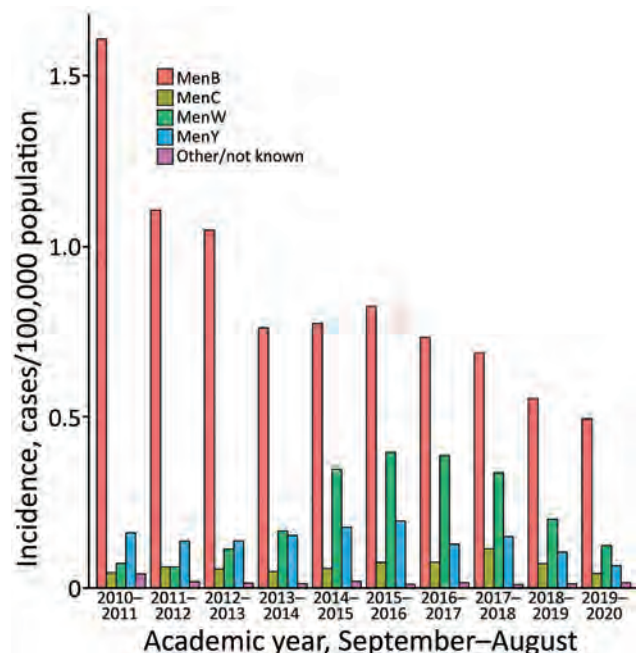

Figure. Cases of invasive meningococcal disease, by academic year, England, 2015–2020. Men, meningococcal conjugate vaccine (by serogroup).

Table. Confirmed cases of meningococcal disease during April–August 2019 and April–August 2020, England*

Category	April–Aug 2019, no. (%)	April–Aug 2020, no. (%)	RR (95% CI)
Group			
Total (N)	179	45	0.25 (0.18–0.35)
MenB	104 (58)	33 (73)	0.32 (0.21–0.47)
MenC	14 (8)	5 (11)	0.36 (0.13–0.99)
MenW	42 (23)	5 (11)	0.12 (0.05–0.30)
MenY	16 (9)	0	0
Other	3 (2)	2 (4)	0.67 (0.11–3.97)
Age group, y			
Total	179	45	0.25 (0.18–0.35)
<5	39 (22)	17 (38)	0.44 (0.25–0.78)
5–14	20 (11)	4 (9)	0.2 (0.07–0.58)
15–24	24 (13)	4 (9)	0.17 (0.06–0.48)
25–64	53 (30)	14 (31)	0.26 (0.15–0.47)
≥65	43 (24)	6 (13)	0.14 (0.06–0.32)

*The numbers of typeable strains during the specified time frame by age group are shown. RR, relative risk.

with 134 (2.7%) of 5,025 samples during the same period in 2019 (p = 0.016). Combining culture-confirmed and PCR-confirmed cases, IMD incidence was 75% lower (IRR 0.25, 95% CI 0.18–0.35) during April–August 2020 than during April–August 2019 (Table). In contrast, IMD incidence during September 2019–March 2020 (the 7 months before national lockdown) was similar to that for September 2018–March 2019 (IRR 1.06, 95% CI 0.91–1.23). Declines were observed for all age groups and serogroups (Appendix Table). During lockdown, compared with the same period during the previous year, MenB was overrepresented (33/45 [73%] vs. 104/179 [58%] cases), whereasMenW (5/45 [11%] vs. 42/179 [23%] cases) and MenY (0/45 [0%] vs. 16/179 [9%] cases) were underrepresented (Appendix Table, Figure 1).

A total of 45 IMD cases were diagnosed during April–August 2020. The median age of patients was 67 (interquartile range 20–85) years. Linkage with national SARS-CoV-2 data identified 2 patients with IMD who were also positive for SARS-CoV-2 by reverse transcription PCR; both were <90 days of age with late-onset MenB meningitis, and 1 died. Meningitis (with or without septicemia) was proportionally more frequent during the lockdown months compared with the same period in 2019 (27/45 [60%] v. 71/179 [39.7%] cases; p = 0.014). Three (6.7%) of the 45 patients died within 28 days of diagnosis: the infant with co-infection, an adult with MenB meningitis, and an older adult with MenB septicemia.

Limitations of our study include limited clinical data collected for undiagnosed IMD cases. Cases and case-fatality rates during the lockdown period might also be underestimated if some patients died of IMD at home because they did not seek medical help earlier as a result of the stay at home messaging during lockdown.

In summary, IMD incidence in England has been declining since the early 2000s (8) because of the MenC immunization program and natural trends in MenB disease and further declined because of 2 new meningococcal immunization programs. National lockdown in March 2020 led to a 75% reduction in cases compared with the same period in the previous year, with MenB cases overrepresented. Declines in IMD cases after national lockdown were also reported in France (9), which is reassuring because viral infections are known to precede IMD; therefore, SARS-CoV-2 could potentially have increased the risk of secondary bacterial infections. Our findings do not support wider vaccination against IMD during the COVID-19 pandemic.

About the Author

Dr. Subbarao is a microbiology and infectious diseases registrar for Public Health England in London. Her main interests are vaccine-preventable diseases, antimicrobial stewardship, and *M. tuberculosis*.

References

1. Harrison LH, Trotter CL, Ramsay ME. Global epidemiology of meningococcal disease. Vaccine. 2009;27(Suppl 2):B51–63. https://doi.org/10.1016/j.vaccine.2009.04.063
2. Ramsay ME, Andrews NJ, Trotter CL, Kaczmarski EB, Miller E. Herd immunity from meningococcal serogroup C conjugate vaccination in England: database analysis. BMJ. 2003;326:365–6. https://doi.org/10.1136/bmj.326.7385.365
3. Campbell H, Edelstein M, Andrews N, Borrow R, Ramsay M, Ladhani S. Emergency meningococcal ACWY vaccination program for teenagers to control group W meningococcal eisease, England, 2015–2016. Emerg Infect Dis. 2017;23:1184–7. https://doi.org/10.3201/eid2307.170236
4. Ladhani SN, Andrews N, Parikh SR, Campbell H, White J, Edelstein M, et al. Vaccination of infants with meningococcal group B vaccine (4CMenB) in England. N Engl J Med. 2020;382:309–17. https://doi.org/10.1056/NEJMoa1901229
5. Parikh SR, Andrews NJ, Beebeejaun K, Campbell H, Ribeiro S, Ward C, et al. Effectiveness and impact of a reduced infant schedule of 4CMenB vaccine against group B meningococcal disease in England: a national observational cohort study. Lancet. 2016;388:2775–82. https://doi.org/10.1016/S0140-6736(16)31921-3
6. Ladhani SN, Waight PA, Ribeiro S, Ramsay ME. Invasive meningococcal disease in England: assessing disease burden

through linkage of multiple national data sources. BMC Infect Dis. 2015;15:551. https://doi.org/10.1186/s12879-015-1247-7

7. Public Health England. Research and analysis: national COVID-19 surveillance reports: GOV.UK; 2021 [cited 2020 Oct 2]. https://www.gov.uk/government/publications/national-covid-19-surveillance-reports

8. Ladhani SN, Flood JS, Ramsay ME, Campbell H, Gray SJ, Kaczmarski EB, et al. Invasive meningococcal disease in England and Wales: implications for the introduction of new vaccines. Vaccine. 2012;30:3710–6. https://doi.org/10.1016/j.vaccine.2012.03.011

9. Taha MK, Deghmane AE. Impact of COVID-19 pandemic and the lockdown on invasive meningococcal disease. BMC Res Notes. 2020;13:399. https://doi.org/10.1186/s13104-020-05241-9

Addresses for correspondence: Shamez Ladhani or Sathyavani Subbarao, Immunisation and Countermeasures Division, Public Health England, 61 Colindale Ave, London NW9 5EQ, UK; email: shamez.ladhani@phe.gov.uk or vani.subbarao@phe.gov.uk

SARS-CoV-2 Infection among Pregnant and Postpartum Women, Kenya, 2020–2021

Nancy A. Otieno,[1] Eduardo Azziz-Baumgartner,[1] Bryan O. Nyawanda, Eunice Oreri, Sascha Ellington, Clayton Onyango, Gideon O. Emukule

Author affiliations: Kenya Medical Research Institute, Kisumu, Kenya (N.A. Otieno, B.O. Nyawanda); Centers for Disease Control and Prevention, Atlanta, Georgia, USA (E. Azziz-Baumgartner, S. Ellington); Ministry of Health, Siaya, Kenya (E. Oreri); Centers for Disease Control and Prevention, Kisumu, Kenya (C. Onyango); Centers for Disease Control and Prevention, Nairobi, Kenya (G.O. Emukule)

We determined incidence of severe acute respiratory syndrome coronavirus 2 and influenza virus infections among pregnant and postpartum women and their infants in Kenya during 2020–2021. Incidence of severe acute respiratory syndrome coronavirus 2 was highest among pregnant women, followed by postpartum women and infants. No influenza virus infections were identified.

[1]These authors contributed equally to this article.

Information about the incidence of severe acute respiratory syndrome coronavirus 2 (SARS-CoV-2) infection among hospitalized pregnant women is available (1), but information about incidence among pregnant women in the community is not. We therefore quantified the incidence of symptomatic laboratory-confirmed SARS-CoV-2 and influenza infections among pregnant and postpartum women and their infants in Kenya during 2020–2021. The study was reviewed and approved by the Kenya Medical Research Institute Scientific and Ethics Review Unit (KEMRI SSC. 2880) and the Centers for Disease Control and Prevention (CDC) Institutional Review Board (CDC protocol 6709; 45 C.F.R. part 46; 21 C.F.R. part 56). All participants provided written consent.

We adapted an ongoing prospective multiyear influenza mother/baby cohort to include SARS-CoV-2 testing (2). Pregnant women at <31 weeks of gestation who were seeking prenatal care in Siaya County, Kenya, were approached for enrollment. Those who provided informed consent completed a survey about their demographics and antenatal history and were tested for HIV infection. Women were then phoned or visited at home once weekly until delivery and through their postpartum period, together with their infants, for 6 months to

Table. Characteristics of pregnant and postpartum women and their infants with laboratory-confirmed severe acute respiratory syndrome coronavirus 2 infection, Kenya, May 2020–February 2021*

Characteristic	Values
Women, n = 16	
Days from onset to swabbing, mean (SD)	2.6 (1.9)
Care-seeking from onset, d	
≤2	11 (68.8)
>2	5 (31.3)
Self-reported symptoms	
Fever in past 48 h	2 (12.5)
Measured fever ≥38.0°C	2 (12.5)
Cough	16 (100)
Shortness of breath	1 (6.3)
Runny nose	10 (62.5)
Headache	10 (62.5)
Muscle/ joint pain	2 (12.5)
Antimicrobial medication	16 (100)
Infants, n = 2	
Days from onset to swabbing, mean (SD)	2.5 (2.1)
Care-seeking from onset, d	
≤2	1 (50.0)
>2	1 (50.0)
Clinical signs reported by mother	
Fever in previous 48 h	1 (50.0)
Measured fever ≥38.0°C	1 (50.0)
Cough	2 (100)
Runny nose	1 (50.0)
Diarrhea	1 (50.0)
Antimicrobial medication	2 (100)

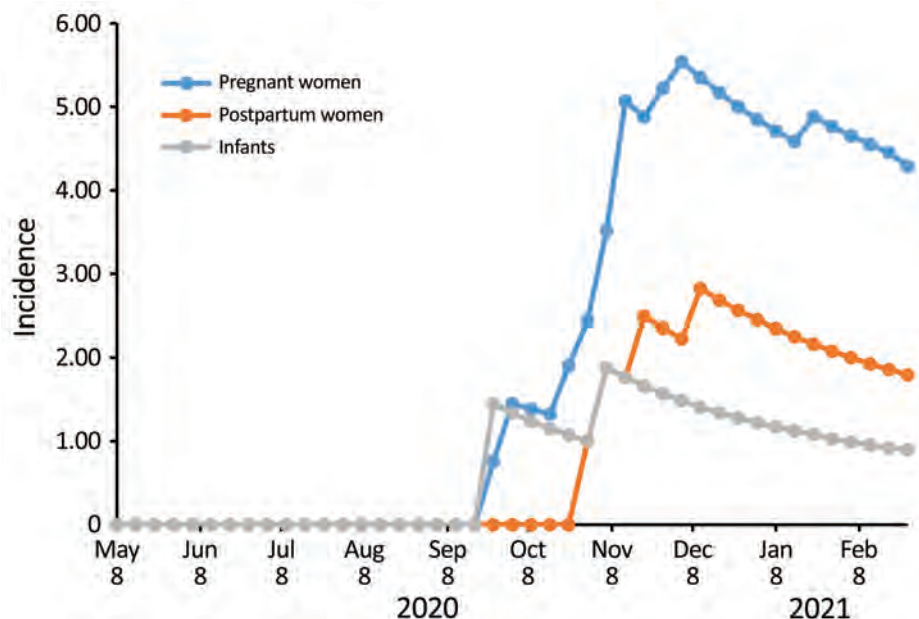*Values are no. (%) unless otherwise indicated.

Figure. Incidence (cases/1,000 person-months) of severe acute respiratory syndrome coronavirus 2 infection among pregnant and postpartum women, Kenya, 2020–2021.

identify coronavirus disease (COVID-19)–like illness (CLI) as defined by CDC (*3*). Those reporting CLI underwent nasopharyngeal and oropharyngeal swabbing at study clinics. Specimens were tested for SARS-CoV-2 and influenza viruses by real-time reverse transcription PCR at the KEMRI laboratory in Kisumu, Kenya.

During May 2020–February 2021, KEMRI staff approached 1,056 pregnant or postpartum women and enrolled 1,023 (97%). Half of enrolled women had primary school education, and 40% ran small businesses. A total of 180 (18%) were HIV infected, of which 177 (98%) were receiving antiretroviral medication. A total of 116 (11%) were vaccinated against influenza. Each of 3 women had hypertension, diabetes mellitus, or tuberculosis.

As of February 2021, staff had followed 886 pregnant women, who contributed 2,786 person-months, and 695 postpartum women and infants, who contributed 2,264 person-months (some women were represented in both groups). CLI developed in 274 (31%) pregnant women (348 episodes), 133 (19%) postpartum women (162 episodes), and 231 (33%) infants (277 episodes). Swab samples were collected within ≤10 days of illness from 58%; positive SARS-CoV-2 results were obtained for 12/200 (6%) pregnant women, 4/100 (4%) postpartum women, and 2/200 (1%) infants. None had positive influenza virus test results. The most common clinical manifestations of COVID-19 among pregnant and postpartum women were cough (16/16; 100%), runny nose (10/16; 63%) and head-

ache (10/16; 63%). Cough was identified for each of the 2 SARS-CoV-2–infected infants (Table). The rate of SARS-CoV-2 infection rapidly increased during follow-up. In the population tested, the cumulative incidence of SARS-CoV-2 infection per 1,000 person-months was 4.3 (pregnant women), 1.8 (postpartum women), and 0.9 (infants) (Figure).

CLI occurred in 19%–33% of participants, of which a small percentage had laboratory-confirmed SARS-CoV-2 infection. The incidence of SARS-CoV-2 infection in this population, however, was rapidly rising during the study period. No influenza viruses were identifiable during the historic influenza epidemic period (*4*). SARS-CoV-2 rates seemed higher among pregnant women, then postpartum women, and lowest among infants.

A study limitation is our inability to exhaustively assess symptoms of CLI among infants (e.g., headache, sore throat, loss of taste and smell) because we relied on the mothers' reports. This limitation would potentially underestimate the burden of COVID-19 among infants. In addition, we did not quantify asymptomatic and mildly symptomatic infections that might have been missed. However, we plan to test acute-phase and convalescent-phase serum, cord blood, and placentas to identify asymptomatic infections and explore whether risk for SARS-CoV-2 infection truly differs.

In summary, our findings suggest a higher burden of COVID-19 during pregnancy. These results highlight the potential benefit of prioritizing COVID-19 vaccination for pregnant women.

Financial support for conducting the research was provided by the Influenza Division, National Center for Immunization and Respiratory Diseases, CDC (grant no. 5U01GH002133–04–00). CDC also participated in the design of the study, analysis and interpretation of data, writing of the report, and decision to submit the article for publication.

About the Author

Ms. Otieno is an assistant principal research scientist at the Kenya Medical Research Institute, Centre for Global Health Research. Her primary research interests are infectious diseases, specifically maternal and child health.

References

1. Zambrano LD, Ellington S, Strid P, Galang RR, Oduyebo T, Tong VT, et al.; CDC COVID-19 Response Pregnancy and Infant Linked Outcomes Team. Update: characteristics of symptomatic women of reproductive age with laboratory-confirmed SARS-CoV-2 infection by pregnancy status — United States, January 22–October 3, 2020. MMWR Morb Mortal Wkly Rep. 2020;69:1641–7. https://doi.org/10.15585/mmwr.mm6944e3
2. Nyawanda BO, Otieno NA, Otieno MO, Emukule GO, Bigogo G, Onyango CO, et al. The impact of maternal human immunodeficiency virus infection on the burden of respiratory syncytial virus among pregnant women and their infants, Western Kenya. J Infect Dis. 2020 Aug 10 [Epub ahead of print].
3. Centers for Disease Control and Prevention. National Notifiable Diseases Surveillance System: surveillance case definitions. Coronavirus disease 2019 (COVID-19) 2020 interim case definition, approved April 5, 2020 [cited 2021 Feb 24]. https://wwwn.cdc.gov/nndss/conditions/coronavirus-disease-2019-covid-19/case-definition/2020
4. Olsen SJ, Azziz-Baumgartner E, Budd AP, Brammer L, Sullivan S, Pineda RF, et al. Decreased influenza activity during the COVID-19 pandemic—United States, Australia, Chile, and South Africa, 2020. MMWR Morb Mortal Wkly Rep. 2020;69:1305–9. https://doi.org/10.15585/mmwr.mm6937a6
5. Flannery DD, Puopolo KM. Perinatal COVID-19: guideline development, implementation, and challenges. Curr Opin Pediatr. 2021;33:188–94. https://doi.org/10.1097/MOP.0000000000000997

Address for correspondence: Nancy A. Otieno, Kenya Medical Research Institute, Centre for Global Health Research, PO Box 1578-40100, Kisumu, Kenya; email: notieno@kemricdc.org, nancyotieno@gmail.com.

Genomic Evolution of SARS-CoV-2 Virus in Immunocompromised Patient, Ireland

Maureen Lynch,[1] Guerrino Macori,[1] Séamus Fanning, Edel O'Regan, Eoin Hunt, Dermot O'Callaghan, Brian McCullagh, Cormac Jennings, Anne Fortune

Author affiliations: Mater Misericordiae University Hospital, Dublin, Ireland (M. Lynch, E. O'Regan, E. Hunt, D. O'Callaghan, B. McCullagh, C. Jennings, A. Fortune); University College Dublin-Centre for Food Safety School of Public Health, Physiotherapy & Sports Science, Dublin (G. Macori, S. Fanning)

We examined virus genomic evolution in an immunocompromised patient with prolonged severe acute respiratory syndrome coronavirus 2 infection. Genomic sequencing revealed genetic variation during infection: 3 intrahost mutations and possible superinfection with a second strain of the virus. Prolonged infection in immunocompromised patients may lead to emergence of new virus variants.

The coronavirus disease (COVID-19) pandemic, caused by severe acute respiratory syndrome coronavirus 2 (SARS-CoV-2), has led to substantial illness and death in immunocompromised patients (1). Outcomes for patients with hematologic malignancies can be poor because of immune suppression associated with cancer itself and chemoimmunotherapy regimens used to treat these cancers (2).

Persistent shedding of SARS-CoV-2 RNA has been described since early in the pandemic; quantitative reverse transcription PCR (qRT-PCR) results have remained positive for 63 days (3). Recent studies of immunocompromised patients have detected infectious virus until 143 days after diagnosis (4–6). Phylogenetic analysis showed that single-nucleotide polymorphisms (SNPs) could be used to elucidate the transmission routes of SARS-CoV-2 in communities (7). Moreover, it has been demonstrated that intrahost single-nucleotide variants are restricted to specific lineages (8); however, no clear evidence supports a link between prolonged infection and intra-evolutionary dynamics (9).

We report a case of a prolonged clinical infection with persistent virus shedding in a patient with functional B-cell deficiency, hypogammaglobulinemia,

---

[1]These authors contributed equally to this article.

and COVID-19. We describe the sequence polymorphisms over time among the 9 whole-virus genome sequences obtained by following the ARTIC tiling-amplicon approach (https://artic.network/resources/ncov/ncov-amplicon-v3.pdf) and using the Illumina MiSeq platform as described (7).

In April 2020, a 52-year-old woman in Dublin, Ireland, sought emergency care for a 5-day history of fever, diarrhea, and fatigue. Five months earlier, she had received a diagnosis of stage 4, grade 1 follicular lymphoma and had since completed 3 cycles of chemotherapy with cyclophosphamide, vincristine, doxorubicin, prednisolone, and obinutuzumab (B-cell monoclonal antibody); the last therapy cycle had been completed 7 days before the emergency department visit. During the emergency department visit, SARS-CoV-2 was detected on a nasopharyngeal swab sample by qRT-PCR (Roche FLOW Flex, https://diagnostics.roche.com) with a cycle threshold (C_t) value of 25.04. Chest radiographs showed a typical pattern for COVID-19 infection. The patient received hydroxychloroquine and azithromycin for 5 days. At the time of admission, she had hypogammaglobulinemia and received intravenous immunoglobulin every 4 weeks as supportive therapy.

During her 100-day hospital stay, the patient's clinical course of illness was protracted, with fevers and oxygen requirements, requiring a 17-day stay in a critical care unit (Appendix, https://wwwnc.cdc.gov/EID/article/27/9/21-1159-App1.pdf). In the hospital, the patient was in a single room with transmission-based air-handling precautions.

During her entire hospital stay, SARS-CoV-2 was detected at varying C_t values in nasopharyngeal swab samples, except for days 31 and 85 when SARS-CoV-2 was not detected. Bronchoalveolar lavage (BAL) performed on day 95 to exclude other pathogens detected SARS-CoV-2 (C_t 30). Serologic testing did not detect antibodies to SARS-CoV-2 (Roche anti-SARS-CoV-2) on days 30, 84, and 103.

The patient was tested 17 times, and we sequenced all samples that were positive by qRT-PCR with C_t <32.8. All 9 samples that underwent whole-virus genome sequencing (Appendix Figure) belonged to clade 20B, lineage B.1.1. SNP analysis clustered these genomes into 3 groups. Genomes sequenced from the positive samples taken on days 5, 19, and 26 were indistinguishable at the sequence level (Figure). A sample taken on day 47 showed the first mutation event; 3 point mutations were identified in the whole-virus genome sequence data until day 76 after diagnosis. On day 82, genome analysis detected a new SNP (second mutation event). Sequencing of the BAL sample taken on day 95 detected a different set of sequence polymorphisms that most likely originated from a new infection event. SNP analysis indicated 11 point mutations (Appendix Table 1) giving rise to 3 amino acid substitutions in the gene coding for the spike protein (S:S50L, S:A653V, and S:L1186F).
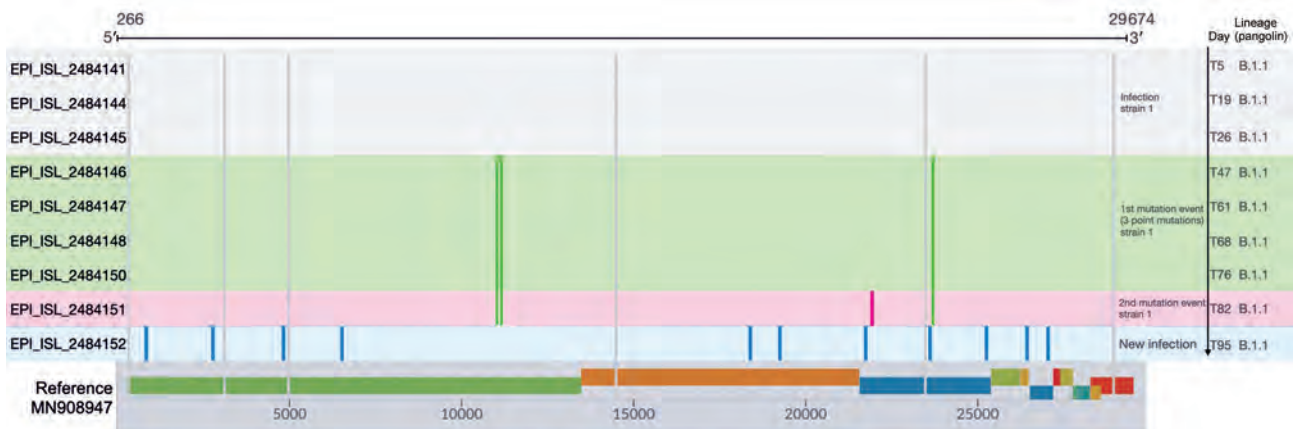

Figure. Sequence polymorphisms detected over time among the 9 whole-virus genome sequences from an immunocompromised patient with prolonged severe acute respiratory syndrome coronavirus 2 (SARS-CoV-2) infection, Ireland. The mutations are represented by different colors; gray lines indicate the polymorphisms common to the 9 whole-virus genome sequences compared with the reference whole-virus genome (GenBank accession no. MN908947, SARS-CoV-2 isolate Wuhan-Hu-1). The infection was confirmed on day 5 of infection (at admission to the emergency department), and the sequencing demonstrated stability of the virus genome sequence on days 19 (T19) and 26 (T26) after the first detection. Green indicates mutations detected in the sample at 47 days after first the emergency department admission (T47), T61, T68, and T76. At sample time T82, the strain exhibited a fourth mutation (pink) corresponding to the second mutation event. On day 95, a bronchoalveolar lavage sample from the patient was positive for SARS-CoV-2 and the whole-virus genome had a different set sequence polymorphism that probably originated from a new infection event. GISAID (https://www.gisaid.org) identification numbers are provided.

SARS-CoV-2 shedding in this patient with lymphoma, ongoing fevers, and oxygen requirements for 6 months was prolonged. The antibody-mediated ablation of B-cell precursors by B-cell directed monoclonal antibody therapy was most likely responsible for the prolonged virus shedding. This effect, combined with hypogammaglobulinemia, explains the lack of seroconversion and the protracted clinical course.

Sequential sequencing demonstrated intrahost mutations of ≥ 2 events (Figure) and accumulation of 4 SNPs. Analysis of a BAL sample taken on day 95 showed 11 point mutations giving rise to 3 aa substitutions in the gene coding for the spike protein. This observation is in accordance with findings of a recent study that detected 7 new mutations in a second virus strain in an immunocompromised patient (10). The BAL findings, along with ongoing symptoms, are suggestive of probable superinfection with cohabitation of 2 virus strains. However, considering that this was the only BAL sampled, we cannot exclude the possibility that the origin of this strain is the result of a different evolutionary path of the original population responsible for the first infection.

The superinfection that we describe was probably a nosocomial infection despite the transmission-based precautions taken in the patient's single room during her hospital stay. However, no sequence data from other patients or healthcare workers on the ward could be explored to identify the source of infection.

Our report highlights the complex clinical course of SARS-CoV-2 in immunocompromised patients. This genomic analysis identified the ability of the virus to mutate and possibly coexist with another strain, resulting in superinfection in this immunocompromised patient.

Acknowledgment

About the Author

Dr. Lynch is a clinical microbiologist in the Mater Misericordiae University Hospital, Dublin, Ireland, with a special interest in molecular diagnostics of respiratory and enteric viruses. Dr. Macori is a research scientist-bioinformatician at University College Dublin, working on the application of novel sequencing technologies for genome diagnosis and epidemiology of major pathogens, including SARS-CoV-2, in Ireland.

References

1. Fung M, Babik JM. COVID-19 in immunocompromised hosts: what we know so far. Clin Infect Dis. 2021;72:340–50. https://doi.org/10.1093/cid/ciaa863
2. Rubinstein SM, Warner JL. COVID-19 and haematological malignancy: navigating a narrow strait. Lancet Haematol. 2020;7:e701–3. https://doi.org/10.1016/S2352-3026(20)30252-0
3. Li J, Zhang L, Liu B, Song D. Case report: viral shedding for 60 days in a woman with COVID-19. Am J Trop Med Hyg. 2020;102:1210–3. https://doi.org/10.4269/ajtmh.20-0275
4. Avanzato VA, Matson MJ, Seifert SN, Pryce R, Williamson BN, Anzick SL, et al. Case study: prolonged infectious SARS-CoV-2 shedding from an asymptomatic immunocompromised individual with cancer. Cell. 2020; 183:1901–1912.e9. https://doi.org/10.1016/j.cell.2020.10.049
5. Baang JH, Smith C, Mirabelli C, Valesano AL, Manthei DM, Bachman MA, et al. Prolonged severe acute respiratory syndrome coronavirus 2 replication in an immunocompromised patient. J Infect Dis. 2021;223:23–7. https://doi.org/10.1093/infdis/jiaa666
6. Choi B, Choudhary MC, Regan J, Sparks JA, Padera RF, Qiu X, et al. Persistence and evolution of SARS-CoV-2 in an immunocompromised host. N Engl J Med. 2020;383:2291–3. https://doi.org/10.1056/NEJMc2031364
7. Lucey M, Macori G, Mullane N, Sutton-Fitzpatrick U, Gonzalez G, Coughlan S, et al. Whole-genome sequencing to track severe acute respiratory syndrome coronavirus 2 (SARS-CoV-2) transmission in nosocomial outbreaks. Clin Infect Dis. 2021;72:e727-e735. https://doi.org/10.1093/cid/ciaa1433
8. Armero A, Berthet N, Avarre JC. Intra-host diversity of SARS-Cov-2 should not be neglected: case of the state of Victoria, Australia. Viruses. 2021;13:133. https://doi.org/10.3390/v13010133
9. Wang Y, Wang D, Zhang L, Sun W, Zhang Z, Chen W, et al. Intra-host variation and evolutionary dynamics of SARS-CoV-2 populations in COVID-19 patients. Genome Med. 2021;13:30. https://doi.org/10.1186/s13073-021-00847-5
10. Tarhini H, Recoing A, Bridier-Nahmias AB, Rahi M, Lambert C, Martres P, et al. Long term SARS-CoV-2 infectiousness among three immunocompromised patients: from prolonged viral shedding to SARS-CoV-2 superinfection. J Infect Dis,2021;223:1522–7.

Address for correspondence: Maureen Lynch, Department of Clinical Microbiology, Mater Hospital, Eccles St, Dublin 7, Ireland; email: lynchm@mater.ie

Prevalence of *mcr-1* in Colonized Inpatients, China, 2011–2019

Cong Shen,[1] Lan-Lan Zhong,[1] Zhijuan Zhong,[1] Yohei Doi, Jianzhong Shen, Yang Wang, Furong Ma, Mohamed Abd El-Gawad El-Sayed Ahmed, Guili Zhang, Yong Xia, Cha Chen, Guo-Bao Tian

Author affiliations: Sun Yat-sen University Zhongshan School of Medicine, Guangzhou, China (C. Shen, L.-L. Zhong, M.A.E.-G.E.-S. Ahmed, G. Zhang, G.-B. Tian); Sun Yat-sen University Key Laboratory of Tropical Diseases Control, Guangzhou (C. Shen, L.-L. Zhong, M.A.E.-G.E.-S. Ahmed, G. Zhang, G. Tian); Guangzhou University of Chinese Medicine The Second Clinic Medical College, Guangzhou (C. Shen, C. Chen); The Second Affiliated Hospital of Guangzhou University of Chinese Medicine, Guangdong Provincial Hospital of Traditional Chinese Medicine, Guangzhou (C. Shen, C. Chen); Sun Yat-Sen University The Fifth Affiliated Hospital, Zhuhai, China (Z. Zhong); University of Pittsburgh School of Medicine, Pittsburgh, Pennsylvania, USA (Y. Doi); Fujita Health University School of Medicine, Aichi, Japan (Y. Doi); China Agricultural University, College of Veterinary Medicine, Beijing, China (J. Shen, Y. Wang); China Agricultural University, College of Animal Science and Technology, Beijing (J. Shen, Y. Wang); Third Affiliated Hospital of Guangzhou Medical University, Guangzhou (F. Ma, Y. Xia); Misr University for Science and Technology, Cairo, Egypt (M.A.E.-G.E.-S. Ahmed); Xizang Minzu University School of Medicine, Xianyang, China (G. Tian)

In response to the spread of colistin resistance gene *mcr-1*, China banned the use of colistin in livestock fodders. We used a time-series analysis of inpatient colonization data from 2011–2019 to accurately reveal the associated fluctuations of *mcr-1* that occurred in inpatients in response to the ban.

Heavy use of antimicrobials in agricultural, human, and veterinary applications correlates directly with emergence and spread of antimicrobial resistance, thereby threatening the effective management of clinical infections (*1,2*). An example of this association is the global dissemination of the antimicrobial resistance gene (ARG) *mcr-1*, conferring resistance to the last-line antimicrobial drug colistin. The *mcr-1* gene has been prevalent in ecosystems that use colistin as a growth promoter in food-producing animals, as seen in China before 2017 (*2–5*).

To counteract the high prevalence of *mcr-1* and align with One Health principles, the government in China formally banned colistin as an animal feed additive on April 30, 2017 (*6*). Previous research demonstrated that colistin resistance rates and *mcr-1* prevalence in *Escherichia coli* from human and animal samples declined substantially in China, according to a regional study conducted in Guangzhou during 2015–2019 (p<0.0001). These data suggest the effectiveness of colistin stewardship in reducing colistin resistance in both livestock and humans (*4,5*). However, the sampling strategy of these studies was limited to evaluating only several cross-sectional timepoints from before and after the ban, resulting in uncertainty about the exact timing of the effect.

To characterize the complete prevalence dynamics of human *mcr-1* colonization, including the periban period, we constructed a 9-year monthly time series for April 2011–December 2019, over which time 13,630 fecal samples from colonized inpatients were previously taken, by further evaluating *mcr-1* prevalence of 3,823 stored fecal samples collected during April–September 2016, January–September 2017–2018, and January–December 2019. We combined these data with those from our previous studies (*3,5*) (Appendix Table 1, https://wwwnc.cdc.gov/EID/article/27/9/20-3642-App1.pdf). We used a 3-month moving average approach to remove noise and substituted missing data for 7 months of the time series by using the mean values of the 2 months flanking any month with missing data (Appendix). Through changepoint analysis (Appendix) (*7*), we identified 5 changepoints, dividing the time series into 6 periods (Figure).

We observed that *mcr-1* prevalence in human fecal samples was low (<3%) in the early period, before October 2013, demonstrating that the *mcr-1* gene was circulating to a limited extent in human populations before late 2013 in period 1 (P1). We observed a significant increase in *mcr-1* colonization prevalence after November 2013 in period 2 (P2) that lagged behind increases of *mcr-1* prevalence observed in livestock from 2011 (*2*) and was consistent with dissemination from this reservoir. The third period (P3) showed a sharp increase in *mcr-1* human colonization prevalence, followed by a peak in October 2016, suggesting that *mcr-1* was rapidly spreading in human settings, potentially attributable to an extremely high *mcr-1* prevalence (>60%) in livestock around the time (*4,5,8*). Beginning in November 2016, in period 4 (P4), pilot decreases in colistin use as an animal feed additive were already being implemented (*4*) before the complete ban in 2017. We observed declines in human *mcr-1* colonization prevalence during this period

---

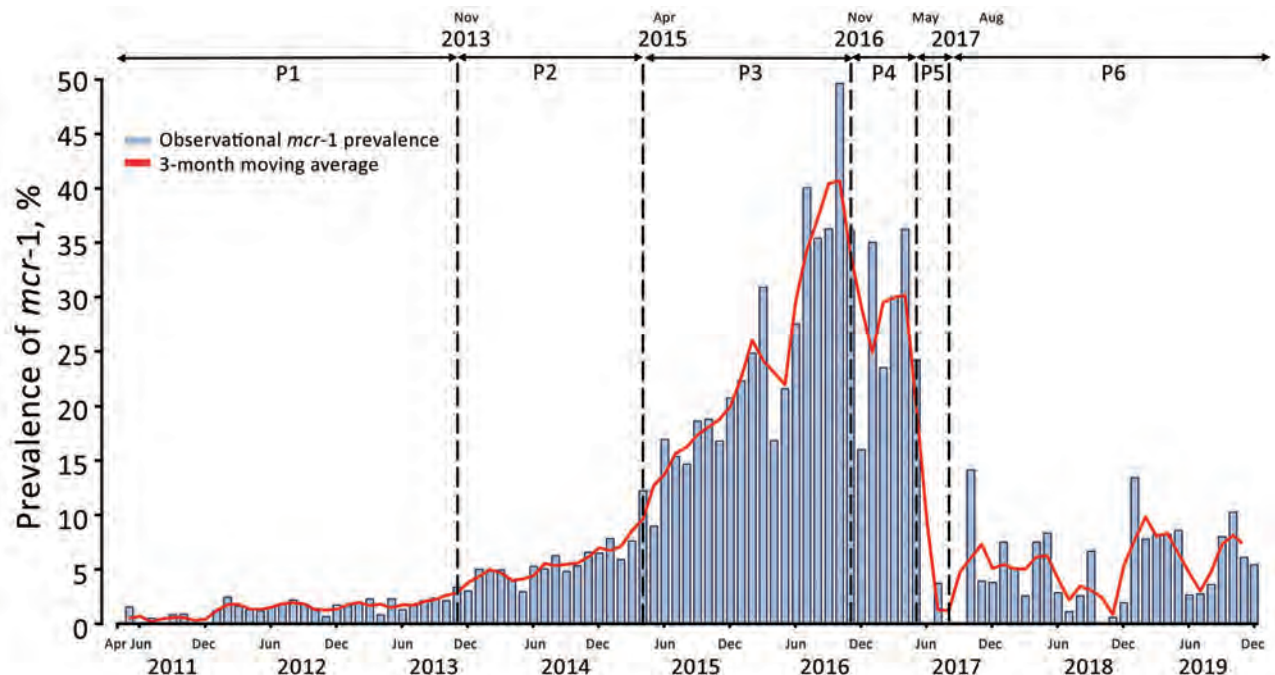[1]These authors contributed equally to this article.

Figure. Time series of monthly *mcr-1* prevalence in colonized inpatients, China, April 2011–December 2019. The *mcr-1* prevalence was recorded each month in observed data (blue histogram) and 3-month moving average data (solid red line). Vertical dashed lines indicate significant changepoints identified in the changepoint analysis: November 2013, May 2015, November 2016, May 2017, and August 2018. The government of China formally banned colistin as an animal feed additive on April 30, 2017. P, time period.

that were temporally consistent with declines in *mcr-1* prevalence observed in livestock (*8*). The fifth period (P5) showed a dramatic decline in human *mcr-1* colonization prevalence, correlating with the complete ban of colistin in animal feed (*6*). The rapid impact of this intervention is indicative of the dramatic effect that curtailing a selection pressure can have in constraining ARG prevalence and could be a template for combatting other ARGs. In the last period evaluated, period 6 (P6), *mcr-1* prevalence fluctuated at a low level (monthly average 5.3%), in accordance with the *mcr-1* prevalence observed in healthy human carriers, pigs, and chickens after the colistin ban (*5*). Although currently at low levels, *mcr-1* prevalence should be monitored continually to detect any signs of its resurgence, particularly given that colistin was approved for human clinical use in China in January 2017 (*9*).

In conclusion, we characterized the dynamic landscape of *mcr-1* over a 9-year period in China and found that colistin stewardship interventions in livestock were reflected in the *mcr-1* prevalence in human fecal colonization samples within a month of a large-scale, national ban on colistin usage. Partial reductions in colistin use beginning in November 2016 rapidly reduced the *mcr-1* prevalence and turned around the alarming increases observed during 2015–2016. The complete ban implemented on April 30, 2017,

significantly and immediately reduced *mcr-1* prevalence to near pre-2015 levels. Of interest, however, the background *mcr-1* prevalence in 2019 was still higher than that observed during 2011–2013, perhaps associated with the approval of colistin for human clinical use in China in January 2017 (*9*). As a result of our findings, we strongly encourage interdisciplinary surveillance involving clinicians, veterinary specialists, and environmentalists to further investigate and evaluate changes in ARG prevalence across different human, animal, and environmental niches to improve holistic understanding of the impact and timeframe of different stewardship interventions.

About the Author

Mr. Shen is a doctoral student at Zhongshan School of Medicine, Sun Yat-sen University, Guangzhou, China. His primary research interests include infectious disease epidemiology, antimicrobial resistance, microbial population genomics, and genomic epidemiology.

References

1. Tang KL, Caffrey NP, Nóbrega DB, Cork SC, Ronksley PE, Barkema HW, et al. Restricting the use of antibiotics in food-producing animals and its associations with antibiotic resistance in food-producing animals and human beings: a systematic review and meta-analysis. Lancet Planet Health. 2017;1:e316–27. https://doi.org/10.1016/S2542-5196(17)30141-9
2. Shen Z, Wang Y, Shen Y, Shen J, Wu C. Early emergence of *mcr-1* in *Escherichia coli* from food-producing animals. Lancet Infect Dis. 2016;16:293. https://doi.org/10.1016/S1473-3099(16)00061-X
3. Zhong LL, Phan HTT, Shen C, Vihta KD, Sheppard AE, Huang X, et al. High rates of human fecal carriage of *mcr-1*-positive multidrug-resistant *Enterobacteriaceae* emerge in China in association with successful plasmid families. Clin Infect Dis. 2018;66:676–85. https://doi.org/10.1093/cid/cix885
4. Wang Y, Xu C, Zhang R, Chen Y, Shen Y, Hu F, et al. Changes in colistin resistance and *mcr-1* abundance in *Escherichia coli* of animal and human origins following the ban of colistin-positive additives in China: an epidemiological comparative study. Lancet Infect Dis. 2020;20:1161–71. https://doi.org/10.1016/S1473-3099(20)30149-3
5. Shen C, Zhong L, Yang Y, Doi Y, Paterson D, Stoesser N, et al. Dynamics of *mcr-1* prevalence and *mcr-1*-positive *Escherichia coli* after the cessation of colistin use as a feed additive for animals in China: a prospective cross-sectional and whole genome sequencing-based molecular epidemiological study. Lancet Microbe. 2020;1:e34–43. https://doi.org/10.1016/S2666-5247(20)30005-7
6. Walsh TR, Wu Y. China bans colistin as a feed additive for animals. Lancet Infect Dis. 2016;16:1102–3. https://doi.org/10.1016/S1473-3099(16)30329-2
7. Killick R, Eckley I. Changepoint: an R package for changepoint analysis. J Stat Softw. 2014;58:1–19. https://doi.org/10.18637/jss.v058.i03
8. Li W, Hou M, Liu C, Xiong W, Zeng Z. Dramatic decrease in colistin resistance in *Escherichia coli* from a typical pig farm following restriction of colistin use in China. Int J Antimicrob Agents. 2019;53:707–8. https://doi.org/10.1016/j.ijantimicag.2019.03.021
9. Zhang R, Shen Y, Walsh TR, Wang Y, Hu F. Use of polymyxins in Chinese hospitals. Lancet Infect Dis. 2020;20:1125–6. https://doi.org/10.1016/S1473-3099(20)30696-4

Address for correspondence: Guo-Bao Tian, Zhongshan School of Medicine, Sun Yat-sen University, 74 Zhongshan 2nd Rd, Guangzhou 510080, China; email: tiangb@mail.sysu.edu.cn

Haemophilus influenzae Type a Sequence Type 23, Northern Spain

Maddi López-Olaizola, Amaia Aguirre-Quiñonero, Andrés Canut, José Luis Barrios, Gustavo Cilla, Diego Vicente, José María Marimón

Author affiliations: Biodonostia Health Research Institute, Infectious Diseases Area, Osakidetza Basque Health Service, Donostialdea Integrated Health Organization, San Sebastián, Spain (M. López-Olaizola, G. Cilla, D. Vicente, J.M. Marimón); Osakidetza Basque Health Service, Araba Integrated Health Organization, Vitoria-Gasteiz, Spain (A. Aguirre-Quiñonero, A. Canut); Osakidetza Basque Health Service, Ezkerraldea-Enkarterri-Cruces Integrated Health Organization, Bilbao, Spain (J.L. Barrios)

Two consecutive cases of *Haemophilus influenzae* type a sequence type 23 invasive infection in 2 children attending the same daycare in 2019 triggered epidemiologic surveillance of *H. in luenzae* infections in northern Spain. Despite the invasiveness potential of this bacterial strain, we detected no additional cases for 2013–2020.

Since the introduction of the *Haemophilus influenzae* type b (Hib) conjugate vaccine in the infant immunization schedule in 1998, the incidence of invasive *H. influenzae* (Hi) infections in Spain decreased to 0.7 episodes/100,000 population (*1*). Higher incidence rates are observed in children ≤2 years of age (1.88/100,000 population) and adults ≥65 years of age (1.89 cases/100,000 population) (*2*). Invasive disease caused by Hib has nearly disappeared, and most cases are caused by nontypeable strains (*3*).

Invasive infections caused by *H. influenzae* type a (Hia) are uncommon in Europe, particularly in Spain. However, Hia incidence is as high in other regions as among indigenous communities in North America (*4*) and as has emerged in Brazil during the 2000s (*5*). We describe 2 cases of Hia invasive disease in Gipuzkoa, northern Spain.

Both cases of Hia invasive disease occurred in children in a village with ≈15,000 inhabitants during November 2–3, 2019. The first patient, a 2-year-old boy, was admitted to the pediatric emergency department with good general aspect and persistent low-grade fever without a clear source. The child was not vaccinated according to the routine immunization schedule. Results for pulmonary auscultation and respiratory and cardiac rates were unremarkable, and a chest radiograph showed no abnormalities.

The second patient, a 19-month-old girl, was admitted to the pediatric emergency department with a nonproductive cough and a 39°C fever that was nonresponsive to antipyretics. The infant was vaccinated according to the routine immunization schedule, including Hib vaccination. No dyspnea was observed, and the chest radiograph showed pulmonary infiltrates suggesting pneumonia.

Both children showed increased C-reactive protein, procalcitonin, and white cell counts and had *H. influenzae* grown in the blood culture taken at admission. The boy was treated with ceftriaxone (50 mg/kg/12 h) for 5 days and the girl with ceftriaxone (50 mg/kg/12 h) for 4 days. Both children were discharged without symptoms or sequelae. Neither patient required additional antibiotic treatment after admission.

Both children attended the same daycare center, where no other children showed symptoms of infection. In Gipuzkoa, no additional cases of Hia invasive infection have been observed since 2013 (Table). However, 1 Hia was isolated 1 week later in the blood-culture of a 51-year-old patient in the adjacent province of Bizkaia.

We identified isolates with matrix-assisted laser desorption/ionization time-of-flight mass spectrometry (Beckman Coulter, https://www.beckmancoulter.com). Both case-patients scored >2.000. We biotyped isolates using the API 20E system of bacterial identification and serotyped using multiplex-PCR (*6*) and confirmed serotypes using BD Difco *Haemophilus influenzae* Antisera (Fisher Scientific, https://www.fishersci.com). We performed genotyping by multilocus sequenced typing and pulsed-field gel electrophoresis (PFGE) (Figure) after *Sma*I digestion with the following running conditions: switch angle 120°, 6 V/cm, ramped switch time from 1–30 s over 23 h. The presence of a deletion in the *IS1016-bexA* genes of the capsular operon was studied by PCR as described (*7*). We determined antimicrobial susceptibility by broth microdilution method according to EUCAST version 9.0 guidelines and criteria (EUCAST, https://www.eucast.org).

The isolates of both children were biotype II, serotype a, sequence type (ST) 23; showed an indistinguishable PFGE pattern; did not show the *IS1016-bexA* partial deletion; and were susceptible to ampicillin, azithromycin, and trimethoprim/sulfamethoxazole. The Hia that was isolated 1 week later in Bizkaia was similar to the 2 previous isolates of Gipuzkoa (biotype II, serotype a, not partial *IS1016-bexA* deletion) but was ST2053 (SLV of ST23) and had a closely related, but not identical, PFGE pattern.

We also characterized all invasive *H. influenzae* isolates reported since 2013 in Gipuzkoa (Table). Of the 48 isolates, 41 (85.4%) were nontypeable and 5 (10.4%) were serotype b; only the 2 cases described in this article were serotype a. All serotype b isolates were biotype I; showed the *IS1016-bexA* partial deletion; and belonged to ST6 (n = 2), ST190, or ST995.

Hia ST23 isolates have been described in different parts of the world, especially in Canada (*4*) and Brazil (*5*). In Europe, Hia ST23 has been found infrequently in Portugal (*8*) and recently in Italy (*9*). The *H. influenzae* multilocus sequence typing database (https://pubmlst.org/organisms/haemophilus-influenzae) lists only 29 ST23 isolates from the United States, Canada, Malaysia, France, and Spain (the 2 isolates in this article), most of them serotype a from invasive diseases.

Hia ST23 isolates from our region and from Canada did not show the virulence-enhancing *IS1016-bexA* partial deletion that has been more commonly associated with increased Hia virulence (*10*). However, isolates from our region only caused a mild and self-limiting infection, as compared with the severe disease observed among native North American Arctic

Table. Epidemiologic and microbiological characteristics of *Haemophilus influenzae* invasive isolates, Gipuzkoa, Northern Spain, January 2013–December 2020*

Year	No. isolates†*	Biotype					Capsulated serotypes/ST			Nonencapsulated serotypes (no. isolates)	
		I	II	III	IV	V	a	b	e	NT	ST‡
2013	7	4	2	1				1/ST6		6	41, 368 (2), 388, 996, 2381§
2014	5	1	4					1/ST190		4	105, 249, 1034, 1608
2015	4		3	1						4	40, 155 (2), 2382§
2016	7	1	4	1						6	3, 85, 103, 266, 937, 2383§
2017	5	2	2			1		1/ST6		4	134, 567, 653, 986
2018	9	2		1		4		1¶		6	14, 145, 165, 838, 1472, 2384§
2019	11	1	6	1	2		2/ST23	1/ST995	1/ST760	6	6, 14, 103, 393, 603, 2110
2020	5	2	3							5	143, 183, 280, 334, 349
Total	53	13	24	5	2	5	2	5	1	41	

*NT, nontypeable; ST, sequence type.
†Four isolates were not available for microbiological characterization: 1 in 2016, 2 in 2018, 1 in 2019.
‡If the number of isolates of a specific ST was not 1, the number of isolates corresponding to that ST is indicated in brackets.
§New ST found in this study.
¶Serotype was determined but the isolate was not available for multilocus sequence typing.
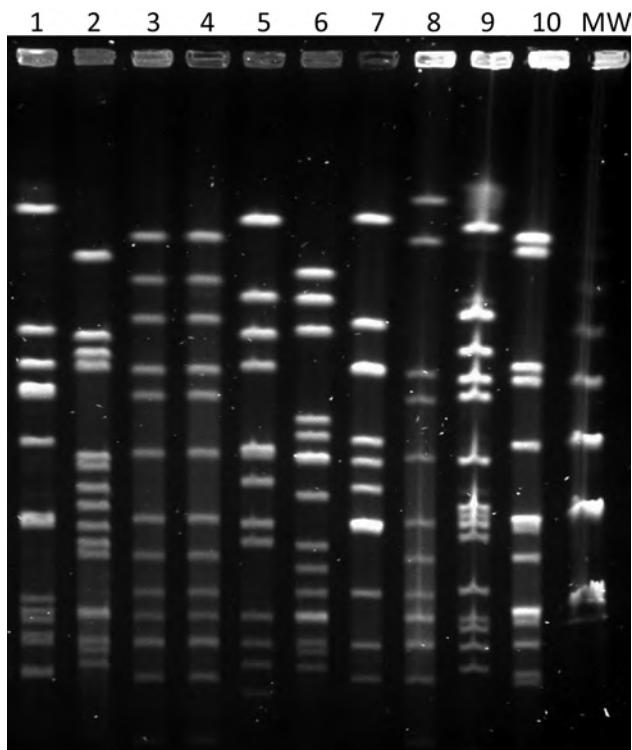
Figure. Pulsed-field gel electrophoresis patterns of invasive *Haemophilus influenzae* isolates collected during 2019–2020, Gipuzkoa, northern Spain. Lane 1, ST103; lane 2, ST760; lanes 3–4, ST23 isolates; lane 5, ST393; lane 6, ST6; lane 7, ST995; lane 8, ST2053; lane 9, ST46; lane 10, control isolate ATCC49766; lane MW, 50 kb DNA ladder. ST, sequence type; MW, molecular weight.

populations that required intensive care unit admission and had notable sequelae (*4*).

As was the case in Italy, transmission of the highly virulent ST23 clone was substantially limited in Gipuzkoa. Although ST23 is a virulent Hia clone, its sustained spread appears to be limited, primarily among indigenous populations of North America. The origin of the isolates described in this article is unknown because Hia ST23 had not been previously described in Spain.

About the Author

Ms. López-Olaizola is a clinical microbiologist in the bacteriology section, University Hospital Donostia. Her research focus on antimicrobial resistance and the epidemiology of infectious agents.

References

1. European Centre for Disease Prevention and Control. *Haemophilus influenzae*—annual epidemiological report for 2017 [cited 2019 Apr 23]. https://www.ecdc.europa.eu/en/publications-data/haemophilus-influenzae-annual-epidemiological-report-2017
2. Ciruela P, Martínez A, Izquierdo C, Hernández S, Broner S, Muñoz-Almagro C, et al.; Microbiological Reporting System of Catalonia Study Group. Epidemiology of vaccine-preventable invasive diseases in Catalonia in the era of conjugate vaccines. Hum Vaccin Immunother. 2013;9:681–91. https://doi.org/10.4161/hv.23266
3. Campos J, Hernando M, Román F, Pérez-Vázquez M, Aracil B, Oteo J, et al.; Group of Invasive Haemophilus Infections of the Autonomous Community of Madrid, Spain. Analysis of invasive *Haemophilus influenzae* infections after extensive vaccination against *H. influenzae* type b. J Clin Microbiol. 2004;42:524–9. https://doi.org/10.1128/JCM.42.2.524-529.2004
4. Tsang RSW, Proulx J-F, Hayden K, Shuel M, Lefebvre B, Boisvert A-A, et al. Characteristics of invasive *Haemophilus influenzae* serotype a (Hia) from Nunavik, Canada and comparison with Hia strains in other North American Arctic regions. Int J Infect Dis. 2017;57:104–7. https://doi.org/10.1016/j.ijid.2017.02.003
5. Tuyama M, Corrêa-Antônio J, Schlackman J, Marsh JW, Rebelo MC, Cerqueira EO, et al. Invasive *Haemophilus influenzae* disease in the vaccine era in Rio de Janeiro, Brazil. Mem Inst Oswaldo Cruz. 2017;112:196–202. https://doi.org/10.1590/0074-02760160391
6. Falla TJ, Crook DW, Brophy LN, Maskell D, Kroll JS, Moxon ER. PCR for capsular typing of *Haemophilus influenzae*. J Clin Microbiol. 1994;32:2382–6. https://doi.org/10.1128/jcm.32.10.2382-2386.1994
7. Leaves NI, Falla TJ, Crook DW. The elucidation of novel capsular genotypes of *Haemophilus influenzae* type b with the polymerase chain reaction. J Med Microbiol. 1995;43:120–4. https://doi.org/10.1099/00222615-43-2-120
8. Heliodoro CIM, Bettencourt CR, Bajanca-Lavado MP; Portuguese Group for the Study of Haemophilus influenzae Invasive Infection. Molecular epidemiology of invasive *Haemophilus influenzae* disease in Portugal: an update of the post-vaccine period, 2011–2018. Eur J Clin Microbiol Infect Dis. 2020;39:1471–80. https://doi.org/10.1007/s10096-020-03865-0
9. Giufrè M, Cardines R, Brigante G, Orecchioni F, Cerquetti M. Emergence of invasive *Haemophilus influenzae* type a disease in Italy. Clin Infect Dis. 2017;64:1626–8. https://doi.org/10.1093/cid/cix234
10. Kapogiannis BG, Satola S, Keyserling HL, Farley MM. Invasive infections with *Haemophilus influenzae* serotype a containing an IS1016-bexA partial deletion: possible association with virulence. Clin Infect Dis. 2005;41:e97–103. https://doi.org/10.1086/498028

Address for correspondence: José María Marimón, Microbiology Department, University Hospital Donostia, Paseo Dr, Beguristain s/n, 20014 San Sebastián, Spain; email: josemaria.marimonortizdez@osakidetza.eus

SARS-CoV-2 Superspread in Fitness Center, Hong Kong, China, March 2021

Linsey C. Marr

Author affiliation: Virginia Polytechnic Institute and State University, Blacksburg, Virginia, USA

To the Editors: I read with interest the article by Chu et al. (*1*), which concluded that poor ventilation might have contributed to a severe acute respiratory syndrome coronavirus 2 (SARS-CoV-2) superspreading event at a fitness center in Hong Kong, China. As an example of SARS-CoV-2 not spreading in a converse environment, I report the absence of apparent transmission at a gym in Montgomery County, Virginia, USA, that emphasized ventilation as part of its coronavirus disease (COVID-19) precautions upon reopening in June 2020. The gym (Appendix Figure 1, https://wwwnc.cdc.gov/EID/article/27/9/21-1177-App1.pdf) increased ventilation by opening 10 exterior doors and keeping them open even during cold or inclement weather. The gym also limited class sizes, stressed hygiene, and required ≥10 feet of distancing. Masks were not worn.

With the doors closed, the air change rate was estimated to be 0.07 air changes/hour, corresponding to a ventilation rate of 7.6 L/second/person (L/s/p) on the basis of an occupancy of 10 persons, below the 10 L/s/p minimum recommended by ASHRAE (American Society of Heating and Air-Conditioning Engineers) for health clubs (*2*). With the doors open, these values were estimated to be 2.4 air changes/hour and 240 L/s/p (Appendix).

On September 24, 2020, an instructor at the gym developed upper respiratory symptoms and lost his sense of smell and taste. He was tested for SARS-CoV-2 infection and received a positive result on September 28, 2020. That day, the gym owner contacted 50 persons who had attended ≥1 of the instructor's classes during September 21–25, 2020 to notify them of potential exposure. During subsequent follow-up, none of these 50 persons reported any COVID-19 symptoms, and 5 people who got tested received negative results (Appendix Figure 2). It is likely that increasing ventilation greatly mitigated the risk of transmission (*3*). Subsequently, the gym acquired a CO_2 sensor and kept the CO_2 level, an indicator of respiratory emissions, well below 600 ppm (*4*) by adjusting the number of open doors.

References

1. Chu DKW, Gu H, Chang LDJ, Cheuk SSY, Gurung S, Krishnan P, et al. SARS-CoV-2 superspread in fitness center, Hong Kong, China, March 2021. Emerg Infect Dis. 2021 May 18 [Epub ahead of print]. https://doi.org/10.3201/eid2708.210833
2. American Society of Heating, Refrigerating and Air-Conditioning Engineers. Ventilation for acceptable indoor air quality. ANSI/ASHRAE Standard 62.1–2019. 2019 [cited 2021 Jan 7]. https://www.ashrae.org/technical-resources/bookstore/standards-62-1-62-2
3. Yang W, Marr LC. Dynamics of airborne influenza A viruses indoors and dependence on humidity. PLoS One. 2011;6:e21481. https://doi.org/10.1371/journal.pone.0021481
4. Peng Z, Jimenez JL. Exhaled CO_2 as a COVID-19 infection risk proxy for different indoor environments and activities. Environ Sci Technol Lett. 2021;8:392–7. https://doi.org/10.1021/acs.estlett.1c00183

Address for correspondence: Linsey C. Marr, Civil and Environmental Engineering, Virginia Tech, 1145 Perry St, Durham 411, Blacksburg, VA 24061, USA; email: lmarr@vt.edu

Fecal Excretion of *Mycobacterium leprae*, Burkina Faso

Ajay Vir Singh, Rajbala Yadav, Harpreet Singh Pawar, Devendra Singh Chauhan

Author affiliation: ICMR–National JALMA Institute for Leprosy and Other Mycobacterial Diseases, Agra, India

To the Editor: Millogo et al. (*1*) documented presence of *Mycobacterium leprae* in a fecal sample from a patient in Burkina Faso, raising questions about the role of fecal excretion of *M. leprae* in the natural history and diagnosis of leprosy. They speculated that *M. leprae* were swallowed by the patient along with blood

or upper respiratory secretions during leprosy rhinitis and epistaxis (*1*) but failed to address other factors that could influence fecal excretion of *M. leprae* and utility of fecal specimens in diagnosing leprosy.

Previous studies have demonstrated the presence of *M. leprae* in water and soil samples from habitations of patients with leprosy (*2,3*). This finding means that patients, contacts, or healthy persons can ingest *M. leprae* from environmental sources through drinking contaminated water or eating *M. leprae*–containing food and may excrete leprosy bacilli in their feces without establishing an infection. The role of environmental sources and simple passthrough phenomena in fecal excretion of *M. leprae* has not been investigated by Millogo et al. (*1*) and other studies (*4,5*).

Koshy et al. (*4*) reported the presence of leprosy bacilli in gastric juice of 9 of 16 patients with lepromatous leprosy; 3 were found to excrete the bacilli in their feces. Manzullo et al. (*5*) demonstrated the presence of acid-fast bacilli in biliary secretions of 7 of 20 patients with leprosy and in 2 of 7 fecal samples. These observations indicate that clinical manifestation of leprosy varies widely. The exact mechanism of fecal excretion of *M. leprae* can be more complex, as presumed in previous studies (*1,4,5*), and may be associated with high bacillary burden (as in lepromatous leprosy), gastrointestinal symptoms (abdominal pain or diarrhea),

disseminated disease, environmental factors, or combinations of these aspects. Verification of transmission routes of *M. leprae* to fecal samples using genotyping techniques (i.e., whole-genome sequencing) is crucial to establish the diagnostic utility of fecal specimens in leprosy.

References

1. Millogo A, Loukil A, L'Ollivier C, Djibougou DA, Godreuil S, Drancourt M. Fecal excretion of *Mycobacterium leprae*, Burkina Faso. Emerg Infect Dis. 2021;27:1758–60. https://doi.org/10.3201/eid2706.200748
2. Mohanty PS, Naaz F, Katara D, Misba L, Kumar D, Dwivedi DK, et al. Viability of *Mycobacterium leprae* in the environment and its role in leprosy dissemination. Indian J Dermatol Venereol Leprol. 2016;82:23–7. https://doi.org/10.4103/0378-6323.168935
3. Turankar RP, Lavania M, Singh M, Sengupta U, Siva Sai K, Jadhav RS. Presence of viable *Mycobacterium leprae* in environmental specimens around houses of leprosy patients. Indian J Med Microbiol. 2016;34:315–21. https://doi.org/10.4103/0255-0857.188322
4. Koshy A, Karat ABA. A study of acid-fast bacilli in the urine, gastric juice and faeces of patients with lepromatous leprosy. Lepr India. 1971;43:3–7.
5. Manzullo A, Manzi RO, Lefevre A, Oteiza ML. Investigation of acid-fast bacilli in the digestive tract of leprosy patients. Leprologia. 1965;10:14–6.

Address for correspondence: Ajay Vir Singh, Department of Microbiology and Molecular Biology, ICMR-National JALMA Institute for Leprosy and Other Mycobacterial Diseases, Agra, Uttar Pradesh, Pin-282001, India; email: avsjalma@gmail.com

CORRECTION

Vol. 26, No. 6

The rate of pregnancy-related invasive group B *Streptococcus* episodes was misstated in Invasive Group B *Streptococcus* Infections in Adults, England, 2015–2016 (S.M. Collins et al.). The correct rate is 4.09/10,000 live births. The article has been corrected online (https://wwwnc.cdc.gov/eid/article/26/6/19-1141_article).

People Count: Contact-Tracing Apps and Public Health

Susan Landau; The MIT Press, Cambridge, MA, USA, 2021; ISBN-10: 0262045710; Pages: 184; Price: $37.99

In *People Count: Contact-Tracing Apps and Public Health*, computer scientist Susan Landau advocates for a public discussion on using contact-tracing applications (apps) in public health. Landau puts her arguments in a succinct, easy-to-read narrative in 6 chapters.

Chapter 1 sets the scene for contact tracing by introducing the basics of epidemiology. Through examples, Chapter 2 explains the implementation of contact tracing and that, for it to succeed, governments must earn the public's trust by maintaining confidentiality and engaging with communities.

Chapter 3 introduces smartphone technologies proposed to add to contact tracing, focusing on apps with centralized databases, such as Singapore's TraceTogether, which exchanges identifiers with other users through Bluetooth Low Energy technology. Users authorize the government to view all the information collected from the app. Chapter 4 introduces coronavirus disease (COVID-19) exposure-notification apps, including SwissCovid and COVID Tracker Ireland, which are based on the Google Apple Exposure Notification (GAEN) system. Landau raises cybersecurity issues, including data storage and access policies, developers' accountability, and data theft. She is concerned that data will be used for other purposes (e.g., criminal investigations), engendering users' distrust.

Chapter 5 discusses whether contact-tracing apps are truly effective public health tools and if they exacerbate inequalities in societies. Landau cautions against measurement inaccuracies and low adoption rates. She provides examples that aid contact tracing while protecting users' privacy, such as the UK NHS (National Health Service) COVID-19 app; this app scans NHS-supplied QR (Quick Response) codes at venues, then downloads hotspot identifiers that match the scanned codes to remind users if they have been to an infection hotspot.

Chapter 6 advocates for a public policy discussion regarding the role of COVID-19 contact-tracing app in society. Landau makes policy recommendations in addition to safeguarding user data. First, COVID-19 should not trump other dimensions of well-being: if contact-tracing apps cause someone to isolate or lose a paycheck unnecessarily, they are not protecting all aspects of one's well-being. Second, contact-tracing app usage must be a genuine choice; access to venues, transportation, or services should not be denied because someone refuses to use an app. Third, data collected should be used only for COVID-19 proximity checking; other uses should be prohibited. Fourth, contact-tracing apps should be evaluated before and during deployment in different communities. Fifth, app software should be open source to maintain transparency, and contact-tracing apps should undergo formal independent testing.

Although Landau covers contact-tracing apps of many countries, she does not directly comment on China's health QR code, which is used for tracing citizens and denying venue and transportation access based on individuals' risk status (1–4). In general, Landau cautions us against the surveillance state: should we normalize the idea of collecting proximity data via contact-tracing apps, governments could use the data to track political opponents and activists. She warns against accepting that it is normal for electronic devices to track our contacts. *People Count* reminds us that protecting citizens' privacy and wellbeing are prerequisites for successful contact tracing, whether app-assisted or not.

Isaac Chun-Hai Fung, Benedict S.B. Chan

Author affiliations: Georgia Southern University, Statesboro, Georgia, USA (I.C.-H. Fung); Hong Kong Baptist University, Hong Kong, China (B.S.B. Chan)

References

1. Pan XB. Application of personal-oriented digital technology in preventing transmission of COVID-19, China. Ir J Med Sci. 2020;189:1145–6. https://doi.org/10.1007/s11845-020-02215-5
2. Yu A. Digital surveillance in post-coronavirus China: a feminist view on the price we pay. Gend Work Organ. 2020; 27:774–7. [Epub ahead of print]. https://doi.org/10.1111/gwao.12471
3. Wang T, Jia F. The impact of health QR code system on older people in China during the COVID-19 outbreak. Age Ageing. 2021;50:55–6. https://doi.org/10.1093/ageing/afaa222
4. Liang F. COVID-19 and health code: how digital platforms tackle the pandemic in China. Soc Media Soc. 2020;6:2056305120947657. https://doi.org/10.1177/2056305120947657

Address for correspondence: Isaac Chun-Hai Fung, Department of Biostatistics, Epidemiology, and Environmental Health Sciences, Jiann-Ping Hsu College of Public Health, Georgia Southern University, Statesboro, GA 30460, USA; email: cfung@georgiasouthern.edu

Considering Mycological Rarities

Byron Breedlove

Neither plant nor animal, fungal organisms—including lichen, mildew, mushrooms, molds, rusts, smuts, and yeasts—are found in nearly every possible terrestrial habitat, even aboard the International Space Station. There are millions of species of fungi, and according to the Centers for Disease Control and Prevention, a few hundred fungal species cause illness in people, ranging from allergies and asthma, to skin rashes and infections, to deadly infections of the bloodstream or lungs.

In a 2013 EID article, Mary Brandt and Benjamin Park note the growing number of human infections from traditional and new fungal agents. Factors driving this emergence, they explain, include medical treatments that make immunocompromised patients more susceptible. They also state that "Risk factors such as changes in land use, seasonal migration, international travel, extreme weather, and natural disasters, and the use of azole antifungal agents in large-scale agriculture are believed to underlie many of the increases in community-acquired fungal infections."

The recent emergence of *Candida auris* infections, for instance, underscores those concerns on a broad scale because *C. auris* is often multidrug-resistant, difficult to identify, and causes outbreaks in healthcare settings. A recent study from Finland that reported life-threatening fungal bloodstream infections associated with consuming probiotic supplements that contain *Saccharomyces boulardii* reveals a route of infection that may represent another mycological issue.

Fungi also have beneficial medicinal and culinary attributes. They were used in traditional medicine long before Alexander Fleming identified and extracted the therapeutic ingredient penicillin from *Penicillium* in 1928. They have subsequently been used to develop antibiotics, fungicides, anticancer drugs, and cholesterol inhibitors. Mushrooms and truffles are highly desirable foods; yeast is essential for baking, brewing, and fermenting; and molds flavor and color cheeses.

Another attribute of fungi, spalted wood—that is, wood colonized and stained by certain species of

Mattia di Nanni di Stefano (1403–1433), *Scipio Africanus* **ca. 1425–1430.** Poplar, bog oak and other wood inlay, rosewood, tin, bone, traces of green coloring, 24.19 in x 17.13 in/61.5 cm x 43.3 cm. Public domain image courtesy of The Metropolitan Museum of Art, New York, NY, USA.

fungi—was a prized commodity among European artisans who practiced the form of wood inlaying called intarsia. Spalted wood may be naturally created or stained by an artist; colors may be green, red, yellow, brown, or black. Writer David Elkind explains that green wood discolored by the green elf cup fungus *Chlorociboria aeruginascens* "happened to fill a lucrative niche in a burgeoning luxury trade, and that made it, for a time at least, as precious as some rare metals."

Intarsia, described as painting with wood to create mosaics as opposed to painting directly onto wood, is

Author affiliation: Centers for Disease Control and Prevention, Atlanta, Georgia, USA

thought to have originated before the seventh century CE. Its zenith was in Italy during the Renaissance (c. 1400−1600). The Tuscan city of Siena, Italy, known for producing many accomplished painters, was home to several *intarsiatori*, including Domenico di Niccolo and his apprentice Mattia di Nanni. *Intarsiatori* inlayed varied shapes, sizes, and species of wood—each with distinct patterns and tones—to fashion decorative items, panels, and elaborate pieces of furniture.

Featured on this month's cover is a wooden panel depicting Roman general Scipio Africanus, crafted by Mattia. According to the Metropolitan Museum of Art, this panel came from what must have been a quite large intarsia bench created for the council chamber of the Palazzo Pubblico in Siena and placed under Simone Martini's fresco the *Maestà*, a 7.62 m × 9.98 m painting that fills the north wall of the chamber. The bench comprised several panels depicting figures from Roman Republican history considered to be "models of civic virtue, such as the illustrious general Publius Cornelius Scipio Africanus." Scipio is remembered for the strategic and diplomatic skills that enabled him to defeat Hannibal in the Battle of Zama and end the Second Punic War in 202 BCE.

Mattia portrays Scipio gesturing with his hands—perhaps making the point that a leader must follow his head and his heart—and fixing an unyielding gaze on the viewer. The whorls and details in the interlocked wood pieces show muscles, eyes, hair, a draped tunic. A rich, patterned background adds contrast and texture. Noted woodworker Silas Kopf writes that Mattia's skills surpassed those of Domenico, from whom he had learned "how to create a strong graphic presentation through contrast, developing the craft further by laminating small pieces of wood into larger shapes."

Intarsiatori mapped out patterns and colors on paper and then created a matrix or framework to be filled in with different types, shapes, and sizes of wood. Their toolbox included saws, planes, chisels, clamps, knives, pigments, and varnishes. Intarsia projects required large amounts of different colored and textured types of wood, including oak, cypress, walnut, fruitwoods, boxwood, and spindle-wood. The artist would attach sections and pieces of wood called *tesserae* to the frame, following the paper template, incorporating larger pieces, and filling in with smaller ones to add details and depth. Mattia was among those who used additional materials: his *Scipio Africanus* features teeth made from bone and a helmet inlaid with metal strips.

Art historian Antoine Wilmering notes that Mattia meticulously tapered the ends of the *tesserae*, "enabling precise and smooth interweaving of the

different, naturally coloured woods. This technique allowed Mattia to create images with carefully modelled details, and some of the inlaid slivers are as fine as a painter's brush." The greenish tints in this panel may be slivers of naturally spalted wood, likely *griinfaule* or "green oak." As intarsia expanded across Europe, such wood became highly prized. Elkind notes that green wood discolored by the green elf cup fungus *C. aeruginascens* was "a mycological rarity."

The craft of intarsia continued to evolve, but spalted wood fell into disfavor once inorganic dyes and stains were readily available. Interest in incorporating spalted wood into intarsia was rekindled in the 1950s, and Professor Sara C. Robinson oversees a laboratory at Oregon State University focused on finding new uses for spalted wood not limited to the creative arts. A recent article by Hyde et. al. in the journal *Fungal Diversity* takes a broader view and examines 50 ways to exploit fungi as an untapped resource, including applications as antibacterials, antimycotics, fungicides, and biofilm inhibitors. Ubiquitous and unique, fungi have a fascinating array of yet unexplored uses.

Bibliography

1. Brandt ME, Park BJ. Think fungus–prevention and control of fungal infections. Emerg Infect Dis. 2013;19:1688–9. https://doi.org/10.3201/eid1910.131092
2. Centers for Disease Control and Prevention. Fungal diseases [cited 2021 Jul 17]. https://www.cdc.gov/fungal/index.html
3. Elkind D. Exquisite rot: spalted wood and the lost art of intarsia [cited 2021 Jul 8]. https://publicdomainreview.org/essay/exquisite-rot-spalted-wood-and-the-lost-art-of-intarsia
4. Hyde KD, Xu J, Rapior S, Jeewon R, Lumyong S, Niego AG, et al. The amazing potential of fungi: 50 ways we can exploit fungi industrially. Fungal Divers. 2019;97:1–136. https://doi.org/10.1007/s13225-019-00430-9
5. Jackson FH. Intarsia and marquetry [cited 2021 Jul 15]. https://www.gutenberg.org/files/30215/30215-h/30215-h.htm
6. Kopf S. A marquetry odyssey: historical objects and personal work. Manchester (Vermont): Hudson Hills Press; 2008. p. 31–36, 48.
7. Metropolitan Museum of Art. Scipio Africanus [cited 2021 Jul 8]. https://www.metmuseum.org/art/collection/search/208569
8. Rannikko J, Holmberg V, Karppelin M, Arvola P, Huttunen R, Mattila E, et al. Fungemia and other fungal infections associated with use of *Saccharomyces boulardii* probiotic supplements. Emerg Infect Dis. 2021;27:2043–51.
9. Robinson SC. The fine art of decay [cited 2021 Jul 17]. https://www.americanscientist.org/article/the-fine-art-of-decay
10. Wilmering A. Domenico Di Niccolò, Mattia Di Nanni and the development of Sienese intarsia techniques [cited 2021 Jul 21]. https://www.jstor.org/stable/887576

Address for correspondence: Byron Breedlove, EID Journal, Centers for Disease Control and Prevention, 1600 Clifton Rd NE, Mailstop H16-2, Atlanta, GA 30329-4027, USA; email: wbb1@cdc.gov

EMERGING INFECTIOUS DISEASES®

Upcoming Issue • October, 2021

- Characteristics, Comorbidities, and Data Gaps for Coronavirus Disease Deaths, Tennessee, USA

- Fatal Exacerbations of Systemic Capillary Leak Syndrome Complicating Coronavirus Disease

- Distribution and Characteristics of Human Plague Cases and Yersinia pestis Isolates from 4 Marmota Plague Foci, China, 1950–2019

- Novel Outbreak-Associated Food Vehicles and Outbreak Investigation, Prevention, and Communications Needs, United States

- Severe Acute Respiratory Syndrome Coronavirus 2 and Pregnancy Outcomes According to Gestational Age at Time of Infection

- Bloodstream Infection Risk, Incidence, and Deaths for Hospitalized Patients during Coronavirus Disease Pandemic

- Direct and Indirect Effectiveness of mRNA Vaccination against Severe Acute Respiratory Syndrome Coronavirus 2 in Long-Term Care Facilities, Spain

- Epidemiology of the Early COVID-19 Epidemic in Orange County, California, USA

- Fatal Cowpox Virus Infection in Human Fetus, France, 2017

- Severe Acute Respiratory Syndrome Coronavirus 2 Transmission in Georgia, USA, February 1– July 13, 2020

- Risk Assessment for Highly Pathogenic Avian Influenza A(H5Nx) Clade 2.3.4.4 Viruses

- Widespread Disease in Hedgehogs (*Erinaceus europaeus*) Caused by Toxigenic *Corynebacterium ulcerans*

- Genetic Diversity of SARS-CoV-2 in Travelers Arriving in Hong Kong

- Point-of-Care Antigen Test for SARS-CoV-2 in Asymptomatic College Students

- Human Babesiosis Reinfection

- Breakthrough Infections of SARS-CoV-2 Gamma Variant in Fully Vaccinated Gold Miners, French Guiana, 2021

- Seoul Virus Associated with Pet Rats, Scotland, United Kingdom, 2019

- Emergence of SARS-COV-2 Spike Protein Escape Mutation Q493R after Treatment for COVID-19

- Natural *Plasmodium inui* Infections among Humans and *Anopheles cracens* Mosquitoes, Malaysia

- Outbreak of Oropouche Virus in French Guiana

- SARS-CoV-2 Neutralization Resistance Mutations in Patient with HIV/AIDS, California, USA

- Rapid Increase in Lymphogranuloma Venereum among HIV-Negative Men Who Have Sex with Men, England, 2019

- Genomic Sequencing of SARS-CoV-2 E484K Variant B.1.243.1, Arizona, USA

- Multiple Transmission Chains within COVID-19 Cluster, Connecticut, USA, 2020

Complete list of articles in the October issue at
http://www.cdc.gov/eid/upcoming.htm

Earning CME Credit

To obtain credit, you should first read the journal article. After reading the article, you should be able to answer the following, related, multiple-choice questions. To complete the questions (with a minimum 75% passing score) and earn continuing medical education (CME) credit, please go to http://www.medscape.org/journal/eid. Credit cannot be obtained for tests completed on paper, although you may use the worksheet below to keep a record of your answers.

You must be a registered user on http://www.medscape.org. If you are not registered on http://www.medscape.org, please click on the "Register" link on the right hand side of the website.

Only one answer is correct for each question. Once you successfully answer all post-test questions, you will be able to view and/or print your certificate. For questions regarding this activity, contact the accredited provider, CME@medscape.net. For technical assistance, contact CME@medscape.net. American Medical Association's Physician's Recognition Award (AMA PRA) credits are accepted in the US as evidence of participation in CME activities. For further information on this award, please go to https://www.ama-assn.org. The AMA has determined that physicians not licensed in the US who participate in this CME activity are eligible for AMA PRA Category 1 Credits™. Through agreements that the AMA has made with agencies in some countries, AMA PRA credit may be acceptable as evidence of participation in CME activities. If you are not licensed in the US, please complete the questions online, print the AMA PRA CME credit certificate, and present it to your national medical association for review.

Article Title

Maternal Carriage in Late-Onset Group B *Streptococcus* Disease, Italy

CME Questions

1. Your patient is a 29-year-old woman found to have group B *Streptococcus* (GBS) colonization at her prenatal screening. According to the retrospective study by Berardi and colleagues, which of the following statements about the dynamics of GBS mother-to-infant transmission based on maternal vaginal-rectal (VR) colonization at prenatal screening and at time of commencement of late-onset disease (LOD), and on additional maternal urine and breast milk cultures collected at LOD onset, is correct?
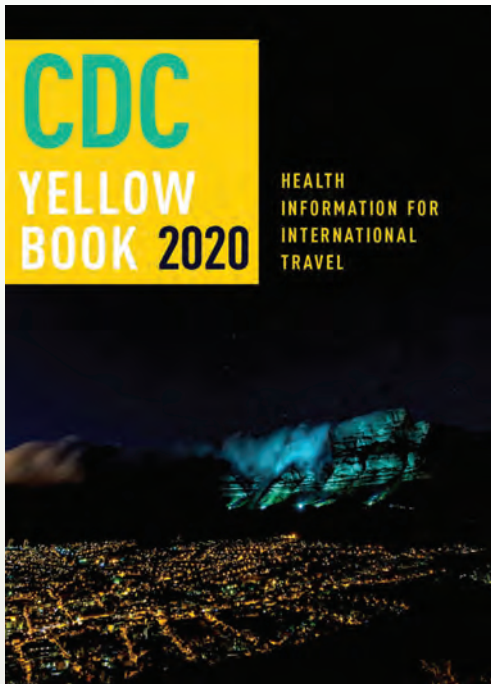
A. One-third of mothers with full assessment of VR carriage (at prenatal screening [APS] and at the time of late-onset disease onset [ATLO]) had VR colonization at either time point
B. Most women given adequate intrapartum antibiotic prophylaxis (IAP) were not GBS carriers at the time of LOD diagnosis
C. Mothers with VR colonization ATLO had high rates of GBS bacteriuria (33.9%) and positive breast milk culture (27.5%), independent of VR status at prenatal screening
D. Most women with positive breast milk culture had mastitis (1 million colony-forming units [CFU]/mL)

2. According to the retrospective study by Berardi and colleagues, which of the following statements about the dynamics of GBS mother-to-infant transmission based on molecular typing and antibiotic resistance is correct?

A. GBS strains from mother-infant pairs were serotype II
B. All but 1 GBS strain from mother-infant pairs belonged to clonal complex 17
C. Antimicrobial susceptibility differed widely among mother-infant pairs
D. Strains from most mother-infant pairs were resistant to both erythromycin and clindamycin

3. According to the retrospective study by Berardi and colleagues, which of the following statements about clinical implications of the dynamics of GBS mother-to-infant transmission is correct?

A. The study proves that mother-to-infant GBS transmission occurs via breastfeeding
B. The findings suggest that maternal transmission after delivery is relatively unlikely
C. Findings regarding GBS bacteriuria suggest that mothers are a relatively minor source of GBS exposure for their infants
D. The findings may facilitate predicting the impact of maternal GBS vaccination